

**Modular Approaches to Skeletally Diverse and
Stereochemically-rich 7- to 11-membered Ring Sultams**

By

Joanna Kejun Loh

Submitted to the graduate degree program in the Department of Chemistry and
the Graduate Faculty of the University of Kansas in partial fulfillment of the
requirements of the degree of Doctor of Philosophy

Paul R. Hanson, chair

Robert G. Carlson

Apurba Dutta

Minae Mure

Jon A. Tunge

May 15th, 2015
Date Defended

The Dissertation Committee for Joanna Kejun Loh
certifies that this is the approved version of the following dissertation:

**Modular Approaches to Skeletally Diverse and
Stereochemically-rich 7- to 11-membered Ring Sultams**

Paul R. Hanson, chair

May 15th, 2015
Date Approved

Abstract

Joanna Kejun Loh

Department of Chemistry

University of Kansas, May 15th, 2015

The overarching goal of this dissertation is the development of efficient methods for the generation of medium- and large-sized heterocycles, specifically 7- to 11-membered sultams, for facilitating probe and drug discovery. Chapter One summarizes the structural components that are prevalent in current marketed pharmaceutical agents, highlighting underrepresented rings, rings systems and frameworks, which have the potential to introduce chemical novelty into the existing limited list of chemical ring systems that describe the majority of the drugs.

Chapter Two introduces the concept of pairing of a reaction triad, namely sulfonylation, S_NAr addition and Mitsunobu alkylation, in varying order via the use of central *o*-fluorobenzene sulfonyl chloride building blocks that afford rapid access to both bridged- and fused-tricyclic, 7- to 10-membered benzofused sultams. This simple approach obviates the need for the construction of elaborate multi-functional scaffolds and merely requires use of *o*-fluorobenzene sulfonyl chlorides, amines and alcohols as building blocks. Simple changes in the reaction pair sequence (e.g., sulfonylation–S_NAr vs sulfonylation–S_NAr–Mitsunobu vs sulfonylation–Mitsunobu–S_NAr), or changes in the building blocks (1,2-amino alcohol vs 1,3-amino alcohol), allows access to skeletal and stereochemical diversity.

Chapter Three presents the concept of complementary pairing of activated

sulfonyl aziridines (simple 6-atom bis-electrophilic synthon) *via* "chemo- and regioselective" aziridine ring-opening with an amino component of an amino alcohol (bis-nucleophiles). Subsequent intramolecular S_NAr cyclization with the alcohol component of the amino alcohol affords unprecedented, functionally rich medium-sized benzofused sultams in overall, chemoselective "6+4" and "6+5" heterocyclization pathways. Moreover, the use of primary amines for the sulfonyl aziridine ring-opening step, whereby the resulting secondary amines cyclize via a subsequent intramolecular S_NAr reaction, enables the generation of 7-membered benzofused sultams via an overall "6+1" atom cyclization sequence

Chapter Four describes efforts aimed at the use of one-pot, sequential 3- or 4-component sulfonylation–aza-Michael–amide cyclization protocols to generate a library of skeletally and stereochemically diverse 7/4, 7/5 and 7/6-fused bicyclic acyl sultams. In this library effort, sulfonylation of different amines with 2-chloroethane sulfonyl chloride, followed by Michael reaction with a variety of amino acids, and subsequent amide cyclization provides access to the titled bicyclic sultams, which are currently being screened for biological activity as well as unique chemical properties.

*To my dearest family, Dad, Mum, sisters Christine and Lena for
love, help and support provided*

Acknowledgments

I want to first acknowledge my family – Daddy, Mummy, my two older sisters, Christine and Lena – for their patience, unconditional love and support during the last five years. Also to my extended family for all the love, concern and food provided when I returned for vacations. My niece, Jojo who was born in 2010, provided all the fun and annoyance that I missed at home. I am deeply grateful to everyone in my family for being there for me always, although we are really far apart from each other.

Next, are my friends, whom supported me throughout the five years here at KU, a special thanks to Sharon and Max, for providing food and a room to me. Jeremiah and Cynthia for taking care of me when I first came and left Lawrence, for being a chauffeur and having dinners together. Also, special thanks to Stephen and Mike for travelling together, for having fun times watching football (soccer) games. Erika, Iris and Jiahui for all their support too.

I want to give special acknowledgement to my boss, Professor Paul R. Hanson for his support and patience. The “pickup at a train station in England” has been mentioned and described in numerous meetings and conferences, and has reminded me of how my “Ph.D. Journey” began way back in 2009/2010. You taught me many things including chemistry, people skills, never give up on some people and the list goes on. It has been great to work in a group so diverse like yours, where I learned about so many different cultures. I am very grateful for what you have done for me and am glad that I chose you as my supervisor.

I would like to thank Susanthi, Soma, Moon Young and Naeem for the help, support and guidance during my Ph.D. and also former post docs including Alan, Thiwanka, Qin and Rambabu for their advice as well. My first undergraduate, Sun Young, was a great student and I loved working with her. I appreciate and really grateful to all Hanson Group members – past and present – that have helped me with my dissertation.

I would also like to acknowledge my thesis committee members: Professors Tunge, Carlson, Mure and Dutta for their help and guidance during my Ph.D. Thank you for your patience. In addition, special thanks to other research groups in Malott Hall, including all of the Tunge, Rubin, Malinakova, Clift and Prisinzano group members.

Lastly, I am very thankful to Dr. Gerald Lushington, Patrick Porubsky and Ben Neuenswander for providing enormous help with both purification and *in-silico* analysis as well as NMR and X-Ray personnel, Justin, Sarah and Victor for their help with gathering the NMR data and X-Ray structures. In addition, I would like to acknowledge our front office staffs, Susan, Beth, Beverly, Ruben, Dan and Donnie for all the excellent help and work that they have provided me.

Modular Approaches to Skeletally Diverse and
Stereochemically-rich 7- to 11-membered Ring Sultams

CONTENTS	Page #
Title Page	i
Acceptance Page	ii
Abstract	iii
Acknowledgments	v
Table of Contents	viii
Abbreviations	xiii
Chapter 1: Analysis of Ring Sizes and Structural Diversity Among Top 200 and U.S. FDA Approved Pharmaceuticals	1
1.1 Introduction	2
1.1.1 Molecular Descriptors of Drug Molecules	7
1.2 Background and Significance of Medium-sized and Macrocyclic Lactams	9
1.2.1 Ring Enumeration and Study of Ring Properties	11
1.3 Analysis of Ring Sizes and Structural Diversity from the Top 200 Drugs List and Orange Book of the FDA	
1.3.1 Introduction	13
1.3.2 Analysis of Top 200 US Pharmaceuticals and US FDA Approved Drugs: Ring Sizes, Structural Diversity and Frequency of Nitrogen Heterocycles	
1.3.2.1 Analysis of Top 200 US Pharmaceuticals	16
1.3.2.2 Analysis of FDA Approved Drugs (Frequency of	

Nitrogen Heterocycles)	20
1.3.3 Examples of Macrocyclic Nitrogen Heterocycles	24
1.3.4 Conclusion	25
1.4 Analysis of Top 100 Most Frequently Used Ring Systems in FDA Orange Book: Ring Sizes and Structural Diversity	
1.4.1 Introduction	26
1.4.2 Analysis of Ring Systems with Amides or Amide-types Motifs	28
1.4.3 Analysis of Ring System Sultams: Bridged and Azepine Scaffolds	29
1.4.4 Conclusion	32
1.5 Summary and Outlook	32
1.6 References cited	34
Chapter 2: A Modular Reaction Pairing Approach to the Diversity-Oriented Synthesis of Fused- and Bridged-Polycyclic Sultams	48
2.1 Introduction	49
2.1.1 Biological Profiles of Sultams (Cyclic Sulfonamides)	51
2.1.2 Chemical Profiles of Sulfonamides and Sultams	52
2.1.3 Synthesis of Sultams: Intramolecular S _N Ar methods	57
2.2 Results and Discussion	64
2.2.1 Optimization Studies	66
2.2.2 Scope of Reactions	67
2.2.3 Sulfonylation–Mitsunobu–Intramolecular S _N Ar Strategy	70
2.2.4 Mitsunobu–S _N Ar–[3+2] Cycloaddition Reaction Pairing	74
2.2.5 Chemical Informatics Analysis	75
2.2.6 Conclusion	77
2.3 Exploring Chemical Diversity via a Modular Reaction Pairing Strategy	

2.3.1 Introduction	77
2.3.2 Results and Discussion	78
2.3.2.1 Optimization of Conditions	79
2.3.2.2 Library Design	81
2.3.2.3 Validation and Library Generation	83
2.3.3 In Silico Analysis of Chemical Diversity and Drug-likeness	85
2.3.3.1 Cartesian Grid-based Chemical Diversity Analysis	85
2.3.3.2 Overlay Analysis	86
2.3.3.3 Principal moments of inertia (PMI) analysis	87
2.3.3.4 Conformational Analysis	88
2.3.3.5 Quantitative estimate of drug-like (QED) values and Z-scores	89
2.3.4 Conclusion	91
2.4 Summary and Outlook	92
2.5 References Cited	93

Chapter 3: Complementary Pairing: A Modular, One-pot, Sequential Aziridine Ring-Opening–S_NAr Strategy to Benzofused Sultams	118
3.1 Introduction	119
3.1.1 Basics of Macrocyclization	122
3.1.2 Synthesis of Macrocycles for Drug Discovery	124
3.1.2.1 Macrolactamization and Macrolactonization	125
3.1.2.2 Substitution Chemistry: S _N 2 and S _N Ar Reactions	128
3.1.2.3 Miscellaneous Methods: Mitsunobu reaction, Ring Expansion/Opening and MCR-Ugi-type Macrocyclization	131
3.1.3 Importance of Stereochemically (sp ³)-Rich Molecules	134
3.2 Complementary Ambiphile Pairing (CAP) and Complementary Pairing	

(CP) Strategies to Benzofused Sultams	137
3.3 Results and Discussion	140
3.3.1 Optimization Studies	140
3.3.2 Synthesis of 10- and 11-membered Benzofused Sultams	143
3.3.3 Synthesis of Stereochemically-rich Benzofused Sultams	145
3.3.4 Synthesis of 7-membered Benzofused Sultams	146
3.3.5 Mitsunobu Reaction to Bridge Benzofused Sultams	148
3.3.6 ¹⁹ F NMR of Benzenesulfonamides Intermediates	149
3.3.7 “Click, Click, Click, Cyclize” to Stereochemically-rich, 10-membered Benzofused sultams	151
3.3.8 Principal Moments of Inertia (PMI) Analysis	152
3.3.9 Overlay Analysis	154
3.4 Summary and Outlook	156
3.5 References cited	156
Chapter 4: Modular One-pot, Sequential Protocols Towards Diverse Acyl Sultam Libraries	180
4.1 Introduction	181
4.1.1 Acyl sulfonamides/sultams	182
4.1.2 Applications: Covalent Protein Modification via Residue-specific Electrophiles	184
4.1.2.1 Covalent Modification of Serine	186
4.1.2.2 Covalent Modification of Cysteine	187
4.1.2.3 Covalent Modification of Lysine	189
4.1.3 One-pot, Sequential Multi-component Protocols	191
4.2 Results and Discussion	192
4.2.1 Optimization Studies	194

4.2.2 Library Design and Scope of Reagents	196
4.2.3 Validation and Library Generation	198
4.2.4 Computer Analysis of Molecular Properties and Shape Diversity	200
4.2.4.1 Molecular Properties	200
4.2.4.2 Principal Moments of Inertia (PMI) Analysis	202
4.2.4.3 Overlay Analysis	203
4.2.5 Conclusion	204
4.2.6 Reactivity Profiling of Potential Electrophilic Modifiers	205
4.2.6.1 Initial Reactivity Profiling of Acyl Sultams	205
4.3 Summary and Outlook	211
4.4 References cited	211
Chapter 5: Experimental Data for Chapters 2–4	221
Appendix A: ^1H and ^{13}C NMR Spectra	221
Appendix B: X-Ray Structure Reports	502

Abbreviations

ADME	absorption, distribution, metabolism and excretion
ABPP	activity-based protein profiling
ATP	Adenosine triphosphate
MeCN	acetonitrile
aq	aqueous
BEAD	benzylethyl azodicarboxylate
Bn	benzyl
BnBr	benzyl bromide
BCP	build-couple-pair
Boc	<i>tert</i> -butyloxycarbonyl
<i>t</i> -BuOH	<i>t</i> -Butanol
CHCl ₃	chloroform
CuI	copper iodide
CAP	complementary ambiphilic pairing
cat.	catalytic
COSY	correlation spectroscopy
C	carbon
Cs ₂ CO ₃	cesium carbonate
CsF	cesium fluoride
Cl	chlorine
CA	chloroacetamides
CP	complementary pairing
CMLD	Center of methodology and library development
CuBr	copper bromide
CDK2	Cyclin-dependent kinase 2
DABCO	1,4-Diazabicyclo[2.2.2]octane
DBU	1,8-diazabicycloundec-7-ene

DCM (CH ₂ Cl ₂)	dichloromethane
Et ₂ O	diethyl ether
DIAD	diisopropyl azodicarboxylate
DIC	<i>N,N'</i> -Diisopropylcarbodiimide
DIPEA/Hünig's base	<i>N,N'</i> -Diisopropylethylamine
DMF	dimethylformamide
DMSO	dimethylsulfoxide
Boc ₂ O	Di-tert-butyl dicarbonate
DOS	diversity oriented synthesis
DMAP	4-(dimethylamino)pyridine
DTT	Dithiothreitol
Da	daltons
E ⁺	electrophile
Eq.	equivalent
Et	ethyl
EtOAc	ethyl acetate
EDC (EDCI)	1-ethyl-3-(3-dimethylaminopropyl)carbodiimide
FG	functional group
FP	fluorophosphonate
FDA	Food and Drug Administration
FCMA	formimidate carboxylate mixed anhydride
GC	gas chromatography
GSTO1	glutathione S-transferase omega 1
HFIP	hexa-fluoroisopropyl
HCl	hydrochloric acid
HPLC	high performance liquid chromatography
HRMS	high resolution mass spectrometry
ABHD6	α - β hydrolase-6
NHS	hydroxysuccinimidyl

h	hours
Hsp90	heat shock protein 90
Hz	hertz
HCV	hepatitis C virus
HTS	high throughput screening
HIV	human immunodeficiency virus
HSA	human serum albumin
HOBt	1-hydroxybenzotriazole
HBA	hydrogen bond acceptor
HBD	hydrogen bond donor
IA	iodoacetamides
IR	infrared radiation
IC ₅₀	inhibitory concentration at 50%
IMDA	Intermolecular Diels-Alder
ⁱ Bu	isobutyl
ⁱ Pr	isopropyl
Leu	Leucine
LiOH	Lithium hydroxide
LCMS	Liquid chromatography–mass spectrometry
LG	leaving group
M	molarity
<i>mW</i>	microwave
MeOH	Methanol
MeI	methyl iodide
MW	molecular weight
MLPCN	Molecular Libraries Probe Production Centers Network
MAGL	monoacylglycerol lipase
Mmol	millimole(s)
MsCl	methanesulfonyl chloride

7-mmc	7-mercapto-4-methyl-coumarin
MCR	multi-component reactions
MFS	multifusion similarity
NSAIDs	Non-steroidal anti-inflammatory drugs
NMR	nuclear magnetic resonance
NIH	National Institute of Health
NEP	neutral endopeptidase 24.11
Nuc/Nu	nucleophile
ⁿ Bu	n-Butyl
OMe	methoxy
PMB	<i>para</i> -methoxybenzyl
ppm	parts per million
PBPs	penicillin binding proteins
Ph	phenyl
PTSA	<i>p</i> -toluenesulfonic Acid
XLogP	partition coefficient
PI3K	phosphoinositide 3'OH kinase
K ₂ CO ₃	potassium carbonate
PCA	principal component analysis
PMI	principal moments of inertia
PEM	protein epitope mimics
PKC	protein kinase C
RCM	ring closing metathesis
rt	room temperature
S	sulfur
Sat'd	saturated
SAR	structure activity relationship
SHs	serine hydrolases
Si	silicon

NaN ₃	sodium azide
NaO ^t Bu	sodium <i>tert</i> -Butoxide
NaHMDS	sodium hexamethyldisilazide
SL-PTC	solid-liquid phase transfer catalysis
SPE	solid phase extraction
SM	starting material
SAR	structure-activity-relationship
TACE	TNF- α converting enzyme
TBAF	Tetrabutyl ammonium fluoride
ⁿ Bu ₄ NBr	tetra-n-butylammonium bromide
TBS	<i>tert</i> -butyldimethylsilyl
TFA	trifluoroacetic acid
K ₃ PO	tripotassium phosphate
PPh ₃	triphenylphosphine
TLC	thin layer chromatography
^t Bu	<i>tert</i> -butyl
Et ₃ N	triethylamine
TEBA	triethylbenzylammonium chloride
THF	tetrahydrofuran
THIQ	tetrahydroisoquinoline
TLC	thin layer chromatography
TLR4	Toll-like receptor 4
TopoPSA	topological polar surface area
TPP	triphenylphosphine
TOS	target oriented synthesis
Val	valine
VEGF-R2	vascular endothelial growth factor receptor-2
H ₂ O	water

Chapter 1

Analysis of Ring Sizes and Structural Diversity

Among Top 200 Drugs and

U.S. FDA Approved Pharmaceuticals

1.1 Introduction

The development of efficient methods¹ for the generation of medium- and large-sized heterocycles¹ is an emerging area for use in probe advancement for chemical biology and drug discovery (Figure 1.1).² In particular, 7- to 11-membered³ lactams have recently surfaced as both novel probes and drugs (Figure 1.1).^{2,4} Naturally occurring cyclic peptides have also been discovered to selectively bind proteins or small molecules, which has led many researchers to design and synthesize unique heterocycles as novel peptidomimetics.⁵ These strained rings are more easily adapted to biological targets than their more flexible linear peptide counterparts. Due to their physicochemical properties, macrocycles are often more stable to hydrolysis, exhibit enhanced lipophilicity, cell permeability and bioavailability when compared to their linear counterparts. These

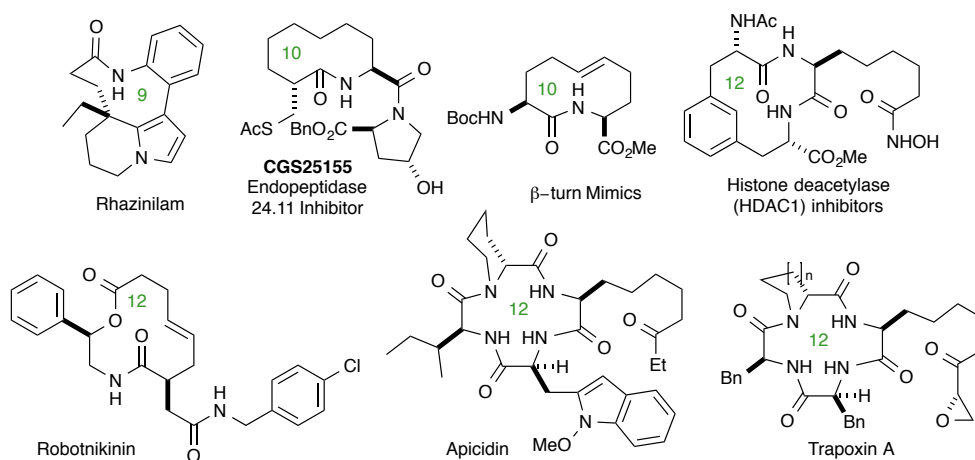


Figure 1.1. Biologically significant natural and synthetic medium- and large-sized heterocycles.

- [I] It should be noted that the definition of ring sizes are based on the number of atoms in the S_N2 cyclization as defined in Reference 3 reported for instance, (a) small rings are 3- to 4-membered (b) common rings are 5- to 7-membered, (c) medium rings are 8- to 11-membered and lastly (c) macrocycles are ≥ 12 -membered.

attributes have motivated several groups to develop methods aimed at the generation of a number of natural product-like medium-sized⁶ and macrocyclic ring systems,⁷ which has in turn, enabled efforts to address difficult drug targets such as those involving protein-protein interactions,⁸ as well as, epigenetic targets.⁹

In contrast, the production of medium-sized sultams (lactam surrogates), with diverse biological activities and medicinal value were relatively rare in the literature at the beginning of this dissertation. Since 2010, more synthetic groups have developed methods for the construction of benzofused sultams, with the majority being 8-membered ring scaffolds,¹⁰ as well as a select number of 9- to 15-membered sultams.¹¹ Two prominent examples of recently discovered bioactive sultams are the macrocyclic inhibitor of HIV-1 developed by Ghosh in 2009,¹¹ and the recently developed inhibitor of lysosomal acidification reported by Schreiber in 2015¹² (Figure 1.2).

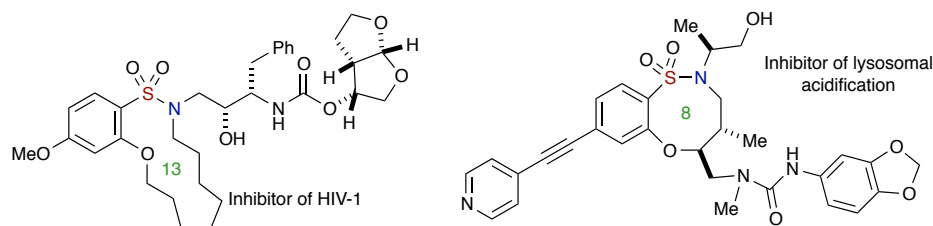


Figure 1.2. Two prominent examples of bioactive sultams.

It is the purpose of this thesis to report studies aimed at the development of several facile and modular strategies for the generation of 7- to 11-membered, polycyclic and bridged sp^3 -rich, benzofused sultams and non-aryl 7/4-, 7/5- and 7/6-fused bicyclic acyl sultams (Figure 1.3). In particular, the syntheses to furnish 7- to 10-membered bridged benzofused sultams will be covered in Chapter 2, Chapter 3 will detail new chemical methods to construct 7- and 10-/11-membered polycyclic benzofused sultams,

while Chapter 4 will finish with a detailed account of efforts to novel, non-aryl 7/4-, 7/5- and 7/6-fused bicyclic acyl sultams.

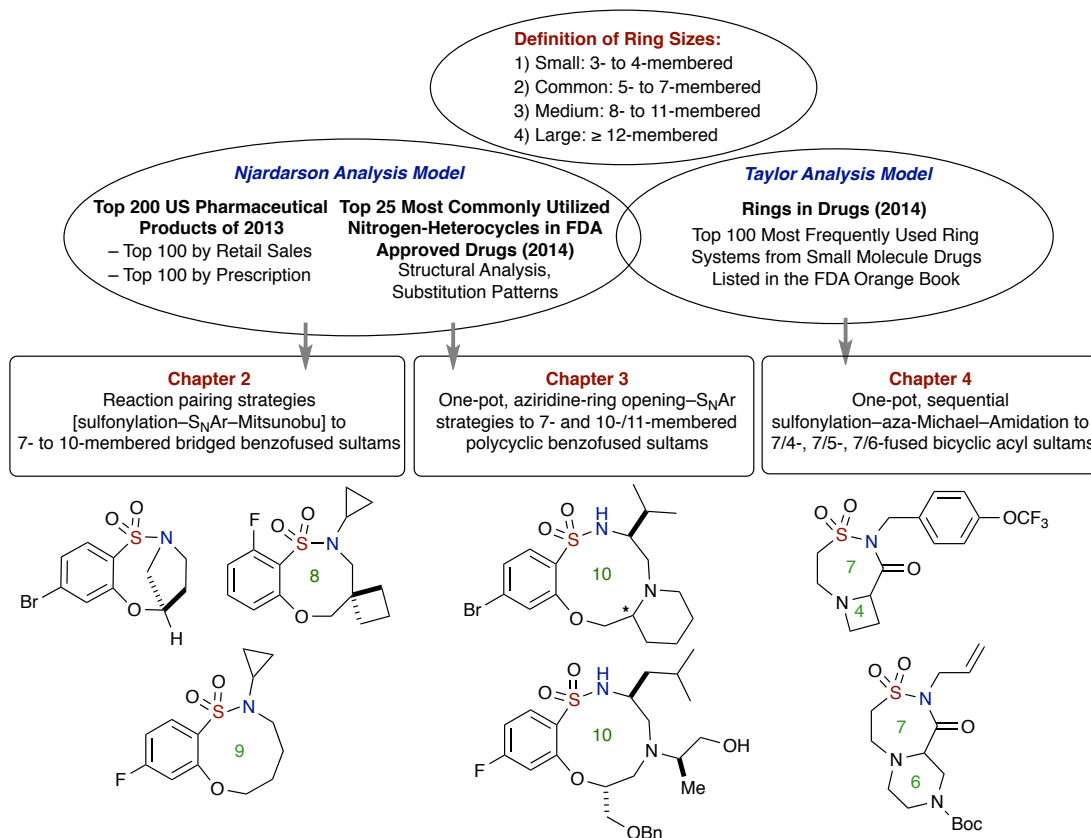


Figure 1.3. Heterocyclic Rings in Drugs Analysis Models reviewed in Chapter 1 and their respective connectivity to Chapters 2–4.

The aim of this chapter is to highlight two recent analysis models developed by Njardarson and Taylor,¹³ which examine the prevalence of heterocyclic rings in currently marketed drugs. Their collective analyses highlight the variety of rings, ring sizes, structural diversity, and substitution patterns found in currently marketed drugs. For the purpose of this chapter, emphasis is placed on the frequencies of common, medium and large-sized lactams, as well as on cyclic scaffolds containing amides or related motifs.

The two drug analysis models provided in this chapter (Njardarson and Taylor) are analyzed in a manner to aid in the identification of underrepresented chemical space that has the potential to be "drug- or probe-like" (Figure 1.3, page 4). As summarized in Figure 1.3 (page 4), the heterocyclic rings in the drugs analysis models are covered in two reviews, which are derived mainly from the Orange Book of the US FDA,¹⁴ but compiled with different parameters by each respective investigator. The first list is the Njardarson Analysis Model and is comprised of the recently tabulated top 200 US pharmaceuticals agents as of 2013. The Njardarson Analysis Model is augmented with 1,086 drugs in a mini-perspective that covers the frequency of nitrogen heterocycles.^{13a-c} The second list of heterocyclic rings is the Taylor Analysis Model that contains 1,175 drugs compiled by Taylor and co-workers in a 2014 report entitled "Rings in Drugs".^{13d}

The identification of scarcely represented structural components in both analyses has the potential to guide the design of new synthetic methods toward the generation of underrepresented, unique scaffolds. In combination with chemical methods development, this data can be used to direct the design and synthesis of diverse scaffolds possessing inadequately represented ring systems, which in turn can provide tools for drug discovery and biological probe studies. Understanding the various factors that make up a drug-like scaffold is highly significant, and will in turn enable the development of robust, scalable and efficient syntheses of new and unique nitrogen heterocycles.

Among the underrepresented heterocycles, we became interested in synthetic methods to generate 7- to 11-membered benzofused sultams and non-aryl 7/4-, 7/5- and 7/6-fused bicyclic acyl sultams. In this regard, sultams represent a class of non-natural

chemotypes that have gained interest in recent years due to their numerous biological activities including several with medicinal value. However, they occupy a much smaller collective area of chemical space when compared with other heterocycles, yet possess innate properties that convey unique chemical characteristics, thus warranting their development, a detailed summary of which can be found in Chapters 2–4.^{II}

In addition to the synthetic methods developed to generate these unique scaffolds, the sultams frameworks have been evaluated with several computational analyses, as outlined in Table 1.1. As will be detailed in Chapters 2–4, cheminformatic studies reveal that the sultams detailed in this thesis lie within new chemical space when mapped using several analyses. The focus of this thesis is to develop synthetic methods for the construction of distinct sultam scaffolds, mainly 8- to 11-membered benzofused sultams and non-aryl 7/4-, 7/5- and 7/6-fused bicyclic acyl sultams that are scarcely represented as evident from both the Njardarson and Taylor Analysis Models. Although 7-membered heterocycles are more common, 7-membered heterocyclic scaffolds containing stereogenic centers and functional handles for diversification are still relatively deficient in both Analysis Models. Hence, there is a demand for new chemical methods for the generation of unique and diverse 7-membered benzofused sultams as well as non-aryl 7/4-, 7/5- and 7/6-fused bicyclic acyl sultams.

[II] Several of the chemical properties and guidelines such as ADMET, Lipinski “rule of 5” and ring systems will be briefly described in section 1.1.1, providing the necessary parameters for a small-molecule new molecular entities (NMEs).

Table 1.1. Chemical Space Analysis.

Chapter 2

- Cartesian grid-based chemical diversity analysis
- Overlay Analysis
- Principal Moments of Inertia (PMI)
- Conformational Analysis
- Quantitative estimate of drug-like (QED) values

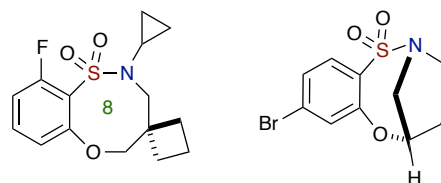
Chapter 3

- Principal Moments of Inertia (PMI)
- Overlay Analysis
-

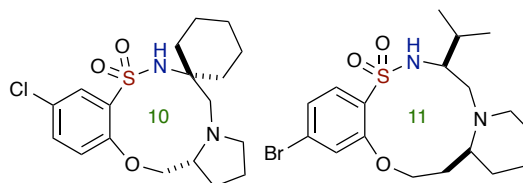
Chapter 4

- Principal Moments of Inertia (PMI)
- Overlay Analysis

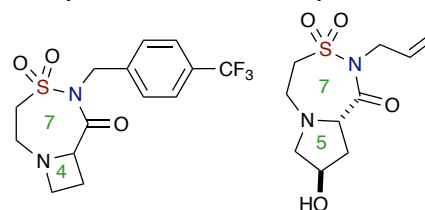
Chapter 2 8-/9-membered Bridged Benzofused Sultams



Chapter 3 10-/11-membered Polycyclic Sultams



Chapter 4 7/4- and 7/5- fused Acyl Sultams



1.1.1 Molecular Descriptors of Drug Molecules

The philosophic view-point of scaffolds occupying drug-like space has been a pervasive issue in medicinal chemistry for a long period of time.¹⁵ The development of molecular descriptors of currently marketed drugs, which can aid in the design of new drugs, is a commonly accepted strategy adopted in order to improve the downstream success of small molecules in clinical trials.¹⁶ Indeed, the failure of new experimental drugs in the clinic can often be attributed to poor physicochemical characteristics, which resulted in poor efficacy, toxicology and safety.¹⁷ However, it is challenging to tabulate the number of failures, as many times chemical problems connected to the structure or

substructure occur during the early phase of discovery and involve issues like undesirable absorption, distribution, metabolism, excretion and toxicity (ADMET).

A full understanding of a successful drug profile is essential to the development of future small-molecule new molecular entities (NMEs).¹⁸ Optimal drug-like parameters and characteristics are generally directed by the Lipinski “rule of 5”^{15a}, which have become steadfast guidelines in medicinal chemistry. The Lipinski “rule of 5” postulates a way of improving drug-like characteristics based on a set of molecular descriptors for small molecule marketed oral drugs. These properties include molecular weight, cLogP, polar surface area, and the number of hydrogen bond donors and acceptors.

In addition to the current drug-like parameters, there have been many extensions and improvements to categorize drug-like space of small molecules, including accounting for chemical composition, substructure scaffolds¹⁹ and ring systems within drugs. Ring systems^{13d} are the basic building blocks of most marketable drugs today as they play a pivotal role in molecular properties like electronic distribution, three dimensionality and scaffold rigidity; and these are key factors in the determination of lipophilicity, molecular reactivity, metabolism stability and toxicity.²⁰ Hence, identifying ring systems that prevail in current marketed drugs will enable underrepresented structures to be highlighted as well, thus enhancing the probability of generating the unique scaffolds such as the aforementioned 7- to 11-membered benzofused sultams and non-aryl 7/4-, 7/5- and 7/6-fused bicyclic sultams.

Taken collectively, the aforementioned analyses can potentially assist in the development of screening collections of structurally diverse compounds that can aid in

the discovery of lead compounds in drug discovery. Small-molecule probes continue to gain in importance as new biological targets emerge from the human genome project. These probes, which often initiate as hits from screening numerous compound collections via high-throughput screening (HTS), can be further developed into powerful tools in chemical biology that aid in the identification of fundamental processes in disease-associated biological problems.²¹ As stated above, the quality and identity of the screening collections is intricately important to the success of the screening approach, which in turn emphasizes the significance that synthetic organic chemistry plays and the importance of generating quality collections of small-molecules to be screened.²² In the end, diversity and suitable physicochemical properties such as sp^3 -rich compounds will undoubtedly play a role in order for probe development to advance further.

1.2 Background and Significance of Medium-sized and Macrocyclic Lactams

During the past decade, an increasing interest has focused on the generation of medium-sized and macrocyclic lactams. Due to their intriguing physico properties and a range of complex natural products being characterized by having lactam structures, their total synthesis is a broad field for organic chemists towards the development of new strategies and methods to access such ring systems. In 2001, Nubbemeyer reported a relatively extensive review on the synthesis of medium-sized ring lactams covering several major methods toward the generation of medium-sized rings, including ring-closure reactions, cycloadditions, ring-expansion reactions by *N*-insertion, ring expansion reactions by *C*-insertion, and fragmentation reactions.²³

In 2009, Troin and coworkers reported the asymmetric synthesis of 7- and higher-membered ring nitrogen heterocycles.²⁴ In 2010, Hassan described the recent applications of ring-closing metathesis in the synthesis of lactams and macrolactams.²⁵ In 2011, van der Eycken and co-workers reported a mini review, about microwave-assisted synthesis of medium-sized heterocycles, where a diverse range of *N*-, *O*- and *S*-containing rings were obtained utilizing various reactions.^{1b} In 2011, Aubé and coworkers reported an emerging area of medium-bridged lactams synthesized by the intramolecular Schmidt reaction, which they defined as a new class of non-planar amides.²⁶ In 2014, Azev and coworkers disclosed a mini-review on employing aminoacyl incorporation reactions of peptides for the synthesis of medium-sized heterocycles, where rigid building blocks such as pyrrolizidines proceeded with a transamidation reaction, followed by nucleophilic substitution at a carbon atom of an activated imide group and ring expansion.²⁷

Taken collectively, the chemistry of medium and macrocyclic lactams has undergone a period of intense growth with numerous publications appearing throughout the years. In contrast, only three reviews on the synthesis of sultams have been reported in the literature, this is surprising considering their broad biological profile (an extensive list of chemical and biological properties of sultams will be reviewed in Chapter 2, providing details to the structural uniqueness of sultams). The first sultam review was reported by Mustafa in 1954, and covered the chemistry of sultones and sultams.²⁸ Over five decades later in 2010, Majumdar and coworkers, reported recent developments in the synthesis of fused sultams, covering the period from 2000–2010.²⁹ In 2012, Sokolov and

coworkers presented a second review on methods enabling the synthesis of mono- and polycyclic sultams.³⁰ However, a full account of specified sultam ring sizes such as 8-, 9-, 10-, and 11-membered, as well as stereochemically-rich sultams, is noticeably absent in the literature, warranting the development of additional strategies to facilitate the synthesis of these unique structural scaffolds.

1.2.1 Ring Enumeration and Study of Ring Properties

In 2010, it was reported that the cost of drug discovery for a new molecular entity (NME) is estimated to be from \$166 million for hit-to-lead and \$414 million for lead optimization, stressing the significance of efficient and timely choices for both the adoption of the initial scaffold as well as subsequent development.³¹ These alarming figures have prompted a number of studies aimed at scaffold analysis. The following is a short summary of contributions in this area.

A significant report in 1996 by Bemis and co-workers,³² concluded that the shapes of half of the 5,120 drugs currently marketed, up till 1995, could be described by using 32 most frequently occurring frameworks. The structural data is organized by grouping the atoms of each drug molecule accordingly into ring, linker, framework and side chains atoms where it was suggested that the diversity of shapes in the set of known drugs is extremely low. In 2003 and 2006, Lewell and co-workers³³ and Ertl and co-workers,³⁴ constructed web-based databases of drug rings, where the second database of Ertl consists of five and six-membered rings showing bioactivity that was sparsely distributed among a small groups of compounds. In addition, Vieth and co-workers reported that

30% of the 1,386 currently marketed drugs contain another drug as a scaffold building block.¹⁹ In 2010, Wang and co-workers³⁵ applied a systematic and comprehensive approach to detail the scaffolds and rings in drugs and showed that there was important overlap between approved drugs and experimental drugs. Several databases of rings and scaffolds were compared between various groups like Bemis, Lee and co-workers,³⁶ and Vieth, noting substantial differences that were associated to the core databases, thus demonstrating the significance of a well-documented data set for this type of analysis.

The aforementioned investigations have revolved around categorizing drug-like rings and several research groups have concluded that the number of ring systems in drugs, as well as bioactive space, is presently very small, and relegated to sparsely populated groups. Other groups have focused on larger data sets,³⁷ and have showed that the number of new molecular frameworks per year has increased since 1959, but these frameworks are comprised of a narrow distribution of building blocks derived by the assembly of the same small set of building blocks in novel ways, such as through the use of Pd-catalyzed cross-coupling chemistry.

In 2008, Lipkus and co-workers³⁸ analyzed the Chemical Abstracts Service (CAS) registry for structural diversity and concluded that a small percentage of frameworks occur in a large percentage of compounds. In contrast, in 2009 Pitt and co-workers³⁹ compiled a list of possible ring systems that have not been synthesized. In 2012, Ertl and co-workers extended their earlier work,⁴⁰ and analyzed databases from ChEMBL,⁴¹ DrugBank,⁴² and ZINC⁴³ in order to generate a database of rings and scaffolds for scaffold hopping. Taken collectively, all of these analyses suggest that synthetic cost is

a key factor, and that “chemical decision-making” must become a vital part of the drug discovery process.

Various groups have investigated the properties of rings. In 1996, Gibson⁴⁴ and co-workers explored the 100 most common heterocyclic rings and derived a principal components model for *in vitro* biological activity. More recently, two different groups explored the importance of aromatic ring count, concluding that more than three aromatic rings in a molecule corresponded with an increased risk of attrition in development.⁴⁵ In addition, they defined a new molecular descriptor to assess the potential for a compound to be developed further, claiming it to be the second most important descriptor after hydrophobicity.

1.3 Analysis of Ring Sizes and Structural Diversity from the Top 200 Drugs List and Orange Book of the FDA

1.3.1 Introduction

As stated earlier, the Njardarson Analysis Model contains two parts, the first portion is the top 200 U.S. Pharmaceutical Products of 2013, recently published by Njardarson and co-workers,^{13a-b} and the second portion includes 1,086 drugs covered in a recent mini-perspective by the same group about the structural diversity, substitution patterns and frequency of nitrogen heterocycles among the pharmaceuticals.^{13c} Njardarson and co-workers have annually assembled a pharmaceutical product list since 2006, with the ultimate goal of generating new research and teaching tools that exploit the pictorial language of organic chemistry in order to gain insight on topics such as

structural patterns, frequency of atoms and substructures while also acquiring information on the type of chemical structures that are deficient from approved pharmaceuticals. The group has also reported investigations on sulfur, which is the fifth most prevalent element, as well as fluorine, a key element in about 20% of recently approved pharmaceuticals drugs.⁴⁶

The primary intent of the Njardarson Analysis Model is to critically analyze the top 200 drugs list by retail sales and prescription, where 47/100 drugs defined by retail sales are cyclic pharmaceutical agents excluding aromatic rings. Furthermore, this list is comprised mainly of 4- to 7-membered rings, as well as two macrocycles. Similarly, 40/100 drugs defined by prescription were comprised of the same structural component; small and common-sized rings and one macrocycle. Although the data set is relatively tiny, the top 200 pharmaceuticals list encompasses only a narrow window of rings, rings systems and frameworks, underlining the deficiency of numerous unique heterocycles such as 8- to 11-membered heterocycles.

A second major point brought to light in the Njardarson Analysis Model is the validation that nitrogen heterocycles are among the most significant structural components of pharmaceuticals in the list of FDA-approved drugs. Their analysis displays the top 25 most frequent nitrogen heterocycles, which highlights the majority of the rings as small and common-sized. Evaluation of their database of FDA-approved drugs reveals that 59% (640/1086) of unique small-molecules drugs contain a nitrogen heterocycle. However, within the 59%, only a few components contain 3- to 8-membered ring sizes as well as > 12-membered ring sizes, with the majority being small

and common-sized cyclic scaffolds. Likewise, to date, there are no 8- to 11-membered nitrogen heterocycles among the 1,086 small-molecules drugs reported by Njardarson and co-workers. This is surprising when one considers the number of papers alluding to their activity,^{2,4} as well as potential to modulate protein-protein interactions⁸ and epigenetic targets.⁹ For the purpose of this discussion, we will be examining the limited list of 7- and 8-membered rings, as well as some examples of macrocyclic nitrogen heterocycles.

Before analyzing ring sizes, several definitions as abbreviated by Taylor⁴⁷ need to be explained. The first is how to define a molecular series that is based on the core “rings”, “ring systems” and “frameworks”. Therefore, by definition, a ring is defined as the smallest non-fused moiety with no acyclic (either hydrocarbon and/or heteroatom containing) linkers or terminal groups (Figure 1.4). Next, a ring system is defined as a complete ring or rings formed by removing all terminal and acyclic linking groups without breaking any ring bonds. Finally, a framework is defined as containing all the ring systems as well as ring systems that are linked by non-terminal acyclic groups (Figure 1.4).

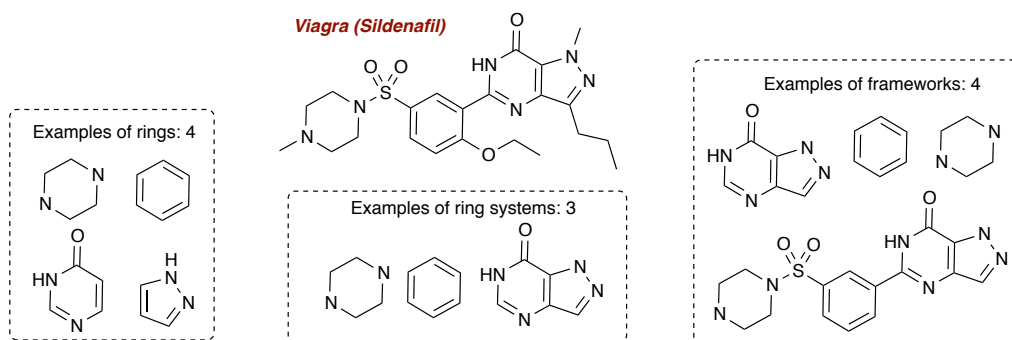


Figure 1.4. Using Viagra as an example for the definitions of rings, ring systems and frameworks.

1.3.2 Analysis of Top 200 US Pharmaceuticals and US FDA-Approved Drugs: Ring Sizes, Structural Diversity and Frequency of Nitrogen Heterocycles

1.3.2.1 Analysis of Top 200 US Pharmaceuticals

The first part of the Top 200 US Pharmaceuticals list is comprised of two segments, which includes the top 100 pharmaceuticals by retail sales and the top 100 by prescription. This is a relatively small list, but contains detailed analysis based on retail sales and prescriptions by medical doctors within the USA. This data set highlights the top 200 out of almost 2000 pharmaceuticals established in the Orange Book of the FDA, and demonstrates the prevalence and importance of these 200 current drugs and their structural components. One other significant factor of this list is that it categorizes non-nitrogen heterocyclic small-molecule drugs, whereas other data sets are focused on the frequency of nitrogen heterocycles that are FDA-approved.

Among the 100 drugs listed by retail sales, 33 drugs belong to oligopeptides, long chain polymers, proteins, and antibodies that were all removed from the data set. In addition, for obvious reasons, three drugs that contain no rings such as lyrica (pregabalin–musculo-skeletal and nervous drug),⁴⁸ lovaza (omega 3-acid ethyl esters–cardiovascular drug)⁴⁹ and Tecfidera (dimethyl fumarate– musculo-skeletal drug)⁵⁰ were disregarded. Similarly, drugs that contain only aromatic rings were not included as the molecular properties of aromatic rings are different than regular rings, namely in the absence of sp^3 stereogenic centers. This accounts for the elimination of 17 out of the remaining 64 drugs, which implies that only 47 are left to analyze. Out of the remaining 47, two drugs are macrocycles⁵¹ (cyclosporine–immunosuppressant and sensory organ drug and everolimus–anti-cancer and oncology drug), four are sulfonamide-containing

scaffolds (darunavir⁵²—anti-infective drug and sildenafil⁵³—genito-urinary and sex hormone drug) and 41 pharmaceuticals contain rings of different sizes (Figure 1.5).

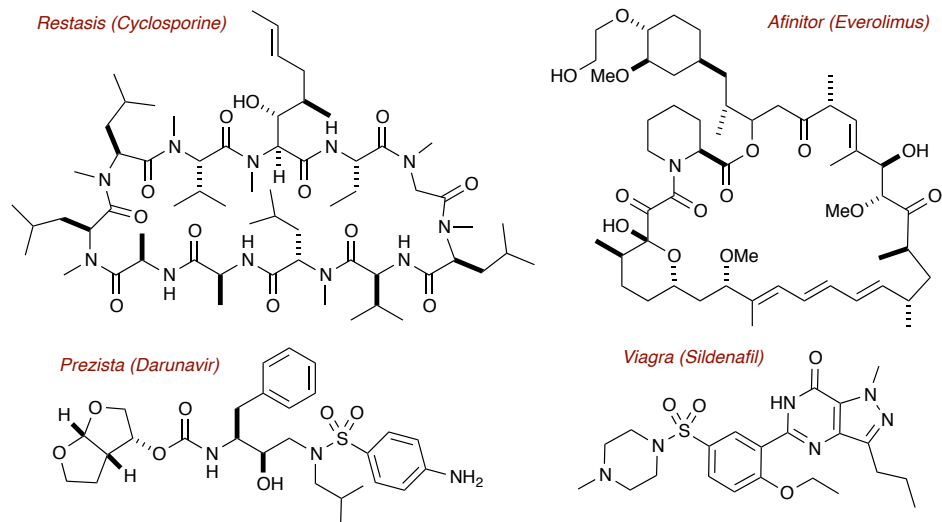


Figure 1.5. Two macrocycles and two sulfonamides from the top 100 list by retail sales.

As shown in the top 100 drugs list, macrocyclic and sulfonamide-bearing drugs represent two unique sets of scaffolds that have attained prominence as pharmaceutical agents. Although benzene-sulfonamide-containing compounds do not possess the “sulfonamide moiety within the ring”, and are comprised of mainly common-sized rings as substituents that are extending out from the central skeleton, they do play a pivotal role, suggesting the importance of ArSO_2NR_2 motifs. These highlighted motifs and their respective flexible core structure might be assisting in the interaction between the binding sites and their respective targets as proven by several structure-activity-relationship (SAR) studies that were completed.⁵⁴

From these aforementioned 41 pharmaceutical agents, only one drug, Zetia (ezetimibe—cholesterol level drug) and a second, Vytarin (cholesterol level drug) in

combination with Simvastatin, have a four-membered lactam surrounded by several substituents (Figure 1.6), while 39 compounds are comprised of different types of ring sizes in distinctive combinations. These 39 pharmaceutical agents consist of combination drugs, some which cannot be taken individually. Since this analysis is focused on the

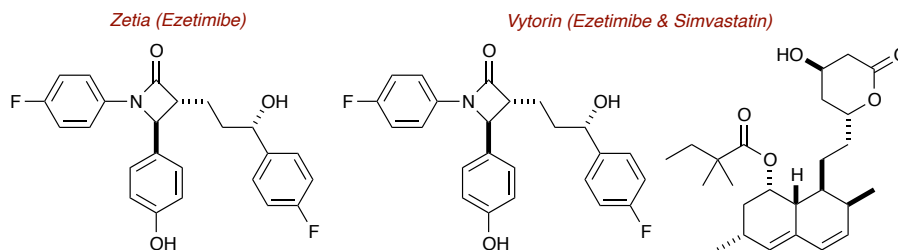


Figure 1.6. 4-membered lactams within the list of the top 100 drugs by retail sales.

frequency of rings, ring systems and frameworks, these combination drugs were included as part of the study. Within these 39 pharmaceutical agents, most of them consist of a combination of 5-, 6-membered and their respective benzofused systems as shown in Figure 1.7. Different combinations of rings like 6/5-, 6/6-, 7/3- and 6/7/6-fused polycyclic systems are among the list.

Many of the drugs are also comprised of rings such as pyrimidin-4-one, morpholin-3-one and oxazolidin-2-one as well as several bridged, *N*-heterocycles in the 6/5- and 6/6-fused systems. Only one example in the list is a dibenzothiazepine (Seroquel XR–quetiapine), which is a 7-membered nitrogen heterocycle fused with two aromatic rings (Figure 1.7). This is the next largest ring size before macrocycles, contain more than 12 atoms in a ring. There are also examples of polycyclic ring systems without nitrogen such as fluticasone propionate, demonstrating the importance of fixed

conformations that are associated with the binding cavity of their respective targets.

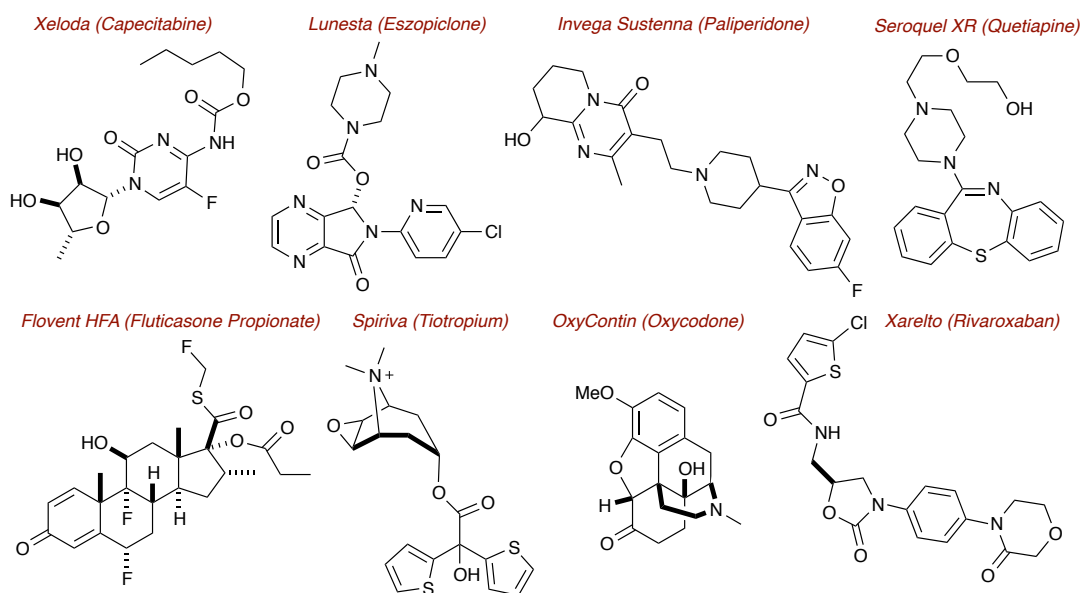


Figure 1.7. Examples of different structural pattern in the list of the top 100 drugs by retail sales.

The second segment within the Top 200 US Pharmaceuticals list is the top 100 list of drugs by prescription. This list of pharmaceutical agents is quite similar to the top 100 list of drugs by retail sales, differing by only four drugs, and signifying the importance of the utilization of these drugs by both doctors and patients. Nearly similar numbers were derived from the top 100 list of drugs by prescription as compared to the top 100 by retail sales, where 40 out of 100 drugs are comprised of small and common ring sizes, highlighting the pivotal role that rings and ring systems play in drug development. Of notable importance, is that there is only a single macrocycle within the current list, underscoring the importance of current efforts in the field, including this thesis, in developing new chemistry and the corresponding biological assays associated with macrocycles.

An initial summary on the Top 200 US Pharmaceuticals list has described the prevailing rings, ring systems and frameworks among the current marketed drugs to be 4- to 7-membered heterocycles, two macrocyclic drugs and four sulfonamide-containing pharmaceuticals. The medium-sized heterocyclic rings, in particular 8- to 11-membered lactams and sultams are deficient from the top 200 US Pharmaceutical compounds, justifying the demand for novel synthetic methods to generate underrepresented cyclic scaffolds, as well as generate opportunities for broad biological screening from the corresponding molecular libraries.

1.3.2.2 Analysis of FDA Approved Drugs (Frequency of Nitrogen Heterocycles)

The second portion of Njardarson Analysis Model includes 1,086 drugs compiled from the US FDA approved pharmaceutical compounds and the analysis reports on the frequency of nitrogen heterocycles amongst the approved drugs.^{13c} Overall, the database contains 1,994 pharmaceuticals and the focus of the investigation is small-molecule drugs that are structurally unique; hence, removing combination drugs (253), biologics (146), peptides (23) and drug duplications (537), which leaves 1,035 small-molecule remaining drugs in the analysis. The number increased to 1,086 when combination drugs are accounted for, where there were 51 small-molecule drugs that were not approved on their own but only as part of a combination. After the compilation, there are 640 small-molecule drugs containing nitrogen heterocycles, with the list being categorized according to the most common structures. Within the sub-list of 640 small-molecules, the top 25 most commonly utilized nitrogen heterocycles were sorted out. The study was

then further divided into seven sections: (a) 3- and 4-membered rings, (b) 5-membered rings, (c) 6-membered rings, (d) fused rings, (e) 7- and 8-membered rings, (f) bicyclic rings, and (g) macro- and metallocycles (Figure 1.8).^{13c} For the purpose of the discussion, we will be examining the 7- and 8-membered nitrogen heterocycles as well as some examples of macrocyclic nitrogen heterocycles.

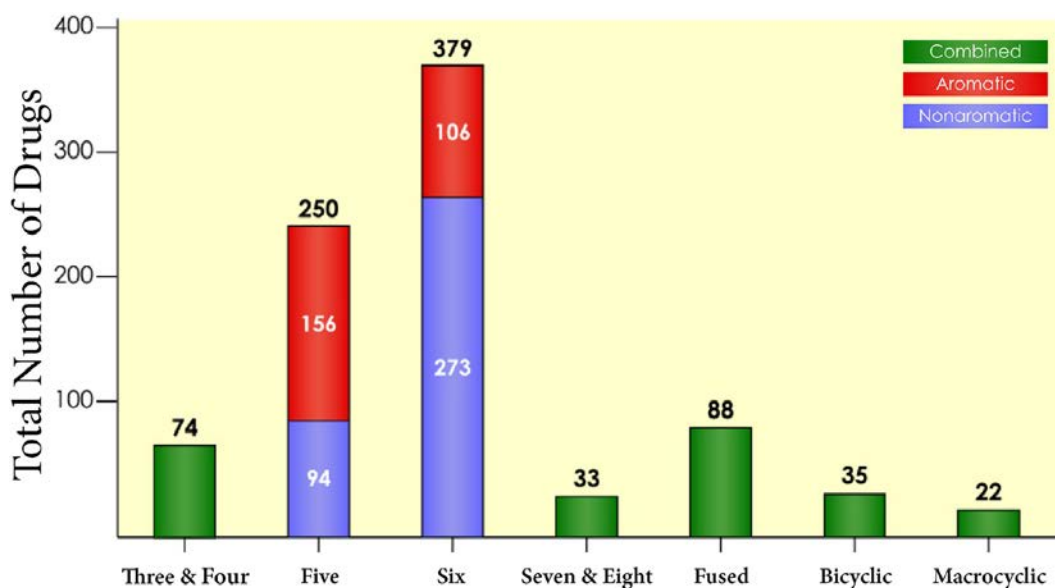


Figure 1.8. Nitrogen heterocyclic drugs grouped into their relative distributions.^{13c}

As is evident from Figure 1.8, the prevalence of the rings varies significantly ranging from the most common sizes: 6-membered (59%) and 5-membered (39%) (common-sized) to the least: 7- and 8-membered, macrocycles and bicyclic compounds. Aromatic rings, are no exception, and are common structural features of many approved pharmaceuticals. Based on the bar graph, the two sizes differ greatly with 62% of 5-membered nitrogen heterocycles being aromatic, compared to only 28% of six-membered rings (Figure 1.8, five- and six-membered rings). The fused ring section focuses on ring systems that contain more than one nitrogen heterocycle fused together.

Ending the graph is the least prevalent ring sizes comprised of macrocyclic rings, followed by 7- and 8-membered heterocycles.

The analysis outlined in Figure 1.8 also provides data on the breakdown with respect to the number of nitrogen atoms within the top 25 most commonly utilized heterocycles; such as the fact that 56% contain a single nitrogen atom, 33% contain two, 4% contains three nitrogens (1,2,4-triazole), and 7% contain four nitrogen atoms (tetrazole and purine). In the list, 56% of the top 25 consist of a single ring, with even representation by 6- (7/15) and 5-membered (8/15) rings, and the remaining 44% of the top 25 that contain more than a single ring. These analyses suggest that poorly represented ring systems include drugs with more than a single ring (\geq two rings), such as bicyclic or tricyclic frameworks, as well as drugs with more than two nitrogen atoms. Hence, there is demand for the development of new synthetic methods to facilitate the generation of distinct structural components, in particular, bicyclic and tricyclic sultams with two or more heteroatoms.

7- and 8-membered nitrogen heterocycles are predominantly less common than their 5- and 6-membered ring counterparts, but as noted previously, they are gaining prominence in recent years with significant scaffolds addressing difficult targets. These heterocycles are rapidly emerging as important pharmaceutical core fragments with selected scaffolds being considered privileged structures due to their desirable properties in tackle challenging targets, as well as more efficient synthetic methods being developed to generate these heterocycles.⁵⁵ The top five most frequently utilized 7-membered heterocyclic scaffolds are shown in Figure 1.9, where the first structural class is the

benzodiazepine core, followed by similar but reduced analogues such as dibenzo-azepine, azepane, dibenzo-oxazepine and benzo-azepine. All scaffolds assessed are benzofused except one, implying that the majority are unsaturated and flat.

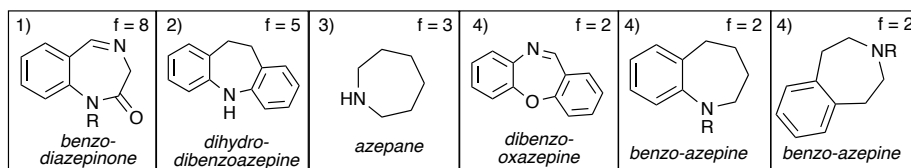


Figure 1.9. *The top five most common 7-membered nitrogen heterocycles.*

As shown in Figure 1.10, the top four most commonly occurring structures contain bridged bicyclic cores. The most frequent nature-derived or inspired structural component is the morphinan architecture, followed closely by the tropane family of alkaloids and quinuclidine core, representing the third most commonly used core. As seen earlier in Figure 1.7 (page 19), oxycodone is one of the examples, which contains the morphinan core, as well as others such as buprenorphine, which is the most complex structure with an intriguing bridging carbon chain installed. Included in this list is the tropane-containing drugs, including the most infamous member, cocaine, which contains the carboxylate group, whereas other examples lack it (Figure 1.10).

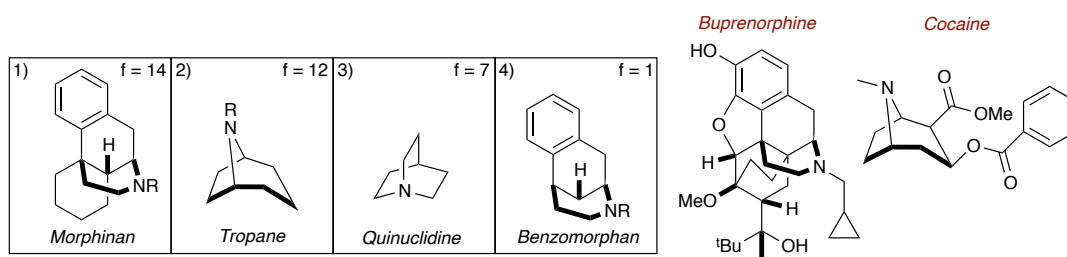


Figure 1.10. *The top four most common bridged bicyclic nitrogen heterocycles and examples of morphinan and tropane core drugs.*

The overarching goal of the aforementioned assessments is the establishment of a

limited list of structural components by which the majority of the small-molecule drugs are comprised of mainly small- to common-sized (4- to 7-membered) cyclic scaffolds, aromatic derivatives and approximately nine macrocycles. Many of the small-molecule drugs are single ring, although statistics have shown that about 44% are more than a single ring. The majority of the ring combinations are 6/5-, 6/5-, 7/6-, 6/7/6-, 6/6/6- as well as many others. But to-date, there are numerous underrepresented ring sizes, ring systems and frameworks, namely 8- to 11-membered benzofused sultams, which if supplemented, would provide chemical novelty to the entire data set of FDA-approved drugs.

1.3.3 Examples of Macrocyclic Nitrogen Heterocycles

Nitrogen-containing macrocycles have emerged as promising pharmaceuticals with cyclosporine and everolimus, a derivative of sirolimus (rapamycin), occurring within the top 200 drugs list (Figure 1.5, page 17). Furthermore, almost all of the macrocycles are natural products or analogues of natural products (Figure 1.11). Tacrolimus,⁵⁶ is a derivative of sirolimus, while rifaximin⁵⁷ is derived from rifamycin,⁵⁸ an antibiotic. Plerixafor is a bicyclam derivative, where all eight nitrogen atoms are strongly basic.⁵⁹ In addition, the two macrocyclic rings chelate with metals like zinc, copper and nickel to form complexes, where the biologically active form occurs upon chelation with zinc (Figure 1.11).⁶⁰

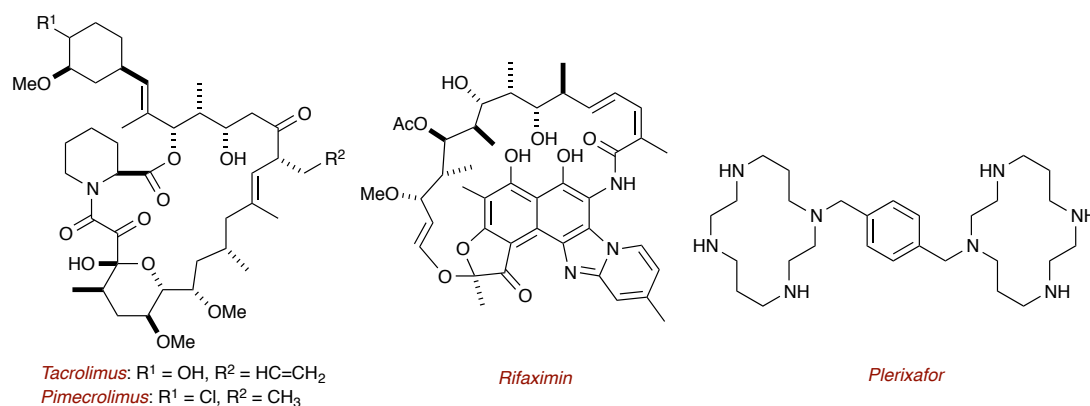


Figure 1.11. Representative examples of nitrogen macrocycles derived pharmaceuticals.

1.3.4 Conclusion

In short, the critical information provided by both drug lists—top 200 drugs by retail sales and by prescription and nitrogen heterocycles in the FDA approved drugs—is the prevalence of small-molecules pharmaceuticals in the FDA approved drugs. In this regard, the prevailing structural components are 4- to 7-membered cyclic scaffolds, of which 59% contain a nitrogen heterocycle and the remaining comprised of carbon and sulfur rings. In addition, data was presented with nine macrocyclic drugs (> 12-membered rings), as well as many aromatic-bearing pharmaceutical agents. Most importantly, underrepresented structural components include a diverse collection of rings, ranging from 8-, 9-, 10-, 11- and 12-membered and their respective benzofused derivatives. Fused and bicyclic systems containing nitrogen and sulfur atoms are less than 44% as well as the count of–nitrogen in the ring(s), where more than 2 nitrogen atoms are contained in a ring(s) are less than 11%. This inadequately represented space provides an impetus to incorporate and synthesize new heterocycles as well as the

development of efficient, adaptable, robust and scalable methods to provide more significant and unique scaffolds for biological assays.

1.4 Analysis of Top 100 Most Frequently Used Ring Systems in FDA Orange Book: Ring Sizes and Structural Diversity

1.4.1 Introduction

The second list analyzed is the Taylor Analysis Model, which contains 1,175 drugs in a 2014 report entitled “Rings in Drugs”, adapted from Taylor and co-workers.^{13d} The list is compiled from the FDA Orange Book¹⁴ for NMEs till the end of 2012 as the basic resource and then cross-referenced against ChEMBL,⁴¹ DrugBank,⁴² Wikipedia,⁶¹ Nature Drug Reviews,⁶² the FDA Web site¹⁴ and the Annual Reports in Medicinal Chemistry.⁶³ A well-combined list of drugs obtained from different resources will enable the various nitrogen heterocycles prevailing in the FDA-approved pharmaceuticals to be highlighted and helps in the identification of underrepresented ring sizes, ring systems and frameworks.

A brief summary of the rings in current marketed drugs is the discovery of only 351 ring systems and 1,197 frameworks in drugs, which came onto the market before 2013 based on the existing list of 1,175 marketable drugs. In addition, prior to 1983, the most frequently used ring systems were first used in drugs 83% of the time, and prior to this time, it was very seldom for a drug to contain more than one new ring system. Furthermore, on average, six new ring systems enter drug space on a yearly basis while only ~28% of new drugs contain a new ring system. In light of this fact, the most

frequent non-aryl bicyclic lactams consist mainly of 6/4-, 5/4-, 7/6- and 6/5-fused systems. In addition, there are more single lactams than bicyclic lactams. Other heterocycles, that are less frequent, include benzofused sultams, bridged, bicyclic *N*-heterocycles and 7-membered cyclic scaffolds, that will be discussed further in the subsequent two sub-sections. Syntheses of 6-membered benzofused sultams and bridged, bicyclic *N*-heterocycles will be briefly discussed, as they are relevant to Chapters 2–4.

These observations provide insights into the chemical novelty of drugs in a molecular scaffold design process and highlight the potential demand for new ring systems or frameworks, with low synthetic cost to develop compound libraries efficiently—based on the core ring systems/molecular fragments derived—from hit identification to lead optimization and beyond. In addition, this documentation of ring systems and frameworks provides an innate description of chemical space that is invaluable when translated to medicinal chemistry and early phase drug discovery.

1.4.2 Analysis of Ring Systems with Amides or Amide-types Motifs

The aforementioned Taylor Analysis Model of 1,175 drugs derived from FDA-approved drugs, and cross-referenced with different resources, furnishes the ring sizes and structural diversity analysis of top 100 most frequently used ring systems. The analysis discussed in this section involves an assessment of the Taylor database for ring systems with amides or amide-type motifs, and begins by removing other groups of drugs, such as oligopeptides, long chain polymers, proteins, antibodies, acyclic drugs and large macrocycles, as well as applying other filters from the data set, resulting in the basis set of 1,175 drugs.

Based on this new basis set of drugs, the top 100 most frequently used ring systems were generated, and from this list, the ring systems that contain amides or amide-type of functional motifs were compiled. From this list, 20 out of the top 100 ring systems were small (4-membered fused and non-fused) and common (5-, 6- and 7-membered fused and non-fused) in different possible combinations, with the exception of 7/4- and 7/5-fused bicyclic scaffolds that were absent (Figure 1.12). In regards to frequencies, these 20 motifs are only moderately common (122 out of 1,501 reported), and underscore the demand for developing facile, dynamic and highly adaptable methods to construct new and unique ring systems and frameworks such as non-aryl 7/4- and 7/5-fused bicyclic sultams.

Also, within the list, only a handful of ring systems have stereocenters. Moreover, those which possess stereogenic centers, have them located between fused

rings, substantiating the need for scaffolds possessing more broad ranging sp^3 stereogenic centers. Taken collectively, many of the scaffolds in this analysis are relatively flat and unsaturated, accentuating the need for new methods to install these properties or characteristics.

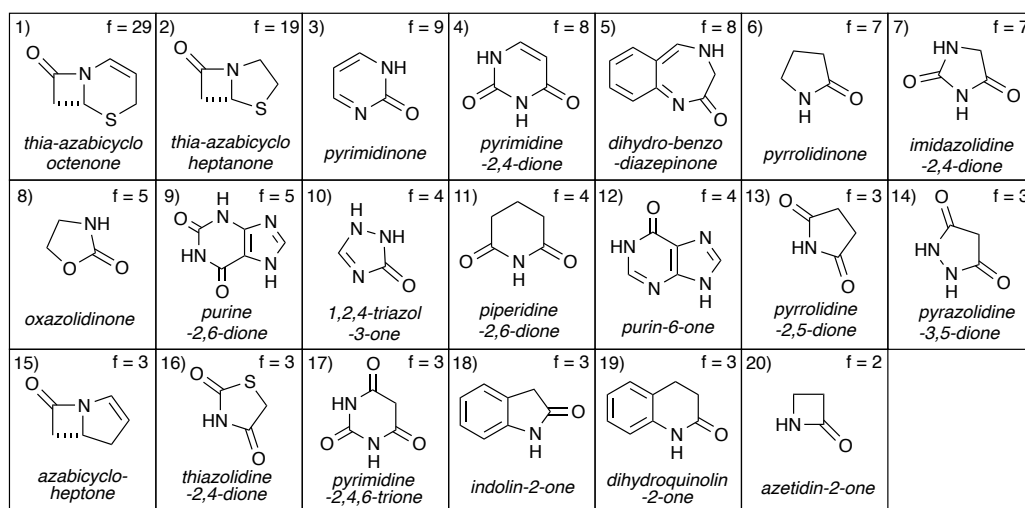


Figure 1.12. Representative examples of motifs within the top 100 most frequently used ring systems sorted by descending frequency (*f*).

1.4.3 Analysis of Ring Systems: Sultams, Bridged and Azepine Scaffolds

In addition to the first 20 out of 100 ring systems as previously described in section 1.4.2, there are certain unique ring systems added to the compilation, including: 6-membered benzofused cyclic sulfonamides (benzo-thiadiazine 1,1-dioxides), bridged bicyclic heterocycles (quinuclidine and 8-azabicyclo[3.2.1]-octane), simple secondary amines (azepane), tricyclic benzofused rings (dibenzoazepine and benzotriazolo diazepine), and a more complex ring system (dihydro-5*H*-benzo-cyclohepta-pyridine),

where 8 out of 100 ring systems are accounted in this section as denoted in Figure 1.13. Likewise, these systems are even less frequent (34 out of 1501 reported) than the aforementioned examples, and many understated ring sizes and ring systems are not found in the list (e.g. 7- to 11-membered benzofused bridged and non-bridged sultams and medium-sized heterocycles). Also, these scaffolds lack 3-dimensionality as well as contain a small fraction of sp^3 carbons, heightening the demand for more synthetic methods to produce novel rings, ring systems and frameworks comprising more drug-like physical properties, preferably with low synthetic cost.

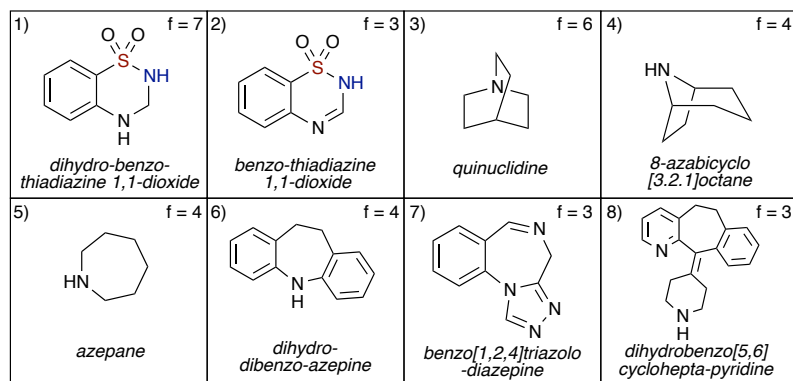


Figure 1.13. Unique examples of motifs within the top 100 most frequently used ring systems sorted by descending frequency (f).

Two drug classes that are relevant to this thesis, namely, benzothiadiazine 1,1-dioxides and quinuclidines will be presented. Benzothiadiazine 1,1-dioxides, also known as sultams, have been utilized as non-steroidal anti-inflammatory drugs (NSAIDs), such as piroxicam⁶⁴ which relieves symptoms of pain, inflammation, swelling, stiffness, and pain associated with rheumatoid arthritis; meloxicam⁶⁵ and isoxicam⁶⁶ that possess

analgesic, anti-inflammatory and anti-pyretic properties (Figure 1.14). A slightly more extensive list of biologically active sultams can be found in Chapter 2.

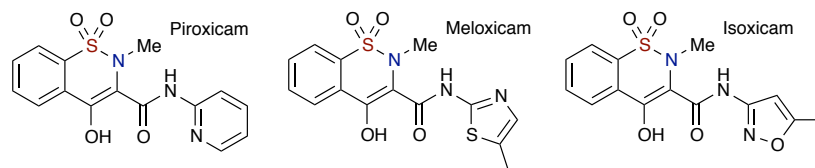


Figure 1.14. Examples of benzo-thiadiazine 1,1-dioxides-containing drugs.

The second core component is quinuclidine, which is an interesting [2.2.2]-bridged bicyclic nitrogen heterocycle found in some drugs for instance quinine, quinidine, aclidinium and palonosetron (Figure 1.15) and relevant to the 8-/9-membered, bridged bicyclic sultams developed in Chapter 2, *vide infra*. Both quinine and quinidine, derived from natural products are stereoisomers of each other, and have different therapeutic effects. Quinine is a fever-reducing, anti-malarial and anti-inflammatory drug, while quinidine is a class I anti-arrhythmic agent.⁶⁷ Acclidinium is an inhaled muscarinic antagonist, and is used in the treatment of chronic obstructive pulmonary disease (COPD),⁶⁸ whereas palonosetron is a 5-HT₃ antagonist used in the prevention and treatment of chemotherapy-induced nausea and vomiting (Figure 1.15).⁶⁹

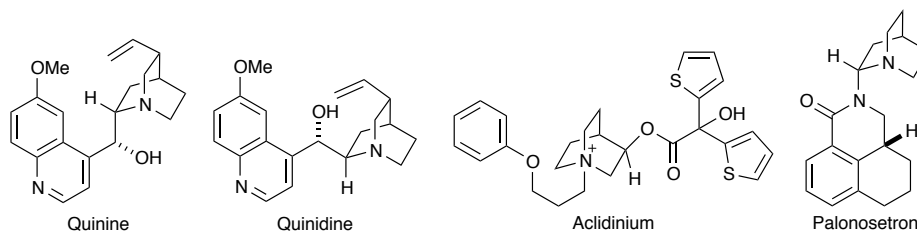


Figure 1.15. Examples of quinuclidine-derived drugs.

1.4.4 Conclusion

As concluded previously, the prevailing rings and ring systems in the current marketed pharmaceuticals are the common-sized (5- to 7-membered) heterocycles, as well as 6/5- and 6/6-fused bicyclic scaffolds, as seen by the number of reported syntheses and examples of drugs. The data provided emphasizes the importance of investigating understudied ring systems and frameworks that are not on the radar of the current analysis., thus heightening the demand for new chemical methods that will be able to furnish the novel rings and ring systems.

1.5 Summary and Outlook

In conclusion, the analyses summarized within Chapter 1 provide insight into scaffold mining, by providing a number of important categories of analysis, such as (i) the limited size of chemical space⁷⁰ being occupied by ring systems of all current drugs, and (ii) the insufficient number of new chemotypes introduced into drug space; The analyses also postulate insight to the design of hit-finding libraries, where libraries can be benchmarked to assist in the search of different combinations of drug ring systems and in the optimization of molecules. Useful data for known novel ring systems can be retrieved from databases and evaluated during optimization for either the initial hit molecule or more developed lead if the ring systems are present in the candidates. The plethora of valuable and extensive data that can be gleaned from the Njardarson and Taylor databases will be of assistance, with respect to scaffold and library design, intellectual property, and potential biological activity.

The ring system chemical space of all currently available drugs is a very small fraction, as indicated by the ring sizes and structural diversities analyses. Ideally, novelty is often assessed by the nature of the scaffold and since only 30% of the drugs on the market contain novel ring systems, there is a demand for chemical novelty to be introduced into new scaffolds. However, it was also suggested that chemical novelty is not as important as bringing together the correct ring systems from drug space. If the arrangement of ring systems is new and can be uniquely introduced, it may provide an optimal solution. In addition, it seems that medicinal chemists depend heavily on a subset of ring systems that has not changed since 1982, which is partially due to synthetic expediency and time-constraints of industrial projects.⁷¹

Upon the evaluation of several databases, it is quite evident that there is a huge void of medium-sized heterocycles within all the lists described in this Chapter, hence warranting the development of facile and efficient methods for the synthesis of new cyclic scaffolds. Preferentially, this will occur with economical cost in mind as there are many new chemical vendors providing unique and interesting building blocks. With the new scaffolds in place, it will be possible to explore unknown or underrepresented chemical space, which will be guided by drug-like molecular properties, as well as a broad biological screening. This in turn could enhance the number of hits, leads, probes and possibly drugs to treat diseases and syndromes that affect human health. The remaining chapters summarize work related towards this goal.

1.6 References cited

- [1] For recent reviews, see (a) Sun, C.-L.; Li, B.-J.; Shi, Z.-J. Macrolactones and macrolactams. In *Handbook of Cyclization Reactions*; Ma, S. Ed.: Wiley-VCH Verlag GmbH & Co. KGaA: **2010**; pp 1055–1097 and references cited therein. (b) Sharma, A.; Appukkuttan, P.; Van der Eycken, E. Microwave-assisted synthesis of medium-sized heterocycles. *Chem. Commun.* **2012**, *48*, 1623–1637 and references cited therein. (c) Kudo, F.; Miyanaga, A.; Eguchi, T., Biosynthesis of natural products containing β -amino acids. *Nat. Prod. Rep.* **2014**, *31*, 1056–1073. (d) Jun, J. H.; Javed, S.; Ndi, C. Hanson, P. R. Synthesis of P-, S-, Si-, B- and Se- Heterocycles via Rings-Closing Metathesis. **2015**, In print.
- [2] (a) Mallinson, J.; Collins, I. Macrocycles in new drug discovery. *Future Med. Chem.* **2012**, *4*, 1409–1438. (b) Marsault, E. Macrocycles as templates for diversity generation in drug discovery. In *Diversity-Oriented Synthesis*; Trabocchi, A. Ed.: John Wiley & Sons, Inc., **2013**; pp 253–287. (c) Vendeville, S.; Cummings, M. D. Synthetic Macrocycles in Small-Molecule Drug Discovery. *Annu. Rep. Med. Chem.* **2013**, *48*, 371–386. (d) Yu, X.; Sun, D. Macrocyclic drugs and synthetic methodologies toward macrocycles. *Molecules* **2013**, *18*, 6230–6268. (e) Giordanetto, F.; Kihlberg, J. Macrocyclic Drugs and Clinical Candidates: What Can Medicinal Chemists Learn from Their Properties? *J. Med. Chem.* **2014**, *57*, 278–295. (f) Hussain, A.; Yousuf, S. K.; Mukherjee, D. Importance and synthesis of benzannulated medium-sized and macrocyclic rings (BMRs). *RSC Adv.* **2014**, *4*, 43241–43257 and references cited therein.
- [3] (a) Evans, P. A.; Holmes, A. B. Medium Ring Nitrogen Heterocycles. *Tetrahedron* **1991**, *47*, 9131–9166. (b) Illuminati, G.; Mandolini, L. Ring Closure Reactions of Bifunctional Chain Molecules. *Acc. Chem. Res.* **1981**, *14*, 95–102 and refs cited therein. (c) Casadei, M. A.; Calli, C.; Mandolini, L. Ring-Closure Reactions. 22. Kinetics of Cyclization of Diethyl (ω -Bromoalkyl)malonates in

the Range of 4- to 21-Membered Rings. Role of Ring Strain. *J. Am. Chem. Soc.* **1984**, *106*, 1051–1056.

- [4] (a) David, B.; Sevenet, T.; Thoison, O.; Awang, K.; Pais, M.; Wright, M.; Guenard, D. Hemisynthesis of rhazinilam analogs: structure-activity relationships on tubulin-microtubule system. *Bioorg. Med. Chem. Lett.* **1997**, *7*, 2155–2158. (b) Johnson, E. P.; Chen, G.-P.; Fales, K. R.; Lenk, B. E.; Szendroi, R. J.; Wang, X.-J.; Carlson, J. A. Macrolactamization via Palladium π -Allyl Alkylation. Preparation of CGS25155: A 10-Membered Lactam Neutral Endopeptidase 24.11 Inhibitor. *J. Org. Chem.* **1995**, *60*, 6595–6598. (c) Kaul, R.; Surprenant, S.; Lubell, W. D. Systematic Study of the Synthesis of Macrocyclic Dipeptide β -Turn Mimics Possessing 8-, 9-, and 10- Membered Rings by Ring-Closing Metathesis. *J. Org. Chem.* **2005**, *70*, 3838–3844. (d) Liu, T.; Kapustin, G.; Etzkorn, F. A. Design and Synthesis of a Potent Histone Deacetylase Inhibitor. *J. Med. Chem.* **2007**, *50*, 2003–2006. (e) Stanton, B. Z.; Peng, L. F.; Maloof, N.; Nakai, K.; Wang, X.; Duffner, J. L.; Taveras, K. M.; Hyman, J. M.; Lee, S. W.; Koehler, A. N.; Chen, J. K.; Fox, J. L.; Mandinova, A.; Schreiber, S. L. A small molecule that binds Hedgehog and blocks its signaling in human cells. *Nat. Chem. Biol.* **2009**, *5*, 154–156. (f) Khan, N.; Jeffers, M.; Kumar, S.; Hackett, C.; Boldog, F.; Khramtsov, N.; Qian, X.; Mills, E.; Berghs, S. C.; Carey, N.; Finn, P. W.; Collins, L. S.; Tumber, A.; Ritchie, J. W.; Jensen, P. B.; Lichenstein, H. S.; Sehested, M. Determination of the class and isoform selectivity of small-molecule histone deacetylase inhibitors. *Biochem. J.* **2008**, *409*, 581–589. (g) Furumai, R.; Komatsu, Y.; Nishino, N.; Khochbin, S.; Yoshida, M.; Horinouchi, S. Potent histone deacetylase inhibitors built from trichostatin A and cyclic tetrapeptide antibiotics including trapoxin. *Proc. Natl. Acad. Sci. U. S. A.* **2001**, *98*, 87–92.
- [5] (a) Fairlie, D. P.; Abbenante, G.; March, D. R. Macrocyclic peptidomimetics-forcing peptides into bioactive conformations. *Curr. Med. Chem.* **1995**, *2*, 654–686. (b) Avan, I.; Hall, C. D.; Katritzky, A. R. Peptidomimetics via modifications

- of amino acids and peptide bonds. *Chem. Soc. Rev.* **2014**, *43*, 3575–3594. (c) Thapa, P.; Espiritu, M. J.; Cabaltea, C.; Bingham, J.-P. The Emergence of Cyclic Peptides: The Potential of Bioengineered Peptide Drugs. *Int. J. Pept. Res. Ther.* **2014**, *20*, 545–551.
- [6] (a) van den Broek, S. A. M. W.; Meeuwissen, S. A.; van Delft, F. L.; Rutjes, F. P. J. T. Natural products containing medium-sized nitrogen heterocycles synthesized by ring-closing alkene metathesis. In *Metathesis in Natural Product Synthesis*; Cossy, J.; Arseniyadis, S.; Meyer, C. Eds.: Wiley-VCH Verlag GmbH & Co. KGaA: **2010**; pp 45–85. (b) Bonney, K. J.; Braddock, D. C. A Unifying Stereochemical Analysis for the Formation of Halogenated C15-Acetogenin Medium-Ring Ethers From *Laurencia* Species via Intramolecular Bromonium Ion Assisted Epoxide Ring-Opening and Experimental Corroboration with a Model Epoxide. *J. Org. Chem.* **2012**, *77*, 9574–9584. (c) Bogdan, A. R.; Jerome, S. V.; Houk, K. N.; James, K. Strained Cyclophane Macrocycles: Impact of Progressive Ring Size Reduction on Synthesis and Structure. *J. Am. Chem. Soc.* **2012**, *134*, 2127–2138. (d) Bauer, R. A.; Wenderski, T. A.; Tan, D. S. Biomimetic diversity-oriented synthesis of benzannulated medium rings via ring expansion. *Nat. Chem. Biol.* **2013**, *9*, 21–29. (e) Dow, M.; Marchetti, F.; Nelson, A. Diversity-oriented synthesis of natural product-like libraries. In *Diversity-Oriented Synthesis*; Trabocchi, A. Ed.: John Wiley & Sons, Inc., **2013**; pp 291–323 and references cited therein.
- [7] (a) Gradillas, A.; Perez-Castells, J. Synthesis of natural products containing macrocycles by alkene ring-closing metathesis. In *Metathesis in Natural Product Synthesis*; Cossy, J.; Arseniyadis, S.; Meyer, C. Eds.: Wiley-VCH Verlag GmbH & Co. KGaA: **2010**; pp 149–182. (b) Madsen, C. M.; Clausen, M. H. Biologically Active Macrocyclic Compounds-from Natural Products to Diversity-Oriented Synthesis. *Eur. J. Org. Chem.* **2011**, 3107–3115. (c) Prunet, J. Progress in

- Metathesis Through Natural Product Synthesis. *Eur. J. Org. Chem.* **2011**, 2011, 3634–3647.
- [8] (a) Villar, E. A.; Beglov, D.; Chennamadhavuni, S.; Porco, J. A., Jr.; Kozakov, D.; Vajda, S.; Whitty, A. How proteins bind macrocycles. *Nat. Chem. Biol.* **2014**, *10*, 723–731. (b) Nero, T. L.; Morton, C. J.; Holien, J. K.; Wielens, J.; Parker, M. W. Oncogenic protein interfaces: small molecules, big challenges. *Nat. Rev. Cancer* **2014**, *14*, 248–262. (c) Vendeville, S.; Cummings, M. D. Synthetic Macrocycles in Small-Molecule Drug Discovery. *Annu. Rep. Med. Chem.* **2013**, *48*, 371–386.
- [9] (a) Mai, A. Targeting Epigenetics in Drug Discovery. *ChemMedChem* **2014**, *9*, 415–417. (b) Knapp, S.; Weinmann, H. Small-Molecule Modulators for Epigenetics Targets. *ChemMedChem* **2013**, *8*, 1885–1891.
- [10] (a) Gerard, B.; Duvall, J. R.; Lowe, J. T.; Murillo, T.; Wei, J.; Akella, L. B.; Marcaurelle, L. A. Synthesis of a Stereochemically Diverse Library of Medium-Sized Lactams and Sultams via S_NAr Cycloetherification. *ACS Comb. Sci.* **2011**, *13*, 365–374. (b) Pizzirani, D.; Kaya, T.; Clemons, P. A.; Schreiber, S. L. Stereochemical and Skeletal Diversity Arising from Amino Propargylic Alcohols. *Org. Lett.* **2010**, *12*, 2822–2825.
- [11] Kulkarni, S.; Anderson, D. D.; Hong, L.; Baldrige, A.; Wang, Y.-F.; Chumanovich, A. A.; Kovalevsky, A. Y.; Tojo, Y.; Amano, M.; Koh, Y.; Tang, J.; Weber, I. T.; Mitsuya, H.; Ghosh, A. K. Design, Synthesis, Protein-Ligand X-ray Structure, and Biological Evaluation of a Series of Novel Macrocytic Human Immunodeficiency Virus-1 Protease Inhibitors to Combat Drug Resistance. *J. Med. Chem.* **2009**, *52*, 7689–7705.
- [12] Aldrich, L. N.; Kuo, S.-Y.; Castoreno, A. B.; Goel, G.; Petric Kuballa, P.; Rees, M. G.; Seashore-Ludlow, B. A.; Cheah, J. H.; Latorre, I. J.; Stuart L. Schreiber, S.

- L.; Shamji, A. F.; Xavier, R. J.; Discovery of a Small-Molecule Probe for V-ATPase Function. *J. Am. Chem. Soc.* **2015**, *137*, 5563–5568.
- [13] (a) McGrath, N. A.; Brichacek, M.; Njardarson, J. T. A Graphical Journey of Innovative Organic Architectures That Have Improved Our Lives. *J. Chem. Ed.* **2010**, *87*, 1348–1349. (b) Vitaku, E.; Smith, B. R.; Smith, D. T. Njarharson, J. T. Top US Pharmaceutical Products of 2013. *J. Chem. Ed.* **2010**, *87*, 1348–1349. (c) Vitaku, E.; Smith, D. T.; Njardarson, J. T. Analysis of the Structural Diversity, Substitution Patterns, and Frequency of Nitrogen Heterocycles among U.S. FDA Approved Pharmaceuticals. *J. Med. Chem.* **2014**, *57*, 10257–10274. (d) Taylor, R. D.; MacCoss, M.; Lawson, A. D. G. Rings in Drugs. *J. Med. Chem.* **2014**, *57*, 5845–5859.
- [14] <http://www.accessdata.fda.gov/scripts/cder/ob/> (accessed on April 15, 2015)
- [15] (a) Lipinski, C. A.; Lombardo, F.; Dominy, B. W.; Feeney, P. J. Experimental and Computational Approaches To Estimate Solubility and Permeability in Drug Discovery and Development Settings. *Adv. Drug Delivery Rev.* **2001**, *46*, 3–26. (b) Sadowski, J.; Kubinyi, H. A Scoring Scheme for Discriminating between Drugs and Nondrugs. *J. Med. Chem.* **1998**, *41*, 3325–3329.
- [16] Leeson, P. D.; Springthorpe, B. The Influence of Drug-like Concepts on Decision-Making in Medicinal Chemistry. *Nat. Rev. Drug Discovery* **2007**, *6*, 881–890.
- [17] Kola, I.; Landis, J. Can the Pharmaceutical Industry Reduce Attrition Rates? *Nat. Rev. Drug Discovery* **2004**, *3*, 711–715.
- [18] Walters, W. P.; Murcko, M. A. Can We Learn To Distinguish between “Drug-like” and “Nondrug-like” Molecules? *J. Med. Chem.* **1998**, *41*, 3314–3324.
- [19] Siegel, M. G.; Vieth, M. Drugs in Other Drugs: A New Look at Drugs as Fragments. *Drug Discovery Today* **2007**, *12*, 71–79.

- [20] Dalvie, D.; Sajiv, N.; Kang, P.; Loi, C.-M. Influence of Aromatic Rings on ADME Properties of Drugs. In *Metabolism, Pharmacokinetics and Toxicity of Functional Groups*; Royal Society of Chemistry: Cambridge, U.K., **2010**; pp 275–327.
- [21] (a) Schreiber, S. L. Molecular Diversity by Design. *Nature* **2009**, *457*, 153–154.
(b) Schreiber, S. L. Small molecules: The missing link in the central dogma. *Nat. Chem. Biol.* **2005**, *1*, 64–66.
- [22] Payne, D. J.; Gwynn, M. N.; Holmes, D. J.; Pompliano, D. L. Drugs for bad bugs: Confronting the challenges of antibacterial discovery. *Nat. Rev. Drug. Discov.* **2007**, *6*, 29–40.
- [23] Nubbemeyer, U. Synthesis of Medium-Sized Ring Lactams. *Top. Curr. Chem.* **2001**, *216*, 125–196 and references cited therein.
- [24] Troin, Y.; Sinibaldi, M.-E. Asymmetric synthesis of seven- and more-membered ring heterocycles. In *Asymmetric Synthesis of Nitrogen Heterocycles*; Royer, J. Ed.: Wiley-VCH Verlag GmbH & Co. KGaA: **2009**; pp 139–186.
- [25] Hassan, H. M. A. Recent applications of ring-closing metathesis in the synthesis of lactams and macrolactams. *Chem. Commun.* **2010**, *46*, 9100–9106.
- [26] Szostak, M.; Aubé, J. Medium-bridged lactams: a new class of non-planar amides. *Org. Biomol. Chem.* **2011**, *9*, 27–35 and references cited therein.
- [27] Azev, V. N.; Chulin, A. N.; Rodionov, I. L. At the Crossroads of Heterocyclic and Peptide Chemistries. The Aminoacyl Incorporation Reaction in the Synthesis of Medium-Sized Ring Heterocycles. *Chem. Heterocycl. Compd.* **2014**, *50*, 145–159.
- [28] Mustafa, A. The chemistry of sultones and sultams. *Chem. Rev.* **1954**, *54*, 195–223.
- [29] Majumdar, K. C.; Mondal, S. Recent developments in the synthesis of fused sultams. *Chem. Rev.* **2011**, *111*, 7749–7773 and references cited therein.

- [30] Rassadin, V. A.; Grosheva, D. S.; Tomashevskii, A. A.; Sokolov, V. V. Methods of Sultam Synthesis. *Chem. Heterocycl. Compd.* **2013**, *49*, 39–65 and references cited therein.
- [31] Paul, S. M.; Mytelka, D. S.; Dunwiddie, C. T.; Persinger, C. C.; Munos, B. H.; Lindborg, S. R.; Schacht, A. L. How To Improve R&D Productivity: The Pharmaceutical Industry's Grand Challenge. *Nat. Rev. Drug Discovery* **2010**, *9*, 203–214.
- [32] Bemis, G. W.; Murcko, M. A. The Properties of Known Drugs. 1. Molecular Frameworks. *J. Med. Chem.* **1996**, *39*, 2887–2893.
- [33] Lewell, X. Q.; Jones, A. C.; Bruce, C. L.; Harper, G.; Jones, M. M.; McLay, I. M.; Bradshaw, J. Drug Rings Database with Web Interface. A Tool for Identifying Alternative Chemical Rings in Lead Discovery Programs. *J. Med. Chem.* **2003**, *46*, 3257–3274.
- [34] Ertl, P.; Jelfs, S.; Mühlbacher, J.; Schuffenhauer, A.; Selzer, P. Quest for the Rings. In Silico Exploration of Ring Universe To Identify Novel Bioactive Heteroaromatic Scaffolds. *J. Med. Chem.* **2006**, *49*, 4568–4573.
- [35] Wang, J.; Hou, T. Drug and Drug Candidate Building Block Analysis. *J. Chem. Inf. Model.* **2010**, *50*, 55–67.
- [36] Lee, M. L.; Schneider, G. Scaffold Architecture and Pharmacophoric Properties of Natural Products and Trade Drugs: Application in the Design of Natural Product-Based Combinatorial Libraries. *J. Comb. Chem.* **2001**, *3*, 284–289.
- [37] Walters, W. P.; Green, J.; Weiss, J. R.; Murcko, M. A. What Do Medicinal Chemists Actually Make? A 50-Year Retrospective. *J. Med. Chem.* **2011**, *54*, 6405–6416.

- [38] Lipkus, A. H.; Yuan, Q.; Lucas, K. A.; Funk, S. A.; Bartelt, W. F., 3rd; Schenck, R. J.; Trippe, A. J. CAS Registry. Structural Diversity of Organic Chemistry. A Scaffold Analysis of the CAS Registry. *J. Org. Chem.* **2008**, *73*, 4443–4451.
- [39] Pitt, W. R.; Parry, D. M.; Perry, B. G.; Groom, C. R. Heteroaromatic Rings of the Future. *J. Med. Chem.* **2009**, *52*, 2952–2963.
- [40] Ertl, P. Database of Bioactive Ring Systems with Calculated Properties and Its Use in Bioisosteric Design and Scaffold Hopping. *Bioorg. Med. Chem.* **2012**, *20*, 5436–5442.
- [41] Gaulton, A.; Bellis, L. J.; Bento, A. P.; Chambers, J.; Davies, M.; Hersey, A.; Light, Y.; McGlinchey, S.; Michalovich, D.; Al-Lazikani, B.; Overington, J. P. ChEMBL: A Large-Scale Bioactivity Database for Drug Discovery. *Nucleic Acids Res.* **2012**, *40*, D1100–D1107.
- [42] Knox, C.; Law, V.; Jewison, T.; Liu, P.; Ly, S.; Frolkis, A.; Pon, A.; Banco, K.; Mak, C.; Neveu, V.; Djoumbou, Y.; Eisner, R.; Guo, A. C.; Wishart, D. S. DrugBank 3.0: A Comprehensive Resource for “Omics” Research on Drugs. *Nucleic Acids Res.* **2011**, *39*, D1035–D1041.
- [43] Irwin, J. J.; Sterling, T.; Mysinger, M. M.; Bolstad, E. S.; Coleman, R. G. ZINC: A Free Tool To Discover Chemistry for Biology. *J. Chem. Inf. Model.* **2012**, *52*, 1757–1768.
- [44] Gibson, S.; McGuire, R.; Rees, D. C. Principal Components Describing Biological Activities and Molecular Diversity of Heterocyclic Aromatic Ring Fragments. *J. Med. Chem.* **1996**, *39*, 4065–4072.
- [45] (a) Ritchie, T. J.; Macdonald, S. J. F. The Impact of Aromatic Ring Count on Compound Developability—Are Too Many Aromatic Rings a Liability in Drug Design? *Drug Discovery Today* **2009**, *14*, 1011–1020. (b) Young, R. J.; Green, D. V. S.; Luscombe, C. N.; Hill, A. P. Getting Physical in Drug Discovery II: The

- Impact of Chromatographic Hydrophobicity Measurements and Aromaticity. *Drug Discovery Today* **2011**, *16*, 822–830.
- [46] Ilardi, E. A.; Vitaku, E.; Njardarson, J. T. Data-mining for Sulfur and Fluorine: An Evaluation of Pharmaceuticals To Reveal Opportunities for Drug Design and Discovery. *J. Med. Chem.* **2014**, *57*, 2832–2842.
- [47] See reference 13d. The ring definitions are adopted from a modified approach to the original work by Murcko and co-worker, see reference 32.
- [48] Papazisis, G.; Tzachanis, D. Pregabalin's abuse potential a mini review focusing on the pharmacological profile. *Int. J. Clin. Pharmacol. Ther.* **2014**, *52*, 709–716 and references cited therein.
- [49] Hoy, S. M.; Keating, G. M. Omega-3 ethylester concentrate: A review of its use in secondary prevention post-myocardial infarction and the treatment of hypertriglyceridaemia. *Drugs* **2009**, *69*, 1077–1105 and references cited therein.
- [50] Burness, C. B.; Deeks, E. D. Dimethyl Fumarate: A Review of Its Use in Patients with Relapsing-Remitting Multiple Sclerosis. *CNS Drugs* **2014**, *28*, 373–387 and references cited therein.
- [51] (a) Borel, J. F. History of the discovery of cyclosporin and of its early pharmacological development. *Wien Klin Wochenschr* **2002**, *114*, 433–437 and references cited therein. (b) Drew, J.; Maimon, N.; Kalansky, A.; Refaely, Y.; Alnasasra, H.; Waldman, M. The Use of Cyclosporine in Respiratory Diseases. *Curr. Respir. Med. Rev.* **2013**, *9*, 344–348 and references cited therein. (c) Bachegowda, L. S.; Barta, S. K. Genetic and molecular targets in lymphoma: implications for prognosis and treatment. *Future Oncol.* **2014**, *10*, 2509–2528 and references cited therein. (d) Casanovas, T. The role of mTOR inhibitors in the prevention of organ rejection in adult liver transplant patients: a focus on everolimus. *Transplant Res. Risk Manage.* **2014**, *6*, 31–43 and references cited

- therein. (e) Merli, M.; Ferrario, A.; Maffioli, M.; Arcaini, L.; Passamonti, F. Everolimus in diffuse large B-cell lymphomas. *Future Oncol.* **2015**, *11*, 373–383 and references cited therein.
- [52] (a) Ghosh, A. K.; Chapsal, B. D. In *Design of the anti-HIV protease inhibitor darunavir*, Elsevier Ltd.: **2013**; pp 355–384 and references cited therein. (b) Kakuda, T. N.; Brochot, A.; Tomaka, F. L.; Vangeneugden, T.; Van De Castele, T.; Hoetelmans, R. M. W. Pharmacokinetics and pharmacodynamics of boosted once-daily darunavir. *J. Antimicrob. Chemother.* **2014**, *69*, 2591–2605 and references cited therein. (c) Kogawa, A. C.; Salgado, H. R. N. Characteristics, complexation and analytical methods of Darunavir. *Br. J. Pharm. Res.* **2014**, *4*, 1276–1286 and references cited therein.
- [53] (a) Albackr, H. B.; Albacker, T. B.; Alkhorayyef, A. A. Epostoperative use of sildenafil for pulmonary hypertension after adult cardiac surgery, a review article. *Exp. Clin. Cardiol.* **2014**, *20*, 3871–3879 and references cited therein. (b) Bhatt-Mehta, V.; Donn, S. M. Sildenafil for pulmonary hypertension complicating bronchopulmonary dysplasia. *Expert Rev. Clin. Pharmacol.* **2014**, *7*, 393–395 and references cited therein. (c) Das, A.; Durrant, D.; Salloum, F. N.; Xi, L.; Kukreja, R. C. PDE5 inhibitors as therapeutics for heart disease, diabetes and cancer. *Pharmacol. Ther.* **2015**, *147*, 12–21 and references cited therein. (d) Kurian, J. K.; Kumar, P. A.; Kulkarni, S. V. Influence of natural, synthetic polymers and fillers on sustained release matrix tablets of sildenafil citrate. *Pharm. Lett.* **2014**, *6*, 106–117 and references cited therein.
- [54] (a) Bi, Y.; Stoy, P.; Adam, L.; He, B.; Krupinski, J.; Normandin, D.; Pongrac, R.; Seliger, L.; Watson, A.; Macor, J. E. The discovery of novel, potent and selective PDE5 inhibitors. *Bioorg. Med. Chem. Lett.* **2001**, *11*, 2461–2464. (b) El-Abadelah, M. M.; Sabri, S. S.; Khanfar, M. A.; Voelter, W.; Maichle-Mossmer, C. X-ray structure analysis of iso-Sildenafil (iso-Viagra). *Z. Naturforsch. B:*

Chem. Sci. **1999**, *54*, 1323–1326. (c) Jiang, W.; Alford, V. C.; Qiu, Y.; Bhattacharjee, S.; John, T. M.; Haynes-Johnson, D.; Kraft, P. J.; Lundeen, S. G.; Sui, Z. Synthesis and SAR of tetracyclic pyrroloquinolones as phosphodiesterase 5 inhibitors. *Bioorg. Med. Chem.* **2004**, *12*, 1505–1515. (d) Rotella, D. P.; Sun, Z.; Zhu, Y.; Krupinski, J.; Pongrac, R.; Seliger, L.; Normandin, D.; Macor, J. E. Optimization of Substituted N-3-Benzylimidazoquinazolinone Sulfonamides as Potent and Selective PDE5 Inhibitors. *J. Med. Chem.* **2000**, *43*, 5037–5043. (e) Terrett, N. K.; Bell, A. S.; Brown, D.; Ellis, P. Sildenafil (Viagra), a potent and selective inhibitor of type 5 cGMP phosphodiesterase with utility for the treatment of male erectile dysfunction. *Bioorg. Med. Chem. Lett.* **1996**, *6*, 1819–1824. (f) Ghosh, A. K.; Chapsal, B. D.; Weber, I. T.; Mitsuya, H. Design of HIV Protease Inhibitors Targeting Protein Backbone: An Effective Strategy for Combating Drug Resistance. *Acc. Chem. Res.* **2008**, *41*, 78–86. (g) Ghosh, A. K.; Sridhar, P. R.; Kumaragurubaran, N.; Koh, Y.; Weber, I. T.; Mitsuya, H. Bis-tetrahydrofuran: a privileged ligand for darunavir and a new generation of HIV protease inhibitors that combat drug resistance. *ChemMedChem* **2006**, *1*, 939–950. (h) Ghosh, A. K.; Sridhar, P. R.; Leshchenko, S.; Hussain, A. K.; Li, J.; Kovalevsky, A. Y.; Walters, D. E.; Wedekind, J. E.; Grum-Tokars, V.; Das, D.; Koh, Y.; Maeda, K.; Gatanaga, H.; Weber, I. T.; Mitsuya, H. Structure-based design of novel HIV-1 protease inhibitors to combat drug resistance. *J. Med. Chem.* **2006**, *49*, 5252–5261. (i) Taiwo, B. O.; Hicks, C. B. Darunavir: an overview of an HIV protease inhibitor developed to overcome drug resistance. *AIDS Read* **2007**, *17*, 151–156. (j) King, N. M.; Prabu-Jeyabalan, M.; Nalivaika, E. A.; Wigerinck, P.; de, B. M.-P.; Schiffer, C. A. Structural and thermodynamic basis for the binding of TMC114, a next-generation human immunodeficiency virus type 1 protease inhibitor. *J. Virol.* **2004**, *78*, 12012–12021. (k) Tie, Y.; Boross, P. I.; Wang, Y.-F.; Gaddis, L.; Hussain, A. K.; Leshchenko, S.; Ghosh, A. K.; Louis, J. M.; Harrison, R. W.; Weber, I. T. High resolution crystal structures

- of HIV-1 protease with a potent non-peptide inhibitor (UIC-94017) active against multi-drug-resistant clinical strains. *J. Mol. Biol.* **2004**, *338*, 341–352. (I) Koh, Y.; Nakata, H.; Maeda, K.; Ogata, H.; Bilcer, G.; Devasamudram, T.; Kincaid, J. F.; Boross, P.; Wang, Y.-F.; Tie, Y.; Volarath, P.; Gaddis, L.; Harrison, R. W.; Weber, I. T.; Ghosh, A. K.; Mitsuya, H. Novel bis-tetrahydrofuranylurethane-containing nonpeptidic protease inhibitor (PI) UIC-94017 (TMC114) with potent activity against multi-PI-resistant human immunodeficiency virus in vitro. *Antimicrob. Agents Chemother.* **2003**, *47*, 3123–3129.
- [55] Smith, S. G.; Sanchez, R.; Zhou, M.-M. Privileged Diazepine Compounds and Their Emergence as Bromodomain Inhibitors. *Chem. Biol.* **2014**, *21*, 573–583 and references cited therein.
- [56] Kino, T.; Hatanaka, H.; Hashimoto, M.; Nishiyama, M.; Goto, T.; Okuhara, M.; Kosaka, M.; Aoki, H.; Imanaka, H. FK-506, a novel immunosuppressant isolated from a Streptomyces. I. Fermentation, isolation, and physicochemical and biological characteristics. *J. Antibiot.* **1987**, *40*, 1249–1255.
- [57] (a) DuPont, H. L. Therapy for and prevention of traveler's diarrhea. *Clin. Infect. Dis.* **2007**, *45 Suppl 1*, S78–84. (b) Ruiz, J.; Mensa, L.; Pons, M. J.; Vila, J.; Gascon, J. Development of Escherichia coli rifaximin-resistant mutants: frequency of selection and stability. *J. Antimicrob. Chemother.* **2008**, *61*, 1016–1019.
- [58] Thiemann, J. E.; Hengeller, C.; Virgilio, A. Rifamycin. XXV: A group of actinophages active on Streptomyces mediterranei. *Nature* **1962**, *193*, 1104–1105.
- [59] Anon, Plerixafor: AMD 3100, AMD3100, JM 3100, SDZ SID 791. *Drugs R&D* **2007**, *8*, 113–119.
- [60] Este, J. A.; Cabrera, C.; De Clercq, E.; Struyf, S.; Van Damme, J.; Bridger, G.; Skerlj, R. T.; Abrams, M. J.; Henson, G.; Gutierrez, A.; Clotet, B.; Schols, D.

Activity of different bicyclam derivatives against human immunodeficiency virus depends on their interaction with the CXCR4 chemokine receptor. *Mol. Pharmacol.* **1999**, *55*, 67–73.

- [61] Wikipedia Home Page. <http://www.wikipedia.org> (accessed April 20, 2015).
- [62] Mullard, A. 2012 FDA Drug Approvals. *Nat. Rev. Drug Discovery* **2013**, *12*, 87–90.
- [63] Cumulative NCE Introduction Index, 1983–2011 (by Indication). In *Annual Reports in Medicinal Chemistry*; Desai, M. C., Ed.; Academic Press: San Diego, CA, **2012**; Vol. 47, pp 629–652.
- [64] Brogden, R. N.; Heel, R. C.; Speight, T. M.; Avery, G. S. Piroxicam: a review of its pharmacological properties and therapeutic efficacy. *Drugs* **1981**, *22*, 165–187.
- [65] Turck, D.; Roth, W.; Busch, U. A review of the clinical pharmacokinetics of meloxicam. *Brit. J. Rheumatol.* **1996**, *35*, 13–16.
- [66] Downie, W. W.; Gluckman, M. I.; Ziehmer, B. A.; Boyle, J. A. Isoxicam. *Clin. Rheum. Dis.* **1984**, *10*, 385–99.
- [67] (a) Kaufman, T. S.; Rúveda, E. A. The Quest for Quinine: Those Who Won the Battles and Those Who Won the War. *Angew. Chem., Int. Ed.* **2005**, *44*, 854–885. (b) Ueda, C. T. In *Quinidine, Appl. Pharmacokinet.* Appl. Ther., Inc.: **1980**; pp 436–463. (c) Mason, D. T.; Braunwald, E. Mechanisms of action and therapeutic uses of cardiac drugs. *Mod. Trends Pharmacol. Ther.* **1967**, *1*, 112–166.
- [68] (a) Damera, G.; Jiang, M.; Zhao, H.; Fogle, H. W.; Jester, W. F.; Freire, J.; Panettieri, R. A. Jr. Aclidinium bromide abrogates allergen-induced hyperresponsiveness and reduces eosinophilia in murine model of airway inflammation. *Eur. J. Pharmacol.* **2010**, *649*, 349–353. (b) Maltais, F.; Milot, J. The potential for aclidinium bromide, a new anticholinergic, in the management

- of chronic obstructive pulmonary disease. *Ther. Adv. Respir. Dis.* **2012**, *6*, 345–361.
- [69] (a) Yang, L. P. H.; Scott, L. J. Palonosetron. In the prevention of nausea and vomiting. *Drugs* **2009**, *69*, 2257–2278. (b) Celio, L.; Agustoni, F.; Testa, I.; Dotti, K.; de Braud, F. Palonosetron: an evidence-based choice in prevention of nausea and vomiting induced by moderately emetogenic chemotherapy. *Tumori* **2012**, *98*, 279–286.
- [70] Dobson, C. M. Chemical Space and Biology. *Nature* **2004**, *432*, 824–828.
- [71] Roughley, S. D.; Jordan, A. M. The Medicinal Chemist's Toolbox: An Analysis of Reactions Used in the Pursuit of Drug Candidates. *J. Med. Chem.* **2011**, *54*, 3451–3479.

Chapter 2

*A Modular Reaction Pairing Approach to
the Diversity-Oriented Synthesis of
Fused- and Bridged-Polycyclic Sultams*

2.1 Introduction

Medium-sized heterocycles ranging from 8- to 11-membered cyclic scaffolds comprise an underrepresented structural ring component as detailed in Chapter 1. The various analyses of pharmaceutical agents crafted in the Njardarson and Taylor Heterocyclic Rings in Drugs Analysis Models summarized in Chapter 1 highlight the prevalence of rings and ring systems for 4- to 7-membered rings consisting of nitrogen and oxygen heterocycles, all-carbon core scaffolds and selected examples of fluorine/sulfur-bearing rings among more than 1,000 existing pharmaceuticals.¹ The Njardarson and Taylor analysis models also provide insight into the chemical innovation of drug development and emphasize conceivable, low-cost strategies that are necessary to increase the likelihood of developing new frameworks from hit identification to lead optimization and beyond. In Chapter 2, we report a facile strategy termed “Reaction Pairing” that is a method comprised of three simple reactions, namely sulfonylation, S_NAr , and Mitsunobu alkylation reactions, which can be carried out in different pairing sequences using simple building blocks to facilitate the construction of unique, bridged- and fused-tricyclic, 7- to 10-membered benzofused sultams.² These sultam scaffolds lie within new chemical space when mapped using the cartesian grid-based chemical diversity analysis, overlay analysis, principal moments of inertia (PMI) analysis, conformational analysis and quantitative estimate of drug-like (QED) values provided at the end of the Chapter 2, *vida infra*.²

The development of new strategies to access diverse heterocyclic collections for high throughput screening (HTS) are an important aspect in modern drug discovery.

Advances in the fields of genomics and proteomics during the “post-genome era” have progressed rapidly, resulting in an increase in potential therapeutic targets for which there are no known small-molecule modulators.³ Thus, there is an ever growing demand for functionally diverse and complex libraries of small molecules. Despite considerable efforts in this area, the lack of adequate screening technologies and diverse libraries of molecules has remained a hurdle within the scientific community.⁴ As early as 1997, Armstrong and coworkers utilized the concept of Scaffold-from-Scaffold⁵ to demonstrate the enhanced of skeletal diversity from a single scaffold. This elegant concept has been utilized by others in the field and was an early example of what has become known as Diversity-Oriented Synthesis (DOS). In this regard, DOS has emerged in recent years as an enabling strategy for the production of diverse collections of heterocycles.⁶ Representative examples of DOS strategies include numerous uses of build-couple-pair (BCP),⁷ functional group pairing,⁸ and split-pool synthesis.⁹ These methods as well as other innovative strategies have advanced the generation of chemical libraries that are rich in functional diversity, consisting of appendage, functional group, stereochemical and skeletal diversity.¹⁰ Taken collectively, these methods have emerged to address modern biological challenges and also offer new chemical opportunities. In this regard, the continual identification of unique, underexplored subsets of chemical space that are sparsely populated, has the potential to continue to affect probe design and basic chemical biology.

The Hanson group has been interested in the development of new motifs that are underrepresented subsets of chemical space. In particular, as part of a program aimed at

developing new chemistry toward novel phosphorus- and sulfur-based heterocycles, efforts have been devoted toward the exploration of sulfonamides and their corresponding cyclic analogs (sultams). The goal of this study is aimed at studying the unique properties of sulfonamides and sultams utilizing chemical methods and molecular library development, as well as biological screening, for ultimate use in drug discovery.¹¹

2.1.1 Biological Profiles of Sultams (Cyclic Sulfonamides)

Sultams are cyclic sulfonamides that represent a class of non-natural chemotypes that have gained interest in recent years due to their activities against a broad spectrum of biological targets,¹² including several with medicinal value. In addition, their innate properties have enabled their widespread use as reagents,¹³ chiral auxiliaries in asymmetric catalysis¹⁴ and ionic liquids as novel reaction medium.¹⁵ In particular, common- and large-sized benzofused sultams (benzannulated sultams), possessing a rich content of sp³ amine functionality, have shown a wide biological profile. They include inhibitory properties against a variety of enzymes such as HIV integrase,¹⁶ Calpain I,¹⁷ TNF α -converting,¹⁸ cyclin-dependent kinases (CDKs)/vascular endothelial growth factor receptor tyrosine kinase (VEGF-RTK)¹⁹ with anti-proliferative activities and trypsin-like serine protease Factor XIa involved in blood coagulation.²⁰ Moreover, sultams have displayed activities such as anti-psychotic,²¹ anti-HIV,²² and anti-leukemic,²³ as well as small-molecule inhibitor of lysosomal acidification,²⁴ allosteric modulation of AMPA receptor,²⁵ modulation of histamine H3-receptor,²⁶ and glucokinase activation,²⁷ to name a few (Figure 2.1).

Sultams have also been utilized as non-steroidal anti-inflammatory drugs (NSAIDs), such as tenoxicam,²⁸ which relieve symptoms of inflammation, swelling, stiffness, and pain associated with rheumatoid arthritis; and lornoxicam²⁹ that possess analgesic, anti-inflammatory and anti-pyretic properties (Figure 2.1). There are also numerous reported syntheses of biologically active benzo-thiadiazine 1,1-dioxides and the related analogues,³⁰ and some examples include inhibitors of the proliferation of non-small cell lung cancer³¹ and HCV NS5B polymerase,³² as well as SUR1-selective K_{ATP} channel openers.³³

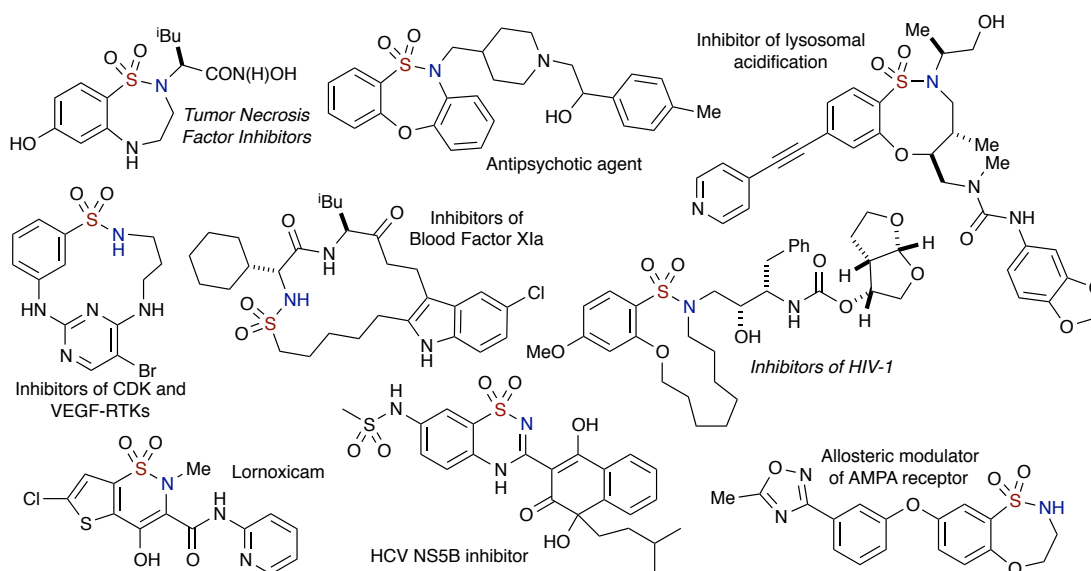


Figure 2.1. Representative examples of bioactive sultams and sultams as drugs.

2.1.2 Chemical Profiles of Sulfonamides and Sultams

Sulfonamides and their cyclic analogs (sultams) have distinct and unique chemical properties that not only aid in their synthesis, but also impart physical properties

that have the potential of effecting biological systems, and thus warrant continued investigations of these non-natural core motifs in drug discovery. Sultams are often referred to as lactam surrogates with molecular properties that differ greatly. While a number of heterocycles have been extensively studied in the field, the sultam class occupies a much smaller segment of chemical space as evident by the comparison to all heterocycles in the Pubchem database.³⁴ The comparison parameters in the Pubchem database were setup using molecular properties such as CLogP, polar surface area and molecular weight]. In addition, chemical properties such as hydrolytic stability and crystallinity, further impart differences between sultams and other comparable heterocycles. Most strikingly, the sp^3 character of a sulfonamide/sultam is vastly different than their planar amide counterparts, relegating them to “non-flatland status” in molecular architecture as demonstrated by the X-ray structures of several benzofused sultams displayed in Figure 2.2.

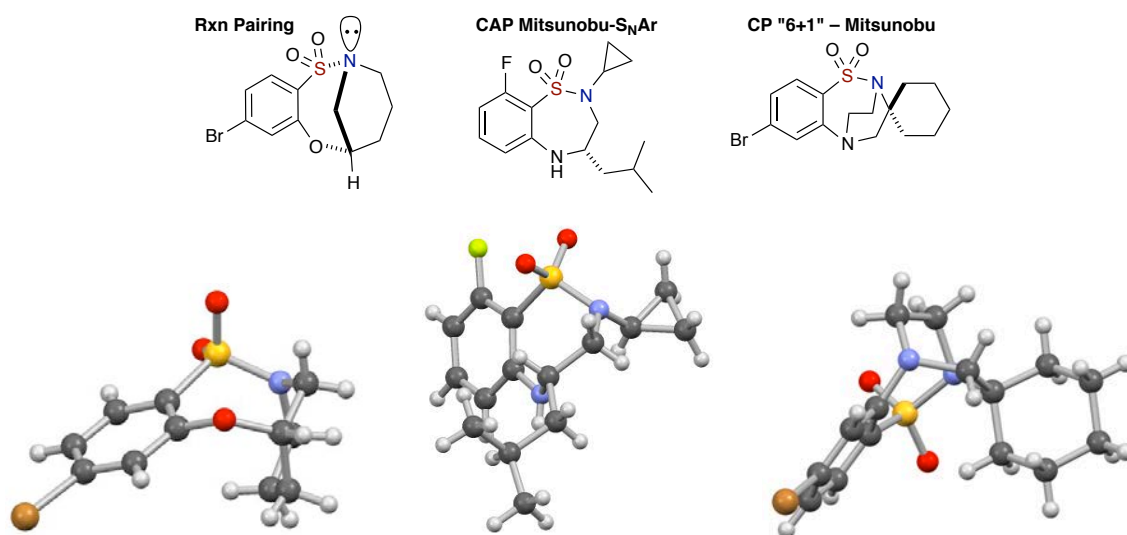


Figure 2.2. Examples of sultams and their corresponding X-rays.

In 2004, Hofmann and co-workers³⁵ reported a systematic study of the conformation of the sulfonamide bond and the respective amides at different levels of *ab initio* MO theory. The distinct differences between the two motifs are as follows: (a) different values of the torsion angle ω ($\angle C^{\alpha}SNC^{\alpha}$), which are about -100 and 60° in the two basic conformers of the sulfonamide bond, and 180 and 0° for the peptide bond, (b) the rotation barriers around the S–N bond, are distinctly lower than that for the peptide bond, hence imparting more flexibility in sulfonamido peptides, and (c) the nature of the sulfonamide nitrogen is pyramidal in comparison to a planar arrangement of the peptide amide bond. Calculations also indicated that during the *cis/trans* isomerization of an amide peptide bond, the *trans* isomer is favored over the *cis* isomer due to the lower energetic values, and because of the structural conformation, this ultimately limits the reactivity of amides (Figure 2.3).

In 2013, in collaboration with Lushington, Mulliken charges³⁶ were calculated (Figure 2.4) for three different moieties—*o*-fluoro sulfonamide, phosphonamide and amide—where *o*-fluoro-*N*-methylbenzenesulfonamide was found to be more electropositive than *o*-fluoro-*N*-methylbenzamide, which are the least electropositive. These calculated values further substantiated the known lower pK_a values of sulfonamides when compared with amides and phosphonamides. This latter property

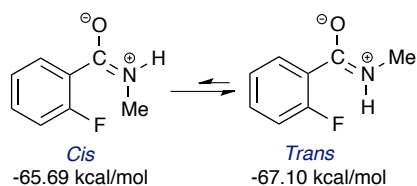


Figure 2.3. *Cis/trans* equilibrium of the amide bond.

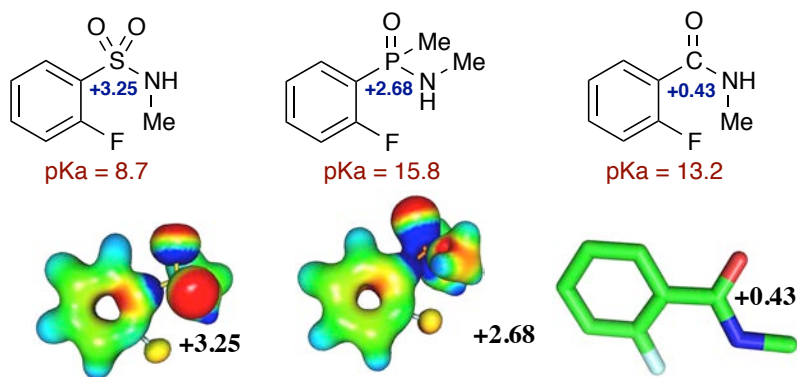


Figure 2.4. Mulliken charges for an *o*-fluoro sulfonamide, phosphonamide and amide.

(pK_a), imparts unique chemistry with sulfonamides that can be exploited in sultam synthesis, such as mild alkylation conditions and the ability to undergo facile Mitsunobu reactions as well as intramolecular S_NAr cyclization reactions, *vide infra* (Figure 2.5).

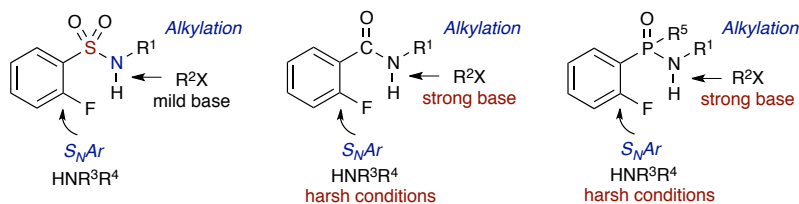


Figure 2.5. Mild reaction conditions for sulfonamide and harsher conditions for others.

A beneficial feature in the chemistry of sulfonamides is the ability to use high yielding click reactions in their formation, as well as in subsequent reactions, as shown in Figure 2.6. In 2001, Sharpless and co-workers³⁷ coined the term “click chemistry” to describe an approach that consists of a set of highly reliable and selective reactions for the rapid synthesis of valuable new compounds. In this work, Sharpless further defined a set of stringent criteria that reactions must meet to be useful in this context. The reaction must be modular, wide in scope, high yielding and must occur with simple reaction conditions, be stereospecific and produce benign by-products. The most common

examples of carbon-heteroatom bond-forming reactions, including the following classes of chemical transformations are: (i) cycloaddition transformations, (ii) nucleophilic substitution chemistry particularly ring-opening reactions of strained heterocycles, (iii) carbonyl chemistry of the “non-aldol” types and (iv) additions to carbon-carbon multiple bonds. In this seminal work, Sharpless also defined many reactions which are useful in sultam synthesis as “click reactions”, including: sulfonylation, sulfonamide alkylation, epoxide-opening, and sulfonyl aziridine-opening (Figure 2.6). The importance of this latter point will become evident throughout this thesis.

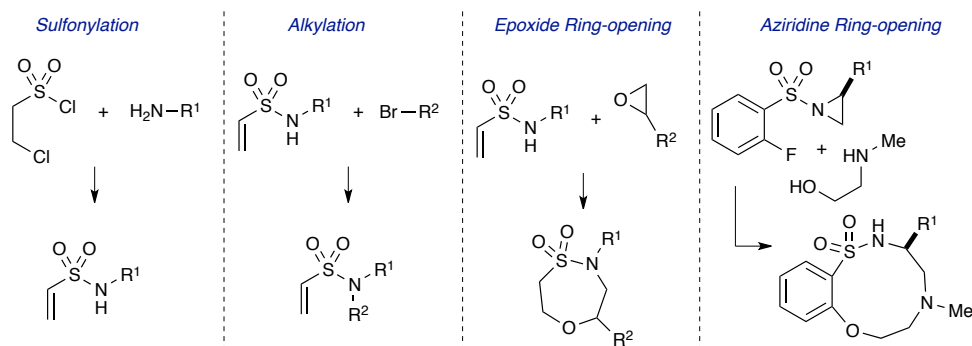


Figure 2.6. Representative examples of “Click” chemistry.

In summary, the promising biological and chemical profiles of sultams/sulfonamides engender properties that promote them as attractive motifs for facile compound synthesis and drug discovery. In this regard, it is the goal of this thesis to synthesize unique and underexplored sultam scaffolds and evaluate their properties by the several computational analyses in order to produce underrepresented ring systems with potential biological significance. With this intention in mind, the remainder of this thesis describes the development of new chemical methods for synthesis of unique

sultams. All compounds produced have been submitted for broad biological screening within the NIH Molecular Library Probe Center Network.

2.1.3 Synthesis of Sultams: Intramolecular S_NAr Methods

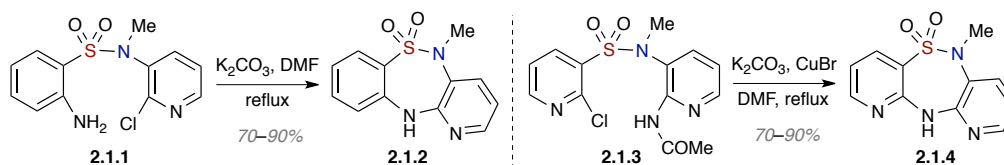
Several classical methodologies have been developed for the synthesis of the sultam ring systems including use of Diels-Alder reaction,³⁸ [2+2],³⁹ [3+2],⁴⁰ and [4+2]⁴¹ cycloadditions, Michael-epoxide-opening cyclizations,⁴² base-, coupling reagents- and halogens-promoted cyclizations,⁴³ S_N2 reactions,⁴⁴ and use of the Baylis-Hillman reaction.⁴⁵ More recently, transition metal-catalyzed reactions for the construction of sultam skeletons have gained prominence, including: (a) Cu-catalyzed,⁴⁶ (b) Pd-catalyzed,⁴⁷ (c) Rh-catalyzed,⁴⁸ (d) Ir-catalyzed⁴⁹ cyclizations, as well as (e) ring-closing metathesis (RCM).⁵⁰ In addition, radical cyclization procedures have also been utilized for the generation of sultam cores.⁵¹ Some of these methods have been covered in the recent two reviews reported in 2011 and 2013, respectively.⁵² Despite several innovative methods outlined in these recent reports, DOS strategies employing intramolecular S_NAr reactions for the synthesis of sultams are much less prevalent than other reported approaches.

Long standing interest in the facile generation of sultam scaffolds has prompted the exploration of a new approach we term reaction-pairing strategy described below. *o*-Haloaryl sulfonyl chlorides and their corresponding sulfonamides have emerged as highly versatile synthons for the generation of sultam scaffolds,⁵³ which our group has developed, and which will be discussed more in Chapter 3. For the remainder of Chapter

2, focus will be placed on the development and extension of the concept of reaction pairing and the corresponding pathways that have been investigated. Before discussing our efforts, a summary of S_NAr methods to generate sultams by other researchers will be reviewed.

Reports of intramolecular heteroaryl cyclizations *en route* to sultams first surfaced in the 1990's, when Giannotti and co-workers⁵⁴ reported ring closure on 2-amino-*N*-(2-chloropyridin-3-yl)-*N*-methylbenzenesulfonamides in the presence of K_2CO_3 and DMF at reflux temperature to afford sultam **2.1.2** (Scheme 2.1). In contrast, if an amide was employed, CuBr/Cu powder was required in the reaction to provide dihydro-dipyrido-thiadiazepine 5,5-dioxide **2.1.4** in good yields.

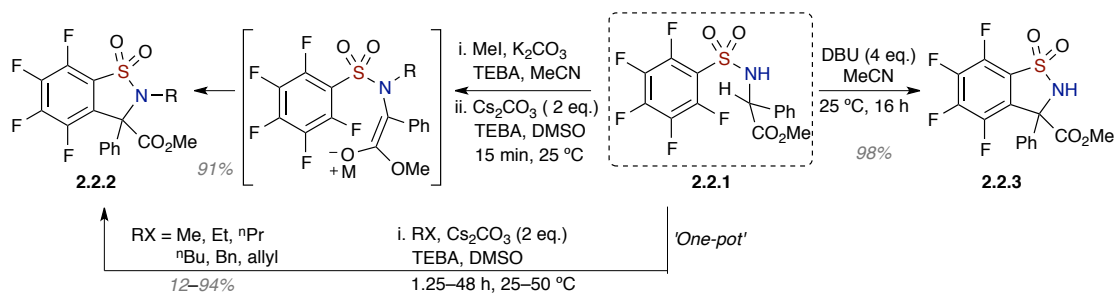
Scheme 2.1. Intramolecular heteroaryl cyclizations *en route* to sultams



In 2008, Penso and co-workers⁵⁵ described the synthesis of polyfunctionalized benzo[*d*]sultams **2.2.2** and **2.2.3** that contain an α -amino ester unit, utilizing complementary solid-liquid phase transfer catalysis (SL-PTC) and homogeneous protocols (Scheme 2.2). The investigations commenced with the optimization of cyclization reaction conditions using *N*-alkylated sulfonamides resulting from the alkylation of (pentafluorobenzene)sulfonamide with MeI, K_2CO_3 and triethylbenzylammonium chloride additive (TEBA) in MeCN using SL-PTC conditions (Cs_2CO_3 , TEBA), in which the choice of solvent was crucial. DMSO was the optimal

solvent, indicated by the formation of an equimolar adduct (enolate:DMSO) as the plausible activated species to provide sultam **2.2.2**. Next, the homogeneous conditions with different bases, solvents and temperatures were studied, where the optimal conditions are DBU in MeCN at 25 °C for 16 h, to afford the non-*N*-alkylated benzofused sultam **2.2.3** in excellent yield (Scheme 2.2). The method was extended to a “one-pot” alkylation/cyclization employing SL-PTC reaction conditions, to generate a range of benzo-isothiazole-3-carboxylate 1,1-dioxides in modest to excellent yields depending on the alkylating reagents, with more sterically hindered alkylating reagents (BnBr and allylBr) furnishing lower yields.

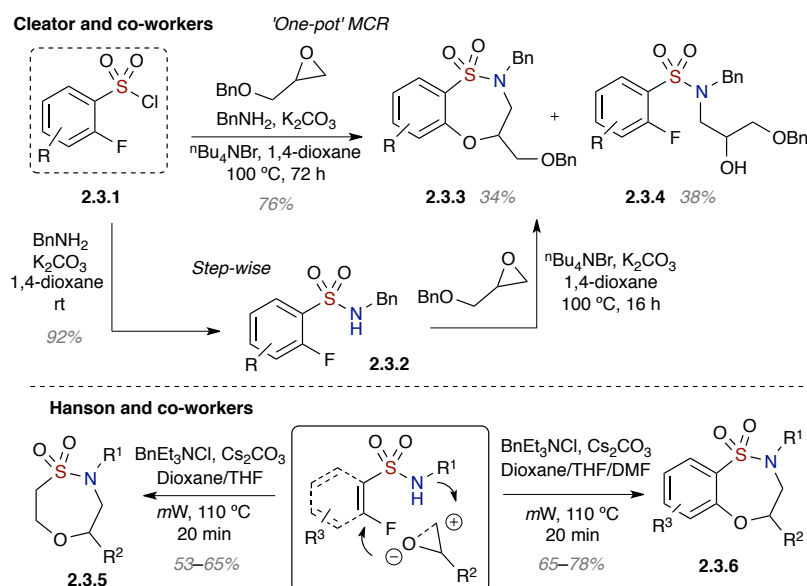
Scheme 2.2. *Synthesis of polyfunctionalized benzo[d]sultams*



In 2010, Cleator and co-workers⁵⁶ reported a one-pot multi-component (MCR) for the synthesis of benzoxathiazepine-1,1-dioxides employing commercially available amines and epoxides (Scheme 2.3). Concurrently, our group was investigating similar work⁵⁷ and the results were published almost simultaneously in the literature. The Cleator synthesis began in a stepwise fashion, with similar reaction conditions as the one-pot protocol; benzylamine and K₂CO₃ in 1,4-dioxane at room temperature afforded the corresponding sulfonamide in 92% isolated yield, followed by heating the mixture in 1,4-

dioxane at 100 °C in the presence of tetra-*n*-butylammonium bromide (${}^n\text{Bu}_4\text{NBr}$), K_2CO_3 and *O*-benzyl glycidyl ether to furnish the corresponding product **2.3.3** in 34% yield and the uncyclized, epoxide-ring opened sulfonamide **2.3.4** in 38% yield. This initial observation lead the authors to proceed with the one-pot procedure where both amine and *O*-benzyl glycidyl ether were added to the mixture with ${}^n\text{Bu}_4\text{NBr}$ and K_2CO_3 in 1,4-dioxane at 100 °C for 72 h to afford the anticipated product in a higher yield of 75% (Scheme 2.3). Different halogen substituents on the aryl ring were investigated, as well as an extension to Pd-catalyzed cross coupling, with the brominated scaffolds derived from the aforementioned method.

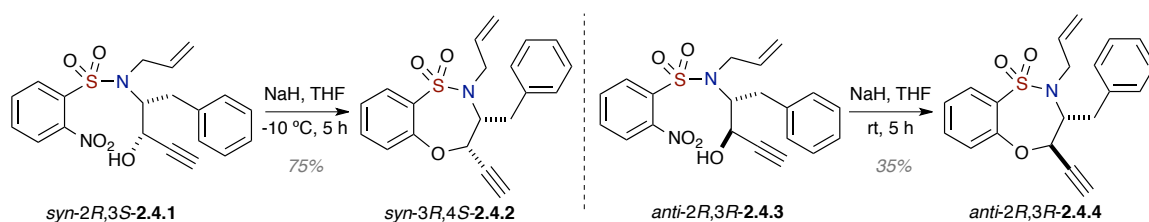
Scheme 2.3. *One-pot multi-component (MCR) for the synthesis of sultams*



In 2010, Schreiber and co-workers⁵⁸ employed a build-couple-pair DOS strategy to effect an intramolecular cyclization pathway using an $\text{S}_\text{N}\text{Ar}$ reaction for the ring closure of *syn*-amino propargylic alcohol (*2R,3S*) benzenesulfonamides **2.4.1** under basic

reaction conditions (NaH in THF) (Scheme 2.4). Control of the temperature between -10 and 0 °C was needed to obtain the endocyclic product **2.4.2** selectively in 75% yield. In comparison, the *anti*-diastereomer (*2R,3R*)-**2.4.3** only reacted at room temperature under the same conditions, generating (*3R,4R*) benzo-oxathiazepine 1,1-dioxide **2.4.4** in moderate yield due to lower selectivity of the *ipso*-substitution relative to the Smiles rearrangement.

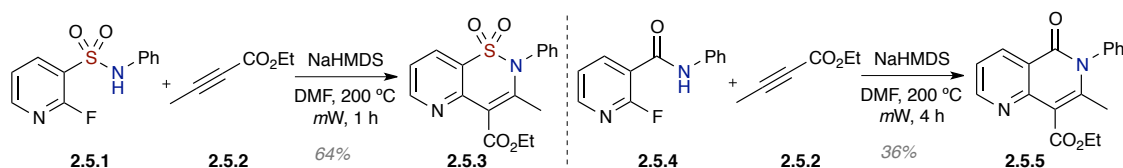
Scheme 2.4. *S_NAr* cyclization pathway to sultams



In 2010, Juhl and co-workers⁵⁹ reported a versatile conjugate addition–*S_NAr* domino reaction for the synthesis of bicyclic benzo- and pyridyl-fused lactam and sultam derivatives. The optimized reaction conditions are NaHMDS in DMF at 200 °C for 1–4 h under *mW* irradiation to generate products **2.5.3** and **2.5.5** (Scheme 2.5). These conditions were plagued with several problems, where oligomerization of the conjugate addition intermediates, decomposition of some substrates and incomplete conversion of starting material were observed. In order to circumvent these issues, the authors modified the conditions, where slow addition of a dilute solution of the alkyne **2.5.2** to a pre-heated, deprotonated amide solution, was effective for certain substrates. The authors found that use of 2 equivalents of alkyne allowed full conversion of starting material, and that controlling the temperature between 100 to 200 °C prevented decomposition of the starting materials. When similar reaction conditions were employed for the amide

substrate, a lower yield of 35% was observed, substantiating the fact that sulfonamides are better substrates than amides for this reaction pathway (Scheme 2.5). This observation is most plausibly due to the higher electron-withdrawing ability of sulfonamides, which allows for a more facile ring-closing step with shorter reaction times. Moreover, very little oligomerization of the resulting intermediates was noted.⁵⁹

Scheme 2.5. Conjugate addition– S_NAr domino reaction for the synthesis of sultams

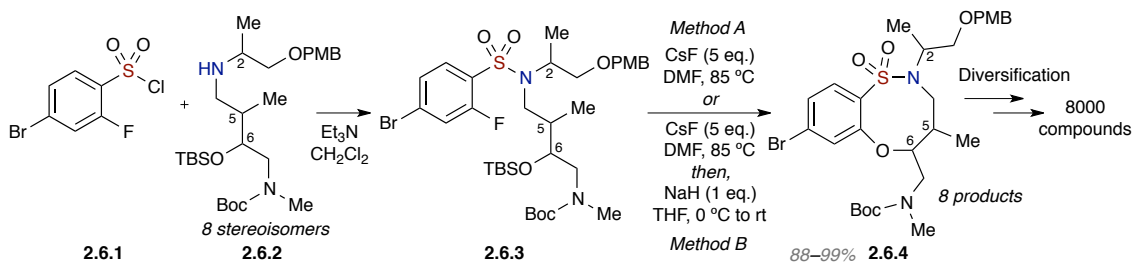


While these aforementioned strategies synthesized mostly common ring sizes (5- to 7-membered), to the best of our knowledge, there are only a handful of reports on the synthesis of medium sized (8- to 11-membered) sultams. In 2011, Marcaurelle and co-workers^{7c} reported an aldol-based, “Build-Couple-Pair” (BCP) strategy for the synthesis of stereochemically diverse 8-membered sultam and lactam scaffolds *via* S_NAr cycloetherification (Scheme 2.6). In this method, each scaffold contained two handles, an amine and aryl bromide for solid-phase diversification *via* N -capping, and Pd-mediated cross coupling. For this section, only the Marcaurelle synthesis of sultams will be discussed. In this regard, the build phase involved a series of asymmetric *syn*- and *anti*-aldol reactions, where four stereoisomers of a Boc-protected β -hydroxy- γ -amino acid were produced. In the couple step, the chiral acid and resulting protected amines were coupled and reduced to generate elaborate building blocks comprised of all 8 stereoisomers. Lastly, in the pair phase, S_NAr cyclization was utilized to pair all 8

stereoisomers with 4-bromo-2-fluorobenzenesulfonyl chloride **2.6.1** in order to furnish a series of benzofused sultams **2.6.4** in good yields (Scheme 2.6).

In this BCP method, two sets of reaction conditions were employed for the cycloetherification step. Thus, depending on the stereochemistry of the building blocks, sulfonamides bearing *2R,5S,6R* and *2S,5S,6R* stereochemistry derived from the *syn*-aldol were easily converted in a single step using method A (CsF, DMF at 85 °C), whereas for sulfonamides bearing *2R,5S,6S* and *2S,5S,6S* stereochemistry and derived from an *anti*-aldol, were converted in a two-step approach employing method B (CsF, DMF at 85 °C, then NaH, THF, 0 °C to rt) (Scheme 2.6). Use of just CsF initially yielded a mixture of TBS-protected, uncyclized material along with some product. However, treatment of the mixture with NaH in THF provided the complete conversion of starting material to the respective products **2.6.4** (Scheme 2.6). With the scaffolds in hand, library diversification proceeded to generate 8000 compounds that were evaluated by various chemical informatics analysis, such as multifusion similarity (MFS) maps, Tanimoto coefficient and principal component analysis (PCA).

Scheme 2.6. Aldol-based “build-couple-pair” strategy for the synthesis of stereochemically diverse 8-membered sultams



In summary, while the S_NAr reaction has been used for the construction of benzofused sultams, the methods outlined above, focused mainly on small ring sizes (5- to 7-membered),⁵⁴⁻⁵⁹ and more recently by Marcaurelle and co-workers in 2011,^{7e} accessing 8-membered benzofused sultams. In this regard, it was the aim of this thesis to extend the scope of the sultam methods using more unique building blocks. In the following section (Section 2.2), we describe a strategy termed “reaction pairing”, which employs *o*-fluoroaryl sulfonamide SMs that undergo facile nucleophilic aromatic substitution (S_NAr) for the rapid generation of 7- to 10-membered benzofused sultam scaffolds.

2.2 Results and Discussion

In the course of designing new methods for sultam synthesis, we have developed an orthogonal reaction pairing strategy we term “Reaction Pairing” that employs the use of three reactions, namely sulfonylation, Mitsunobu alkylation and S_NAr for the facile, efficient and modular synthesis of sultams (Figure 2.7).² The main concept in reaction pairing is the “pairing of reaction pathways” that are orthogonal (mutually exclusive) to each other. The utility of this related strategy lies in its potential to generate diverse skeletons from a single central bi-functional core without the need for the construction of an elaborate multi-functional scaffold (Figure 2.7). The reaction probability of bi-functional scaffolds can be exploited to obtain skeletally diverse motifs by simply pairing the core scaffold with compatible synthons via suitable orthogonal reaction pathways, allowing access to skeletally distinct motifs in a facile manner.

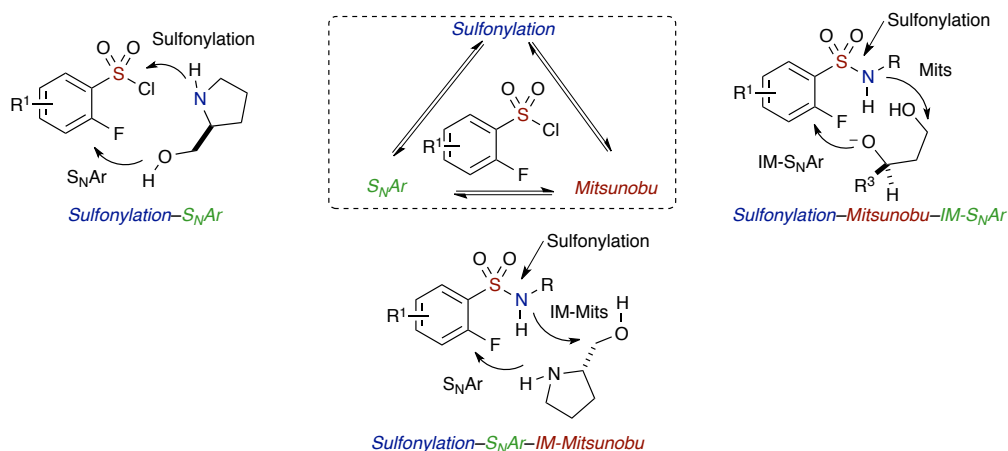


Figure 2.7. Three different reaction pathways to diverse benzofused sultams.

While sulfonylation and Mitsunobu alkylation are well preceded for sulfonamides,⁶⁰ the ability of these synthons to undergo facile S_NAr is far less prevalent, as previously noted in the section above. Collectively, it was therefore envisioned that pairing of the reaction triad (sulfonylation, S_NAr addition and Mitsunobu alkylation) in varying order alongside the central *o*-fluorobenzene sulfonyl chloride building blocks could afford rapid access to both bridged- and fused-tricyclic sultams (Figure 2.8). This simple approach obviates the need for construction of elaborate multifunctional scaffolds and merely requires *o*-fluorobenzene sulfonyl chlorides, amines and alcohols as building blocks. Simple changes in the reaction pair sequence (e.g., sulfonylation- S_NAr vs sulfonylation- S_NAr -Mitsunobu vs sulfonylation-Mitsunobu- S_NAr) or changes in building blocks (1,2-amino alcohol vs 1,3-amino alcohol) allows access to skeletal and stereochemical diversity (Figure 2.8).

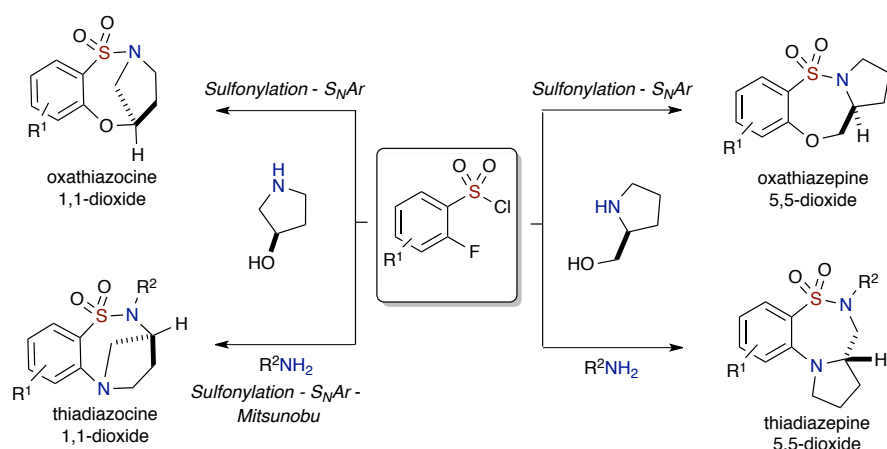
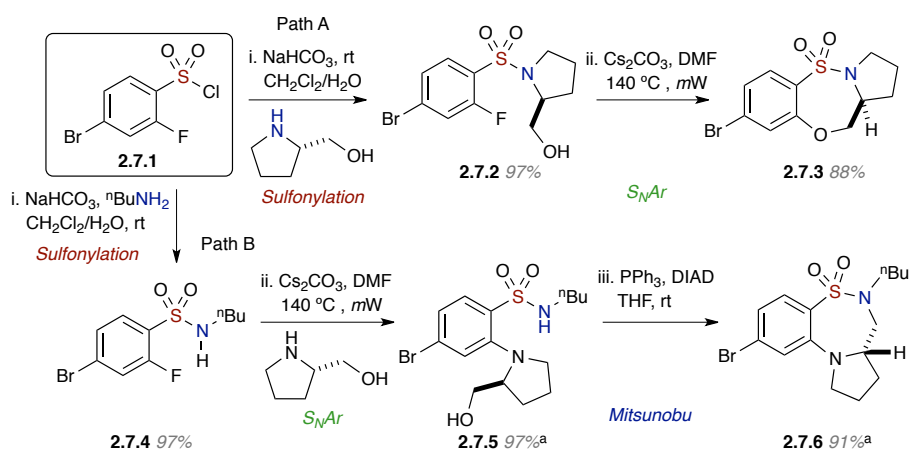


Figure 2.8. Reaction pairing strategies to diverse benzofused sultams.

2.2.1 Optimization Studies

Investigations commenced with the exploration of pairing (*S*)-prolinol with 4-bromo-2-fluorobenzenesulfonyl chloride **2.7.1** via a combination of sulfonation, S_NAr and Mitsunobu methods (Scheme 2.7). Thus, (*S*)-prolinol was sulfonated with 4-bromo-2-fluorobenzenesulfonyl chloride in CH₂Cl₂/H₂O, in the presence of NaHCO₃, to provide β-hydroxy *o*-fluorobenzene sulfonamide **2.7.2** in 97% yield. Subjection of the sulfonamide to microwave (*mW*) irradiation at 150 °C for 30 min in DMF in the presence of Cs₂CO₃ gratifyingly produced the benzofused tricyclic sultam **2.7.3** in 88% yield. In contrast, S_NAr addition of (*S*)-prolinol to *n*-butyl-derived *o*-fluorobenzene sulfonamide **2.7.4** under *mW* irradiation in DMSO at 140 °C for 30 min afforded the desired S_NAr adducts **2.7.5** in 97% yield (Scheme 2.7). Addition of PPh₃ to a stirring solution of the prolinol-derived S_NAr adduct in THF (0.05 M), followed by slow addition of DIAD, was found to proceed quickly (10 min) to furnish the desired tricyclic benzothiadiazepine-1,1-dioxide **2.7.6** in 91% yield. Overall, this approach rapidly furnishes different sultam

Scheme 2.7. Two distinct reaction pairing pathways with amino alcohols



^a See reference 61 for full characterization data.

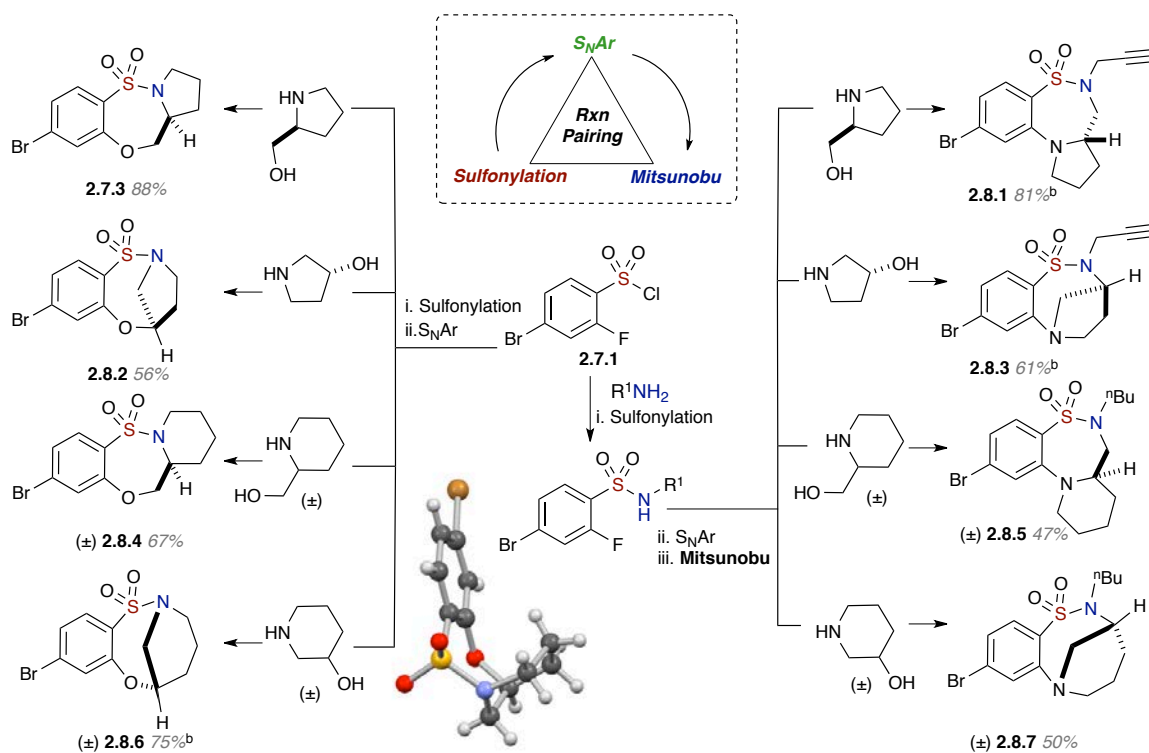
skeletons by implementing a single sulfonyl chloride in conjunction with an amino alcohol by merely changing the order of reaction pairing.

2.2.2 Scope of Reactions

With these results in hand, the generation of diverse benzofused sultams was explored by utilizing the reaction pairing strategy. Thus, use of (*S*)-prolinol alongside propargylamine derived *o*-fluorobenzene sulfonamides in the established S_NAr –Mitsunobu pairing afforded the desired tricyclic sultam **2.8.1** in good yield (Scheme 2.8). A simple switch in the amino alcohol component to (*R*)-(+)-3-hydroxypyrrolidine gratifyingly afforded the corresponding bridged, tricyclic benzofused sultams **2.8.2** and **2.8.3** in moderate to good yield. Of notable importance is the facile production of the unique bridged tricyclic sultam **2.8.2** containing a bridge-head nitrogen connected to an SO_2 moiety. It is proposed that this “bridged sultam”, like corresponding twisted amides,

could cause a deviation in the geometry of the sulfonamide group leading to potential hybridization and geometry changes at nitrogen, ultimately affecting physical properties.^{62,63} It has been reported that twisted amides (anti-Bredt) possess a distorted amide bond, which dramatically affect stability and reactivity in comparison to their standard planar amides while increasing the basicity of the N atom (or bridgehead N).⁶⁴

Scheme 2.8. Reaction pairing strategy to access skeletally diverse sultams with an array of amino alcohols^a



^a **Sulfonylation:** R¹NH₂ (Compounds **2.8.1** and **2.8.3**: R¹ = Propargyl; **2.8.5** and **2.8.7**: R¹ = ⁿBu). **S_NAr:** Cs₂CO₃, DMF, 140 °C, *mW*. **Mitsunobu:** PPh₃, DIAD, THF, rt. ^b See reference 61 for full characterization data.

In considering potential physical property changes within constrained sulfonamides one must start with the preferred conformation of a sulfonamide as outlined in Figure 2.9, which places the nitrogen lone pair anti-periplanar to the S–Ar bond to

maximize the σ^* orbital delocalization.^{62f} This conformation effectively allows the orientation of the lone pair to bisect the O=S=O internuclear angle.⁶⁵ As seen in the X-ray of bridged sultam (\pm)-**2.8.6**, the preferred conformation of the Ar-SO₂NR¹R² moiety is conserved. Despite this conservation of geometry—between normal and bridged sultams, bridged sultams are structurally different than their twisted amide counterparts and thus represent interesting probe molecules that we will continue to pursue [Note also: a twisted amide is structurally different from a typical amide for reasons outlined above].

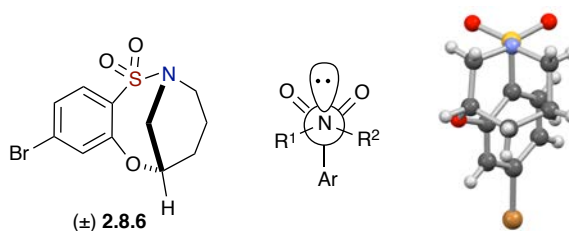
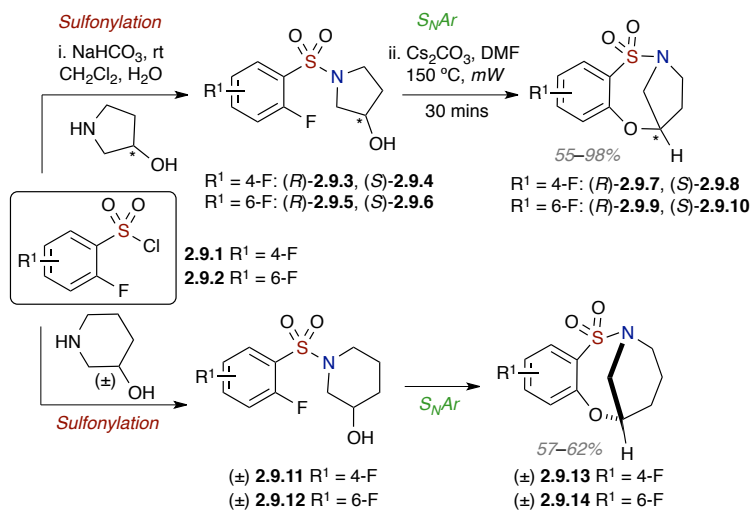


Figure 2.9. Preferred conformation of sultam **2.8.6**.

While (*R*)-(+)-3-hydroxypyrrolidine was first used in the reaction sequence, the *S*-isomer was also exploited to provide desired benzo-oxathiazocine 1,1-dioxides **2.9.7**–**2.9.10**, with both stereoisomers having 4- and 6-fluoro substituents on benzenesulfonyl chlorides (Scheme 2.9). With the four scaffolds on hand, a peripherally diverse 80-member library of bridged and benzofused sultams were generated, as described in Section 2.3.

Building on these results, utilization of 2-piperidinemethanol in the established reaction pairing protocol generated the corresponding benzofused tricyclic sultams **2.8.4** and **2.8.5** in good yields (Scheme 2.8). In contrast, use of 3-hydroxypiperidine and 4-bromo-benzenesulfonyl chloride allowed for the synthesis of bridged benzofused sultams

Scheme 2.9. *Sulfonylation–S_NAr reaction pathway to bridged, benzofused sultams*



2.8.6 and **2.8.7** in satisfactory yields (Scheme 2.8), with **2.8.6** [see X-ray crystallographic analysis in the experimental section, Chapter 5] possessing similar bridged sultam structural characteristics as **2.8.2**. Similarly, 3-hydroxypiperidine and 4- and 6-fluorobenzenesulfonyl chlorides were employed to generate fluoro-substituted 9-membered bridged benzofused sultams **2.9.13–2.9.14** in satisfactory yields (Scheme 2.9).

Overall, this reaction pairing sequence allowed for the rapid construction of a skeletally and stereochemically diverse collection of benzofused sultams by simple variation of the amine component.

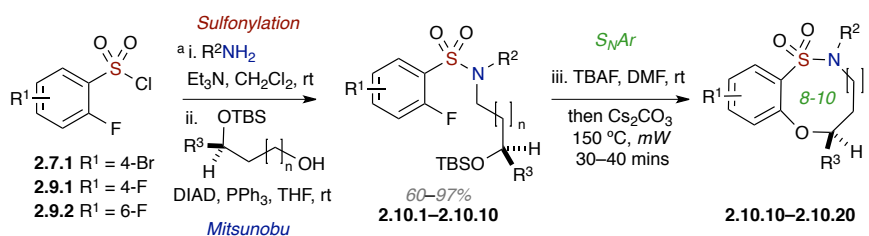
2.2.3 Sulfonylation–Mitsunobu–Intramolecular S_NAr Strategy

Alternatively, it was envisioned that utilization of mono protected 1,3-, 1,4- and 1,5-diols, alongside *o*-fluorobenzene sulfonamides in a Mitsunobu alkylation–intramolecular S_NAr *O*-arylation would allow access to oxygen-containing benzofused

sultams **2.10.10–2.10.20** (Scheme 2.10). This method began with use of a simple mono-protected 3-silyloxy-1-propanol, whereby subsection to Mitsunobu alkylation with *n*-butyl-derived *o*-fluorobenzene sulfonamide, furnished the 3° sulfonamides **2.10.1–2.10.10** in good yields.

It was envisioned that deprotection of the TBS group under basic conditions would allowed for an intramolecular S_NAr cyclization to take place. Hence, a THF solution of sulfonamide **2.10.1** was stirred in the presence of TBAF for 30 min under *mW* irradiation at 150 °C to our delight, yielded the desired sultam **2.10.11** in 88% yield (Scheme 2.10 and Table 2.1, entry 1). Application of the enantiomers (*R*)- and (*S*)-3-((*tert*-butyldimethylsilyl)oxy)-butan-1-ol in the above Mitsunobu–S_NAr pairing sequence was again found to cleanly furnished the corresponding benzothiazocine- 1,1-dioxides **2.10.14** and **2.10.17** in good yields, albeit longer reaction times for deprotection of secondary alcohols before the cyclization process (Table 2.1, entries 4 and 7). The substrate scope was investigated with commercially available benzenesulfonyl chlorides, where 4-bromo, 4-fluoro and 6-fluoro substituents work satisfactory in the reaction sequence, as well as simple alkyl amines including cyclopropylamine for the synthesis of 2° sulfonamides.

Scheme 2.10. Mitsunobu–intramolecular S_NAr strategy to 8- to 10-membered sultams



^aAlternate reaction condition for step i. sulfonylation: NaHCO₃, CH₂Cl₂/H₂O.

Table 2.1. Substrate scope of Mitsunobu–intramolecular S_NAr strategy

entry	R ¹	R ²	R ³	n/ring size	yield (%)	product
1	4-Br	ⁿ Bu	H	1/8	88%	2.10.11
2	4-F	cyclopropyl	H	1/8	90%	2.10.12
3	6-F	cyclopropyl	H	1/8	72%	2.10.13
4	4-Br	ⁿ Bu	(<i>R</i>)-Me	1/8	90%	2.10.14^a
5	4-F	cyclopropyl	(<i>R</i>)-Me	1/8	90%	2.10.15^a
6	6-F	cyclopropyl	(<i>R</i>)-Me	1/8	98%	2.10.16^a
7	4-Br	ⁿ Bu	(<i>S</i>)-Me	1/8	87%	2.10.17^a
8	4-F	cyclopropyl	H	2/9	31%	2.10.18
9	6-F	cyclopropyl	H	2/9	66%	2.10.19
10	4-F	cyclopropyl	H	3/10	59%	2.10.20

^aIM- S_NAr : TBAF, rt, 12 h, then CS_2CO_3 , 150 °C, *mW*, 30 mins.

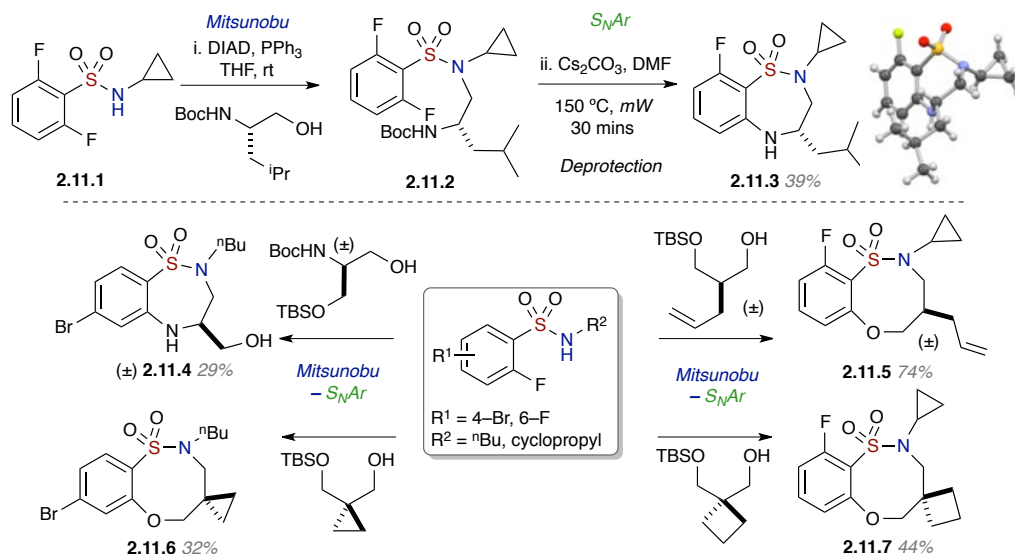
Next, mono-protected 1,4-diols were examined where benzo-oxathiazonine 1,1-dioxides **2.10.18** and **2.10.19** (9-membered) were synthesized in satisfactory yields (Table 2.1, entries 8 and 9). Lastly, an ether-containing 1,5 mono-protected diol (2-(2-((*tert*-butyldimethylsilyl)-oxy)ethoxy)-ethanol) was utilized in the Mitsunobu- S_NAr pathway to generate the 10-membered sultam **2.10.20** in 59% yield (Table 2.1, entry 10).

The scope was further expanded to unique 1,2 amino alcohols and 1,3 diols where skeletally diverse 7- and 8-membered sultams were synthesized in a facile Mitsunobu–intramolecular S_NAr sequence. In a similar approach, a range of 2° sulfonamides were obtained *via* a sulfonylation reaction with benzenesulfonyl chlorides and alkyl amines,

followed by intermolecular Mitsunobu alkylation with the respective mono-protected 1,2 amino alcohols and 1,3 diols. These substrates include protected amino alcohols – (*S*)-*tert*-butyl (1-hydroxy-4-methylpentan-2-yl)carbamate, olefin-containing diols – 2-(((*tert*-butyl-dimethylsilyl)oxy)methyl)pent-4-en-1-ol and spiro-cycloalkyl diols – (1-(((*tert*-butyldimethyl-silyl)oxy)methyl)cyclobutyl)methanol (Scheme 2.11). Upon the synthesis of these 3° sulfonamides, an intramolecular S_NAr cyclization was executed to provide diverse benzofused sultams **2.11.3–2.11.7** in decent yields (Scheme 2.11). The structure of sultam **2.11.3** was confirmed by X-ray crystallography analysis (Scheme 2.11).

A nice caveat to this method occurred when mono-protected 1,3-diols were employed, the removal of the TBS-protecting group with TBAF at rt for 12 h preceded the cyclization with Cs₂CO₃ under *mW* irradiation for 30 mins at 150 °C (Scheme 2.11).

Scheme 2.11. Expanded substrate scope of 1,2 amino alcohols and 1,3 diols in a Mitsunobu–S_NAr pathway



^a For mono protected 1,3 diols, reaction conditions for step ii, TBAF, rt, 12 h, then Cs₂CO₃, 150 °C, *mW*, 30 mins.

This resulted in an overall, one-pot, TBS-deprotection–cyclization to afford benzofused sultams, as well as the spiro-cycloalkyl substituents scaffolds. In cases when protected amino alcohols were used in the reaction sequence, a one-pot TBS-deprotection–cyclization–Boc-deprotection was accomplished as the Boc group was removed after ring closure, under *mW* irradiation at high temperatures.

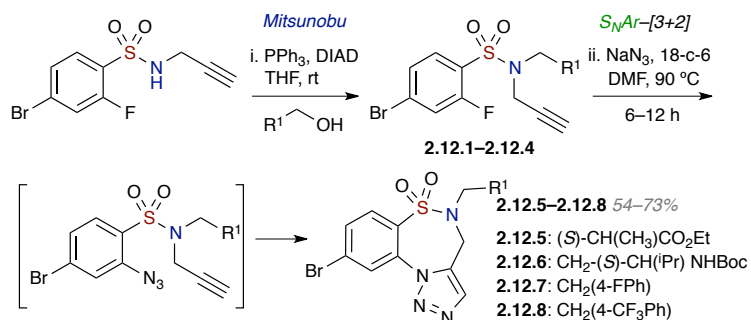
Overall, simply changing of the order of pairing for the sulfonylation–intermolecular S_NAr –Mitsunobu sequence to sulfonylation–Mitsunobu–intramolecular S_NAr allows for facile access to skeletally, as well as stereochemically, diverse benzofused sultams.

2.2.4 Mitsunobu– S_NAr –[3+2] Cycloaddition Reaction Pairing

Utilization of a [3+2] Huisgen cycloaddition reaction for the production of triazole-containing sultams was next explored. Hemming and co-workers reported the elegant use of a one pot, tandem alkynylation–[3+2] cycloaddition approach to triazolosultams,⁶⁶ while a recent report by Yao and co-workers outline the utilization of a Cu-catalyzed tandem [3+2] dipolar cycloaddition–*N*-arylation approach to these motifs utilizing *o*-bromo and *o*-iodobenzenesulfonamides.⁶⁷ However, there are no reports of the use of non-metal catalyzed, S_NAr –[3+2] Huisgen cycloaddition for the generation of benzofused sultams. Thus, a sulfonylation–Mitsunobu protocol using propargyl alcohol and *o*-fluorobenzene sulfonamide as the Mitsunobu partners produced the desired propargylated *o*-fluorobenzene sulfonamides **2.12.1–2.12.4** in excellent overall yield (Scheme 2.12). Azidation of sulfonamides **2.12.1–2.12.4** was carried out using NaN_3 in

DMF at 90 °C in the presence of 18-crown-6 (1 eq.) for 12 h to afford the tricyclic triazole-containing sultams **2.12.5–2.12.8**⁶¹ which had participated in an intramolecular [3+2] Huisgen cycloaddition ring closure following intermolecular S_NAr azidation. To the best of our knowledge, in 2011, this represented the first report of a one-pot tandem S_NAr-intramolecular [3+2] Huisgen cycloaddition for the synthesis of benzofused sultams.⁶⁸ The reported method was reviewed in a dissertation (Thiwanka Samarakoon).⁶¹ Overall, the sulfonylation–Mitsunobu–S_NAr protocol is augmented by pairing with an intramolecular [3+2] cycloaddition protocol for the synthesis of triazol-bearing benzofused sultams in 3 steps.

Scheme 2.12. Mitsunobu–Azido S_NAr–[3+2] cycloaddition RP approach to benzothia-diazepine-6,6-Dioxides



2.2.5 Chemical Informatic Analysis

From chemical informatics analysis, utilizing a multi-fusion similarity (MFS) analysis,⁶⁹ it is apparent that sultams synthesized in Chapter 2 (red) are fairly unique relative to the manifold of currently available analogs,² (April 2012) and that there is a reasonable amount of structural diversity present (Figure 2.10).⁷⁰ Selected sultams are a distance from the populated region, suggesting that these compounds may be identifying new or

unpopulated chemical space. Analysis was conducted against all 1198 compounds (blue) in the NIH Molecular Libraries Probe Production Center Network (MLPCN) as of 2010 that contained the maximum common substructure (4-bromo-*N*-propylbenzene sulfonamide) evident within our own (Figure 2.10). The graph is guided by the chemical space defined by BCUT polarizability metrics where the x-axis reports values of an AM1 polarizability metric scaled by molecular bond-order profile and the y-axis reports an AM1 polarizability metric scaled by an inverse topological distance profile.

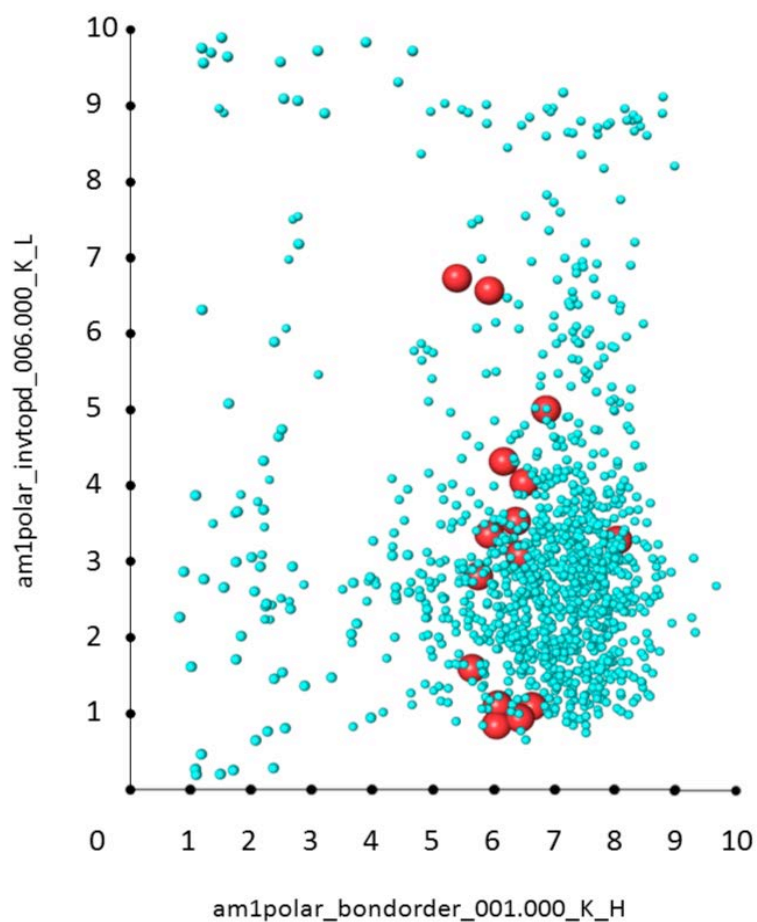


Figure 2.10. Diversity distribution of sultams (red spheres) relative to analogous MLPCN compounds (blue) currently present in the NIH Molecular Libraries Probe Production Center Network (MLPCN) as of 2010.

2.2.6 Conclusion

In conclusion, we have developed a reaction pairing strategy employing the reaction triad–sulfonylation, Mitsunobu, S_NAr for the rapid synthesis of a diverse collection of benzofused sultams. Simple changes to the order of the pairing sequence and/or building blocks, allows for access to skeletal and stereochemical diversity. Overall, this strategy affords a diverse set of heterocycles in 2–3 steps from commercially available building blocks. These results are highly amenable for library production to generate collections of skeletally diverse sultams for high throughput screening.

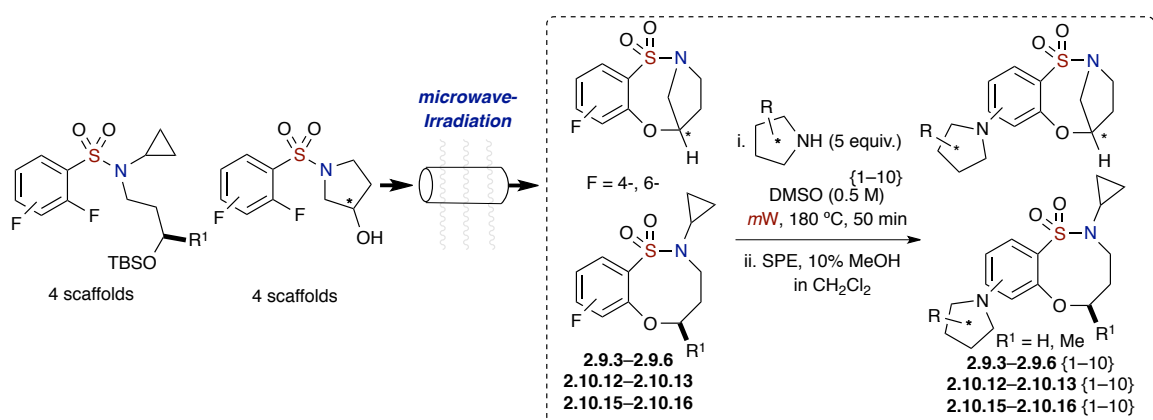
2.3 Exploring Chemical Diversity via a Modular Reaction Pairing Strategy

2.3.1 Introduction

While there are numerous methods reported in the literature for the synthesis of 5-, 6- and 7-membered benzofused sultams, reports on the generation of 8-membered benzofused sultams have been sparse.^{7e,71} In this regard, our group has focused on the development of several protocols for the generation of diverse sultam collections.⁷² Recent highlights towards these goals include, “click-click-cyclize”,⁷³ and complementary ambiphile pairing (CAP).^{57,71a} In 2011 and in the preceding part of this Chapter 2, we reported the development and application of an efficient reaction pairing strategy utilizing three simple reactions, namely sulfonylation, Mitsunobu alkylation and S_NAr , which when combined in different sequences or with different coupling reagents, provided access to skeletally diverse 7- and 8-membered sultams (*vide supra*).² Building on this strategy, we report the design and synthesis of an 80-member library of

benzofused sultams by a microwave-assisted, intermolecular S_NAr diversification of core benzo-oxathiazocine 1,1-dioxide scaffolds (Scheme 2.13).⁷⁴

Scheme 2.13. Proposed library generation by microwave-assisted intermolecular S_NAr diversification reaction

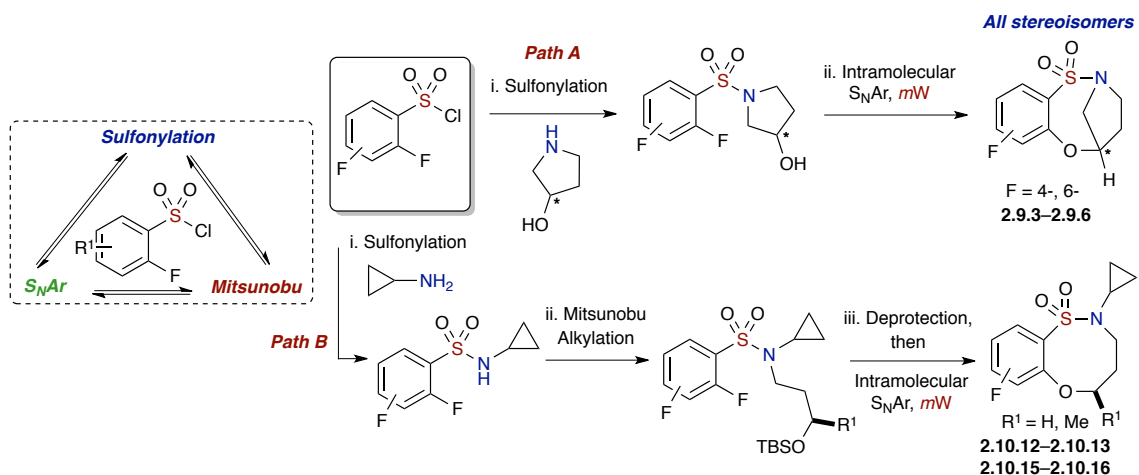


2.3.2 Results and Discussion

Initial efforts focused on the synthesis of eight core scaffolds **2.9.3–2.9.6**, **2.10.12–2.10.13**, **2.10.15–2.10.16** on multi-gram scale through the use of three efficient steps, namely sulfonylation, Mitsunobu alkylation and S_NAr (Scheme 2.14).⁷⁵ The bridged benzofused sultam scaffolds were prepared by a sulfonylation–intramolecular S_NAr protocol, reported previously,² utilizing 3-hydroxypyrrolidine in combination with 2,4-difluoro- and 2,6-difluoro-benzenesulfonyl chloride. Both *R* and *S* isomers of 3-hydroxypyrrolidine were employed for the synthesis. Likewise, the non-bridged scaffolds were also prepared as reported by a sulfonylation–intermolecular Mitsunobu alkylation–intramolecular S_NAr protocol.² Cyclopropyl amine was sulfonylated with 2,4-difluoro- and 2,6-difluoro-benzenesulfonyl chlorides, followed by Mitsunobu alkylation

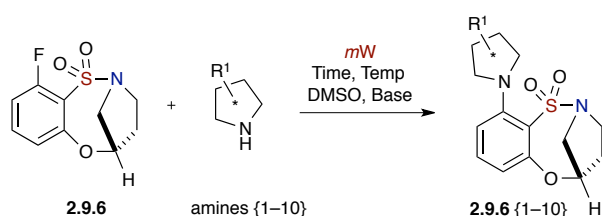
with 3-silyloxybutan-1-ol and subsequent one-pot desilylation–intramolecular S_NAr alkoxylation (Scheme 2.14). Each of the scaffolds **2.9.3–2.9.6**, **2.10.12–2.10.13**, **2.10.15–2.10.16** was prepared on a 2.5 gram scale.

Scheme 2.14. Utilization of a reaction pairing strategy for the synthesis of benzo-oxathiazocine 1,1-dioxides core scaffolds **2.9.3–2.9.6**, **2.10.12–2.10.13**, **2.10.15–2.10.16**



2.3.2.1 Optimization of Conditions

With scaffolds **2.9.3–2.9.6**, **2.10.12–2.10.13**, **2.10.15–2.10.16** in hand, efforts were focused on the diversification of these core scaffolds with a variety of chiral, non-racemic amines/amino alcohols, using intermolecular S_NAr with benzo-oxathiazocine 1,1-dioxide **2.9.6** as the test substrate (Table 2.2). A variety of reaction conditions (eq. of amine, presence of base, concentration of solvent, time and temperature) were examined to identify the optimal conditions. Our initial attempt gave an excellent yield of 94% when 4.4 equivalents of amine were employed, in the absence of base, at a concentration of 0.1 M in DMSO, and under *mW* irradiation at 150 °C for 20 min. (Table 2.2, entry 2).

Table 2.2. Optimization studies for the S_NAr reaction utilizing sultam **2.9.6**

Entry	Amine	Eq.	Conc. (M)	Time (mins)	Temp (°C)	Yields ^a (%)
1 ^c	(<i>R</i>)-3-Pyrrolidinol	1.3	0.1	30	150	NA
2	(<i>R</i>)-3-Pyrrolidinol	4.4	0.1	20	150	94
3	(<i>S</i>)-2-Pyrrolidine methanol	4.4	0.1	30	150	29
4	(<i>S</i>)-2-Methoxymethyl pyrrolidine	4.3	0.1	50	180	NA
5	(<i>S</i>)-3- Dimethylamino pyrrolidine	5.0	0.1	50	180	88
5	(<i>R</i>)-2-Methylpyrrolidine	5.0	0.1	30	150	42
6	(<i>R</i>)-2-Methylpyrrolidine	5.0	0.1	40	180	62 ^b
7	(<i>R</i>)-2-Methylpyrrolidine	5.0	0.1	50	180	70
8	(<i>R</i>)-2-Methylpyrrolidine	5.0	0.1	60	180	35
9	(<i>R</i>)-2-Methylpyrrolidine	5.0	0.5	50	180	95 ^b
10	(<i>R</i>)-2-Methylpyrrolidine	5.0	1.0	50	180	83 ^b

^aYields are reported after flash column chromatography on silica gel. ^bCrude yield as judged by ¹H NMR. ^cCs₂CO₃ was added to the reaction.

However, when a hindered amine was utilized, it resulted in low (29%) or no yield, even when the reaction time was extended (Table 2.2, entry 3) or when slightly harsher conditions were used (Table 2.2, entry 4). The equivalents of amine were increased and the choice of substrate was changed to examine further, with the substrates listed on the series of building blocks proposed in the Library Design section. Hence, more experiments were executed to investigate other factors, in which the nature and equivalents of amine remained the same while the concentration of solvent, temperature and reaction time were increased. Finally, the optimal results were obtained in the absence of base, with 5 equivalents of amine, at a concentration of 0.5 M in DMSO, and

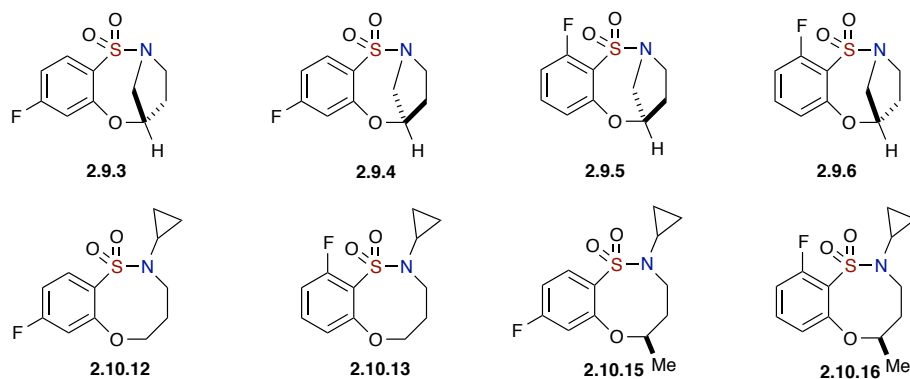
under 50 min of *mW* irradiation at 180 °C (Table 2.2, entry 9). All reactions were performed under identical conditions, thus attempts were not made to optimize the conditions further for individual substrates.

2.3.2.2 Library Design

An 80-member, full matrix library was designed by using *in silico* analysis.⁷⁶ Eight benzo-oxathiazocine 1,1-dioxide scaffolds **2.9.3–2.9.6**, **2.10.12–2.10.13**, **2.10.15–2.10.16** were designed, of which library **I** (**2.9.3–2.9.6**) was composed of the entire spectrum of possible stereoisomers, and library **II** (**2.10.12–2.10.13**, **2.10.15–2.10.16**) was composed of two sets of benzofused sultams having an H or Me group at the R¹ position (Figure 2.11). The use of all possible stereoisomers provides the opportunity to generate stereochemical SAR (SSAR) for each building block combination.^{7a} With the core sultams in hand, a virtual library incorporating all possible combinations of the building blocks of the secondary amines {1–10} was constructed for each scaffold. Physico-chemical property filters were applied, guiding the elimination of undesirable building blocks that led to products with undesirable *in silico* properties (see Chapter 5 for the Supporting Information for full *in silico* data and detailed information on the calculations). These metric filters included standard Lipinski's rule of five parameters (molecular weight <500, ClogP <5.0, number of H-acceptors <10, and number of H-donors <5), in addition to consideration of the number of rotatable bonds (<5) and polar surface area. Absorption, distribution, metabolism and excretion (ADME) properties were calculated by using the Volsurf program.⁷⁷ Cartesian grid based chemical diversity

analysis was performed according to the method described previously,⁷⁸ by using standard H-aware 3D BCUT descriptors comparing against the MLSMR screening set (ca. 7/2010; ~330,000 unique chemical structures). Guided by this library design analysis, benzoxathiazocine 1,1-dioxides scaffolds **2.9.3–2.9.6**, **2.10.12–2.10.13**, **2.10.15–2.10.16** and amines {1–10} were chosen to generate the aforementioned 80-member library.

Benzo-oxathiazocine 1,1-dioxides core scaffolds



Amine nucleophiles

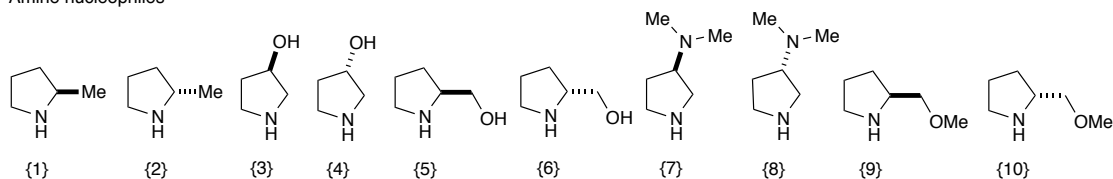


Figure 2.11. Benzo-oxathiazocine 1,1-dioxides **2.9.3–2.9.6**, **2.10.12–2.10.13**, **2.10.15–2.10.16** and amine library building blocks {1–10}.

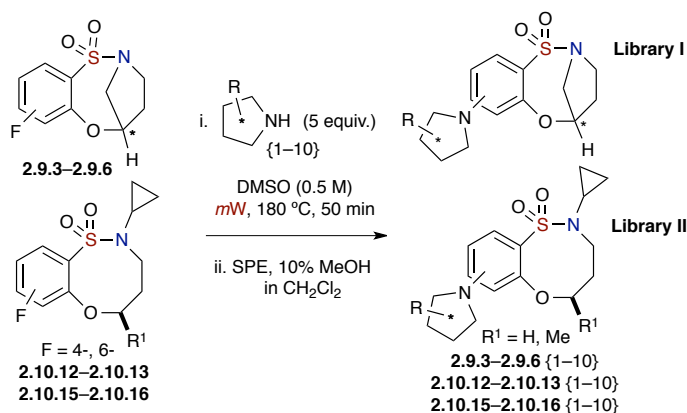
2.3.2.3 Validation and Library Generation

With the optimized conditions in hand, a 20-member validation library was prepared by using scaffolds selected from **2.9.3–2.9.6**, **2.10.12** and amines {1–10} in DMSO (0.5 M) at 180 °C for 50 min, in 1 dram vials, using the Anton Parr Synthos 3000® platform (Table 2.3).⁷⁹ Upon completion, the crude reaction mixtures were diluted, filtered through silica SPE, and purified by automated mass-directed HPLC. Library validation was essential to assess both substrate and reaction scope, along with evaluating the application of automated mass-directed HPLC as the final analysis and purification method. Key goals for this compound collection were the synthesis of compounds in >90% purity in 40–50 mg quantities, which would be sufficient for HTS screening in the Molecular Library Probe Center Network (MLPCN) (20 mg), for external biological outreach screening partners (20 mg), and to retain a sample (10 mg) for follow-up evaluation or to resupply the NIH MLPCN. Evaluation of this validation library demonstrated that all 20 members were successfully prepared (average purity = 99.7%, yield = 70%, quantity = 73.0 mg) in the desired sultam final masses, with all 20 possessing a final purity >98%.

With the validation completed, the remaining 60 compounds of both libraries **I** and **II** were synthesized by the diversification of core benzo-oxathiazocine 1,1-dioxides scaffolds **2.9.3–2.9.6**, **2.10.12–2.10.13**, **2.10.15–2.10.16** and amines {1–10}. Under the optimal S_NAr reaction conditions, libraries **I** and **II** were generated and purified by automated mass-directed HPLC. A total of 80 compounds were prepared and isolated in good yields (average yield 65%), and all compounds had purities greater than 95% after

automated purification (see Supporting Information for all compounds with full numeric data). Final assessment of both libraries **I** and **II** demonstrated that the primary objectives set out in the library design were achieved; final masses ranged between 18–127 mg and the average final mass was 68 mg (original target being 50 mg).

Table 2.3. Use of a 20-member validation library to probe the reaction scope



Sultam ^a	Purity (%) ^b	Yield (%) ^b	Quantity (mg)	Sultam ^a	Purity (%) ^b	Yield (%) ^b	Quantity (mg)
2.9.3 {3}	99.8	78	79.5	2.10.12 {1}	100	80	79.8
2.9.4 {3}	99.4	69	70.0	2.10.12 {2}	100	80	79.4
2.9.5 {3}	100	48	49.3	2.10.12 {3}	100	76	75.8
2.9.6 {3}	99.7	53	54.1	2.10.12 {4}	100	79	79.1
2.9.3 {1}	100	71	71.7	2.10.12 {5}	100	83	85.7
2.9.3 {2}	100	72	73.4	2.10.12 {6}	100	80	83.1
2.9.3 {4}	99.8	75	76.7	2.10.12 {7}	98.2	17	18.7 ^c
2.9.3 {5}	99.7	69	73.6	2.10.12 {8}	99.9	46	49.2
2.9.3 {6}	99.6	85	90.2	2.10.12 {9}	99.1	79	85.3
2.9.3 {8}	100	86	94.9	2.10.12 {10}	99.1	78	83.7

^aReaction conditions: Benzo-oxathiazocine-1,1-dioxides **2.9.3–2.9.6**, **2.10.12–2.10.13**, **2.10.15–2.10.16** (1 eq., 80 mg), dry DMSO (0.5 M) and amine (5 equiv.). ^bPurified by automated preparative reverse phase HPLC (detected by mass spectroscopy); purity was assessed by HPLC (214nm). ^cThe low yield obtained was due to instrumental error (see Supporting Information for more information).

2.3.3 In Silico Analysis of Chemical Diversity and Drug-likeness

In silico analysis of the molecular library was performed to achieve enhanced drug-like and lead-like properties, as well as to assess the molecular diversity. In order to assess diversity, five computational analyses were performed, including

1. Cartesian grid-based chemical diversity analysis⁷⁸ [Section 2.3.3.1]
2. Overlay analysis⁸⁰ [Section 2.3.3.2]
3. Principal moments of inertia (PMI) analysis⁸¹ [Section 2.3.3.3]
4. Conformational analysis [Section 2.3.3.4]
5. Quantitative estimate of drug-like (QED) values⁸² [Section 2.3.3.5]

2.3.3.1 Cartesian Grid-based Chemical Diversity Analysis

The grid-based diversity analysis protocol, described previously in the Library Design section 2.3.2.2, provides a simple measure of the relative novelty of a compound. By computing the position of a compound within the molecular property space defined by a large reference set of other interesting compounds, chemical novelty can be estimated from the density of reference compounds in close proximity to the compound of interest. This analysis suggests that our compounds consistently occupy regions of chemical space that are under-represented within the MLSMR reference set as of April-2010. Specifically, all 80 compounds were located in regions with local compound densities of less than the mean value, with compounds **2.9.5**{3}, **2.9.6**{3}, **2.9.6**{4}, **2.10.12**{3} and **2.10.12**{4} occupying a particularly sparse region of space (all co-locating within a cell whose density was 3.5% of the mean density experienced by the

reference compounds), while the least unique eight compounds (**2.10.12**{5}, **2.10.12**{6}, **2.10.15**{3}, **2.10.15**{4}, **2.10.15**{5}, **2.10.15**{6}, **2.10.16**{3} and **2.10.16**{4}) all co-located in a cell with density equal to 78.9% of the mean density experienced by the reference compounds. The mean local density experienced by the 80 compounds reported herein, was only 31.7% of the mean density experienced by the reference compounds. All related information can be found in Chapter 5 (Experimental Data).

2.3.3.2 Overlay Analysis

The overlay produced for the 80 compounds reported herein is depicted in Figure 2.12 and provides a rudimentary indication of the shape distribution and diversity evident in this library. Orientations **2.12iv** and **2.12v** collectively suggest that the library

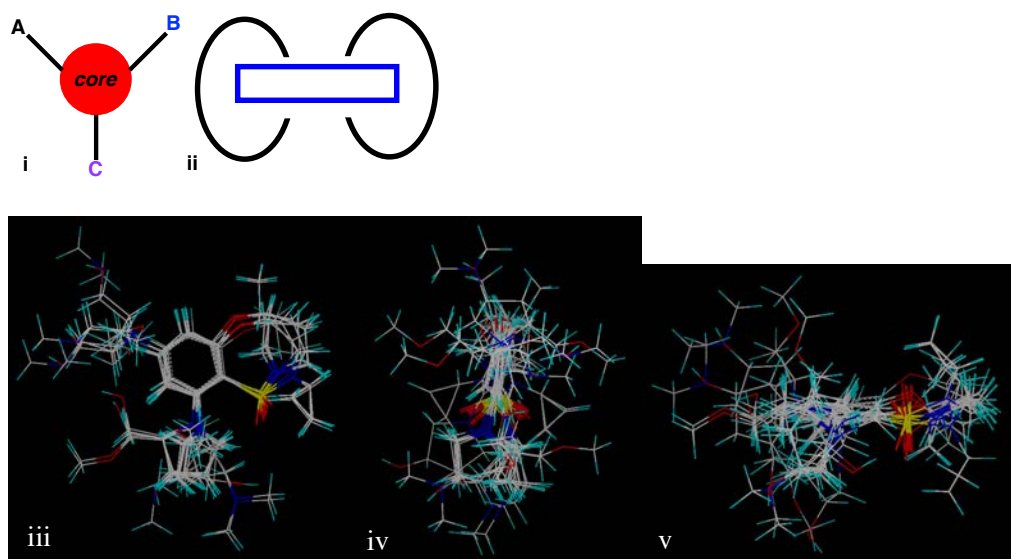


Figure 2.12. (i) Simple cartoon of the library compounds, with a core of MW ~ 80, based on Lipinski's rules (MW < 500), and comprising three substituents, each having MW < 140, to establish different functional groups. (ii) This cartoon demonstrates that the substituents extend out of the core in a circular motion. (iii) Overlay images exhibiting the common core in these 80 compounds. (iv) and (v) both overlay images revealing that the substituents are extending outwards in the circular motion as mentioned in (ii).

generally tends toward elongated (rod-like) structures, while the apparent distribution of functional substituents across angles spanning the better part of the whole sphere surrounding the conserved core, suggests that the library as a whole achieves a reasonable level of shape-based diversity.

2.3.3.3 Principal Moments of Inertia (PMI) Analysis

The rudimentary information gleaned from overlay analysis can be quantified more rigorously via principal moments of inertia (PMI) analysis, which is also employed herein to assess the molecular diversity (Figure 2.13).⁸¹ PMI analysis utilizes shape-based descriptors: The minimum energy conformation of each library member is determined, PMI ratios are calculated and normalized, and a subsequent triangular plot

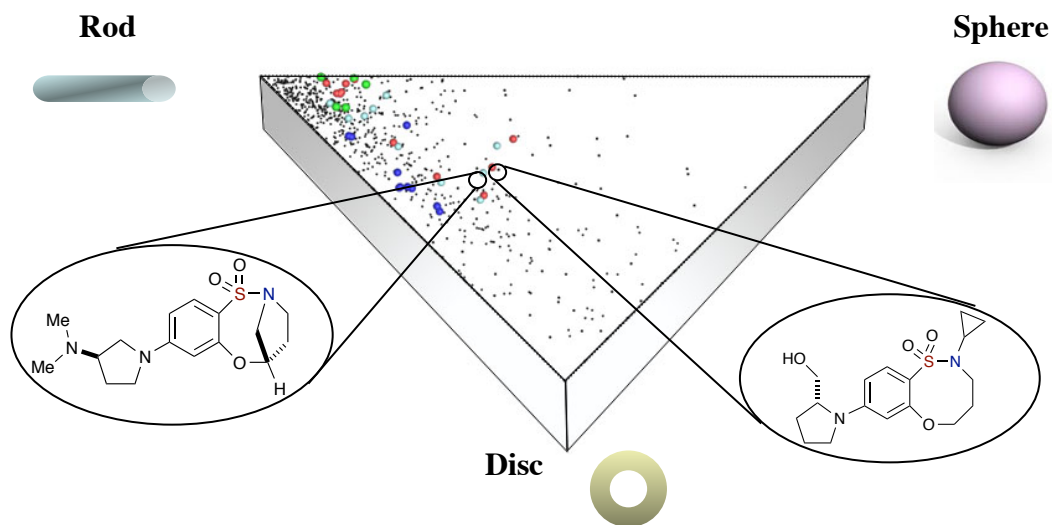


Figure 2.13. Distribution of 80 compounds (colored spheres) relative to the set of 771 known orally available drugs (black dots).⁷⁹

depicts the shape diversity of the library. The analysis reveals that the 80 compounds generally mirror the shape distribution of the set of 771 known drugs (Figure 2.13), thus demonstrating the potential drug-likeness of our scaffold. In contrast, some of the compounds are located in the unpopulated region of chemical space, illustrating the novel nature of some of our compounds from the perspective of molecular shape.

2.3.3.4 Conformational Analysis

While overlay and PMI analysis tend to focus on the shape diversity of libraries as a function of the combined structure of the core scaffold and all known substituents, it is useful to quantify the conformational diversity of the core alone, since this provides additional insight into the prospects for sampling new diversity space as a function of hitherto untested substituents. To quantify this, computations were generated for the mean pairwise atomic root-mean-squared distance (RMSD) using a small set of representative products from the library that was synthesized and compared this value with similar pairwise RMSD calculations for other analogous libraries (Figure 2.14). In all cases, the structures have been sketched and optimized in SYBYL,⁸³ according to default molecular mechanics settings, and the resulting optimized structures were then all mutually aligned in order to minimize the total pairwise RMSD among conserved scaffold core atoms. The pairwise RMSD values reported in Figure 2.14 also only correspond to conserved core atoms. The fact that the highlighted core scaffold achieves a 0.33 value, a much higher RMSD than the other libraries suggests that the scaffold conformation is more sensitive to the choice of substituents, whereas the other libraries

exhibit little variation as a function of different substituents. This greater sensitivity on the part of the highlighted library should correspond to greater conformational diversity, which implies sampling of a broader range of property and pharmacophore space than those libraries with lesser conformational diversity.

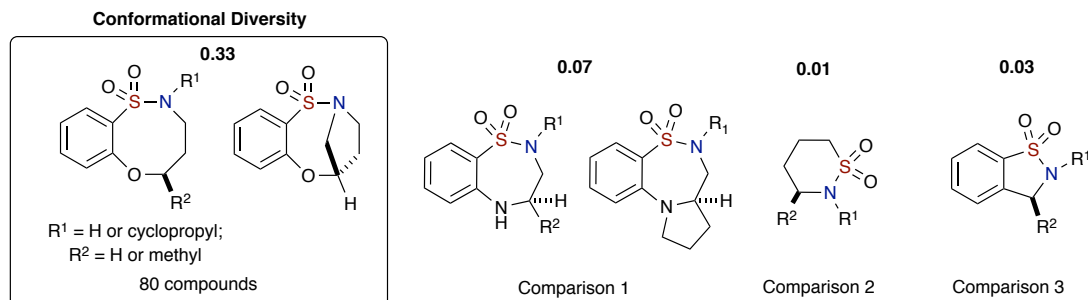


Figure 2.14. Comparison using RMSD calculations of a small set of our representative compounds versus two sultams synthesized by our group as well as a biologically active compound.^{12d}

2.3.3.5 Quantitative Estimate of Drug-like (QED) Values and Z-scores

While molecular diversity is in itself a topic of intellectual value, in applied sciences it is important to balance this intellectual aspect with suitability toward the intended application. In other words, if one intends to synthesize novel compounds for potential pharmacological applications it is critical that the compounds not only be unique but also be drug-like. Quantifying drug-likeness is one of the numerous methods that are regularly utilized as useful guidelines for early stage drug discovery. A measure of drug-likeness based on the concept of desirability called the quantitative estimate of drug-likeness (QED) has been proposed.⁸² The QED concept is a simple approach to multi-criteria optimization whereby compound desirability is defined as a function of

eight molecular properties, i.e., molecular weight, ALogP, polar surface area, H-bond donor, acceptor, rotatable bond and aryl ring counts, and the presence of structural alerts. The weighted QED values were calculated based on the equation provided by Hopkins et al., mapping compounds to a range from 0 to 1, in which a value of 1 indicates that all properties are within a favorable range. Based on this measure, the 80 compounds reported herein may have elevated prospects for interesting chemical biology: the lowest QED values among these 80 compounds (QED = 0.819 for **2.9.3**{3} and **2.9.3**{4}) are actually significantly above the mean value (QED = 0.615) for the 771 known drugs analyzed by Hopkins *et al.*, while several distinct scaffolds within our library produced QED values of greater than 0.90 (Figure 2.15).

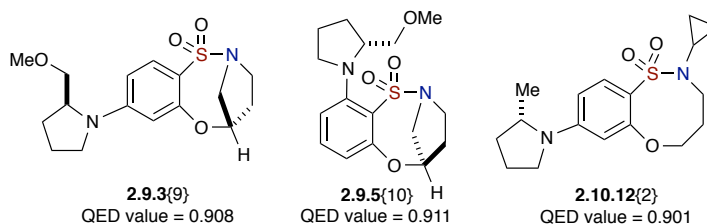


Figure 2.15. Three representative compounds with high QED values.

To characterize the QED scores of our scaffolds relative to the reference set of 771 known drugs, we computed mean Z-scores for each scaffold and plotted them in Figure 2.16. Since Z-scores of 1.64 and 1.0 correspond to percentile rankings of 95 and 84.1, respectively, it is apparent that all of the reported scaffolds contain compounds with QED values in the upper 80th to lower 90th percentile. The 80 compounds exhibited an average Z-score of 1.29, which corresponds to a mean percentile ranking of 90.

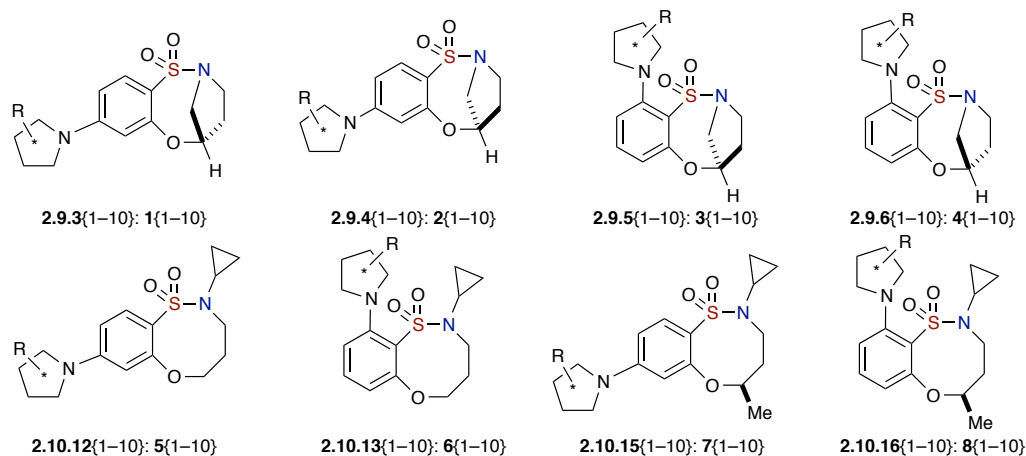
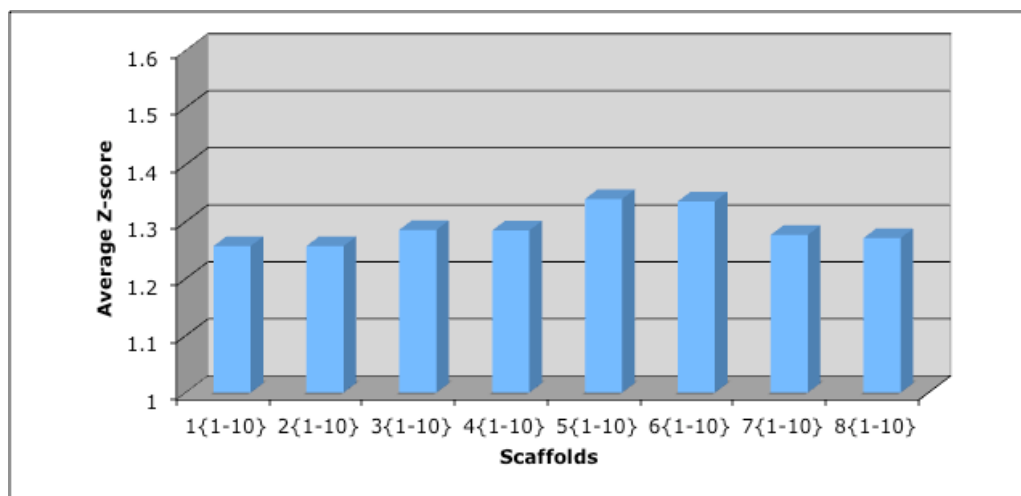


Figure 2.16. Representation of Z-scores for the 80 compounds.

2.3.4 Conclusion

In conclusion, an efficient microwave-assisted intermolecular- S_NAr method for the synthesis of amino benzoxa-thiazocine 1,1-dioxides has been developed. Employing a variety of commercially available chiral, nonracemic amines, the 80-member library of bridged, benzofused, bicyclic sultams was generated by the microwave assisted- S_NAr diversification at 4-F and 6-F positions. A series of computational analyses was performed in order to provide pertinent information that guided the second part of the

reaction pairing strategy, which will be reported in due course. Further computational analysis revealed that the compounds reported herein generally occupy underrepresented chemical space relative to the MLSMR screening set, and are drug-like both in terms of their distribution in shape space (as compared to a collection of 771 known orally available drugs depicted according to molecular PMI profiles) and according to the QED measure (by which all of this library of compounds are predicted to be significantly more drug-like than the average real drug). Structural overlays and PMI analysis suggest that the highlighted compounds tend to sample a reasonable array of shape space within the range between rod-like and disk-like compounds. RMSD comparisons of a selection of representative structures from this library suggest that the core scaffold has a greater inherent flexibility than comparable products from other related libraries. This flexibility can produce libraries with greater molecular diversity as a function of a fixed number of substituents than is observed for comparably sized libraries arising from more rigid scaffolds. It is our hope that the combination of drug-likeness and inherent molecular diversity evident in this library will produce products that demonstrate interesting behavior in biological screening. To gauge these prospects rigorously, these compounds have been submitted for evaluation of their biological activity in high-throughput screening assays at the NIH MLPCN and the results will be reported in due course.

2.4 Summary and Outlook

In summary, facile, efficient and modular methods to synthesize skeletally diverse and unique medium-sized (8- to 10-membered) polycyclic sultams have been developed.

The scope of sultams synthesized, includes: (i) bridged benzofused sultams with both possible stereoisomers of different ring sizes, as well as (ii) non-bridged benzofused sultams consisting of all possible stereochemistries. The reported strategy was extended to library development that comprised a library of 80 compounds, demonstrating the reliability of the method. In addition, the cheminformatics derived from the several computational analyses suggested that these sultams are populating the gap of underrepresented chemical space and ring systems.

2.5 References Cited

- [1] (a) McGrath, N. A.; Brichacek, M.; Njardarson, J. T. A Graphical Journey of Innovative Organic Architectures That Have Improved Our Lives. *J. Chem. Ed.* **2010**, *87*, 1348–1349. (b) Vitaku, E.; Smith, B. R.; Smith, D. T. Njarharson, J. T. Top US Pharmaceutical Products of 2013. *J. Chem. Ed.* **2010**, *87*, 1348–1349. (c) Vitaku, E.; Smith, D. T.; Njardarson, J. T. Analysis of the Structural Diversity, Substitution Patterns, and Frequency of Nitrogen Heterocycles among U.S. FDA Approved Pharmaceuticals. *J. Med. Chem.* **2014**, *57*, 10257–10274. (d) Taylor, R. D.; MacCoss, M.; Lawson, A. D. G. Rings in Drugs. *J. Med. Chem.* **2014**, *57*, 5845–5859.
- [2] (a) Samarakoon, T. B.; Loh, J. K.; Rolfe, A.; Le, L. S.; Yoon, S. Y.; Lushington, G. H.; Hanson, P. R. A Modular Reaction Pairing Approach to the Diversity-Oriented Synthesis of Fused- and Bridged-Polycyclic Sultams. *Org. Lett.* **2011**, *13*, 5148–5151. (b) Loh, J. K.; Yoon, S. Y.; Samarakoon, T. B.; Rolfe, A.; Porubsky, P.; Neuenswander, B.; Lushington, G. H.; Hanson, P. R. Exploring Diversity via a Modular Reaction Pairing Strategy. *Beilstein J. Org. Chem.* **2012**, *8*, 1293–1302.

- [3] Macarron, R.; Banks, M. N.; Bojanic, D.; Burns, D. J.; Cirovic, D. A.; Garyantes, T.; Green, D. V. S.; Hertzberg, R. P.; Janzen, W. P.; Paslay, J. W.; Schopfer, U.; Sittampalam, G. S. Impact of high-throughput screening in biomedical research. *Nat. Rev. Drug Discovery* **2011**, *10*, 188–195.
- [4] Galloway, W. R. J. D.; Isidro-Llobet, A.; Spring, D. R. Diversity-oriented synthesis as a tool for the discovery of novel biologically active small molecules. *Nat. Commun.* **2010**, *1*, No. 8, Gal1/1–Gal1/13.
- [5] **Scaffold-from-Scaffold:** (a) Tempest, A. P.; Armstrong, W. R. Cyclobutenedione Derivatives on Solid Support: Toward Multiple Core Structure Libraries. *J. Am. Chem. Soc.* **1997**, *119*, 7607–7608. (b) Castellano, S.; Fiji, H. D. G.; Kinderman, S. S.; Watanabe, M.; de Leon, P.; Tamanoi, F.; Kwon, O. Small-Molecule Inhibitors of Protein Geranylgeranyltransferase Type I. *J. Am. Chem. Soc.* **2007**, *129*, 5843–5845. (c) Huigens, R. W.; Morrison, K. C.; Hicklin, R. W.; Flood, T. A.; Richter, M. F.; Hergenrother, P. J. A Ring Distortion Strategy to Construct Stereochemically Complex and Structurally Diverse Compounds from Natural Products. *Nature Chem.* **2013**, *5*, 195–202. (d) McLeod, M. C.; Singh, G.; Plampin, J. N., III; Rane, D.; Wang, J. L.; Day, V. W.; Aubé, J. Probing chemical space with alkaloid-inspired libraries. *Nat. Chem.* **2014**, *6*, 133–140.
- [6] (a) Schreiber, S. L. Target-oriented and diversity-oriented organic synthesis in drug discovery. *Science* **2000**, *287*, 1964–1969. (b) Burke, M. D.; Berger, E. M.; Schreiber, S. L. Generating Diverse Skeletons of Small Molecules Combinatorially. *Science* **2003**, *302*, 613–618. (c) Spring, D. R. Diversity-oriented synthesis; a challenge for synthetic chemists. *Org. Biomol. Chem.* **2003**, *1*, 3867–3870. (d) Burke, M. D.; Schreiber, S. L. A Planning Strategy for Diversity-Oriented Synthesis. *Angew. Chem. Int. Ed.* **2004**, *43*, 46–58. (e) Tan, D. S. Diversity-oriented synthesis: exploring the intersections between chemistry and biology. *Nat. Chem. Biol.* **2005**, *1*, 74–84. (f) Schreiber, S. L. Molecular diversity

by design. *Nature* **2009**, *457*, 153–154. (g) Galloway, W. R. J. D.; Isidro-Llober, A.; Spring, D. R. Diversity-oriented synthesis as a tool for the discovery of novel biologically functional small molecules. *Nat. Commun.* **2010**, *1*, 80–92. (h) Fergus, S.; Bender, A.; Spring, D. R. Assessment of structural diversity in combinatorial synthesis. *Curr. Opin. Chem. Biol.* **2005**, *9*, 304–309. (i) Spandl, R. J.; Bender, A.; Spring, D. R. Diversity-oriented synthesis; a spectrum of approaches and results. *Org. Biomol. Chem.* **2008**, *6*, 1149–1158. (j) Spandl, R. J.; Diaz-Gavilan, M.; O'Connell, K. M. G.; Thomas, G. L.; Spring, D. R. Diversity-oriented synthesis. *Chem. Rec.* **2008**, *8*, 129–142

- [7] **Build-Couple-Pair:** (a) Nielsen, T. E.; Schreiber, S. L. Towards the Optimal Screening Collection: A Synthesis Strategy. *Angew. Chem. Int. Ed.* **2008**, *47*, 48–56. (b) Uchida, T.; Rodriguez, M.; Schreiber, S. L. Skeletally Diverse Small Molecules Using a Build/Couple/Pair Strategy. *Org. Lett.* **2009**, *11*, 1559–1562. (c) Luo, T.; Schreiber, S. L. Gold (I)-Catalyzed Coupling Reactions for the Synthesis of Diverse Small Molecules Using the Build/Couple/Pair Strategy. *J. Am. Chem. Soc.* **2009**, *131*, 5667–5674. (d) Marcaurelle, L. A.; Comer, E.; Dandapani, S.; Duvall, J. R.; Gerard, B.; Kesavan, S.; Lee, M. D. IV; Liu, H.; Lowe, J. T.; Marie, J.-C.; Mulrooney, C. A.; Pandya, B. A.; Rowley, A.; Ryba, T. D.; Suh, B.-C.; Wei, J.; Young, D. W.; Akella, L. B.; Ross, N. T.; Zhang, Y.-L.; Fass, D. M.; Reis, S. A.; Zhao, W.-N.; Haggarty, S. J.; Palmer, M.; Foley, M. A. An Aldol-Based Build/Couple/Pair Strategy for the Synthesis of Medium- and Large-Sized Rings: Discovery of Macrocyclic Histone Deacetylase Inhibitors. *J. Am. Chem. Soc.* **2010**, *132*, 16962–16976. (e) Gerard, B.; Duvall, J. R.; Lowe, J. T.; Murillo, T.; Wei, J.; Akella, L. B.; Marcaurelle, L. A. Synthesis of a Stereochemically Diverse Library of Medium-Sized Lactams and Sultams via S_NAr Cycloetherification. *ACS Comb. Sci.* **2011**, *13*, 365–374. (f) Beckmann, H. S. G.; Nie, F.; Hagerman, C. E.; Johansson, H.; Tan, Y. S.; Wilcke, D.; Spring, D. R. A strategy for the diversity-oriented synthesis of macrocyclic scaffolds using

multidimensional coupling. *Nat. Chem.* **2013**, *5*, 861–867. (g) Comer, E.; Beaudoin, J. A.; Kato, N.; Fitzgerald, M. E.; Heidebrecht, R. W.; Lee, M. d.; Masi, D.; Mercier, M.; Mulrooney, C.; Muncipinto, G.; Rowley, A.; Crespo-Llado, K.; Serrano, A. E.; Lukens, A. K.; Wiegand, R. C.; Wirth, D. F.; Palmer, M. A.; Foley, M. A.; Munoz, B.; Scherer, C. A.; Duvall, J. R.; Schreiber, S. L. Diversity-Oriented Synthesis-Facilitated Medicinal Chemistry: Toward the Development of Novel Antimalarial Agents. *J. Med. Chem.* **2014**, *57*, 8496–8502. (h) Mamidala, R.; Babu Damerla, V. S.; Gundla, R.; Chary, M. T.; Murthy, Y. L. N.; Sen, S. Pyrrolidine and piperidine based chiral spiro and fused scaffolds via build/couple/pair approach. *RSC Adv.* **2014**, *4*, 10619–10626. (i) Flagstad, T.; Hansen, M. R.; Le Quement, S. T.; Givskov, M.; Nielsen, T. E. Combining the Petasis 3-Component Reaction with Multiple Modes of Cyclization: A Build/Couple/Pair Strategy for the Synthesis of Densely Functionalized Small Molecules. *ACS Comb. Sci.* **2015**, *17*, 19–23.

[8] **FG-Pairing**: (a) Comer, E.; Rohan, E.; Deng, L.; Porco, J. A., Jr. An Approach to Skeletal Diversity Using Functional Group Pairing of Multifunctional Scaffolds. *Org. Lett.* **2007**, *9*, 2123–2126. (b) Dandapani, S.; Marcaurelle, L. A. Current strategies for diversity-oriented synthesis. *Curr. Opin. Chem. Biol.* **2010**, *14*, 362–370. (c) Yang, Y.; Dai, M. Total Syntheses of Lyconadins: Finding Efficiency and Diversity. *Synlett* **2014**, *25*, 2093–2098. (d) Zhang, J.; Wu, J.; Hong, B.; Ai, W.; Wang, X.; Li, H.; Lei, X. Diversity-oriented synthesis of Lycopodium alkaloids inspired by the hidden functional group pairing pattern. *Nat. Commun.* **2014**, *5*, 4614–4622.

[9] (a) Huang, J.; Schreiber, S. L. A yeast genetic system for selecting small molecule inhibitors of protein-protein interactions in nanodroplets. *Proc. Natl. Acad. Sci. U. S. A.* **1997**, *94*, 13396–13401. (b) Kapoor, T. M.; Andreotti, A. H.; Schreiber, S. L. Exploring the Specificity Pockets of Two Homologous SH3 Domains Using Structure-Based, Split-Pool Synthesis and Affinity-Based Selection. *J. Am. Chem.*

- Soc.* **1998**, *120*, 23–29. (c) Morken, J. P.; Kapoor, T. M.; Feng, S.; Shirai, F.; Schreiber, S. L. Exploring the Leucine-Proline Binding Pocket of the Src SH3 Domain Using Structure-Based, Split-Pool Synthesis and Affinity-Based Selection. *J. Am. Chem. Soc.* **1998**, *120*, 30–36. (d) Habashita, H. Drug development using combinatorial synthesis. *Farumashia* **2000**, *36*, 19–23. (e) Sun, Y.; Chan, B. C.; Ramanathan, R.; Leventry, W. M.; Mallouk, T. L. Split-Pool Method for Synthesis of Solid-State Material Combinatorial Libraries. *J. Comb. Chem.* **2002**, *4*, 569–575. (f) Weller, H. N. An introduction to combinatorial chemistry. In *Analytical Techniques in Combinatorial Chemistry*; Swartz, M. E. Ed.: Marcel Dekker, Inc. New York, N. Y.: **2000**; pp 1–28. (g) Winssinger, N.; Pianowski, Z.; Barluenga, S. Chemical technologies: probing biology with small molecules. In *Chemical and Functional Genomic Approaches to Stem Cell Biology and Regenerative Medicine.*; Ding, S. Ed.: John Wiley & Sons, Inc.: **2008**; pp 109–144. (h) Joo, S. H. Cyclic peptides as therapeutic agents and biochemical tools. *Biomol. Ther.* **2012**, *20*, 19–26.
- [10] (a) Frankowski, K. J.; Hirt, E. E.; Zeng, Y.; Neuenswander, B.; Fowler, D.; Schoenen, F.; Aubé, J. Synthesis of N-Alkyl-octahydroisoquinolin-1-one-8-carboxamide Libraries Using a Tandem Diels-Alder/Acylation Sequence. *J. Comb. Chem.* **2007**, *9*, 1188–1192. (b) Mukherjee, S.; Hill, D.; Neuenswander, B.; Schoenen, F.; Hanson, P. R.; Aubé, J. Three-component synthesis of 1,4-diazepin-5-ones and the construction of γ -turn-like peptidomimetic libraries. *J. Comb. Chem.* **2008**, *10*, 230–234. (c) Aubé, J. Small-molecule libraries, naturally inspired oligomers. *Nat. Chem.* **2012**, *4*, 71–72. (d) Fenster, E.; Hill, D.; Reiser, O.; Aubé, J. Automated three-component synthesis of a library of γ -lactams. *Beilstein J. Org. Chem.* **2012**, *8*, 1804–1813. (e) Beeler, A. B.; Acquilano, D. E.; Su, Q.; Yan, F.; Roth, B. L.; Panek, J. S.; Porco, J. A., Jr. Synthesis of a Library of Complex Macrodilides Employing Cyclodimerization of Hydroxy Esters. *J. Comb. Chem.* **2005**, *7*, 673–681. (f) Lei, X.; Zaarur, N.; Sherman, M. Y.; Porco, J.

A., Jr. Stereocontrolled Synthesis of a Complex Library via Elaboration of Angular Epoxyquinol Scaffolds. *J. Org. Chem.* **2005**, *70*, 6474–6483. (g) Villar, E. A.; Beglov, D.; Chennamadhavuni, S.; Porco, J. A., Jr.; Kozakov, D.; Vajda, S.; Whitty, A. How proteins bind macrocycles. *Nat. Chem. Biol.* **2014**, *10*, 723–731. (h) Rafferty, R. J.; Hicklin, R. W.; Maloof, K. A., Hergenrother, P. J. Synthesis of Complex and Diverse Compounds through Ring Distortion of Abietic Acid. *Angew. Chem.* **2014**, *53*, 220–224. (i) Comer, E.; Beaudoin, J. A.; Kato, N.; Fitzgerald, M. E.; Heidebrecht, R. W.; Lee, M. d.; Masi, D.; Mercier, M.; Mulrooney, C.; Muncipinto, G.; Rowley, A.; Crespo-Llado, K.; Serrano, A. E.; Lukens, A. K.; Wiegand, R. C.; Wirth, D. F.; Palmer, M. A.; Foley, M. A.; Munoz, B.; Scherer, C. A.; Duvall, J. R.; Schreiber, S. L., Diversity-Oriented Synthesis-Facilitated Medicinal Chemistry: Toward the Development of Novel Antimalarial Agents. *J. Med. Chem.* **2014**, *57*, 8496–8502. (j) Dandapani, S.; Germain, A. R.; Jewett, I.; Le Quement, S.; Marie, J.-C.; Muncipinto, G.; Duvall, J. R.; Carmody, L. C.; Perez, J. R.; Engel, J. C.; Gut, J.; Kellar, D.; Lage de Siqueira-Neto, J.; McKerrow, J. H.; Kaiser, M.; Rodriguez, A.; Palmer, M. A.; Foley, M.; Schreiber, S. L.; Munoz, B. Diversity-Oriented Synthesis Yields a New Drug Lead for Treatment of Chagas Disease. *ACS Med. Chem. Lett.* **2014**, *5*, 149–153. (k) O' Connor, C. J.; Beckmann, H. S. G.; Spring, D. R. Diversity-oriented synthesis: producing chemical tools for dissecting biology. *Chem. Soc. Rev.* **2012**, *41*, 4444–4456. (l) Dockendorff, C.; Faloon, P. W.; Pu, J.; Yu, M.; Johnston, S.; Bennion, M.; Penman, M.; Nieland, T. J. F.; Dandapani, S.; Perez, J. R.; Munoz, B.; Palmer, M. A.; Schreiber, S. L.; Krieger, M. Benzo-fused lactams from a diversity-oriented synthesis (DOS) library as inhibitors of scavenger receptor BI (SR-BI)-mediated lipid uptake. *Bioorg. Med. Chem. Lett.* **2015**, *25*, 2100–2105.

- [11] (a) Drews, J. Drug discovery: A historical perspective. *Science* **2000**, 287, 1960–1963. (b) Scozzafava, A.; Owa, T.; Mastrolorenzo, A.; Supuran, C. T. Anticancer and antiviral sulfonamides. *Curr. Med. Chem.* **2003**, 10, 925–953.
- [12] (a) Palani, A.; Qin, J.; Zhu, X.; Aslanian, R. G.; McBriar, M. D. Preparation of imidazolylphenylethanesulfonamide derivatives for use as gamma secretase modulators. *PCT Int. Appl.* WO 2009020579 A1 20090212 2009. (b) Page, M. I. β -Sultams—Mechanism of Reactions and Use as Inhibitors of Serine Proteases. *Acc. Chem. Res.* **2004**, 37, 297–303. (c) Hanessian, S.; Sailes, H.; Therrien, E. Synthesis of functionally diverse bicyclic sulfonamides as constrained proline analogs and application to the design of potential thrombin inhibitors. *Tetrahedron* **2003**, 59, 7047–7056. (d) Cherney, R. J.; Mo, R.; Meyer, D. T.; Hardman, K. D.; Liu, R.-Q.; Covington, M. B.; Qian, M.; Wasserman, Z. R.; Christ, D. D.; Trzaskos, J. M.; Newton, R. C.; Decicco, C. P. Sultam Hydroxamates as Novel Matrix Metalloproteinase Inhibitors. *J. Med. Chem.* **2004**, 47, 2981–2983. (e) Van Nhien, A. N.; Tomassi, C.; Len, C.; Marco-Contelles, J. L.; Balzarini, J.; Pannecouque, C.; De Clercq, E.; Postel, D. First Synthesis and Evaluation of the Inhibitory Effects of Aza Analogues of TSAO on HIV-1 Replication. *J. Med. Chem.* **2005**, 48, 4276–4284. (f) Cordi, A.; Lacoste, J. M.; Audinot, V.; Millan, M. Design, synthesis and structure-activity relationships of novel strychnine-insensitive glycine receptor ligands. *Bioorg. Med. Chem. Lett.* **1999**, 9, 1409–1414. (g) Chen, Z.; Demuth, T. P.; Wireko, F. C. Stereoselective synthesis and antibacterial evaluation of 4-amidoisothiazolidinone oxides. *Bioorg. Med. Chem. Lett.* **2001**, 11, 2111–2115.
- [13] (a) Differding, E.; Lang, R. W. New Fluorinating Reagents Part II. Preparation and Synthetic Application of a Saccharin Derived *N*-Fluorosultams. *Helv. Chim. Acta* **1989**, 72, 1248–1252. (b) Differding, E.; Rüegg, G. M.; Lang, R. W. Selective Mono- and Difluorination of Enolates. *Tetrahedron Lett.* **1991**, 32,

- 1779–1782. (c) Davies, F. A.; Chen, B-C. Asymmetric Hydroxylation of Enolates with *N*-Sulfonyloxaziridines. *Chem. Rev.* **1992**, *92*, 919–934.
- [14] (a) Oppolzer, W. Metal-Directed Stereoselective Functionalizations of Alkenes in Organic Synthesis. *Pure Appl. Chem.* **1988**, *60*, 39–48. (b) Oppolzer, W. Camphor as a Natural Source of Chirality in Asymmetric Synthesis. *Pure Appl. Chem.* **1990**, *62*, 1241–1250. (c) For reviews see: (i) Kim, B. H.; Curran, D. P. Asymmetric Thermal Reactions with Oppolzer's Camphor Sultam. *Tetrahedron* **1993**, *49*, 293–318. (ii) Pellissier, H. Asymmetric Domino Reactions. Part a: Reactions Based on the Use of Chiral Auxiliaries. *Tetrahedron* **2006**, *62*, 1619–1665. (iii) Pellissier, H. Asymmetric 1,3-Dipolar Cycloadditions. *Tetrahedron* **2007**, *63*, 3235–3285 and references cited therein. (d) Vandewalle, M.; van der Eycken, J.; Oppolzer, W.; Vullioud, C. Iridoids: Enantioselective Synthesis of Loganin via an Asymmetric Diels-Alder Reaction. *Tetrahedron* **1986**, *42*, 4035–4043. (e) Curran, D. P.; Kim, B. H.; Daugherty, J.; Heffner, T. A. The Preparation of Optically Active δ^2 -Isoxazolines. A Model for Asymmetric Induction in the Non Lewis Acid Catalyzed Reactions of Oppolzer's Chiral Sultam. *Tetrahedron Lett.* **1988**, *29*, 3555–3558. (f) Srirajan, V.; Puranik, Vedavati G.; Deshmukh, A. R. A. S.; Bhawal, B. M. An efficient use of Oppolzer sultam for Diastereospecific Synthesis of *cis*- β -Lactams. *Tetrahedron* **1996**, *52*, 5579–5584. (g) Kiegiel, K.; Jurczak, J. Diastereoselective addition of allylic reagents to chiral α -ketoimides derived from Oppolzer's sultam. *Tetrahedron Lett.* **1999**, *40*, 1009–1012.
- [15] Hough-Troutmana, W. L.; Smiglaka, M.; Griffina, S.; Reichertb, W. M.; Mirskac, I.; Jodynis-Liebertd, J.; Adamskad, T.; Nawrote, J.; Stasiewicz, M.; Rogers, R. D.; Pernak, J. Ionic Liquids with Dual Biological Function: Sweet and Anti-microbial, Hydrophobic Quaternary Ammonium-Based Salts. *New J. Chem.* **2009**, *33*, 26–33.

- [16] (a) Brzozowski, Z.; Saczewski, F.; Neamati, N. Synthesis and anti-HIV-1 activity of a novel series of 1,4,2-benzodithiazine-dioxides. *Bioorg. Med. Chem. Lett.* **2006**, *16*, 5298–5302. (b) Zhuang, L.; Wai, J. S.; Embrey, M. W.; Fisher, T. E.; Egbertson, M. S.; Payne, L. S.; Guare, J. P. Jr.; Vacca, J. P.; Hazuda, D. J.; Felock, P. J.; Wolfe, A. L.; Stillmock, K. A.; Witmer, M. V.; Moyer, G.; Schleif, W. A.; Gabryelski, L. J.; Leonard, Y. M.; Lynch, Jr.; Michelson, S. R.; Young, S. D. Design and synthesis of 8-hydroxy-[1,6]naphthyridines as novel inhibitors of HIV-1 integrase in vitro and in infected cells. *J. Med. Chem.* **2003**, *46*, 453–456.
- [17] Wells, G. J.; Tao, M.; Josef, K. A.; Bihovsky, R. 1,2-Benzothiazine 1,1-dioxide P2-P3 peptide mimetic aldehyde calpain I inhibitors. *J. Med. Chem.* **2001**, *44*, 3488–3503.
- [18] Cherney, R. J.; Duan, J. J.-W.; Voss, M. E.; Chen, L.; Wang, L.; Meyer, D. T.; Wasserman, Z. R.; Hardman, K. D.; Liu, R.-Q.; Covington, M. B.; Qian, M.; Mandlekar, S.; Christ, D. D.; Trzaskos, J. M.; Newton, R. C.; Magolda, R. L.; Wexler, R. R.; Decicco, C. P. Design, synthesis, and evaluation of benzothiadiazepine hydroxamates as selective tumor necrosis factor- α converting enzyme inhibitors. *J. Med. Chem.* **2003**, *46*, 1811–1823.
- [19] Siemeister, G.; Schäfer, M.; Briem, H.; Krüger, M.; Lienau, P.; Jautelat, R.; Lücking, U. Macrocyclic Aminopyrimidines as Multitarget CDK and VEGF-R Inhibitors with Potent Antiproliferative Activities *ChemMedChem* **2007**, *2*, 63–77.
- [20] Larsson, A.; Fex, T.; Knecht, W.; Blomberg, N.; Hanessian, S. Design and synthesis of macrocyclic indoles targeting blood coagulation cascade Factor XIa *Bioorg. Med. Chem. Lett.* **2010**, *20*, 6925–6928.
- [21] Rocher, J.-P. Preparation of diarylsultam derivatives as antipsychotic agents. *PCT Int. Appl.* WO 9730038 A1 19970821 1997.

- [22] Kulkarni, S.; Anderson, D. D.; Hong, L.; Baldrige, A.; Wang, Y.-F.; Chumanovich, A. A.; Kovalevsky, A. Y.; Tojo, Y.; Amano, M.; Koh, Y.; Tang, J.; Weber, I. T.; Mitsuya, H.; Ghosh, A. K. Design, Synthesis, Protein-Ligand X-ray Structure, and Biological Evaluation of a Series of Novel Macrocyclic Human Immunodeficiency Virus-1 Protease Inhibitors to Combat Drug Resistance. *J. Med. Chem.* **2009**, *52*, 7689–7705.
- [23] Silvestri, R.; Marfe, G.; Artico, M.; La Regina, G.; Lavecchia, A.; Novellino, E.; Morgante, M.; Di Stefano, C.; Catalano, G.; Filomeni, G.; Abruzzese, E.; Ciriolo, M. R.; Russo, M. A.; Amadori, S.; Cirilli, R.; La Torre, F.; Salimei, P. S. Pyrrolo[1,2-*b*][1,2,5]benzothiadiazepines (PBTDS): A new class of agents with high apoptotic activity in chronic myelogenous leukemia K562 cells and in cells from patients at onset and who were imatinib-resistant. *J. Med. Chem.* **2006**, *49*, 5840–5844.
- [24] Aldrich, L. N.; Kuo, S.-Y.; Castoreno, A. B.; Goel, G.; Petric Kuballa, P.; Rees, M. G.; Seashore-Ludlow, B. A.; Cheah, J. H.; Latorre, I. J.; Stuart L. Schreiber, S. L.; Shamji, A. F.; Xavier, R. J.; Discovery of a Small-Molecule Probe for V-ATPase Function. *J. Am. Chem. Soc.* **2015**, *137*, 5563–5568.
- [25] Cordi, A.; Desos, P.; Lestage, P.; Danober, L. Preparation of phenoxy dihydrobenzoxathiazepine derivatives and their use as positive allosteric modulators of AMPA receptors. *Can. Pat. Appl.* CA 2752131 A1 20120316 2012.
- [26] Santora, V. J.; Covel, J. A.; Ibarra, J. B.; Semple, G.; Smith, B.; Smith, J.; Weinhouse, M. I.; Schultz, J. A. Biphenylsulfonamides as modulators of the histamine H3-receptor useful for the treatment of disorders related thereto and their preparation. *PCT Int. Appl.* WO 2008005338 A1 20080110 2008.
- [27] (a) McKerrecher, D.; Pike, K. G.; Waring, M. J. Preparation of heteroaryl benzamide derivatives for use as glucokinase activators in the treatment of type 2 diabetes. *PCT Int. Appl.* WO 2006125972 A1 20061130 2006. (b) Campbell, L.;

- Pike, K. G.; Suleman, A.; Waring, M. J. Preparation of benzoyl amino heterocyclyl compounds as glucokinase activators for treating type 2 diabetes and other diseases mediated by GLK. *PCT Int. Appl.* WO 2008050101 A2 20080502 2008.
- [28] Todd, P. A.; Clissold, S. P. Tenoxicam. An update of its pharmacology and therapeutic efficacy in rheumatic diseases. *Drugs* **1991**, *41*, 625–646.
- [29] Balfour, J. A.; Fitton, A.; Barradell, L. B. Lornoxicam. A review of its pharmacology and therapeutic potential in the management of painful and inflammatory conditions. *Drugs* **1996**, *51*, 639–657.
- [30] (a) Lachenicht, S.; Fischer, A.; Schmidt, C.; Winkler, M.; Rood, A.; Lemoine, H.; Braun, M. Synthesis of Modified 4*H*-1,2,4-Benzothiadiazine-1,1-dioxides and Determination of their Affinity and Selectivity for Different Types of KATP Channels. *ChemMedChem* **2009**, *4*, 1850–1858. (b) Tedesco, R.; Chai, D.; Darcy, M. G.; Dhanak, D.; Fitch, D. M.; Gates, A.; Johnston, V. K.; Keenan, R. M.; Lin-Goerke, J.; Sarisky, R. T.; Shaw, A. N.; Valko, K. L.; Wiggall, K. J.; Zimmerman, M. N.; Duffy, K. J. Synthesis and biological activity of heteroaryl 3-(1,1-dioxo-2*H*-(1,2,4)-benzothiadiazin-3-yl)-4-hydroxy-2(1*H*)-quinolinone derivatives as hepatitis C virus NS5B polymerase inhibitors. *Bioorg. Med. Chem. Lett.* **2009**, *19*, 4354–4358. (c) Wang, G.; Lei, H.; Wang, X.; Das, D.; Hong, J.; MacKinnon, C. H.; Coulter, T. S.; Montalbetti, C. A. G. N.; Mears, R.; Gai, X.; Bailey, S. E.; Ruhmund, D.; Hooi, L.; Misialek, S.; Rajagopalan, P. T. R.; Cheng, R. K. Y.; Barker, J. J.; Felicetti, B.; Schoenfeld, D. L.; Stoycheva, A.; Buckman, B. O.; Kossen, K.; Seiwert, S. D.; Beigelman, L. HCV NS5B polymerase inhibitors 2: Synthesis and in vitro activity of (1,1-dioxo-2*H*-[1,2,4]benzothiadiazin-3-yl) azolo[1,5-*a*]pyridine and azolo[1,5-*a*]pyrimidine derivatives. *Bioorg. Med. Chem. Lett.* **2009**, *19*, 4480–4483. (d) Wang, G.; Zhang, L.; Wu, X.; Das, D.; Ruhmund, D.; Hooi, L.; Misialek, S.; Ravi Rajagopalan, P. T.; Buckman, B. O.; Kossen, K.;

Seiwert, S. D.; Beigelman, L. HCV NS5B polymerase inhibitors 3: Synthesis and in vitro activity of 3-(1,1-dioxo-2*H*-[1,2,4]benzothiadiazin-3-yl)-4-hydroxy-2*H*-quinolizin-2-one derivatives. *Bioorg. Med. Chem. Lett.* **2009**, *19*, 4484–4487. (e) Pirotte, B.; de Tullio, P.; Nguyen, Q.-A.; Somers, F.; Fraikin, P.; Florence, X.; Wahl, P.; Hansen, J. B.; Lebrun, P. Chloro-Substituted 3-Alkylamino-4*H*-1,2,4-benzothiadiazine 1,1-Dioxides as ATP-Sensitive Potassium Channel Activators: Impact of the Position of the Chlorine Atom on the Aromatic Ring on Activity and Tissue Selectivity. *J. Med. Chem.* **2010**, *53*, 147–154. (f) Restrepo, J.; Salazar, J.; Lopez, S. E. Microwave-Assisted Direct Synthesis of 4*H*-1,2,4-Benzothiadiazine 1,1-Dioxide Derivatives. *Phosphorus, Sulfur Silicon Relat. Elem.* **2011**, *186*, 2311–2320. (g) Khelili, S.; Kihal, N.; Yekhlef, M.; de Tullio, P.; Lebrun, P.; Pirotte, B. Synthesis and pharmacological activity of *N*-(2,2-dimethyl-3,4-dihydro-2*H*-1-benzopyran-4-yl)-4*H*-1,2,4-benzothiadiazine-3-carboxamides 1,1-dioxides on rat uterus, rat aorta and rat pancreatic β -cells. *Eur. J. Med. Chem.* **2012**, *54*, 873–878. (h) Francotte, P.; Goffin, E.; Fraikin, P.; Graindorge, E.; Lestage, P.; Danober, L.; Challal, S.; Rogez, N.; Nosjean, O.; Caignard, D.-H.; Pirotte, B.; de Tullio, P. Development of Thiophenic Analogues of Benzothiadiazine Dioxides as New Powerful Potentiators of 2-Amino-3-(3-hydroxy-5-methylisoxazol-4-yl)propionic Acid (AMPA) Receptors. *J. Med. Chem.* **2013**, *56*, 7838–7850. (i) Pirotte, B.; de Tullio, P.; Florence, X.; Goffin, E.; Somers, F.; Boverie, S.; Lebrun, P. 1,4,2-Benzo/pyridodithiazine 1,1-Dioxides Structurally Related to the ATP-Sensitive Potassium Channel Openers 1,2,4-Benzo/pyridothiadiazine 1,1-Dioxides Exert a Myorelaxant Activity Linked to a Distinct Mechanism of Action. *J. Med. Chem.* **2013**, *56*, 3247–3256. (j) Varano, F.; Catarzi, D.; Colotta, V.; Squarzialupi, L.; Matucci, R. 1,2,4-Benzothiadiazine-1,1-dioxide Derivatives as Ionotropic Glutamate Receptor Ligands: Synthesis and Structure-Activity Relationships. *Arch. Pharm.* **2014**, *347*, 777–785.

- [31] Gobis, K.; Foks, H.; Slawinski, J.; Augustynowicz-Kopec, E.; Napiorkowska, A. Synthesis and biological activity of novel 3-heteroaryl-2*H*-pyrido[4,3-*e*][1,2,4]thiadiazine and 3-heteroaryl-2*H*-benzo[*e*][1,2,4]thiadiazine 1,1-dioxides. *Monatsh. Chem.* **2013**, *144*, 1197–1203.
- [32] Wang, G.; He, Y.; Sun, J.; Das, D.; Hu, M.; Huang, J.; Ruhmund, D.; Hooi, L.; Misialek, S.; Ravi Rajagopalan, P. T.; Stoycheva, A.; Buckman, B. O.; Kossen, K.; Seiwert, S. D.; Beigelman, L. HCV NS5B polymerase inhibitors 1: Synthesis and in vitro activity of 2-(1,1-dioxo-2*H*-[1,2,4]benzothiadiazin-3-yl)-1-hydroxynaphthalene derivatives. *Bioorg. Med. Chem. Lett.* **2009**, *19*, 4476–4479.
- [33] de Tullio, P.; Servais, A.-C.; Fillet, M.; Gillotin, F.; Somers, F.; Chiap, P.; Lebrun, P.; Pirotte, B. Hydroxylated Analogues of ATP-Sensitive Potassium Channel Openers Belonging to the Group of 6- and/or 7-Substituted 3-Isopropylamino-4*H*-1,2,4-benzothiadiazine 1,1-Dioxides: Toward an Improvement in Sulfonylurea Receptor 1 Selectivity and Metabolism Stability. *J. Med. Chem.* **2011**, *54*, 8353–8361.
- [34] <http://pubchem.ncbi.nlm.nih.gov/> (Accessed on April 20, 2015).
- [35] Baldauf, C.; Günther, R.; Hofmann, H.-J. Conformational properties of sulfonamido peptides. *J. Mol. Struc-Theochem.* **2004**, *675*, 19–28.
- [36] The calculations were completed by Gerald H. Lushington using the link provided. MOPAC 2012 [HTTP://OpenMOPAC.net](http://OpenMOPAC.net)
- [37] Kolb, H. C.; Finn, M. G.; Sharpless, K. B. Click Chemistry: Diverse Chemical Function from a Few Good Reactions. *Angew. Chem. Int. Ed.* **2001**, *40*, 2004–2021.
- [38] (a) Ghandi, M.; Sheibani, S.; Sadeghzadeh, M.; Daha, F. J.; Kubicki, M. Synthesis of novel tetra- and pentacyclic benzosultam scaffolds via domino Knoevenagel hetero-Diels-Alder reactions in water. *J. Iran. Chem. Soc.* **2013**, *10*,

- 1057–1065. (b) Ma, C.; Gu, J.; Teng, B.; Zhou, Q.-Q.; Li, R.; Chen, Y.-C. 1-Azadienes as Regio- and Chemoselective Dienophiles in Aminocatalytic Asymmetric Diels-Alder Reaction. *Org. Lett.* **2013**, *15*, 6206–6209. (c) Veremeichik, Y. V.; Merabov, P. V.; Chuiko, A. V.; Lodochnikova, O. A.; Plemenkov, V. V. Synthesis of benzo-*ortho*-thiazines S-oxides by Diels-Alder reaction of *N*-sulfinylanilines with norbornadiene. *Russ. J. Org. Chem.* **2013**, *49*, 1605–1609.
- [39] (a) Rai, A.; Rai, V. K.; Singh, A. K.; Yadav, L. D. S. [2+2] Annulation of Aldimines with Sulfonic Acids: A Novel One-Pot *cis*-Selective Route to β -Sultams. *Eur. J. Org. Chem.* **2011**, *2011*, 4302–4306. (b) Zarei, M. Phosphonitrilic chloride as an efficient reagent for the synthesis of β -sultams. *Tetrahedron Lett.* **2013**, *54*, 1100–1102. (c) Zarei, M. Convenient Propylphosphonic Anhydride (T3P)-Mediated Synthesis of β -Sultams. *Mendeleev Commun.* **2013**, *23*, 39–40.
- [40] Scott, J. P.; Oliver, S. F.; Brands, K. M. J.; Brewer, S. E.; Davies, A. J.; Gibb, A. D.; Hands, D.; Keen, S. P.; Sheen, F. J.; Reamer, R. A.; Wilson, R. D.; Dolling, U.-H. Practical Asymmetric Synthesis of a δ -Secretase Inhibitor Exploiting Substrate- Controlled Intramolecular Nitrile Oxide-Olefin Cycloaddition. *J. Org. Chem.* **2006**, *71*, 3086–3092.
- [41] Chen, X.-Y.; Ye, S. Phosphane-Catalyzed [4+2] Annulation of Allenates with Ketimines: Synthesis of Sultam-Fused Tetrahydropyridines. *Eur. J. Org. Chem.* **2012**, *29*, 5723–5728.
- [42] (a) Wang, M.; Wang, Y.; Qi, X.; Xia, G.; Tong, K.; Tu, J.; Pittman, C. U.; Zhou, A. Selective Synthesis of Seven- and Eight-Membered Ring Sultams via Two Tandem Reaction Protocols from One Starting Material. *Org. Lett.* **2012**, *14*, 3700–3703. (b) Ji, T.; Wang, Y.; Wang, M.; Niu, B.; Xie, P.; Pittman, C. U.;

- Zhou, A. Parallel Syntheses of Eight-Membered Ring Sultams via Two Cascade Reactions in Water. *ACS Comb. Sci.* **2013**, *15*, 595–600.
- [43] (a) Jakopin, Z.; Dolenc, M. S. Microwave-assisted preparation of N-alkylated saccharins and their reactions with potassium t-butoxide. *Synth. Commun.* **2010**, *40*, 2464–2474. (b) Foschi, F.; Tagliabue, A.; Mihali, V.; Pilati, T.; Pecnikaj, I.; Penso, M. Memory of Chirality Approach to the Enantiodivergent Synthesis of Chiral Benzo[d]sultams. *Org. Lett.* **2013**, *15*, 3686–3689. (c) Lad, N.; Sharma, R.; Marquez, V. E.; Mascarenhas, M. A new synthesis of sultams from amino alcohols. *Tetrahedron Lett.* **2013**, *54*, 6307–6309. (d) McMaster, C.; Fulopova, V.; Popa, I.; Grepl, M.; Soural, M. Solid-Phase Synthesis of Anagrelide Sulfonyl Analogues. *ACS Comb. Sci.* **2014**, *16*, 221–224. (e) Barange, D. K.; Kavala, V.; Kuo, C.-W.; Wang, C.-C.; Rajawinslin, R. R.; Donala, J.; Yao, C.-F. Regioselective synthesis of thiophene fused sultam derivatives via iodocyclization approach and their application towards triazole linker. *Tetrahedron* **2014**, *70*, 7598–7605.
- [44] (a) Dominguez, L.; Nhien, A. N. V.; Tomassi, C.; Len, C.; Postel, D.; Contelles, J. M. Synthesis of 4-Amino-5-*H*-2,3-dihydroisothiazole-1,1-dioxide Ring Systems on Sugar Templates via Carbanion-Mediated Sulfonamide Intramolecular Cyclization Reactions (CSIC Protocols) of Glyco- α -sulfonamidonitriles. *J. Org. Chem.* **2004**, *69*, 843–856. (b) Lee, J.; Zhong, Y.-L.; Reamer, R. A.; Askin, D. Practical Synthesis of Sultams via Sulfonamide Dianion Alkylation: Application to the Synthesis of Chiral Sultams. *Org. Lett.* **2003**, *5*, 4175–4177.
- [45] (a) Vasudevan, A.; Tseng, P.-S.; Djuric, S. W. A Post Aza Baylis-Hillman/Heck Coupling Approach Towards the Synthesis of Constrained Scaffolds. *Tetrahedron Lett.* **2006**, *47*, 8591–8593. (b) Tong, K.; Tu, J.; Qi, X.; Wang, M.; Wang, Y.; Fu, H.; Pittman, C. U.; Zhou, A. Syntheses of five- and seven-membered ring sultam derivatives by Michael addition and Baylis-Hillman reactions. *Tetrahedron* **2013**,

- 69, 2369–2375. (c) Ghandi, M.; Feizi, S.; Ziaie, F.; Notash, B. Solvent-dependent Baylis-Hillman reactions for the synthesis of 3-benzyl-3-hydroxyoxindoles and benzo- δ -sultams. *Tetrahedron* **2014**, *70*, 2563–2569.
- [46] (a) Majumdar, K. C.; Taher, A.; Nandi, R. K. Copper (II) acetate promoted intramolecular carboamination of alkenes: an efficient synthesis of pentacyclic sultams. *Synlett* **2010**, 1389–1393. (b) Kaneko, K.; Yoshino, T.; Matsunaga, S.; Kanai, M. Sultam Synthesis via Cu-Catalyzed Intermolecular Carboamination of Alkenes with *N*-Fluorobenzenesulfonimide. *Org. Lett.* **2013**, *15*, 2502–2505.
- [47] (a) Chen, W.; Li, Z.; Ou, L.; Giulianotti, M. A.; Houghten, R. A.; Yu, Y. Solid-phase synthesis of skeletally diverse benzofused sultams via palladium-catalyzed cyclization. *Tetrahedron Lett.* **2011**, *52*, 1456–1458. (b) Dadiboyena, S.; Nefzi, A. Parallel synthesis of structurally diverse aminobenzimidazole tethered sultams and benzothiazepinones. *Tetrahedron Lett.* **2012**, *53*, 6897–6900. (c) Yang, G.; Zhang, W. A Palladium-Catalyzed Enantioselective Addition of Arylboronic Acids to Cyclic Ketimines. *Angew. Chem., Int. Ed.* **2013**, *52*, 7540–7544. (d) Laha, J. K.; Dayal, N.; Jain, R.; Patel, K. Palladium-Catalyzed Regiocontrolled Domino Synthesis of *N*-Sulfonyl Dihydrophenanthridines and Dihydrodibenzo[*c,e*]azepines: Control over the Formation of Biaryl Sultams in the Intramolecular Direct Arylation. *J. Org. Chem.* **2014**, *79*, 10899–10907. (e) Laha, J. K.; Jethava, K. P.; Dayal, N. Palladium-Catalyzed Intramolecular Oxidative Coupling Involving Double C(sp²)-H Bonds for the Synthesis of Annulated Biaryl Sultams. *J. Org. Chem.* **2014**, *79*, 8010–8019. (f) Nagarjuna Reddy, M.; Kumara Swamy, K. C. Palladium-catalyzed reactions of allenes with 2-iodobenzene-sulfonamides: simple synthesis of benzosultams under green conditions. *Synthesis* **2014**, *46*, 1091–1099. (g) Joardar, S.; Chakravorty, S.; Das, S. Palladium-Mediated Reductive Heck Cyclization for the Formation of Tricyclic Sultams. *Synlett* **2015**, *26*, 359–362. (h) Song, B.; Yu, C.-B.; Huang, W.-X.; Chen, M.-W.;

- Zhou, Y.-G. Formal Palladium-Catalyzed Asymmetric Hydrogenolysis of Racemic *N*-Sulfonyloxaziridines. *Org. Lett.* **2015**, *17*, 190–193.
- [48] (a) Pham, M. V.; Ye, B.; Cramer, N. Access to sultams by rhodium(III)-catalyzed directed C-H activation. *Angew. Chem., Int. Ed.* **2012**, *51*, 10610–10614. (b) Dong, L.; Qu, C.-H.; Huang, J.-R.; Zhang, W.; Zhang, Q.-R.; Deng, J.-G. Rhodium-Catalyzed Spirocyclic Sultam Synthesis by [3+2] Annulation with Cyclic *N*-Sulfonyl Ketimines and Alkynes. *Chem.-Eur. J.* **2013**, *19*, 16537–16540. (c) Xie, W.; Yang, J.; Wang, B.; Li, B. Regioselective Ortho Olefination of Aryl Sulfonamide via Rhodium-Catalyzed Direct C-H Bond Activation. *J. Org. Chem.* **2014**, *79*, 8278–8287. (d) Yang, Z.; Xu, J. Synthesis of benzo- γ -sultams via the Rh-catalyzed aromatic C-H functionalization of diazosulfonamides. *Chem. Commun.* **2014**, *50*, 3616–3618. (e) Li, X.; Dong, Y.; Qu, F.; Liu, G. Synthesis of Benzofused Five-Ring Sultams via Rh-Catalyzed C-H Olefination Directed by an *N*-Ac-Substituted Sulfonamide Group. *J. Org. Chem.* **2015**, *80*, 790–798.
- [49] Ichinose, M.; Suematsu, H.; Yasutomi, Y.; Nishioka, Y.; Uchida, T.; Katsuki, T. Enantioselective Intramolecular Benzylic C-H Bond Amination: Efficient Synthesis of Optically Active Benzosultams. *Angew. Chem., Int. Ed.* **2011**, *50*, 9884–9887.
- [50] Mondal, S.; Debnath, S. Synthesis of sultams by ring-closing metathesis. *Synthesis* **2014**, *46*, 368–374,
- [51] (a) Biswas, D.; Samp, L.; Ganguly, A. K. Synthesis of conformationally restricted sulfonamides via radical cyclisation. *Tetrahedron Lett.* **2010**, *51*, 2681–2684. (b) Feuillastre, S.; Pelotier, B.; Piva, O. Merging cross-metathesis and radical cyclization: a straightforward access to 4-substituted benzosultams. *Synthesis* **2013**, *45*, 810–816. (c) Li, Y.; Ding, Q.; Qiu, G.; Wu, J. Synthesis of benzosultams via an intramolecular sp² C-H bond amination reaction of o-

- arylbenzenesulfonamides under metal-free conditions. *Org. Biomol. Chem.* **2014**, *12*, 149–155.
- [52] (a) Majumdar, K. C.; Mondal, S. Recent developments in the synthesis of fused sultams. *Chem. Rev.* **2011**, *111*, 7749–7773. (b) Rassadin, V. A.; Grosheva, D. S.; Tomashevskii, A. A.; Sokolov, V. V. Methods of Sultam Synthesis. *Chem. Heterocycl. Compd.* **2013**, *49*, 39–65.
- [53] Rayabharapu, D. K.; Zhou, A.; Jeon, K. O.; Samarakoon, T.; Rolfe, A.; Siddiqui, H.; Hanson, P. R. α -Haloarylsulfonamides: multiple cyclization pathways to skeletally diverse benzofused sultams. *Tetrahedron* **2009**, *65*, 3180–3188.
- [54] (a) Viti, G.; Sbraci, P.; Pestellini, V.; Volterra, G.; Borsini, F.; Lecci, A.; Meli, A.; Dapporto, P.; Paoli, P.; Giannotti, D. New Dibenzothiadiazepine Derivatives with Antidepressant Activities. *J. Med. Chem.* **1991**, *34*, 1356–1362 and references cited therein. (b) Viti, G.; Nannicini, R.; Pestellini, V.; Bellarosa, D.; Giannotti, D. Synthesis and Anti HIV-1 Activity of New Thiadiazepindioxides. *Bioorg. Med. Chem. Lett.* **1995**, *5*, 1461–1466.
- [55] Penso, M.; Albanese, D.; Landini, D.; Lupi, V.; Tagliabue, A. Complementary Heterogeneous/Homogeneous Protocols for the Synthesis of Densely Functionalized Benzo[*d*]sultams: C-C Bond Formation by Intramolecular Nucleophilic Aromatic Fluorine Displacement. *J. Org. Chem.* **2008**, *73*, 6686–6690.
- [56] Baxter, C. A.; O'Hagan, M.; O'Riordan, T. J. C.; Sheen, F. J.; Stewart, G. W.; Cleator, E. Synthesis of novel benzoxathiazepine-1,1-dioxides by means of a one-pot multicomponent reaction. *Tetrahedron Lett.* **2010**, *51*, 1079–1082.
- [57] Rolfe, A.; Samarakoon, T. B.; Hanson, P. R. Formal [4+3] Epoxide Cascade Reaction via a Complementary Ambiphilic Pairing Strategy. *Org. Lett.* **2010**, *12*, 1216–1219.

- [58] Pizzirani, D.; Kaya, T.; Clemons, P. A.; Schreiber, S. L. Stereochemical and Skeletal Diversity Arising from Amino Propargylic Alcohols. *Org. Lett.* **2010**, *12*, 2822–2825.
- [59] Noerager, N. G.; Juhl, K. Conjugate addition- S_NAr domino reaction for the synthesis of benzo- or pyridyl-fused lactams and sultams. *Synthesis* **2010**, 4273–4281.
- [60] (a) Golantsov, N. E.; Karchava, A. V.; Yurovskaya, M. A. The Mitsunobu reaction in the chemistry of nitrogen-containing heterocyclic compounds. The formation of heterocyclic systems. *Chem. Heterocycl. Compd.* **2008**, *44*, 263–294. (b) Suzuki, M.; Kambe, M.; Tokuyama, H.; Fukuyama, T. Facile construction of N-hydroxybenzazocine: enantioselective total synthesis of (+)-FR900482. *Angew. Chem., Int. Ed.* **2002**, *41*, 4686–4688. (c) Rujirawanich, J.; Gallagher, T. Substituted 1,4-Benzoxazepines, 1,5-Benzoxazocines, and N- and S-Variants. *Org. Lett.* **2009**, *11*, 5494–5496.
- [61] Samarakoon, T. B. S_NAr -based DOS strategies for the Facile Synthesis of Benzofused Sultam Libraries. Ph. D. Thesis, University of Kansas, Lawrence, KS, 2010.
- [62] Review: (a) Paquette, L. A. Synthesis and unprecedented reactivity characteristics of unsaturated bridgehead sultams. *Chemtracts* **2006**, *19*, 1–10. (b) Dura, R. D.; Modolo, I.; Paquette, L. A. Contrasting Responses of Pyrido[2,1-a]isoindol-6-ones and Their Sultam Counterparts to Photochemical Activation. *J. Org. Chem.* **2009**, *74*, 1982–1987. (c) Dura, R. D.; Modolo, I.; Paquette, L. A. Effective synthetic routes to 4H- and 10bH-pyrido[2,1-a]isoindol-6-ones. *Heterocycles* **2007**, *74*, 145–148. (d) Paquette, L. A.; Dura, R. D.; Fosnaugh, N.; Stepanian, M. Direct Comparison of the Response of Bicyclic Sultam and Lactam Dienes to Photoexcitation. Concerning the Propensity of Differing Bond Types to Bridgehead Nitrogen for Homolytic Cleavage. *J. Org. Chem.* **2006**, *71*, 8438–

8445. (e) Preston, A. J.; Gallucci, J. C.; Paquette, L. A. Synthesis and Selected Reactions of a Bicyclic Sultam Having Sulfur at the Apex Position. *J. Org. Chem.* **2006**, *71*, 6573–6578. (f) Dura, R. D.; Paquette, L. A. Ring Contraction of Bridgehead Sultams by Photoinduced Di- π -methane Rearrangement. *J. Org. Chem.* **2006**, *71*, 2456–2459. (g) Paquette, L. A.; Barton, W. R. S.; Gallucci, J. C. Synthesis of 1-Aza-8-thiabicyclo[4.2.1]nona-2,4-diene 8,8-Dioxide and Its Conversion to a Strained Spirocycle via Photoinduced SO₂-N Bond Cleavage. *Org. Lett.* **2004**, *6*, 1313–1315. (h) Rassadin, V. A.; Grosheva, D. S.; Tomashevskiy, A. A.; Sokolov, V. V.; Yufit, D. S.; Kozhushkov, S. I.; de Meijere, A. Bicyclic Sultams with a Nitrogen at the Bridgehead and a Sulfur Atom in the Apex Position: Facile Preparation and Conformational Properties. *Eur. J. Org. Chem.* **2010**, 3481–3486.

- [63] For reviews of twisted amides, see: (a) Greenberg, A.; Breneman, C. M.; Liebman, J. F. Amide Linkage: Selected Structural Aspects in Chemistry, Biochemistry, and Materials Science. Wiley: New York, **2000**. (b) Greenberg, A. Twisted bridgehead bicyclic lactams. *Mol. Struct. Energ.* **1988**, *7*, 139–178. (c) Hall, H. K., Jr.; El-Shekeil, A. Anti-Bredt bridgehead nitrogen compounds in ring-opening polymerization. *Chem. Rev.* **1983**, *83*, 549–555.
- [64] (a) Szostak, M.; Aubé, J. Medium-bridged lactams: a new class of non-planar amides. *Org. Biomol. Chem.* **2011**, *9*, 27–35 and references cited therein. (b) Szostak, M.; Yao, L.; Day, V. W.; Powell, D. R.; Aubé, J. Structural Characterization of *N*-Protonated Amides: Regioselective *N*-Activation of Medium-Bridged Twisted Lactams. *J. Am. Chem. Soc.* **2010**, *132*, 8836–8837. (c) Szostak, M.; Yao, L.; Aubé, J. Proximity Effects in Nucleophilic Addition Reactions to Medium-Bridged Twisted Lactams: Remarkably Stable Tetrahedral Intermediates. *J. Am. Chem. Soc.* **2010**, *132*, 2078–2084. (d) Szostak, M.; Aubé, J. Direct Synthesis of Medium-Bridged Twisted Amides via a Transannular Cyclization Strategy. *Org. Lett.* **2009**, *11*, 3878–3881. (e) Tani, K.; Stoltz, B. M.

- Synthesis and structural analysis of 2-quinuclidonium tetrafluoroborate. *Nature* **2006**, *441*, 731–734. (f) Lei, Y.; Wroblewski, A. D.; Golden, J. E.; Powell, D. R.; Aubé, J. Facile C-N Cleavage in a Series of Bridged Lactams. *J. Am. Chem. Soc.* **2005**, *127*, 4552–4553. (g) Greenberg, A.; Venanzi, C. A. Structures and energetics of two bridgehead lactams and their N- and O-protonated forms: an ab initio molecular orbital study. *J. Am. Chem. Soc.* **1993**, *115*, 6951–6957.
- [65] (a) Beddoes, R. L.; Dalton, L.; Joule, J. A.; Mills, O. S.; Street, J. D.; Watt, C. I. F. The geometry at nitrogen in N-phenylsulfonylpyrroles and -indoles. The geometry of sulfonamides. *J. Chem. Soc., Perkin Trans. 2* **1986**, 787–797. (b) Klug, H. P. The crystal structure of methanesulfonanilide. *Acta Crystallogr., Sect. B* **1968**, *24*, 792–802. (c) Oppolzer, W.; Rodriguez, I.; Starkemann, C.; Walther, E. Chiral toluene-2, α -sultam auxiliaries: asymmetric alkylations, acylations and aldolizations of N-acyl derivatives. *Tetrahedron Lett.* **1990**, *31*, 5019–5022.
- [66] Chambers, C. S.; Patel, N.; Hemming, K. Intramolecular 1,3-dipolar cycloaddition as a route to triazolobenzodiazepines and pyrrolobenzodiazepines. *Tetrahedron Lett.* **2010**, *51*, 4859–4861.
- [67] (a) Barange, D. K.; Tu, Y.-C.; Kavala, V.; Kuo, C.-W.; Yao, C.-F. One-pot synthesis of triazolothiadiazepine 1,1-dioxide derivatives via copper-catalyzed tandem [3+2] cycloaddition/*N*-arylation. *Adv. Synth. Catal.* **2011**, *353*, 41–48. (b) Sai Sudhir, V.; Nasir Baig, R. B.; Chandrasekaran, S. Facile Entry to 4,5,6,7-Tetrahydro[1,2,3]triazolo[1,5-*a*]pyrazin-6-ones from Amines and Amino Acids. *Eur. J. Org. Chem.* **2008**, *14*, 2423–2429. (c) Mohapatra, D. K.; Maity, P. K.; Gonnade, R. G.; Chorghade, M. S.; Gurjar, M. K. Synthesis of New Chiral 4,5,6,7-Tetrahydro[1,2,3]triazolo[1,5-*a*]pyrazines from α -Amino Acid Derivatives under Mild Conditions. *Synlett* **2007**, *12*, 1893–1896. (d) Brawn, R. A.; Welzel, M.; Lowe, J. T.; Panek, J. S. Regioselective Intramolecular Dipolar Cycloaddition of Azides and Unsymmetrical Alkynes. *Org. Lett.* **2010**, *12*, 336–339.

- [68] (a) Wu, P.; Fokin, V. V. Catalytic azide-alkyne cycloaddition: reactivity and applications. *Aldrichimica Acta* **2007**, *40*, 7–17. (b) Moses, J. E.; Moorhouse, A. D. The growing applications of Click chemistry. *Chem. Soc. Rev.* **2007**, *36*, 1249–1262. (c) Kolb, H. C.; Sharpless, K. B. The growing impact of click chemistry on drug discovery. *Drug Discovery Today* **2003**, *8*, 1128–1137. (d) Looper, R. E.; Pizzirani, D.; Schreiber, S. L. Macrocycloadditions Leading to Conformationally Restricted Small Molecules. *Org. Lett.* **2006**, *8*, 2063–2066.
- [69] See Chapter 5 Supporting Information for detailed description of analysis.
- [70] (a) Pearlman, R. S.; Smith, K. M. Metric Validation and the Receptor-Relevant Subspace Concept. *J. Chem. Inf. Comput. Sci.* **1999**, *39*, 28–35. (b) *DiverseSolutions 8.1*; Tripos Inc.: St. Louis, MO, 2009.
- [71] (a) Samarakoon, T. B.; Hur, M. Y.; Kurtz, R. D.; Hanson, P. R. A Formal [4+4] Complementary Ambiphile Pairing Reaction: A New Cyclization Pathway for *ortho*-Quinone Methides. *Org. Lett.* **2010**, *12*, 2182–2185. (b) Wang, M.; Wang, Y.; Qi, X.; Xia, G.; Tong, K.; Tu, J.; Pittman, C. U.; Zhou, A. Selective Synthesis of Seven- and Eight-Membered Ring Sultams via Two Tandem Reaction Protocols from One Starting Material. *Org. Lett.* **2012**, *14*, 3700–3703. (c) See ref 9e.
- [72] (a) Rolfe, A.; Hanson, P. R. Microwave-assisted sequential one-pot protocol to benzothiadiazin-3-one-1,1-dioxides via a copper-catalyzed *N*-arylation strategy. *Tetrahedron Lett.* **2009**, *50*, 6935–6937. (b) Rolfe, A.; Young, K.; Volp, K.; Schoenen, F.; Neuenswander, B.; Lushington, G. H.; Hanson, P. R. One-Pot, Three-Component, Domino Heck-aza-Michael Approach to Libraries of Functionalized 1,1-Dioxido-1,2-benzisothiazoline-3-acetic Acids. *J. Comb. Chem.* **2009**, *11*, 732–738. (c) Jeon, K. O.; Rayabarapu, D.; Rolfe, A.; Volp, K.; Omar, I.; Hanson, P. R. Metathesis cascade strategies (ROM-RCM-CM): a DOS approach to skeletally diverse sultams. *Tetrahedron* **2009**, *65*, 4992–5000. (d)

- Rayabarapu, D. K.; Zhou, A.; Jeon, K. O.; Samarakoon, T.; Rolfe, A.; Siddiqui, H.; Hanson, P. R. α -Haloarylsulfonamides: multiple cyclization pathways to skeletally diverse benzofused sultams. *Tetrahedron* **2009**, *65*, 3180–3188.
- [73] (a) Zhou, A.; Rayabarapu, D.; Hanson, P. R. "Click, click, cyclize": a DOS approach to sultams utilizing vinyl sulfonamide linchpins. *Org. Lett.* **2009**, *11*, 531–534. (b) Zhou, A.; Hanson, P. R. Synthesis of sultam scaffolds via intramolecular oxa-Michael and diastereoselective Baylis-Hillman reactions. *Org. Lett.* **2008**, *10*, 2951–2954.
- [74] (a) Chen, W.; Li, Z.; Ou, L.; Giulianott, M. A.; Houghten, R. A.; Yu, Y. Solid-phase synthesis of skeletally diverse benzofused sultams via palladium-catalyzed cyclization. *Tetrahedron Lett.* **2011**, *52*, 1456–1458. (b) Rolfe, A.; Samarakoon, T. B.; Klimberg, S. V.; Brzozowski, M.; Neuenswander, B.; Lushington, G. H.; Hanson, P. R. S_NAr -Based, Facile Synthesis of a Library of Benzothioxazepine-1,1'-dioxides. *J. Comb. Chem.* **2010**, *12*, 850–854. (c) Rolfe, A.; Probst, D. A.; Volp, K. A.; Omar, I.; Flynn, D. L.; Hanson, P. R. High-Load, Oligomeric Dichlorotriazine: A Versatile ROMP-Derived Reagent and Scavenger. *J. Org. Chem.* **2008**, *73*, 8785–8790. (d) Rolfe, A.; Ullah, F.; Samarakoon, T. B.; Kurtz, R. D.; Porubsky, P.; Neuenswander, B.; Lushington, G. H.; Santini, C.; Organ, M. G.; Hanson, P. R. Synthesis of Amino-Benzothioxazepine-1,1-dioxides Utilizing a Microwave-Assisted, S_NAr Protocol. *ACS Comb. Sci.* **2011**, *13*, 653–658.
- [75] Ullah, F.; Samarakoon, T.; Rolfe, A.; Kurtz, R. D.; Hanson, P. R.; Organ, M. G. Scaling out by microwave-assisted, continuous flow organic synthesis (MACOS): multi-gram synthesis of bromo- and fluoro-benzofused sultams, benzothiazepine 1,1-dioxides. *Chem. Eur. J.* **2010**, *16*, 10959–10962.
- [76] Akella, L. B.; Marcaurelle, L. A. Application of a Sparse Matrix Design Strategy to the Synthesis of DOS Libraries. *ACS Comb. Sci.* **2011**, *13*, 357–364.

- [77] Cruciani, G.; Pastor, M.; Guba, W. VolSurf: a new tool for the pharmacokinetic optimization of lead compounds. *Eur. J. Pharm. Sci.* **2000**, *11* (Suppl. 2), S29–S39.
- [78] Rolfe, A.; Painter, T. O.; Asad, N.; Hur, M. Y.; Jeon, K. O.; Brzozowski, M.; Klimberg, S. V.; Porubsky, P.; Neuenswander, B.; Lushington, G. H.; Santini, C.; Hanson, P. R. Triazole-Containing Isothiazolidine 1,1-Dioxide Library Synthesis: One-Pot, Multi-Component Protocols for Small Molecular Probe Discovery. *ACS Comb. Sci.* **2011**, *13*, 511–517.
- [79] Description of the Synthos 3000 microwave synthesis system. <http://www.anton-paar.com/us-en/products/group/microwave-synthesis/> (accessed April 20, 2015).
- [80] All of the compounds were sketched using the Avogadro suite of molecular modeling programs (a), and were subsequently subjected to molecular mechanics optimization at default minimization constraints according to the MMFF94 force field and charge parametrization (b). Compounds were then mutually aligned using PyMol (c) according to least-squares positional fitting across the atoms corresponding to the conserved sultam and adjacent carbonyl functional groups. The resulting molecular alignments were then visualized in PyMol. (a) Hanwell, M. D.; Curtis, D. E.; Lonie, D. C.; Vandermeersch, T.; Zurek E.; Hutchison, G. R. Avogadro: an advanced semantic chemical editor, visualization, and analysis platform. *J. Cheminf.* **2012**, *4*, 1–17. (b) Halgren, T. A.; Merck molecular force field. I. Basis, form, scope, parameterization, and performance of MMFF94. *J. Comp. Chem.* **1996**, 490–519. (c) PyMol Molecular Graphics System, Version 1.6, 2014. <http://sourceforge.net/projects/pymol/>
- [81] Sauer, W. H. B.; Schwarz, M. K. Molecular Shape Diversity of Combinatorial Libraries: A Prerequisite for Broad Bioactivity. *J. Chem. Inf. Comput. Sci.* **2003**, *43*, 987–1003.

- [82] Bickerton, G. R.; Paolini, G. V.; Besnard, J.; Muresan, S.; Hopkins, A. L. Quantifying the chemical beauty of drugs. *Nat. Chem.* **2012**, *4*, 90–98.
- [83] *SYBYL 8.0*; The Tripos Associates: St. Louis, MO, 2008.

Chapter 3

*A Modular, One-pot, Sequential
Aziridine Ring-Opening– S_NAr Strategy
to Benzofused Sultams*

3.1 Introduction

The development of efficient methods for the generation of medium- and large-sized heterocycles¹ is an important facet of screening campaigns for facilitating drug discovery.² In particular, medium and macrocyclic lactams^{1,3} constitute an important group of molecules in compound collections derived from target-oriented- and diversity-oriented⁴ synthetic approaches. Furthermore, macrocycles are also known to be a pharmacological and physicochemical relevant molecular class for which numerous methods have been developed to synthesize the collections of molecules in a facile and effective manner.¹ Their distinct properties that were also detailed in Chapter 1 include conformational constraint, lower rotatable bond count, reduced polarity, increased proteolytic stability and potential for higher target binding and selectivity.⁵ Macrocycles are also manifested in improved pharmacokinetics and pharmacodynamics, rendering them as attractive lead molecules for drug development.² Taken collectively, these attributes have inspired limited production of natural product-like⁶ medium-sized and macrocyclic ring systems, enabling efforts to address emerging difficult drug targets such as those involving protein-protein interactions⁷ and epigenetic targets.⁸ However, the strategy for the development of novel macrocycle-based drugs or probes is still an emerging field as the synthetic challenges of assembling macrocycles that are stereochemically-rich, and enhanced in terms of their fraction of sp³ carbons,⁹ have began surfacing in this area.

Accordingly, the innate properties of medium and large-sized strained rings (10- to 13-membered)¹⁰ can conceivably produce uncommon molecular shapes, alternative

bond geometries and spatial orientations of functional groups that are different from unstrained or acyclic motifs. While the chemical space of these unique systems represent an intriguing target in synthesis,ⁱ they also exemplify difficult scaffolds to access chemically.

Macrocycles, both macrolactones and macrolactams, in general have exhibited broad biological activity¹¹ in a variety of areas ranging from antibiotics,¹² inhibitors of CDK2/cyclin A,¹³ Hsp90 inhibitors,¹⁴ protein kinase C (PKC) inhibitors,¹⁵ anti-fungal activity,¹⁶ anthelmintic activity,¹⁷ hepatitis C virus (HCV) NS3/4A serine protease¹⁸ in drug discovery¹⁹ to insecticidal agents in agriculture.²⁰ As previously mentioned in Chapter 1, while medium and macrocyclic lactams are well documented in the literature, their sulfonamide-based counterparts, medium and macrocyclic sultams, are unnatural and less prevalent synthetically but have been found to exhibit a variety of biological activities ranging from anti-proliferative,²¹ anti-HIV activity,²² treatment of feline immunodeficiency virus,²³ inhibitory activity of trypsin-like serine protease Factor XIa involved in blood coagulation,²⁴ inhibitors of phosphoinositide 3'OH kinase (PI3K class I sub-type)²⁵ and inhibitors of hepatitis C virus (HCV)²⁶ where in fact, several examples of macrocyclic sultams are treatments of HCV (Figure 3.1).

Based on the studies of Heterocyclic Rings in Drugs Analysis Models in Chapter 1, the underrepresented ring systems were highlighted and in particular, medium-sized

[i] Note: A short section towards the end of this chapter, is used to describe the chemical space that some of the chemically constructed unique rings systems occupy

sultams such as 10-/11-membered rings will be discussed in the remaining of this chapter. In Chapter 3, a one-pot, sequential aziridine-ring opening and intramolecular S_NAr cyclization employing heretofore unknown *o*-fluoroaryl-sulfonyl aziridines and amino alcohols in a “6+4” and “6+5” heterocyclization pathways to generate 10-/11-membered polycyclic benzofused sultams. The method was extended for the construction of 7-membered benzofused sultams with functional handles for diversification by exploiting amines in a “6+1” cyclization sequence. These sultam scaffolds lie within new chemical space when mapped using the principal moments of inertia (PMI) analysis and overlay analysis presented at the end of Chapter 3, *vida infra*.

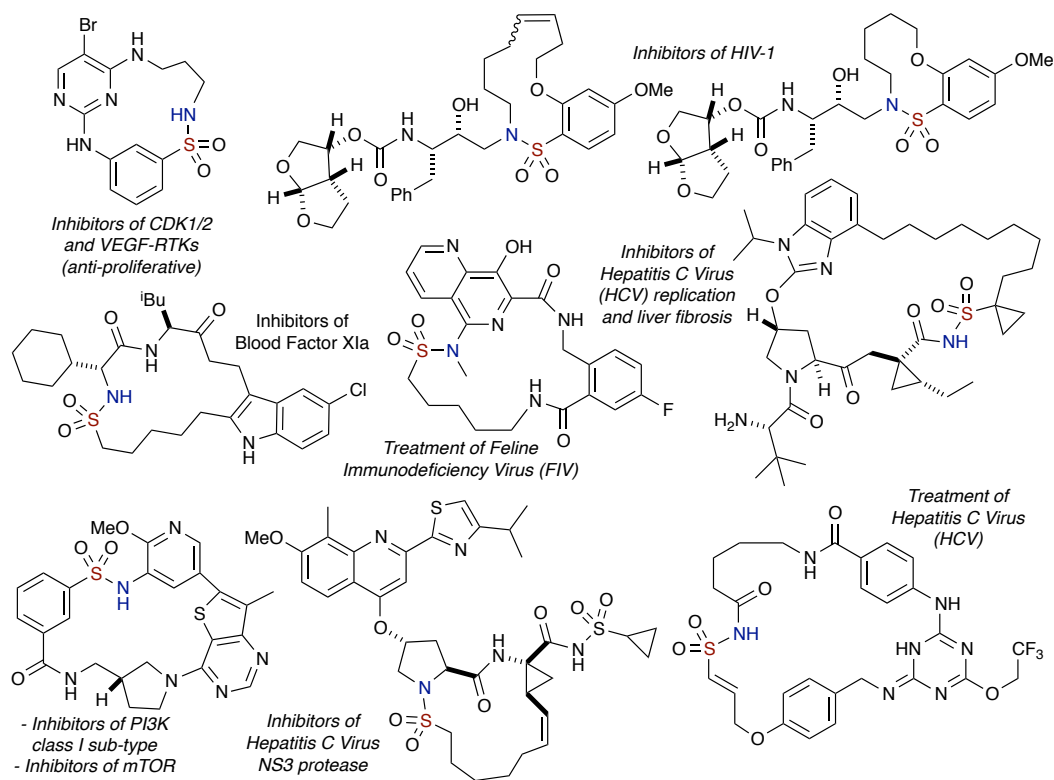


Figure 3.1. Representative examples of biologically active macrocyclic sultams.

3.1.1 Basics of Macrocyclization

In 1981 and 1984, respectively, Illuminati and Mandolini carried out investigations that illustrated the physical aspects of cyclization reactions that imply the use of bi-functional substrates undertaking a ring closure by an intramolecular reaction.²⁷ Studies by Mandolini and co-workers on the macrolactonization of ω -bromo alkanic acids, $\text{Br}-(\text{CH}_2)_{n-2}\text{CO}_2\text{H}$ via intramolecular nucleophilic substitution ($\text{S}_{\text{N}}2$) have shown that medium ring (8- to 11-membered) cyclizations have the most strain energy due to the medium-ring effects based on the data provided,²⁸ whereas for other ring sizes—including small rings (3- to 4-membered), common rings (5- to 7-membered) and large rings (>12-membered)—are less obvious (Figure 3.2).²⁷ Since $\text{S}_{\text{N}}\text{Ar}$ reactions belong to the realm of substitution chemistry, cyclization studies carried out using $\text{S}_{\text{N}}2$ reactions are quite relevant when discussing $\text{S}_{\text{N}}\text{Ar}$ reactions based on certain similarities that they collectively share.

The $\text{S}_{\text{N}}2$ macrocyclization studies revealed that the formation of medium size rings (8- to 11-membered) is in many instances the most difficult to effect, even under high dilution conditions. These results were relatively similar to other profiles that were investigated, for instance, the formation of catechol polymethylene ethers²⁹ from o - $\text{OC}_6\text{H}_4\text{O}(\text{CH}_2)_{n-4}\text{Br}$ and lactones³⁰ from $\text{Br}(\text{CH}_2)_{n-2}\text{CO}_2^-$ and even earlier work by Ruzicka³¹ and Ziegler.³²

In 2013, Campagne and coworkers assembled an elegant review entitled “Macrolactonizations in the Total Synthesis of Natural Products”³³ that substantiated the aforementioned Illuminati and Mandolini studies, and again detailed the various factors

one needs to consider when designing a macrocyclization event. For the purpose of convenience, these are summarized as follows: the difficulties seen in medium ring cyclizations are primarily due to the high strain energy (enthalpic factor) in the ring being formed that outweighs the entropic factor (Figure 3.2). In contrast, intramolecular reaction in large ring sizes, the entropic factor is increased further, but the enthalpic factor has decreased significantly since the rings formed are almost strain free. Hence, medium ring formation are the most difficult cases due to entropic and enthalpic factors. Several reasons cited in these investigations are ring strain (enthalpic factor) that consist mainly of (a) angle strain; (b) conformational strain and (c) transannular strain, as well as the relative rates of ring formation (entropic factor), which is inversely proportional to the length of the acyclic chain.

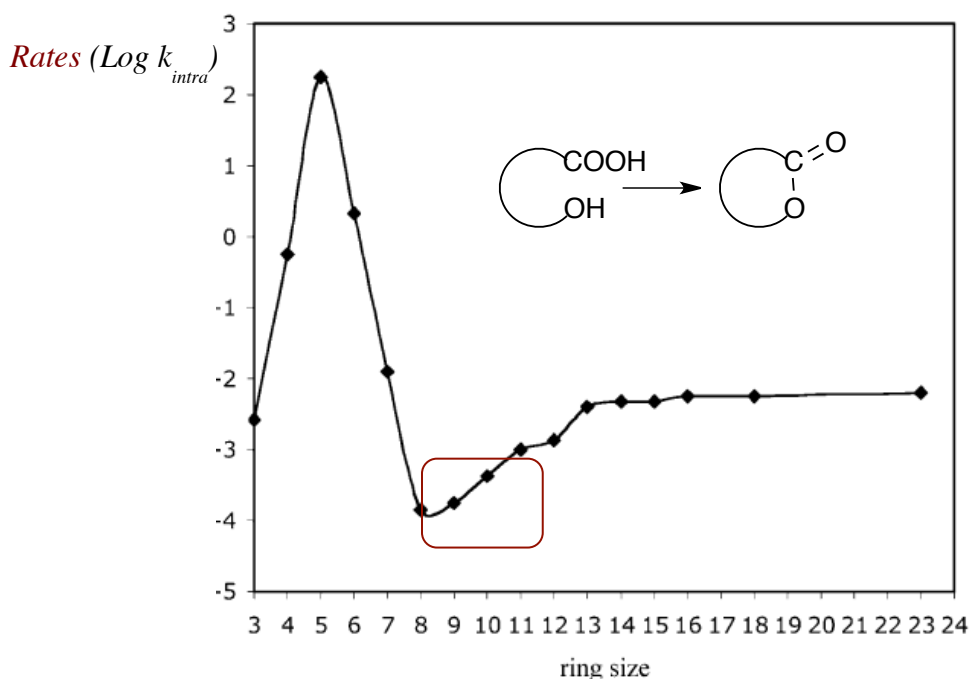


Figure 3.2. Reactivity profile for lactone formation as noted in the Campaign review.

Since larger chains can assume a greater total number of conformations, the likelihood of the chain assuming “the one reactive conformation,” is reduced. Moreover, a portion of the entropic cost of forming a ring comes from the fact that the conformational degrees of freedom are being lost in a ring-like transition state that is considerably more ordered than the flexible acyclic starting material. Thus, entropic costs start to increase sharply at medium ring sizes, as the transition states remain fairly rigid, while the number of degrees of freedom that are being lost, increases greatly. For macrocycles, the ability to bend and twist in space increases as the size increases thus reducing ring strain, which is thought to partially compensate for the freezing of rotors.

3.1.2 Synthesis of Macrocycles for Drug Discovery

Due to the aforementioned difficulties in macrocycle synthesis, and Lipinski’s ‘rule of 5’ physicochemical properties, applications in medicinal chemistry have been limited until recently, as more methods have been developed to address the issues. The focus of the present section will be on synthetic approaches to macrocyclic compounds, as well as libraries related to the parent molecules. Several of these strategies possess some general advantages: (a) well-developed chemistry and procedures; (b) broad selection of readily available reagents; (c) suitability for a wide range of ring sizes and (d) efficient formation of acyclic precursors with high diversity. In contrast, the challenges common to all macrocyclizations include: (a) high dilution conditions to prevent formation of oligomeric side-products; (b) the efficiency of the cyclization

guided by kinetics which play a major role and (c) linear precursors to adopt an appropriate conformation suitable for cyclization.

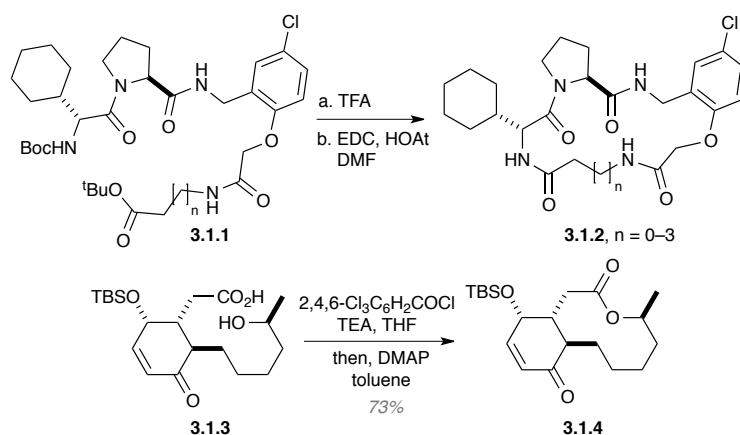
These macrocyclization approaches include a collection of methods that range from standard processes like macrolactamization/macrolactonization and substitution chemistry (S_N2 and S_NAr), to more intricate ring-closing metathesis (RCM), organometallic methods (Pd, Ru and Ni), multi-component reactions (MCR) and cycloadditions, and reactions that are significant in the synthetic realm; Wittig chemistry, Mitsunobu reactions, ring expansion/opening and finally some miscellaneous reactions (Cope rearrangement and Staudinger-type ring closure).³⁴ However, for brevity, only a short list of reactions will be discussed in this chapter.

3.1.2.1 Macrolactamization and Macrolactonization

Historically, the two most established reactions for the formation of macrocycles are macrolactamization and macrolactonization, both of which are still in regular use. This is due partially to the peptidomimetic nature of many of those structures, whose targets are typically protease enzyme inhibitors. Thus, amide bond formation *via* macrolactamization or macrolactonization is traditionally a viable option for the synthesis of cyclodepsipeptide-like compounds.³⁵ Classical examples of the two general transformations are shown in Scheme 3.1, where **3.1.2** is a thrombin inhibitor and **3.1.4** is an inhibitor of bacterial DNA primase (Sch 642305).

For both macrolactamization and macrolactonization, there is an extensive selection of coupling reagents available, including carbodiimides, phosphonium salts,

Scheme 3.1. *Examples of macrolactamization and macrolactonization*



other phosphorus derivatives, pyridinium salts, triazines, acylazoles and halogenating reagents, and for the latter, comprised of thioesters activation of acids in the absence or presence of metal salts, Mukaiyama's salt, mixed anhydrides [2,4,6-trichlorobenzoyl chloride (Yamaguchi's reagent) and 2-methyl-6-nitrobenzoic anhydride (Shiina's reagent)], mixed anhydrides under Lewis acid activation and phosphorus-based reagents with more, constantly adding to the lists.³⁶ Several of these reagents are now available on polymer support, which provide ease of use in parallel synthesis and library production.

More often, macrolactamization has been the strategy for peptidomimetic macrocycles and has successfully synthesized a broad range of structures from small ring inhibitors, such as neutral endopeptidase 24.11 (NEP),³⁷ to large macrocycles, such as protein epitope mimics (PEM) (Figure 3.3).³⁸ This list also includes macrocyclic peptidomimetic and non-peptide compounds, comprising human immunodeficiency (HIV) protease inhibitors,³⁹ renin inhibitors,⁴⁰ thrombin inhibitors,⁴¹ β -secretase (BACE-1) inhibitors,⁴² and TNF- α converting enzyme (TACE) inhibitors,⁴³ among many other more targets.⁴⁴ In addition, using a non-traditional amine-acid coupling has provided a

series of finger loop inhibitors of hepatitis C virus (HCV) nonstructural protein 5B (NS5b) polymerase, leading to the discovery of the clinical candidate TMC647055 currently in phase II trials (Figure 3.3).⁴⁵

While there are many efficient macrolactamization methods for the preparations of peptidomimetic and non-peptide compounds, the use of macrolactonization for the generation of *de novo* macrocyclic molecules are still limited. The majority of synthetic efforts for macrolactonization have been to synthesize the myriad of macrolide natural products, their derivatives and analogues. This could be due to the fact that the ester of the lactone has a greater hydrolytic lability than its counterpart-lactam, thus the slight bias. Nonetheless, a 14-membered macrolactone that is a naturally occurring kinase inhibitor against MEK (mitogen-activated protein kinase enzyme) was accessed by Yamaguchi's conditions for the pivotal ring closure (Figure 3.3).⁴⁶

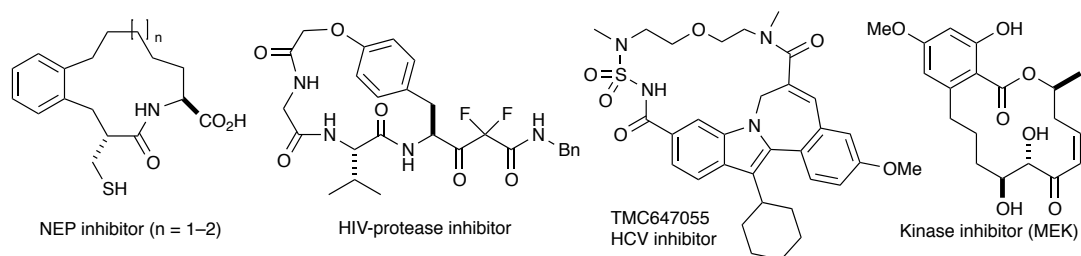


Figure 3.3. Examples of macrolactamization and macrolactonization products.

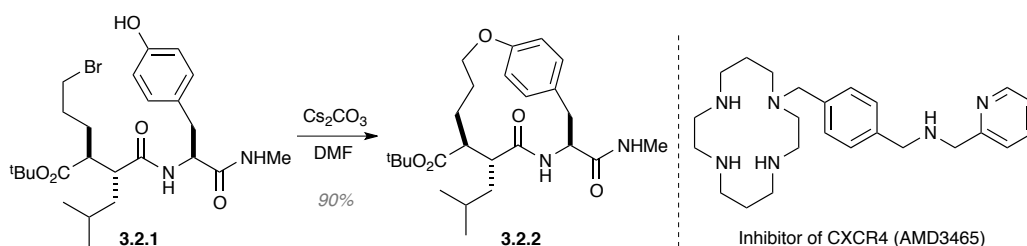
The two strategies, macrolactamization and macrolactonization, together with innovative technologies have been used for generating macrocyclic libraries up to 44,000 analogues, with wide level of diversity initiating from commercially available building blocks and use of solid supports to minimize possible side reactions.

3.1.2.2 Substitution Chemistry: S_N2 and S_NAr Reactions

A chemical reaction during which one functional group in a chemical compound is directly displaced by another functional group is known as substitution chemistry, also one of the common strategies used to build macrocyclic motifs. Other than the aforementioned considerations, additional advantages to utilization of substitution chemistry are that more possibilities are available to investigate different sites of ring closure. In contrast, however, a drawback of substitution chemistry is potential incompatibilities of functional groups or reactive motifs that will require tedious protection/deprotection protocols.

The classic intramolecular S_N2 displacement reaction has various applications in certain macrocyclic structures, usually the simpler, less complex molecules with limited functionality. For example, the intramolecular S_N2 reaction under the conditions of Cs₂CO₃ in DMF was used to synthesize 14-membered macrocycle **3.2.2**, inhibitors of matrix metalloproteinases (MMP-1, -3 and -9) (Scheme 3.2).⁴⁷ Likewise, inhibitors of

Scheme 3.2. S_N2 reaction towards macrocycles and AMD3465



CXCR4-targeted immunostimulating cyclams AMD3100 (plerixafor)⁴⁸ and AMD3465⁴⁹ were also constructed under similar conditions. Their therapeutic effects are primarily anti-cancer and/or anti-viral.

In addition to the intramolecular S_N2 displacement approach, sequential or pseudo-simultaneous substitution reactions have been used to produce ring systems, whereby reactants are used, that are equipped with two electrophilic sites in the same acyclic precursor together with two nucleophilic groups. Furthermore, these latter transformations have successfully provided both complex structures as well as some bioactive macrocyclic compounds. These examples include macroheterocyclic peptidomimetic BACE inhibitors,⁵⁰ macrocyclic peptidomimetics designed to mimic β -turns,⁵¹ thiazole-containing RGD analogues,⁵² cyclin-dependent kinase (CDK) inhibitors,⁵³ hydroxamic acid MMP and TACE inhibitors (Figure 3.4).^{47,54} The synthesis of β -turns mimics using solid support was extended to library assembly and more than 3,600 derivatives were prepared.⁵⁵ With a similar strategy, using the S_N2 process, produced up to 4,000 derivatives and analogues.⁵⁶

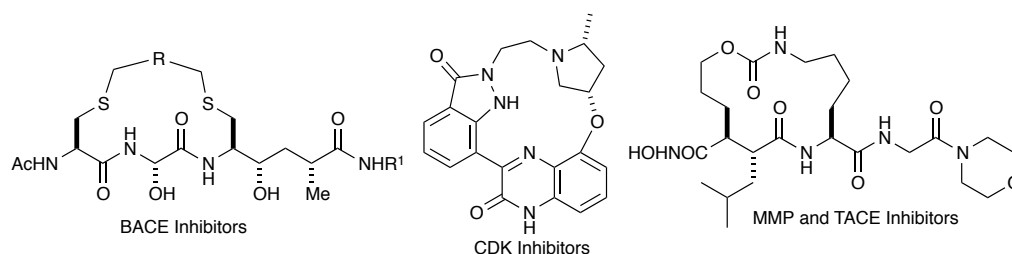
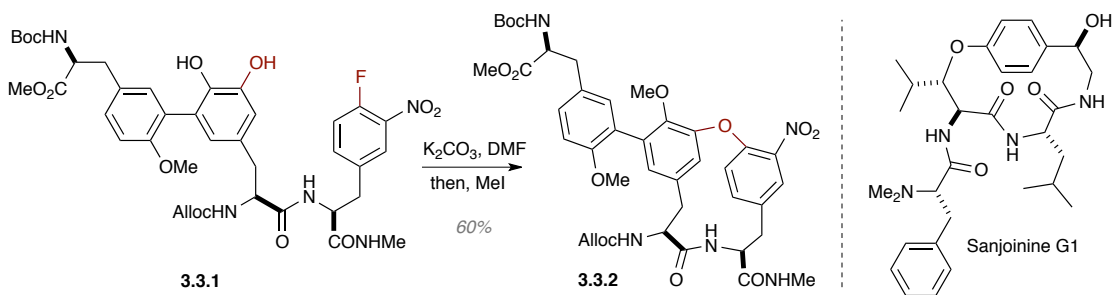


Figure 3.4. Selected macrocycles from S_N2 chemistry.

Equally important is the use of substitution reactions with aromatic rings also known as a nucleophilic aromatic substitution (S_NAr) reaction that has been applied to the generation of macrocyclic compounds. For example, the key cyclization for the synthesis of RP-66453 **3.3.2** was accomplished under defined conditions (K_2CO_3 , 0.002 M in DMF) deemed complete by TLC analysis, whereby an excess of methyl iodide was

introduced to the reaction mixture to promote the methylation of the remaining free hydroxyl function to afford the desired cyclized compound (Scheme 3.3).⁵⁷ Intramolecular S_NAr cyclizations have been utilized to access unique structures comprising (1) 5-membered indoles and indolines,⁵⁸ (2) “privileged structure” in bioactive natural products such as complestatin,⁵⁹ vancomycin⁶⁰ and many others⁶¹ that contain the biaryl ether moiety, as well as (3) cyclopeptide alkaloids like sanjoinine G1 that are peptidomimetics-like and its related motifs. Despite these successful applications of S_NAr cyclizations, there are still many other reactions being employed for the generation of more complex macrocyclic compounds.^{57,62}

Scheme 3.3. S_NAr reaction towards macrocyclic natural products



Although this effective transformation has been applied to mainly bioactive natural products, there are increasing examples of *de novo* macrocyclic compounds being synthesized via S_NAr cyclization. To name a few, aminopyrimidine macrocycles that possessed inhibitory activity against both CDK and vascular endothelial growth factor receptor-2 (VEGF-R2) and exhibited *in vivo* oral activity in a tumor xenograft model,⁶³ agonists of the TrkC neurotrophin-3 receptor and the TrkA nerve growth factor receptor,⁶⁴ as well as TrkC antagonists,⁶⁵ and lastly, a series of macrocyclic piperazinone and imidazole farnesyltransferase (FTase) inhibitors (Figure 3.5).⁶⁶ In addition to facile

use of intramolecular S_NAr cyclization, the ease and speed of executions for this transformation have been greatly enhanced with technologies available like solid phase synthesis and microwave irradiation. Several different libraries capitalized on this existing assistance, whereby almost 14,000 derivatives were synthesized for biological screening, resulting in various lead compounds being identified.⁶⁷

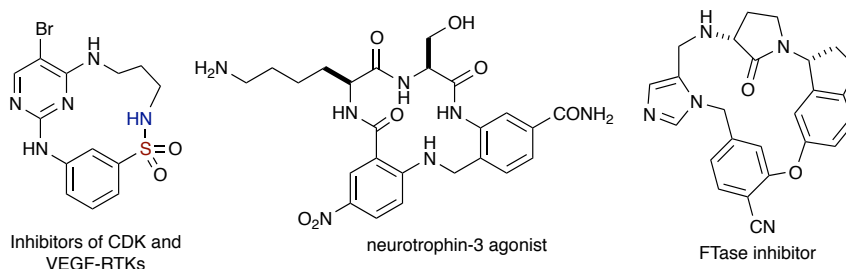


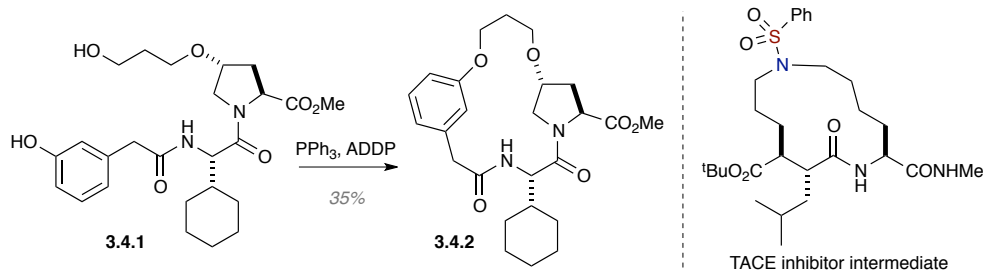
Figure 3.5. Selected macrocycles from S_NAr chemistry.

3.1.2.3 Miscellaneous Methods: Mitsunobu reaction, Ring Expansion/Opening and MCR-Ugi-type Macrocyclization

Several other reaction methods, which have limited applications to macrocyclic structures but have been exploited in the synthetic arena, are the Mitsunobu reaction, ring expansion/opening and Ugi-type macrocyclizations. Examples of utilization of the Mitsunobu reaction are in the production of key intermediates *en route* to MMP⁶⁸ and HCV NS3-4A protease inhibitors⁶⁹ **3.4.2**, as well as a TACE inhibitor (Scheme 3.4).⁷⁰

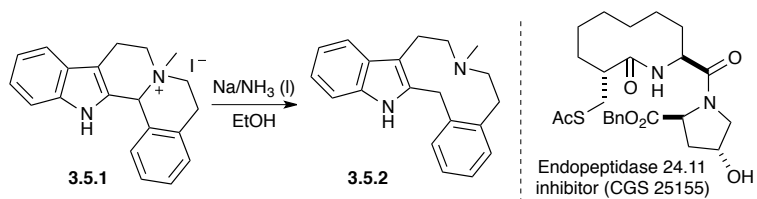
In contrast to the previous list, ring expansion/opening chemistry has more applications in methods development space and is less obvious for the synthesis of macrocycles. However, macrocyclic structures can be generated by cleavage of appropriate bonds in multi-ring systems, although only certain reactions can withstand the harsher conditions that it will required. Nonetheless, examples of

Scheme 3.4. Mitsunobu reaction to key intermediates of inhibitors



macrocycles obtained *via* ring expansion/opening chemistry are phosphatase cdc25B inhibitors and their 500 analogues,⁷¹ cyclic dopamine antagonists azecine LE300⁷² (10-membered ring) **3.5.2** and also neutral endopeptidase 24.11 inhibitor CGS 25155 and related analogues (Scheme 3.5).⁷³ Furthermore, a similar process is utilization of nitrogen insertion/ring expansion of cyclic ketones that have yielded either macrolactones or macrolactams, with the relative proportions dependent on the ring size of the precursor and the pH of the reaction medium.⁷⁴ The limitations of the ring expansion/opening approaches become more apparent, when taking into account the relative simplicity of the molecules produced.

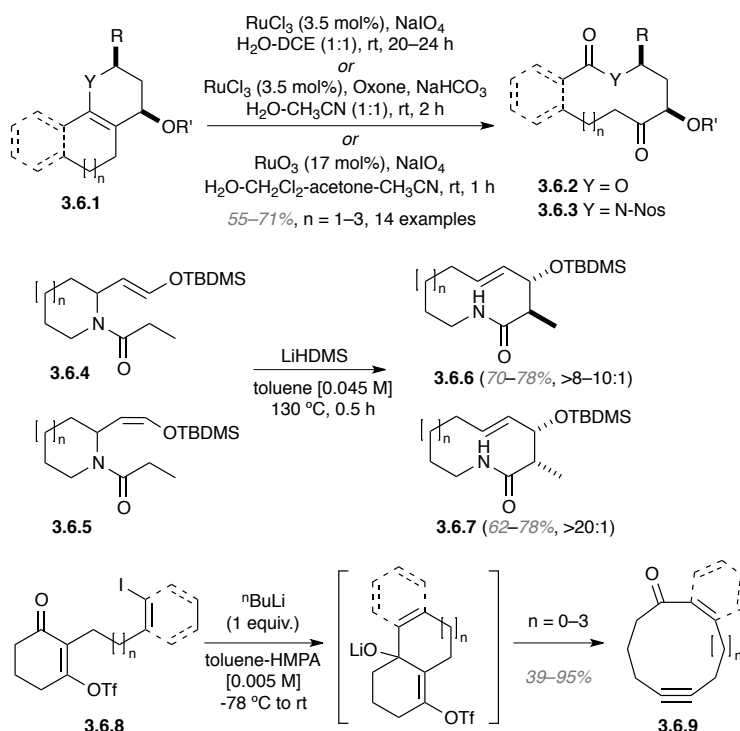
Scheme 3.5. Ring expansion/opening chemistry towards macrocyclic products



In addition to the previously mentioned methods, a number of newer strategies have been developed to access more complex and diversified structures. In this regard, in 2012, Tan and coworkers developed an oxidative ring expansion using polycyclic precursors in a diversity-oriented approach to provide macrolactones **3.6.2** or

macrolactams **3.6.3**.⁷⁵ In 2011, Suh and coworkers utilized readily prepared, smaller exocyclic lactam-containing precursors to generate functionalized macrolactams **3.6.6** and **3.6.7** via aza-Claisen rearrangement.⁷⁶ In 2011, Dudley and coworkers used a reductive cyclization, followed by a ring-expanding fragmentation, en route to cyclic alkynyl ketones **3.6.9** (Scheme 3.6).⁷⁷

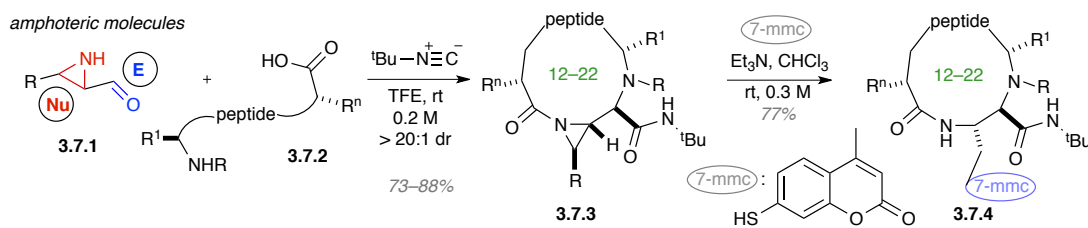
Scheme 3.6. Macrocyclic compounds from different ring expansion/opening chemistries.



Finally, in 2010, Yudin and co-workers reported a high yielding macrocyclization process to generate challenging medium and large-sized cyclic peptide products with high diastereoselectivity and no dimerization or oligomerization products.⁷⁸ In this approach (Scheme 3.7), a multi-component Ugi-type reaction was utilized in a macrocyclization of linear peptides enabled by amphoteric aziridine aldehydes, which consists of both nucleophilic and electrophilic sites on a molecule. Investigations began

with nucleophilic aziridine aldehydes **3.7.1** as core building blocks together with a range of amino acids **3.7.2** and *tert*-butyl isocyanide in trifluoroethanol to provide the desired cyclic peptide products **3.7.3** in good yields with varying peptide chain lengths, as it affects the reaction outcome in terms of selectivity. Gratifyingly for the authors, the medium and large-sized rings were readily synthesized. In addition, the authors found that the resulting cyclic products which incorporated an activated aziridine ring, provided a valuable point for conjugation to different side chains *via* nucleophilic ring-opening, for example, the commonly used fluorescent tag 7-mercapto-4-methyl-coumarin (7-mmc) was attached in a site-specific manner to the cyclic peptides at a late stage of the synthesis, as shown in Scheme 3.7.

Scheme 3.7. *Macrocyclic compounds from MCR Ugi-type reaction*



3.1.3 Importance of Stereochemically (sp^3)-Rich Molecules

Since the introduction of the Lipinski “rule of 5” guidelines,⁷⁹ the medicinal chemistry community has become more aware of the value of these physical properties of potential drug candidates. These properties include molecular weight (MW), topological polar surface area (pTSA), rotatable bonds and hydrogen bond donors and acceptors. These properties are not only incorporated to the medicinal chemistry dictionary but are also often used in ADME prediction models.⁸⁰ Resulting from these properties was the

shift to high-throughput synthesis of compounds over the past years that may have given an inclination for molecules to fail by directing discovery efforts toward achiral, aromatic compounds. As such, two simple and interpretable measures of the complexity of molecules prepared were hypothesized in relation to the potential of drug candidates. The first is carbon bond saturation as described by fraction sp^3 (F_{sp^3}) where $F_{sp^3} = (\text{number of } sp^3 \text{ hybridized carbons} / \text{total carbon count})$ (Figure 3.6). The second is whether or not a chiral carbon exists in the molecule. Considering both aspects [e.g. carbon bond saturation (as measured by F_{sp^3}) and the presence of chiral centers], is now deemed important when associated with potential success, as compounds transition from discovery, through clinical testing to drugs.⁹ Judicial use of these parameters may permit the generation of architecturally more complex molecules, as well as more chemically diverse space, without increasing the molecular weight considerably. This point is brought to light by looking at two simple examples outlined in Figure 3.6, whereby dimethyl pyridine has only five possible isomers, in contrast to the saturated structure of dimethylpiperidine, possessing two stereogenic centers, which is able to accommodate up to 34 isomers (Figure 3.6).

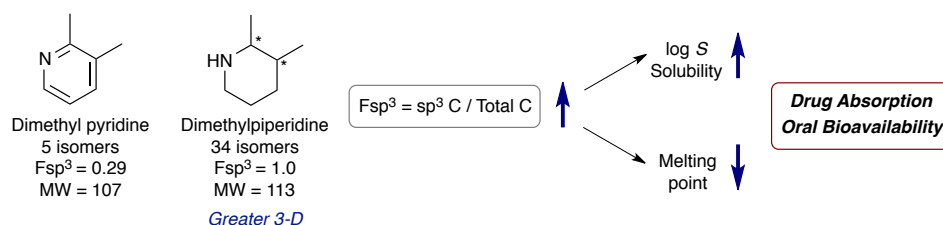


Figure 3.6. Comparison between isomers of dimethyl pyridine and dimethylpiperidine.

In addition to an increase in diversity, increasing sp^3 character may also improve other molecular properties that contribute to clinical success. Two recent studies⁸¹

substantiate this claim, as well as the medicinal chemistry belief⁸² that reducing the aromatic character of a molecule might improve physical characteristics, namely solubility. Using the formula provided, investigations were executed to interpret that highly complex molecules, as measured by saturation, increased the likelihood of higher solubility and lower melting points. As such, if the compounds have appropriate values for these properties, they will be more likely to succeed as drugs. The presence of stereocenters, another descriptor for complexity, also increases the likelihood.

In addition to higher solubility and lower melting points, saturation and presence of stereocenters also allow more complex molecules to access larger chemical space, which leads to a greater probability to identify compounds that better complement the spatial intricacies of target proteins (Figure 3.7). Other properties that influence the shape complementarity between ligands and its binding site are as follow: (a) size, a molecule needs to have an appropriate size to enter the binding pocket, (b) shape, a molecule needs to be able to exhibit a comparable shape to prevent clashes with the protein, and (c) electrostatics, whereby a molecule needs to ensure ideal positioning of its functional groups in the molecular setting to finally establish the essential electrostatic complementarity with the target protein (Figure 3.7).⁸³

The molecular properties of drug molecules were first introduced in Chapter 1, and further illustrated in the current section, suggesting that the molecular descriptors portray a pivotal role when small-molecule is *en route* to a potential druggable compound. With the desired molecular properties in hand, there is a higher probability of achieving high impact small-molecule hits through a high-throughout screening platform

and thus reaching a hit identification to lead optimization and beyond process. Hence, there is the growing need to incorporate all the relevant properties when designing the synthetic methods to generate unique small-molecules.

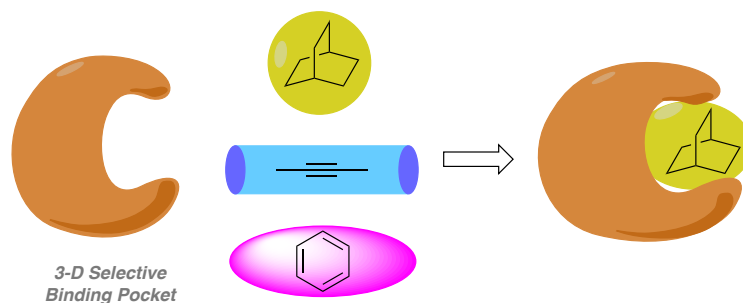


Figure 3.7. Shape complementarity of ligands and 3D binding pocket of target protein.

3.2 Complementary Amphiphile Pairing (CAP) and Complementary Pairing (CP) Strategies to Benzofused Sultams

As described in Chapter 2 and Section 3.1, sulfonamides⁸⁴ and sultams are unnatural and less prevalent in the literature, but have been found to exhibit some biological activities. Despite advances in the field,⁸⁵ methods to generate medium- to large-sized lactams and sultams remain a challenge.

Previously, our group has reported two strategies termed complementary pairing (CP) and complementary amphiphile pairing (CAP)⁸⁶ for the synthesis of skeletally diverse common ring sultams (5–7 membered rings) in a modular and efficient fashion. As shown in Figure 3.8A, CP involves simple coupling of *bis*-electrophile components reacting with complementary *bis*-nucleophiles, namely amino alcohols or amines. In contrast, CAP strategies unite a pair of amphiphilic compounds—possessing both electrophilic and nucleophilic components—in a synergistic complementary manner. On a similar note, Yudin and co-workers have developed amphoteric molecules (amphiphiles)

such as aziridine aldehydes that contain a nucleophile and electrophile on the same molecule (Figure 3.8B).⁷⁸ A high yielding macrocyclization of linear peptides using aziridine aldehydes as core building block under mild conditions were reported, which afforded medium and large-sized rings with high diastereoselectivity and no dimerization or oligomerization byproducts. The nucleophilic aziridine functionality is retained in their synthesis, whereas our current work of activated electrophilic sulfonyl aziridine opens up upon reacting with nucleophiles to generate cyclic scaffolds in an atom-economical fashion.

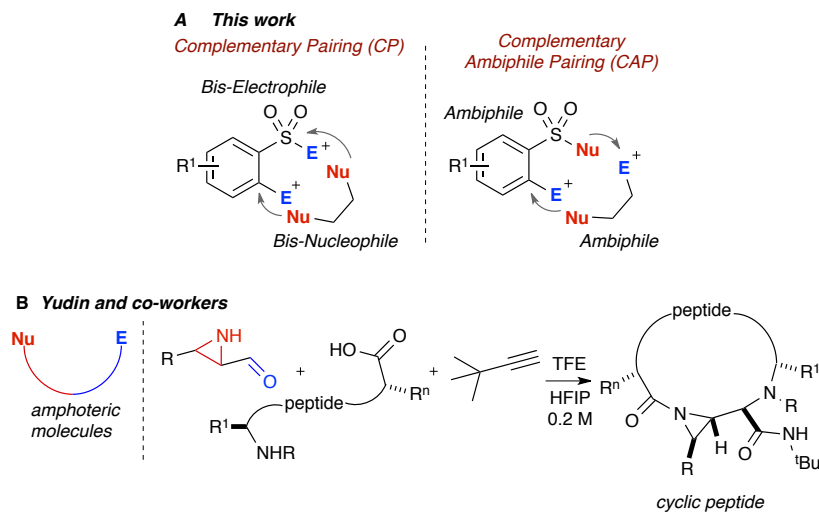


Figure 3.8. CP, CAP and amphoteric molecules.

We have previously investigated and reported the use of *o*-haloaryl sulfonyl chlorides in a number of CP/CAP strategies, including: CP ‘4+1’,⁸⁷ CP ‘3+4’,⁸⁸ CAP ‘4+3’,^{86a} CAP ‘4+4’,^{86b} and lastly CP/CAP reaction pairing⁸⁹ to generate a variety of bridged and benzofused sultams (Figure 3.9). Based on these studies, we sought to expand the scope to another unique class of *bis*-electrophiles, namely, heretofore unknown *o*-fluoroaryl-sulfonyl aziridines for use in pairing to *bis*-nucleophilic

counterparts, such as amino alcohols, as well as consecutive coupling with primary amines.⁹⁰ We envisioned complementary pairing of activated sulfonyl aziridines (simple 6-atom bis-electrophilic synthon) *via* "chemo- and regioselective" ring-opening by the amino component of the amino alcohol (*bis*-nucleophiles) and subsequent S_NAr cyclization with the alcohol component to furnish unprecedented, functionally rich medium-sized benzofused sultams in a chemoselective "6+4" and "6+5" heterocyclization pathways. Moreover, we envisioned the use of *o*-fluoroaryl-sulfonyl aziridines to generate complex 7-membered benzofused sultams via "6+1" atom cyclization sequence, when primary amines are utilized for sulfonyl aziridine ring-opening and the resulting secondary amines cyclize via a subsequent S_NAr reaction (Figure 3.9).

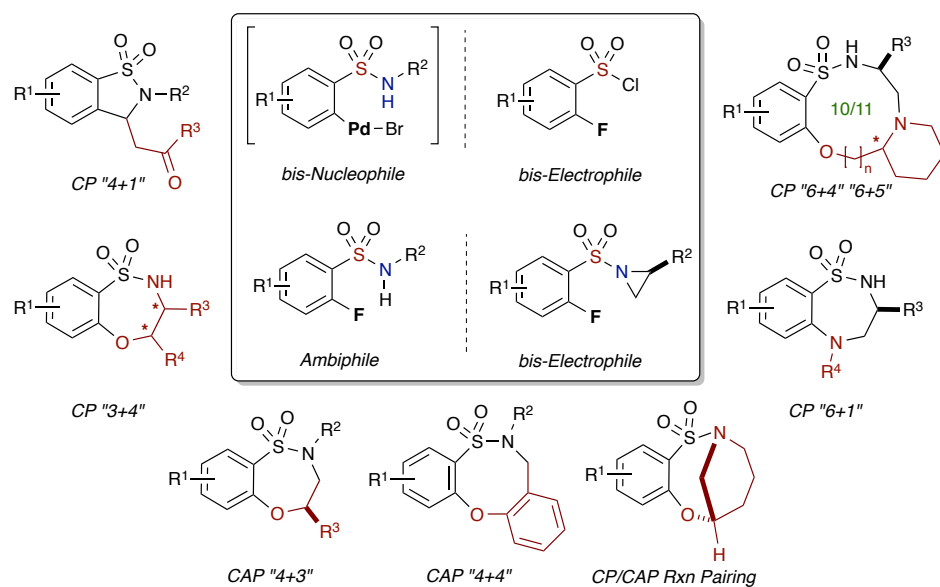


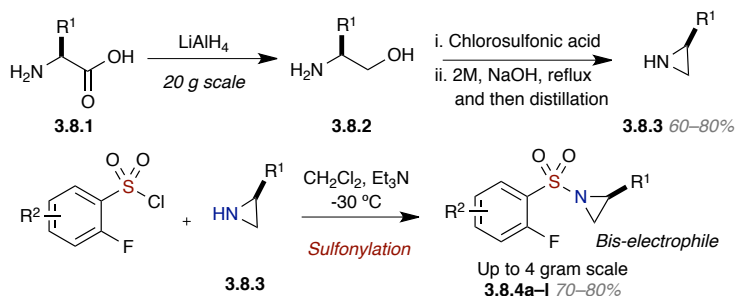
Figure 3.9. Summary of CP and CAP routes to benzofused sultams.

3.3 Results and Discussion

3.3.1 Optimization Studies

The titled investigation commenced with the preparation of chiral aziridines **3.8.3** *via* a mild Wenker synthesis⁹¹ from the respective amino alcohols, with all preparations occurring in excellent yields. Sulfonylation of aziridines with *o*-fluorobenzene sulfonyl chlorides furnished a variety of 1-((2-fluorophenyl)sulfonyl)aziridines **3.8.4a–l** in good yields ranging from 70–80% (Scheme 3.8). The variety of sulfonyl aziridines can be observed from the sultams constructed *via* the reported methodology.

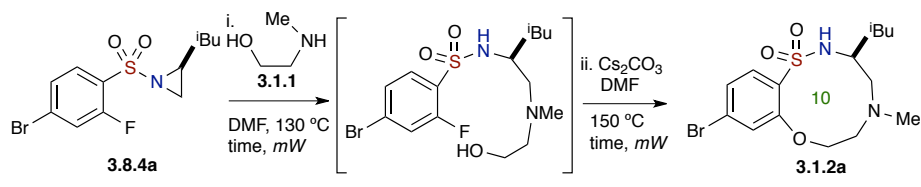
Scheme 3.8. Generation of various aziridines *via* Wenker synthesis and sulfonylation of the derived aziridines



Studies on the one-pot, sequential process began with (*S*)-1-((4-bromo-2-fluorophenyl)sulfonyl)-2-isobutylaziridine **3.8.4a** (aziridine ring-opening), which was reacted with *N*-methylethanolamine **3.1.1** (1.2 eq.) in DMF at 130 °C, using microwave (*mW*) irradiation for 30 mins (Table 3.1, entry 1). The reaction was monitored by TLC and upon disappearance of starting material—Cs₂CO₃ (2.5 eq.) was added to the crude mixture. The mixture was next subjected to 30 additional min. of *mW* irradiation at 150 °C in order to facilitate the S_NAr reaction, and ultimately afford the desired benzo-oxathiadiazecine 1,1-dioxide **3.1.2a** in moderate yield (43% over 2 rxns; 66% avg/rxn).

With this result in hand, optimization of reaction conditions was carried out. Notably, it was found that solvent concentrations, reaction time and temperature were key factors since the aziridine ring-opening and S_NAr reactions are inter- and intramolecular pathways, respectively. In particular, increased reaction time and temperature were found to effect reaction decomposition. It should also be noted that the first reaction (aziridine ring-opening) was carried out under relatively high concentrations, while the subsequent intramolecular S_NAr reactions required dilute concentrations (Table 3.1, entries 3–5). Furthermore, it should also be noted that while aziridine ring-opening proceeds at rt, the reaction took 5 days to go to completion; while utilization of *mW* irradiation allowed for completion of reaction in 30 mins. Efforts to improve this reaction by screening other bases for instance CsF, K_2CO_3 , K_3PO_4 , DBU and NaH revealed that use of Cs_2CO_3 was optimal. After thorough investigation, the optimized conditions for this one-pot, sequential aziridine ring-opening– S_NAr protocol were achieved, whereby, arylsulfonyl aziridine **3.8.4a** and amino alcohol **3.1.1** were subjected to *mW* irradiation in DMF at 130 °C for 30 mins and 150 °C for 40 mins, respectively. This led to 10-membered sultam **3.1.2a** in good yield (66% over 2 rxns; 81% avg/rxn) (Table 3.1, entry 5). The structure of sultam **3.1.2a** was confirmed by X-ray crystallographic analysis (Figure 3.10). This set of optimized conditions was also utilized for the synthesis of 7-membered benzofused sultams, with some substrates having a shorter reaction time for S_NAr cyclization.

Table 3.1. Optimization of reaction conditions



entry ^c	conc (i to ii M)	time (i, ii mins)	yield (%) ^a
1	0.3	30, 30	43 ^b
2	0.3	30, 40	50 ^b
3	0.3 to 0.1	30, 40	58 ^b
4	0.3 to 0.08	30, 40	66 ^b
5	0.3 to 0.05	30, 40	34 ^b

^aFinal isolated yield over 2 reactions after flash chromatography. ^b**Aziridine-opening:** **3.8.4a** (1.0 equiv) and **3.1.1** (1.05–1.3 equiv) in DMF at 130 °C. **S_NAr:** Cs₂CO₃ (2.5 equiv) in DMF at 150 °C. ^cReactions were monitored by TLC.

As seen in the X-ray crystallographic analysis of the cyclic products shown in Figure 3.10, the preferred conformation⁹² as noted in Chapter 2 of the Ar-SO₂NR¹R² moiety is also conserved, however in this case, it renders the core macrocycle in a unique conformation, whereby the N–H bond points inward.

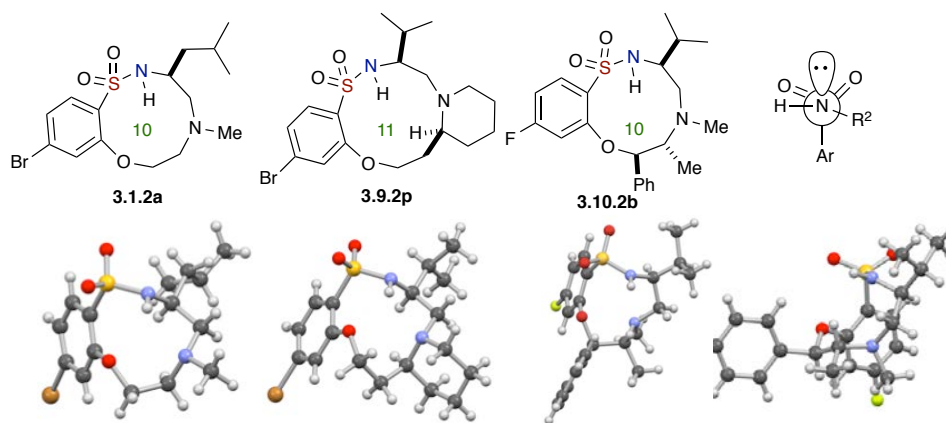
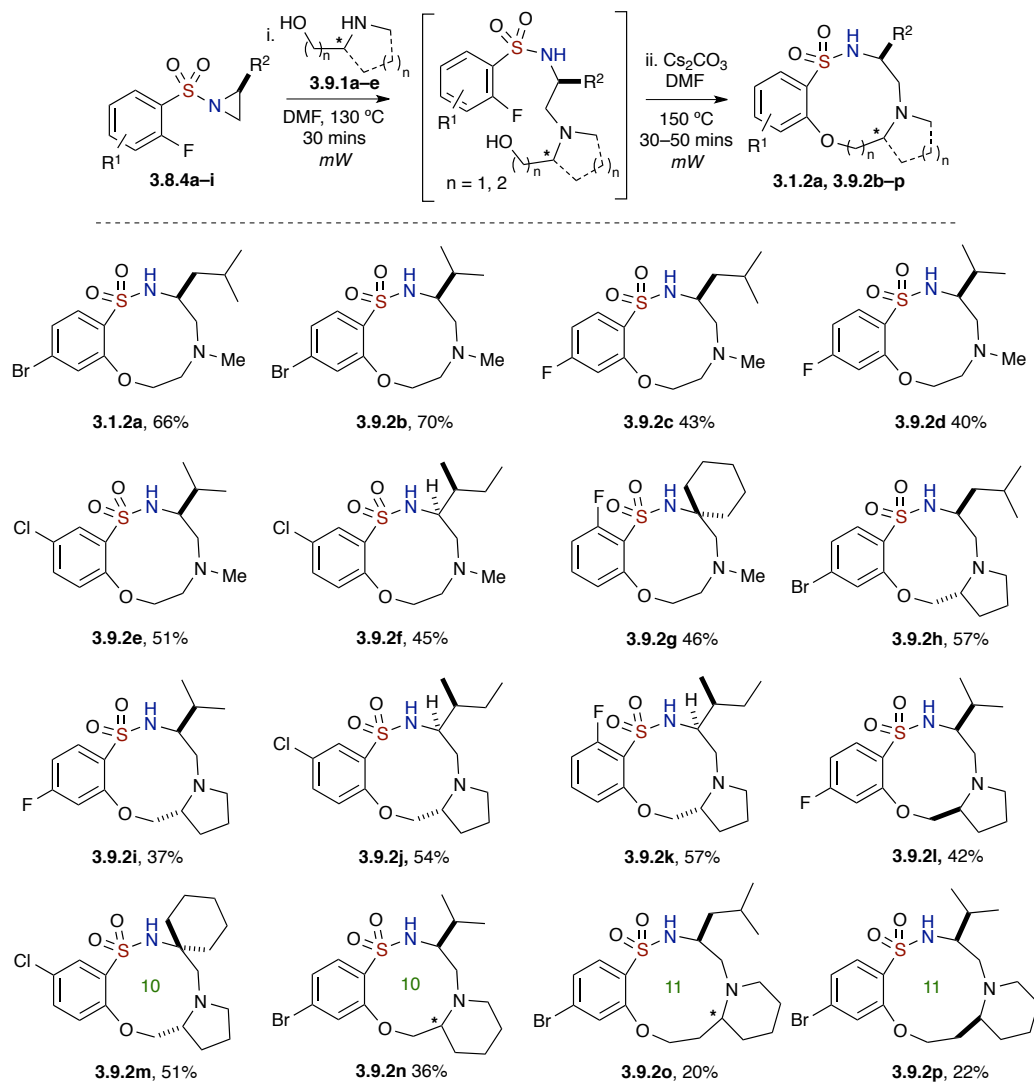


Figure 3.10. Absolute stereochemistry and structures of **3.1.2a**, **3.9.2p** and **3.10.2b**.

3.3.2 Synthesis of 10- and 11-membered Benzofused Sultams

With the optimization conditions in hand, substrate scope studies commenced with the synthesis of medium-sized, fused polycyclic and spirocyclic benzofused sultams using various secondary acyclic and cyclic amino alcohols **3.9.1a–e**, which proceeded to occur in average to good overall yields (Scheme 3.9). Notable applications include both *R* and *S*-prolinol, racemic 2-piperidinemethanol and 2-piperidine-ethanol to afford the 6,10,5-fused, 6,10,6- fused and 6,11,6-fused tricyclic systems, respectively. The synthesized structures have stereocenters on the core medium-sized rings, which consequently imparts “non-flatland” architecture. During the investigation, it was determined that by increasing the reaction time for some substrates, slightly higher yields were obtained thus, sultam **3.9.2b** was generated in 70% yield over 2 reactions (84% avg/rxn) when the reaction time for S_NAr reaction was extended to 50 mins, while maintaining all other reaction conditions (Scheme 3.9). Also, the 10-membered benzofused sultams **3.9.2g** and **3.9.2m** were synthesized from sulfonamides derived from spiro-cyclohexyl aziridine in good yields. Another interesting reaction occurred in the production of the 6,11,6-fused tricyclic sultam, **3.9.2p**, that was furnished as a single diastereomer as confirmed by X-ray crystallographic analysis (Figure 3.10, page 25), albeit it in lower yield, when racemic 2-piperidine-ethanol was utilized in the opening of non-racemic aziridine. Presumably only one of the diastereomeric intermediates underwent the S_NAr cyclization reaction, although studies confirming this are underway.

Scheme 3.9. “6+4” and “6+5” cyclization to bi- and tricyclic, 10- and 11-membered sultams

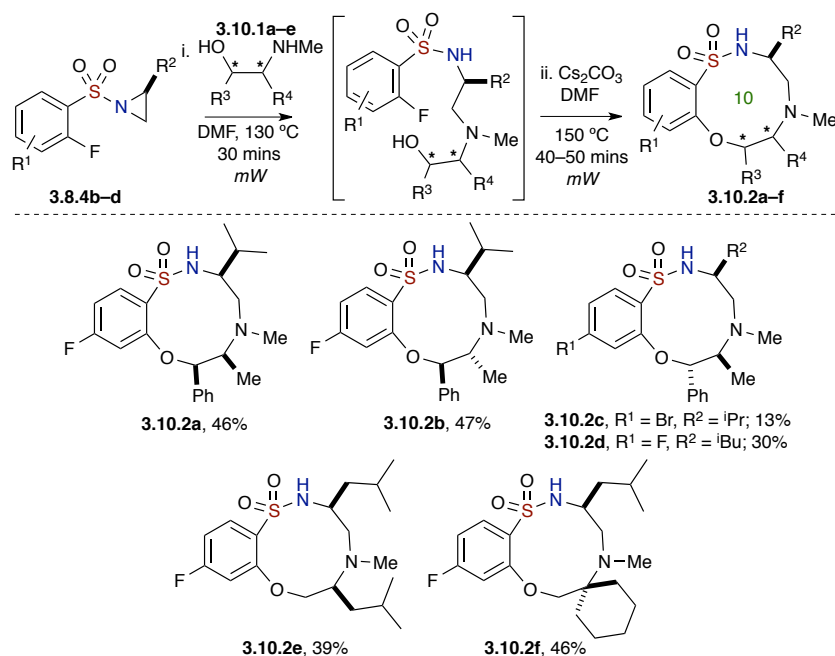


The proposed plausible mechanism for all substrates is that the secondary amino group proceeded with the aziridine-ring opening, *vide infra*, and the resulting tertiary amine which is incapable of executing a subsequent intramolecular $\text{S}_{\text{N}}\text{Ar}$ cyclization reaction, allowed the unprotected primary or secondary hydroxyl group to cyclize under basic conditions and afford the various benzo-oxathiadiazecine 1,1-dioxides.

3.3.3 Synthesis of Stereochemically-rich Benzofused Sultams

Next, we further investigated the scope of this one-pot, sequential procedure by using chiral, non-racemic, substituted secondary amino alcohols (Scheme 3.10). Derivatives of ephedrine **3.10.1a–e** were subjected to the "Click" aziridine ring-opening– S_NAr reaction conditions and to our delight, the secondary alcohols proceeded smoothly to afford medium-sized sultams (**3.10.2a–f**) in average to good yields over 2 reactions, albeit lower yield for (1*S*,2*S*)-(+)-pseudoephedrine derived **3.10.2c**. Sultam **3.10.2b** was confirmed by X-ray crystallography where the respective stereocenters (*6R*,*7R*) correspond to the structure as shown in Figure 3.10 (page 25). In addition, regardless of the substrate, both primary and branched secondary hydroxyl groups were able to undergo the aziridine-ring opening– S_NAr protocol to furnish the respective sultams. Also, use of the *N*-(methylamino) cyclohexyl methanol in the aforementioned method,

Scheme 3.10. Spiro and stereochemically-rich 10-membered sultams



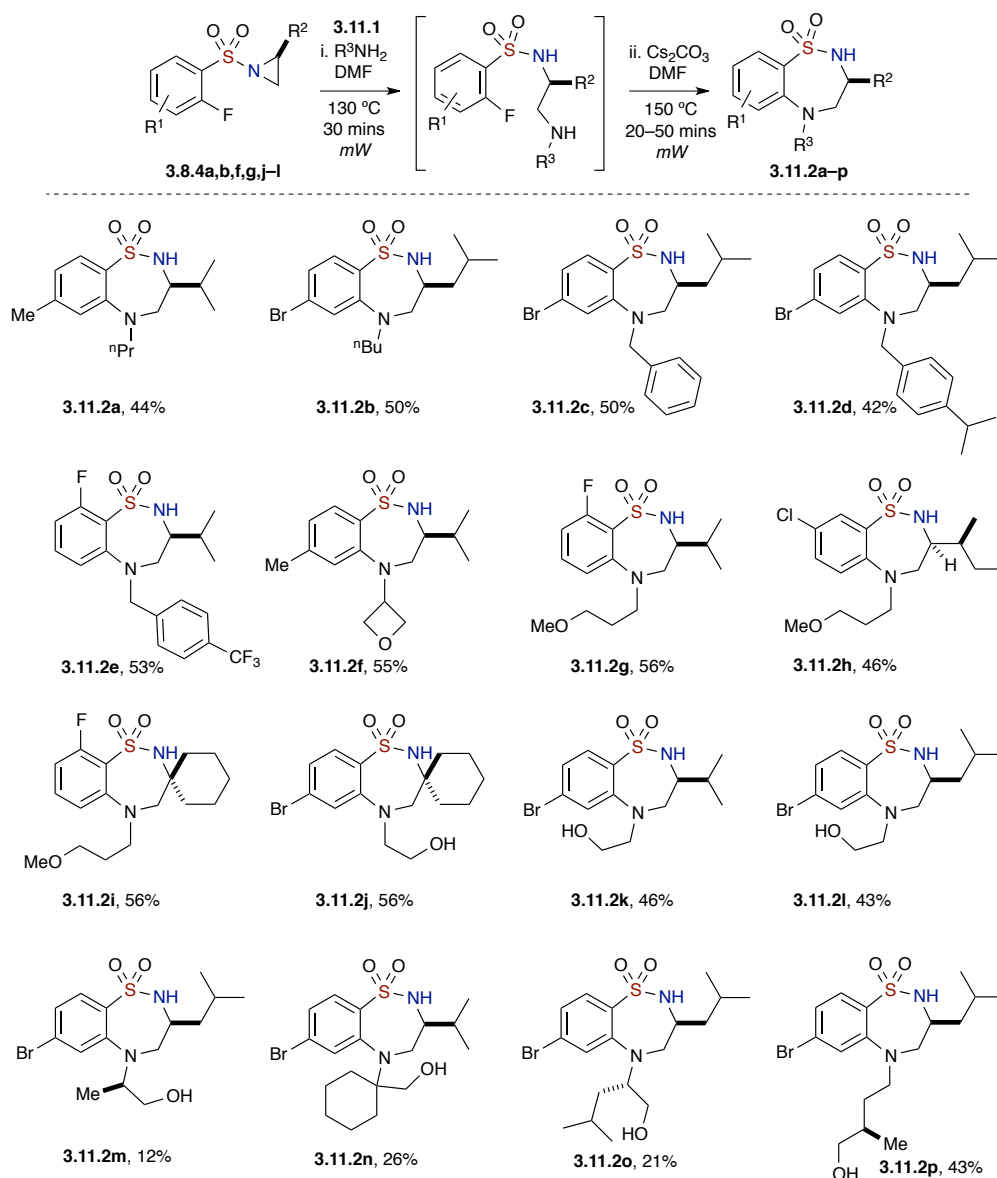
provided the spiro-benzo-oxathiadiazecine-cyclohexane 1,1-dioxide **3.10.2f** in 46% yield over 2 reactions (68% avg/rxn) (Scheme 3.10). On a similar note, secondary amino alcohols that react with the sulfonyl-aziridines generated tertiary amine-containing intermediates (incapable of intramolecular S_NAr cyclization), whereby the adjacent free secondary hydroxyl groups underwent facile cyclization to provide sultams bearing three stereogenic centers.

3.3.4 Synthesis of 7-membered Benzofused Sultams

This one-pot, sequential strategy was extended to several amines **3.11.1** whereby their dual reactivity facilitates access to 7-membered (common-sized) benzofused sultams in an overall “6+1” atom cyclization sequence involving consecutive aziridine ring-opening and intramolecular S_NAr reaction (Scheme 3.11). The use of simple alkyl and aromatic amines containing different substituents furnished benzo-thiadiazepine 1,1-dioxides **3.11.2a–3.11.2e** in satisfactory yields (44–53% over 2 rxns, 67–73% avg/rxn). Amines with both cyclic and linear ether moieties were also employed successfully to provide 7-membered benzofused sultams **3.11.2f–3.11.2i** in moderate yields (46–56% over 2 rxns, 68–75% avg/rxns). The primary amines proceeded with aziridine-ring opening and the secondary amines derived after the first reaction, were then cyclized to form cyclic sulfonamides. Similarly, common-sized benzofused sultams **3.11.2j–3.11.2p** consisting of amines having hydroxyl moieties were resulted from different aziridinyl sulfonamides (cyclohexyl, ⁱPr and ^tBu) in albeit slightly lower yields (12–56% over 2 rxns, 35–75% avg/rxn). Likewise, a plausible mechanism was proposed; when the

nucleophiles are primary amines with free hydroxyl groups, the secondary amines generated after aziridine-ring opening proceeded with the S_NAr cyclization instead of free hydroxyl groups for the formation of benzo-thiadiazepine 1,1-dioxides. A high degree of chemoselective was observed in all the cases, except formation of side-product during the S_NAr reaction and possibly decomposition of the final product.

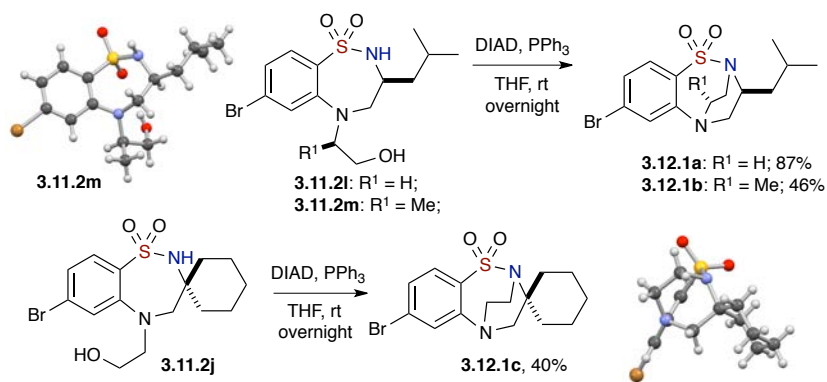
Scheme 3.11. Substrate scope of “6+1” cyclization to 7-membered benzofused sultams



3.3.5 Mitsunobu Reaction to Bridge Benzofused Sultams

An added feature of the 7-membered sultams is their ability to undergo facile and unprecedented intramolecular Mitsunobu alkylation reactions to synthesize the strained [3.2.2] bridge bicyclic sultams (Scheme 3.12). Thus, sultam **3.11.2i** was treated with PPh_3 and DIAD in THF at room temperature, stirred overnight and upon completion, provided ethanobenzo-thiadiazepine 1,1-dioxide **3.12.1a** in 87% yield. The structure of sultam **3.11.2m** was confirmed by X-ray crystallography and shown to display an optimal positioning of the hydroxyl group on order to participate in facile Mitsunobu alkylation to afford sultam **3.12.1b** bearing a two-carbon bridgehead. Further demonstration of this notable intramolecular Mitsunobu reaction was realized in the production of the spiro-cyclohexyl-containing [3.2.2] bridged benzofused sultam **3.12.1c**, albeit in a lower yield of 40%. The structure was confirmed by X-ray crystallographic analysis (Scheme 3.12).

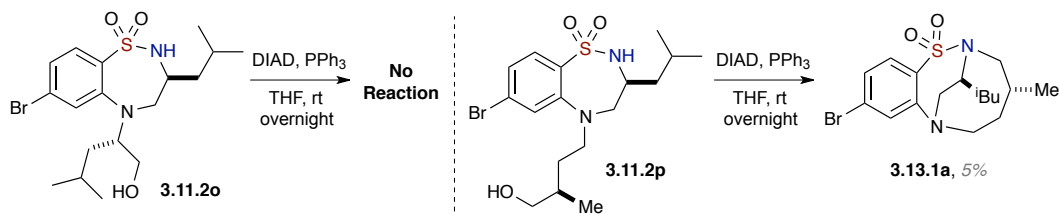
Scheme 3.12. Utilization of the Mitsunobu reaction to access bridged, 7-membered sultams



In contrast, the more sterically hindered sultam **3.11.2o** was unsuccessful in yielding the two-carbon bridged sultam after several attempts using similar reaction conditions (Figure 3.13). The recovery of starting material, several side-products present

in the various Mitsunobu reaction attempts, as well as excess reagents that were used in the reaction, were isolated. While sultam **3.11.2o** was unsuccessful, a unique [4.3.2] bridged, 9-membered benzofused sultam **3.13.1a** was observed when hydroxyl-containing sultam **3.11.2p** underwent the intramolecular Mitsunobu reaction with the same reaction conditions, albeit a much lower yield of 5% was obtained (Scheme 3.13).

Scheme 3.13. Utilization of the Mitsunobu reaction to access [4.3.2] bridged 9-membered benzofused sultam



3.3.6 ¹⁹F NMR of Benzenesulfonamides Intermediates

A key finding during these studies was the isolation of the intermediate, aziridine-ring-opened product, which was observable using ¹⁹F NMR as detailed in Figure 3.11. In this experiment, aziridinyl-sulfonamide **A** was chosen and shown to contain a single resonance (triplet) in the ¹⁹F NMR spectrum (Figure 3.11.A). Reaction with racemic 2-piperidinemethanol furnished the ring-opened intermediate **B**, which was detected as a single resonance (triplet) in the ¹⁹F NMR spectrum (Figure 3.11.B) but shifted upfield marginally due to the electronic changes within the molecule. After S_NAr reaction, the ¹⁹F NMR of the desired product **C** was obtained and shown to have complete absence of any fluorine resonances (Figure 3.11.C). As this particular *bis*-nucleophile is racemic, only one favored diastereomeric intermediate from the aziridine-ring opening would

generate the cyclic product, resulting in slightly lower yield (36% over 2 rxns, 60% avg/rxn).

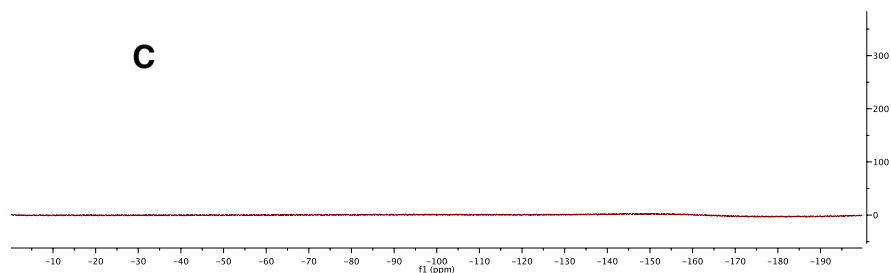
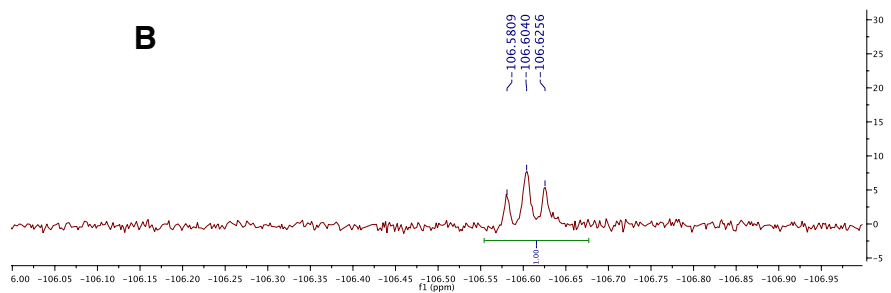
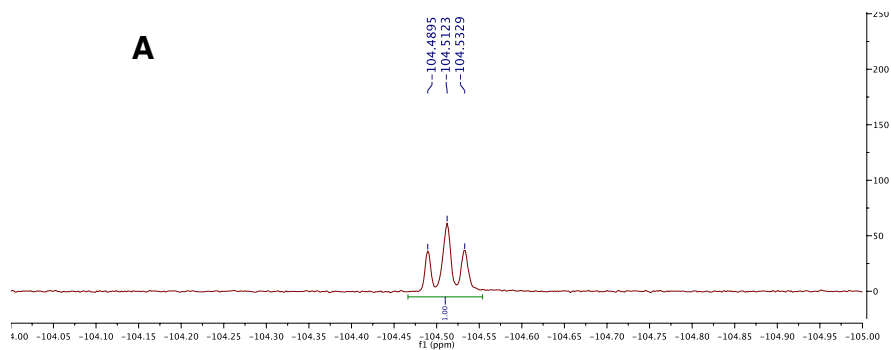
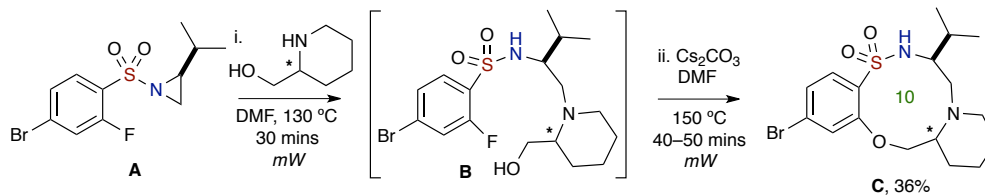
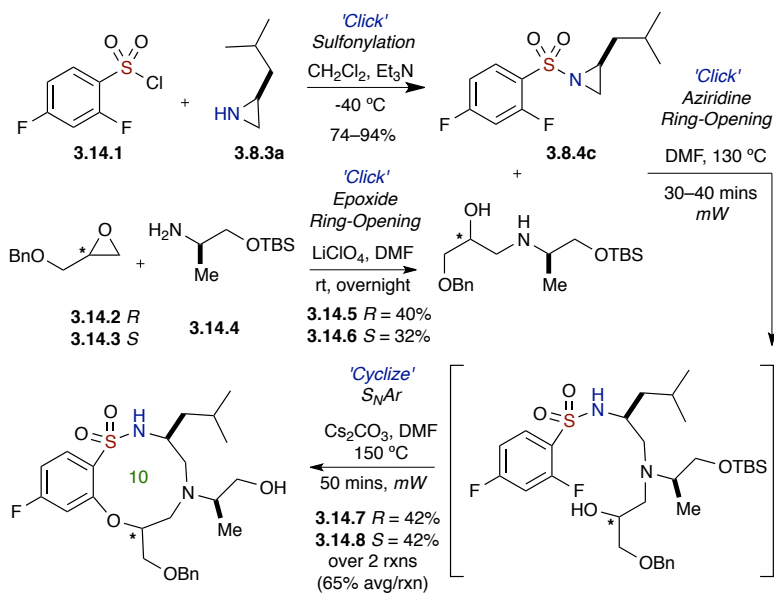


Figure 3.11. ^{19}F NMR studies: comparison of sulfonamide **A**, ring-opened **B** and product **C**.

3.3.7 “Click, Click, Click, Cyclize” to Stereochemically-rich, 10-membered Benzofused sultams

Encouraged by these results, efforts were focused toward the extension of the method using distinct building blocks that were obtained in one step (Scheme 3.14). Hence, both *R*- and *S*-benzyl glycidyl ethers were subjected to "Click" epoxide ring-opening⁹⁰ with TBS-protected *D*-alaninol, to furnish elaborate amino alcohols **3.14.5** and **3.14.6**. These chiral, non-racemic building blocks were then utilized in the established aziridine ring-opening– S_NAr procedure to afford 10-membered sultams **3.14.7** and **3.14.8** bearing three stereogenic centers, along with pendant free hydroxy group, in moderate yields. In addition, it should be noted that the displaced fluoride anion in the intramolecular S_NAr reaction served an additional role by deprotecting the TBS-ether, thus representing an overall atom economical one-pot, sequential aziridine ring-opening– S_NAr –desilylation protocol.

Scheme 3.14. “Click, Click, Click, Cyclize” to stereochemically-rich, 10-membered sultams



3.3.8 Principal Moments of Inertia (PMI) Analysis

The small strained macrocycles denoted an intriguing region of chemical space that can be difficult to access chemically. As so, principal moments of inertia (PMI) analyses as developed by Sauer and Schwarz⁹³ were computed to quantify more rigorously the chemical space that the common and medium-sized sultams might occupy, which was employed herein to assess the molecular diversity. PMI analysis utilizes shape-based descriptors: the minimum energy conformation of each compound is determined, PMI ratios are calculated and normalized, and a subsequent triangular plot depicts the shape diversity of the library. The analysis reveals that the 7-membered and 10/11-membered benzofused sultams generally mirror the shape distribution of the set of FDA approved drugs (Figure 3.12), thus demonstrating the potential drug-likeness of the scaffolds. The most populated region has the majority of sultams as well as the hybrid region, which is the center of the triangular plot, and contains some of the 10/11-membered sultams. In addition, the area also has lesser unpopulated regions of chemical

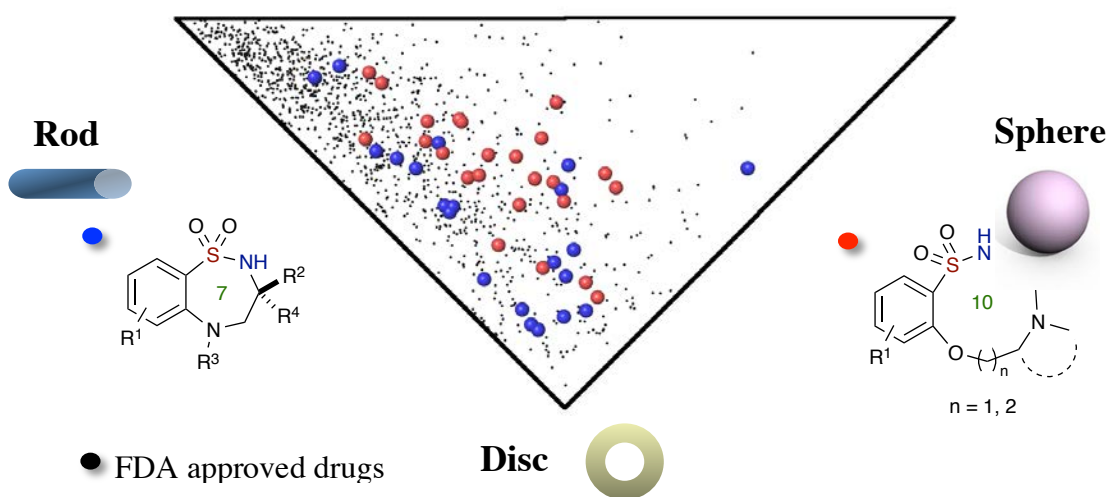


Figure 3.12. Distribution of 7-membered and 10/11-membered sultams vs FDA-approved drugs.

space, illustrating the novel nature of some FDA-approved drugs, as well as sultams generated in this method, from the perspective of molecular shape.

In addition, a second analysis was tabulated, plotted against medium to large-sized rings (10- to 14-membered rings) extracted from the ZINC database (Figure 3.13).⁹⁴ Although these compounds are not necessarily drugs, they could be utilized as probes or leads in different screens. The presence of these molecules in the ZINC database is an indication that there is also demand for such analyses, which further substantiates that macrocyclic-based drug discovery/development, is a recently evolving field. With similar calculations in Figure 3.12, the plot demonstrates that 10- to 14-membered rings in the database are relatively widespread in terms of chemical space, suggesting they are not necessarily a specified shape. Upon comparison, both the 7- and 10-/11-membered benzofused sultams are also outspread, parallel to the rings extracted from the database. The compounds are located in both the populated and underrepresented regions, signifying their diverse molecular shape distribution.

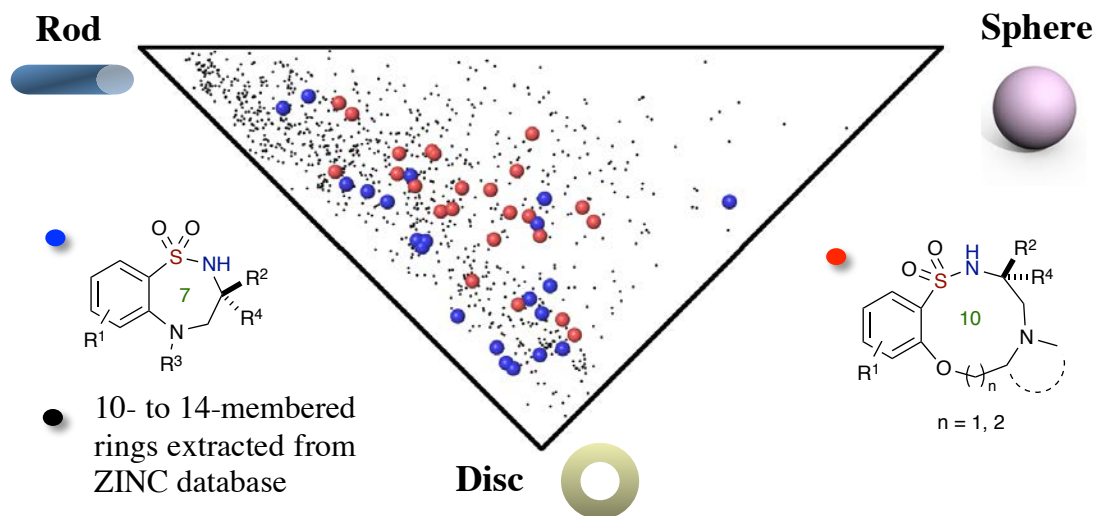


Figure 3.13. Distribution of 7-membered and 10/11-membered sultams versus 10- to 14-membered rings from ZINC database.

3.3.9 Overlay Analysis⁹⁵

The overlay produced for the sultam scaffolds reported herein is depicted in Figure 3.14 and provides a simple indication of the diversity and shape distribution evident in this library. The peripheral spatial variation seems to be portraying a non-trivial role in the shape-diversity although the critical source of diversity comes from the core. Both sources of diversity are interrelated as the cores have sufficient torsional flexibility that varying the side chains can influence the core backbone orientation. Hence, the orientations in Figure 3.14iii and 3.14v collectively suggest that the 7-membered sultams (benzo[*f*][1,2,5]-thiadiazepine 1,1-dioxides) have a good combination of elongated (rod-like) and flat (disc-like) structures, depending on the substituents extending out from the conserved core, benzofused rings. Also, the orientations in Figures 3.14iv and 3.14vi together, propose a likewise scenario, although the 10-membered sultams (benzo[*b*][1,4,5,8]oxathia-diazecine 1,1-dioxides, benzo[*b*]pyrrolo[1,2-*h*][1,4,5,8]oxathiadiazecine 8,8-dioxides and benzo[*b*]-pyrido[1,2-*h*][1,4,5,8]oxathiadiazecine 5,5-dioxide and benzo[*b*]-pyrido[1,2-*h*][1,4,5,8]-oxathiadiazacycloundecine 5,5-dioxides) are more hybrid, where it is a good mixture of elongated, flat and sphere-like characteristics than the 7-membered scaffolds. By varying the substituents or ring sizes, it can influence the shape as seen in Figure 3.14vi where some motifs are covering different space than others. The distribution of functional substituents across angles spanning some parts of the whole sphere surrounding the conserved core, suggests that the two sets of compounds as a whole achieves a reasonable level of shape-based diversity.

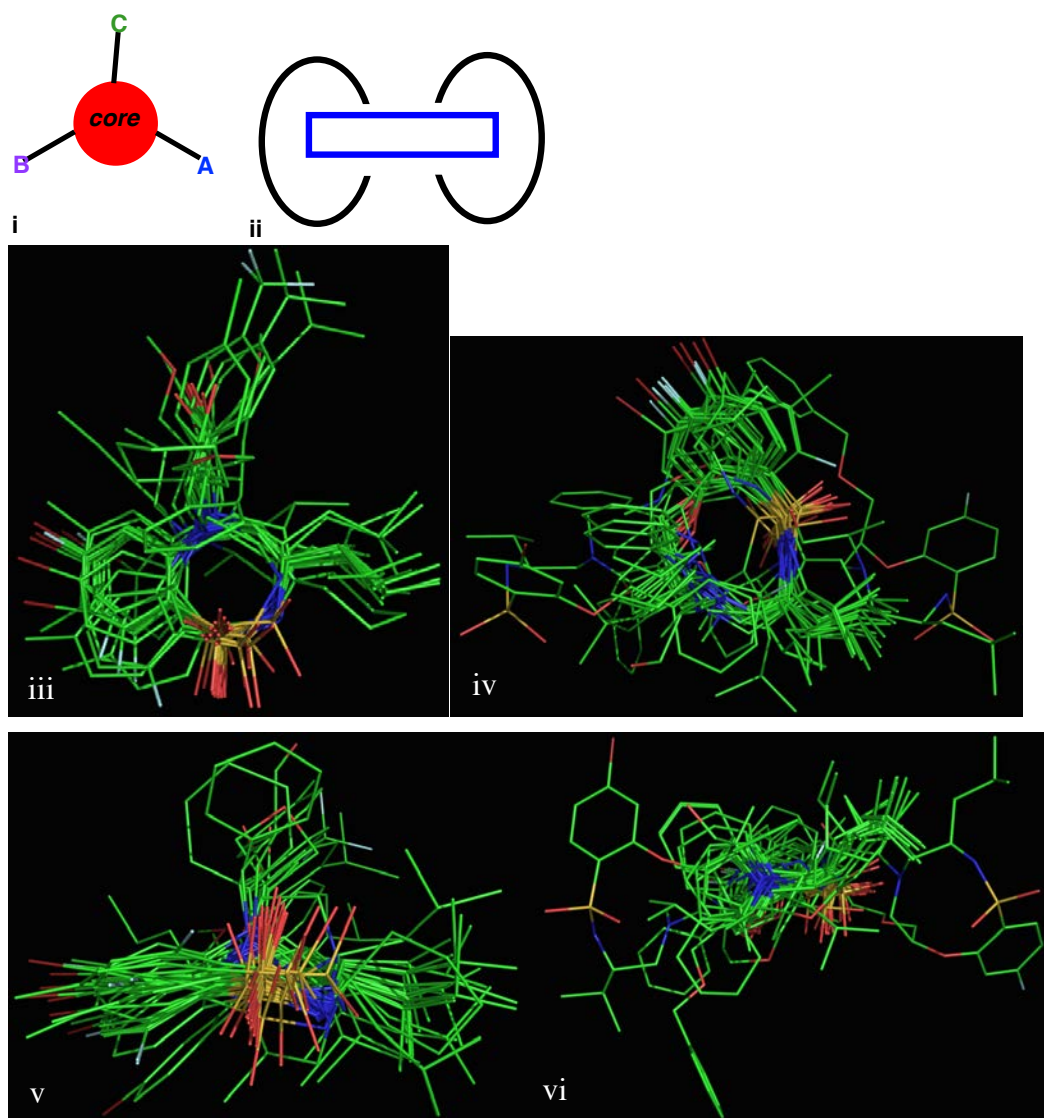


Figure 3.14. (i) Simple cartoon of the library compounds, with a core of MW ~ 150–193, based on Lipinski's rules (MW < 500), and comprising three substituents, each having MW < 180, to establish different functional groups. (ii) This cartoon demonstrates that the substituents extend out of the core in a circular motion. (iii) and (iv) both overlay images exhibiting the conserved core of 7-membered and 10-membered sultams respectively. (v): 7-membered and (vi): 10-membered, both overlay images revealing that the substituents are extending outwards in a semi-circular or circular motion as mentioned in (ii).

3.4 Summary and Outlook

In summary, we have developed a one-pot, CP strategy introducing the 1-((2-fluoroaryl)sulfonyl)aziridine building block as a versatile *bis*-electrophilic species for reaction with amino alcohols/amines for the preparation of common and medium-sized benzofused sultams containing up to three stereogenic centers. This approach was extended to the utilization of elaborate chiral, non-racemic building blocks as well as cyclic and spirocyclic amino alcohols to afford a diverse array of polycyclic scaffolds. Furthermore, the method is highly modular and adaptable for the preparation of sultam libraries in an atom economical, one-pot, sequential manner. Work in this regard is underway and will be reported in due course.

3.5 References cited

- [1] For reviews, see (a) Nubbemeyer, U. Synthesis of Medium-Sized Ring Lactams. *Top. Curr. Chem.* **2001**, *216*, 125–196 and references cited therein. (b) Sharma, A.; Appukkuttan, P.; Van der Eycken, E. Microwave-assisted synthesis of medium-sized heterocycles. *Chem. Commun.* **2012**, *48*, 1623–1637 and references cited therein. For recent methods, see (c) Bogdan, A. R.; Jerome, S. V.; Houk, K. N.; James, K. Strained Cyclophane Macrocycles: Impact of Progressive Ring Size Reduction on Synthesis and Structure. *J. Am. Chem. Soc.* **2012**, *134*, 2127–2138.
- [2] (a) McGeary, R. P.; Fairlie, D. P. Macrocyclic peptidomimetics: potential for drug development. *Curr. Opin. Drug Discovery Dev.* **1998**, *1*, 208–217. (b) Driggers, E. M.; Hale, S. P.; Jinbo Lee, J.; Terrett, N. K. The exploration of macrocycles for drug discovery—an underexploited structural class. *Nat. Rev. Drug Discovery* **2008**, *7*, 608–624. (c) Marsault, E.; Peterson, M. L. Macrocycles Are Great

Cycles: Applications, Opportunities, and Challenges of Synthetic Macrocycles in Drug Discovery. *J. Med. Chem.* **2011**, *54*, 1961–2004. (d) Mallinson, J.; Collins, I. Macrocycles in new drug discovery. *Future Med. Chem.* **2012**, *4*, 1409–1438. (e) Marsault, E. Macrocycles as templates for diversity generation in drug discovery. In *Diversity-Oriented Synthesis*; Trabocchi, A. Ed.: John Wiley & Sons, Inc., **2013**; pp 253–287. (f) Vendeville, S.; Cummings, M. D. Synthetic Macrocycles in Small-Molecule Drug Discovery. *Annu. Rep. Med. Chem.* **2013**, *48*, 371–386. (g) Giordanetto, F.; Kihlberg, J. Macrocyclic Drugs and Clinical Candidates: What Can Medicinal Chemists Learn from Their Properties? *J. Med. Chem.* **2014**, *57*, 278–295. (h) Hussain, A.; Yousuf, S. K.; Mukherjee, D. Importance and synthesis of benzannulated medium-sized and macrocyclic rings (BMRs). *RSC Adv.* **2014**, *4*, 43241–43257 and references cited therein.

- [3] (a) Wessjohann, L. A.; Ruijter, E. Strategies for Total and Diversity-Oriented Synthesis of Natural Product(-Like) Macrocycles *Top. Curr. Chem.* **2005**, *243*, 137–184. For selected examples of heterocycles derived from target-oriented, see: (b) Lou, L.; Qian, G.; Xie, Y.; Hang, J.; Chen, H.; Zaleta-Rivera, K.; Li, Y.; Shen, Y.; Dussault, P. H.; Liu, F.; Du, L. Biosynthesis of HSAF, a Tetramic Acid-Containing Macrolactam from *Lysobacter enzymogenes*. *J. Am. Chem. Soc.* **2011**, *133*, 643–645. (c) Yang, S.; Xi, Y.; Zhu, R.; Wang, L.; Chen, J.; Yang, Z. Asymmetric Total Syntheses of Ansamacrolactams (+)-Q-1047H-A-A and (+)-Q-1047H-R-A. *Org. Lett.* **2013**, *15*, 812–815. (d) Floss, H. G.; Yu, T.-W. Rifamycins Mode of Action, Resistance, and Biosynthesis. *Chem. Rev.* **2005**, *105*, 621–632. For selected examples of heterocycles derived from diversity-oriented, see: (e) Bauer, R. A.; Wenderski, T. A.; Tan, D. S. Biomimetic diversity-oriented synthesis of benzannulated medium rings via ring expansion. *Nat. Chem. Biol.* **2013**, *9*, 21–29. (f) Hussain, A.; Yousuf, S. K.; Sharma, D. K.; Mallikharjuna Rao, L.; Singh, B.; Mukherjee, D. Design and synthesis of carbohydrate based medium sized sulfur containing benzannulated macrocycles: applications of

Sonogashira and Heck coupling. *Tetrahedron* **2013**, *69*, 5517–5524.

- [4] (a) Schreiber, S. L. Target-Oriented and Diversity-Oriented Organic Synthesis in Drug Discovery. *Science* **2000**, *287*, 1964–1969. (b) Nielsen, T. E.; Schreiber, S. L. Towards the Optimal Screening Collection: A Synthesis Strategy. *Angew. Chem., Int. Ed.* **2008**, *47*, 48–56. (c) Burke, M. D.; Schreiber, S. L. A Planning Strategy for Diversity-Oriented Synthesis. *Angew. Chem., Int. Ed.* **2004**, *43*, 46–58.
- [5] (a) Udugamasooriya, D. G.; Spaller, M. R. Conformational constraint in protein ligand design and the inconsistency of binding entropy. *Biopolymers* **2008**, *89*, 653–667. (b) Gilon, C.; Halle, D.; Chorev, M.; Selinger, Z.; Byk, G. Backbone cyclization: A new method for conferring conformational constraint on peptides. *Biopolymers* **1991**, *31*, 745–750. (c) Veber, D. F.; Johnson, S. R.; Cheng, H. Y.; Smith, B. R.; Ward, K. W.; Kopple, K. D. Molecular Properties That Influence the Oral Bioavailability of Drug Candidates. *J. Med. Chem.* **2002**, *45*, 2615–2623. (d) Adessi, C.; Soto, C. Converting a Peptide into a Drug: Strategies to Improve Stability and Bioavailability. *Curr. Med. Chem.* **2002**, *9*, 963–978.
- [6] (a) de Greef, M.; Abeln, S.; Belkasmi, K.; Dömling, A.; Orru, R. V. A.; Wessjohann, L. A. Rapid Combinatorial Access to Macrocyclic Ansapeptoids and Ansapeptides with Natural-Product-like Core Structures. *Synthesis* **2006**, *23*, 3997–4004. (b) Wessjohann, L. A. Synthesis of natural-product-based compound libraries. *Curr. Opin. Chem. Biol.* **2000**, *4*, 303–309. (c) Su, Q.; Beeler, A. B.; Lobkovsky, E.; Porco, J. A., Jr.; Panek, J. S. Stereochemical Diversity through Cyclodimerization: Synthesis of Polyketide-like Macrodiolides. *Org. Lett.* **2003**, *5*, 2149–2152. (d) Lee, D.; Sello, J. K.; Schreiber, S. L. A Strategy for Macrocyclic Ring Closure and Functionalization Aimed toward Split-Pool Syntheses. *J. Am. Chem. Soc.* **1999**, *121*, 10648–10649. (e) Ruijter, E.; Wessjohann, L. A. Macrocycles rapidly produced by multiple multicomponent

reactions including bifunctional building blocks (MiBs). *Molec. Divers.* **2005**, *9*, 159–169. (f) Clardy, J.; Walsh, C. Lessons from natural molecules. *Nature*, **2004**, *432*, 829–837. (g) Bonney, K. J.; Braddock, D. C. A Unifying Stereochemical Analysis for the Formation of Halogenated C15-Acetogenin Medium-Ring Ethers From *Laurencia* Species via Intramolecular Bromonium Ion Assisted Epoxide Ring-Opening and Experimental Corroboration with a Model Epoxide. *J. Org. Chem.* **2012**, *77*, 9574–9584. (h) Bogdan, A. R.; Jerome, S. V.; Houk, K. N.; James, K. Strained Cyclophane Macrocycles: Impact of Progressive Ring Size Reduction on Synthesis and Structure. *J. Am. Chem. Soc.* **2012**, *134*, 2127–2138. (i) Bauer, R. A.; Wenderski, T. A.; Tan, D. S. Biomimetic diversity-oriented synthesis of benzannulated medium rings via ring expansion. *Nat. Chem. Biol.* **2013**, *9*, 21–29. (j) Dow, M.; Marchetti, F.; Nelson, A. Diversity-oriented synthesis of natural product-like libraries. In *Diversity-Oriented Synthesis*; Trabocchi, A. Ed.: John Wiley & Sons, Inc., **2013**; pp 291–323 and references cited therein.

- [7] (a) Villar, E. A.; Beglov, D.; Chennamadhavuni, S.; Porco, J. A., Jr.; Kozakov, D.; Vajda, S.; Whitty, A. How proteins bind macrocycles. *Nat. Chem. Biol.* **2014**, *10*, 723–731. (b) Nero, T. L.; Morton, C. J.; Holien, J. K.; Wielens, J.; Parker, M. W. Oncogenic protein interfaces: small molecules, big challenges. *Nat. Rev. Cancer* **2014**, *14*, 248–262.
- [8] (a) Mai, A. Targeting Epigenetics in Drug Discovery. *ChemMedChem* **2014**, *9*, 415–417. (b) Knapp, S.; Weinmann, H. Small-Molecule Modulators for Epigenetics Targets. *ChemMedChem* **2013**, *8*, 1885–1891.
- [9] Bikker, J.; Humblet, C.; Lovering, F. Escape from Flatland: Increasing Saturation as an Approach to Improving Clinical Success. *J. Med. Chem.* **2009**, *52*, 6752–6756.

- [10] Evans, P. A.; Holmes, A. B. Medium Ring Nitrogen Heterocycles. *Tetrahedron* **1991**, *47*, 9131–9166.
- [11] (a) Newman, D. J.; Cragg, G. M. Bioactive macrocycles from nature. *RSC Drug Discovery Ser.* **2015**, *40*, 1–36. (b) Kudo, F.; Miyanaga, A.; Eguchi, T. Biosynthesis of natural products containing β -amino acids. *Nat. Prod. Rep.* **2014**, *31*, 1056–1073. (c) Bornhovd, E. C.; Burgdorf, W. H. C.; Wollenberg, A. Immunomodulatory macrolactams for topical treatment of inflammatory skin diseases. *Curr. Opin. Invest. Drugs* **2002**, *3*, 708–712. (d) Sharma, G. V. M.; Doddi, V. R. Macrolactones. In *Natural Lactones and Lactams*; Janecki, T. Ed.: Wiley-VCH Verlag GmbH & Co. KGaA: **2014**; pp 229–272.
- [12] Albaugh, D.; Albert, G.; Bradford, P.; Cotter, V.; Froyd, J.; Gaughran, J.; Kirsch, D. R.; Lai, M.; Rehnig, A.; Sieverding, E.; Silverman, S. Cell wall active antifungal compounds produced by the marine fungus *Hypoxylon oceanicum* LL-15G256. III. Biological properties of 15G256 γ . *J. Antibiot.* **1998**, *51*, 317–322.
- [13] (a) Xu, J.; Chen, A.; Go, M.-L.; Nacro, K.; Liu, B.; Chai, C. L. L. Exploring Aigialomycin D and Its Analogues as Protein Kinase Inhibitors for Cancer Targets. *ACS Med. Chem. Lett.* **2011**, *2*, 662–666. (b) Patocka, J.; Soukup, O.; Kuca, K. Resorcylic Acid Lactones as the Protein Kinase Inhibitors, Naturally Occurring Toxins. *Mini-Rev. Med. Chem.* **2013**, *13*, 1873–1878.
- [14] (a) De Boer, C.; Meulman, P. A.; Wnuk, R. J.; Peterson, D. H. Geldanamycin, a new antibiotic. *J. Antibiot.* **1970**, *23*, 442–447. (b) Taldone, T.; Gozman, A.; Maharaj, R.; Chiosis, G. Targeting Hsp90: small-molecule inhibitors and their clinical development. *Curr Opin Pharmacol* **2008**, *8*, 370–374.
- [15] (a) Ruan, B. F.; Zhu, H. L. The chemistry and biology of the bryostatins: potential PKC inhibitors in clinical development. *Curr. Med. Chem.* **2012**, *19*, 2652–2664. (b) Kollar, P.; Rajchard, J.; Balounova, Z.; Pazourek, J. Marine natural products: Bryostatins in preclinical and clinical studies. *Pharm. Biol.* **2014**, *52*, 237–242.

- [16] Hegde, V. R.; Patel, M. G.; Gullo, V. P.; Ganguly, A. K.; Sarre, O.; Puar, M. S. Macrolactams: A New Class of Antifungal Agents. *J. Am. Chem. Soc.* **1990**, *112*, 6403–6405.
- [17] (a) Ayers, S.; Zink, D. L.; Mohn, K.; Powell, J. S.; Brown, C. M.; Murphy, T.; Grund, A.; Genilloud, O.; Salazar, O.; Thompson, D.; Singh, S. B. Anthelmintic Macrolactams from *Nonomuraea turkmeniaca* MA7364. *J. Nat. Prod.* **2007**, *70*, 1371–1373. (b) Ayers, S.; Zink, D. L.; Powell, J. S.; Brown, C. M.; Grund, A.; Genilloud, O.; Salazar, O.; Thompson, D.; Singh, S. B. Anthelmintic Macrolactams from *Nonomuraea turkmeniaca* MA7381. *J. Antibiot.* **2008**, *61*, 59–62.
- [18] Lin, T.-I.; Lenz, O.; Fanning, G.; Verbinnen, T.; Delouvroy, F.; Scholliers, A.; Vermeiren, K.; Rosenquist, A.; Edlund, M.; Samuelsson, B.; Vrang, L.; de Kock, H.; Wigerinck, P.; Raboisson, P.; Simmen, K. In Vitro Activity and Preclinical Profile of TMC435350, a Potent Hepatitis C Virus Protease Inhibitor. *Antimicrob. Agents Chemother.* **2009**, *53*, 1377–1385.
- [19] (a) Kaul, R.; Surprenant, S.; Lubell, W. D. Systematic Study of the Synthesis of Macrocyclic Dipeptide β -Turn Mimics Possessing 8-, 9-, and 10-Membered Rings by Ring-Closing Metathesis. *J. Org. Chem.* **2005**, *70*, 3838–3844. (b) Lesma, G.; Colombo, A.; Silvani, A.; Sacchetti, A. A new spirocyclic proline-based lactam as efficient type II' β -turn inducing peptidomimetic. *Tetrahedron Lett.* **2008**, *49*, 7423–7425. (c) Yu, X.; Sun, D. Macrocyclic Drugs and Synthetic Methodologies toward Macrocycles. *Molecules* **2013**, *18*, 6230–6268. (d) de Jesus, R.; Yuan, A.; Ghai, R. D.; McMartin, C.; Bohacek, R.; Ksander, G. M. Meta-Substituted Benzofused Macrocyclic Lactams as Zinc Metalloprotease Inhibitors. *J. Med. Chem.* **1997**, *40*, 506–514. (e) Ding, G.; Liu, F.; Yang, T.; Fu, H.; Zhao, Y.; Jiang, Y. A novel kind of nitrogen heterocycle compound induces

- apoptosis of human chronic myelogenous leukemia K562 cells. *Bioorg. Med. Chem.* **2006**, *14*, 3766–3774.
- [20] Velten, R.; Erdelen, C.; Gehling, M.; Gohrt, A.; Gondol, D.; Lenz, J.; Lockhoff, O.; Wachendorff, U.; Wendisch, D. Cripowellin A and B, a Novel Type of Amaryllidaceae Alkaloid from *Crinum powellii*. *Tetrahedron Lett.* **1998**, *39*, 1737–1740.
- [21] Siemeister, G.; Schäfer, M.; Briem, H.; Krüger, M.; Lienau, P.; Jautelat, R.; Lücking, U. Macrocyclic Aminopyrimidines as Multitarget CDK and VEGF-R Inhibitors with Potent Antiproliferative Activities. *ChemMedChem* **2007**, *2*, 63–77.
- [22] Kulkarni, S.; Anderson, D. D.; Hong, L.; Baldrige, A.; Wang, Y.-F.; Chumanovich, A. A.; Kovalevsky, A. Y.; Tojo, Y.; Amano, M.; Koh, Y.; Tang, J.; Weber, I. T.; Mitsuya, H.; Ghosh, A. K. Design, Synthesis, Protein-Ligand X-ray Structure, and Biological Evaluation of a Series of Novel Macrocyclic Human Immunodeficiency Virus-1 Protease Inhibitors to Combat Drug Resistance. *J. Med. Chem.* **2009**, *52*, 7689–7705.
- [23] Thuring, J. W. J. Preparation of macrocyclic naphthyridine compounds as integrase inhibitors for use in the treatment of feline immunodeficiency virus. WO2012112345 A1 20120823, 2012.
- [24] Larsson, A.; Fex, T.; Knecht, W.; Blomberg, N.; Hanessian, S. Design and synthesis of macrocyclic indoles targeting blood coagulation cascade Factor XIa. *Bioorg. Med. Chem. Lett.* **2010**, *20*, 6925–6928.
- [25] Pastor Fernandez, J.; Alvarez Escobar, R. M.; Riesco Fagundo, R. C.; Garcia Garcia, A. B.; Rodriguez Hergueta, A.; Martin Hernando, J. I.; Blanco Aparicio, C.; Cebrian Munoz, D. A. Preparation of N-pyridyl benzenesulfonamide contg.

macrocyclic compds. as inhibitors of protein or lipid kinase useful in treatment of cancer. WO2012156756 A2 20121122, 2012.

- [26] (a) Wang, T.; Pendri, A.; Zhang, Z.; Zhai, W.; Li, G.; Gerritz, S.; Scola, P. M.; Sun, L.-Q.; Zhao, Q.; Mull, E. Preparation of macrocyclic 2-amino-4-phenylamino-1,3,5-triazine compounds for the treatment of hepatitis C virus infection. WO2012141704 A1 20121018, 2012. (b) Buckman, B.; Nicholas, J. B.; Serebryany, V.; Seiwert, S. D. Preparation of macrocyclic peptides, especially proline-containing peptides, as inhibitors of hepatitis C virus replication for treating hepatitis C infection and liver fibrosis. WO2012037259 A1 20120322, 2012. (c) Kirschberg, T. A.; Squires, N. H.; Yang, H.; Corsa, A. C.; Tian, Y.; Tirunagari, N.; Sheng, X. C.; Kim, C. U. Novel, sulfonamide linked inhibitors of the hepatitis C virus NS3 protease. *Bioorg. Med. Chem. Lett.* **2014**, *24*, 969–972.
- [27] (a) Illuminati, G.; Mandolini, L. Ring Closure Reactions of Bifunctional Chain Molecules. *Acc. Chem. Res.* **1981**, *14*, 95–102 and references cited therein. (b) Casadei, M. A.; Calli, C.; Mandolini, L. Ring-Closure Reactions. 22. Kinetics of Cyclization of Diethyl (ω -Bromoalkyl)malonates in the Range of 4- to 21-Membered Rings. Role of Ring Strain. *J. Am. Chem. Soc.* **1984**, *106*, 1051–1056.
- [28] Casadei, M. A.; Galli, C.; Mandolini, L. Ring-closure reactions. 18. Application of the malonic ester synthesis to the preparation of many-membered carbocyclic rings. *J. Org. Chem.* **1981**, *46*, 3127–3128.
- [29] Dalla Cort, A.; Illuminati, G.; Mandolini, L.; Masci, B. Ring-closure reactions. Part 15. Solvent effects on cyclic aralkyl ether formation by intramolecular Williamson synthesis. *J. Chem. Soc., Perkin Trans. 2* **1980**, 1774–1777.
- [30] Galli, C.; Illuminati, G.; Mandolini, L.; Tamborra, P. Ring-closure reactions. 7. Kinetics and activation parameters of lactone formation in the range of 3- to 23-membered rings. *J. Am. Chem. Soc.* **1977**, *99*, 2591–2597.

- [31] Ruzicka, L.; Stoll, M.; Schinz, H. Carbon rings. II. Synthesis of carbocyclic ketones of 10- to 18-membered rings. *Helv. Chim. Acta.* **1926**, *9*, 249–264.
- [32] Ziegler, K.; Eberle, H.; Ohlinger, H. Polymembered ring systems. I. Synthesis of polymethylene ketones with more than six-membered rings *Liebigs Ann. Chem.* **1933**, *504*, 94–130.
- [33] Parenty, A.; Moreau, X.; Niel, G.; Campagne, J.-M. Macrolactonizations in the Total Synthesis of Natural Products. *Chem. Rev.* **2013**, *113*, PR1–PR40.
- [34] Peterson, M. L. The synthesis of macrocycles for drug discovery. In RSC Drug Discovery Series.; Levin, J. Ed.: Royal Society of Chemistry; Cambridge, U.K., **2015**, *40*, 398–486 and references cited therein.
- [35] Davies, J. S. The cyclization of peptides and depsipeptides. *J. Pept. Sci.* **2003**, *9*, 471–501.
- [36] (a) Albericio, F.; Carpino, L. A. Coupling reagents and activation. *Methods Enzymol.* **1997**, *289*, 104–126. (b) Albericio, F.; Chinchilla, R.; Dodsworth, D. J.; Najera, C. New trends in peptide coupling reagents. *Org. Prep. Proced. Int.* **2001**, *33*, 203–303. (c) Albericio, F. Developments in peptide and amide synthesis. *Curr. Opin. Chem. Biol.* **2004**, *8*, 211–221. (d) Han, S.-Y.; Kim, Y.-A. Recent development of peptide coupling reagents in organic synthesis. *Tetrahedron* **2004**, *60*, 2447–2467. (e) El-Faham, A.; Albericio, F. Peptide Coupling Reagents, More than a Letter Soup. *Chem. Rev.* **2011**, *111*, 6557–6602. (f) Corey, E. J.; Nicolaou, K. C. Efficient and mild lactonization method for the synthesis of macrolides. *J. Am. Chem. Soc.* **1974**, *96*, 5614–5616. (g) Mukaiyama, T. New Synthetic Methods Based on the Onium Salts of Aza-Arenes. *Angew. Chem., Int. Ed. Engl.* **1979**, *18*, 707–721. (h) Mukaiyama, T.; Usui, M.; Saigo, K. The facile synthesis of lactones. *Chem. Lett.* **1976**, 49–50. (i) Inanaga, J.; Hirata, K.; Saeki, H.; Katsuki, T.; Yamaguchi, M. A rapid esterification by mixed anhydride and its application to large-ring lactonization. *Bull. Chem. Soc. Jpn.* **1979**, *52*, 1989–

1993. (j) Shiina, I.; Kubota, M.; Ibuka, R. A novel and efficient macrolactonization of ω -hydroxycarboxylic acids using 2-methyl-6-nitrobenzoic anhydride (MNBA). *Tetrahedron Lett.* **2002**, *43*, 7535–7539. (k) Mukaiyama, T.; Izumi, J.; Miyashita, M.; Shiina, I. Facile synthesis of lactones from silyl ω -siloxycarboxylates using p-(trifluoromethyl)benzoic anhydride and a catalytic amount of active Lewis acid. *Chem. Lett.* **1993**, 907–910. (l) Ishihara, K.; Kubota, M.; Kurihara, H.; Yamamoto, H. Scandium Trifluoromethanesulfonate as an Extremely Active Lewis Acid Catalyst in Acylation of Alcohols with Acid Anhydrides and Mixed Anhydrides. *J. Org. Chem.* **1996**, *61*, 4560–4567. (m) Kaiho, T.; Masamune, S.; Toyoda, T. Macrolide synthesis: narbonolide. *J. Org. Chem.* **1982**, *47*, 1612–1614. (n) Corey, E. J.; Hua, D. H.; Pan, B. C.; Seitz, S. P. Total synthesis of aplasmomycin. *J. Am. Chem. Soc.* **1982**, *104*, 6818–6820.
- [37] (a) Ksander, G. M.; de Jesus, R.; Yuan, A.; Ghai, R. D.; Trapani, A.; McMartin, C.; Bohacek, R. Ortho-Substituted Benzofused Macrocyclic Lactams as Zinc Metalloprotease Inhibitors. *J. Med. Chem.* **1997**, *40*, 495–505. (b) Ksander, G. M.; de Jesus, R.; Yuan, A.; Ghai, R. D.; McMartin, C.; Bohacek, R. Meta-Substituted Benzofused Macrocyclic Lactams as Zinc Metalloprotease Inhibitors. *J. Med. Chem.* **1997**, *40*, 506–514. (c) Chen, G.-P.; Fales, K. R.; Lenk, B. E.; Szendroi, R. J.; Wang, X.-J.; Carlson, J. A.; Johnson, E. P. Macrolactamization via Palladium π -Allyl Alkylation. Preparation of CGS25155: A 10-Membered Lactam Neutral Endopeptidase 24.11 Inhibitor. *J. Org. Chem.* **1995**, *60*, 6595–6598.
- [38] Robinson, J. A. Protein epitope mimetics in the age of structural vaccinology. *J. Pept. Sci.* **2013**, *19*, 127–140.
- [39] (a) Podlogar, B. L.; Farr, R. A.; Friedrich, D.; Tarnus, C.; Huber, E. W.; Cregge, R. J.; Schirlin, D. Design, Synthesis, and Conformational Analysis of a Novel Macrocyclic HIV-Protease Inhibitor. *J. Med. Chem.* **1994**, *37*, 3684–3692. (b)

- Abbenante, G.; Bergman, D. A.; Brinkworth, R. I.; March, D. R.; Reid, R. C.; Hunt, P. A.; James, I. W.; Dancer, R. J.; Garnham, B.; Stoermer, M. L. Structure-activity relationships for macrocyclic peptidomimetic inhibitors of HIV-1 protease. *Bioorg. Med. Chem. Lett.* **1996**, *6*, 2531–2536.
- [40] (a) Sham, H. L.; Bolis, G.; Stein, H. H.; Fesik, S. W.; Marcotte, P. A.; Plattner, J. J.; Rempel, C. A.; Greer, J. Renin inhibitors. Design and synthesis of a new class of conformationally restricted analogs of angiotensinogen. *J. Med. Chem.* **1988**, *31*, 284–295. (b) Weber, A. E.; Halgren, T. A.; Doyle, J. J.; Lynch, R. J.; Siegl, P. K. S.; Parsons, W. H.; Greenlee, W. J.; Patchett, A. A. Design and synthesis of P2-P1'-linked macrocyclic human renin inhibitors. *J. Med. Chem.* **1991**, *34*, 2692–2701. (c) Dhanoa, D. S.; Parsons, W. H.; Greenlee, W. J.; Patchett, A. A. The synthesis of potent macrocyclic renin inhibitors. *Tetrahedron Lett.* **1992**, *33*, 1725–1728. (d) Reily, M. D.; Thanabal, V.; Lunney, E. A.; Repine, J. T.; Humblet, C. C.; Wagner, G. Design, synthesis and solution structure of a renin inhibitor. Structural constraints from NOE, and homonuclear and heteronuclear coupling constants combined with distance geometry calculations. *FEBS Lett.* **1992**, *302*, 97–103. (e) Sund, C.; Belda, O.; Wikteliuss, D.; Sahlberg, C.; Vrang, L.; Sedig, S.; Hamelink, E.; Henderson, I.; Agback, T.; Jansson, K.; Borkakoti, N.; Derbyshire, D.; Eneroth, A.; Samuelsson, B. Design and synthesis of potent macrocyclic renin inhibitors. *Bioorg. Med. Chem. Lett.* **2011**, *21*, 358–362.
- [41] (a) Greco, M. N.; Powell, E. T.; Hecker, L. R.; Andrade-Gordon, P.; Kauffman, J. A.; Lewis, J. M.; Ganesh, V.; Tulinsky, A.; Maryanoff, B. E. Novel thrombin inhibitors that are based on a macrocyclic tripeptide motif. *Bioorg. Med. Chem. Lett.* **1996**, *6*, 2947–2952. (b) Nantermet, P. G.; Barrow, J. C.; Newton, C. L.; Pellicore, J. M.; Young, M.; Lewis, S. D.; Lucas, B. J.; Krueger, J. A.; McMasters, D. R.; Yan, Y.; Kuo, L. C.; Vacca, J. P.; Selnick, H. G. Design and synthesis of potent and selective macrocyclic thrombin inhibitors. *Bioorg. Med. Chem. Lett.* **2003**, *13*, 2781–2784.

- [42] Stachel, S. J.; Coburn, C. A.; Sankaranarayanan, S.; Price, E. A.; Pietrak, B. L.; Huang, Q.; Lineberger, J.; Espeseth, A. S.; Jin, L.; Ellis, J.; Holloway, M. K.; Munshi, S.; Allison, T.; Hazuda, D.; Simon, A. J.; Graham, S. L.; Vacca, J. P. Macrocyclic inhibitors of β -secretase: functional activity in an animal model. *J. Med. Chem.* **2006**, *49*, 6147–6150.
- [43] Xue, C.-B.; He, X.; Corbett, R. L.; Roderick, J.; Wasserman, Z. R.; Liu, R.-Q.; Jaffee, B. D.; Covington, M. B.; Qian, M.; Trzaskos, J. M.; Newton, R. C.; Magolda, R. L.; Wexler, R. R.; Decicco, C. P. Discovery of Macrocyclic Hydroxamic Acids Containing Biphenylmethyl Derivatives at P1', a Series of Selective TNF- α Converting Enzyme Inhibitors with Potent Cellular Activity in the Inhibition of TNF- α Release. *J. Med. Chem.* **2001**, *44*, 3351–3354.
- [44] (a) Cherney, R. J.; Wang, L.; Meyer, D. T.; Xue, C.-B.; Wasserman, Z. R.; Hardman, K. D.; Welch, P. K.; Covington, M. B.; Copeland, R. A.; Arner, E. C.; DeGrado, W. F.; Decicco, C. P. Macrocyclic Amino Carboxylates as Selective MMP-8 Inhibitors. *J. Med. Chem.* **1998**, *41*, 1749–1751. (b) Dumez, E.; Snaith, J. S.; Jackson, R. F. W.; McElroy, A. B.; Overington, J.; Wythes, M. J.; Withka, J. M.; McLellan, T. J. Synthesis of Macrocyclic, Potential Protease Inhibitors Using a Generic Scaffold. *J. Org. Chem.* **2002**, *67*, 4882–4892. (c) Chen, H.; Jiao, W.; Jones, M. A.; Coxon, J. M.; Morton, J. D.; Bickerstaffe, R.; Pehere, A. D.; Zvarec, O.; Abell, A. D. New Tripeptide-Based Macrocyclic Calpain Inhibitors Formed by N-Alkylation of Histidine. *Chem. Biodiversity* **2012**, *9*, 2473–2484. (d) Bolton, G. L.; Roth, B. D.; Trivedi, B. K. Synthesis of conformationally constrained macrocyclic analogs of the potent and selective CCK-B antagonist CI-988. *Tetrahedron* **1993**, *49*, 525–536. (e) Suich, D. J.; Mousa, S. A.; Singh, G.; Liapakis, G.; Reisine, T.; DeGrado, W. F. Template-constrained cyclic peptide analogues of somatostatin: subtype-selective binding to somatostatin receptors and antiangiogenic activity. *Bioorg. Med. Chem.* **2000**, *8*, 2229–2241. (f) Lee, K.; Zhang, M.; Liu, H.; Yang, D.; Burke, T. R. Jr. Utilization of a β -

- Aminophosphotyrosyl Mimetic in the Design and Synthesis of Macrocyclic Grb2 SH2 Domain-Binding Peptides. *J. Med. Chem.* **2003**, *46*, 2621–2630. (g) Mwakwari, S. C.; Patil, V.; Guerrant, W.; Oyelere, A. K. Macrocyclic histone deacetylase inhibitors. *Curr. Top. Med. Chem.* **2010**, *10*, 1423–1440. (h) Suda, A.; Koyano, H.; Hayase, T.; Hada, K.; Kawasaki, K.-i.; Komiyama, S.; Hasegawa, K.; Fukami, T. A.; Sato, S.; Miura, T.; Ono, N.; Yamazaki, T.; Saitoh, R.; Shimma, N.; Shiratori, Y.; Tsukuda, T. Design and synthesis of novel macrocyclic 2-amino-6-arylpyrimidine Hsp90 inhibitors. *Bioorg. Med. Chem. Lett.* **2012**, *22*, 1136–1141. (i) Udugamasooriya, G.; Saro, D.; Spaller, M. R. Bridged Peptide Macrocycles as Ligands for PDZ Domain Proteins. *Org. Lett.* **2005**, *7*, 1203–1206. (j) Singh, Y.; Stoermer, M. J.; Lucke, A. J.; Glenn, M. P.; Fairlie, D. P. Regioselective Synthesis of Antiparallel Loops on a Macrocyclic Scaffold Constrained by Oxazoles and Thiazoles. *Org. Lett.* **2002**, *4*, 3367–3370. (k) Nielsen, M. C.; Ulven, T. Macrocyclic G-quadruplex ligands. *Curr. Med. Chem.* **2010**, *17*, 3438–3448.
- [45] Vendeville, S.; Lin, T.-I.; Hu, L.; Tahri, A.; McGowan, D.; Cummings, M. D.; Amsoms, K.; Canard, M.; Last, S.; Van den Steen, I.; Devogelaere, B.; Rouan, M.-C.; Vijgen, L.; Berke, J. M.; Dehertogh, P.; Franssen, E.; Cleiren, E.; van der Helm, L.; Fanning, G.; Van Emelen, K.; Nyanguile, O.; Simmen, K.; Raboisson, P. Finger loop inhibitors of the HCV NS5b polymerase. Part II. Optimization of tetracyclic indole-based macrocycle leading to the discovery of TMC647055. *Bioorg. Med. Chem. Lett.* **2012**, *22*, 4437–4443.
- [46] Choi, H. G.; Son, J. B.; Park, D.-S.; Ham, Y. J.; Hah, J.-M.; Sim, T. An efficient and enantioselective total synthesis of naturally occurring L-783277. *Tetrahedron Lett.* **2010**, *51*, 4942–4946.
- [47] Xue, C.-B.; He, X.; Roderick, J.; Degrado, W. F.; Cherney, R. J.; Hardman, K. D.; Nelson, D. J.; Copeland, R. A.; Jaffee, B. D.; Decicco, C. P. Design and synthesis

- of cyclic inhibitors of matrix metalloproteinases and TNF- α production. *J. Med. Chem.* **1998**, *41*, 1745–1748.
- [48] (a) Bridger, G. J.; Skerlj, R. T.; Thornton, D.; Padmanabhan, S.; Martellucci, S. A.; Henson, G. W.; Abrams, M. J.; Yamamoto, N.; Vreese, K. D.; Pauwels, R.; De Clercq, E. Synthesis and Structure-Activity Relationships of Phenylenebis-(methylene)-Linked Bis-Tetraazamacrocycles That Inhibit HIV Replication. Effects of Macrocyclic Ring Size and Substituents on the Aromatic Linker. *J. Med. Chem.* **1995**, *38*, 366–378. (b) Fricker, S. P. A novel CXCR4 antagonist for hematopoietic stem cell mobilization. *Expert Opin. Invest. Drugs* **2008**, *17*, 1749–1760.
- [49] (a) Bridger, G. J.; Skerlj, R. T.; Hernandez-Abad, P. E.; Bogucki, D. E.; Wang, Z.; Zhou, Y.; Nan, S.; Boehringer, E. M.; Wilson, T.; Crawford, J.; Metz, M.; Hatse, S.; Princen, K.; De Clercq, E.; Schols, D. Synthesis and Structure-Activity Relationships of Azamacrocyclic C-X-C Chemokine Receptor 4 Antagonists: Analogues Containing a Single Azamacrocyclic Ring are Potent Inhibitors of T-Cell Tropic (X4) HIV-1 Replication. *J. Med. Chem.* **2010**, *53*, 1250–1260. (b) Ling, X.; Spaeth, E.; Chen, Y.; Shi, Y.; Zhang, W.; Schober, W.; Hail, N., Jr.; Konopleva, M.; Andreeff, M. The CXCR4 antagonist AMD3465 regulates oncogenic signaling and invasiveness in vitro and prevents breast cancer growth and metastasis in vivo. *PLoS One* **2013**, *8*, e58426.
- [50] Hanessian, S.; Yang, G.; Rondeau, J.-M.; Neumann, U.; Betschart, C.; Tintelnot-Blomley, M. Structure-Based Design and Synthesis of Macroheterocyclic Peptidomimetic Inhibitors of the Aspartic Protease β -Site Amyloid Precursor Protein Cleaving Enzyme (BACE). *J. Med. Chem.* **2006**, *49*, 4544–4567.
- [51] Virgilio, A. A.; Ellman, J. A. Simultaneous Solid-Phase Synthesis of β -Turn Mimetics Incorporating Side-Chain Functionality. *J. Am. Chem. Soc.* **1994**, *116*, 11580–11581.

- [52] (a) Nefzi, A.; Arutyunyan, S.; Fenwick, J. E. Two-step Hantzsch based macrocyclization approach for the synthesis of thiazole-containing cyclopeptides. *J. Org. Chem.* **2010**, *75*, 7939–7941. (b) Nefzi, A.; Fenwick, J. E. N-terminus 4-chloromethylthiazole peptide as a macrocyclization tool in the synthesis of cyclic peptides: application to the synthesis of conformationally constrained RGD-containing integrin ligands. *Tetrahedron Lett.* **2011**, *52*, 817–819.
- [53] Kawanishi, N.; Sugimoto, T.; Shibata, J.; Nakamura, K.; Masutani, K.; Ikuta, M.; Hirai, H. Structure-based drug design of a highly potent CDK1,2,4,6 inhibitor with novel macrocyclic quinoxalin-2-one structure. *Bioorg. Med. Chem. Lett.* **2006**, *16*, 5122–5126.
- [54] Xue, C.-B.; Voss, M. E.; Nelson, D. J.; Duan, J. J. W.; Cherney, R. J.; Jacobson, I. C.; He, X.; Roderick, J.; Chen, L.; Corbett, R. L.; Wang, L.; Meyer, D. T.; Kennedy, K.; DeGrado, W. F.; Hardman, K. D.; Teleha, C. A.; Jaffee, B. D.; Liu, R.-Q.; Copeland, R. A.; Covington, M. B.; Christ, D. D.; Trzaskos, J. M.; Newton, R. C.; Magolda, R. L.; Wexler, R. R.; Decicco, C. P. Design, synthesis, and structure-activity relationships of macrocyclic hydroxamic acids that inhibit tumor necrosis factor α release in vitro and in vivo. *J. Med. Chem.* **2001**, *44*, 2636–2660.
- [55] (a) Virgilio, A. A.; Bray, A. A.; Zhang, W.; Trinh, L.; Snyder, M.; Morrissey, M. M.; Ellman, J. A. Synthesis and evaluation of a library of peptidomimetics based upon the β -turn. *Tetrahedron* **1997**, *53*, 6635–6644. (b) Souers, A. J.; Virgilio, A. A.; Schurer, S. S.; Ellman, J. A.; Kogan, T. P.; West, H. E.; Ankener, W.; Vanderslice, P. Novel inhibitors of $\alpha 4\beta 1$ integrin receptor interactions through library synthesis and screening. *Bioorg. Med. Chem. Lett.* **1998**, *8*, 2297–2302. (c) Souers, A. J.; Virgilio, A. A.; Rosenquist, S. A.; Fenuik, W.; Ellman, J. A. Identification of a Potent Heterocyclic Ligand To Somatostatin Receptor Subtype

- 5 by the Synthesis and Screening of β -Turn Mimetic Libraries. *J. Am. Chem. Soc.* **1999**, *121*, 1817–1825.
- [56] (a) An, H.; Haly, B. D.; Cook, P. D. New piperazinyl polyazacyclophane scaffolds, libraries and biological activities. *Bioorg. Med. Chem. Lett.* **1998**, *8*, 2345–2350. (b) Wang, T.; An, H.; Vickers, T. A.; Bharadwaj, R.; Cook, P. D. Synthesis of novel polyazadipyridinocyclophane scaffolds and their application for the generation of libraries. *Tetrahedron* **1998**, *54*, 7955–7976.
- [57] Boisnard, S.; Zhu, J. Studies toward the total synthesis of RP-66453. *Tetrahedron Lett* **2002**, *43*, 2577–2580.
- [58] Chen, C.-Y.; Reamer, R. A. A facile synthesis of N,3-disubstituted indoles and 3-hydroxyl indolines via an intramolecular S_NAr of fluorinated amino alcohols. *Tetrahedron Lett.* **2009**, *50*, 1529–1532.
- [59] Wang, Z.; Bois-Choussy, M.; Jia, Y.; Zhu, J. Total Synthesis of Complestatin (Chloropeptin II). *Angew. Chem., Int. Ed.* **2010**, *49*, 2018–2022.
- [60] (a) Beugelmans, R.; Singh, G. P.; Bois-Choussy, M.; Chastanet, J.; Zhu, J. S_NAr -Based Macrocyclization: An Application to the Synthesis of Vancomycin Family Models. *J. Org. Chem.* **1994**, *59*, 5535–5542. (b) Ma, N.; Jia, Y.; Liu, Z.; Gonzalez-Zamora, E.; Bois-Choussy, M.; Malabarba, A.; Brunati, C.; Zhu, J. Design and synthesis of macrocycles active against vancomycin-resistant enterococci (VRE): the interplay between D-Ala-D-Lac binding and hydrophobic effect. *Bioorg. Med. Chem. Lett.* **2005**, *15*, 743–746. (c) Borzilleri, R. M.; Nukui, S.; Beresis, R. T.; Boger, D. L. Synthesis of the Vancomycin CD and DE Ring Systems. *J. Org. Chem.* **1997**, *62*, 4721–4736.
- [61] (a) Zhu, J. S_NAr -based macrocyclization via biaryl ether formation. Application in natural product synthesis. *Synlett* **1997**, 133–144. (b) Pitsinos, E. N.; Vidali, V. P.;

- Couladouros, E. A. Diaryl Ether Formation in the Synthesis of Natural Products. *Eur. J. Org. Chem.* **2011**, 1207–1222.
- [62] Temal-Laïb, T.; Chastanet, J.; Zhu, J. A Convergent Approach to Cyclopeptide Alkaloids: Total Synthesis of Sanjoinine G1. *J. Am. Chem. Soc.* **2002**, *124*, 583–590.
- [63] Lücking, U. Siemeister, G.; Schäfer, M.; Briem, H.; Krüger, M.; Lienau, P.; Jautelat, R. Macrocyclic Aminopyrimidines as Multitarget CDK and VEGF-R Inhibitors with Potent Antiproliferative Activities. *ChemMedChem* **2007**, *2*, 63–77.
- [64] (a) Maliartchouk, S.; Feng, Y.; Ivanisevic, L.; Debeir, T.; Cuello, A. C.; Burgess, K.; Saragovi, H. U. A designed peptidomimetic agonistic ligand of TrkA nerve growth factor receptors. *Mol. Pharmacol.* **2000**, *57*, 385–391. (b) Pattarawarapan, M.; Zaccaro, M. C.; Saragovi, U. H.; Burgess, K. New Templates for Syntheses of Ring-Fused, C10 β -Turn Peptidomimetics Leading to the First Reported Small-Molecule Mimic of Neurotrophin-3. *J. Med. Chem.* **2002**, *45*, 4387–4390. (c) Zaccaro, M. C.; Lee, H. B.; Pattarawarapan, M.; Xia, Z.; Caron, A.; L'Heureux, P.-J.; Bengio, Y.; Burgess, K.; Saragovi, H. U. Selective Small Molecule Peptidomimetic Ligands of TrkC and TrkA Receptors Afford Discrete or Complete Neurotrophic Activities. *Chem. Biol.* **2005**, *12*, 1015–1028.
- [65] Brahim, F.; Malakhov, A.; Lee, H. B.; Pattarawarapan, M.; Ivanisevic, L.; Burgess, K.; Saragovi, H. U. A peptidomimetic of NT-3 acts as a TrkC antagonist. *Peptides* **2009**, *30*, 1833–1839.
- [66] (a) Dinsmore, C. J.; Bogusky, M. J.; Culberson, J. C.; Bergman, J. M.; Homnick, C. F.; Zartman, C. B.; Mosser, S. D.; Schaber, M. D.; Robinson, R. G.; Koblan, K. S.; Huber, H. E.; Graham, S. L.; Hartman, G. D.; Huff, J. R.; Williams, T. M. Conformational Restriction of Flexible Ligands Guided by the Transferred NOE Experiment: Potent Macrocyclic Inhibitors of Farnesyltransferase. *J. Am. Chem.*

Soc. **2001**, *123*, 2107–2108. (b) Beshore, D. C.; Bell, I. M.; Dinsmore, C. J.; Homnick, C. F.; Culberson, J. C.; Robinson, R. G.; Fernandes, C.; Walsh, E. S.; Abrams, M. T.; Bhimnathwala, H. G.; Davide, J. P.; Ellis-Hutchings, M. S.; Huber, H. A.; Koblan, K. S.; Buser, C. A.; Kohl, N. E.; Lobell, R. B.; Chen, I. W.; McLoughlin, D. A.; Olah, T. V.; Graham, S. L.; Hartman, G. D.; Williams, T. M. Evaluation of amino acid-based linkers in potent macrocyclic inhibitors of farnesyl-protein transferase. *Bioorg. Med. Chem. Lett.* **2001**, *11*, 1817–1821. (c) Bell, I. M.; Gallicchio, S. N.; Abrams, M.; Beese, L. S.; Beshore, D. C.; Bhimnathwala, H.; Bogusky, M. J.; Buser, C. A.; Culberson, J. C.; Davide, J.; Ellis-Hutchings, M.; Fernandes, C.; Gibbs, J. B.; Graham, S. L.; Hamilton, K. A.; Hartman, G. D.; Heimbrook, D. C.; Homnick, C. F.; Huber, H. E.; Huff, J. R.; Kassahun, K.; Koblan, K. S.; Kohl, N. E.; Lobell, R. B.; Lynch, J. J., Jr.; Robinson, R.; Rodrigues, A. D.; Taylor, J. S.; Walsh, E. S.; Williams, T. M.; Zartman, C. B. 3-Aminopyrrolidinones Farnesyltransferase Inhibitors: Design of Macrocyclic Compounds with Improved Pharmacokinetics and Excellent Cell Potency. *J. Med. Chem.* **2002**, *45*, 2388–2409.

- [67] (a) Jefferson, E. A.; Arakawa, S.; Blyn, L. B.; Miyaji, A.; Osgood, S. A.; Ranken, R.; Risen, L. M.; Swayze, E. E. New Inhibitors of Bacterial Protein Synthesis from a Combinatorial Library of Macrocycles. *J. Med. Chem.* **2002**, *45*, 3430–3439. (b) Jefferson, E. A.; Swayze, E. E.; Osgood, S. A.; Miyaji, A.; Risen, L. M.; Blyn, L. B. Antibacterial activity of quinolone-Macrocycle conjugates. *Bioorg. Med. Chem. Lett.* **2003**, *13*, 1635–1638. (c) Giulianotti, M.; Nefzi, A. Efficient approach for the diversity-oriented synthesis of macro-heterocycles on solid-support. *Tetrahedron Lett.* **2003**, *44*, 5307–5309. (d) Comer, E.; Liu, H.; Joliton, A.; Clabaut, A.; Johnson, C.; Akella, L. B.; Marcaurelle, L. A. Fragment-based domain shuffling approach for the synthesis of pyran-based macrocyclic compounds. *Proc. Natl. Acad. Sci. U. S. A.* **2011**, *108*, 6751–6756.

- [68] (a) Steinman, D. H.; Curtin, M. L.; Garland, R. B.; Davidsen, S. K.; Heyman, H. R.; Holms, J. H.; Albert, D. H.; Magoc, T. J.; Nagy, I. B.; Marcotte, P. A.; Li, J.; Morgan, D. W.; Hutchins, C.; Summers, J. B. The design, synthesis, and structure-activity relationships of a series of macrocyclic MMP inhibitors. *Bioorg. Med. Chem. Lett.* **1998**, *8*, 2087–2092. (b) Cherney, R. J.; Wang, L.; Meyer, D. T.; Xue, C.-B.; Arner, E. C.; Copeland, R. A.; Covington, M. B.; Hardman, K. D.; Wasserman, Z. R.; Jaffee, B. D.; Decicco, C. P. Macrocyclic hydroxamate inhibitors of matrix metalloproteinases and TNF- α production. *Bioorg. Med. Chem. Lett.* **1999**, *9*, 1279–1284.
- [69] (a) Arasappan, A.; Chen, K. X.; Njoroge, F. G.; Parekh, T. N.; Girijavallabhan, V. Novel Dipeptide Macrocycles from 4-Oxo, -Thio, and -Amino-Substituted Proline Derivatives. *J. Org. Chem.* **2002**, *67*, 3923–3926. (b) Arasappan, A.; Njoroge, F. G.; Chen, K. X.; Venkatraman, S.; Parekh, T. N.; Gu, H.; Pichardo, J.; Butkiewicz, N.; Prongay, A.; Madison, V.; Girijavallabhan, V. P2-P4 Macrocyclic inhibitors of hepatitis C virus NS3-4A serine protease. *Bioorg. Med. Chem. Lett.* **2006**, *16*, 3960–3965. (c) Chen, K. X.; Njoroge, F. G.; Pichardo, J.; Prongay, A.; Butkiewicz, N.; Yao, N.; Madison, V.; Girijavallabhan, V. Potent 7-hydroxy-1,2,3,4-tetrahydroisoquinoline-3-carboxylic acid-based macrocyclic inhibitors of hepatitis C virus NS3 protease. *J. Med. Chem.* **2006**, *49*, 567–574.
- [70] Xue, C.-B.; Voss, M. E.; Nelson, D. J.; Duan, J. J. W.; Cherney, R. J.; Jacobson, I. C.; He, X.; Roderick, J.; Chen, L.; Corbett, R. L.; Wang, L.; Meyer, D. T.; Kennedy, K.; DeGrado, W. F.; Hardman, K. D.; Teleha, C. A.; Jaffee, B. D.; Liu, R.-Q.; Copeland, R. A.; Covington, M. B.; Christ, D. D.; Trzaskos, J. M.; Newton, R. C.; Magolda, R. L.; Wexler, R. R.; Decicco, C. P. Design, synthesis, and structure-activity relationships of macrocyclic hydroxamic acids that inhibit tumor necrosis factor α release in vitro and in vivo. *J. Med. Chem.* **2001**, *44*, 2636–2660.

- [71] (a) Baurle, S.; Blume, T.; Mengel, A.; Parchmann, C.; Skuballa, W.; Basler, S.; Schafer, M.; Sulzle, D.; Wrona-Metzinger, H.-P. From rigidity to conformational flexibility: macrocyclic templates derived from ansa-steroids. *Angew Chem Int Ed Engl* **2003**, *42*, 3961–3964. (b) Baurle, S.; Blume, T.; Leroy, E.; Mengel, A.; Parchmann, C.; Schmidt, K.; Skuballa, W. Novel macrocyclic templates by ring enlargement of ansa-steroids. *Tetrahedron Lett.* **2004**, *45*, 9569–9571. (c) Baurle, S.; Blume, T.; Gunther, J.; Henschel, D.; Hillig, R. C.; Husemann, M.; Mengel, A.; Parchmann, C.; Schmid, E.; Skuballa, W. Design and synthesis of macrocyclic inhibitors of phosphatase cdc25B. *Bioorg Med Chem Lett* **2004**, *14*, 1673–1677.
- [72] Witt, T.; Hock, F. J.; Lehmann, J. 7-Methyl-6,7,8,9,14,15-hexahydro-5H-benz[d]indolo[2,3-g]azecine: a new heterocyclic system and a new lead compound for dopamine receptor antagonists. *J. Med. Chem.* **2000**, *43*, 2079–2081.
- [73] MacPherson, L. J.; Bayburt, E. K.; Capparelli, M. P.; Bohacek, R. S.; Clarke, F. H.; Ghai, R. D.; Sakane, Y.; Berry, C. J.; Peppard, J. V.; Trapani, A. J. Design and synthesis of an orally active macrocyclic neutral endopeptidase 24.11 inhibitor. *J. Med. Chem.* **1993**, *36*, 3821–3828.
- [74] Forsee, J. E.; Aube, J. Hydrolysis of Iminium Ethers Derived from the Reaction of Ketones with Hydroxy Azides: Synthesis of Macrocyclic Lactams and Lactones. *J. Org. Chem.* **1999**, *64*, 4381–4385.
- [75] Kopp, F.; Stratton, C. F.; Akella, L. B.; Tan, D. S. A diversity-oriented synthesis approach to macrocycles via oxidative ring expansion. *Nat. Chem. Biol.* **2012**, *8*, 358–365.
- [76] Suh, Y.-G.; Lee, Y.-S.; Kim, S.-H.; Jung, J.-K.; Yun, H.; Jang, J.; Kim, N.-J.; Jung, J.-W. A stereo-controlled access to functionalized macrolactams via an aza-Claisen rearrangement. *Org. Biomol. Chem.* **2012**, *10*, 561–568.

- [77] Tummatorn, J.; Dudley, G. B. Generation of Medium-Ring Cycloalkynes by Ring Expansion of Vinylogous Acyl Triflates. *Org. Lett.* **2011**, *13*, 1572–1575.
- [78] (a) Hili, R.; Rai, V.; Yudin, A. K. Macrocyclization of Linear Peptides Enabled by Amphoteric Molecules. *J. Am. Chem. Soc.* **2010**, *132*, 2889–2891. (b) He, Z.; Zajdlik, A.; Yudin, A. K. Air- and moisture-stable amphoteric molecules: Enabling reagents in synthesis. *Acc. Chem. Res.* **2014**, *47*, 1029–1040 and references cited therein.
- [79] Lipinski, C. A.; Lombardo, F.; Dominy, B. W.; Feeney, P. J. Experimental and computational approaches to estimate solubility and permeability in drug discovery and development settings. *Adv. Drug Delivery Rev.* **1997**, *23*, 3–25.
- [80] (a) Gleeson, M. P. Generation of a set of simple, interpretable ADMET rules of thumb. *J. Med. Chem.* **2008**, *51*, 817–834. (b) Martin, Y. C. A bioavailability score. *J. Med. Chem.* **2005**, *48*, 3164–3170. (c) Pajouhesh, H.; Lenz, G. R. Medicinal chemical properties of successful central nervous system drugs. *NeuroRx* **2005**, *2*, 541–553.
- [81] (a) Delaney, J. S. ESOL: estimating aqueous solubility directly from molecular structure. *J. Chem. Inf. Comp. Sci.* **2004**, *44*, 1000–1005. (b) Lamanna, C.; Bellini, M.; Padova, A.; Westerberg, G.; Maccari, L. Straightforward recursive partitioning model for discarding insoluble compounds in the drug discovery process. *J. Med. Chem.* **2008**, *51*, 2891–2897.
- [82] Ando, H. Y.; Radebaugh, G. W. Property-based drug design and preformulation. *In Remington: The Science and Practice of Pharmacy*; Lippincott, Williams and Wilkins; Philadelphia, **2005**; pp 720–744.
- [83] Wirth, M.; Volkamer, A.; Zoete, V.; Rippmann, F.; Michielin, O.; Rarey, M.; Sauer, W. H. B. Protein pocket and ligand shape comparison and its application in virtual screening. *J. Comput. Aided Mol. Des.* **2013**, *27*, 511–524.

- [84] Baldauf, C.; Günther, R.; Hofmann, H.-J. Conformational properties of sulfonamido peptides. *J. Mol. Struct-Theochem.* **2004**, *675*, 19–28.
- [85] (a) See references 1, 3, 6 and 34 and references cited therein. (b) Hassan, H. M. Recent applications of ring-closing metathesis in the synthesis of lactams and macrolactams. *A. Chem. Commun.* **2010**, *46*, 9100–9106. (c) White, C. J.; Yudin A. K. Contemporary strategies for peptide macrocyclization. *Nat. Chem.* **2011**, *3*, 509–524.
- [86] (a) Rolfe, A.; Samarakoon, T. B.; Hanson, P. R. Formal [4+3] Epoxide Cascade Reaction via a Complementary Ambiphilic Pairing Strategy. *Org. Lett.* **2010**, *12*, 1216–1219. (b) Samarakoon, T. B.; Hur, M. Y.; Kurtz, R. D.; Hanson, P. R. A Formal [4+4] Complementary Ambiphile Pairing Reaction: A New Cyclization Pathway for *ortho*-Quinone Methides. *Org. Lett.* **2010**, *12*, 2182–2185. (c) For convergent two-component synthesis, Dow, M.; Fisher, M.; James, T.; Marchetti, F.; Nelson, A. Towards the systematic exploration of chemical space. *Org. Biomol. Chem.* **2012**, *10*, 17–28 and references cited therein. (d) For reactions using amphoteric building blocks, see reference 78.
- [87] Rolfe, A.; Young, K.; Volp, K.; Schoenen, F.; Neuenswander, B.; Lushington, G. H.; Hanson, P. R. One-Pot, Three-Component, Domino Heck-aza-Michael Approach to Libraries of Functionalized 1,1-Dioxido-1,2-benzisothiazoline-3-aceticAcids. *J. Comb. Chem.* **2009**, *11*, 732–738.
- [88] Ullah, F.; Samarakoon, T.; Rolfe, A.; Kurtz, R. D.; Hanson, P. R.; Organ, M. G. Scaling out by microwave-assisted, continuous flow organic synthesis (MACOS): multi-gram synthesis of bromo- and fluoro-benzofused sultams, benzoxathiazepine 1,1-dioxides. *Chem. Eur. J.* **2010**, *16*, 10959–10962.
- [89] Samarakoon, T. B.; Loh, J. K.; Yoon, S. Y.; Rolfe, A.; Le, L. S.; Hanson, P. R. A Modular Reaction Pairing Approach to the Diversity-Oriented Synthesis of Fused- and Bridged-Polycyclic Sultams. *Org. Lett.* **2011**, *13*, 5148–5151.

- [90] Ring-opening of sulfonyl aziridines and epoxides with amines are among the original “Click” reactions detailed by Sharpless in this seminal paper. Kolb, H. C.; Finn, M. G.; Sharpless, K. B. Click Chemistry: Diverse Chemical Function from a Few Good Reactions. *Angew. Chem., Int. Ed.*, **2001**, *40*, 2004–2021.
- [91] Li, X.; Chen, N.; Xu, J. An Improved and Mild Wenker Synthesis of Aziridines. *Synthesis*, **2010**, *20*, 3423–3428.
- [92] (a) Beddoes, R. L.; Dalton, L.; Joule, J. A.; Mills, O. S.; Street, J. D.; Watt, C. I. F. The geometry at nitrogen in N-phenylsulfonylpyrroles and -indoles. The geometry of sulfonamides. *J. Chem. Soc., Perkin Trans. 2* **1986**, 787–797. (b) Klug, H. P. The crystal structure of methanesulfonanilide. *Acta Crystallogr., Sect. B* **1968**, *24*, 792–802. (c) Oppolzer, W.; Rodriguez, I.; Starkemann, C.; Walther, E. Chiral toluene-2, α -sultam auxiliaries: asymmetric alkylations, acylations and aldolizations of N-acyl derivatives. *Tetrahedron Lett.* **1990**, *31*, 5019–5022.
- [93] Sauer, W. H. B.; Schwarz, M. K. Molecular Shape Diversity of Combinatorial Libraries: A Prerequisite for Broad Bioactivity. *J. Chem. Inf. Comput. Sci.* **2003**, *43*, 987–1003.
- [94] (a) Irwin, J. J.; Sterling, T.; Mysinger, M. M.; Bolstad, E. S.; Coleman, R. G. *J. Chem. Inf. Model.*, **2012**, *52*, 1757–1768. (b) <http://zinc.docking.org/> (accessed on April 20th, 2015).
- [95] All of the compounds were sketched using the Avogadro suite of molecular modeling programs (a), and were subsequently subjected to molecular mechanics optimization at default minimization constraints according to the MMFF94 force field and charge parametrization (b). Compounds were then mutually aligned using PyMol (c) according to least-squares positional fitting across the atoms corresponding to the conserved sultam and adjacent carbonyl functional groups. The resulting molecular alignments were then visualized in PyMol. (a) Hanwell, M. D.; Curtis, D. E.; Lonie, D. C.; Vandermeersch, T.; Zurek E.;

Hutchison, G. R. Avogadro: an advanced semantic chemical editor, visualization, and analysis platform. *J. Cheminf.* **2012**, *4*, 1–17. (b) Halgren, T. A.; Merck molecular force field. I. Basis, form, scope, parameterization, and performance of MMFF94. *J. Comp. Chem.* **1996**, 490–519. (c) PyMol Molecular Graphics System, Version 1.6, 2014. <http://sourceforge.net/projects/pymol/>

Chapter 4

Modular One-pot, Sequential Protocols

Toward Diverse Acyl Sultam Libraries

4.1 Introduction

As analyzed in Chapter 1, there are only 351 ring systemsⁱ and 1,197 frameworks among more than 1,000 current marketed small-molecule drugs, which came onto the market before 2013.¹ Moreover, the most frequently used ring systems (83%) were first used in drugs developed prior to 1983, and it is also very unusual for a drug to contain more than one new ring system. Furthermore, on average, six new ring systems enter drug space on a yearly basis and only ~28% of new drugs contain a new ring system. In light of these facts, the most frequent non-aryl, bicyclic lactams consist mainly of 6/4-, 5/4-, 7/6-, 6/5-fused systems. These observations provide insights into the chemical novelty of drugs and highlight the potential demand for new ring systems or frameworks, with low synthetic cost to develop compound libraries efficiently from hit identification to lead optimization and beyond. Herein, is reported a facile one-pot, sequential 3-component approach employing sulfonylation–aza-Michael addition–intramolecular amidation to generate 79/90-member library of 7/4-, 7/5-, 7/6-fused bicyclic sultams with attenuated electronic, steric and stereochemical properties, depending on the selected building blocks for each scaffold. These sultam scaffolds lie within new chemical space when mapped using the principal moments of inertia (PMI) analysis and overlay analysis presented at the end of Chapter 4, *vide infra*.

Based on the ring systems within the top 100 most frequently used, and sorted by descending frequency in Chapter 1, the top two most frequent frameworks are thia-

[i] A ring system is a complete ring or rings formed by removing all terminal and acyclic linking groups without breaking any ring bonds.

azabicyclo octenone and thia-azabicyclo heptanone, which contain the 6/4- and 5/4-fused bicyclic lactam motifs, respectively. There are numerous pharmaceutical compounds that contain the highlighted motifs and the two examples are penicillins and cephalosporins, which are both acylating agents. They are capable of acylating nucleophilic residues in a diverse range of viral, bacterial and mammalian enzymes. More recently, fine-tuning of the β -lactam scaffold has enabled the development of not only serine-based enzyme inhibitors but also inhibitors of cysteine-based and metalloenzymes.² However, due to the rapidly eroding effectiveness of this class of compounds as a result of the ever-evolving microbial development of β -lactamases, there is an exponentially growing need for new compounds to facilitate or replace the current class of drugs. In this regard, the targets in Chapter 4, namely non-aryl 7/4-, 7/5- and 7/6-fused bicyclic acyl sultams, could be regarded in this light. One potential application of the acyl sultams is the development of probes as acylating agents, by acylating the nucleophilic residues in biological systems. A brief summary of the current landscape of electrophiles for covalent modification with the numerous nucleophiles (amino acids-selectivity) on the chemical-proteomic platforms will be discussed in Section 4.1.2.

4.1.1 Acyl sulfonamides/sultams

Acyl sultams, which are a subset of sultams, represent an interesting and unnatural motif for the development of probes in biological systems due to their distinct physical and chemical properties. Several of the physico-chemical properties include hydrolytic stability, crystallinity and unique sp^3 characteristic, where an extensive list can

be found in Chapter 2. These properties make them an attractive target where they exhibit a variety of biological activities, including anti-inflammatory, anti-bacterial, and anti-cancer, as well as unique biological profiles in different cell assays.³ Shown in Figure 4.1 are a few important examples of bioactive acyl sulfonamides and sultams, however an extensive list of biological activities can be found in a recent dissertation from our laboratory.⁴

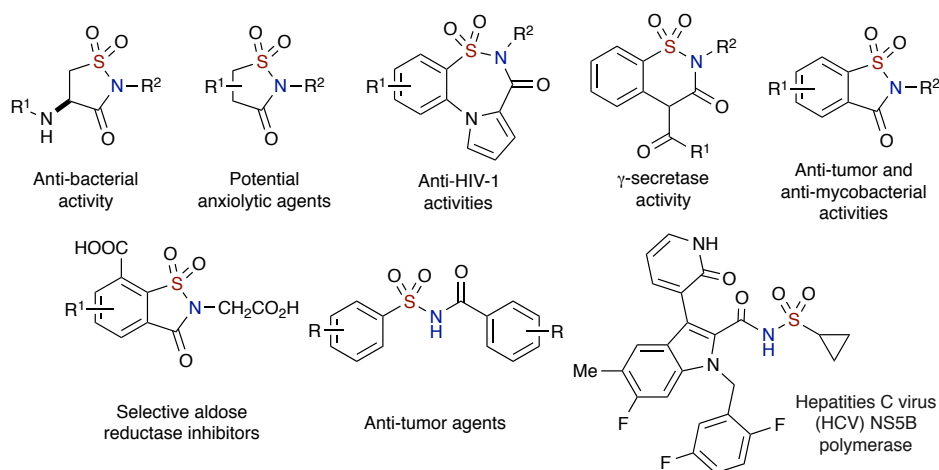


Figure 4.1. Bioactive acyl sultams and sulfonamides.

The prevalence of acyl sulfonamides/sultams as biologically active molecules³ has inspired the present study aimed at the development of a facile and efficient synthesis of non-aryl, 7/4-, 7/5- and 7/6-fused bicyclic acyl sultams, bearing stereogenic centers with different substituents.⁵ In this regard, the growing need to develop streamlined synthetic strategies to access diverse libraries of acyl sulfonamides/sultams has led to this present study; we herein report a complementary ambiphilic pairing (CAP) strategy, *vide infra*, employing 2-chloroethane sulfonyl chloride with different amines and unprotected amino acids in a one-pot, sequential, 3- and 4-component (sulfonylation–aza-Michael addition–

intramolecular amidation–click or carbamoylation) procedures for the generation of sp^3 -rich, 7/4, 7/5 and 7/6-fused bicyclic acyl sultams.

Upon the generation of approximately 203-member library of bicyclic acyl sultams, there are several interesting electrophilic motifs on these acyl sultams, which will be useful in future, applications that include reactivity studies with various nucleophiles (Figure 4.2). Some of the electrophilic motifs are the acyl functional group within the sultam, the carbamate motifs and aryl-halogens, as well as sulfonamides containing aziridines and epoxides, and vinylsulfonamides. The existing landscape of electrophiles for covalent modifications with their respective nucleophiles will be briefly reviewed in the following Section (4.1.2).

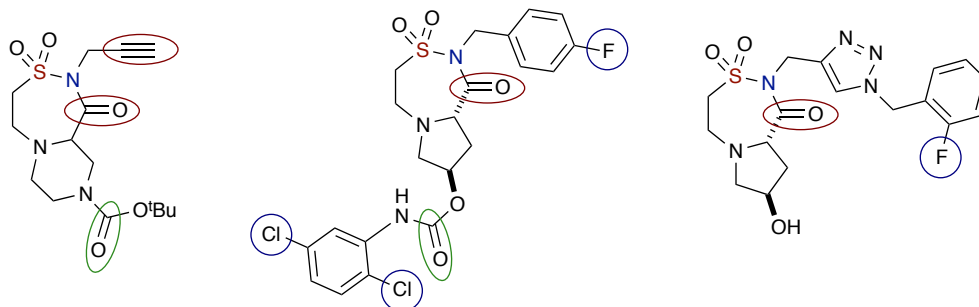


Figure 4.2. *Different electrophilic motifs on acyl sultams.*

4.1.2 Application: Covalent Protein Modification via Residue-specific Electrophiles

One possible application for acyl sultams is the investigation of electrophilic reactivity toward amino acids within the complex proteome. This is based on the numerous functional amino acids that portray vital roles in catalysis and regulation, and which are known to demonstrate elevated nucleophilicity, and which can potentially be

selectively targeted for covalent modification by reactive electrophiles.⁶ The concepts of electrophilicity and nucleophilicity establish the basic principles of organic chemistry are of utmost importance to understanding the fundamentals of chemical reactivity. The formation of covalent bond occurs when a nucleophile attacks an electrophilic center, where the affinity is facilitated primarily by the relative hardness/softness of the two entities. Also, most frequently, nucleophiles are present in proteins provided by the functional side chains of several amino acids, including, serine,⁷ threonine,⁸ cysteine,⁹ lysine,¹⁰ as well as biological molecules like DNA¹¹ and other compounds such as glutathione.¹² Within each class, nucleophilicity depends on the protein microenvironment, where side chains such as lysine exist in the predominantly protonated form at physiological pH. Nucleophiles often react or bind with their counterparts such as electrophilic natural products, covalently acting drugs¹³ and small-molecules probes allowing nature to affect a wide range of biological functions.¹⁴ Chemical-proteomic platforms like activity-based protein profiling (ABPP),¹⁵ exploit this covalently modified reactivity with a chemical probe to selectively target a single enzyme or a functionally related family of proteins. There are different examples of ABPP including the use of fluorophosphonate (FP)-based probes for targeting serine hydrolases (SHs), and vinyl sulfone and epoxide-based probes for lysosomal cysteine proteases and also non-directed strategies by utilizing electrophiles such as sulfonate esters and chloroacetamides to profile the enzymes for which cognate affinity labels do not yet exist.¹⁶

4.1.2.1 Covalent Modification of Serine

An activated serine can be found within a catalytic dyad or triad in the SH enzyme family and this covers approximately 1% of the human proteome.¹⁷ However, the serine residue will have a low reactivity if it is found outside of a typical catalytic site, thus limiting certain electrophiles. The sensitivity of SHs to inhibition by fluoro-phosphonates and FPs was well investigated and the use of probes has enabled the functional explanation of novel SHs, the discovery of selective inhibitors and characterization of dis-regulated SH activities in diseases such as cancer.¹⁸ Furthermore, the high affinity of FPs toward hydroxyl nucleophiles over other reactive groups, like thiols and amines, has rendered the serine-FPs reaction highly effective for proteomic applications (Figure 4.3i).

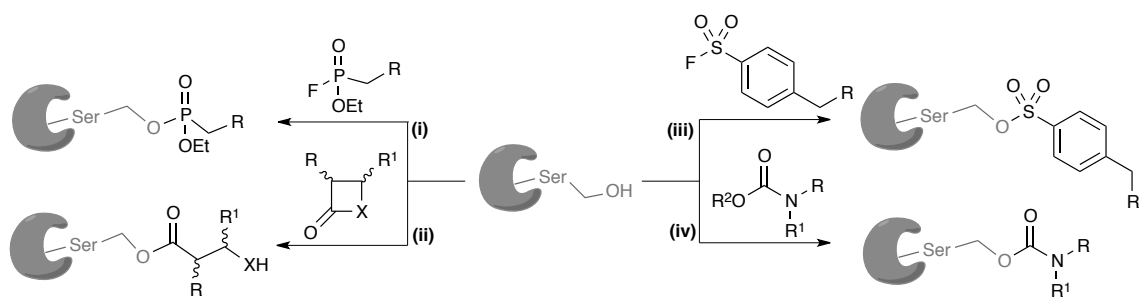


Figure 4.3. Serine-mediated electrophiles for covalent protein modification.⁶

Another important class of serine-reactive electrophiles are β -lactams as they are well characterized by the covalent modification of the serine nucleophile in penicillin binding proteins (PBPs) (Figure 4.3ii). β -lactams activity-based probes libraries were synthesized and evaluated in bacterial proteomes as well as probes originating from several known antibiotics like ampicillin and related analogues, have revealed various SHs being labeled (ATP-dependent caseinolytic protease Clp) and insights on targets

preferences of these privileged scaffolds.¹⁹ The labeling work disclosed that some of these β -lactam-bearing electrophiles are not selective for serine nucleophiles but a similar electrophile β -sultam reacted with an activated threonine-residue in azoreductases.²⁰

Sulfonyl-fluoride derivatives such as 4-(2-aminoethyl) benzenesulfonyl fluoride (pan-serine protease inhibitor) were shown to covalently label multiple serine protease sub-classes, indicating utility as a serine-reactive electrophile (Figure 4.3iii).²¹ Although it is widely utilized in protease cocktails, the reactivity of the sulfonyl-fluoride electrophile was poorly characterized.

Other common serine-reactive electrophiles include carbamates where several carbamate-based inhibitors happen for various SHs and recently, investigations on the balance between affinity and reactivity of this electrophile were completed (Figure 4.3iv).²² A group of carbamates with various leaving groups for instance O-aryl, O-hexafluoroisopropyl (HFIP), and N-hydroxysuccinimidyl (NHS) was shown to be highly selective for SHs; where an HFIP-containing carbamate showed excellent selectivity for two SHs, α - β hydrolase-6 (ABHD6) and monoacylglycerol lipase (MAGL), and was further developed into a fluorescent activity-based imaging probe (JW912).²³

4.1.2.2 Covalent Modification of Cysteine

The cysteine thiol is very reactive due to the electron-rich nature and polarizability of sulfur, facilitating a range of functions, including nucleophilic and redox catalysis, allosteric regulation and metal binding.²⁴ Diverse proteins such as proteases, oxidoreductases and kinases contain functional cysteines, which enables cysteine-

targeted electrophiles to expand the protein families amenable to ABPP. Epoxides are found in many electrophilic natural products like fosfomycin²⁵ and also cysteine protease inhibitor E-64,²⁶ which target cysteine proteases (Figure 4.4i). In addition, studies²⁷ have shown that epoxides are relatively promiscuous to different amino acids. The properties (steric, electronics and stereoelectronics) of the peptide backbone which the mild-electrophile epoxide is connected to, can be attenuated to enable selectivity specific for an amino acid.

Two widely utilized electrophiles in various ABPP applications are chloroacetamides (CA) and iodoacetamides (IA) (Figure 4.4ii). The more reactive IA covalently modifies ~1000 cysteines in the proteome,²⁸ sanctioning the global description of changes in cysteine reactivity. Several instrumental results were identified including bacterial redox modulators,²⁹ cellular targets of electrophilic lipids,³⁰ and zinc-binding cysteines within complex proteomes.³¹ These studies emphasize the benefits of a highly-reactive, yet residue-selective electrophile to gain understanding into modulators of amino-acid nucleophilicity. IA has been shown to react with other nucleophiles, such as the amine group of lysine,³² albeit at high millimolar concentrations.²⁸ In contrast, CA is less reactive than IA but has been also integrated into libraries based on peptide^{16d,33} and piperidine³⁴ scaffolds, leading to the identification of covalent modifiers for nitrilases and glutathione S-transferase omega 1 (GSTO1), respectively.

Other chemotypes that covalently modify cysteine include Michael accepting motifs; acrylamides and vinylsulfonamides (Figure 4.4iii and iv). Two groups were first examined for preferential reactivity toward cysteine over lysine³⁵ as well as evaluated for

fragment-screening applications related to thiol reactivity.³⁶ Among these, reactivity can be attenuated based on the substituents/substituent effect on the electrophiles and this was highlighted by the acrylamide reactivity with different substituents where >2000-fold deviation was observed.³⁶ Finally, the reversibility of Michael adducts with cysteine has been analyzed and can be tuned in a predictable manner where concerns related to off-target protein modification can be obviated.³⁷ Likewise for vinyl sulfonamides can be modulated accordingly to suit the appropriate nucleophiles.

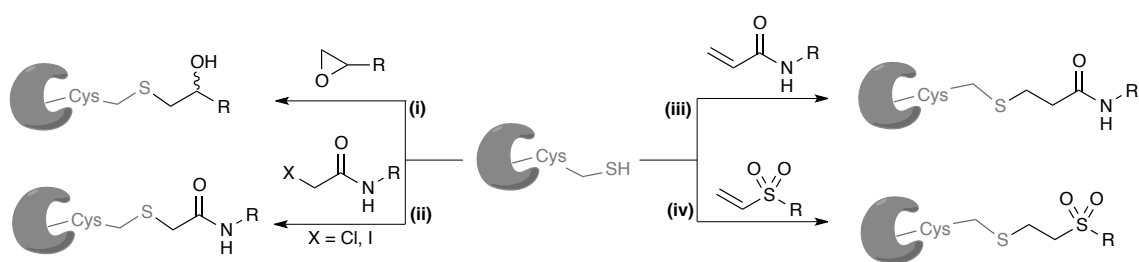


Figure 4.4. Cysteine-mediated electrophiles for covalent protein modification.⁶

4.1.2.3 Covalent Modification of Lysine

A significant challenge of selective modification of functional lysine residues is the abundance of non-functional lysines and *N*-terminal protein amines. However, recent work on aryl halides as protein-reactive electrophiles revealed that the lysine-reactive dichlorotriazine function through a S_NAr mechanism (Figure 4.5i). Advantages including identification of sites of acetylation, active-sites residues and ATP-binding sites by labeling the lysine residues.³⁸ The general reactivity of *N*-phenyl-sulfonamides is poorly studied, although there is an example where the *N*-phenylsulfonamide-containing Toll-like receptor 4 (TLR4) inhibitor TAK-242 covalently modifies Lys64 on human serum

albumin (HSA) (Figure 4.5ii).³⁹ Additional investigation is required to demonstrate more fittingly the potential utility as a lysine-reactive electrophile.

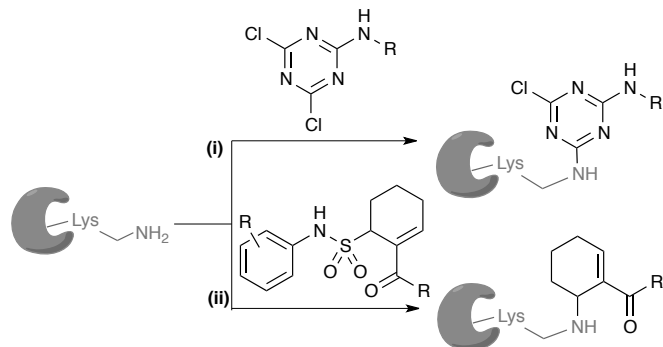


Figure 4.5. *Lysine-mediated electrophiles for covalent protein modification.*⁶

While the current prospect of reactive electrophiles and their respective nucleophiles is promising, electrophiles typically react with more than a single residue (nucleophile). In this regard, continued expansion and development of novel electrophilic species is highly warranted, as is the need for more investigations on their respective reactivity patterns and chemoselectivity. Several properties that can be attenuated include electronic, steric, stereo-electronic and ring-strain of selected electrophiles. Hence, the demand for new small-molecules bearing electrophilic groups with the potential of modulation has motivate efforts to develop efficient syntheses of unique scaffolds. In this regard, this Chapter details efforts to 7/4, 7/5 and 7/6-fused bicyclic acyl sultams that are sp^3 -rich. In the final section of Chapter 4, these sultam scaffolds are evaluated by several computational analyses to demonstrate their underrepresentation in chemical space and with regard to ring systems.

4.1.3 One-pot, Sequential Multi-component Protocols

One-pot, sequential multi-component protocols are versatile strategies to rapidly generate structurally distinct and complex moieties in an efficient manner.⁴⁰ These methods have important ramifications in economical, environmental and synthetic aspects and as a result, these procedures have gained prominence in modern organic synthesis.^{40b} One-pot, sequential strategies are utilized to effect multiple transformations in the same flask thus, negating several purification steps and minimizing hazardous chemical waste making this process green and eco-friendly. In contrast, the one-pot/one-pot, sequential transformations have several obstacles that need to be circumvented. Some of these hurdles include, (i) compatibility of multiple reactions: (ii) side products from earlier reactions that may interfere with the one-pot protocols, and (iii) minimal usage of solvents and reagents. Nevertheless, these one-pot protocols are highly desirable with regards to time, energy, efficiency and purification.

Application of one-pot, sequential protocols to diversity-oriented synthesis (DOS) has emerged as a facilitating platform for the synthesis of new heterocyclic small molecules for high throughput screening (HTS) toward unveiling their biological activity profiles. Within the realms of DOS, accessing diversity elements including skeletal, stereochemical, functional and appendage on small multiple scaffold libraries are highly coveted.⁴¹ Incorporating these essential elements—with high emphasis given to molecular skeletal diversity—into library synthesis generally affords considerable ‘molecular shape space’ coverage, which correlates to broad biological space and also potentially higher biological hit rates.⁴² In contrast, traditional libraries having similar core skeletons

possess only peripheral diversity occupy narrow chemical space, which typically leads to lower biological hit rates. In view of that, the construction of libraries with enhanced structural diversity has the potential to address these challenges. Introduced in the following section, is an efficient strategy that allows for rapid access to structural diverse libraries encompassing molecular complexity, as well as stereochemical and functional diversity.

4.2 Results and Discussion

We previously demonstrated a highly scalable, one-pot complementary ambiphile pairing (CAP) method employing vinyl sulfonamides and amino acids for the preparation of skeletally, stereochemically and peripherally diverse sp^3 -rich acyl sultam scaffolds (Figure 4.6).⁵ The method employs an aza-Michael and amide coupling reactions in a one-pot, sequential protecting group-free protocol utilizing both linear and cyclic amino

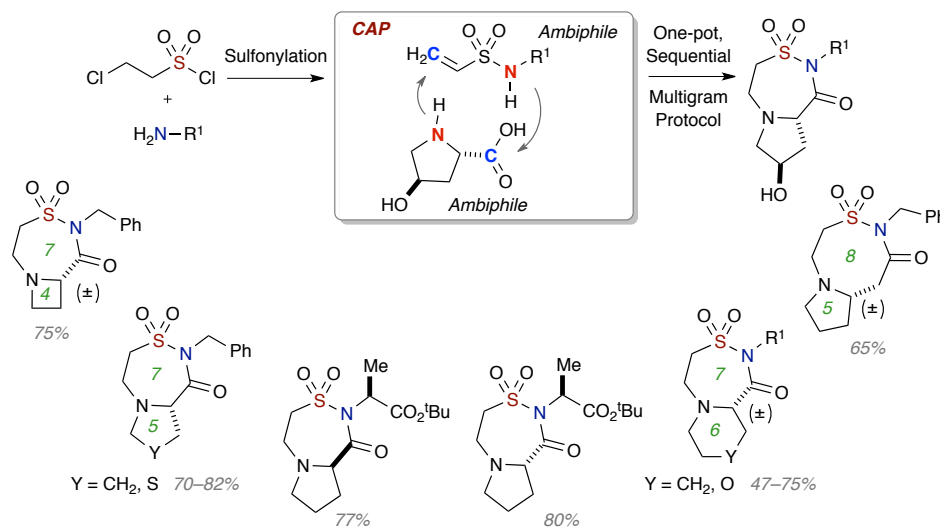


Figure 4.6. One-pot, sequential 3- and 4-component pathways to diverse acyl sultams.

acids building blocks. Use of cyclic amino acids in this protocol, generated an array of sp^3 -rich 7/4-, 7/5- and 7/6-fused bicyclic acyl sultams. The CAP method employed utilizes the ambiphilic nature of both vinyl sulfonamides and amino acids, whereby sulfonamides, can readily undergo hetero-Michael additions as well as facile amidation. The one-pot, sequential aza-Michael–amidation method was also extended to include an initial sulfonylation reaction in a protecting-group free protocol.

With the core strategy in place, we next extended the method to include one-pot, sequential 3- or 4-component protocols in a library platform. In this approach, sulfonylation of different amines with 2-chloroethane sulfonyl chloride, followed by Michael reaction with variety of amino acids and subsequent amide cyclization, enables access to skeletally and stereochemically diverse acyl sultam scaffolds (Figure 4.7). The next objective was to further extrapolate the one-pot, sequential process to a 4-component protocol. Two pathways were envisioned – (i) sulfonylation with propargylamine, followed by a click reaction as the fourth step would provide triazolated products and

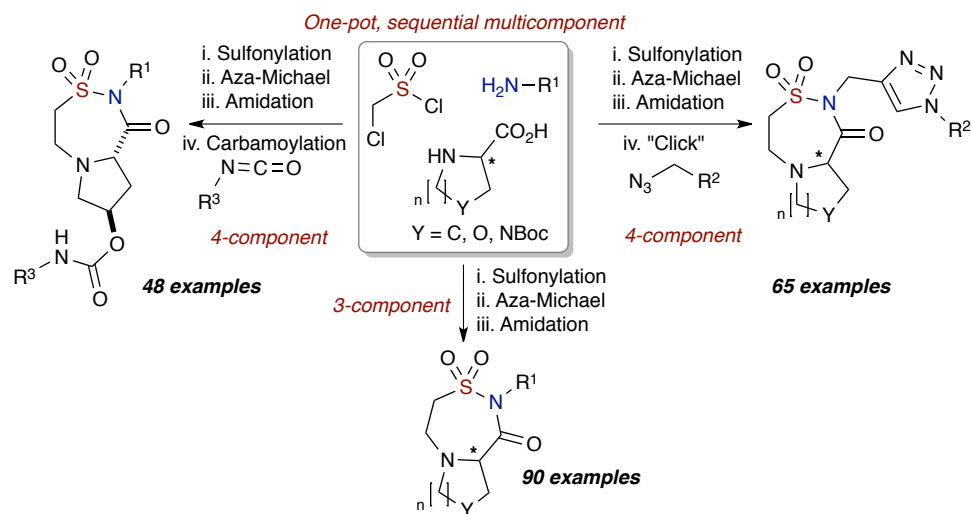


Figure 4.7. One-pot, sequential 3- and 4-component pathways to diverse acyl sultams.

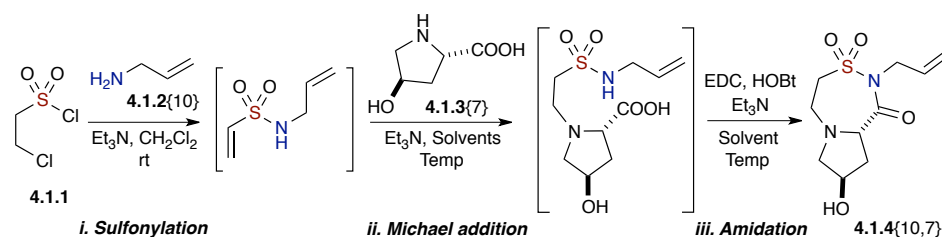
(ii) aza-Michael reaction with hydroxyproline to afford a hydroxyl functional handle for carbamoylation with isocyanates (Figure 4.7). However, for this chapter, only the generation of 90-member library employing the one-pot, sequential 3-component approach will be discussed in detail. The 4-component pathways were reviewed in a recent dissertation (Naeem Asad).⁴

4.2.1 Optimization Studies

The one-pot, sequential 3-component method was first investigated in 2014 and based on the reported protocol, the first experiment was setup and optimized utilizing the initial reaction conditions provided. The preliminary reaction conditions were employed for the synthesis of vinyl sulfonamide *via* a sulfonylation of allylamine **4.1.2**{10} with 2-chloroethane sulfonyl chloride **4.1.1** in the presence of Et₃N and CH₂Cl₂ (Table 4.1, entry 1a), followed by a one-pot aza-Michael addition and an intramolecular amide coupling provided the desired acyl sultam in good yield (86% over 2 rxns; 93% avg/rxn) (Table 4.1, entry 1b). With the result, efforts were made for the one-pot, sequential, 3-component reaction protocol, by examining equivalents of reagents, as this is vital for one-pot, multicomponent reactions-to prevent excess reagents/by-products from advancing to the next reaction. Hence, the equivalents of amino acid **4.1.3**{7} were increased to ensure full conversion of the starting material to the Michael adduct intermediate, and also the equivalents of Et₃N was decreased to prevent excess of reagent. Lastly, for the intramolecular amidation, the amount of hydroxybenzotriazole (HOBt) and solvent were investigated to facilitate the full conversion of starting material (Table 4.1,

entry 2). Finally, the optimal reaction conditions were achieved with sulfonylation [1.5 eq. of **4.1.2**{10}, 2.0 eq. of Et₃N, and CH₂Cl₂ (0.5 M)] at room temperature, followed by aza-Michael addition [1.2 eq. of **4.1.3**{7}, 2.0 eq. of Et₃N and MeOH/H₂O (0.5 M)] at 60 °C for 12 h and lastly, intramolecular amidation [2.0 eq. of EDC, 1.5 eq. of HOBT, 2.0 eq. of Et₃N, DMF (0.08 M)] at room temperature afforded acyl sultam **4.1.4**{10,7} in satisfactory yield (30% over 3 rxns; 67% avg/rxn) (Table 4.1, entry 3).

Table 4.1. Optimization of one-pot, sequential 3-component reaction protocol



entry	reactions	reagents (eq.)	T/time	yield
1a	sulfonylation	4.1.2 {10} (1.5), Et ₃ N (2.0), CH ₂ Cl ₂ (0.5 M)	rt/12 h	88%
1b	Michael	4.1.3 {7} (1.0), Et ₃ N (3.0), MeOH/H ₂ O (0.5 M)	60 °C /12 h	-
	amidation	EDC (2.0), HOBT (0.2), Et ₃ N (2.0), DMF (0.05 M)	rt/12 h	86%
2	sulfonylation	4.1.2 {10} (1.5), Et ₃ N (2.0), CH ₂ Cl ₂ (0.5 M)	rt/12 h	-
	Michael	4.1.3 {7} (1.2), Et ₃ N (2.0), MeOH/H ₂ O (0.5 M)	60 °C /12 h	-
	amidation	EDC (2.0), HOBT (1.0), Et ₃ N (2.0), DMF (0.08 M)	rt/12 h	29% ^a
3	sulfonylation	4.1.2 {10} (1.5), Et ₃ N (2.0), CH ₂ Cl ₂ (0.5 M)	rt/12 h	-
	Michael	4.1.3 {7} (1.2), Et ₃ N (2.0), MeOH/H ₂ O (0.5 M)	60 °C /12 h	-
	amidation	EDC (2.0), HOBT (1.5), Et ₃ N (2.0), DMF (0.08 M)	rt/12 h	30% ^a

^aIsolated yield over three reactions.

4.2.2 Library Design and Scope of Reagents

A 90-member, full matrix library was designed by using in silico analysis.⁴³ Nine amines were selected based on the physico-chemical property filters that were applied, to guide the elimination of undesirable building blocks that led to products with undesirable in silico properties (see Supporting Information in Chapter 5 for full in silico data and detailed information on the calculations). Simple aliphatic and aromatic with different substituents amines were introduced as well as others with functional motifs like olefins to modulate the physico-chemical properties of the substrates. Furthermore, the amino acids were carefully chosen and investigated with the one-pot protocol.

Simple alkyl amino acids with both stereochemistry (*R* and *S*) and ring sizes were studied and selected as the resulting core bicyclic acyl sultams will be skeletally diverse within the group of scaffolds. In addition, inclusion of heteroatoms in the core introduces diversity and moderates the properties, however, selected examples proved to be problematic, thus the elimination of some building block, but retainment of the non-challenging substrates **4.1.3**{8–9}.

Hydroxyl-containing amino acids **4.1.3**{6–7} were favored as they are able to enhance the physico-chemical properties like solubility and CLogP values. Hence, the desired diversity reagents were selected and a virtual library incorporating all possible combinations of the building blocks amines **4.1.2**{1–10} and amino acids **4.1.3**{1–9} was constructed (Figure 4.8). Physico-chemical property filters were applied and these metric filters included standard Lipinski's rule of five parameters (molecular weight <500, ClogP <5.0, number of H-acceptors <10, and number of H-donors <5), in addition to

consideration of the number of rotatable bonds (<5) and polar surface area. Absorption, distribution, metabolism and excretion (ADME) properties were calculated by using the Volsurf program.⁴⁴ Cartesian grid based chemical diversity analysis was performed according to the method described previously,⁴⁵ by using standard H-aware 3D BCUT descriptors comparing against the MLPCN screening set (ca. 7/2010; ~330,000 unique chemical structures). Guided by this library design analysis, amines **4.1.2**{1–10} and amino acids **4.1.3**{1–9} were chosen to generate the aforementioned 90-member library.

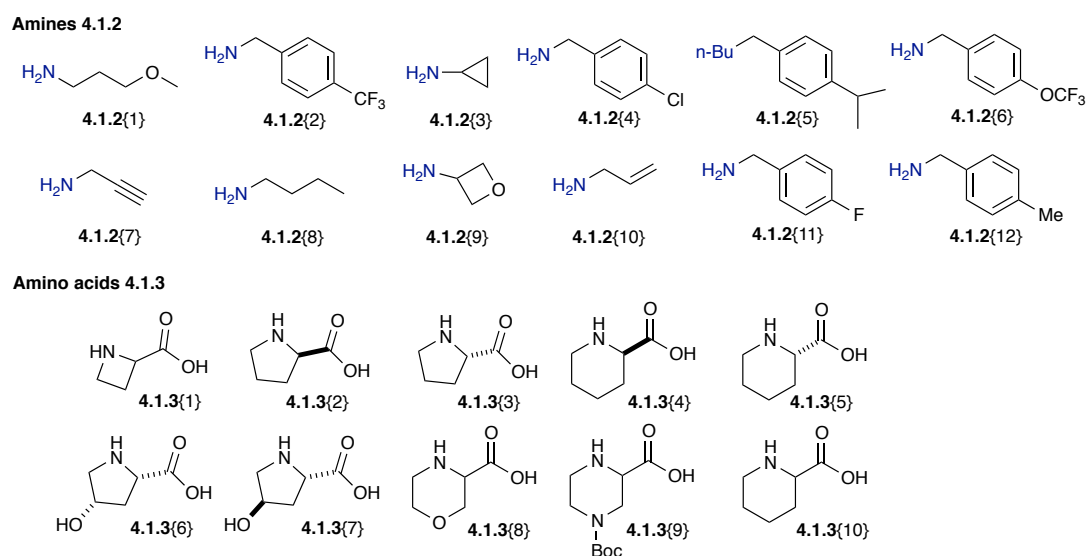
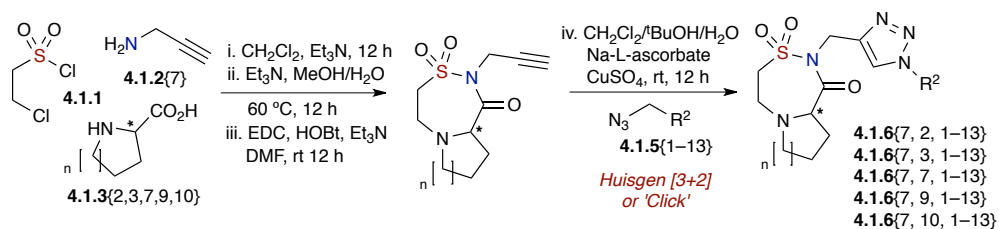


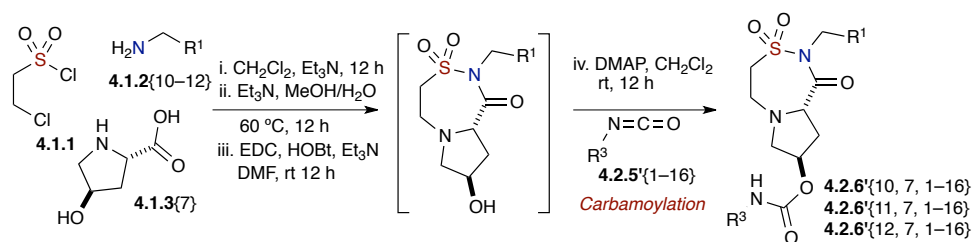
Figure 4.8. Diversity reagents of 12 amines **4.1.2**{1–12} and ten amino acids **4.1.3**{1–10}.

Efforts next extended the one-pot, sequential protocol via the inclusion of a fourth component, namely a click reaction with the corresponding azides **4.1.5**{1–13} and a propargylic amine to provide a number of triazolated scaffolds (Scheme 4.1). Alternatively, carbamylation with the addition of isocyanates **4.2.5'**{1–16} afforded the carbamates containing acyl sultams (Scheme 4.2). More detailed description of this current method can be found in a recently reported dissertation (Naeem Asad).⁴

Scheme 4.1. Reaction pathway with Huisgen [3+2] or 'Click' reaction as the 4-component



Scheme 4.2. Reaction pathway with carbamoylation as the 4-component

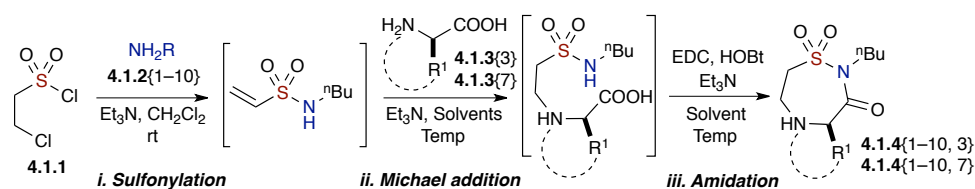


4.2.3 Validation and Library Generation

With the optimal reaction conditions in hand, a 20-member validation library was prepared by using ten amines **4.1.2**{1–10} and two different amino acids—**4.1.3**{3} and **4.1.3**{7}—in pressure tubes and carousel for stirring and heating purposes (Table 4.2). Upon completion of the three reactions, all 20 crude reaction mixtures were diluted with water, extracted with EtOAc (2x), and the layers were separated. The resulting organic layers were filtered through a silica SPE, and purified by automated mass-directed HPLC. Library validation was vital to assess both substrate and reaction scope, along with evaluating the application of automated mass-directed HPLC as the final analysis and purification method. Evaluation of the validation library demonstrated that all 20 members were successfully prepared (average yield = 33% over 3 rxns; 69% avg/rxn) in

nearly all of the desired acyl sultam final masses (20–40 mg), with all 20 possessing a final purity >90%. These sultams were purified several times due to the properties of the substrates/structures, resulting in yields that are relatively lower than average. The protocol is very dependent on the polarity of the substrates as well as the extraction method, which led to the isolated yields being relatively different.

Table 4.2. Optimization of one-pot, sequential 3-component reaction protocol



entry	sultam	yield (%) ^a	entry	sultam	yield (%) ^a
1	4.1.4 {1,3}	56	1	4.1.4 {1,7}	4 ^b
2	4.1.4 {2,3}	49	2	4.1.4 {2,7}	4 ^b
3	4.1.4 {3,3}	29	3	4.1.4 {3,7}	16
4	4.1.4 {4,3}	50	4	4.1.4 {4,7}	14
5	4.1.4 {5,3}	41	5	4.1.4 {5,7}	8
6	4.1.4 {6,3}	64	6	4.1.4 {6,7}	25
7	4.1.4 {7,3}	32	7	4.1.4 {7,7}	48
8	4.1.4 {8,3}	7 ^b	8	4.1.4 {8,7}	11
9	4.1.4 {9,3}	16	9	4.1.4 {9,7}	33
10	4.1.4 {10,3}	54	10	4.1.4 {10,7}	30

^aIsolated yield after three reactions. ^bRe-purified thrice.

With the validation completed, the remaining 70 compounds were synthesized via the one-pot, sequential 3-component protocol that consists of sulfonylation–aza-Michael–

amidation with ten amines **4.1.2**{1–10} and seven other amino acids **4.1.3**{1–2}, **4.1.3**{4–6} and **4.1.3**{8–9}. Under the optimized reaction conditions, the 70-member library were constructed and purified by automated mass-directed HPLC, although some scaffolds had to be purified thrice. A total of 90 compounds were prepared, isolated in satisfactory yields (average yield: 30% over 3 rxns; 67% avg/rxn) and 79/90 compounds had purity greater than 90% after automated purification (see Supporting Information for all compounds with full numeric data). Final assessment of the library established that the diverse compounds could be generated in a facile manner *via* a one-pot, sequential protocol.

4.2.4 Computer Analysis of Molecular Properties and Shape Diversity

4.2.4.1 Molecular Properties

Molecular properties for the library were calculated (Figure 4.9) and average property values for the respective core acyl sultams are displayed in Table 4.3. Analysis of molecular properties suggests some compounds may have desirable qualities for biological or reactivity probes, while others could have a more appropriate role as drug lead discovery (Table 4.3).⁴⁶ The average molecular weights of all acyl sultams fall within the acceptable range (molecular weight less than 500 Da) for drug-like compounds,^{46a} as well as the lack of hydrogen bond donors may alternatively allowed them as suitable biological probes for disrupting protein–protein interactions.^{46b}

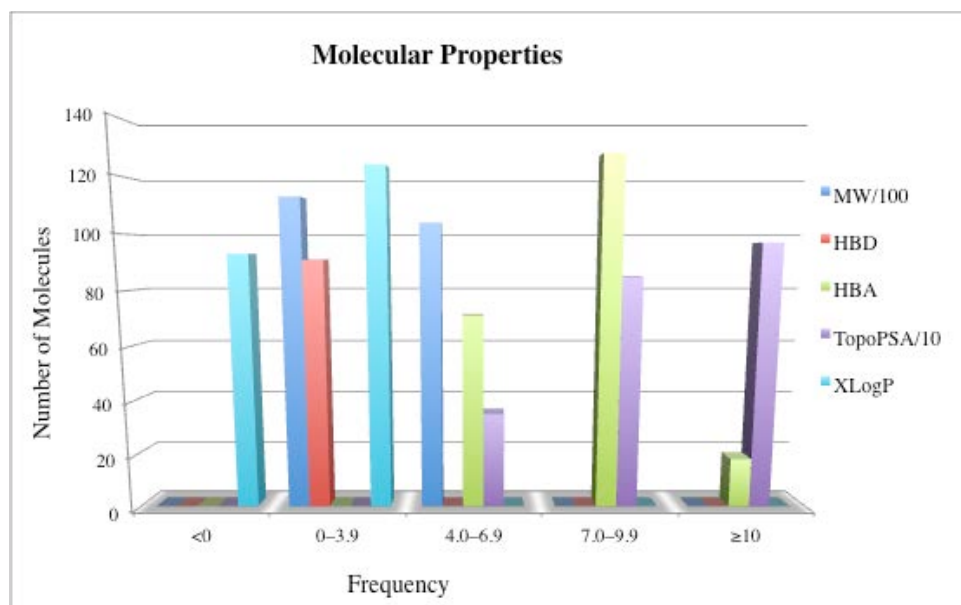


Figure 4.9. Molecular properties of the 90-member library. HBD: hydrogen bond donor, HBA: hydrogen bond acceptor, TopoPSA: topological polar surface area, XLogP: partition coefficient.

Table 4.3. Average molecular property values.

property	4.1.4 {1-10,1}	4.1.4 {1-10,2} 4.1.4 {1-10,3}	4.1.4 {1-10,4} 4.1.4 {1-10,5}	4.1.4 {1-10,6} 4.1.4 {1-10,7}	4.1.4 {1-10,8} 4.1.4 {1-10,9}
MW	279	293	307	309	358
HBD	0	0	0	1	0
HBA	5.3	5.3	5.3	6.3	7.3
cLogP	-0.1171	0.2409	0.5989	-0.7891	-0.0136

4.2.4.2 Principal Moments of Inertia (PMI) Analysis

As described in previous chapters, the basic information can be quantified more thoroughly *via* principal moments of inertia (PMI) analysis,⁴⁷ which was used herein to assess the molecular shape diversity. PMI analysis utilizes shape-based descriptors: The minimum energy conformation of each library member is determined, PMI ratios are calculated and normalized, and a subsequent triangular plot depicts the shape diversity of the library. From it, the greater shape diversity of a library associates with increased probability of the library containing bioactive molecules.

The analysis reveals three sets of acyl sultams (green, red and cayenne spheres) largely emulate the shape distribution of the set of FDA approved drugs (Figure 4.10), thus demonstrating the potential drug-likeness of the scaffolds and populating the chemical space with more unique scaffolds. The synthesis of 90 compounds represented by the green spheres was described in the earlier sections and is the highlight of this chapter. However, for the purpose of the discussion here, based on the graphics provided in Figure 4.10, four sets of bicyclic acyl sultams are briefly mentioned. The most populated region contains the majority of the acyl sultams as well as the hybrid region, situated in the center of the triangle, which contains a mixture of acyl sultams with different peripheral substituents. The hybrid region has a smaller amount of the FDA-approved drugs where the majority of the blue spheres representing the carbamate-containing acyl sultams, occupy an underrepresented region of chemical space, thus illustrating the novel nature of some compounds from the perspective of molecular shape. Overall, the shape diversity of the library implies a potential influence in compound

binding to a biological target.

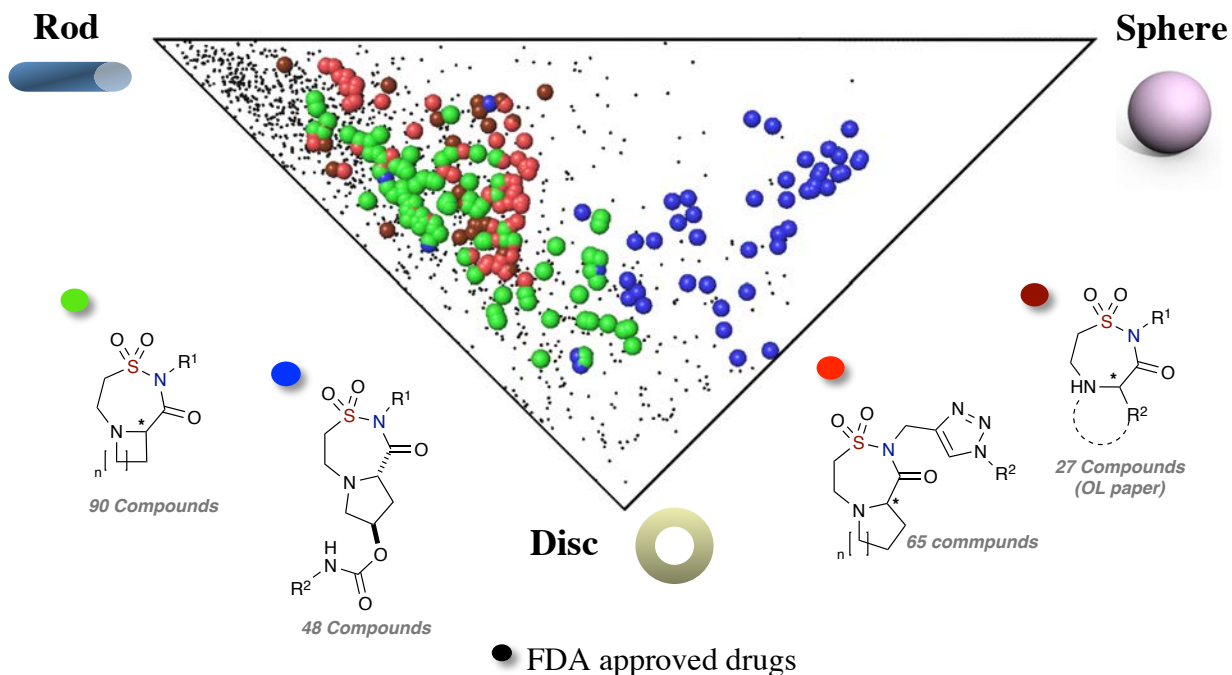


Figure 4.10. Distribution of four acyl sultam libraries.

4.2.4.3 Overlay Analysis⁴⁸

The overlay produced for the 90 compounds reported herein is depicted in Figure 4.11 and provides a fundamental indication of the shape distribution and diversity evident in this library. The peripheral spatial distinction is the main source of diversity, however, the conserved core has several distinct differences derived from the building blocks, which consists of 7/4, 7/5 or 7/6-fused bicyclic system, where some have substituents extending outwards. Hence, orientations **4.11iii** and **4.11iv** collectively suggest that the library generally tends to lie between elongated (rod-like) and flat (disc-like) structures, while the distribution of functional substituents across angles covering most part of the whole sphere adjoining the conserved core, suggests that the library as a whole attains a

realistic level of shape-based diversity.

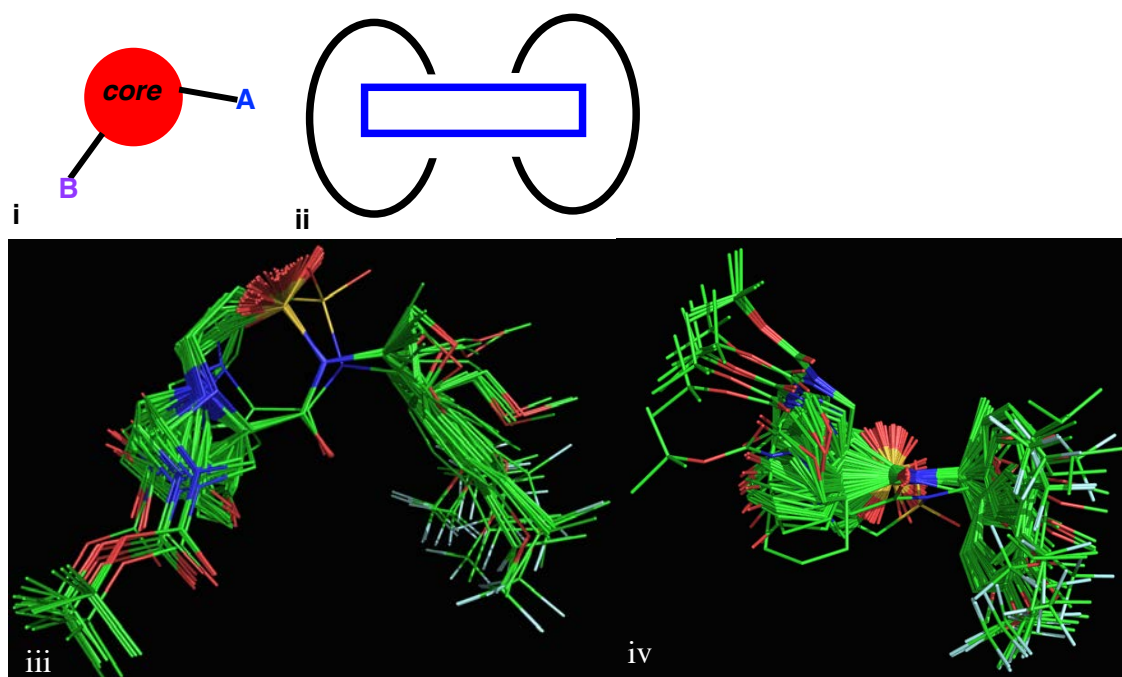


Figure 4.11. (i) Simple cartoon of the library compounds, with a core of MW~189–217, based on Lipinski's rules (MW<500), and comprising one substituent having MW~50–180, to establish different functional groups and the second substituent that influence the core structure with MW~10–100. (ii) This cartoon reveals that the substituents extend out of the core in a circular motion. (iii) Overlay image exhibiting the common core in these 90 compounds. (iv) Overlay image revealing that the substituents are extending outwards in a semi-circular motion as mentioned in overlay image (ii).

4.2.5 Conclusion

Overall, a one-pot, sequential 3-component reaction protocol employing sulfonylation–aza-Michael addition–Intramolecular amidation has been developed. Utilizing various commercially available amines and amino acids, a 79/90-member library of 7/4, 7/5 and 7/6-fused bicyclic acyl sultams was generated. A series of computational analyses was performed, and revealed that the compounds reported herein occupy a good combination of populated and underrepresented chemical space relative to

FDA-approved drugs. The compounds also sample a reasonable array of shape space within all three rod-like, disc-like and sphere-like structures. The products have been submitted for evaluation of their biological activity in high-throughput screening assays at the NIH MLPCN and the results will be reported in due course.

4.2.6 Reactivity Profiling of Potential Electrophilic Modifiers

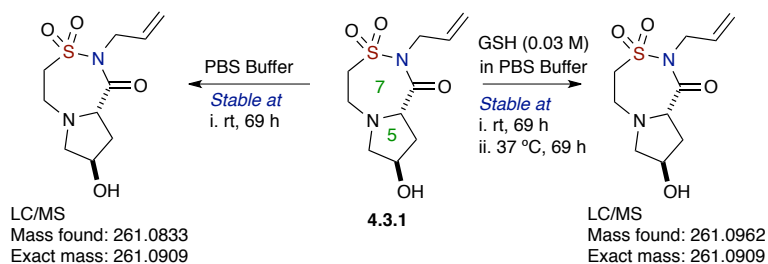
4.2.6.1 Initial Reactivity Profiling of Acyl Sultams

Recent interest in drugs that covalently modify their protein targets or other biomacromolecules has motivated the search for small molecules with enhanced efficacy and selectivity towards the suppression of enzymatic activity by targeting uniquely positioned nucleophilic amino acid residues.⁴⁹ As described in Section 4.1.2, one of the potential applications for the non-aryl 7/4-, 7/5- and 7/6-fused bicyclic acyl sultams is the ability to serve as unique electrophilic modifiers by reacting in the presence of biologically relevant nucleophiles such as cysteine, serine and lysine, among other examples.⁶ In this regard, preliminary investigations have begun to study the reactivity of the cyclic and bicyclic acyl sultams detailed in this Chapter. This is with respect to their ability to serve as novel electrophilic modifiers with ultimate potential as probes in chemical biology and/or targeted small-molecule covalent inhibitors.

Initial studies on electrophilic reactivity describe reactions of acyl sultams with the nucleophiles glutathione (GSH), cysteine (Cys) and serine (Ser). Before these studies began, we aimed to investigate the stability of various acyl sultams in 100 mM phosphate buffered saline (PBS) solution at pH 7.4 as traditionally, experiments with GSH often

occur in this buffered media. The exposure time of acyl sultam **4.3.1** in PBS was extended up to 69 h to determine its stability over a long period of time at room temperature (Scheme 4.3). Subsequently, GSH and **4.3.1** were stirred in PBS at a concentration of 0.03 M and at room temperature, and the reaction mixture was monitored by TLC, for up to 69 h. When **4.3.1** did not show reactivity as evidenced by TLC, the reaction mixture was then heated to 37 °C and monitoring by TLC was continued over another 69 h. Mass spectral data analyses for acyl sultam **4.3.1** supported the TLC findings, which indicated that the starting material was still present in the reaction mixture. These results suggest that the acyl sultam is relatively stable in PBS buffer with both absence and presence of GSH, as described in Scheme 4.3.

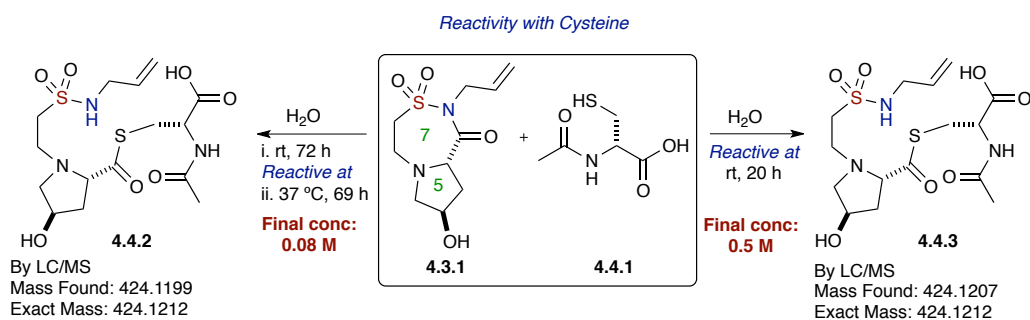
Scheme 4.3. Initial reactivity studies in phosphate buffer and with glutathione (GSH)



Reactivity with *N*-acetyl-*L*-cysteine was next investigated, whereby acyl sultam **4.3.1** was reacted with this nucleophilic residue at different solvent concentrations. The initial experiment reacted within a shorter reaction time of 20 h for complete SM consumption when the concentration was at 0.5 M in H₂O, and a longer reaction time with heating up to 37 °C when the condition was more diluted (0.08 M) (Scheme 4.4). *N*-acetyl-*L*-cysteine was added in excess up to five equivalents in both reactions. These

preliminary results revealed that the thiol of cysteine reacts with the electrophilic acyl sultam to a certain extent as shown by the initial TLC findings, implying the disappearance of the SM with new products being formed. This is supported by mass spectrometry data for both reactions.

Scheme 4.4. *Initial reactivity studies with cysteine.*



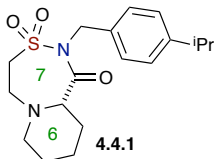
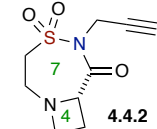
The primary goal of this project that is currently at the infancy stage is to determine if there is chemoselectivity for the reactions between the electrophilic acyl sultams and nucleophilic residues such as cysteine, serine and lysine under various conditions. With the initial data highlighted in Scheme 4.4, investigations were extended to acyl sultams containing different ring systems, and thus varying the ring strain, with a preliminary array of nucleophiles.

Hence, the investigations began with the 7/6-fused acyl sultam **4.4.1** where reaction with *N*-acetyl-*L*-cysteine only occurred after prolonged heating for several hours at both 37 °C and 60 °C (Table 4.4, entry 1), as supported by both TLC and mass spectral analyses. As a second nucleophile, *N*-Boc-*D*-alaninol was employed for preliminary investigations with oxygen nucleophiles. This study showed the disappearance of

starting material within 63.5 h of heating at 37 °C, with mass spectral data supporting the TLC analysis (Table 4.4, entry 3). In addition, the 7/6-fused acyl sultam **4.4.1** reacted with K₂CO₃ in MeOH at room temperature and within 15 h of stirring afforded the corresponding sulfonamide methyl ester, which was also supported by ¹H NMR data (Table 4.4, entry 4).

The substrate for this preliminary investigation was the novel, 7/4-fused bicyclic acyl sultam **4.4.2**, which was presumed to be an interesting electrophilic modifier due to enhanced ring strain, and thus could potentially react faster with a range of nucleophiles under milder reaction conditions. These assumptions were substantiated via reaction with *N*-acetyl-*L*-cysteine when performed in H₂O at room temperature to yield the ring-opened product sulfonamide as verified again by mass spectral data, together with the initial TLC analysis, although this initial reaction was conducted at a higher concentration of 1.3 M (Table 4.4, entry 2). However, the reaction with *N*-acetyl-*L*-cysteine at a lower

Table 4.4. Analysis of reactivity with different nucleophiles and 7/6- and 7/4-fused ring systems.

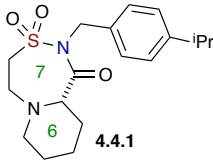
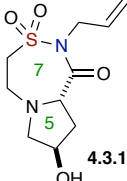
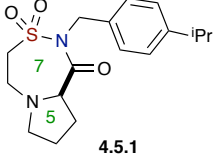
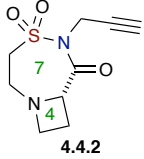
	1	2	3	4
	rt, 37 °C, 60 °C N-Acetyl-L-Cys in PBS Buffer	rt, 37 °C, 60 °C N-Acetyl-L-Cys in H ₂ O	rt, 37 °C, 60 °C D-Alaninol in PBS Buffer	rt, 37 °C, 60 °C K₂CO₃ in MeOH
	Stable @ 37 °C, 63.5 h Reactive @ 60 °C, 73 h ^a (0.022 M)	–	Reactive @ 37 °C, 63.5 h ^a (0.022 M)	Reactive @ rt, 15 h 0.2 M, ¹ H NMR
	No SM by TLC @ rt, 7 h	Reactive @ rt, 7 h ^a (1.3 M)	Reactive @ rt, 7 h ^a (0.066 M)	Reactive @ rt, 10 h ^a (0.2 M)

concentration [0.066 M] in PBS buffer solution was inconclusive, as the mass spectral data did not confirm the formation of the expected product although the starting material was consumed as attributed by TLC (Table 4.4, entry 1). Likewise, the 7/4-fused ring system **4.4.2** reacted with *N*-Boc-*D*-alaninol and provided the sulfamoyl-carboxylate derivative, as supported by both TLC and mass spectral data (Table 4.4, entry 3). Furthermore, this electrophilic motif reacted with K_2CO_3 in MeOH at room temperature within 10 h of stirring to furnish a similar methyl ester-analogue with mass spectral data substantiating the TLC analysis (Table 4.4, entry 4).

As described in Table 4.5 is the overall summary of four different acyl sultams and their respective results with the different nucleophilic residues. The final substrate for this study is the un-substituted 7/5-fused bicyclic acyl sultam **4.5.1** where harsher reaction conditions were employed for the three nucleophiles (GSH, *N*-acetyl-*L*-cysteine and *N*-Boc-*D*-alaninol) that were not reacting with the aforementioned electrophile at room temperature (Table 4.5, entries 2–4). Heating up to 60 °C and prolonged reaction times were required and the complete disappearance of SM **4.5.1** was seen only after the extended period of time. This is based on the TLC findings although the mass spectral data supporting this observation was inconclusive. Thus, more experiments are required to further analyze this substrate. A final, but notable result that was carried out involving the comparison between the reactions of 7/6-, 7/5- and 7/4-fused acyl sultams (**4.4.1**, **4.5.1** and **4.4.2**) with GSH, whereby both larger systems remained unreactive, and whereas the more strained 7/4-fused ring system **4.4.2** reacted with GSH with complete

SM disappearance in under 72 h heated at 60 °C (Table 4.5, entry 2). This is based on the TLC findings together with the mass spectral data supporting this observation.

Table 4.5. Summary of electrophilic reactivity of bicyclic acyl sultams.

entry	reaction conditions and nucleophiles	 4.4.1	 4.3.1	 4.5.1	 4.4.2
1	PBS Buffer	Stable @ rt	Stable @ rt	Stable @ rt	Stable @ rt
2	rt, 37 °C, 60 °C in GSH (0.03 M) in PBS Buffer	Stable @ 60 °C, 72 h	Stable @ 37 °C, 69 h	Stable @ 37 °C, 62 h No SM by TLC @ 60 °C, 93 h	Stable @ rt, 15 h Reactive @ 60 °C, 72 h^a
3	rt, 37 °C, 60 °C N-Acetyl-L-Cys in PBS Buffer	Stable @ 37 °C, 63.5 h Reactive @ 60 °C, 73 h^a (0.022 M)	–	No SM by TLC @ 60 °C, 93 h	No SM by TLC @ rt, 7 h
4	rt, 37 °C, 60 °C D-Alaninol in PBS Buffer	Reactive @ 37 °C, 63.5 h^a (0.022 M)	–	No SM by TLC @ 60 °C, 93 h	Reactive @ rt, 7 h^a (0.066 M)
5	rt, 37 °C, 60 °C N-Acetyl-L-Cys in H ₂ O	–	Reactive @ rt, 20 h^a 0.5 M Reactive @ 37 °C, 69 h^a 0.08 M	–	Reactive @ rt, 7 h^a (1.3 M)
6	rt, 37 °C, 60 °C K₂CO₃ in MeOH	Reactive @ rt, 15 h 0.2 M, ¹ H NMR	–	–	Reactive @ rt, 10 h^a (0.2 M)

^awith LC/MS data provided.

In summary, the aforementioned promising preliminary results demonstrate that the titled novel, fused bicyclic acyl sultams are acting as electrophilic modifiers and thus have potential as electrophilic probes. Current and future efforts are aimed at further developing routes to additional acyl sultams that are attenuated electronically, sterically and stereochemically for subsequent reactivity profiling with a range of nucleophiles with the ultimate goal of being able to modulate important proteins in biological systems.

4.3 Summary and Outlook

In summary, with a number of interesting applications readily available for these newly synthesized bicyclic acyl sultams, efforts will be focused on new strategies to modulate the properties of these unique systems. In addition, submission of the 7/4, 7/5 and 7/6-fused bicyclic acyl sultams to biological collaborators will allow for additional screening to potentially reveal interesting biological activity. Efforts along these courses of action are currently in order and will be reported in due course.

4.4 References Cited

- [1] Taylor, R. D.; MacCoss, M.; Lawson, A. D. G. Rings in Drugs. *J. Med. Chem.* **2014**, *57*, 5845–5859.
- [2] (a) Konaklieva, M. I.; Plotkin, B. J. Asymmetric synthesis of β -lactams via the Staudinger reaction. In *Amino Acids, Peptides and Proteins in Organic Chemistry.*; Hughes, A. B. Ed.: Wiley-VCH Verlag GmbH & Co. KGaA: **2011**; pp 293–319. (b) Konaklieva, M. I.; Plotkin, B. J. The relationship between inhibitors of eukaryotic and prokaryotic serine proteases. *Mini-Rev. Med. Chem.* **2004**, *4*, 721–739. (c) Konaklieva, M. I.; Plotkin, B. J.; Herbert, T. β -lactams as neuroprotective agents. *Anti-Infect. Agents Med. Chem.* **2009**, *8*, 28–35.
- [3] (a) Da Settimo, F.; Primofiore, G.; La Motta, C.; Sartini, S.; Taliani, S.; Simorini, F.; Marini, A. M.; Lavecchia, A.; Novellino, E.; Boldrini, E. Naphtho[1,2-*d*]isothiazole acetic acid derivatives as a novel class of selective aldose reductase inhibitors. *J. Med. Chem.* **2005**, *48*, 6897–6907. (b) Di Santo, R.; Costi, R.; Artico, M.; Massa, S.; Marongiu, M. E.; De Montis, A.; La Colla, P. 1,2,5-Benzothiadiazepine and pyrrolo[2,1-*d*][1,2,5]benzo-thiadiazepine derivatives with specific anti-human immunodeficiency virus type 1 activity. *Antiviral Chem.*

Chemother. **1998**, *9*, 127–137. (c) Abou-Gharbia, M.; Moyer, J. A.; Patel, U.; Webb, M.; Schiehser, G.; Andree, T.; Haskins, J. T. Synthesis and structure activity relationship of substituted tetrahydro- and hexahydro-1, 2-benzisothiazol-3-one 1, 1-dioxides and thiadiazinones: potential anxiolytic agents. *J. Med. Chem.* **1989**, *32*, 1024–1033. (d) Klaus, B.; Guenter, T.; Edward, S. L.; Miao, C. K.; Beck, B.; Sams-Dodd, F.; Kugler, D.; Klinder, K.; Dorner-Ciossek, C.; Kostka, M. Treatment of diseases associated with altered level of amyloid beta peptides. PCT Int. Appl. WO 2005110422 A2 20051124, 2005. (e) Chen, Z.; Demuth, T. P., Jr.; Wireko, F. C. Stereoselective synthesis and antibacterial evaluation of 4-amido-isothiazolidinone oxides. *Bioorg. Med. Chem. Lett.* **2001**, *11*, 2111–2115. (f) Groutas, W. C.; Homer-Archield, N.; Chong, L. S.; Venkataraman, R.; Epp, J. B.; Huang, H.; McClenahan, J. J. Stereoselective synthesis and antibacterial evaluation of 4-amido-isothiazolidinone oxides. *J. Med. Chem.* **1993**, *36*, 3178–3181. (g) Guzel, O.; Salman, A. Synthesis, antimycobacterial and antitumor activities of new (1,1-dioxido-3-oxo-1,2-benzisothiazol-2(3*H*)-yl)methyl *N,N*-disubstituted dithiocarbamate/O-alkyldithiocarbonate derivatives. *Bioorg. Med. Chem.* **2006**, *14*, 7804–7815. (h) Seibel, J.; Brown, D.; Amour, A.; Macdonald, S. J.; Oldham, N. J.; Schofield, C. J. Regulation of Jumonji-domain-containing histone demethylases by hypoxia-inducible factor (HIF)-1 alpha. *Bioorg. Med. Chem. Lett.* **2003**, *13*, 387–389. (i) Pomarnacka, E.; Kornicka, A.; Saczewski, F. A facile synthesis and chemical properties of 3,4-dihydro-2*H*-1,5,2-benzof[d]thiazepin-3-ones with potential anticancer activity. *Heterocycles* **2001**, *55*, 753–761. (j) Bhushan, L. V.; Singh, S. K.; Venkateswarlu, A.; Bhushan, L. B.; Reddy, P. G.; Ramanujam, R.; Misra, P. Pyrazoles having antiinflammatory activity. PCT Int. Appl. WO 2000066562 A1 20001109, 2000. (k) Chen, K. X.; Vibulbhan, B.; W.; Yang, Sannigrahi, M.; Velazquez, F.; Chan, T-Y.; Venkatraman, S.; Anilkumar, G. N.; Zeng, O.; Bennet, F.; Jiang, Y.; Lesburg, C.

- A.; Duca, J.; Pinto, P.; Gavalas, S.; Huang, Y.; Wu, W.; Selyutin, O.; Agrawal, S.; Feld, B.; Huang, H.-C.; Li, C.; Cheng, K.-C.; Shih, N.-Y.; Kozlowski, J.-A.; Rosenblum, S. B.; Njoroge, F. B. Structure-activity relationship (SAR) development and discovery of potent indole-based inhibitors of the hepatitis C virus (HCV) NS5B polymerase. *J. Med. Chem.* **2012**, *55*, 754–765. (l) Lobb, K. L.; Hippskind, P. A.; Aikins, J. A.; Alvarez, E.; Cheung, Y. Y.; Considine, E. L.; De Dios, A.; Durst, G. L.; Ferritto, R.; Grossman, C. S.; Giera, D. D.; Hollister, B. A.; Huang, Z.; Iversen, P. W.; Law, K. L.; Li, T.; Lin, H. S.; Lopez, B.; Lopez, J. E.; Cabrejas, L. M.; McCann, D. J.; Molero, V.; Reilly, J. E.; Richett, M. E.; Shih, C.; Teicher, B.; Wikel, J. H.; White, W. T.; Mader, M. M. Acyl sulfonamide anti-proliferatives: benzene substituent structure-activity relationships for a novel class of antitumor agents. *J. Med. Chem.* **2004**, *47*, 5367–5380.
- [4] Asad, N. Methods for Sultam Library Synthesis: One-pot, Sequential Protocols. Ph. D. Thesis, University of Kansas, Lawrence, KS, 2014.
- [5] Asad, N.; Samarakoon, T. B.; Zang, Q.; Loh, J. K.; Javed, S.; Hanson, P. R. Rapid, Scalable Assembly of Stereochemically Rich, Mono- and Bicyclic Acyl Sultams *Org. Lett.* **2014**, *16*, 82–85.
- [6] Shannon, D. A.; Weerapana, E. Covalent protein modification: the current landscape of residue-specific electrophiles. *Curr. Opin. Chem. Biol.* **2015**, *24*, 18–26 and references cited therein.
- [7] Boettcher, T.; Sieber, S. A. β -Lactones as Specific Inhibitors of ClpP Attenuate the Production of Extracellular Virulence Factors of *Staphylococcus aureus*. *J. Am. Chem. Soc.* **2008**, *130*, 14400–14401.
- [8] Fenteany, G.; Standaert, R. F.; Lane, W. S.; Choi, S.; Corey, E. J.; Schreiber, S. L. Inhibition of proteasome activities and subunit-specific amino-terminal threonine modification by lactacystin. *Science* **1995**, *268*, 726–731.

- [9] Barrett, A. J.; Kembhavi, A. A.; Brown, M. A.; Kirschke, H.; Knight, C. G.; Tamai, M.; Hanada, K. L-trans-Epoxy succinyl-leucylamido(4-guanidino)butane (E-64) and its analogs as inhibitors of cysteine proteinases including cathepsins B, H, and L. *Biochem. J.* **1982**, *201*, 189–198.
- [10] Wymann, M. P.; Bulgarelli-Leva, G.; Zvelebil, M. J.; Pirola, L.; Vanhaesebroeck, B.; Waterfield, M. D.; Panayotou, G. Wortmannin inactivates phosphoinositide 3-kinase by covalent modification of Lys-802, a residue involved in the phosphate transfer reaction. *Mol. Cell. Biol.* **1996**, *16*, 1722–1733.
- [11] Armstrong, R. W.; Salvati, M. E.; Nguyen, M. Novel interstrand cross-links induced by the antitumor antibiotic carzinophilin/azinomycin B. *J. Am. Chem. Soc.* **1992**, *114*, 3144–3145.
- [12] Nakamura, Y.; Miyoshi, N. Electrophiles in foods: the current status of isothiocyanates and their chemical biology. *Biosci., Biotechnol., Biochem.* **2010**, *74*, 242–255.
- [13] Gersch, M.; Kreuzer, J.; Sieber, S. A. Electrophilic natural products and their biological targets. *Nat. Prod. Rep.* **2012**, *29*, 659–682.
- [14] Krysiak, J.; Breinbauer, R. Activity-based protein profiling for natural product target discovery. *Top. Curr. Chem.* **2012**, *324*, 43–84.
- [15] (a) Cravatt, B. F.; Wright, A. T.; Kozarich, J. W. Activity-based protein profiling: From enzyme chemistry to proteomic chemistry. *Annu. Rev. Biochem.* **2008**, *77*, 383–414. (b) Zuhl, A. M.; Mohr, J. T.; Bachovchin, D. A.; Niessen, S.; Hsu, K.-L.; Berlin, J. M.; Dochnahl, M.; López-Alberca, M. P.; Fu, G. C.; Cravatt, B. F. Competitive Activity-Based Protein Profiling Identifies Aza- β -Lactams as a Versatile Chemotype for Serine Hydrolase Inhibition. *J. Am. Chem. Soc.* **2012**, *134*, 5068–5071.

- [16] (a) Liu, Y.; Patricelli, M. P.; Cravatt, B. F. Activity-based protein profiling: the serine hydrolases. *Proc. Natl. Acad. Sci. U. S. A.* **1999**, *96*, 14694–14699. (b) Bogyo, M.; Verhelst, S.; Bellingard-Dubouchaud, V.; Toba, S.; Greenbaum, D. Selective targeting of lysosomal cysteine proteases with radiolabeled electrophilic substrate analogs. *Chem. Biol.* **2000**, *7*, 27–38. (c) Adam, G. C.; Sorensen, E. J.; Cravatt, B. F. Proteomic profiling of mechanistically distinct enzyme classes using a common chemotype. *Nat. Biotechnol.* **2002**, *20*, 805–809. (d) Barglow, K. T.; Cravatt, B. F. Discovering disease-associated enzymes by proteome reactivity profiling. *Chem. Biol.* **2004**, *11*, 1523–1531.
- [17] Long, J. Z.; Cravatt, B. F. The metabolic serine hydrolases and their functions in mammalian physiology and disease. *Chem. Rev.* **2011**, *111*, 6022–6063.
- [18] (a) Liu, Y.; Patricelli, M. P.; Cravatt, B. F. Activity-based protein profiling: the serine hydrolases. *Proc. Natl. Acad. Sci. U. S. A.* **1999**, *96*, 14694–14699. (b) Simon, G. M.; Cravatt, B. F. Activity-based Proteomics of Enzyme Superfamilies: Serine Hydrolases as a Case Study. *J. Biol. Chem.* **2010**, *285*, 11051–11055.
- [19] (a) Bottcher, T.; Sieber, S. A. Beta-lactones as privileged structures for the active-site labeling of versatile bacterial enzyme classes. *Angew Chem Int Ed Engl* **2008**, *47*, 4600–4603. (b) Staub, I.; Sieber, S. A. β -Lactams as Selective Chemical Probes for the in Vivo Labeling of Bacterial Enzymes Involved in Cell Wall Biosynthesis, Antibiotic Resistance, and Virulence. *J. Am. Chem. Soc.* **2008**, *130*, 13400–13409.
- [20] Kolb, R.; Bach, N. C.; Sieber, S. A. β -Sultams exhibit discrete binding preferences for diverse bacterial enzymes with nucleophilic residues. *Chem. Commun.* **2014**, *50*, 427–429.

- [21] Shannon, D. A.; Gu, C.; McLaughlin, C. J.; Kaiser, M.; van der Hoorn, R. A. L.; Weerapana, E. Sulfonyl Fluoride Analogues as Activity-Based Probes for Serine Proteases. *ChemBioChem* **2012**, *13*, 2327–2330.
- [22] Bachovchin, D. A.; Ji, T.; Li, W.; Simon, G. M.; Blankman, J. L.; Adibekian, A.; Hoover, H.; Niessen, S.; Cravatt, B. F. Superfamily-wide portrait of serine hydrolase inhibition achieved by library-versus-library screening. *Proc. Natl. Acad. Sci. U. S. A.* **2010**, *107*, 20941–20946.
- [23] Chang, J. W.; Cognetta, A. B., III; Niphakis, M. J.; Cravatt, B. F. Proteome-Wide Reactivity Profiling Identifies Diverse Carbamate Chemotypes Tuned for Serine Hydrolase Inhibition. *ACS Chem. Biol.* **2013**, *8*, 1590–1599.
- [24] Pace, N. J.; Weerapana, E. Diverse Functional Roles of Reactive Cysteines. *ACS Chem. Biol.* **2013**, *8*, 283–296.
- [25] (a) Brown, E. D.; Vivas, E. I.; Walsh, C. T.; Kolter, R. MurA (MurZ), the enzyme that catalyzes the first committed step in peptidoglycan biosynthesis, is essential in *Escherichia coli*. *J. Bacteriol.* **1995**, *177*, 4194–4197. (b) Skarzynski, T.; Mistry, A.; Wonacott, A.; Hutchinson, S. E.; Kelly, V. A.; Duncan, K. Structure of UDP-N-acetylglucosamine enolpyruvyl transferase, and enzyme essential for the synthesis of bacterial peptidoglycan, complexed with substrate UDP-N-acetylglucosamine and the drug fosfomycin. *Structure* **1996**, *4*, 1465–1474.
- [26] Greenbaum, D.; Medzihradzky, K. F.; Burlingame, A.; Bogyo, M. Epoxide electrophiles as activity-dependent cysteine protease profiling and discovery tools. *Chem. Biol.* **2000**, *7*, 569–581.
- [27] (a) Lowther, W. T.; McMillen, D. A.; Orville, A. M.; Matthews, B. W. The anti-angiogenic agent fumagillin covalently modifies a conserved active-site histidine in the *Escherichia coli* methionine aminopeptidase. *Proc. Natl. Acad. Sci. U. S. A.* **1998**, *95*, 12153–12157. (b) Evans, M. J.; Morris, G. M.; Wu, J.; Olson, A. J.;

- Sorensen, E. J.; Cravatt, B. F. Mechanistic and structural requirements for active site labeling of phosphoglycerate mutase by spiroepoxides. *Mol. BioSyst.* **2007**, *3*, 495–506.
- [28] Weerapana, E.; Wang, C.; Simon, G. M.; Richter, F.; Khare, S.; Dillon, M. B. D.; Bachovchin, D. A.; Mowen, K.; Baker, D.; Cravatt, B. F. Quantitative reactivity profiling predicts functional cysteines in proteomes. *Nature* **2010**, *468*, 790–795.
- [29] Deng, X.; Weerapana, E.; Ulanovskaya, O.; Sun, F.; Liang, H.; Ji, Q.; Ye, Y.; Fu, Y.; Zhou, L.; Li, J.; Zhang, H.; Wang, C.; Alvarez, S.; Hicks, L. M.; Lan, L.; Wu, M.; Cravatt, B. F.; He, C. Proteome-wide quantification and characterization of oxidation-sensitive cysteines in pathogenic bacteria. *Cell Host Microbe* **2013**, *13*, 358–370.
- [30] Wang, C.; Weerapana, E.; Blewett, M. M.; Cravatt, B. F. A chemoproteomic platform to quantitatively map targets of lipid-derived electrophiles. *Nat. Methods* **2014**, *11*, 79–85.
- [31] Pace, N. J.; Weerapana, E. A Competitive Chemical-Proteomic Platform To Identify Zinc-Binding Cysteines. *ACS Chem. Biol.* **2014**, *9*, 258–265.
- [32] Nielsen, M. L.; Vermeulen, M.; Bonaldi, T.; Cox, J.; Moroder, L.; Mann, M. Iodoacetamide-induced artifact mimics ubiquitination in mass spectrometry. *Nat. Methods* **2008**, *5*, 459–460.
- [33] (a) Barglow, K. T.; Cravatt, B. F. Substrate mimicry in an activity-based probe that targets the nitrilase family of enzymes. *Angew. Chem., Int. Ed.* **2006**, *45*, 7408–7411. (b) Barglow, K. T.; Saikatendu, K. S.; Bracey, M. H.; Huey, R.; Morris, G. M.; Olson, A. J.; Stevens, R. C.; Cravatt, B. F. Functional Proteomic and Structural Insights into Molecular Recognition in the Nitrilase Family Enzymes. *Biochemistry* **2008**, *47*, 13514–13523.

- [34] Couvertier, S. M.; Weerapana, E. Cysteine-reactive chemical probes based on a modular 4-aminopiperidine scaffold. *MedChemComm* **2014**, *5*, 358–362.
- [35] (a) Doorn, J. A.; Petersen, D. R. Covalent Modification of Amino Acid Nucleophiles by the Lipid Peroxidation Products 4-Hydroxy-2-nonenal and 4-Oxo-2-nonenal. *Chem. Res. Toxicol.* **2002**, *15*, 1445–1450. (b) Lo Pachin, R. M.; Gavin, T.; Petersen, D. R.; Barber, D. S., Molecular Mechanisms of 4-Hydroxy-2-nonenal and Acrolein Toxicity: Nucleophilic Targets and Adduct Formation. *Chem. Res. Toxicol.* **2009**, *22*, 1499–1508.
- [36] Kathman, S. G.; Xu, Z.; Statsyuk, A. V. A Fragment-Based Method to Discover Irreversible Covalent Inhibitors of Cysteine Proteases. *J. Med. Chem.* **2014**, *57*, 4969–4974.
- [37] (a) Krishnan, S.; Miller, R. M.; Tian, B.; Mullins, R. D.; Jacobson, M. P.; Taunton, J. Design of Reversible, Cysteine-Targeted Michael Acceptors Guided by Kinetic and Computational Analysis. *J. Am. Chem. Soc.* **2014**, *136*, 12624–12630. (b) Serafimova, I. M.; Pufall, M. A.; Krishnan, S.; Duda, K.; Cohen, M. S.; Maglathlin, R. L.; McFarland, J. M.; Miller, R. M.; Froedin, M.; Taunton, J. Reversible targeting of noncatalytic cysteines with chemically tuned electrophiles. *Nat. Chem. Biol.* **2012**, *8*, 471–476.
- [38] Shannon, D. A.; Banerjee, R.; Webster, E. R.; Bak, D. W.; Wang, C.; Weerapana, E. Investigating the Proteome Reactivity and Selectivity of Aryl Halides. *J. Am. Chem. Soc.* **2014**, *136*, 3330–3333.
- [39] Asano, S.; Patterson, J. T.; Gaj, T.; Barbas, C. F. Site-selective labeling of a lysine residue in human serum albumin. *Angew. Chem., Int. Ed.* **2014**, *53*, 11783–11786.
- [40] (a) Wender, P. A.; Croatt, M. P.; Witulski, B. New reactions and step economy: the total synthesis of (±)-salsolene oxide based on the type II transition metal-catalyzed intramolecular [4+4] cycloaddition. *Tetrahedron* **2006**, *62*, 7505–7511.

- (b) Wender, P. A.; Verma, V. A.; Paxton, T. J.; Pillow, T. H. Function-Oriented Synthesis, Step Economy, and Drug Design. *Acc. Chem. Res.* **2008**, *41*, 40–49 and references cited therein. (c) Hulme, C.; Nixey, T. Rapid assembly of molecular diversity via exploitation of isocyanide-based multi-component reactions. *Curr. Opin. Drug Discovery Dev.* **2003**, *6*, 921–929. (d) Bienayme, H., Hulme, C., Oddon, G., Schmitt, P. Maximizing synthetic efficiency: multi-component transformations lead the way. *Chem. Eur. J.* **2000**, *6*, 3321–3329. (e) Hulme, C.; Gore, V. Multi-component reactions: emerging chemistry in drug discovery from xylocain to crixivan. *Curr. Med. Chem.* **2003**, *10*, 51–80.
- [41] O' Connor, C. J.; Beckmann, H. S. G.; Spring, D. R. Diversity-oriented synthesis: producing chemical tools for dissecting biology. *Chem. Soc. Rev.* **2012**, *41*, 4444–4456.
- [42] Schawrz, M. K.; Sauer, W. H. B. Molecular shape diversity of combinatorial libraries: a prerequisite for broad bioactivity. *J. Chem. Inf. Comput. Sci.* **2003**, *43*, 987–1003.
- [43] Akella, L. B.; Marcaurelle, L. A. Application of a Sparse Matrix Design Strategy to the Synthesis of DOS Libraries. *ACS Comb. Sci.* **2011**, *13*, 357–364.
- [44] Cruciani, G.; Pastor, M.; Guba, W. VolSurf: a new tool for the pharmacokinetic optimization of lead compounds. *Eur. J. Pharm. Sci.* **2000**, *11* (Suppl. 2), S29–S39.
- [45] Rolfe, A.; Painter, T. O.; Asad, N.; Hur, M. Y.; Jeon, K. O.; Brzozowski, M.; Klimberg, S. V.; Porubsky, P.; Neuenswander, B.; Lushington, G. H.; Santini, C.; Hanson, P. R. Triazole-Containing Isothiazolidine 1,1-Dioxide Library Synthesis: One-Pot, Multi-Component Protocols for Small Molecular Probe Discovery. *ACS Comb. Sci.* **2011**, *13*, 511–517.

- [46] (a) Lipinski, C. A. Lead- and drug-like compounds: the rule-of-five revolution. *Drug Discovery Today: Technol.* **2004**, *1*, 337–341. (b) Arkin, M. R.; Wells, J. A. Small-molecule inhibitors of proteinprotein interactions: progressing towards the dream. *Nat. Rev. Drug Discovery* **2004**, *3*, 301–317.
- [47] Sauer, W. H. B.; Schwarz, M. K. Molecular Shape Diversity of Combinatorial Libraries: A Prerequisite for Broad Bioactivity. *J. Chem. Inf. Comput. Sci.* **2003**, *43*, 987–1003.
- [48] All of the compounds were sketched using the Avogadro suite of molecular modeling programs (a), and were subsequently subjected to molecular mechanics optimization at default minimization constraints according to the MMFF94 force field and charge parametrization (b). Compounds were then mutually aligned using PyMol (c) according to least-squares positional fitting across the atoms corresponding to the conserved sultam and adjacent carbonyl functional groups. The resulting molecular alignments were then visualized in PyMol. (a) Hanwell, M. D.; Curtis, D. E.; Lonie, D. C.; Vandermeersch, T.; Zurek E.; Hutchison, G. R. Avogadro: an advanced semantic chemical editor, visualization, and analysis platform. *J. Cheminf.* **2012**, *4*, 1–17. (b) Halgren, T. A.; Merck molecular force field. I. Basis, form, scope, parameterization, and performance of MMFF94. *J. Comp. Chem.* **1996**, 490–519. (c) PyMol Molecular Graphics System, Version 1.6, 2014. <http://sourceforge.net/projects/pymol/>
- [49] Flanagan, M. E.; Abramite, J. A.; Anderson, D. P.; Aulabaugh, A.; Dahal, U. P.; Gilbert, A. M.; Li, C.; Montgomery, J.; Oppenheimer, S. R.; Ryder, T.; Schuff, B. P.; Uccello, D. P.; Walker, G. S.; Wu, Y.; Brown, M. F.; Chen, J. M.; Hayward, M. M.; Noe, M. C.; Obach, R. S.; Philippe, L.; Shanmugasundaram, V.; Shapiro, M. J.; Starr, J.; Stroh, J.; Che, Y. Chemical and Computational Methods for the Characterization of Covalent Reactive Groups for the Prospective Design of Irreversible Inhibitors. *J. Med. Chem.* **2014**, *57*, 10072–10079.

Chapter 5

Experimental Data for Chapters 2–4

Appendix A

^1H and ^{13}C NMR Spectra

5.1 Experimental for Chapter 2

General Experimental Methods

All air and moisture sensitive reactions were carried out in flame- or oven-dried glassware under argon atmosphere using standard gas tight syringes, cannula, and septa. Stirring was achieved with oven-dried, magnetic stir bars. CH_2Cl_2 was purified by passage through the Solv-Tek purification system employing activated Al_2O_3 [1]. Et_3N was purified by passage through basic alumina and was stored over KOH. Flash column chromatography was performed with SiO_2 from Mallinckrodt Chemicals (V120-25, Silica gel, 60 A, 40–63 μm). Thin layer chromatography was performed on silica gel 60F254 plates (EMD-5715-7, Merck). Deuterated solvents were purchased from Cambridge Isotope Laboratories. ^1H and ^{13}C NMR spectra were recorded on a Bruker Avance spectrometer operating at 400, 500 MHz and 126 MHz, respectively. High-resolution mass spectrometry (HRMS) and FAB spectra were obtained either on a VG Instrument ZAB double-focusing mass spectrometer or on a LCT Premier Spectrometer (Micromass UK Ltd) operating in the ESI mode (MeOH). GC/mass spectrometry was performed using a Quattro micro GC (Micromass UK Limited). Chapter 2 library syntheses were carried out in 1 dram vials utilizing a reaction heating block in an Anton Paar® Synthos 3000 synthesizer. Microwave-assisted reactions were carried out in 1 dram vials utilizing a reaction heating block in an Anton Paar® Synthos 3000 synthesizer and also Biotage® Initiator. Parallel evaporations were performed using a GeneVac EZ-2 Plus evaporator. Automated preparative reverse-phase HPLC purification was performed using a Waters Mass-Directed Fractionation system (Prep Pump 2525, Make-up pump 515, Sample

Manager 2767, UV-DAD detection 2996, and Micromass ZD quadrupole mass spectrometer). Purification via preparative chromatography was achieved utilizing a Waters X-Bridge C18 column (19 x 150 mm, 5 μ m, w/ 19 x 10 mm guard column) at a flow rate of 20 mL/min. Samples were diluted in DMSO and purified using a elution mixture of water (modified to pH 9.8 by the addition of NH_4OH) and CH_3CN , running a concentration gradient which increased to 20% CH_3CN over a 4 min period. The corresponding preparative gradient, triggering thresholds, and UV wavelength were selected based on the HPLC analysis of each crude sample. Analytical analysis of each sample after preparative chromatography utilized a Waters Acquity system with UV-detection and mass-detection (Waters LCT Premier). The analytical method conditions included a Waters Aquity BEH C18 column (2.1 x 50 mm, 1.7 μ m) and elution with a linear gradient of 5% water (modified to pH 9.8 through addition of NH_4OH) to 100% CH_3CN at 0.6 mL/min flow rate. Purity of each sample was determined using UV peak area detected at 214 nm wavelength.

Note:

1. All reactions involving the use and heating of azides were carried out behind a safety shield taking extra precautions due to the explosive nature of these materials.
2. 20 of the 80 compounds in Chapter 2 were fully characterized with mp, FTIR, ^1H , ^{13}C NMR and HRMS.
3. 20 of the 90 compounds in Chapter 4 were fully characterized with mp, FTIR, ^1H , ^{13}C NMR and HRMS.
4. As this is a library synthesis, compounds with a low yield were not re-synthesized.

General Procedure A: preparation of *o*-fluorobenzene sulfonamide via sulfonylation. To a round bottom flask containing a solution of amine (8.77 mmol, 1.2 equiv.) in dry CH₂Cl₂ (0.3 M), was added Et₃N (14.6 mmol, 2.0 equiv.) and DMAP (0.089 g, 0.73 mmol, 0.1 equiv.). The reaction mixture was cooled to 0 °C, stirred for 10–20 min, after which benzenesulfonyl chloride (7.31 mmol, 1.0 equiv.) was added to the reaction mixture, warmed to rt and left to stir overnight. *Alternatively*, to a vigorously stirred solution of amine (7.34 mmol, 2.0 equiv.) in CH₂Cl₂ (12.2 mL, 0.4 M) in a round bottom flask was added NaHCO₃ (3 equiv.) and H₂O (6.1 mL, 0.8 M). A solution of benzenesulfonyl chloride (1.0 g, 3.67 mmol) in CH₂Cl₂ (3.6 mL, 1 M) was added dropwise, and the reaction was stirred for 4–8 hours. Upon disappearance of sulfonyl chloride, the reaction was quenched with 10% aq. HCl (2 mL), organic layer was separated and the aqueous layer was extracted with CH₂Cl₂ (3 x 5 mL). The combined organic layers were washed with brine (10 mL), dried (Na₂SO₄), and concentrated under reduced pressure to afford the desired *o*-fluorobenzene sulfonamide.

General Procedure B: intermolecular S_NAr of amino alcohols with *o*-fluorobenzene sulfonamides. To a flame dried microwave vial under Ar was added *o*-fluorobenzene sulfonamide (0.69 mmol), amino alcohol (2.07 mmol) and DMSO (0.35 mL) and the reaction was heated at 140 °C for 30 min in the microwave. The reaction mixture was transferred to a separatory funnel along with Et₂O (3 mL), EtOAc (1 mL) and H₂O (2 mL) and extracted. The aqueous layer was extracted with Et₂O (4 x 1 mL), and the combined organic layers were dried (Na₂SO₄). The extract was concentrated under

reduced pressure and subject to column chromatography (6:1 hexane:EtOAc) to afford the desired product.

General procedure C: intramolecular S_NAr cyclization for the synthesis of benzo-oxathiazepine-dioxides (7-membered sultams). To a microwave vial charged with fluorobenzene sulfonamide (1.52 mmol, 1.0 equiv.) in dry DMF (0.1 M), was added Cs₂CO₃ (4.56 mmol, 3.0 equiv.). *Alternatively*, to a microwave vial charged with fluorobenzene sulfonamide (1.52 mmol, 1.0 equiv.) in dry DMSO (0.1 M), was added Cs₂CO₃ (4.56 mmol, 3.0 equiv.). The reaction was heated at 150 °C under *mW* irradiation for 30–40 min, which upon completion, the crude reaction was quenched with aq., HCl, diluted EtOAc and stirred for an additional 5 min at rt. After such time, the organic layer was separated and the aqueous layer extracted with EtOAc (3x). The combined organic layers were washed with brine, dried over Na₂SO₄, concentrated under reduced pressure and subject to column chromatography (3:1 hexane:EtOAc) to afford the desired product.

General procedure D: intramolecular Mitsunobu ring closure for the synthesis of sultams. To a flame dried round bottom flask under argon, was added hydroxybenzenesulfonamide (0.25 mmol, 1.0 equiv.), PPh₃ (0.49 mmol, 2.0 equiv.) and dry THF (5 mL, 0.05 M). After stirring to completely dissolve PPh₃, DIAD (0.37 mmol, 1.5 equiv.) was added via slow dropwise to the stirring reaction mixture. The reaction was stirred for 10–30 min (TLC monitoring of SM) up to 12 h, concentrated under reduced pressure and subjected to flash chromatography to afford the desired sultam.

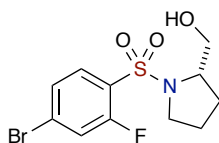
General procedure E: intermolecular Mitsunobu alkylation for the preparation of 3° sulfonamides. To a flame-dried round bottom flask under charged with a solution of sulfonamide (0.81 mmol, 1.0 equiv.) in dry THF (0.05 M), was added PPh₃ (2.42 mmol, 3.0 equiv.) and alcohol (1.38–1.62 mmol, 1.7–2.0 equiv.). The reaction mixture was stirred for 10 min, after which DIAD (2.01 mmol, 2.5 equiv.) was added via slow drop-wise addition to the reaction mixture. *Alternatively*, to a flame-dried round bottom flask under charged with a solution of sulfonamide (0.64 mmol, 1.0 equiv.) in dry THF or CH₂Cl₂ (0.05 M), was added PPh₃ (1.35 mmol, 2.1 equiv.) and alcohol (0.97 mmol, 1.5 equiv.). The reaction mixture was stirred for 10 min, after which DIAD (1.16 mmol, 1.8 equiv.) was added via slow drop-wise addition to the reaction mixture. The reaction was stirred at rt for 12 h, after which it was concentrated under reduced pressure and subjected to chromatography (15:1 hexane:EtOAc) to afford the desired product.

General procedure F: intramolecular S_NAr cyclization to yield 8- to 10-membered sultams. To a microwave vial with protected hydroxyl-fluorobenzenesulfonamide (0.21 mmol, 1.0 equiv.) in dry DMF (0.1 M), was added TBAF (0.403 mmol, 2.0 equiv.) and stirred overnight at rt. The reaction was monitored by TLC and upon absence of starting material, was added Cs₂CO₃ (0.503 mmol, 2.5 equiv.). The reaction was heated at 150 °C under *mW* irradiation for 30 min; upon completion the crude mixture was concentrated and subjected to column chromatography (7:1 hexane:EtOAc) to yield the desired sultams **14b** and **14c**.

General procedure G: intramolecular S_NAr ring closure to yield benzo-thiadiazepine 1,1-dioxides (7-membered sultams). To a microwave vial with alkylated-fluorobenzenesulfonamide (0.23 mmol, 1.0 equiv.) in dry DMSO (0.1 M), was added Cs₂CO₃ (0.46 mmol, 2.0–2.5 equiv.). The reaction mixture was heated at 150 °C under *mW* irradiation for 30 min. The crude mixture was transferred to a separatory funnel along with EtOAc (3 mL) and H₂O (3 mL). The aqueous layer was extracted with EtOAc (3 x 3 mL). The combined organic layers were washed with brine and dried over Na₂SO₄. The extract was concentrated under reduced pressure and subjected to column chromatography (10:1 hexane:EtOAc) to yield the desired sultams

General procedure H: intramolecular S_NAr ring closure to yield benzo-oxathiazocine 1,1-dioxides (8-membered sultams). To a microwave vial with protected-fluorobenzenesulfonamide (0.036 mmol, 1.0 equiv.) in dry DMSO (0.1 M), was added TBAF (0.073 mmol, 2.0 equiv.). The reaction was stirred at rt for 4–12 h until the starting material was consumed based on TLC analysis. Cs₂CO₃ (0.090 mmol, 2.5 equiv.) was then added and the reaction mixture was heated at 150 °C under *mW* irradiation for 30–40 min. The crude mixture was transferred to a separatory funnel along with EtOAc (3 mL) and H₂O (3 mL). The aqueous layer was extracted with EtOAc (3 x 3 mL), the combined organic layers were washed with brine and dried over Na₂SO₄. The extract was concentrated under reduced pressure and subjected to column chromatography (10:1 hexane:EtOAc) to yield the desired sultams.

(S)-1-((4-Bromo-2-fluorophenyl)sulfonyl)pyrrolidin-2-yl)methanol (2.7.2)



According to general procedure **A**, **2.7.2** (1.23 g, 97%) was isolated as dark yellow oil.

FTIR (neat) 3531, 3377, 2953, 1587, 1470, 1346, 1161, 1063, 830 cm^{-1} ;

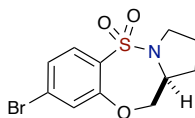
$[\alpha]_D^{20} = -43.3$ ($c = 0.84$, CHCl_3);

^1H NMR (500 MHz, CDCl_3) δ ppm 7.79 (t, $J = 7.8$ Hz, 1H, aromatic), 7.46–7.40 (m, 2H, aromatic), 3.82 (dq, $J = 7.3, 5.0$ Hz, 1H, NCH_2CH_2), 3.68 (qd, $J = 11.5, 4.9$ Hz, 2H, CH_2OH), 3.51–3.35 (m, 2H, NCH_2CH_2), 2.41 (bs, 1H, OH), 1.95–1.78 (m, 3H, $\text{NCH}_2\text{CH}_2\text{H}_b\text{CH}_2$), 1.71–1.62 (m, 1H, $\text{NCH}_2\text{CH}_2\text{H}_a\text{CH}_2$);

^{13}C NMR (126 MHz, CDCl_3) δ ppm 158.5 (d, $^1J_{\text{C-F}} = 260.0$ Hz), 132.8 (d, $^4J_{\text{C-F}} = 1.8$ Hz), 128.6 (d, $^3J_{\text{C-F}} = 9.3$ Hz), 128.0 (d, $^3J_{\text{C-F}} = 3.8$ Hz), 125.2 ($^2J_{\text{C-F}} = 15.8$ Hz), 121.0 ($^2J_{\text{C-F}} = 25.7$ Hz), 65.5, 61.8, 49.5, 28.9, 24.5;

HRMS calculated for $\text{C}_{11}\text{H}_{13}\text{BrFNO}_3\text{SNa}$ ($\text{M}+\text{Na}$) $^+$ 359.9681; found 359.9679 (TOF MS ES^+).

8-Bromo-2,3,11,11a-tetrahydro-1H-benzo[b]pyrrolo[1,2-e][1,4,5] oxathiazepine 5,5-dioxide (2.7.3)



According to general procedure **C**, **2.7.3** was isolated (165 mg, 88%) as a white solid.

mp 132–135 $^{\circ}\text{C}$;

FTIR (neat) 3088, 2970, 2957, 2874, 1580, 1460, 1335, 1161, 1068, 820, 763, 733 cm^{-1} ;

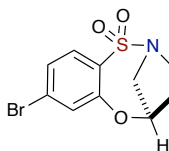
$[\alpha]_D^{20} = +19.5$ ($c = 0.2$, CHCl_3);

^1H NMR (500 MHz, CDCl_3) δ ppm 7.68 (d, $J = 8.4$ Hz, 1H, aromatic), 7.31 (dd, $J = 8.4$, 1.9 Hz, 1H, aromatic), 7.27 (d, $J = 1.9$ Hz, 1H, aromatic), 4.80 (dd, $J = 13.1$, 2.8 Hz, 1H, $\text{OCH}_a\text{H}_b\text{CHN}$), 4.18–4.12 (m, 1H, OCH_2CHN), 3.97 (dd, $J = 13.1$, 4.4 Hz, 1H, $\text{OCH}_a\text{H}_b\text{CHN}$), 3.61–3.57 (m, 1H, NCH_aH_b), 3.09–3.03 (m, 1H, NCH_aH_b), 2.25 (ddd, $J = 10.6$, 8.7, 5.1 Hz, 1H, NCHCH_aH_b), 2.02–1.93 (m, 3H, $\text{NCHCH}_a\text{H}_b\text{CH}_2$);

^{13}C NMR (126 MHz, CDCl_3) δ ppm 155.8, 130.9, 130.2, 127.2, 126.9, 125.2, 73.8, 59.6, 48.6, 28.5, 23.9;

HRMS calculated for $\text{C}_{11}\text{H}_{12}\text{BrNO}_3\text{SH}$ ($\text{M}+\text{H}$) $^+$ 317.9800; found 317.9808 (TOF MS ES^+).

(5*R*)-8-bromo-4,5-dihydro-3*H*-2,5-methanobenzo[*b*][1,4,5]oxathiazocine 1,1-dioxide (2.8.2)



According to general procedure **C**, **2.8.2** (50 mg, 56%) was isolated as a white solid.

mp 164–166 $^{\circ}\text{C}$;

FTIR (neat) 2957, 2924, 1578, 1460, 1340, 1161 cm^{-1} ;

$[\alpha]_D^{20} = -43.6$ ($c = 0.11$, CHCl_3);

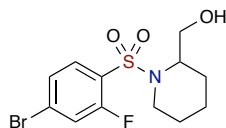
^1H NMR (400 MHz, CD_2Cl_2) δ ppm 7.74 (d, $J = 8.5$ Hz, 1H), 7.37 (dd, $J = 8.5$, 1.9 Hz, 1H), 7.28 (d, $J = 1.8$ Hz, 1H), 5.14 (dd, $J = 6.2$, 2.7 Hz, 1H), 4.33–4.24 (m, 1H), 3.49

(dddd, $J = 14.0, 9.2, 4.8, 1.9$ Hz, 1H), 3.27–3.20 (m, 1H), 3.18 (dd, $J = 2.8, 14.1$ Hz, 1H), 2.06 (ddd, $J = 15.7, 10.9, 5.5$ Hz, 1H), 1.98–1.89 (m, 1H);

^{13}C NMR (126 MHz, CD_2Cl_2) δ ppm 152.1, 132.0, 131.7, 128.6, 128.5, 127.6, 81.6, 57.5, 47.7, 29.7;

HRMS calculated for $\text{C}_{10}\text{H}_{10}\text{BrNO}_3\text{SH}$ ($\text{M}+\text{H}$) $^+$ 303.9643; found 303.9629 (TOF MS ES $^+$).

(1-((4-Bromo-2-fluorophenyl)sulfonyl)piperidin-2-yl)methanol (SI-1)



According to general procedure **A**, **SI-1** (453 mg, 35%) was isolated as a dark yellow solid.

mp 85 °C;

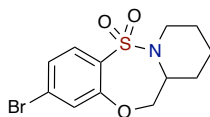
FTIR (neat) 3529, 2941, 2872, 1587, 1398, 1159, 1064, 820 cm^{-1} ;

^1H NMR (500 MHz, CDCl_3) δ ppm 7.79 (dd, $J = 8.6, 7.7$ Hz, 1H, aromatic), 7.44–7.36 (m, 2H, aromatic), 4.07 (dt, $J = 5.8, 4.9$ Hz, 1H, NCHCH_2), 3.91–3.81 (m, 2H, $\text{NCH}_a\text{H}_b\text{CH}_2$, $\text{CH}_a\text{H}_b\text{OH}$), 3.60 (ddd, $J = 11.4, 6.5, 5.9$ Hz, 1H, $\text{CH}_a\text{H}_b\text{OH}$), 3.18–3.09 (m, 1H, $\text{NCH}_a\text{H}_b\text{CH}_2$), 1.81 (dd, $J = 6.6, 5.3$ Hz, 1H, OH), 1.70–1.67 (m, 1H, $\text{NCH}_2\text{CH}_a\text{H}_b$), 1.59 (dd, $J = 12.4, 4.2$ Hz, 2H, NCHCH_aH_b , $\text{NCH}_2\text{CH}_2\text{CH}_a\text{H}_b$), 1.53–1.43 (m, 2H, $\text{NCH}_2\text{CH}_a\text{H}_b$, NCHCH_aH_b), 1.37–1.26 (m, 1H, $\text{NCH}_2\text{CH}_2\text{CH}_a\text{H}_b$);

^{13}C NMR (126 MHz, CDCl_3) δ ppm 158.3 (d, $^1J_{\text{C-F}} = 260.8$ Hz), 131.7, 128.4 (d, $^2J_{\text{C-F}} = 13.9$ Hz), 128.0 (d, $^3J_{\text{C-F}} = 8.8$ Hz), 127.8 (d, $^4J_{\text{C-F}} = 3.8$ Hz), 120.8 (d, $^2J_{\text{C-F}} = 25.2$ Hz), 60.6, 54.7, 41.4, 25.3, 24.8, 18.9;

HRMS calculated for $\text{C}_{12}\text{H}_{15}\text{BrFNO}_3\text{SNa}$ ($\text{M}+\text{Na}$) $^+$ 373.9838; found 373.9840 (TOF MS ESI $^+$).

9-Bromo-1,2,3,4,12,12a-hexahydrobenzo[*b*]pyrido[1,2-*e*][1,4,5]oxathiazepine 6,6-dioxide (2.8.4)



According to general procedure C, **2.8.4** (63.1 mg, 67%) was isolated as a white solid.

mp 163–168 °C;

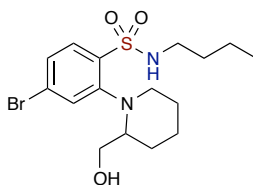
FTIR (neat) 2941, 1578, 1477, 1381, 1340, 1167, 835 cm^{-1} ;

^1H NMR (500 MHz, CDCl_3) δ ppm 7.66 (d, $J = 8.3$ Hz, 1H, aromatic), 7.42–7.33 (m, 2H, aromatic), 4.58–4.49 (m, 1H, $\text{NCH}_2\text{CH}_2\text{O}$), 4.23–4.12 (m, 2H, NCHCH_2O), 3.57–3.47 (m, 1H, $\text{NCH}_a\text{H}_b\text{CH}_2$), 2.57 (td, $J = 11.8, 3.6$ Hz, 1H, $\text{NCH}_a\text{H}_b\text{CH}_2$), 1.97–1.84 (m, 1H, NCHCH_aH_b), 1.80–1.59 (m, 4H, $\text{NCHCH}_a\text{H}_b\text{CH}_a\text{H}_b\text{CH}_2$), 1.20 (dddd, $J = 17.7, 13.7, 7.6, 3.5$ Hz, 1H, $\text{NCHCH}_2\text{CH}_a\text{H}_b\text{CH}_2$);

^{13}C NMR (126 MHz, CDCl_3) δ ppm 156.2, 132.2, 130.9, 127.9, 127.8, 127.0, 69.6, 55.0, 41.3, 26.5, 24.8, 19.4;

HRMS calculated for $\text{C}_{12}\text{H}_{14}\text{BrNO}_3\text{SNa}$ ($\text{M}+\text{Na}$) $^+$ 353.9775; found 353.9777 (TOF MS ES $^+$).

4-Bromo-N-butyl-2-(2-(hydroxymethyl)piperidin-1-yl)benzenesulfonamide (SI-2)



According to general procedure **B**, **SI-2** (100 mg, 15%) was isolated as clear oil.

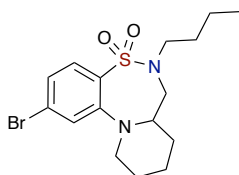
FTIR (neat) 3495, 3246, 2934, 1574, 1555, 1448, 1321, 1165, 1061, 827 cm^{-1} ;

^1H NMR (500 MHz, CDCl_3) δ ppm 7.88 (d, $J = 8.5$ Hz, 1H, aromatic), 7.55 (s, 1H, aromatic), 7.49 (d, $J = 8.4$ Hz, 1H, aromatic), 5.71 (s, 1H, NH), 3.51 (dd, $J = 12.3, 2.2$ Hz, 1H, $\text{CH}_a\text{H}_b\text{OH}$), 3.38 (d, $J = 11.7$ Hz, 1H, $\text{CH}_a\text{H}_b\text{OH}$), 3.16 (d, $J = 11.2$ Hz, 1H, NCH_aH_b), 3.01 (s, 1H, NCHCH_2OH), 2.96–2.78 (m, 3H, NHCH_2 , OH), 2.61 (t, $J = 10.1$ Hz, 1H, NCH_aH_b), 1.95 (dd, $J = 12.0, 5.4$ Hz, 2H, $\text{NCHCH}_a\text{H}_b\text{CH}_a\text{H}_b$), 1.83 (d, $J = 11.1$ Hz, 1H, $\text{NCHCH}_a\text{H}_b\text{CH}_2$), 1.76 (d, $J = 12.9$ Hz, 1H, $\text{NCH}_2\text{CH}_a\text{H}_b$), 1.64 (dd, $J = 24.7, 12.3$ Hz, 1H, $\text{NCH}_2\text{CH}_a\text{H}_b$), 1.54–1.48 (m, 3H, $\text{NHCH}_2\text{CH}_2\text{CH}_2\text{CH}_3$, $\text{NCHCH}_2\text{CH}_a\text{H}_b$), 1.40–1.31 (m, 2H, $\text{NHCH}_2\text{CH}_2\text{CH}_2\text{CH}_3$), 0.91 (t, $J = 7.4$ Hz, 3H, $\text{NHCH}_2\text{CH}_2\text{CH}_2\text{CH}_3$);

^{13}C NMR (126 MHz, CDCl_3) δ ppm 151.8, 136.8, 131.2, 129.3, 129.1, 127.8, 62.9, 62.4, 43.7, 32.0, 29.7, 28.1, 26.3, 24.0, 19.9, 13.7;

HRMS calculated for $\text{C}_{16}\text{H}_{25}\text{BrN}_2\text{O}_3\text{SH}$ ($\text{M}+\text{H}$) $^+$ 405.0848; found 405.0839 (TOF MS ES^+).

2-Bromo-6-butyl-7,7a,8,9,10,11-hexahydro-6H-benzo[*f*]pyrido[2,1-*d*][1,2,5]thiadiazepine 5,5-dioxide (2.8.5)



According to general procedure **D**, **2.8.5** (54 mg, 47%) was isolated as colorless oil.

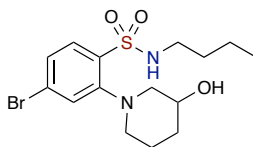
FTIR (neat) 2934, 1576, 1452, 1333, 1153, 812, 770, 731 cm^{-1} ;

^1H NMR (500 MHz, CDCl_3) δ ppm 7.62 (d, $J = 8.5$ Hz, 1H, aromatic), 7.21 (s, 1H, aromatic), 7.11 (d, $J = 8.3$ Hz, 1H, aromatic), 3.91 (s, 1H, NCHCH_2N), 3.61 (s, 1H, $\text{NCHCH}_a\text{H}_b\text{N}$), 3.40 (t, $J = 5.8$ Hz, 2H, NCH_2), 3.18 (d, $J = 13.2$ Hz, 1H, $\text{NCHCH}_d\text{H}_b\text{N}$), 3.14–3.02 (m, 2H, $\text{NCH}_2\text{CH}_2\text{CH}_2\text{CH}_3$), 1.80 (dddd, $J = 14.8, 13.3, 10.6, 5.9$ Hz, 3H, $\text{NCH}_2\text{CH}_2\text{CH}_a\text{H}_b$), 1.68 (dt, $J = 14.6, 5.4$ Hz, 1H, $\text{NCH}_2\text{CH}_2\text{CH}_a\text{H}_b$), 1.64–1.55 (m, 4H, $\text{NCH}_2\text{CH}_2\text{CH}_2\text{CH}_3$, NCHCH_2), 1.39–1.30 (m, 2H, $\text{NCH}_2\text{CH}_2\text{CH}_2\text{CH}_3$), 0.92 (t, $J = 7.4$ Hz, 3H, $\text{NCH}_2\text{CH}_2\text{CH}_2\text{CH}_3$);

^{13}C NMR (126 MHz, CDCl_3) δ ppm 149.9, 130.2 (2C), 126.8, 124.4 (2C), 54.6, 50.5, 49.5, 47.3, 30.9, 27.1, 25.0, 19.7, 18.9, 13.7;

HRMS calculated for $\text{C}_{16}\text{H}_{23}\text{BrN}_2\text{O}_2\text{SH}$ ($\text{M}+\text{H}$) $^+$ 387.0742; found 387.0751 (TOF MS ES^+).

4-Bromo-*N*-butyl-2-(3-hydroxypiperidin-1-yl)benzenesulfonamide (SI-3)



According to general procedure **B**, **SI-3** (1.05 g, 71%) was isolated as a white solid.

mp 93–95 °C;

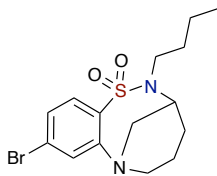
FTIR (neat) 3501, 3204, 2955, 1574, 1555, 1456, 1319, 1161, 1084, 822, 777, 731 cm^{-1} ;

^1H NMR (500 MHz, CDCl_3) δ ppm 7.86 (dd, $J = 8.2, 3.0$ Hz, 1H, aromatic), 7.42 (dd, $J = 7.4, 1.9$ Hz, 2H, aromatic), 6.84 (s, 1H, NH), 4.14 (s, 1H, NCH_2CHOH), 3.38 (s, 1H, $\text{NCH}_a\text{H}_b\text{CH}_2$), 3.12 (s, 1H, $\text{NCH}_a\text{H}_b\text{CHOH}$), 2.93–2.81 (m, 2H, $\text{NCH}_a\text{H}_b\text{CH}_2$, $\text{NCH}_a\text{H}_b\text{CHOH}$), 2.76 (s, 1H, NHCH_aH_b), 2.66 (s, 1H, NHCH_aH_b), 2.33 (bs, 1H, OH), 2.13 (d, $J = 11.1$ Hz, 1H, $\text{NCH}_2\text{CH}_a\text{H}_b$), 1.90 (s, 1H, $\text{NCH}_2\text{CH}_2\text{CH}_a\text{H}_b$), 1.66 (d, $J = 12.0$ Hz, 2H, $\text{NCH}_2\text{CH}_a\text{H}_b\text{CH}_a\text{H}_b$), 1.43 (dd, $J = 13.2, 6.2$ Hz, 2H, NHCH_2CH_2), 1.31 (dd, $J = 14.4, 7.2$ Hz, 2H, $\text{NHCH}_2\text{CH}_2\text{CH}_2$), 0.89–0.82 (m, 3H, $\text{NHCH}_2\text{CH}_2\text{CH}_2\text{CH}_3$);

^{13}C NMR (126 MHz, CDCl_3) δ ppm 152.3, 134.7, 131.7, 128.4, 127.7, 127.2, 65.7, 59.8, 54.1, 43.3, 31.8, 30.1, 21.1, 19.9, 13.6;

HRMS calculated for $\text{C}_{15}\text{H}_{23}\text{BrN}_2\text{O}_3\text{SH}$ ($\text{M}+\text{H}$) $^+$ 391.0691; found 391.0694 (TOF MS ES^+).

9-Bromo-2-butyl-3,4,5,6-tetrahydro-2H-3,7-methanobenzo[*h*][1,2,7]thiadiazonine 1,1-dioxide (2.8.7)



According to general procedure **D**, **2.8.7** (95 mg, 50%) was isolated as a white solid.

mp 83–84 °C;

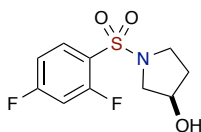
FTIR (neat) 2955, 1578, 1474, 1423, 1308, 1148, 832, 783, 731 cm^{-1} ;

¹H NMR (500 MHz, CDCl₃) δ ppm 7.62 (d, *J* = 8.7 Hz, 1H, aromatic), 7.06 (d, *J* = 1.9 Hz, 1H, aromatic), 6.94 (dd, *J* = 8.6, 1.9 Hz, 1H, aromatic), 4.79 (ddd, *J* = 16.0, 5.0, 2.4 Hz, 1H, NCH_aH_bCH), 3.72 (dd, *J* = 13.7, 1.7 Hz, 1H, NCH_aH_b), 3.59–3.51 (m, 2H, NCH₂CH, SNCH_aH_b), 3.37–3.30 (m, 1H, NCH_aH_b), 3.25 (dd, *J* = 16.0, 1.3 Hz, 1H, NCH_aH_bCH), 3.17–3.10 (m, 1H, SNCH_aH_b), 2.20–2.15 (m, 1H, NCH₂CH₂CH_aH_b), 1.74–1.64 (m, 2H, NCH₂CH_aH_bCH_aH_b), 1.59–1.45 (m, 2H, NCH₂CH₂CH₂CH₃), 1.39–1.22 (m, 3H, NCH₂CH₂CH₂CH₃, NCH₂CH_aH_b), 0.87 (t, *J* = 7.3 Hz, 3H, NCH₂CH₂CH₂CH₃);

¹³C NMR (126 MHz, CDCl₃) δ ppm 149.3, 134.6, 128.0, 126.1, 125.8, 123.2, 55.4, 53.8, 51.6, 45.7, 30.4, 29.7, 28.5, 20.0, 13.8;

HRMS calculated for C₁₅H₂₁BrN₂O₂SH (M+H)⁺ 373.0585; found 373.0586 (TOF MS ES⁺).

(R)-1-((2,4-difluorophenyl)sulfonyl)pyrrolidin-3-ol (2.9.3)



According to general procedure **A**, **2.9.3** (3.65 g, 98%) was isolated as yellow oil.

FTIR (neat) 3508, 3101, 2949, 1601, 1481, 1344, 1161, 1082, 856, 797, 712 cm⁻¹;

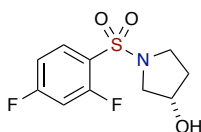
$[\alpha]_D^{20} = -6.7$ (c = 0.36, CHCl₃);

¹H NMR (500 MHz, CDCl₃) δ ppm 7.94 (ddd, *J* = 8.8, 7.9, 6.2 Hz, 1H, aromatic), 7.03–6.93 (m, 2H, aromatic), 4.53–4.46 (m, 1H, CHOH), 3.56–3.51 (m, 2H, NCH₂CH), 3.51–3.46 (m, 1H, NCH_aH_bCH₂), 3.44–3.40 (m, 1H, NCH_aH_bCH₂), 2.08–2.00 (m, 1H, NCH₂CH_aH_b), 1.98–1.90 (m, 1H, NCH₂CH_aH_b), 1.59 (s, 1H, OH);

^{13}C NMR (126 MHz, CDCl_3) δ ppm 165.6 (dd, $J_{\text{C-F}} = 257.2, 11.4$ Hz), 159.8 (dd, $J_{\text{C-F}} = 257.6, 12.6$ Hz), 133.0 (dd, $J_{\text{C-F}} = 10.4, 2.5$ Hz), 122.5 (dd, $J_{\text{C-F}} = 15.5, 3.9$ Hz), 111.7 (dd, $J_{\text{C-F}} = 21.7, 3.8$ Hz), 105.7 (dd, $J_{\text{C-F}} = 26.0, 25.9$ Hz), 70.8, 55.8, 45.6, 34.4;

HRMS calculated for $\text{C}_{10}\text{H}_{11}\text{F}_2\text{NO}_3\text{SH}$ (M+H) $^+$ 264.0506; found 264.0510 (TOF MS ES $^+$).

(S)-1-((2,4-difluorophenyl)sulfonyl)pyrrolidin-3-ol (2.9.4)



According to general procedure **A**, **2.9.4** (3.07 g, 99%) was isolated as yellow oil.

FTIR (neat) 3512, 3027, 2953, 1601, 1481, 1344, 1161, 1082, 856, 797, 712 cm^{-1} ;

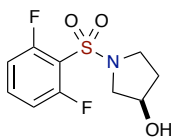
$[\alpha]_D^{20} = +6.1$ ($c = 1.575$, CHCl_3);

^1H NMR (500 MHz, CDCl_3) δ ppm 7.94 (ddd, $J = 8.8, 7.9, 6.2$ Hz, 1H, aromatic), 7.12–6.76 (m, 2H, aromatic), 4.49 (tt, $J = 4.5, 2.2$ Hz, 1H, CHOH), 3.57–3.52 (m, 2H, NCH_2CH), 3.48 (ddd, $J = 9.7, 9.6, 6.8$ Hz, 1H, $\text{NCH}_a\text{H}_b\text{CH}_2$), 3.42 (ddd, $J = 11.3, 1.8, 1.6$ Hz, 1H, $\text{NCH}_a\text{H}_b\text{CH}_2$), 2.13–1.98 (m, 1H, $\text{NCH}_2\text{CH}_a\text{H}_b$), 1.99–1.84 (m, 1H, $\text{NCH}_2\text{CH}_a\text{H}_b$), 1.53 (d, $J = 3.5$ Hz, 1H, OH);

^{13}C NMR (126 MHz, CDCl_3) δ ppm 165.6 (dd, $J_{\text{C-F}} = 257.1, 11.5$ Hz), 159.9 (dd, $J_{\text{C-F}} = 257.5, 12.7$ Hz), 133.0 (dd, $J_{\text{C-F}} = 10.4, 2.3$ Hz), 122.5 (dd, $J = 15.6, 4.0$ Hz), 111.7 (dd, $J_{\text{C-F}} = 21.8, 3.7$ Hz), 105.7 (dd, $J_{\text{C-F}} = 25.9$ Hz), 70.8, 55.8, 45.6, 34.4;

HRMS calculated for $\text{C}_{10}\text{H}_{11}\text{F}_2\text{NO}_3\text{SH}$ (M+H) $^+$ 264.0506; found 264.0514 (TOF MS ES $^+$).

(R)-1-((2,6-difluorophenyl)sulfonyl)pyrrolidin-3-ol (2.9.5)



According to general procedure **A**, **2.9.5** (1.24 g, 99%) was isolated as a brown solid.

mp 122–125 °C;

FTIR (neat) 3489, 3298, 2993, 1612, 1583, 1464, 1346, 1163, 1103, 787, 770, 704 cm⁻¹;

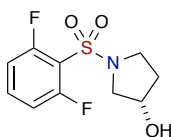
$[\alpha]_D^{20} = -9.7$ (c = 0.248, CHCl₃);

¹H NMR (500 MHz, CDCl₃) δ ppm 7.68–7.31 (m, 1H, aromatic), 7.16–6.89 (m, 2H, aromatic), 4.51 (dddd, *J* = 4.4, 4.2, 2.1, 2.1 Hz, 1H, CHOH), 3.68–3.53 (m, 3H, NCH₂CH, NCH_aH_bCH₂), 3.49 (ddd, *J* = 11.4, 1.8, 1.7 Hz, 1H, NCH_aH_bCH₂), 2.07 (dddd, *J* = 13.3, 9.6, 8.6, 4.6 Hz, 1H, NCH₂CH_aH_b), 2.00–1.92 (m, 1H, NCH₂CH_aH_b), 1.60 (d, *J* = 3.8 Hz, 1H, OH);

¹³C NMR (126 MHz, CDCl₃) δ ppm 159.8 (dd, *J*_{C-F} = 258.1, 4.4 Hz, 2C), 134.2 (t, *J*_{C-F} = 11.0 Hz), 116.5 (dd, *J*_{C-F} = 17.2, 17.0 Hz), 113.1 (dd, *J*_{C-F} = 24.2, 3.8 Hz, 2C), 70.7, 55.8, 45.6, 34.4;

HRMS calculated for C₁₀H₁₁F₂NO₃SH (M+H)⁺ 264.0506; found 264.0513 (TOF MS ES⁺).

(S)-1-((2,6-difluorophenyl)sulfonyl)pyrrolidin-3-ol (2.9.6)



According to general procedure **A**, **2.9.6** (2.46 g, 99%) was isolated as a yellow solid.

mp 124–127 °C;

FTIR (neat) 3487, 2993, 1612, 1583, 1464, 1346, 1163, 1103, 787, 770, 704 cm⁻¹;

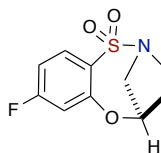
$[\alpha]_D^{20} = +4.4$ ($c = 0.29$, CHCl₃);

¹H NMR (500 MHz, CDCl₃) δ ppm 7.58–7.42 (m, 1H, aromatic), 7.11–6.94 (m, 2H, aromatic), 4.51 (s, 1H, CHOH), 3.67–3.52 (m, 3H, NCH₂CH, NCH_aH_bCH₂), 3.49 (d, $J = 11.2$ Hz, 1H, NCH_aH_bCH₂), 2.14–2.01 (m, 1H, NCH₂CH_aH_b), 2.01–1.88 (m, 1H, NCH₂CH_aH_b), 1.56 (s, 1H, OH);

¹³C NMR (126 MHz, CDCl₃) δ ppm 159.8 (dd, $J_{C-F} = 257.9$, 4.5 Hz, 2C), 134.2 (t, $J_{C-F} = 11.0$ Hz), 116.5, 113.1 (dd, $J_{C-F} = 24.2$, 3.8 Hz, 2C), 70.8, 55.8, 45.6, 34.4;

HRMS calculated for C₁₀H₁₁F₂NO₃SH (M+H)⁺ 264.0506; found 264.0516 (TOF MS ES⁺).

(5R)-8-fluoro-4,5-dihydro-3H-2,5-methanobenzo[*b*][1,4,5]oxathiazocine 1,1-dioxide (2.9.7)



According to general procedure **C**, **2.9.7** (57.3 mg, 62%) was isolated as a white solid.

mp 124–127 °C;

FTIR (thin film) 3105, 2964, 1599, 1583, 1474, 1335, 1153, 1117, 824, 746 cm⁻¹;

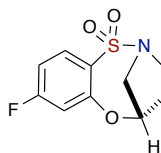
$[\alpha]_D^{20} = -47.6$ ($c = 0.525$, CHCl₃);

¹H NMR (500 MHz, CDCl₃) δ ppm 7.93 (dd, *J* = 8.8, 6.3 Hz, 1H, aromatic), 6.93 (ddd, *J* = 8.9, 7.5, 2.5 Hz, 1H, aromatic), 6.79 (dd, *J* = 9.6, 2.5 Hz, 1H, aromatic), 5.16 (dd, *J* = 6.3, 2.7 Hz, 1H, OCH), 4.38 (ddd, *J* = 14.2, 2.3, 2.2 Hz, 1H, NCH_aH_bCHO), 3.57 (dddd, *J* = 14.0, 9.3, 4.8, 2.0 Hz, 1H, NCH_aH_bCH₂), 3.30–3.23 (m, 1H, NCH_aH_bCH₂), 3.21 (dd, *J* = 14.3, 2.8 Hz, 1H, NCH_aH_bCHO), 2.08 (dddd, *J* = 15.5, 10.9, 6.4, 4.9 Hz, 1H, NCH₂CH_aH_b), 1.98 (dddd, *J* = 15.7, 9.0, 6.5, 2.4 Hz, 1H, NCH₂CH_aH_b);

¹³C NMR (126 MHz, CDCl₃) δ ppm 165.8 (d, ¹*J*_{C-F} = 255.8 Hz), 152.8 (d, ³*J*_{C-F} = 12.7 Hz), 132.5 (d, ³*J*_{C-F} = 10.6 Hz), 128.0 (d, ⁴*J*_{C-F} = 3.2 Hz), 112.0 (d, ²*J*_{C-F} = 23.6 Hz), 111.4 (d, ²*J*_{C-F} = 22.2 Hz), 80.7, 56.9, 47.2, 29.3;

HRMS calculated for C₁₀H₉FNO₃S (M-H)⁻ 242.0287; found 242.0295 (TOF MS ES⁻).

(5*S*)-8-fluoro-4,5-dihydro-3*H*-2,5-methanobenzo[*b*][1,4,5]oxathiazocine 1,1-dioxide (2.9.8)



According to general procedure C, **2.9.8** (51.0 mg, 55%) was isolated as a white solid.

mp 122–125 °C;

FTIR (thin film) 3099, 2972, 1601, 1581, 1474, 1339, 1159, 1117, 820, 741, 706 cm⁻¹;

[α]_D²⁰ = +24.4 (*c* = 0.39, CHCl₃);

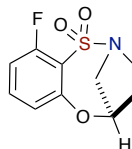
¹H NMR (400 MHz, CDCl₃) δ ppm 7.93 (dd, *J* = 8.9, 6.3 Hz, 1H, aromatic), 6.93 (ddd, *J* = 8.9, 7.4, 2.5 Hz, 1H, aromatic), 6.79 (dd, *J* = 9.6, 2.5 Hz, 1H, aromatic), 5.16 (dd, *J* = 6.2, 2.8 Hz, 1H, OCH), 4.38 (ddd, *J* = 14.3, 2.4, 2.3 Hz, 1H, NCH_aH_bCHO), 3.57 (dddd, *J*

= 14.0, 9.3, 4.9, 2.0 Hz, 1H, NCH_aH_bCH₂), 3.34–3.07 (m, 2H, NCH_aH_bCHO, NCH_aH_bCH₂), 2.23–1.87 (m, 2H, NCH₂CH₂);

¹³C NMR (126 MHz, CDCl₃) δ ppm 165.8 (d, ¹J_{C-F} = 255.7 Hz), 152.8 (d, ³J_{C-F} = 12.7 Hz), 132.5 (d, ³J_{C-F} = 10.6 Hz), 128.0 (d, ⁴J_{C-F} = 3.3 Hz), 112.0 (d, ²J_{C-F} = 23.6 Hz), 111.4 (d, ²J_{C-F} = 22.2 Hz), 80.7, 56.9, 47.2, 29.3;

HRMS calculated for C₁₀H₉FNO₃S (M-H)⁻ 242.0287; found 242.0287 (TOF MS ES⁻).

(5R)-10-fluoro-4,5-dihydro-3H-2,5-methanobenzo[*b*][1,4,5]oxathiazocine 1,1-dioxide (2.9.9)



According to general procedure C, **2.9.9** (90.6 mg, 98%) was isolated as a yellow solid.

mp 130–134 °C;

FTIR (thin film) 3078, 2959, 1601, 1564, 1456, 1348, 1159, 1112, 793, 718 cm⁻¹;

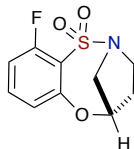
[α]_D²⁰ = -8.0 (c = 0.785, CHCl₃);

¹H NMR (500 MHz, CDCl₃) δ ppm 7.39 (ddd, *J* = 8.3, 5.9 Hz, 1H, aromatic), 6.94 (ddd, *J* = 10.1, 8.3, 1.2 Hz, 1H, aromatic), 6.85 (ddd, *J* = 8.3, 1.3 Hz, 1H, aromatic), 5.11 (ddd, *J* = 5.4, 2.4, 1.4 Hz, 1H, OCH), 4.34 (dd, *J* = 14.2, 2.0, 1.9 Hz, 1H, NCH_aH_bCHO), 3.92–3.72 (m, 1H, NCH_aH_bCH₂), 3.43–3.30 (m, 1H, NCH_aH_bCH₂), 3.21 (dd, *J* = 14.2, 2.5 Hz, 1H, NCH_aH_bCHO), 2.24–2.02 (m, 2H, NCH₂CH₂);

¹³C NMR (126 MHz, CDCl₃) δ ppm 161.5 (d, ¹J_{C-F} = 259.3 Hz), 151.8, 133.9 (d, ³J_{C-F} = 11.3 Hz, 2C), 120.4 (d, ⁴J_{C-F} = 3.3 Hz), 112.4 (d, ²J_{C-F} = 23.8 Hz), 80.5, 55.9, 47.3, 29.8;

HRMS calculated for $C_{10}H_9FNO_3S$ (M-H)⁻ 242.0287; found 242.0264 (TOF MS ES⁻).

(5*S*)-10-fluoro-4,5-dihydro-3*H*-2,5-methanobenzo[*b*][1,4,5]oxathiazocine 1,1-dioxide (2.9.10)



According to general procedure **C**, **2.9.10** (1.38 g, 66%) was isolated as a white solid.

mp 133–135 °C;

FTIR (thin film) 3018, 2959, 1601, 1564, 1456, 1350, 1159, 1112, 793, 717 cm⁻¹;

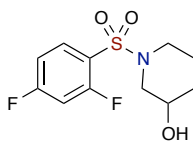
$[\alpha]_D^{20} = +5.0$ ($c = 0.285$, CHCl₃);

¹H NMR (500 MHz, CDCl₃) δ ppm 7.39 (ddd, $J = 8.3, 5.9$ Hz, 1H, aromatic), 6.94 (ddd, $J = 9.8, 8.3, 1.2$ Hz, 1H, aromatic), 6.85 (ddd, $J = 8.2, 1.3$ Hz, 1H, aromatic), 5.11 (ddd, $J = 4.3, 2.3, 2.0$ Hz, 1H, OCH), 4.34 (ddd, $J = 14.2, 2.0, 1.9$ Hz, 1H, NCH_aH_bCHO), 3.82 (dddd, $J = 14.3, 8.0, 5.9, 1.9$ Hz, 1H, NCH_aH_bCH₂), 3.36 (ddd, $J = 13.8, 10.0, 6.9$ Hz, 1H, NCH_aH_bCH₂), 3.21 (dd, $J = 14.2, 2.5$ Hz, 1H, NCH_aH_bCHO), 2.28–2.01 (m, 2H, NCH₂CH₂);

¹³C NMR (126 MHz, CDCl₃) δ ppm 161.5 (d, $^1J_{C-F} = 258.9$ Hz), 151.8 (d, $^4J_{C-F} = 1.9$ Hz), 133.9 (d, $^3J_{C-F} = 11.3$ Hz), 122.2 (d, $^3J_{C-F} = 14.3$ Hz), 120.4 (d, $^3J_{C-F} = 3.5$ Hz), 112.4 (d, $^2J_{C-F} = 23.9$ Hz), 80.5, 55.9, 47.3, 29.8;

HRMS calculated for $C_{10}H_9FNO_3S$ (M-H)⁻ 242.0287; found 242.0320 (TOF MS ES⁻).

1-((2,4-difluorophenyl)sulfonyl)piperidin-3-ol (2.9.11)



According to general procedure **A**, **2.9.11** (1.28 g, 98%) was isolated as a white solid.

mp 96–99 °C;

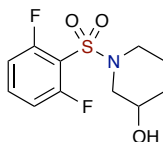
FTIR (neat) 3502, 3101, 2943, 1603, 1481, 1344, 1169, 1074, 856, 752, 708 cm⁻¹;

¹H NMR (500 MHz, CDCl₃) δ ppm 7.89 (ddd, *J* = 8.9, 7.9, 6.1 Hz, 1H, aromatic), 7.15–6.61 (m, 2H, aromatic), 4.00–3.80 (m, 1H, CHOH), 3.49 (ddd, *J* = 12.0, 3.6, 1.3 Hz, 1H, NCH_aH_bCH), 3.37–3.26 (m, 1H, NCH_aH_bCH₂), 3.03 (ddd, *J* = 12.0, 8.2, 3.1 Hz, 1H, NCH_aH_bCH), 2.92 (dd, *J* = 12.0, 7.3 Hz, 1H, NCH_aH_bCH₂), 2.00–1.74 (m, 3H, NCH₂CH₂CH_aH_b), 1.69–1.59 (m, 1H, NCH₂CH₂CH_aH_b), 1.55–1.44 (m, 1H, OH);

¹³C NMR (126 MHz, CDCl₃) δ ppm 165.7 (dd, *J*_{C-F} = 257.6, 11.4 Hz), 159.7 (dd, *J*_{C-F} = 258.4, 12.7 Hz), 132.9 (dd, *J*_{C-F} = 10.4, 2.1 Hz), 122.3 (dd, *J*_{C-F} = 14.9, 3.9 Hz), 112.0 (dd, *J*_{C-F} = 21.8, 3.7 Hz), 105.8 (dd, *J*_{C-F} = 25.8, 25.6 Hz), 65.7, 52.1, 45.9, 31.7, 22.1;

HRMS calculated for C₁₁H₁₃F₂NO₃SH (M+H)⁺ 278.0662; found 278.063 (TOF MS ES⁺).

1-((2,6-difluorophenyl)sulfonyl)piperidin-3-ol (2.9.12)



According to general procedure **A**, **2.9.12** (942 mg, 72%) was isolated as a white solid.

mp 102–105 °C;

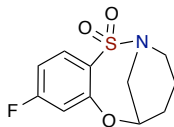
FTIR (neat) 3419, 3092, 2943, 1610, 1585, 1466, 1356, 1173, 1103, 773, 734 cm^{-1} ;

^1H NMR (500 MHz, CDCl_3) δ ppm 7.52 (tt, $J = 8.4, 5.9$ Hz, 1H, aromatic), 7.16–6.86 (m, 2H, aromatic), 4.00–3.83 (m, 1H, CHOH), 3.58 (dd, $J = 12.2, 3.6$ Hz, 1H, $\text{NCH}_a\text{H}_b\text{CH}$), 3.40 (ddd, $J = 11.3, 6.3, 3.8$ Hz, 1H, $\text{NCH}_a\text{H}_b\text{CH}_2$), 3.10 (ddd, $J = 12.0, 8.3, 3.0$ Hz, 1H, $\text{NCH}_a\text{H}_b\text{CH}$), 2.99 (dd, $J = 12.1, 7.3$ Hz, 1H, $\text{NCH}_a\text{H}_b\text{CH}_2$), 2.05–1.76 (m, 3H, $\text{NCH}_2\text{CH}_2\text{CH}_2$), 1.73–1.60 (m, 1H, $\text{NCH}_2\text{CH}_2\text{CH}_a\text{H}_b$), 1.57–1.44 (m, 1H, $\text{NCH}_2\text{CH}_2\text{CH}_a\text{H}_b$);

^{13}C NMR (126 MHz, CDCl_3) δ ppm 159.7 (dd, $J_{C-F} = 258.9, 4.2$ Hz, 2C), 134.5 (t, $J_{C-F} = 11.0$ Hz), 115.9 (dd, $J = 17.5, 15.9$ Hz), 113.2 (dd, $J_{C-F} = 24.0, 3.8$ Hz, 2C), 65.6, 51.9, 45.8, 31.7, 22.1;

HRMS calculated for $\text{C}_{11}\text{H}_{13}\text{F}_2\text{NO}_3\text{SH}$ ($\text{M}+\text{H}$) $^+$ 278.0662; found 278.0638 (TOF MS ES^+).

9-fluoro-3,4,5,6-tetrahydro-2,6-methanobenzo[*b*][1,4,5]oxathiazonine 1,1-dioxide (2.9.13)



According to general procedure **C**, **2.9.13** (53.1 mg, 57%) was isolated as a white solid.

mp 132–135 $^{\circ}\text{C}$;

FTIR (neat) 3097, 2961, 1599, 1583, 1472, 1339, 1163, 1111, 818, 731 cm^{-1} ;

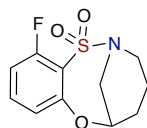
^1H NMR (500 MHz, CDCl_3) δ ppm 7.90–7.79 (m, 1H, aromatic), 7.01–6.83 (m, 2H, aromatic), 4.56 (dddd, $J = 4.3, 2.2, 2.1, 2.0$ Hz, 1H, OCHCH_2N), 4.42 (dddd, $J = 15.3, 2.5, 2.3, 2.1$ Hz, 1H, $\text{OCHCH}_a\text{H}_b\text{N}$), 3.98–3.84 (m, 1H, NCH_aH_b), 3.41 (dd, $J = 15.3, 1.6$

Hz, 1H, OCHCH_aH_bN), 3.33–3.18 (m, 1H, NCH_aH_b), 2.25–2.13 (m, 1H, NCH₂CHCH_aH_b), 2.04–1.82 (m, 1H, NCH₂CHCH_aH_b), 1.28–1.09 (m, 2H, NCH₂CH₂);

¹³C NMR (126 MHz, CDCl₃) δ ppm 165.5 (d, ¹J_{C-F} = 255.4 Hz), 155.1 (d, ³J_{C-F} = 12.3 Hz), 133.4 (d, ⁴J_{C-F} = 3.6 Hz), 130.6 (d, ³J_{C-F} = 10.5 Hz), 112.4 (d, ²J_{C-F} = 23.2 Hz), 111.3 (d, ²J_{C-F} = 22.1 Hz), 72.2, 51.9, 46.2, 27.4, 16.8;

HRMS calculated for C₁₁H₁₂FNO₃SH (M+H)⁺ 258.0600; found 258.0617 (TOF MS ES⁺).

11-fluoro-3,4,5,6-tetrahydro-2,6-methanobenzo[*b*][1,4,5]oxathiazonine 1,1-dioxide (2.9.14)



According to general procedure **C**, **2.9.14** (290 mg, 62%) was isolated as a white solid.

mp 118–120 °C;

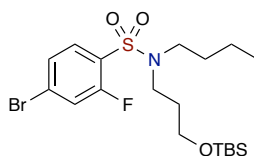
FTIR (neat) 3084, 2957, 1599, 1568, 1458, 1346, 1163, 1105, 798, 754, 721 cm⁻¹;

¹H NMR (500 MHz, CDCl₃) δ ppm 7.40 (ddd, *J* = 8.3, 8.0, 5.8 Hz, 1H, aromatic), 7.01–6.93 (m, 2H, aromatic), 4.55 (dddd, *J* = 4.0, 2.9, 2.7, 1.1 Hz, 1H, OCHCH₂N), 4.38 (dddd, *J* = 15.1, 2.4, 2.2, 2.2 Hz, 1H, OCHCH_aH_bN), 4.14–4.04 (m, 1H, NCH_aH_b), 3.38 (dd, *J* = 15.1, 1.3 Hz, 1H, OCHCH_aH_bN), 3.30 (ddd, *J* = 14.8, 13.4, 4.5 Hz, 1H, NCH_aH_b), 2.26–2.17 (m, 1H, NCH₂CHCH_aH_b), 1.93 (dddd, *J* = 15.4, 12.9, 6.9, 4.1 Hz, 1H, NCH₂CHCH_aH_b), 1.53–1.39 (m, 1H, NCH₂CH_aH_b), 1.33–1.24 (m, 1H, NCH₂CH_aH_b);

^{13}C NMR (126 MHz, CDCl_3) δ ppm 159.8 (d, $^1J_{\text{C-F}} = 259.2$ Hz), 154.3 (d, $^4J_{\text{C-F}} = 1.9$ Hz), 133.7 (d, $^3J_{\text{C-F}} = 11.0$ Hz), 126.7 (d, $^2J_{\text{C-F}} = 13.4$ Hz), 120.7 (d, $^3J_{\text{C-F}} = 3.3$ Hz), 113.0 (d, $^2J_{\text{C-F}} = 23.9$ Hz), 73.0, 51.2, 46.5, 27.5, 16.9;

HRMS calculated for $\text{C}_{11}\text{H}_{12}\text{FNO}_3\text{SNH}_4$ ($\text{M}+\text{NH}_4$) $^+$ 275.0866; found 275.0895 (TOF MS ES^+).

4-Bromo-*N*-butyl-*N*-(3-(*tert*-butyldimethylsilyloxy)propyl)-2-fluorobenzene-sulfonamide (2.10.1)



According to general procedure **E**, **2.10.1** (265 mg, 68%) was isolated as yellow oil.

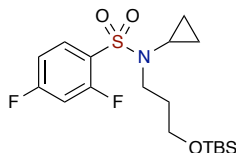
FTIR (neat) 2955, 1589, 1470, 1398, 1348, 1161, 1059, 835, 775 cm^{-1} ;

^1H NMR (500 MHz, CDCl_3) δ ppm 7.78–7.75 (m, 1H, aromatic), 7.41–7.36 (m, 2H, aromatic), 3.58 (t, $J = 5.8$ Hz, 2H, CH_2OTBS), 3.33–3.30 (m, 2H, $\text{NCH}_2\text{CH}_2\text{CH}_2\text{O}$), 3.26–3.23 (m, 2H, $\text{NCH}_2\text{CH}_2\text{CH}_2\text{CH}_3$), 1.74–1.71 (m, 2H, $\text{NCH}_2\text{CH}_2\text{CH}_2\text{O}$), 1.53–1.50 (m, 2H, $\text{NCH}_2\text{CH}_2\text{CH}_2\text{CH}_3$), 1.32–1.25 (m, 2H, $\text{NCH}_2\text{CH}_2\text{CH}_2\text{CH}_3$), 0.89 (t, $J = 7.3$ Hz, 3H, $\text{NCH}_2\text{CH}_2\text{CH}_2\text{CH}_3$), 0.87 (s, 9H, $(\text{CH}_3)_3$), 0.02 (s, 6H, $(\text{CH}_3)_2$);

^{13}C NMR (126 MHz, CDCl_3) δ ppm 158.4 (d, $^1J_{\text{C-F}} = 259.3$ Hz), 131.9 (d, $^4J_{\text{C-F}} = 1.6$ Hz), 127.8 (d, $^3J_{\text{C-F}} = 15.1$ Hz), 127.7 (d, $^3J_{\text{C-F}} = 9.0$ Hz), 127.6, 120.7 (d, $^2J_{\text{C-F}} = 25.0$ Hz), 60.1, 47.8 (2C), 44.8 (2C), 31.8, 30.4, 25.8, 21.6, 19.8, 18.2, 13.7, -5.5;

HRMS calculated for $\text{C}_{19}\text{H}_{33}\text{BrFNO}_3\text{SSiNa}$ ($\text{M}+\text{Na}^+$) 504.1016; found 504.1013 (TOF MS ES^+).

***N*-(3-((*tert*-butyldimethylsilyloxy)propyl)-*N*-cyclopropyl-2,4-difluorobenzene-sulfonamide (2.10.2)**



According to general procedure **E**, **2.10.2** (1.98 g, 88%) was isolated as colorless oil.

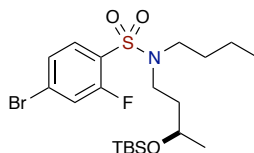
FTIR (thin film) 3098, 2955, 1603, 1487, 1362, 1165, 1096, 835, 775, 715 cm^{-1} ;

^1H NMR (500 MHz, CDCl_3) δ ppm 7.95 (ddd, $J = 8.9, 8.0, 6.2$ Hz, 1H, aromatic), 7.00 (dddd, $J = 8.7, 7.6, 2.4, 1.0$ Hz, 1H, aromatic), 6.94 (ddd, $J = 10.0, 8.5, 2.4$ Hz, 1H, aromatic), 3.65 (t, $J = 6.0$ Hz, 2H, CH_2OTBS), 3.45–3.33 (m, 2H, $\text{NCH}_2\text{CH}_2\text{CH}_2\text{O}$), 2.40–2.24 (m, 1H, NCH), 1.95–1.76 (m, 2H, $\text{NCH}_2\text{CH}_2\text{CH}_2\text{O}$), 0.90 (s, 9H, $(\text{CH}_3)_3$), 0.81–0.73 (m, 2H, $\text{NCHCH}_2\text{CH}_2$), 0.73–0.65 (m, 2H, $\text{NCHCH}_2\text{CH}_2$), 0.05 (s, 6H, $(\text{CH}_3)_2$);

^{13}C NMR (126 MHz, CDCl_3) δ ppm 165.6 (dd, $J_{\text{C-F}} = 257.1, 11.3$ Hz), 159.7 (dd, $J_{\text{C-F}} = 258.6, 12.6$ Hz), 133.0 (dd, $J_{\text{C-F}} = 10.3, 1.9$ Hz), 124.3 (dd, $J_{\text{C-F}} = 14.9, 3.9$ Hz), 111.7 (dd, $J_{\text{C-F}} = 21.8, 3.9$ Hz), 105.6 (dd, $J_{\text{C-F}} = 25.8, 25.6$ Hz), 60.4, 47.9, 32.0, 29.9, 25.9 (3C), 18.2, 7.2 (2C), -5.4 (2C);

HRMS calculated for $\text{C}_{18}\text{H}_{29}\text{F}_2\text{NO}_3\text{SSiH}$ ($\text{M}+\text{H}$) $^+$ 406.1684; found 406.1681 (TOF MS ES^+).

***(R)*-4-Bromo-*N*-butyl-*N*-(3-((*tert*-butyldimethylsilyloxy)butyl)-2-fluorobenzene-sulfonamide (2.10.4)**



According to general procedure **E, 2.10.4** (192 mg, 60%) was isolated as colorless oil.

FTIR (neat) 2957, 1589, 1470, 1398, 1348, 1161, 1136, 1090, 1059, 835 cm^{-1} ;

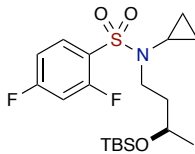
$[\alpha]_D^{20} = -31.5$ ($c = 0.2$, CHCl_3);

^1H NMR (500 MHz, CDCl_3) δ ppm 7.78–7.74 (m, 1H, aromatic), 7.41–7.36 (m, 2H, aromatic), 3.80–3.79 (m, 1H, CH_3CHOTBS), 3.30–3.19 (m, 4H, $\text{NCH}_2\text{CH}_2\text{CH}$, $\text{NCH}_2\text{CH}_2\text{CH}_2\text{CH}_3$), 1.66–1.62 (m, 2H, $\text{NCH}_2\text{CH}_2\text{CH}$), 1.52–1.47 (m, 2H, $\text{NCH}_2\text{CH}_2\text{CH}_2\text{CH}_3$), 1.32–1.24 (m, 2H, $\text{NCH}_2\text{CH}_2\text{CH}_2\text{CH}_3$), 1.11 (d, $J = 6.0$ Hz, 3H, CH_3CHOTBS), 0.89 (t, $J = 7.3$ Hz, 3H, $\text{NCH}_2\text{CH}_2\text{CH}_2\text{CH}_3$), 0.86 (s, 9H, $(\text{CH}_3)_3$), 0.03 (d, $J = 8.0$ Hz, 6H, $(\text{CH}_3)_2$);

^{13}C NMR (126 MHz, CDCl_3) δ ppm 158.4 (d, $^1J_{\text{C-F}} = 259.3$ Hz), 131.9 (d, $^4J_{\text{C-F}} = 1.3$ Hz), 127.9 (d, $^3J_{\text{C-F}} = 15.1$ Hz), 127.7 (d, $^3J_{\text{C-F}} = 3.6$ Hz), 127.6, 120.7 (d, $^2J_{\text{C-F}} = 25.0$ Hz), 66.4, 47.6 (2C), 44.7 (2C), 38.2, 30.5, 25.8, 23.7, 19.8, 18.0, 13.7, -4.3, -5.0;

HRMS calculated for $\text{C}_{20}\text{H}_{35}\text{BrFNO}_3\text{SSiNa}$ ($\text{M}+\text{Na}$) $^+$ 518.1172; found 518.1173 (TOF MS ES^+).

(*R*)-*N*-(3-((*tert*-butyldimethylsilyl)oxy)butyl)-*N*-cyclopropyl-2,4-difluorobenzene-sulfonamide (2.10.5)



According to general procedure **E, 2.10.5** (1.92 g, 89%) was isolated as colorless oil.

FTIR (thin film) 3099, 2955, 1603, 1486, 1358, 1167, 1072, 835, 773, 714 cm^{-1} ;

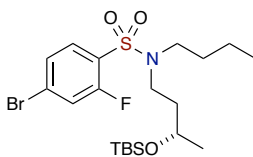
$[\alpha]_D^{20} = -8.8$ ($c = 1.55$, CHCl_3);

¹H NMR (500 MHz, CDCl₃) δ ppm 7.95 (ddd, *J* = 8.8, 8.0, 6.2 Hz, 1H, aromatic), 7.00 (dddd, *J* = 8.8, 7.7, 2.5, 1.0 Hz, 1H, aromatic), 6.94 (ddd, *J* = 10.0, 8.5, 2.4 Hz, 1H, aromatic), 3.84 (dddd, *J* = 6.2, 6.2, 6.1, 6.1, 6.1 Hz, 1H, CH₃CHOTBS), 3.52–3.26 (m, 2H, NCH₂CH₂CH), 2.34 (dddd, *J* = 8.8, 6.1, 3.9, 1.2 Hz, 1H, NCH), 1.78 (ddd, *J* = 9.0, 7.8, 5.8 Hz, 2H, NCH₂CH₂CH), 1.15 (d, *J* = 6.1 Hz, 3H, CH₃CHOTBS), 0.89 (s, 9H, (CH₃)₃), 0.82–0.63 (m, 4H, NCHCH₂CH₂), 0.05 (d, *J* = 4.6 Hz, 6H, (CH₃)₂);

¹³C NMR (126 MHz, CDCl₃) δ ppm 165.6 (dd, *J*_{C-F} = 257.3, 11.3 Hz), 159.6 (dd, *J*_{C-F} = 258.7, 12.8 Hz), 133.0 (d, *J*_{C-F} = 8.7 Hz), 124.4 (d, *J*_{C-F} = 10.8 Hz), 111.7 (dd, *J*_{C-F} = 21.6, 3.8 Hz), 105.6 (dd, *J*_{C-F} = 25.7, 25.3 Hz), 66.6, 47.7, 38.3, 29.6, 25.8 (3C), 23.8, 18.0, 7.2, 7.0, -4.3, -4.9;

HRMS calculated for C₁₉H₃₁F₂NO₃SSiNa (M+Na)⁺ 442.1660; found 442.1667 (TOF MS ES⁺).

(S)-4-Bromo-N-butyl-N-(3-(*tert*-butyldimethylsilyloxy)butyl)-2-fluorobenzene-sulfonamide (2.10.7)



According to general procedure **E**, **2.10.7** (288 mg, 90%) was isolated as colorless oil.

FTIR (neat) 2957, 1589, 1470, 1398, 1348, 1161, 1136, 1090, 835 cm⁻¹;

[α]_D²⁰ = +9.9 (*c* = 0.242, CHCl₃);

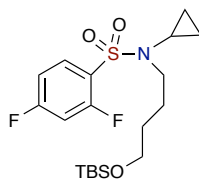
¹H NMR (500 MHz, CDCl₃) δ ppm 7.76 (t, *J* = 7.8 Hz, 1H, aromatic), 7.41–7.36 (m, 2H, aromatic), 3.80–3.79 (m, 1H, CH₃CHOTBS), 3.32–3.19 (m, 4H, NCH₂CH₂CH,

NCH₂CH₂CH₂CH₃), 1.63–1.61 (m, 2H, NCH₂CH₂CH), 1.54–1.47 (m, 2H, NCH₂CH₂CH₂CH₃), 1.32–1.24 (m, 2H, NCH₂CH₂CH₂CH₃), 1.11 (d, *J* = 6.0 Hz, 3H, CH₃CHOTBS), 0.89 (t, *J* = 7.5 Hz, 3H, NCH₂CH₂CH₂CH₃), 0.86 (s, 9H, (CH₃)₃), 0.02 (d, *J* = 8.5 Hz, 6H, (CH₃)₂);

¹³C NMR (126 MHz, CDCl₃) δ ppm 158.4 (d, ¹*J*_{C-F} = 259.3 Hz), 131.9 (d, ⁴*J*_{C-F} = 1.5 Hz), 127.9 (d, ³*J*_{C-F} = 15.2 Hz), 127.7 (d, ³*J*_{C-F} = 3.6 Hz), 127.6, 120.7 (d, ²*J*_{C-F} = 25.1 Hz), 66.4, 47.6 (2C) 44.7 (2C), 38.2, 30.5, 25.8, 23.7, 19.8, 18.0, 13.7, -4.3, -5.0;

HRMS calculated for C₂₀H₃₅BrFNO₃SSiNa (M+Na)⁺ 518.1172; found 518.1176 (TOF MS ES⁺).

***N*-(4-((*tert*-butyldimethylsilyl)oxy)butyl)-*N*-cyclopropyl-2,4-difluorobenzene-sulfonamide (2.10.8)**



According to general procedure **E**, **2.10.8** (284 mg, 85%) was isolated as colorless oil.

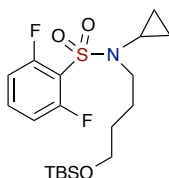
FTIR (thin film) 3099, 2953, 2930, 1603, 1487, 1348, 1165, 1072, 835, 775, 715 cm⁻¹;

¹H NMR (500 MHz, CDCl₃) δ ppm 7.95 (ddd, *J* = 8.9, 7.9, 6.2 Hz, 1H, aromatic), 7.00 (dddd, *J* = 8.8, 7.8, 2.5, 0.9 Hz, 1H, aromatic), 6.94 (ddd, *J* = 10.1, 8.5, 2.4 Hz, 1H, aromatic), 3.63 (t, *J* = 6.2 Hz, 2H, CH₂OTBS), 3.42–3.28 (m, 2H, NCH₂CH₂CH₂CH₂O), 2.39–2.25 (m, 1H, NCH), 1.77–1.66 (m, 2H, NCH₂CH₂CH₂CH₂O), 1.59–1.47 (m, 2H, NCH₂CH₂CH₂CH₂O), 0.89 (s, 9H, (CH₃)₃), 0.76–0.71 (m, 2H, NCHCH₂CH₂), 0.70–0.65 (m, 2H, NCHCH₂CH₂), 0.05 (s, 6H, (CH₃)₂);

^{13}C NMR (126 MHz, CDCl_3) δ ppm 165.6 (dd, $J_{\text{C-F}} = 257.1, 11.5$ Hz), 159.6 (dd, $J_{\text{C-F}} = 258.4, 12.7$ Hz), 132.9 (d, $J_{\text{C-F}} = 2.0$ Hz), 124.5 (d, $J_{\text{C-F}} = 11.0$ Hz), 111.7 (dd, $J_{\text{C-F}} = 21.7, 3.7$ Hz), 105.6 (dd, $J_{\text{C-F}} = 25.9, 25.7$ Hz), 62.6, 50.5, 30.0, 29.4, 25.9 (3C), 25.1, 18.3, 7.0 (2C), -5.3 (2C);

HRMS calculated for $\text{C}_{19}\text{H}_{31}\text{F}_2\text{NO}_3\text{SSiH}$ ($\text{M}+\text{H}$) $^+$ 420.1840; found 420.1799 (TOF MS ES $^+$).

N-(4-((tert-butyldimethylsilyloxy)butyl)-N-cyclopropyl-2,6-difluorobenzene-sulfonamide (2.10.9)



According to general procedure **E**, **2.10.9** (340 mg, 97%) was isolated as colorless oil.

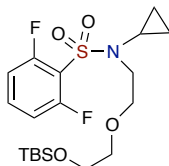
FTIR (thin film) 2928, 1610, 1585, 1466, 1362, 1167, 1055, 835, 775, 698 cm^{-1} ;

^1H NMR (500 MHz, CDCl_3) δ ppm 7.55–7.43 (m, 1H, aromatic), 7.06–6.97 (m, 2H, aromatic), 3.64 (t, $J = 6.2$ Hz, 2H, CH_2OTBS), 3.45–3.34 (m, 2H, $\text{NCH}_2\text{CH}_2\text{CH}_2\text{CH}_2\text{O}$), 2.49–2.35 (m, 1H, NCH), 1.82–1.69 (m, 2H, $\text{NCH}_2\text{CH}_2\text{CH}_2\text{CH}_2\text{O}$), 1.61–1.48 (m, 2H, $\text{NCH}_2\text{CH}_2\text{CH}_2\text{CH}_2\text{O}$), 0.89 (s, 9H, $(\text{CH}_3)_3$), 0.84–0.78 (m, 2H, $\text{NCHCH}_2\text{CH}_2$), 0.78–0.64 (m, 2H, $\text{NCHCH}_2\text{CH}_2$), 0.05 (s, 6H, $(\text{CH}_3)_2$);

^{13}C NMR (126 MHz, CDCl_3) δ ppm 159.8 (dd, $J_{\text{C-F}} = 258.9, 4.2$ Hz, 2C), 134.1 (t, $J_{\text{C-F}} = 10.8$ Hz), 118.3, 113.1 (dd, $J_{\text{C-F}} = 24.0, 3.7$ Hz, 2C), 62.6, 50.4, 30.0, 29.4, 25.9 (3C), 25.1, 18.3, 6.8 (2C), -5.1, -5.3;

HRMS calculated for $C_{19}H_{31}F_2NO_3SSiH$ ($M+H$)⁺ 420.1840; found 420.1860 (TOF MS ES⁺).

***N*-(2-(2-((*tert*-butyldimethylsilyl)oxy)ethoxy)ethyl)-*N*-cyclopropyl-2,6-difluorobenzenesulfonamide (SI-4)**



According to general procedure **E**, **SI-4** (576 mg, 90%) was isolated as colorless oil.

FTIR (thin film) 3092, 2928, 1610, 1585, 1468, 1364, 1146, 1103, 833, 777, 680 cm^{-1} ;

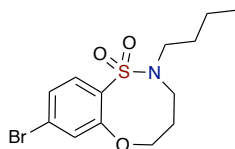
¹H NMR (500 MHz, CDCl₃) δ ppm 7.61–7.40 (m, 1H, aromatic), 7.10–6.94 (m, 2H, aromatic), 3.76–3.62 (m, 4H, CH₂OCH₂), 3.55 (t, $J = 6.1$ Hz, 2H, OCH₂CH₂OTBS), 3.50 (dd, $J = 5.6, 4.9$ Hz, 2H, NCH₂CH₂O), 2.54–2.42 (m, 1H, NCH), 0.90 (s, 9H, (CH₃)₃), 0.89–0.86 (m, 2H, NCHCH₂CH₂), 0.78–0.69 (m, 2H, NCHCH₂CH₂), 0.07 (s, 6H, (CH₃)₂);

¹³C NMR (126 MHz, CDCl₃) δ ppm 159.8 (dd, $J_{C-F} = 259.0, 4.3$ Hz, 2C), 134.2 (t, $J_{C-F} = 11.0$ Hz), 118.0 (dd, $J_{C-F} = 16.7, 16.6$ Hz), 113.1 (dd, $J_{C-F} = 24.0, 3.8$ Hz, 2C), 72.5, 69.7, 62.6, 50.1, 30.5, 25.9 (3C), 18.4, 7.4 (2C), -5.3 (2C);

HRMS calculated for $C_{19}H_{31}F_2NO_4SSiH$ ($M+H$)⁺ 436.1789; found 436.1809 (TOF MS ES⁺).

8-Bromo-2-butyl-2,3,4,5-tetrahydrobenzo[*b*][1,4,5]oxathiazocine
(2.10.11)

1,1-dioxide



According to general procedure **F**, **2.10.11** (64 mg, 88%) was isolated as a white solid.

mp 115–118 °C;

FTIR (neat) 2957, 1574, 1468, 1454, 1371, 1337, 1161, 1061, 831 cm⁻¹;

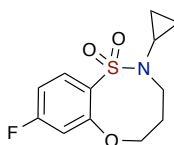
¹H NMR (500 MHz, CDCl₃) δ ppm 7.75 (d, *J* = 8.3 Hz, 1H, aromatic), 7.36 (dt, *J* = 8.3, 1.8 Hz, 2H, aromatic), 4.25 (t, *J* = 6.1 Hz, 2H, OCH₂CH₂CH₂N), 3.83–3.65 (m, 2H, NCH₂CH₂CH₂O), 2.99–2.77 (m, 2H, NCH₂CH₂CH₂CH₃), 1.83 (dt, *J* = 10.6, 6.1 Hz, 2H, NCH₂CH₂CH₂O), 1.63–1.56 (m, 2H, NCH₂CH₂CH₂CH₃), 1.33 (dd, *J* = 15.2, 7.5 Hz, 2H, NCH₂CH₂CH₂CH₃), 0.92 (t, *J* = 7.4 Hz, 3H, NCH₂CH₂CH₂CH₃);

¹³C NMR (126 MHz, CDCl₃) δ ppm 156.8, 134.1, 130.7, 127.3 (2C), 126.8, 75.0, 45.6, 43.2, 30.4, 24.9, 19.8, 13.7;

HRMS calculated for C₁₃H₁₈BrNO₃SNa (M+Na)⁺ 370.0088; found 370.0096 (TOF MS ES⁺).

2-cyclopropyl-8-fluoro-2,3,4,5-tetrahydrobenzo[*b*][1,4,5]oxathiazocine
(2.10.12)

1,1-dioxide



According to general procedure **F**, **2.10.12** (60.9 mg, 90%) was isolated as a white solid.

mp 143–145 °C;

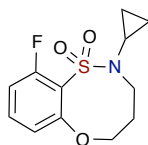
FTIR (thin film) 3103, 2920, 1587, 1474, 1346, 1167, 1070, 851 cm^{-1} ;

^1H NMR (500 MHz, CDCl_3) δ ppm 7.97 (ddd, $J = 8.3, 6.4, 0.7$ Hz, 1H, aromatic), 7.06–6.85 (m, 2H, aromatic), 4.35 (dd, $J = 6.2, 6.1$ Hz, 2H, $\text{OCH}_2\text{CH}_2\text{CH}_2\text{N}$), 3.88–3.61 (m, 2H, $\text{NCH}_2\text{CH}_2\text{CH}_2\text{O}$), 1.96 (tt, $J = 6.9, 3.6$ Hz, 1H, NCH), 1.91–1.81 (m, 2H, $\text{NCH}_2\text{CH}_2\text{CH}_2\text{O}$), 1.01–0.84 (m, 2H, $\text{NCHCH}_2\text{CH}_2$), 0.73 (ddd, $J = 6.7, 4.2, 2.9$ Hz, 2H, $\text{NCHCH}_2\text{CH}_2$);

^{13}C NMR (126 MHz, CDCl_3) δ ppm 165.8 (d, $^1J_{\text{C-F}} = 255.8$ Hz), 157.9 (d, $^3J_{\text{C-F}} = 11.2$ Hz), 132.4 (d, $^3J_{\text{C-F}} = 10.5$ Hz), 129.9 (d, $^4J_{\text{C-F}} = 3.6$ Hz), 111.3 (d, $^2J_{\text{C-F}} = 21.9$ Hz), 111.0 (d, $^2J_{\text{C-F}} = 22.7$ Hz), 75.2, 46.9, 28.0, 24.2, 8.1 (2C);

HRMS calculated for $\text{C}_{12}\text{H}_{14}\text{FNO}_3\text{SH}$ ($\text{M}+\text{H}$) $^+$ 272.0757; found 272.0758 (TOF MS ES^+).

2-cyclopropyl-10-fluoro-2,3,4,5-tetrahydrobenzo[*b*][1,4,5]oxathiazocine 1,1-dioxide (2.10.13)



According to general procedure **F**, **2.10.13** (483 mg, 72%) was isolated as a white solid.

mp 86–88 $^{\circ}\text{C}$;

FTIR (thin film) 3084, 2945, 1599, 1568, 1458, 1352, 1177, 1063, 800, 756 cm^{-1} ;

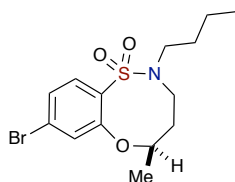
^1H NMR (500 MHz, CDCl_3) δ ppm 7.43 (ddd, $J = 8.3, 6.0$ Hz, 1H, aromatic), 7.07–6.89 (m, 2H, aromatic), 4.30 (dd, $J = 5.5, 5.4$ Hz, 2H, $\text{OCH}_2\text{CH}_2\text{CH}_2\text{N}$), 3.91–3.67 (m, 2H, $\text{NCH}_2\text{CH}_2\text{CH}_2\text{O}$), 2.62 (tt, $J = 7.1, 3.7$ Hz, 1H, NCH), 2.09–1.83 (m, 2H,

NCH₂CH₂CH₂O), 1.11–0.87 (m, 2H, NCHCH₂CH₂), 0.80 (dd, *J* = 6.9, 1.8 Hz, 2H, NCHCH₂CH₂);

¹³C NMR (126 MHz, CDCl₃) δ ppm 160.6 (d, ¹*J*_{C-F} = 258.4 Hz), 156.1 (d, ³*J*_{C-F} = 2.6 Hz), 133.5 (d, ³*J*_{C-F} = 10.9 Hz), 124.7 (d, ²*J*_{C-F} = 13.5 Hz), 119.3 (d, ⁴*J*_{C-F} = 3.6 Hz), 113.2 (d, ²*J*_{C-F} = 23.6 Hz), 75.5, 48.6, 28.7, 24.6, 8.1 (2C);

HRMS calculated for C₁₂H₁₄FNO₃SH (M+H)⁺ 272.0757; found 272.0758 (TOF MS ES⁺).

(R)-8-Bromo-2-butyl-5-methyl-2,3,4,5-tetrahydrobenzo[*b*][1,4,5]oxathiazocine 1,1-dioxide (2.10.14)



According to general procedure **F**, **2.10.14** (66 mg, 90%) was isolated as colorless oil.

FTIR (neat) 2957, 2932, 1574, 1456, 1379, 1333, 1161, 1136, 1090, 1063 cm⁻¹;

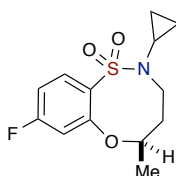
[α]_D²⁰ = +41.1 (*c* = 0.496, CHCl₃);

¹H NMR (500 MHz, CDCl₃) δ ppm 7.76 (d, *J* = 8.5 Hz, 1H, aromatic), 7.36–7.32 (m, 2H, aromatic), 4.13–4.10 (m, 2H, OCHCH₂CH_aH_bN), 3.45–3.42 (m, 1H, OCHCH₂CH_aH_bN), 3.23–3.20 (m, 1H, NCH_aH_bCH₂CH₂CH₃), 2.75–2.72 (m, 1H, NCH_aH_bCH₂CH₂CH₃), 1.91–1.89 (m, 1H, OCHCH_aH_bCH₂N), 1.77–1.75 (m, 1H, OCHCH_aH_bCH₂N), 1.63–1.59 (m, 2H, NCH₂CH₂CH₂CH₃), 1.47 (d, *J* = 6.5 Hz, 3H, OCHCH₃), 1.36–1.30 (m, 2H, NCH₂CH₂CH₂CH₃), 0.92 (t, *J* = 7.5 Hz, 3H, NCH₂CH₂CH₂CH₃);

^{13}C NMR (126 MHz, CDCl_3) δ ppm 156.8, 134.2, 130.9, 127.5, 127.4, 127.1, 82.2, 45.2, 41.6, 31.6, 30.4, 21.2, 19.8, 13.7;

HRMS calculated for $\text{C}_{14}\text{H}_{20}\text{BrNO}_3\text{SNa}$ ($\text{M}+\text{Na}$) $^+$ 384.0245; found 384.0235 (TOF MS ES $^+$).

(R)-2-cyclopropyl-8-fluoro-5-methyl-2,3,4,5-tetrahydrobenzo[*b*][1,4,5]oxathiazocine 1,1-dioxide (2.10.15)



According to general procedure **F**, **2.10.15** (548 mg, 90%) was isolated as a white solid.

mp 93–95 °C;

FTIR (thin film) 3085, 2955, 1585, 1472, 1344, 1167, 1068, 834, 756 cm^{-1} ;

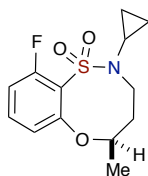
$[\alpha]_D^{20} = -28.8$ ($c = 1.99$, CHCl_3);

^1H NMR (500 MHz, CDCl_3) δ ppm 7.97 (dd, $J = 8.8, 6.4$ Hz, 1H, aromatic), 7.02–6.80 (m, 2H, aromatic), 4.50–4.23 (m, 1H, OCHCH_3), 4.08 (ddd, $J = 15.3, 8.4, 3.0$ Hz, 1H, $\text{NCH}_a\text{H}_b\text{CH}_2\text{CHO}$), 3.46 (ddd, $J = 15.3, 7.1, 3.0$ Hz, 1H, $\text{NCH}_a\text{H}_b\text{CH}_2\text{CHO}$), 2.13–1.93 (m, 2H, NCH_2 , $\text{OCHCH}_a\text{H}_b\text{CH}_2\text{N}$), 1.70 (dddd, $J = 15.8, 7.1, 5.9, 3.1$ Hz, 1H, $\text{OCHCH}_a\text{H}_b\text{CH}_2\text{N}$), 1.50 (d, $J = 6.4$ Hz, 3H, OCHCH_3), 1.08 (dddd, $J = 10.4, 7.0, 5.3, 3.6$ Hz, 1H, $\text{NCHCH}_a\text{H}_b\text{CH}_2$), 0.82 (dddd, $J = 9.6, 7.1, 6.8, 5.3$ Hz, 1H, $\text{NCHCH}_a\text{H}_b\text{CH}_2$), 0.75 (dddd, $J = 10.6, 7.0, 5.1, 3.7$ Hz, 1H, $\text{NCHCH}_2\text{CH}_a\text{H}_b$), 0.64 (dddd, $J = 9.7, 7.2, 7.0, 5.1$ Hz, 1H, $\text{NCHCH}_2\text{CH}_a\text{H}_b$);

^{13}C NMR (126 MHz, CDCl_3) δ ppm 165.6 (d, $^1J_{\text{C-F}} = 255.5$ Hz), 157.7 (d, $^3J_{\text{C-F}} = 11.4$ Hz), 132.3 (d, $^3J_{\text{C-F}} = 10.7$ Hz), 130.1 (d, $^4J_{\text{C-F}} = 3.6$ Hz), 111.5 (d, $^2J_{\text{C-F}} = 21.1$ Hz), 111.4 (d, $^2J_{\text{C-F}} = 20.5$ Hz), 82.2, 44.9, 31.0, 27.8, 21.3, 9.6, 6.3;

HRMS calculated for $\text{C}_{13}\text{H}_{16}\text{FNO}_3\text{SH}$ ($\text{M}+\text{H}$) $^+$ 286.0913; found 286.0909 (TOF MS ES $^+$).

(R)-2-cyclopropyl-10-fluoro-5-methyl-2,3,4,5-tetrahydrobenzo[*b*][1,4,5]oxathiazocine 1,1-dioxide (2.10.16)



According to general procedure **F**, **2.10.16** (67.0 mg, 98%) was isolated as colorless oil.

FTIR (thin film) 3084, 2976, 1599, 1568, 1462, 1340, 1148, 1103, 797, 758, 725 cm^{-1} ;

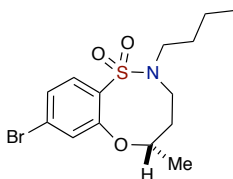
$[\alpha]_D^{20} = -51.3$ ($c = 2.235$, CHCl_3);

^1H NMR (500 MHz, CDCl_3) δ ppm 7.40 (ddd, $J = 8.3, 8.2, 6.0$ Hz, 1H, aromatic), 7.00 (ddd, $J = 9.6, 8.4, 1.2$ Hz, 1H, aromatic), 6.90 (ddd, $J = 8.2, 1.2, 1.1$ Hz, 1H, aromatic), 4.23–4.14 (m, 1H, OCHCH_3), 4.04–3.91 (m, 1H, $\text{NCH}_a\text{H}_b\text{CH}_2\text{CHO}$), 3.61 (ddd, $J = 15.2, 4.5, 4.3$ Hz, 1H, $\text{NCH}_a\text{H}_b\text{CH}_2\text{CHO}$), 2.79–2.70 (m, 1H, NCH), 2.10 (dddd, $J = 14.7, 10.6, 8.8, 3.9$ Hz, 1H, $\text{NCH}_2\text{CH}_a\text{H}_b\text{CHO}$), 1.83–1.67 (m, 1H, $\text{NCH}_2\text{CH}_a\text{H}_b\text{CHO}$), 1.44 (d, $J = 6.3$ Hz, 3H, OCHCH_3), 1.20 (s, 1H, $\text{NCHCH}_a\text{H}_b\text{CH}_2$), 0.94–0.68 (m, 3H, $\text{NCHCH}_a\text{H}_b\text{CH}_2$);

^{13}C NMR (126 MHz, CDCl_3) δ ppm 160.9 (d, $^1J_{\text{C-F}} = 257.7$ Hz), 133.1 (d, $^3J_{\text{C-F}} = 10.9$ Hz, 2C), 119.9, 113.3 (d, $^2J_{\text{C-F}} = 23.5$ Hz, 2C), 83.1, 47.4, 31.6, 28.3, 21.5, 9.5, 6.5;

HRMS calculated for $\text{C}_{13}\text{H}_{16}\text{FNO}_3\text{SH}$ ($\text{M}+\text{H}$) $^+$ 286.0913; found 286.0944 (TOF MS ES $^+$).

(S)-8-Bromo-2-butyl-5-methyl-2,3,4,5-tetrahydrobenzo[*b*][1,4,5]oxathiazocine 1,1-dioxide (2.10.17)



According to general procedure **F, 2.10.17** (64 mg, 87%) was isolated as colorless oil.

FTIR (neat) 2957, 2932, 1574, 1456, 1379, 1333, 1161, 1136, 1061, 833 cm^{-1} ;

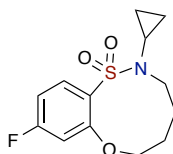
$[\alpha]_D^{20} = -55.0$ ($c = 0.2$, CHCl_3);

^1H NMR (500 MHz, CDCl_3) δ ppm 7.76 (d, $J = 8.5$ Hz, 1H, aromatic), 7.36–7.32 (m, 2H, aromatic), 4.16–4.12 (m, 2H, $\text{OCHCH}_2\text{CH}_a\text{H}_b\text{N}$), 3.46–3.42 (m, 1H, $\text{OCHCH}_2\text{CH}_a\text{H}_b\text{N}$), 3.23–3.20 (m, 1H, $\text{NCH}_a\text{H}_b\text{CH}_2\text{CH}_2\text{CH}_3$), 2.76–2.71 (m, 1H, $\text{NCH}_a\text{H}_b\text{CH}_2\text{CH}_2\text{CH}_3$), 1.91–1.89 (m, 1H, $\text{OCHCH}_a\text{H}_b\text{CH}_2\text{N}$), 1.77–1.75 (m, 1H, $\text{OCHCH}_a\text{H}_b\text{CH}_2\text{N}$), 1.63–1.58 (m, 2H, $\text{NCH}_2\text{CH}_2\text{CH}_2\text{CH}_3$), 1.47 (d, $J = 6.0$ Hz, 3H, OCHCH_3), 1.36–1.30 (m, 2H, $\text{NCH}_2\text{CH}_2\text{CH}_2\text{CH}_3$), 0.92 (t, $J = 7.3$ Hz, 3H, $\text{NCH}_2\text{CH}_2\text{CH}_2\text{CH}_3$);

^{13}C NMR (126 MHz, CDCl_3) δ ppm 156.8, 134.1, 130.9, 127.5, 127.4, 127.1, 82.2, 45.2, 41.6, 31.6, 30.4, 21.2, 19.8, 13.7;

HRMS calculated for $\text{C}_{14}\text{H}_{20}\text{BrNO}_3\text{SNa}$ ($\text{M}+\text{Na}$) $^+$ 384.0245; found 384.0248 (TOF MS ES^+).

2-cyclopropyl-9-fluoro-3,4,5,6-tetrahydro-2H-benzo[*b*][1,4,5]oxathiazonine 1,1-dioxide (2.10.18)



According to general procedure **F**, **2.10.18** (21.4 mg, 31%) was isolated as a white solid.

mp 140–144 °C;

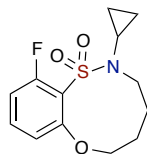
FTIR (thin film) 2920, 1585, 1473, 1334, 1165, 1151, 1068 cm⁻¹;

¹H NMR (500 MHz, CDCl₃) δ ppm 8.02–7.81 (m, 1H, aromatic), 6.92–6.75 (m, 2H, aromatic), 4.45–4.30 (m, 2H, OCH₂CH₂CH₂CH₂N), 3.87 (s, 2H, NCH₂CH₂CH₂CH₂O), 2.09–1.83 (m, 3H, NCH, NCH₂CH₂CH₂CH₂O), 1.73–1.58 (m, 2H, NCH₂CH₂CH₂CH₂O), 0.91 (s, 2H, NCHCH₂CH₂), 0.80–0.56 (m, 2H, NCHCH₂CH₂);

¹³C NMR (126 MHz, CDCl₃) δ ppm 165.9 (d, ¹J_{C-F} = 254.4 Hz), 157.6 (d, ³J_{C-F} = 10.6 Hz), 132.0 (d, ³J_{C-F} = 10.7 Hz), 129.6 (d, ⁴J_{C-F} = 3.4 Hz), 109.8 (d, ²J_{C-F} = 22.0 Hz), 106.7 (d, ²J_{C-F} = 24.0 Hz), 74.2, 47.9, 26.6, 26.4, 26.0, 7.8 (2C);

HRMS calculated for C₁₃H₁₆FNO₃SH (M+H)⁺ 286.0913; found 286.0885 (TOF MS ES⁺).

2-cyclopropyl-11-fluoro-3,4,5,6-tetrahydro-2H-benzo[*b*][1,4,5]oxathiazonine 1,1-dioxide (2.10.19)



According to general procedure **F**, **2.10.19** (44.9 mg, 66%) was isolated as a white solid.

mp 105–108 °C;

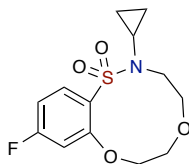
FTIR (thin film) 3018, 2930, 1599, 1570, 1464, 1340, 1165, 1040, 829, 788, 669 cm^{-1} ;

^1H NMR (500 MHz, CDCl_3) δ ppm 7.44 (ddd, $J = 8.4, 8.2, 5.7$ Hz, 1H, aromatic), 6.97–6.77 (m, 2H, aromatic), 4.35 (dd, $J = 6.0, 3.8$ Hz, 2H, $\text{OCH}_2\text{CH}_2\text{CH}_2\text{CH}_2\text{N}$), 3.85 (bs, 2H, $\text{NCH}_2\text{CH}_2\text{CH}_2\text{CH}_2\text{O}$), 2.08 (tt, $J = 7.0, 3.7$ Hz, 1H, NCH), 1.98–1.86 (m, 2H, $\text{NCH}_2\text{CH}_2\text{CH}_2\text{CH}_2\text{O}$), 1.79–1.67 (m, 2H, $\text{NCH}_2\text{CH}_2\text{CH}_2\text{CH}_2\text{O}$), 0.94 (s, 2H, $\text{NCHCH}_2\text{CH}_2$), 0.76 (dt, $J = 6.9, 2.1$ Hz, 2H, $\text{NCHCH}_2\text{CH}_2$);

^{13}C NMR (126 MHz, CDCl_3) δ ppm 160.3 (d, $^1J_{\text{C-F}} = 260.8$ Hz), 157.9 (d, $^3J_{\text{C-F}} = 2.7$ Hz), 133.8 (d, $^3J_{\text{C-F}} = 11.1$ Hz), 121.1 (d, $^2J_{\text{C-F}} = 11.9$ Hz), 113.3 (d, $^4J_{\text{C-F}} = 3.7$ Hz), 111.2 (d, $^2J_{\text{C-F}} = 24.1$ Hz), 73.7, 49.0, 27.0 (2C), 26.1, 7.6 (2C);

HRMS calculated for $\text{C}_{13}\text{H}_{16}\text{FNO}_3\text{SH}$ ($\text{M}+\text{H}^+$) 286.0913; found 286.0904 (TOF MS ES^+).

2-cyclopropyl-10-fluoro-3,4,6,7-tetrahydro-2H-benzo[*e*][1,4,7,8]dioxathiazecine 1,1-dioxide (2.10.20)



According to general procedure **F**, **2.10.20** (41.2 mg, 59%) was isolated as a white solid.

mp 142–144 $^{\circ}\text{C}$;

FTIR (thin film) 2922, 1599, 1572, 1470, 1337, 1151, 1111, 1078 cm^{-1} ;

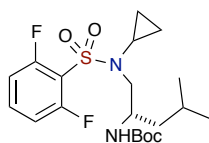
^1H NMR (500 MHz, CDCl_3) δ ppm 7.45 (ddd, $J = 8.4, 8.2, 5.7$ Hz, 1H, aromatic), 6.83 (ddd, $J = 10.4, 8.5, 1.1$ Hz, 1H, aromatic), 6.77 (ddd, $J = 8.3, 1.2, 1.1$ Hz, 1H, aromatic), 4.15 (dd, $J = 4.4, 4.2$ Hz, 2H, $\text{COCH}_2\text{CH}_2\text{O}$), 3.98 (dd, $J = 5.2, 5.1$ Hz, 2H, $\text{NCH}_2\text{CH}_2\text{O}$),

3.90 (dd, $J = 4.9, 3.7$ Hz, 2H, COCH₂CH₂O), 3.81–3.67 (m, 2H, NCH₂CH₂O), 2.52–2.31 (m, 1H, NCH), 0.74–0.53 (m, 4H, NCHCH₂CH₂);

¹³C NMR (126 MHz, CDCl₃) δ ppm 160.7 (d, ¹ $J_{C-F} = 260.9$ Hz), 158.9 (d, ⁴ $J_{C-F} = 2.8$ Hz), 134.3 (d, ² $J_{C-F} = 11.5$ Hz), 119.0 (d, ³ $J_{C-F} = 11.4$ Hz), 111.3 (d, ³ $J_{C-F} = 3.6$ Hz), 110.5 (d, ² $J_{C-F} = 24.8$ Hz), 72.8, 68.6, 67.9, 49.4, 28.8, 6.9 (2C);

HRMS calculated for C₁₃H₁₆FNO₃SH (M+H)⁺ 302.0862; found 302.0858 (TOF MS ES⁺).

(S)-tert-butyl (1-(N-cyclopropyl-2,6-difluorophenylsulfonamido)-4-methylpentan-2-yl)carbamate (2.11.2)



According to general procedure **E**, **2.11.2** (210 mg, 75%) was isolated as a white solid.

mp 131–134 °C;

FTIR (thin film) 3404, 2957, 1697, 1612, 1514, 1468, 1366, 1167, 777, 719 cm⁻¹;

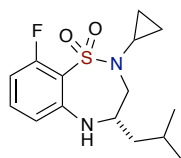
$[\alpha]_D^{20} = -10.7$ ($c = 0.55$, CHCl₃);

¹H NMR (500 MHz, CDCl₃) δ ppm 7.54–7.44 (m, 1H, aromatic), 7.01 (dd, $J = 8.9, 8.6$ Hz, 2H, aromatic), 4.53 (d, $J = 9.5$ Hz, 1H, NH), 4.13–3.98 (m, 1H, NHCH), 3.51 (dd, $J = 14.2, 9.8$ Hz, 1H, NCH_aH_bCHNH), 3.17 (dd, $J = 14.4, 5.1$ Hz, 1H, NCH_aH_bCHNH), 2.58–2.46 (m, 1H, NCH), 1.79–1.68 (m, 1H, CH₃CHCH₃), 1.46 (s, 9H, (CH₃)₃), 1.41 (s, 1H, CHCH_aH_bCHCH₃), 1.34–1.26 (m, 2H CHCH_aH_bCHCH₃, NCHCH_aH_bCH₂), 0.95 (dd, $J = 6.5, 1.7$ Hz, 6H, CH₃CHCH₃), 0.87–0.82 (m, 1H, NCHCH_aH_bCH₂), 0.78–0.70 (m, 2H, NCHCH₂CH₂);

^{13}C NMR (126 MHz, CDCl_3) δ ppm 159.7 (dd, $J_{\text{C-F}} = 258.4, 4.1$ Hz, 2C), 155.8, 134.1 (t, $J_{\text{C-F}} = 11.0$ Hz), 118.8, 113.1 (dd, $J_{\text{C-F}} = 23.7, 3.7$ Hz, 2C), 79.3, 54.0, 46.8, 42.4, 29.4, 28.4 (3C), 24.9, 23.2, 22.1 (2C), 6.5, 6.3;

HRMS calculated for $\text{C}_{20}\text{H}_{30}\text{F}_2\text{N}_2\text{O}_4\text{SNa}$ ($\text{M}+\text{Na}$) $^+$ 455.1792; found 455.1782 (TOF MS ES^+).

(S)-2-cyclopropyl-9-fluoro-4-isobutyl-2,3,4,5-tetrahydrobenzo[f][1,2,5]thiadiazepine 1,1-dioxide (2.11.3)



According to general procedure **G**, **2.11.3** (28 mg, 39%) was isolated as a white solid.

mp 131–135 °C;

FTIR (thin film) 3373, 2957, 2922, 1609, 1578, 1504, 1470, 1344, 1155 cm^{-1} ;

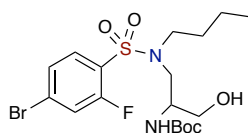
$[\alpha]_D^{20} = -29.6$ ($c = 0.805$, CH_2Cl_2);

^1H NMR (500 MHz, CDCl_3) δ ppm 7.18 (ddd, $J = 8.3, 8.2, 5.8$ Hz, 1H, aromatic), 6.67–6.62 (m, 1H, aromatic), 6.51 (d, $J = 8.2$ Hz, 1H, aromatic), 4.12–4.04 (m, 1H, NHCH), 4.01 (s, 1H, NH), 3.72 (dd, $J = 13.2, 4.4$ Hz, 1H, $\text{NCH}_a\text{H}_b\text{CHNH}$), 3.05 (dd, $J = 12.9, 12.1$ Hz, 1H, $\text{NCH}_a\text{H}_b\text{CHNH}$), 2.81–2.71 (m, 1H, NCH), 1.74–1.65 (m, 1H, CH_3CHCH_3), 1.48–1.37 (m, 2H, $\text{CHCH}_2\text{CHCH}_3$), 1.24–1.16 (m, 1H, $\text{NCHCH}_a\text{H}_b\text{CH}_2$), 0.97 (d, $J = 6.6$ Hz, 3H, CH_3CHCH_3), 0.91 (d, $J = 6.6$ Hz, 3H, CH_3CHCH_3), 0.84–0.74 (m, 1H, $\text{NCHCH}_a\text{H}_b\text{CH}_2$), 0.68–0.59 (m, 2H, $\text{NCHCH}_2\text{CH}_2$);

^{13}C NMR (126 MHz, CDCl_3) δ ppm 161.9 (d, $^1J_{\text{C-F}} = 254.3$ Hz), 148.4 (d, $^3J_{\text{C-F}} = 3.6$ Hz), 132.6 (d, $^3J_{\text{C-F}} = 11.0$ Hz), 116.5 (d, $^2J_{\text{C-F}} = 16.5$ Hz), 114.3 (d, $^4J_{\text{C-F}} = 3.3$ Hz), 107.8 (d, $^2J_{\text{C-F}} = 22.7$ Hz), 59.4, 56.0, 42.7, 33.7, 25.3, 22.7, 22.4, 11.1, 6.4;

HRMS calculated for $\text{C}_{15}\text{H}_{21}\text{FN}_2\text{O}_2\text{SH}$ (M+H) $^+$ 313.1386; found 313.1371 (TOF MS ES $^+$).

***tert*-butyl (1-(4-bromo-*N*-butyl-2-fluorophenylsulfonamido)-3-hydroxypropan-2-yl)-carbamate (SI-5)**



According to general procedure E, **SI-5** (26.9 mg, 35%) was isolated as colorless oil.

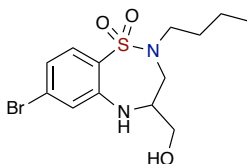
FTIR (thin film) 3599, 3354, 2959, 1714, 1576, 1456, 1387, 1339, 1159, 1061, 852 cm^{-1} ;

^1H NMR (500 MHz, CDCl_3) δ ppm 7.77 (d, $J = 8.3$ Hz, 1H, aromatic), 7.43–7.33 (m, 2H, aromatic), 4.74 (d, $J = 8.6$ Hz, 1H, NH), 4.28 (dd, $J = 11.2, 5.3$ Hz, 1H, $\text{CH}_a\text{H}_b\text{OH}$), 4.21–4.05 (m, 2H, $\text{NCH}_a\text{H}_b\text{CHNH}$), 3.97 (dd, $J = 11.3, 4.2$ Hz, 1H, $\text{CH}_a\text{H}_b\text{OH}$), 3.43 (d, $J = 11.3$ Hz, 1H, $\text{NCH}_a\text{H}_b\text{CHNH}$), 3.28 (dt, $J = 15.1, 7.9$ Hz, 1H, $\text{NCH}_a\text{H}_b\text{CH}_2\text{CH}_2\text{CH}_3$), 2.90 (dt, $J = 14.0, 7.1$ Hz, 1H, $\text{NCH}_a\text{H}_b\text{CH}_2\text{CH}_2\text{CH}_3$), 1.76–1.58 (m, 2H, $\text{NCH}_2\text{CH}_2\text{CH}_2\text{CH}_3$), 1.46 (s, 9H, $(\text{CH}_3)_3$), 1.40–1.28 (m, 2H, $\text{NCH}_2\text{CH}_2\text{CH}_2\text{CH}_3$), 1.27 (s, 1H, OH), 1.03–0.85 (m, 3H, $\text{NCH}_2\text{CH}_2\text{CH}_2\text{CH}_3$);

^{13}C NMR (126 MHz, CDCl_3) δ ppm 156.1 (d, $^1J_{\text{C-F}} = 261.2$ Hz), 154.9, 133.7, 130.7, 127.9, 127.5, 126.8, 80.5, 77.8, 48.2, 47.8, 46.3, 30.5, 28.3 (3C), 19.7, 13.7;

HRMS calculated for $C_{18}H_{28}BrFN_2O_5SNa$ ($M+Na$)⁺ 505.0784; found 505.0770 (TOF MS ES⁺).

7-bromo-2-butyl-4-(hydroxymethyl)-2,3,4,5-tetrahydrobenzo[f][1,2,5]thiadiazepine 1,1-dioxide (2.11.4)



According to general procedure **G**, **2.11.4** (11 mg, 29%) was isolated as colorless oil.

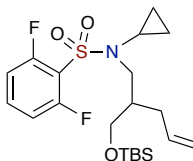
FTIR (thin film) 3501, 3354, 2957, 1582, 1504, 1462, 1325, 1155, 1090, 862, 763 cm^{-1} ;

¹H NMR (500 MHz, CDCl₃) δ ppm 7.69 (d, $J = 8.4$ Hz, 1H, aromatic), 7.13 (dd, $J = 8.4$, 1.8 Hz, 1H, aromatic), 7.10 (d, $J = 1.7$ Hz, 1H, aromatic), 4.65 (s, 1H, NH), 3.83 (dt, $J = 10.4$, 3.4 Hz, 1H, CH_aH_bOH), 3.79–3.71 (m, 1H, NHCH), 3.63 (ddd, $J = 10.3$, 8.5, 5.9 Hz, 1H, CH_aH_bOH), 3.46 (dd, $J = 14.1$, 10.9 Hz, 1H, NCH_aH_bCH), 3.30 (dd, $J = 14.1$, 2.2 Hz, 1H, NCH_aH_bCH), 3.22 (dt, $J = 14.3$, 7.3 Hz, 1H, NCH_aH_bCH₂), 2.94 (dt, $J = 14.0$, 7.1 Hz, 1H, NCH_aH_bCH₂), 1.79 (dd, $J = 5.7$, 3.4 Hz, 1H, OH), 1.62–1.55 (m, 2H, NCH₂CH₂CH₂CH₃), 1.41–1.31 (m, 2H, NCH₂CH₂CH₂CH₃), 0.94 (t, $J = 7.4$ Hz, 3H, NCH₂CH₂CH₂CH₃);

¹³C NMR (126 MHz, CDCl₃) δ ppm 146.3, 130.9, 127.9, 127.1, 123.8, 123.5, 62.6, 55.2, 50.7, 48.6, 30.7, 19.7, 13.7;

HRMS calculated for $C_{13}H_{19}BrN_2O_3SNa$ ($M+Na$)⁺ 385.0197; found 385.0208 (TOF MS ES⁺).

(R)-N-(2-(((*tert*-butyldimethylsilyl)oxy)methyl)pent-4-en-1-yl)-N-cyclopropyl-2,6-difluorobenzenesulfonamide (SI-6)



According to general procedure E, **SI-6** (260 mg, 69%) was isolated as colorless oil.

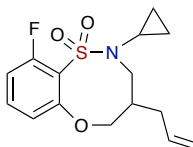
FTIR (thin film) 3150, 2928, 1612, 1585, 1468, 1361, 1174, 1105, 914, 777, 723 cm^{-1} ;

^1H NMR (500 MHz, CDCl_3) δ ppm 7.54–7.47 (m, 1H, aromatic), 7.02 (t, $J = 8.7$ Hz, 2H, aromatic), 5.80 (ddt, $J = 17.1, 10.1, 6.9$ Hz, 1H, $\text{CH}_2\text{HC}=\text{CH}_2$), 5.06 (m, 2H, $\text{CH}_2\text{HC}=\text{CH}_2$), 3.60 (ddd, $J = 23.3, 10.2, 4.6$ Hz, 2H, CH_2OTBS), 3.33 (d, $J = 2$ Hz, NCH_2CH), 2.40–2.34 (m, 1H, NCH), 2.18–2.09 (m, 3H, $\text{NCH}_2\text{CHCH}_2$), 0.92–0.82 (m, 10H, $(\text{CH}_3)_3$, $\text{NCHCH}_a\text{H}_b\text{CH}_2$), 0.73 (m, 3H, $\text{NCHCH}_a\text{H}_b\text{CH}_2$), 0.05 (d, $J = 2.1$ Hz, 6H, $(\text{CH}_3)_2$);

^{13}C NMR (126 MHz, CDCl_3) δ ppm 159.9 (dd, $J_{\text{C-F}} = 258.9, 4.4$ Hz, 2C), 136.4, 134.2 (t, $J_{\text{C-F}} = 11.0$ Hz), 117.7, 116.5, 113.1 (dd, $J_{\text{C-F}} = 23.7, 3.7$ Hz, 2C), 62.8, 52.0, 51.9, 39.4, 33.3, 30.5, 25.9 (3C), 18.2, 6.8, 6.6, -5.5 (2C);

HRMS calculated for $\text{C}_{21}\text{H}_{33}\text{F}_2\text{NO}_3\text{SSiNa}$ ($\text{M}+\text{Na}$) $^+$ 468.1816; found 468.1827 (TOF MS ES^+).

4-allyl-2-cyclopropyl-10-fluoro-2,3,4,5-tetrahydrobenzo[b][1,4,5]oxathiazocine 1,1-dioxide (2.11.5)



According to general procedure **H**, **2.11.5** (41 mg, 74%) was isolated as colorless oil.

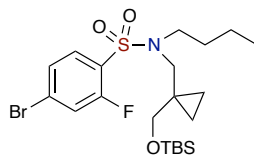
FTIR (thin film) 3078, 2935, 1599, 1568, 1470, 1458, 1348, 1145, 991, 924, 833 cm^{-1} ;

^1H NMR (500 MHz, CDCl_3) δ ppm 7.43 (td, $J = 8.3, 6.0$ Hz, 1H, aromatic), 7.02–6.97 (m, 1H, aromatic), 6.96 (d, $J = 8.2$ Hz, 1H, aromatic), 5.79–5.65 (m, 1H, $\text{HC}=\text{CH}_2$), 5.11 (s, 1H, $\text{HC}=\text{CH}_a\text{H}_b$), 5.09–5.07 (m, 1H, $\text{HC}=\text{CH}_a\text{H}_b$), 4.32–4.23 (m, 1H, OCH_aH_b), 3.95 (dd, $J = 11.0, 10.5$ Hz, 1H, OCH_aH_b), 3.86–3.78 (m, 1H, NCH_aH_b), 3.42 (d, $J = 14.6$ Hz, 1H, NCH_aH_b), 2.62 (s, 1H, NCH), 2.48–2.37 (m, 1H, NCH_2CH), 1.98 (dd, $J = 7.1, 6.6$ Hz, 2H, $\text{CH}_2\text{HC}=\text{CH}_a\text{H}_b$), 1.22 (s, 1H, $\text{NCHCH}_a\text{H}_b\text{CH}_2$), 0.90–0.83 (m, 1H, $\text{NCHCH}_a\text{H}_b\text{CH}_2$), 0.79–0.66 (m, 2H, $\text{NCHCH}_2\text{CH}_2$);

^{13}C NMR (126 MHz, CDCl_3) δ ppm 160.9 (d, $^1J_{\text{C-F}} = 258.8$ Hz), 156.4, 134.4, 133.5 (d, $^3J_{\text{C-F}} = 10.9$ Hz), 119.1 (d, $^4J_{\text{C-F}} = 3.5$ Hz), 117.9, 113.2 (d, $^2J_{\text{C-F}} = 23.1$ Hz, 2C), 79.5, 53.5, 34.0, 33.8, 29.1, 10.0, 6.5;

HRMS calculated for $\text{C}_{15}\text{H}_{18}\text{FNO}_3\text{SNa}$ ($\text{M}+\text{Na}$) $^+$ 334.0889; found 334.0895 (TOF MS ES^+).

4-bromo-*N*-butyl-*N*-((1-(((*tert*-butyldimethylsilyl)oxy)methyl)cyclopropyl)methyl)-2-fluorobenzenesulfonamide (SI-7)



According to general procedure **E**, **SI-7** (265 mg, 81%) was isolated as colorless oil.

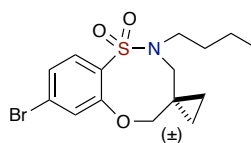
FTIR (thin film) 2955, 1589, 1470, 1398, 1346, 1161, 1082, 837, 775, 730 cm^{-1} ;

¹H NMR (500 MHz, CDCl₃) δ ppm 7.78 (dd, *J* = 8.4, 7.5 Hz, 1H, aromatic), 7.40 (ddd, *J* = 8.4, 1.8, 0.6 Hz, 1H, aromatic), 7.37 (dd, *J* = 9.5, 1.8 Hz, 1H, aromatic), 3.41 (s, 2H, CH₂OTBS), 3.38–3.33 (m, 2H, NCH₂CH₂), 3.31 (s, 2H, NCH₂), 1.54–1.47 (m, 2H, NCH₂CH₂CH₂), 1.31–1.18 (m, 2H, NCH₂CH₂CH₂), 0.93–0.84 (m, 12H, (CH₃)₃, NCH₂CH₂CH₂CH₃), 0.49–0.45 (m, 2H, CCH₂CH₂), 0.41–0.36 (m, 2H, CCH₂CH₂), 0.01 (s, 6H, (CH₃)₂);

¹³C NMR (126 MHz, CDCl₃) δ ppm 158.4 (d, ¹*J*_{C-F} = 258.9 Hz), 131.9 (d, ⁴*J*_{C-F} = 1.8 Hz), 128.5 (d, ²*J*_{C-F} = 15.0 Hz), 127.6 (d, ³*J*_{C-F} = 3.7 Hz), 127.5 (d, ³*J*_{C-F} = 9.1 Hz), 120.6 (d, ²*J*_{C-F} = 25.0 Hz), 65.0, 51.8, 48.3, 30.1, 25.9 (3C), 21.0, 20.0, 18.3, 13.7, 8.7 (2C), -5.4 (2C);

HRMS calculated for C₂₁H₃₅BrFNO₃SSiH (M+H)⁺ 508.1353; found 508.1349 (TOF MS ES⁺).

8-bromo-2-butyl-3,5-dihydro-2H-spiro[benzo[b][1,4,5]oxathiazine-4,1'-cyclopropane]1,1-dioxide (2.11.6)



According to general procedure **H**, **2.11.6** (11 mg, 32%) was isolated as colorless oil.

FTIR (thin film) 2957, 1574, 1454, 1335, 1203, 1155, 1061, 818, 760 cm⁻¹;

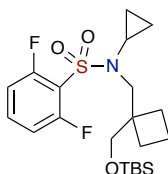
¹H NMR (500 MHz, CDCl₃) δ ppm 7.82 (d, *J* = 8.4 Hz, 1H, aromatic), 7.38 (dd, *J* = 8.4, 1.9 Hz, 1H, aromatic), 7.28 (d, *J* = 1.9 Hz, 1H, aromatic), 3.88 (s, 2H, OCH₂), 3.65 (s, 2H, NCH₂), 3.22 (t, *J* = 7.5 Hz, 2H, NCH₂CH₂), 1.67–1.58 (m, 2H, NCH₂CH₂), 1.40–1.29

(m, 2H, NCH₂CH₂CH₂CH₃), 0.93 (t, $J = 7.4$ Hz, 3H, NCH₂CH₂CH₂CH₃), 0.55 (d, $J = 4.0$ Hz, 4H, CCH₂CH₂);

¹³C NMR (126 MHz, CDCl₃) δ ppm 157.7, 134.1, 131.2, 127.8, 127.2, 127.1, 82.7, 51.0, 46.0, 30.3, 19.9, 17.8, 13.8, 9.2 (2C);

HRMS calculated for C₁₅H₂₀BrNO₃SH (M+H)⁺ 374.0426; found 374.0453 (TOF MS ES⁺).

***N*-((1-(((*tert*-butyldimethylsilyl)oxy)methyl)cyclobutyl)methyl)-*N*-cyclopropyl-2,6-difluorobenzenesulfonamide (SI-8)**



According to general procedure **E**, **SI-8** (16.2 mg, 36%) was isolated as colorless oil.

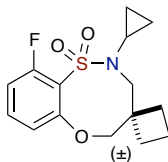
FTIR (thin film) 2928, 1585, 1468, 1364, 1167, 1089, 835, 777, 706 cm⁻¹;

¹H NMR (500 MHz, CDCl₃) δ ppm 7.63–7.37 (m, 1H, aromatic), 7.15–6.89 (m, 2H, aromatic), 3.67 (s, 2H, CH₂OTBS), 3.44 (s, 2H, NCH₂), 2.52 (tt, $J = 7.2, 4.0$ Hz, 1H, NCH), 2.14–1.95 (m, 2H, CCH₂CH₂CH₂), 1.96–1.71 (m, 4H, CCH₂CH₂CH₂), 0.92 (s, 9H, (CH₃)₃), 0.75–0.70 (m, 2H, NCHCH₂CH₂), 0.69–0.64 (m, 2H, NCHCH₂CH₂), 0.09 (s, 6H, (CH₃)₂);

¹³C NMR (126 MHz, CDCl₃) δ ppm 159.7 (d, $J_{C-F} = 258.1$ Hz, 2C), 133.9 (t, $J_{C-F} = 11.0$ Hz), 113.1 (d, $J_{C-F} = 3.7$ Hz), 112.9 (d, $J_{C-F} = 3.7$ Hz, 2C), 66.9, 54.9, 44.0, 30.9, 29.7, 27.2 (2C), 25.9 (3C), 15.6, 7.2 (2C), -5.4 (2C);

HRMS calculated for $C_{21}H_{33}F_2NO_3SSiH$ ($M+H$)⁺ 446.1997; found 446.1974 (TOFMS ESI⁺).

2-cyclopropyl-10-fluoro-3,5-dihydro-2*H*-spiro[benzo[*b*][1,4,5]oxathiazocine-4,1'-cyclo-butane] 1,1-dioxide (2.11.7)



According to general procedure **H**, **2.11.7** (5 mg, 44%) was isolated as colorless oil.

FTIR (thin film) 2930, 1601, 1572, 1456, 1339, 1150, 810, 742 cm^{-1} ;

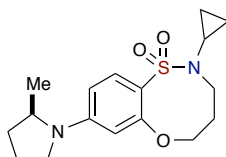
¹H NMR (500 MHz, CDCl₃) δ ppm 7.40 (ddd, $J = 8.3, 8.2, 6.0$ Hz, 1H, aromatic), 7.02–6.96 (m, 1H, aromatic), 6.94 (ddd, $J = 8.2, 1.1, 1.0$ Hz, 1H, aromatic), 4.24 (s, 2H, OCH₂), 3.75 (s, 2H, NCH₂), 2.69–2.60 (m, 1H, NCH), 2.12–1.89 (m, 6H, C(CH₂)₃), 1.06 (s, 2H, NCHCH₂CH₂), 0.78 (dd, $J = 6.8, 1.5$ Hz, 2H, NCHCH₂CH₂);

¹³C NMR (126 MHz, CDCl₃) δ ppm 161.0 (d, $^1J_{C-F} = 257.9$ Hz), 156.8 (d, $^4J_{C-F} = 2.6$ Hz), 133.2 (d, $^3J_{C-F} = 10.9$ Hz), 124.3 (d, $^2J_{C-F} = 13.8$ Hz), 119.3 (d, $^3J_{C-F} = 3.6$ Hz), 113.3 (d, $^2J_{C-F} = 23.1$ Hz), 81.8, 58.1, 41.3, 28.8 (2C), 28.7, 15.9, 9.0 (2C);

HRMS calculated for $C_{15}H_{18}FNO_3SH$ ($M+H$)⁺ 312.1070; found 312.1073 (TOF MS ES⁺).

General procedure I: Microwave-assisted S_NAr diversification of Benzoxathiazocine-1,1-dioxides 2.9.3–2.9.6, 2.10.12–2.10.13, 2.10.15–2.10.16 cores. Into a 1-dram vial was added benzoxathiazocine-1,1-dioxide **2.9.3–2.9.6, 2.10.12–2.10.13, 2.10.15–2.10.16** (1 equiv., 80 mg), dry DMSO (0.5 M) and the corresponding amine (5 equiv.). The reaction vessel was capped, placed in Anton Paar Synthos 3000 ® microwave and heated at 180 °C for 50 min [Power = 1200 W, 8 min ramp then 50 min hold]. After such time, the reaction was diluted with 10% MeOH on CH₂Cl₂, filtered through a SiO₂ SPE and concentrated. The crude reaction was concentrated and QC/purified by an automated preparative reverse phase HPLC (detected by mass spectroscopy).

(R)-2-cyclopropyl-8-(2-methylpyrrolidin-1-yl)-2,3,4,5-tetrahydrobenzo[*b*][1,4,5]oxathiazocine 1,1-dioxide (2.10.12{1})



According to general procedure I, **2.10.12{1}** was isolated (79.8 mg, 80%) as a yellow solid;

mp 92.5 °C;

$[\alpha]_D^{20} = -66.0$ ($c = 0.106$, CH₂Cl₂);

FTIR (thin film) 2964, 2930, 1595, 1497, 1464, 1383, 1335, 1202, 1150, 1049 cm⁻¹;

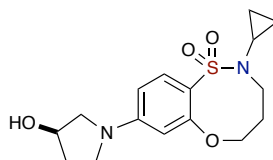
¹H NMR (500 MHz, DMSO) δ ppm 7.51 (d, $J = 8.8$ Hz, 1H), 6.47–6.34 (m, 2H), 4.27–4.16 (m, 2H), 3.98–3.90 (m, 1H), 3.54 (td, $J = 5.8, 2.7$ Hz, 2H), 3.40 (dd, $J = 6.0, 3.8$ Hz,

1H), 3.15 (dd, $J = 17.7, 8.2$ Hz, 1H), 2.10–1.92 (m, 3H), 1.85 (tt, $J = 6.9, 3.6$ Hz, 1H), 1.74–1.66 (m, 3H), 1.10 (d, $J = 6.2$ Hz, 3H), 0.74–0.66 (m, 2H), 0.64–0.56 (m, 2H);

^{13}C NMR (126 MHz, DMSO) δ ppm 157.5, 151.1, 131.1, 117.3, 106.5, 105.4, 74.6, 53.3, 47.6, 46.6, 32.3, 27.6, 22.9, 22.5, 18.4, 7.7, 7.4;

HRMS calculated for $\text{C}_{17}\text{H}_{25}\text{N}_2\text{O}_3\text{S}$ ($\text{M}+\text{H}$) $^+$ 337.1586; found 337.1580 (TOF MS ES $^+$).

(R)-2-cyclopropyl-8-(3-hydroxypyrrolidin-1-yl)-2,3,4,5-tetrahydrobenzo[b][1,4,5]-oxathiazocine 1,1-dioxide (2.10.12{3})



According to general procedure I, **2.10.12{3}** was isolated (75.8 mg, 76%) as yellow oil;

$[\alpha]_D^{20} = +9.88$ ($c = 0.162$, CH_2Cl_2);

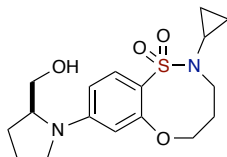
FTIR (neat) 3404, 3394, 2937, 2918, 1597, 1502, 1331, 1254, 1148, 1026 cm^{-1} ;

^1H NMR (500 MHz, DMSO) δ ppm 7.52 (d, $J = 8.8$ Hz, 1H), 6.43 (d, $J = 2.3$ Hz, 1H), 6.35 (dd, $J = 8.8, 2.3$ Hz, 1H), 5.03 (d, $J = 3.7$ Hz, 1H), 4.40 (s, 1H), 4.24 (t, $J = 6.1$ Hz, 2H), 3.57–3.51 (m, 2H), 3.43 (dd, $J = 10.7, 4.6$ Hz, 1H), 3.37 (dd, $J = 9.6, 2.7$ Hz, 2H), 3.14 (d, $J = 10.7$ Hz, 1H), 2.03 (dtd, $J = 13.2, 8.8, 4.6$ Hz, 1H), 1.94–1.87 (m, 1H), 1.82 (dt, $J = 10.4, 3.5$ Hz, 1H), 1.73–1.67 (m, 2H), 0.72–0.68 (m, 2H), 0.61 (dd, $J = 6.7, 2.0$ Hz, 2H);

^{13}C NMR (126 MHz, DMSO) δ ppm 157.4, 151.9, 131.1, 117.5, 106.2, 105.2, 74.5, 69.0, 55.9, 46.7, 45.5, 33.5, 27.6, 22.8, 7.6, 7.5;

HRMS calculated for $\text{C}_{16}\text{H}_{23}\text{N}_2\text{O}_4\text{S}$ ($\text{M}+\text{H}$) $^+$ 339.1379; found 339.1339 (TOF MS ES $^+$).

(S)-2-cyclopropyl-8-(2-(hydroxymethyl)pyrrolidin-1-yl)-2,3,4,5-tetrahydrobenzo[*b*]-[1,4,5]oxathiazocine 1,1-dioxide (2.10.12{5})



According to general procedure I, **2.10.12{5}** was isolated (85.7 mg, 83%) as dark yellow oil;

$[\alpha]_D^{20} = -66.4$ ($c = 0.128$, CH_2Cl_2);

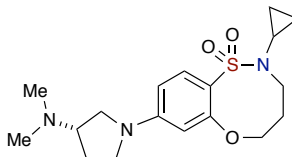
FTIR (neat) 3381, 2918, 1595, 1498, 1331, 1153, 1045, 1026 cm^{-1} ;

^1H NMR (500 MHz, DMSO) δ ppm 7.51 (d, $J = 8.8$ Hz, 1H), 6.51 (d, $J = 2.2$ Hz, 1H), 6.44 (dd, $J = 8.9, 2.3$ Hz, 1H), 4.83 (dd, $J = 6.4, 5.3$ Hz, 1H), 4.23 (t, $J = 6.1$ Hz, 2H), 3.77 (td, $J = 7.8, 3.6$ Hz, 1H), 3.54 (qt, $J = 11.7, 5.9$ Hz, 2H), 3.48–3.42 (m, 1H), 3.39 (t, $J = 7.7$ Hz, 1H), 3.22 (ddd, $J = 10.9, 8.1, 6.7$ Hz, 1H), 3.11 (td, $J = 9.7, 7.3$ Hz, 1H), 2.02–1.83 (m, 5H), 1.75–1.67 (m, 2H), 0.74–0.66 (m, 2H), 0.65–0.57 (m, 2H);

^{13}C NMR (126 MHz, DMSO) δ ppm 157.4, 151.8, 131.0, 117.8, 106.6, 105.7, 74.6, 60.6, 60.1, 48.1, 46.6, 27.8, 27.6, 22.9, 22.5, 7.7, 7.4;

HRMS calculated for $\text{C}_{17}\text{H}_{25}\text{N}_2\text{O}_4\text{S}$ ($\text{M}+\text{H}^+$) 353.1535; found 353.1510 (TOF MS ES^+).

(S)-2-cyclopropyl-8-(3-(dimethylamino)pyrrolidin-1-yl)-2,3,4,5-tetrahydrobenzo[*b*]-[1,4,5]oxathiazocine 1,1-dioxide (2.10.12{8})



According to general procedure I, **2.10.12**{8} was isolated (49.2 mg, 46%) as a light brown solid;

mp 170.5 °C;

$[\alpha]_D^{20} = -32.9$ ($c = 0.140$, CH₂Cl₂);

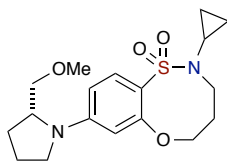
FTIR (thin film) 2947, 2866, 1597, 1501, 1437, 1387, 1333, 1194, 1150, 1074 cm⁻¹;

¹H NMR (500 MHz, DMSO) δ ppm 7.52 (d, $J = 8.8$ Hz, 1H), 6.47 (d, $J = 2.3$ Hz, 1H), 6.37 (dd, $J = 8.9, 2.3$ Hz, 1H), 4.24 (td, $J = 6.1, 1.6$ Hz, 2H), 3.56–3.48 (m, 3H), 3.46–3.41 (m, 1H), 3.27 (td, $J = 10.0, 6.9$ Hz, 1H), 3.08–3.03 (m, 1H), 2.77 (dt, $J = 15.1, 7.5$ Hz, 1H), 2.20 (s, 6H), 2.16 (dd, $J = 11.9, 6.4$ Hz, 1H), 1.81 (ddd, $J = 18.6, 9.2, 6.2$ Hz, 2H), 1.71 (ddd, $J = 9.8, 6.0, 4.0$ Hz, 2H), 0.74–0.66 (m, 2H), 0.61 (d, $J = 6.5$ Hz, 2H);

¹³C NMR (126 MHz, DMSO) δ ppm 157.4, 151.7, 131.0, 117.7, 106.1, 105.3, 74.5, 64.8, 51.9, 46.7, 46.7, 43.9, 40.4, 29.5, 27.6, 22.8, 7.7, 7.4;

HRMS calculated for C₁₈H₂₈N₃O₃S (M+H)⁺ 366.1851; found 366.1826 (TOF MS ES⁺).

(R)-2-cyclopropyl-8-(2-(methoxymethyl)pyrrolidin-1-yl)-2,3,4,5-tetrahydrobenzo[*b*]-[1,4,5]oxathiazocine 1,1-dioxide (2.10.12{10})



According to general procedure I, **2.10.12**{10} was isolated (83.7 mg, 78%) as dark yellow oil;

$[\alpha]_D^{20} = +91.9$ ($c = 0.124$, CH₂Cl₂);

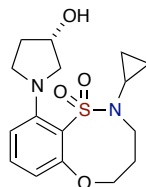
FTIR (neat) 2968, 2922, 2878, 1595, 1498, 1435, 1377, 1333, 1177, 1151, 1024 cm⁻¹;

¹H NMR (500 MHz, DMSO) δ ppm 7.52 (d, *J* = 8.8 Hz, 1H), 6.50 (d, *J* = 2.3 Hz, 1H), 6.45 (dd, *J* = 8.9, 2.3 Hz, 1H), 4.23 (td, *J* = 6.2, 2.7 Hz, 2H), 3.98–3.92 (m, 1H), 3.55 (td, *J* = 7.9, 2.8 Hz, 2H), 3.38 (ddd, *J* = 13.7, 13.1, 6.3 Hz, 2H), 3.28–3.24 (m, 4H), 3.13 (dt, *J* = 13.0, 4.8 Hz, 1H), 2.08–1.98 (m, 1H), 1.97–1.90 (m, 3H), 1.88–1.84 (m, 1H), 1.72 (dd, *J* = 9.4, 4.4 Hz, 2H), 0.71 (dd, *J* = 5.8, 2.7 Hz, 2H), 0.62 (dd, *J* = 6.8, 2.4 Hz, 2H);

¹³C NMR (126 MHz, DMSO) δ ppm 157.4, 151.7, 131.0, 118.1, 106.7, 105.9, 74.6, 72.0, 58.5, 57.5, 48.1, 46.6, 28.3, 27.6, 22.9, 22.6, 7.8, 7.4;

HRMS calculated for C₁₈H₂₇N₂O₄S (M+H)⁺ 367.1692; found 367.1680 (TOF MS ES⁺).

(S)-2-cyclopropyl-10-(3-hydroxypyrrolidin-1-yl)-2,3,4,5-tetrahydrobenzo[*b*][1,4,5]-oxathiazocine 1,1-dioxide (2.10.13{4})



According to general procedure I, **2.10.13{4}** was isolated (61.0 mg, 61%) as dark brown oil;

$[\alpha]_D^{20} = +266.8$ (*c* = 0.196, CH₂Cl₂);

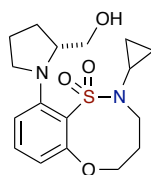
FTIR (neat) 3385, 2943, 2918, 1589, 1549, 1323, 1236, 1151, 1028 cm⁻¹;

¹H NMR (400 MHz, DMSO) δ ppm 7.22 (dd, *J* = 8.5, 8.0 Hz, 1H), 6.58 (dd, *J* = 10.2, 8.3 Hz, 2H), 4.86 (s, 1H), 4.36 (t, *J* = 6.8 Hz, 2H), 4.25 (d, *J* = 2.7 Hz, 1H), 3.72 (s, 2H), 3.49 (d, *J* = 7.0 Hz, 1H), 3.35 (s, 1H), 3.29 (d, *J* = 4.3 Hz, 1H), 3.05 (d, *J* = 10.9 Hz, 1H), 1.95 (ddd, *J* = 12.5, 11.4, 6.9 Hz, 2H), 1.81 (d, *J* = 2.8 Hz, 2H), 1.55 (d, *J* = 3.5 Hz, 1H), 0.73 (s, 1H), 0.52 (ddt, *J* = 14.0, 11.4, 5.8 Hz, 3H);

^{13}C NMR (126 MHz, DMSO) δ ppm 159.6, 151.6, 132.0, 115.5, 109.2, 105.2, 70.1, 68.9, 62.0, 54.9, 49.2, 45.8, 33.2, 27.2, 23.1, 5.8;

HRMS calculated for $\text{C}_{16}\text{H}_{23}\text{N}_2\text{O}_4\text{S}$ ($\text{M}+\text{H}$) $^+$ 339.1379; found 339.1356 (TOF MS ES $^+$).

(R)-2-cyclopropyl-10-(2-(hydroxymethyl)pyrrolidin-1-yl)-2,3,4,5-tetrahydrobenzo-[b][1,4,5]oxathiazocine 1,1-dioxide (2.10.13{6})



According to general procedure I, **2.10.13{6}** was isolated (67.7 mg, 65%) as brown oil;

$[\alpha]_D^{20} = +76.0$ ($c = 0.550$, CH_2Cl_2);

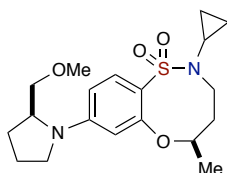
FTIR (neat) 3474, 2945, 2872, 1585, 1474, 1458, 1327, 1237, 1151, 1059 cm^{-1} ;

^1H NMR (500 MHz, DMSO) δ ppm 7.32 (t, $J = 8.2$ Hz, 1H), 6.96 (d, $J = 8.4$ Hz, 1H), 6.77 (d, $J = 7.8$ Hz, 1H), 4.42–4.34 (m, 1H), 4.33–4.24 (m, 1H), 4.14 (dd, $J = 6.9, 4.8$ Hz, 1H), 3.91 (d, $J = 3.5$ Hz, 1H), 3.87–3.76 (m, 2H), 3.43 (ddd, $J = 10.3, 7.0, 3.1$ Hz, 1H), 3.32–3.25 (m, 2H), 2.92–2.87 (m, 1H), 2.13–1.98 (m, 2H), 1.84–1.63 (m, 5H), 0.86–0.78 (m, 1H), 0.58–0.48 (m, 3H);

^{13}C NMR (126 MHz, DMSO) δ ppm 158.4, 151.0, 132.5, 113.7, 110.1, 71.3, 62.4, 60.7, 56.9, 46.7, 28.7, 27.6, 24.6, 23.0, 9.7, 5.1;

HRMS calculated for $\text{C}_{17}\text{H}_{25}\text{N}_2\text{O}_4\text{S}$ ($\text{M}+\text{H}$) $^+$ 353.1530; found 353.1519 (TOF MS ES $^+$).

(R)-2-cyclopropyl-8-((S)-2-(methoxymethyl)pyrrolidin-1-yl)-5-methyl-2,3,4,5-tetrahydrobenzo[*b*][1,4,5]oxathiazocine 1,1-dioxide (2.10.15{9})



According to general procedure I, **2.10.15{9}** was isolated (67.4 mg, 63%) as dark yellow oil;

$[\alpha]_D^{20} = -33.0$ ($c = 0.224$, CH_2Cl_2);

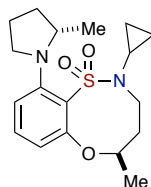
FTIR (neat) 2974, 2930, 2878, 1595, 1489, 1435, 1375, 1329, 1209, 1155, 1074 cm^{-1} ;

^1H NMR (400 MHz, DMSO) δ ppm 7.52 (d, $J = 9.0$ Hz, 1H), 6.49–6.42 (m, 2H), 4.28 (m, 1H), 3.98–3.86 (m, 2H), 3.43–3.31 (m, 4H), 3.31–3.27 (m, 1H), 3.27–3.19 (m, 2H), 3.18–3.10 (m, 1H), 2.06–1.89 (m, 6H), 1.55–1.46 (m, 1H), 1.37 (d, $J = 6.4$ Hz, 3H), 0.91–0.82 (m, 1H), 0.75–0.66 (m, 1H), 0.64–0.49 (m, 2H);

^{13}C NMR (126 MHz, DMSO) δ ppm 157.5, 151.5, 130.9, 118.3, 106.8, 106.3, 81.1, 72.2, 58.5, 57.6, 48.1, 43.9, 29.6, 28.3, 27.3, 22.7, 20.9, 9.8, 5.0;

HRMS calculated for $\text{C}_{19}\text{H}_{29}\text{N}_2\text{O}_4\text{S}$ ($\text{M}+\text{H}$) $^+$ 381.1848; found 381.1831 (TOF MS ES^+).

(R)-2-cyclopropyl-5-methyl-10-((S)-2-methylpyrrolidin-1-yl)-2,3,4,5-tetrahydrobenzo[*b*][1,4,5]oxathiazocine 1,1-dioxide (2.10.16{2})



According to general procedure I, **2.10.16**{2} was isolated (33.9 mg, 35%) as a dark yellow solid;

mp 111.5 °C;

$[\alpha]_D^{20} = -29.4$ ($c = 0.330$, CH_2Cl_2);

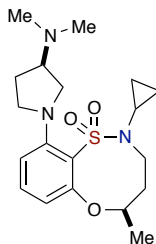
FTIR (thin film) 2968, 2918, 1572, 1454, 1441, 1377, 1319, 1236, 1140, 1055 cm^{-1} ;

^1H NMR (500 MHz, DMSO) δ ppm 7.34 (t, $J = 8.1$ Hz, 1H), 7.03 (d, $J = 8.2$ Hz, 1H), 6.68 (d, $J = 7.7$ Hz, 1H), 4.07 (s, 1H), 3.75 (dd, $J = 16.0, 7.2$ Hz, 3H), 3.50 (d, $J = 14.8$ Hz, 1H), 2.89 (td, $J = 8.5, 4.9$ Hz, 1H), 2.61–2.55 (m, 1H), 2.11–2.04 (m, 1H), 1.93 (dtd, $J = 14.3, 9.6, 4.6$ Hz, 1H), 1.85–1.72 (m, 2H), 1.68 (ddd, $J = 16.5, 8.2, 3.9$ Hz, 1H), 1.47 (dq, $J = 11.8, 8.7$ Hz, 1H), 1.31 (d, $J = 6.2$ Hz, 3H), 0.99 (d, $J = 6.0$ Hz, 3H), 0.92 (d, $J = 9.2$ Hz, 1H), 0.72–0.61 (m, 3H);

^{13}C NMR (126 MHz, DMSO) δ ppm 151.1, 132.6, 117.7, 116.3, 82.4, 56.2, 55.7, 54.9, 46.6, 33.1, 31.6, 27.7, 23.5, 21.2, 18.7, 9.1, 6.2;

HRMS calculated for $\text{C}_{18}\text{H}_{27}\text{N}_2\text{O}_3\text{S}$ ($\text{M}+\text{H}$)⁺ 351.1742; found 351.1700 (TOF MS ES⁺).

(R)-2-cyclopropyl-10-((R)-3-(dimethylamino)pyrrolidin-1-yl)-5-methyl-2,3,4,5-tetrahydrobenzo[b][1,4,5]oxathiazocine 1,1-dioxide (2.10.16{7})



According to general procedure I, **2.10.16**{7} was isolated (37.9 mg, 36%) as a brown solid;

mp 91.5 °C;

$[\alpha]_D^{20} = -158.6$ ($c = 0.140$, CH_2Cl_2);

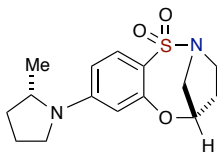
FTIR (thin film) 2972, 2932, 2824, 1583, 1460, 1377, 1323, 1221, 1155, 1103 cm^{-1} ;

^1H NMR (400 MHz, DMSO) δ ppm 7.27–7.21 (m, 1H), 6.71 (d, $J = 8.1$ Hz, 1H), 6.54 (d, $J = 7.2$ Hz, 1H), 4.44–4.35 (m, 1H), 3.71 (s, 1H), 3.56 (dd, $J = 10.4, 6.3$ Hz, 2H), 3.42 (dd, $J = 10.8, 4.7$ Hz, 1H), 3.30 (dd, $J = 9.7, 7.1$ Hz, 1H), 3.21 (dd, $J = 10.4, 5.7$ Hz, 1H), 2.70 (m, 1H), 2.12 (s, 6H), 1.97 (td, $J = 12.6, 6.5$ Hz, 3H), 1.83 (td, $J = 13.7, 7.0$ Hz, 1H), 1.71 (d, $J = 6.9$ Hz, 1H), 1.35 (d, $J = 6.2$ Hz, 3H), 0.72 (s, 2H), 0.56 (td, $J = 6.7, 2.0$ Hz, 2H);

^{13}C NMR (126 MHz, DMSO) δ ppm 158.3, 150.9, 132.4, 119.2, 111.7, 109.4, 79.4, 64.7, 57.2, 54.9, 50.8, 45.4, 43.4, 31.1, 28.9, 27.2, 22.1, 8.2, 6.6;

HRMS calculated for $\text{C}_{19}\text{H}_{30}\text{N}_3\text{O}_3\text{S}$ ($\text{M}+\text{H}^+$) 380.2008; found 380.1976 (TOF MS ES^+).

(5*S*)-8-((*S*)-2-methylpyrrolidin-1-yl)-4,5-dihydro-3*H*-2,5-methanobenzo[*b*][1,4,5]oxathiazocine 1,1-dioxide (2.9.3{2})



According to general procedure I, **2.9.3{2}** was isolated (73.4 mg, 72%) as a pale yellow solid;

mp 143.0 °C;

$[\alpha]_D^{20} = +72.3$ ($c = 0.260$, CH_2Cl_2);

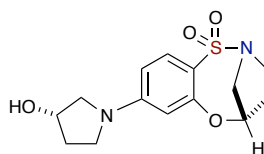
FTIR (thin film) 2964, 2918, 2868, 2847, 1599, 1434, 1327, 1142, 1107 cm^{-1} ;

¹H NMR (400 MHz, DMSO) δ ppm 7.46 (d, *J* = 8.9 Hz, 1H), 6.40 (dd, *J* = 8.9, 2.4 Hz, 1H), 6.12 (d, *J* = 2.4 Hz, 1H), 5.05 (dd, *J* = 6.4, 2.7 Hz, 1H), 4.01–3.89 (m, 2H), 3.38 (t, *J* = 8.8 Hz, 1H), 3.27 (dd, *J* = 8.3, 3.5 Hz, 1H), 3.20–3.08 (m, 3H), 2.05–1.92 (m, 4H), 1.76 (dt, *J* = 15.4, 7.8 Hz, 1H), 1.70–1.62 (m, 1H), 1.08 (d, *J* = 6.2 Hz, 3H);

¹³C NMR (126 MHz, DMSO) δ ppm 152.1, 150.9, 130.8, 116.1, 107.1, 105.4, 80.0, 56.7, 53.3, 47.6, 47.0, 32.3, 28.2, 22.5, 18.4;

HRMS calculated for C₁₅H₂₁N₂O₃S (M+H)⁺ 309.1273; found 309.1243 (TOF MS ES⁺).

(5*S*)-8-((*S*)-3-hydroxypyrrolidin-1-yl)-4,5-dihydro-3*H*-2,5-methanobenzo[*b*][1,4,5]-oxathiazocine 1,1-dioxide (2.9.3{4})



According to general procedure I, **2.9.3{4}** was isolated (76.7 mg, 75%) as a pale yellow solid;

mp 208.0 °C;

[α]_D²⁰ = +63.1 (*c* = 0.160, CH₂Cl₂);

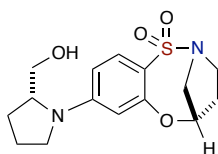
FTIR (thin film) 3406, 3009, 2945, 2920, 1601, 1504, 1437, 1321, 1140, 1107 cm⁻¹;

¹H NMR (400 MHz, DMSO) δ ppm 7.47 (d, *J* = 8.9 Hz, 1H), 6.37 (dd, *J* = 8.9, 2.4 Hz, 1H), 6.09 (d, *J* = 2.3 Hz, 1H), 5.05 (dd, *J* = 6.4, 2.7 Hz, 1H), 5.01 (d, *J* = 3.6 Hz, 1H), 4.39 (s, 1H), 3.99 (d, *J* = 13.9 Hz, 1H), 3.41 (dd, *J* = 10.8, 4.6 Hz, 1H), 3.36 (d, *J* = 6.9 Hz, 1H), 3.32–3.22 (m, 2H), 3.20–3.06 (m, 3H), 2.06–1.94 (m, 2H), 1.93–1.85 (m, 1H), 1.76 (dt, *J* = 15.3, 6.8 Hz, 1H);

^{13}C NMR (126 MHz, DMSO) δ ppm 152.1, 151.7, 130.8, 116.3, 106.8, 105.2, 80.0, 69.0, 56.7, 55.9, 47.0, 45.5, 33.4, 28.1;

HRMS calculated for $\text{C}_{14}\text{H}_{19}\text{N}_2\text{O}_4\text{S}$ ($\text{M}+\text{H}$) $^+$ 311.1066; found 311.1032 (TOF MS ES^+).

(5*S*)-8-((*R*)-2-(hydroxymethyl)pyrrolidin-1-yl)-4,5-dihydro-3*H*-2,5-methanobenzo-*b*][1,4,5]oxathiazocine 1,1-dioxide (2.9.3{6})



According to general procedure I, **2.9.3{6}** was isolated (90.2 mg, 85%) as brown oil;

$[\alpha]_D^{20} = +105.5$ ($c = 0.254$, CH_2Cl_2);

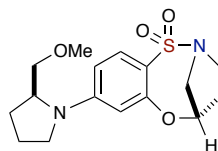
FTIR (neat) 3420, 2972, 2878, 1599, 1497, 1437, 1323, 1140, 1107 cm^{-1} ;

^1H NMR (400 MHz, DMSO) δ ppm 7.46 (d, $J = 8.9$ Hz, 1H), 6.45 (dd, $J = 8.9, 2.3$ Hz, 1H), 6.20 (d, $J = 2.2$ Hz, 1H), 5.05 (dd, $J = 6.4, 2.6$ Hz, 1H), 4.83 (t, $J = 5.8$ Hz, 1H), 3.99 (d, $J = 13.9$ Hz, 1H), 3.74 (td, $J = 7.8, 3.6$ Hz, 1H), 3.41 (ddd, $J = 11.7, 9.4, 4.6$ Hz, 2H), 3.29–3.05 (m, 5H), 2.05–1.95 (m, 3H), 1.94–1.82 (m, 2H), 1.77 (dt, $J = 13.4, 6.8$ Hz, 1H);

^{13}C NMR (126 MHz, DMSO) δ ppm 152.1, 151.6, 130.7, 116.5, 107.3, 105.6, 80.0, 60.5, 60.1, 56.7, 48.1, 47.0, 28.2, 27.7, 22.5;

HRMS calculated for $\text{C}_{15}\text{H}_{21}\text{N}_2\text{O}_4\text{S}$ ($\text{M}+\text{H}$) $^+$ 325.1222; found 325.1183 (TOF MS ES^+).

(5*S*)-8-((*S*)-2-(methoxymethyl)pyrrolidin-1-yl)-4,5-dihydro-3*H*-2,5-methanobenzo-*[b]*[1,4,5]oxathiazocine 1,1-dioxide (2.9.3{9})



According to general procedure I, **2.9.3{9}** was isolated (84.7 mg, 76%) as a light brown solid;

mp 152.0 °C;

$[\alpha]_D^{20} = -36.1$ ($c = 0.180$, CH₂Cl₂);

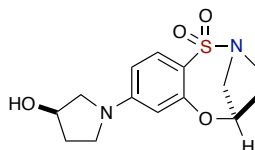
FTIR (thin film) 2972, 2953, 2928, 1597, 1495, 1435, 1381, 1327, 1142, 1107 cm⁻¹;

¹H NMR (500 MHz, DMSO) δ ppm 7.47 (d, $J = 8.9$ Hz, 1H), 6.48 (dd, $J = 8.9, 2.3$ Hz, 1H), 6.17 (d, $J = 2.3$ Hz, 1H), 5.06 (dd, $J = 6.4, 2.6$ Hz, 1H), 4.07–3.95 (m, 1H), 3.93 (d, $J = 10.3$ Hz, 1H), 3.44–3.34 (m, 3H), 3.30–3.22 (m, 5H), 3.22–3.06 (m, 3H), 2.05–1.88 (m, 4H), 1.78 (dd, $J = 14.3, 7.6$ Hz, 1H);

¹³C NMR (126 MHz, DMSO) δ ppm 152.6, 152.0, 131.2, 117.3, 107.9, 106.2, 80.5, 72.4, 59.0, 58.1, 57.2, 48.5, 47.5, 28.8, 28.7, 23.1;

HRMS calculated for C₁₆H₂₃N₂O₄S (M+H)⁺ 339.1379; found 339.1345 (TOF MS ES⁺).

(5*R*)-8-((*R*)-3-hydroxypyrrolidin-1-yl)-4,5-dihydro-3*H*-2,5-methanobenzo-*[b]*[1,4,5]-oxathiazocine 1,1-dioxide (2.9.4{3})



According to general procedure I, **2.9.4**{3} was isolated (70.0 mg, 69%) as a light yellow solid;

mp 202.0 °C;

$[\alpha]_D^{20} = -49.2$ ($c = 0.240$, CH₂Cl₂);

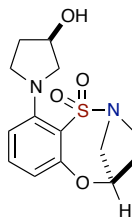
FTIR (thin film) 3394, 2949, 2920, 2858, 1601, 1504, 1437, 1321, 1140, 1107 cm⁻¹;

¹H NMR (400 MHz, DMSO) δ ppm 7.47 (d, $J = 8.8$ Hz, 1H), 6.37 (dd, $J = 8.9, 2.4$ Hz, 1H), 6.09 (d, $J = 2.3$ Hz, 1H), 5.05 (dd, $J = 6.3, 2.6$ Hz, 1H), 5.01 (d, $J = 3.6$ Hz, 1H), 4.39 (s, 1H), 3.99 (d, $J = 13.9$ Hz, 1H), 3.41 (dd, $J = 10.8, 4.6$ Hz, 1H), 3.36 (d, $J = 7.0$ Hz, 1H), 3.27 (ddd, $J = 11.9, 9.8, 4.0$ Hz, 2H), 3.18 (dd, $J = 13.9, 2.7$ Hz, 1H), 3.14–3.06 (m, 2H), 2.06–1.95 (m, 2H), 1.90 (dd, $J = 9.7, 6.2$ Hz, 1H), 1.81–1.71 (m, 1H);

¹³C NMR (126 MHz, DMSO) δ ppm 152.1, 151.7, 130.8, 116.3, 106.8, 105.2, 80.0, 69.0, 56.7, 55.9, 47.0, 45.5, 33.4, 28.1;

HRMS calculated for C₁₄H₁₉N₂O₄S (M+H)⁺ 311.1066; found 311.1014 (TOF MS ES⁺).

(5*R*)-10-((*R*)-3-hydroxypyrrolidin-1-yl)-4,5-dihydro-3*H*-2,5-methanobenzo[*b*][1,4,5]-oxathiazocine 1,1-dioxide (2.9.5{3})



According to general procedure I, **2.9.5**{3} was isolated (49.3 mg, 48%) as dark yellow oil;

$[\alpha]_D^{20} = +183.3$ ($c = 0.084$, CH₂Cl₂);

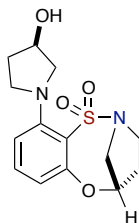
FTIR (neat) 3404, 3394, 2962, 2897, 1585, 1464, 1375, 1327, 1140, 1113 cm^{-1} ;

^1H NMR (500 MHz, DMSO) δ ppm 7.24 (t, $J = 8.2$ Hz, 1H), 6.72 (d, $J = 8.6$ Hz, 1H), 6.37 (d, $J = 7.7$ Hz, 1H), 5.10 (d, $J = 4.7$ Hz, 1H), 4.86 (d, $J = 4.1$ Hz, 1H), 4.22 (dq, $J = 12.4, 6.4$ Hz, 1H), 3.93 (d, $J = 13.2$ Hz, 1H), 3.51 (td, $J = 9.5, 6.7$ Hz, 1H), 3.42–3.35 (m, 2H), 3.31–3.25 (m, 1H), 3.15 (ddd, $J = 15.0, 10.6, 4.5$ Hz, 1H), 3.06 (t, $J = 12.1$ Hz, 2H), 2.10–2.01 (m, 2H), 1.90 (ddd, $J = 14.7, 10.5, 5.9$ Hz, 1H), 1.73 (dq, $J = 11.5, 8.1$ Hz, 1H);

^{13}C NMR (126 MHz, DMSO) δ ppm 153.8, 151.0, 132.0, 119.9, 113.3, 112.2, 79.8, 68.9, 59.8, 56.4, 49.7, 46.4, 33.5, 28.5;

HRMS calculated for $\text{C}_{14}\text{H}_{19}\text{N}_2\text{O}_4\text{S}$ ($\text{M}+\text{H}$) $^+$ 311.1066; found 311.1028 (TOF MS ES^+).

(5*S*)-10-((*R*)-3-hydroxypyrrolidin-1-yl)-4,5-dihydro-3*H*-2,5-methanobenzo[*b*][1,4,5]-oxathiazocine 1,1-dioxide (2.9.6{3})



According to general procedure I, **2.9.6{3}** was isolated (54.1 mg, 53%) as light brown oil;

$[\alpha]_D^{20} = -378.0$ ($c = 2.60$, CH_2Cl_2);

FTIR (neat) 3439, 3418, 1643, 1634, 1589, 1327, 1227, 1138 cm^{-1} ;

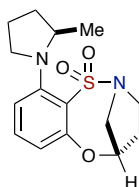
^1H NMR (500 MHz, CDCl_3) δ ppm 7.17 (dd, $J = 8.4, 7.9$ Hz, 1H), 6.71 (dd, $J = 8.6, 1.0$ Hz, 1H), 6.41 (dd, $J = 7.8, 1.0$ Hz, 1H), 4.93 (d, $J = 4.7$ Hz, 1H), 4.47 (s, 1H), 4.37 (d, $J =$

13.2 Hz, 1H), 3.87 (ddd, $J = 14.2, 8.4, 5.4$ Hz, 2H), 3.28–3.13 (m, 4H), 3.05 (dd, $J = 13.2, 1.2$ Hz, 1H), 2.37 (s, 1H), 2.29–2.21 (m, 1H), 2.10–2.00 (m, 2H), 1.93–1.84 (m, 1H);

^{13}C NMR (126 MHz, CDCl_3) δ ppm 154.2, 152.0, 132.0, 121.3, 115.3, 113.3, 80.2, 71.1, 61.7, 58.1, 49.6, 46.6, 33.9, 28.8;

HRMS calculated for $\text{C}_{14}\text{H}_{19}\text{N}_2\text{O}_4\text{S}$ ($\text{M}+\text{H}$) $^+$ 311.1066; found 311.1051 (TOF MS ES^+).

(5*S*)-10-((*R*)-2-methylpyrrolidin-1-yl)-4,5-dihydro-3*H*-2,5-methanobenzo[*b*][1,4,5]-oxathiazocine 1,1-dioxide (2.9.6{1})



According to general procedure I, **2.9.6{1}** was isolated (70.8 mg, 70%) as a pale yellow solid;

mp 139.0 °C;

$[\alpha]_D^{20} = -359.0$ ($c = 0.286$, CH_2Cl_2);

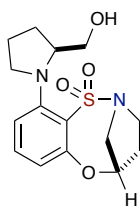
FTIR (thin film) 2964, 2928, 2889, 1583, 1460, 1373, 1333, 1227, 1142, 1115 cm^{-1} ;

^1H NMR (400 MHz, CDCl_3) δ ppm 7.14 (dd, $J = 8.5, 7.8$ Hz, 1H), 6.72 (d, $J = 8.1$ Hz, 1H), 6.36 (dd, $J = 7.7, 1.0$ Hz, 1H), 4.92 (d, $J = 4.7$ Hz, 1H), 4.42 (dd, $J = 13.2, 2.3$ Hz, 1H), 4.03–3.91 (m, 2H), 3.32–3.24 (m, 1H), 3.20–3.11 (m, 2H), 3.04 (dd, $J = 13.2, 1.2$ Hz, 1H), 2.29–2.16 (m, 2H), 1.95–1.81 (m, 2H), 1.72–1.59 (m, 2H), 1.19 (d, $J = 6.0$ Hz, 3H);

^{13}C NMR (126 MHz, CDCl_3) δ ppm 154.5, 151.6, 131.4, 121.8, 114.6, 113.5, 80.1, 58.4, 55.7, 55.3, 46.4, 34.3, 28.7, 25.3, 19.1;

HRMS calculated for $\text{C}_{15}\text{H}_{21}\text{N}_2\text{O}_3\text{S}$ ($\text{M}+\text{H}$) $^+$ 309.1273; found 309.1259 (TOF MS ES^+).

(5*S*)-10-((*S*)-2-(hydroxymethyl)pyrrolidin-1-yl)-4,5-dihydro-3*H*-2,5-methanobenzo-*b*][1,4,5]oxathiazocine 1,1-dioxide (2.9.6{5})



According to general procedure I, **2.9.6{5}** was isolated (72.9 mg, 68%) as a white solid;
mp 149.0 °C;

$[\alpha]_D^{20} = -128.0$ ($c = 0.530$, CH_2Cl_2);

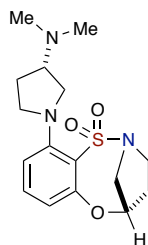
FTIR (thin film) 3472, 2968, 2874, 1582, 1456, 1331, 1142, 1115, 1067 cm^{-1} ;

^1H NMR (400 MHz, CDCl_3) δ ppm 7.21 (t, $J = 8.1$ Hz, 1H), 6.95 (d, $J = 8.1$ Hz, 1H), 6.53 (dd, $J = 7.9, 1.0$ Hz, 1H), 4.97 (dd, $J = 5.1, 1.3$ Hz, 1H), 4.37 (d, $J = 13.5$ Hz, 1H), 4.07 (t, $J = 7.7$ Hz, 1H), 3.98 (td, $J = 9.5, 6.0$ Hz, 1H), 3.77 (dd, $J = 11.3, 2.9$ Hz, 1H), 3.42 (t, $J = 10.0$ Hz, 1H), 3.28–3.14 (m, 4H), 3.10 (dd, $J = 13.5, 1.6$ Hz, 1H), 2.26–2.17 (m, 1H), 2.16–2.07 (m, 1H), 2.03 (ddd, $J = 7.2, 5.6, 2.6$ Hz, 1H), 2.00–1.88 (m, 2H), 1.82–1.70 (m, 1H);

^{13}C NMR (126 MHz, CDCl_3) δ ppm 153.9, 151.6, 132.1, 125.6, 117.7, 115.9, 80.1, 61.3, 60.7, 57.7, 57.3, 46.7, 29.0, 27.4, 25.7;

HRMS calculated for $\text{C}_{15}\text{H}_{21}\text{N}_2\text{O}_4\text{S}$ ($\text{M}+\text{H}$) $^+$ 325.1222; found 325.1194 (TOF MS ES^+).

**(5*S*)-10-((*S*)-3-(dimethylamino)pyrrolidin-1-yl)-4,5-dihydro-3*H*-2,5-methanobenzo-
[*b*][1,4,5]oxathiazocine 1,1-dioxide 2.9.6{8}**



According to general procedure I, **2.9.6{8}** was isolated (86.3 mg, 78%) as dark brown oil;

$[\alpha]_D^{20} = -449.0$ ($c = 0.152$, CH_2Cl_2);

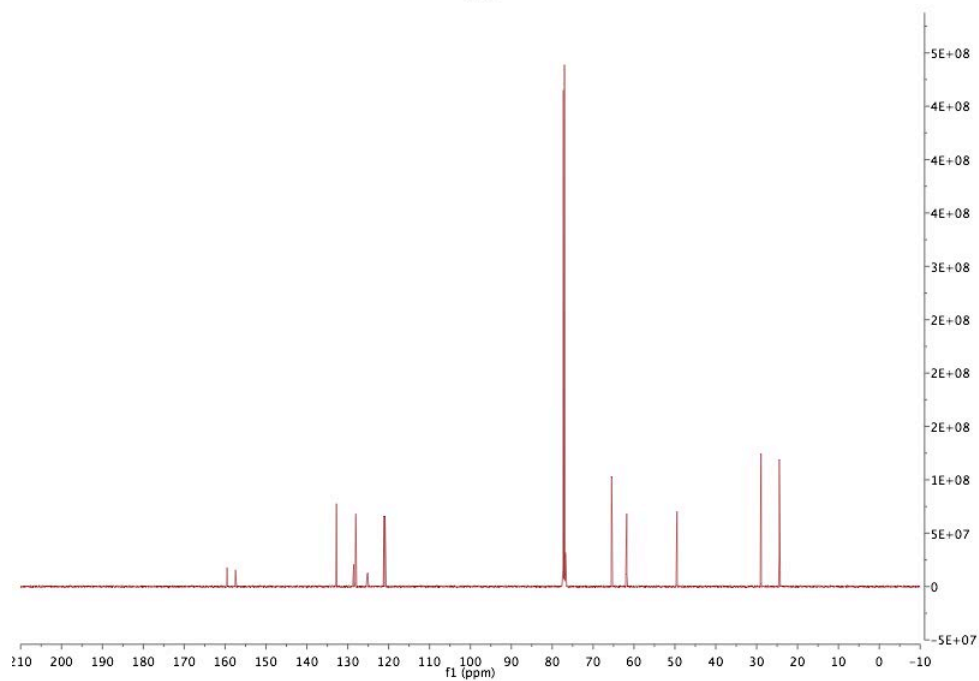
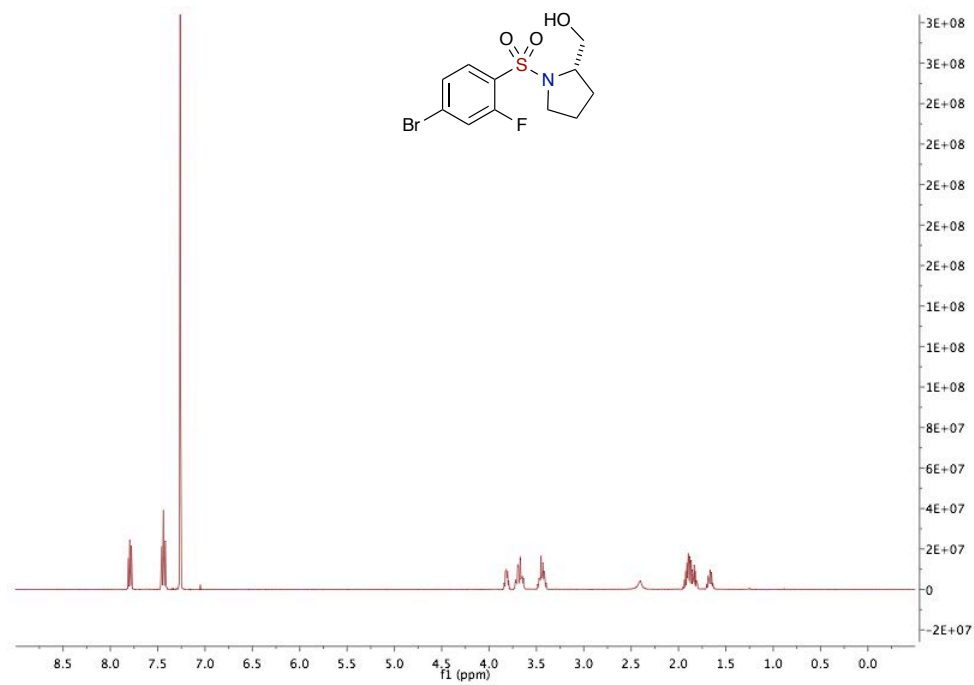
FTIR (neat) 2955, 1637, 1585, 1464, 1375, 1331, 1223, 1142, 1115 cm^{-1} ;

^1H NMR (400 MHz, CDCl_3) δ ppm 7.19–7.09 (m, 1H), 6.66 (d, $J = 8.6$ Hz, 1H), 6.40–6.31 (m, 1H), 4.93 (d, $J = 4.5$ Hz, 1H), 4.41 (d, $J = 13.2$ Hz, 1H), 3.88 (td, $J = 10.8, 6.2$ Hz, 1H), 3.58–3.46 (m, 2H), 3.40 (t, $J = 9.0$ Hz, 1H), 3.16 (dd, $J = 8.8, 6.5$ Hz, 2H), 3.04 (d, $J = 13.1$ Hz, 1H), 2.74 (tt, $J = 10.1, 6.1$ Hz, 1H), 2.31 (s, 6H), 2.28–2.21 (m, 1H), 2.20–2.11 (m, 1H), 1.91–1.72 (m, 2H);

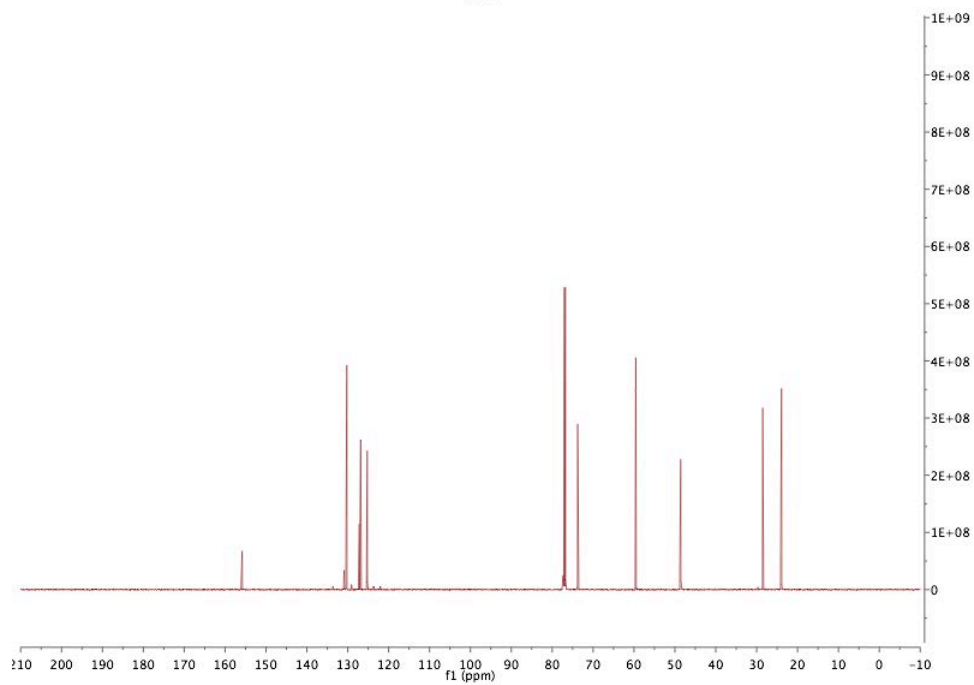
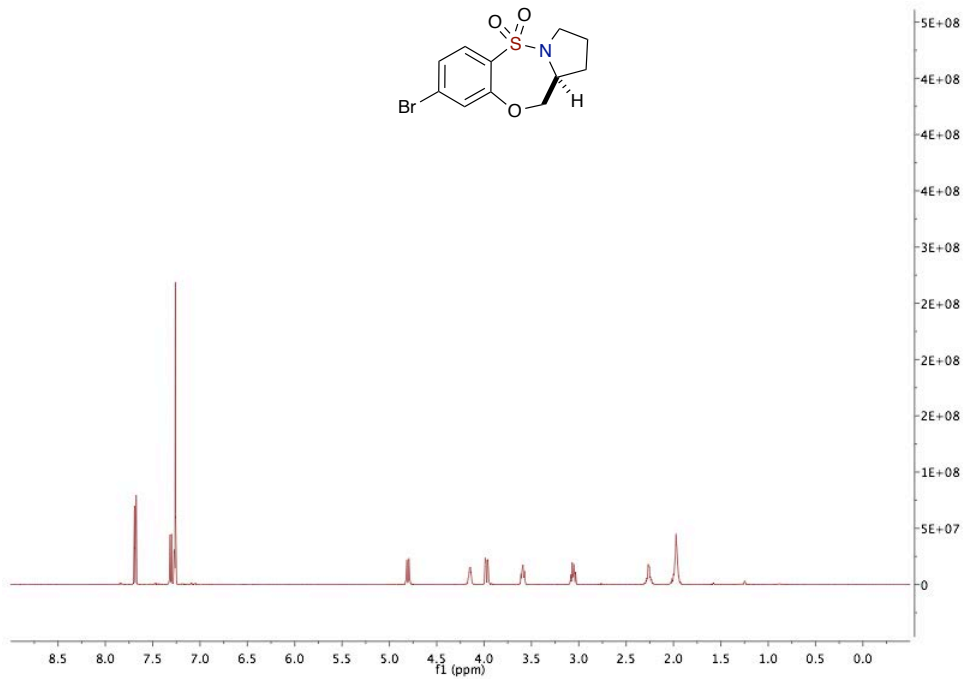
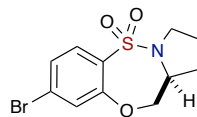
^{13}C NMR (126 MHz, CDCl_3) δ ppm 154.5, 151.9, 131.6, 120.0, 114.4, 112.1, 80.2, 65.5, 58.4, 57.2, 52.3, 46.5, 44.6, 31.0, 29.7, 28.7;

HRMS calculated for $\text{C}_{16}\text{H}_{24}\text{N}_3\text{O}_3\text{S}$ ($\text{M}+\text{H}$)⁺ 338.1538; found 338.1517 (TOF MS ES⁺).

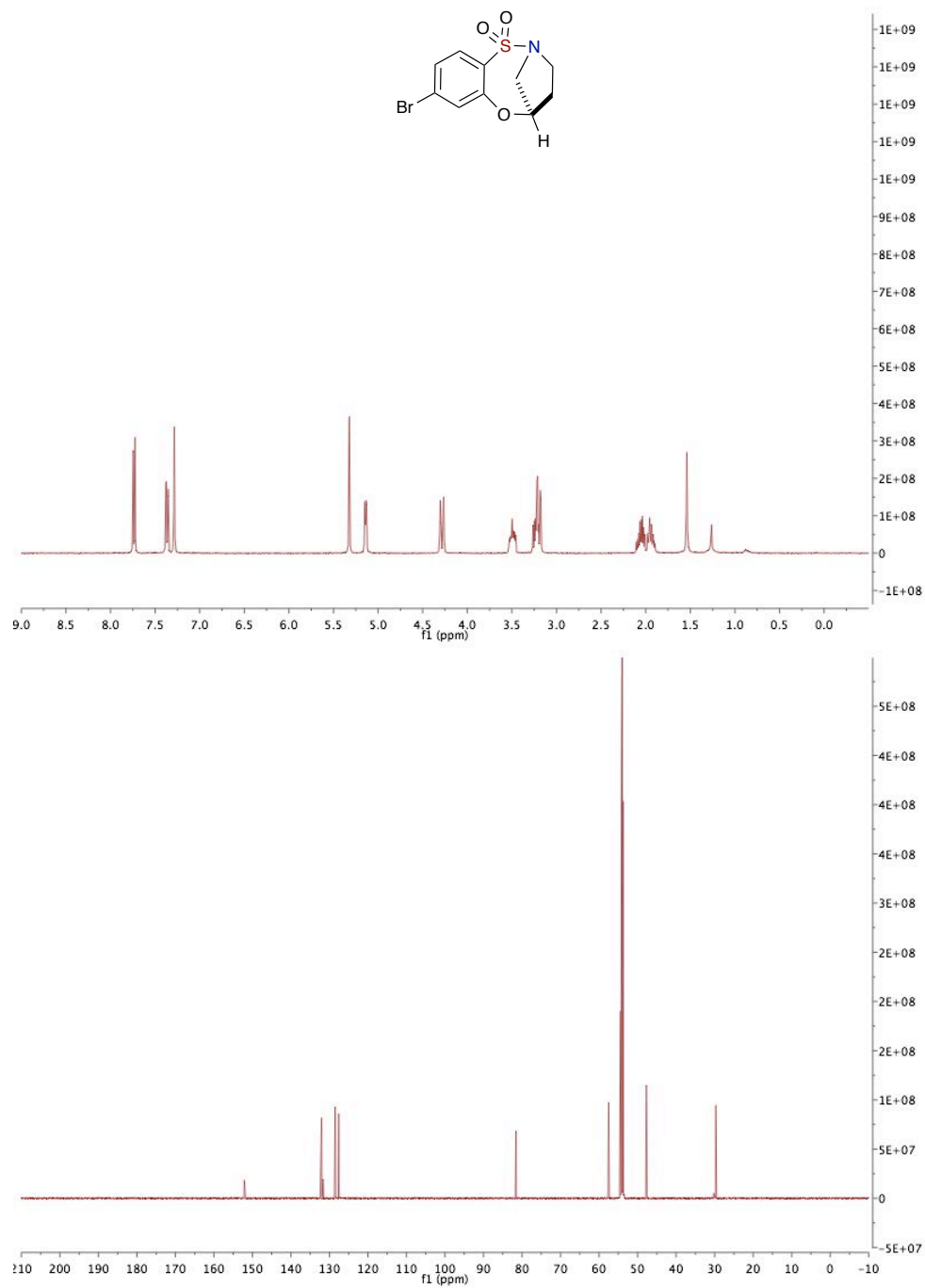
(S)-1-((4-Bromo-2-fluorophenyl)sulfonyl)pyrrolidin-2-yl)methanol (2.7.2)



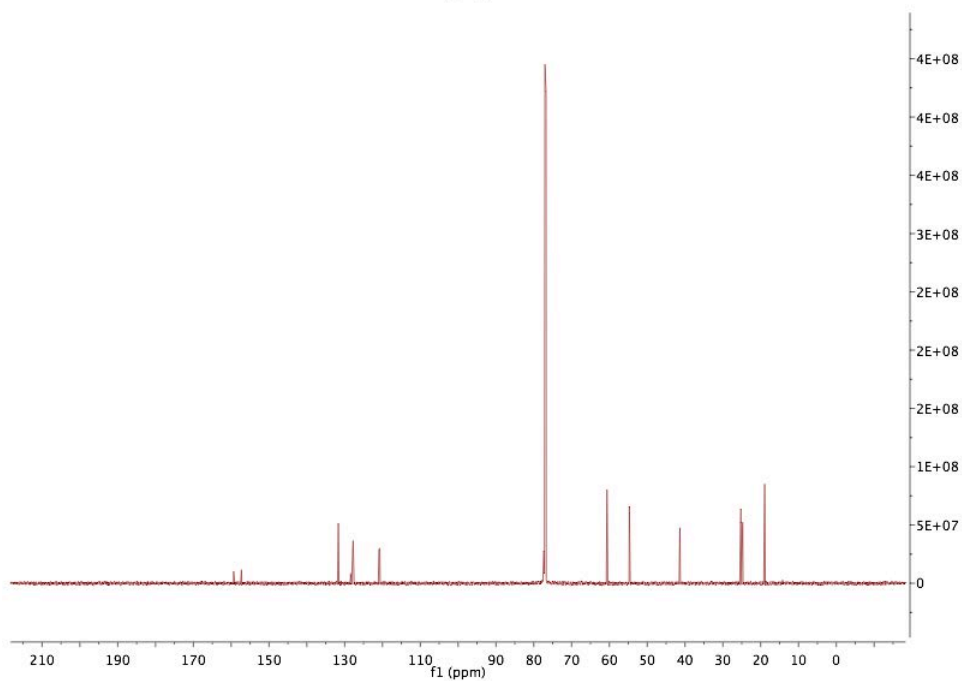
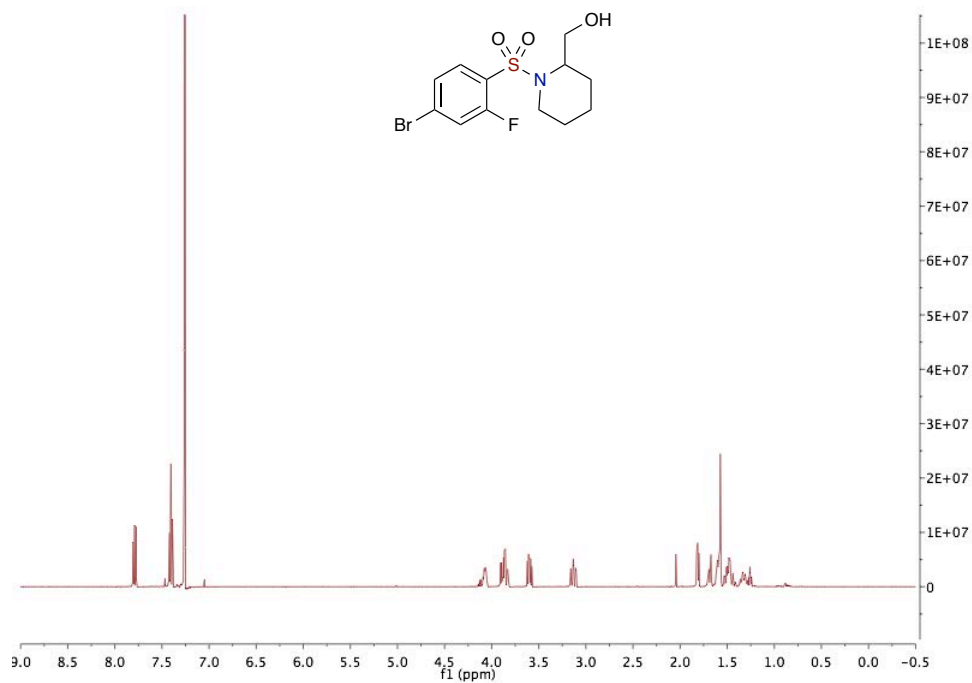
8-Bromo-2,3,11,11a-tetrahydro-1H-benzo[*b*]pyrrolo[1,2-*e*][1,4,5] oxathiazepine 5,5-dioxide (2.7.3)



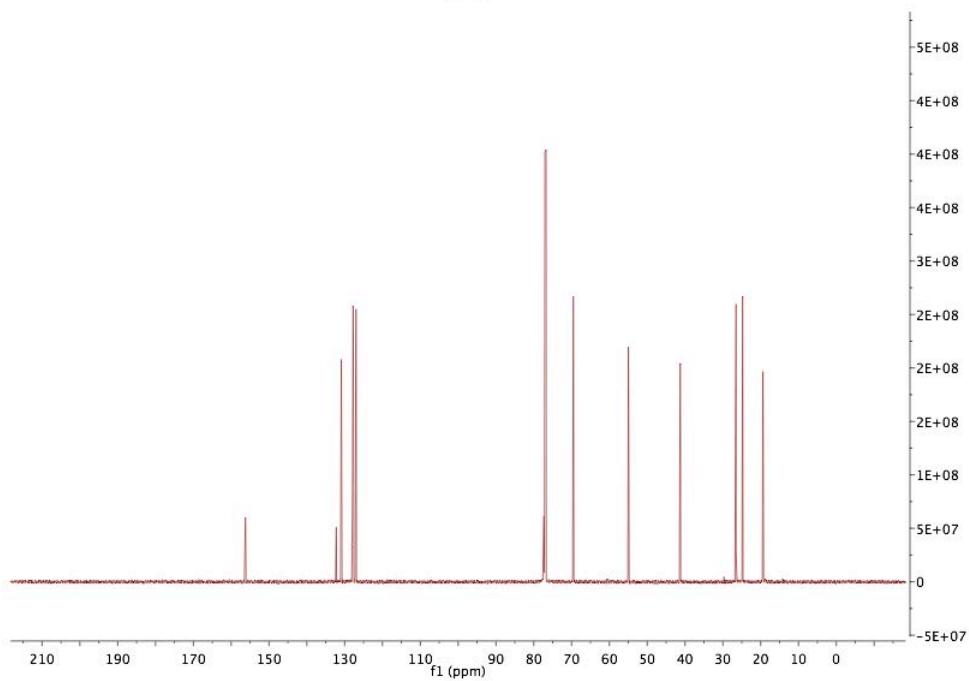
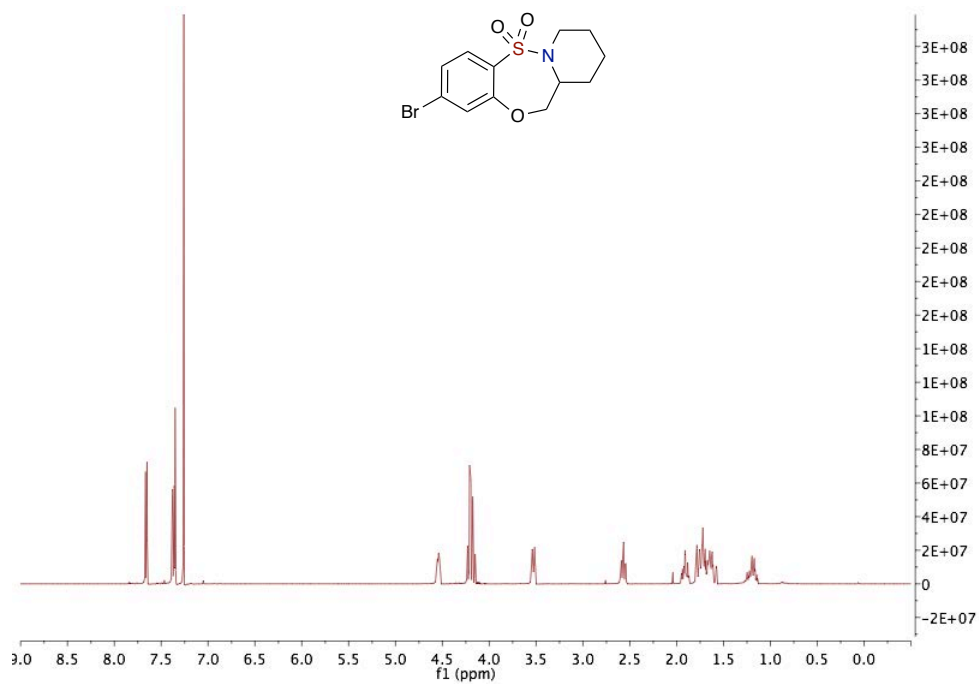
(2*R*,5*S*)-8-Bromo-4,5-dihydro-3*H*-2,5-methanobenzo[*b*][1,4,5]oxathiazocine 1,1-dioxide (2.8.2)



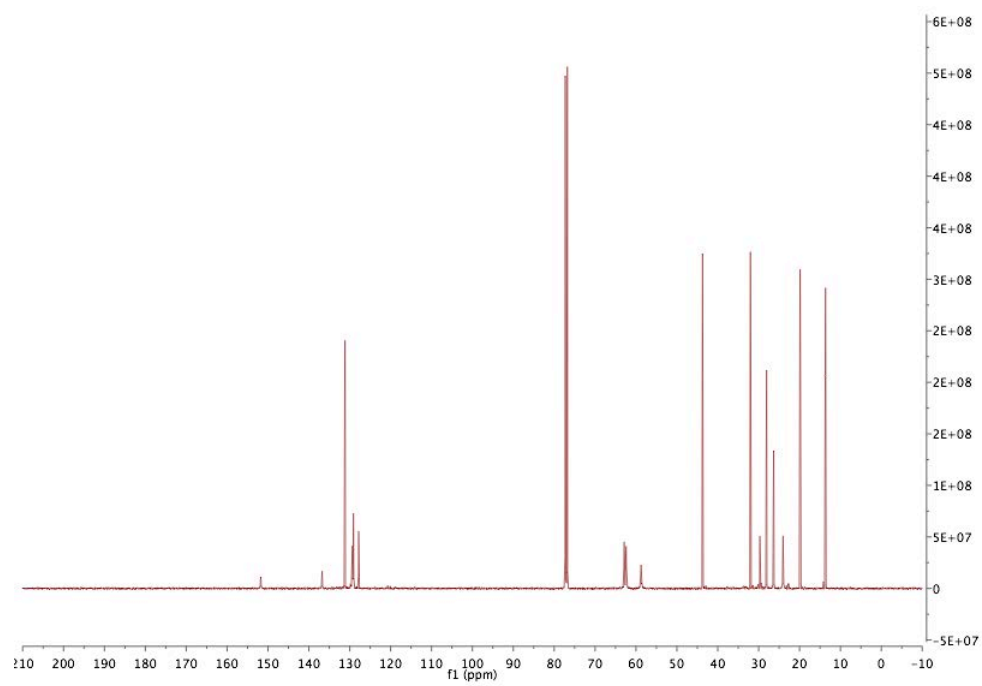
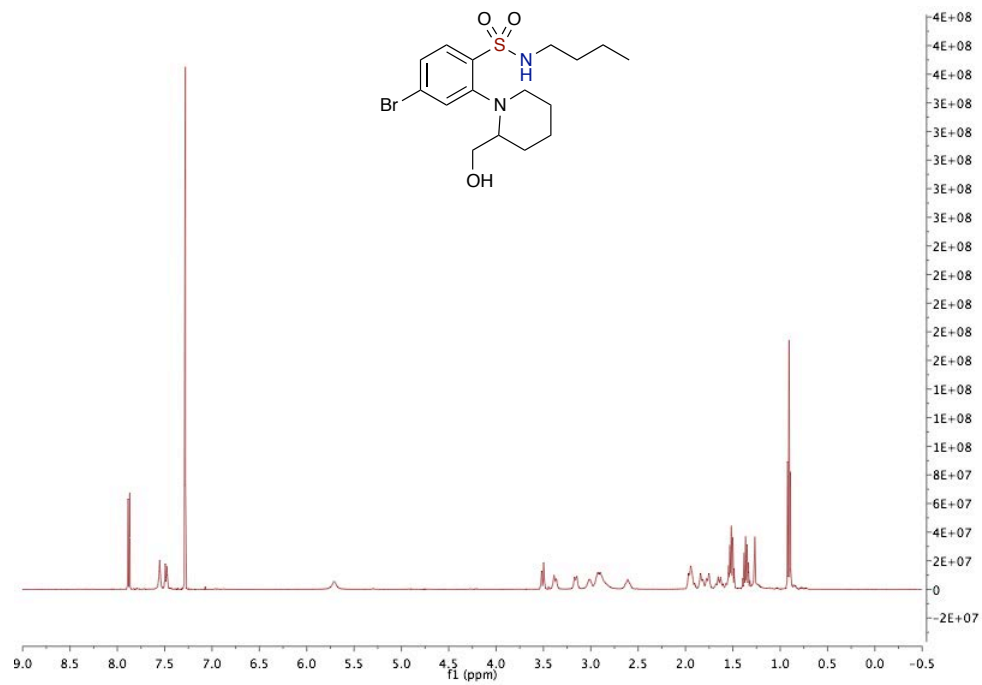
(1-((4-Bromo-2-fluorophenyl)sulfonyl)piperidin-2-yl)methanol (SI-1)



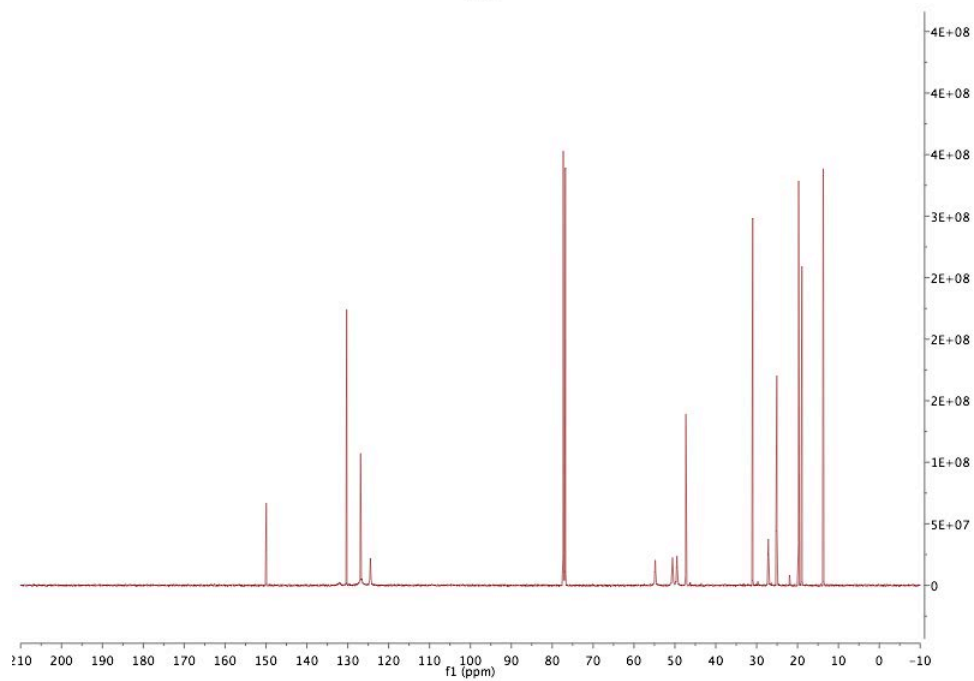
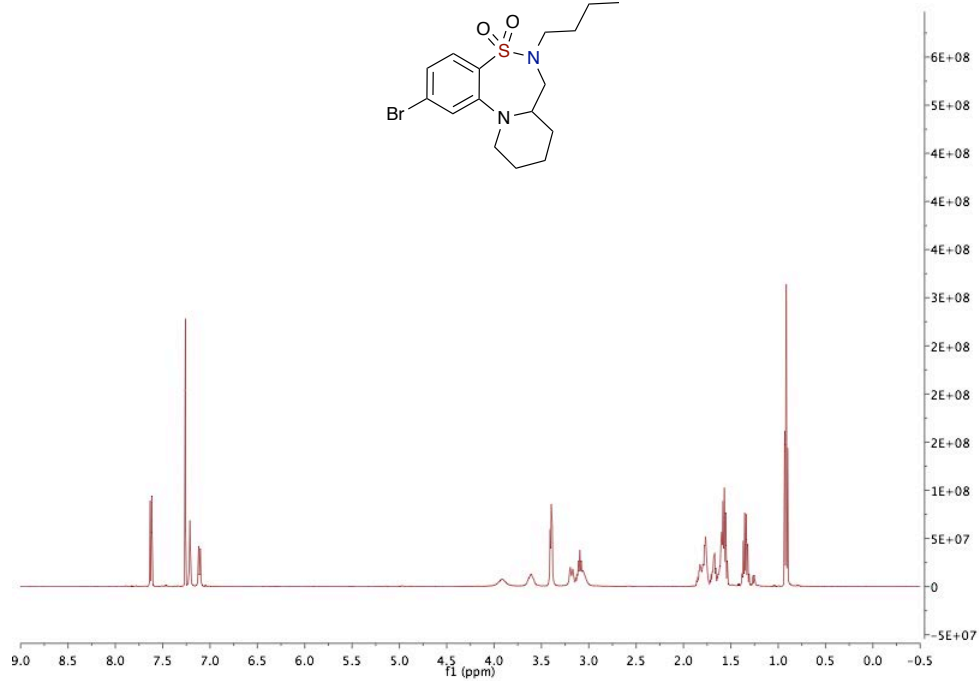
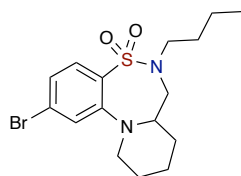
9-Bromo-1,2,3,4,12,12a-hexahydrobenzo[*b*]pyrido[1,2-*e*][1,4,5]oxathiazepine 6,6-dioxide (2.8.4)



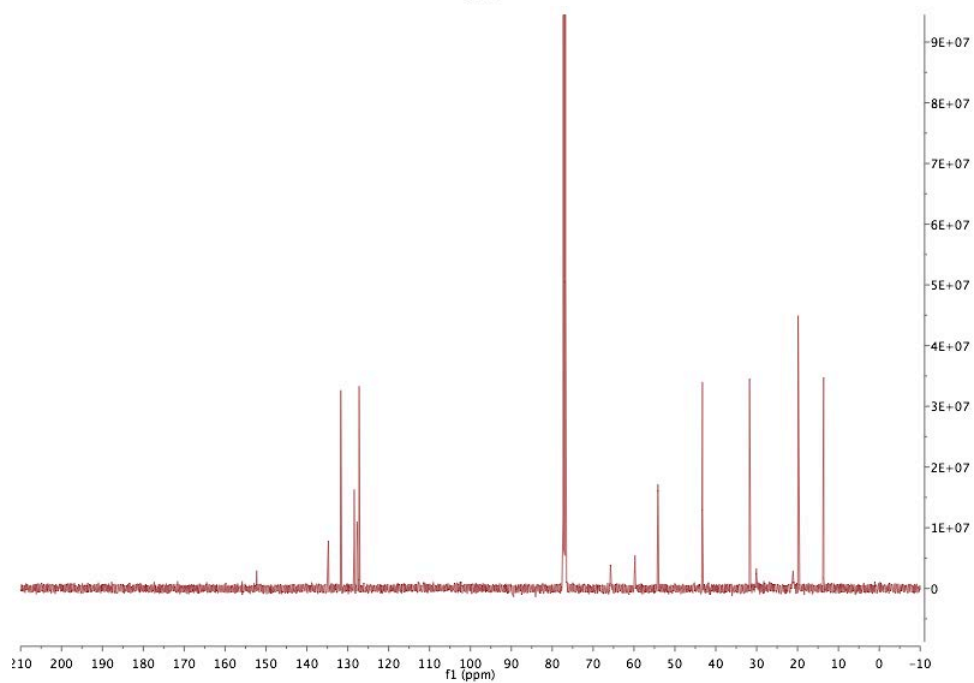
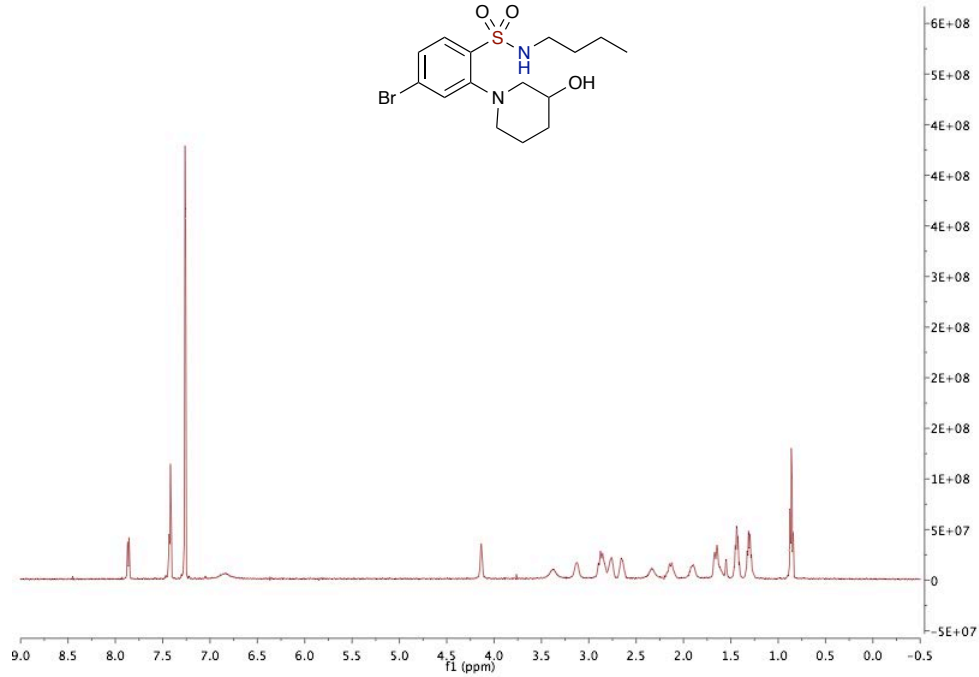
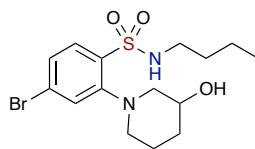
4-Bromo-N-butyl-2-(2-(hydroxymethyl)piperidin-1-yl)benzenesulfonamide (SI-2)



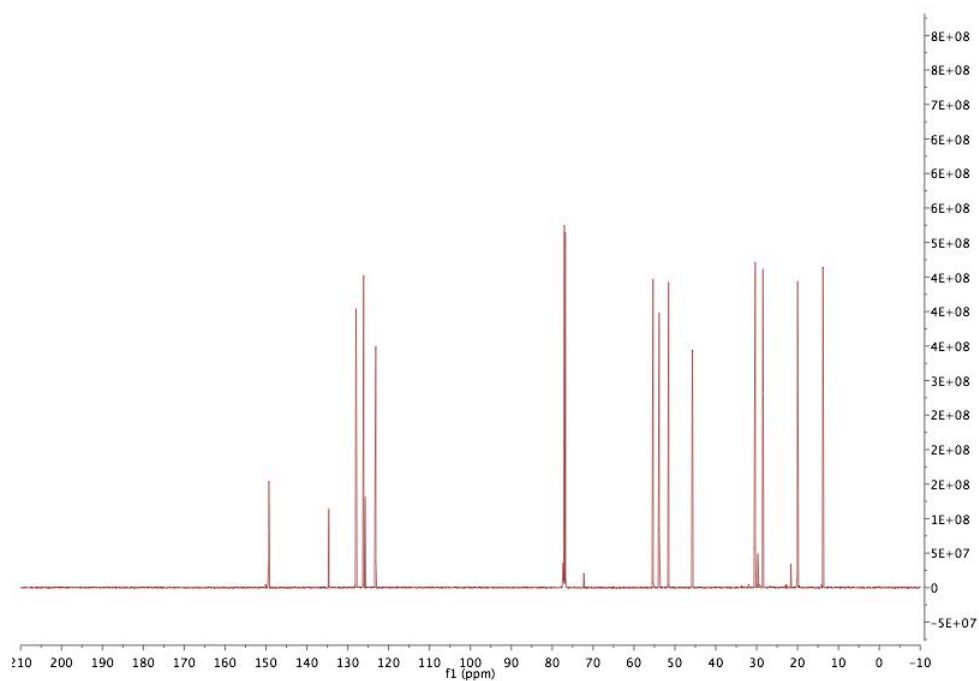
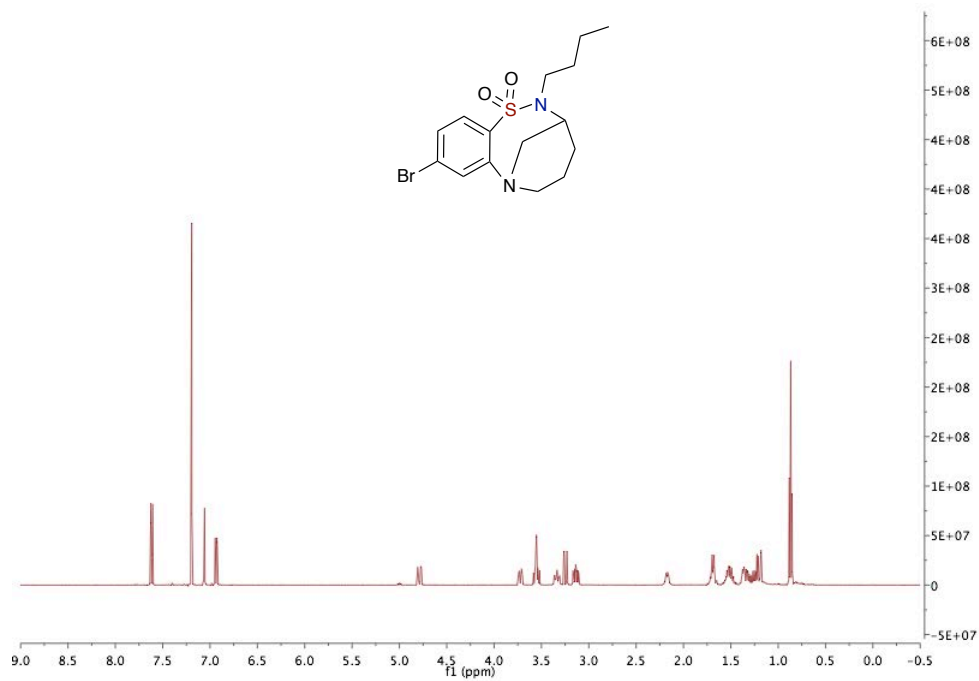
2-Bromo-6-butyl-7,7a,8,9,10,11-hexahydro-6H-benzo[f]pyrido[2,1-d][1,2,5]thiadiazepine 5,5-dioxide (2.8.5)



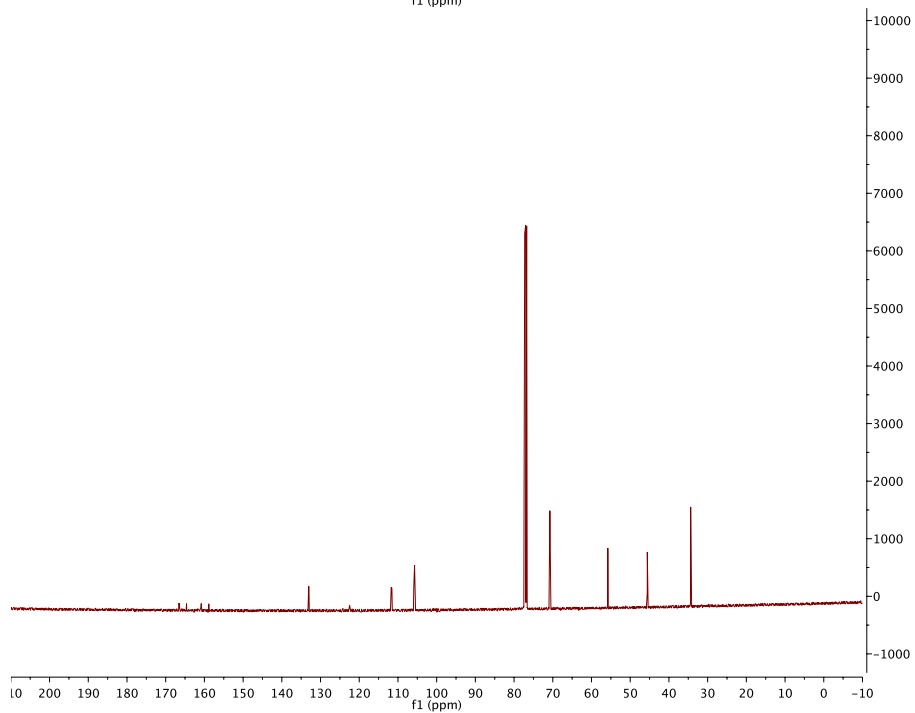
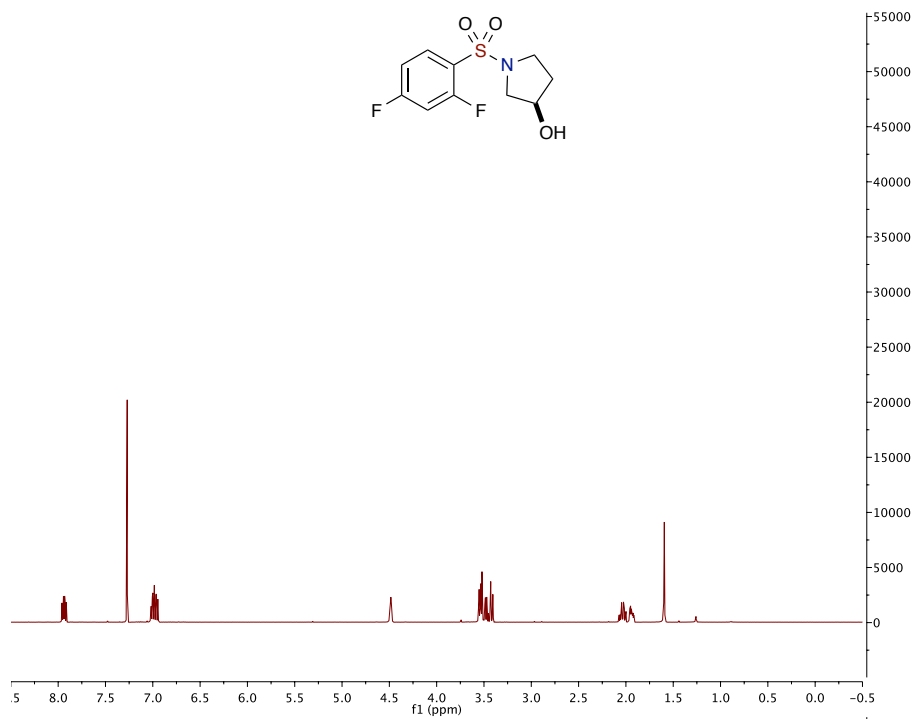
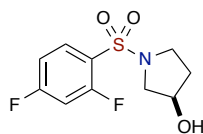
4-Bromo-N-butyl-2-(3-hydroxypiperidin-1-yl)benzenesulfonamide (SI-3)



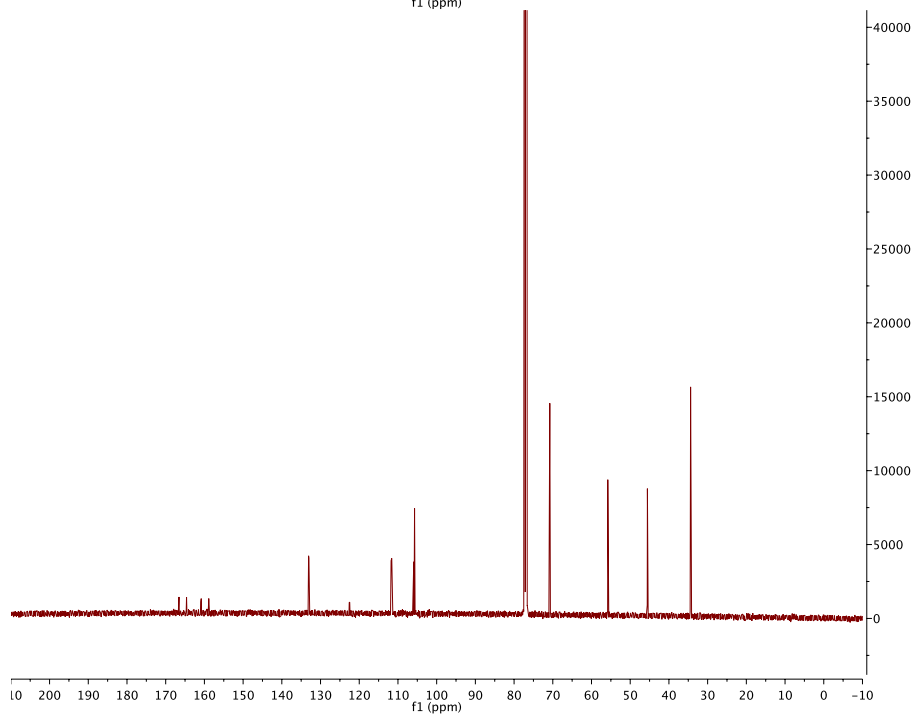
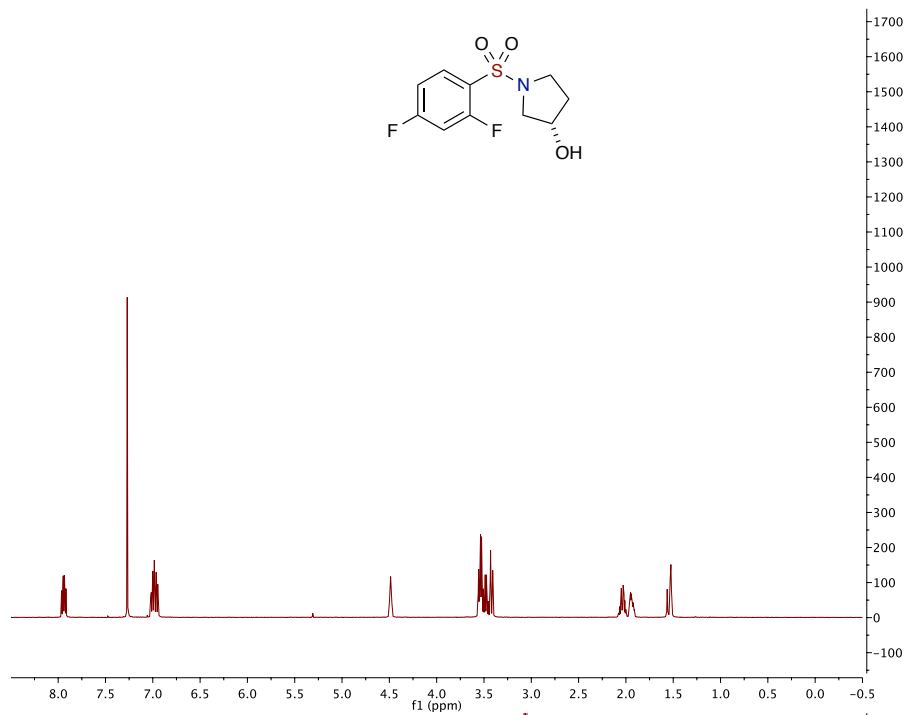
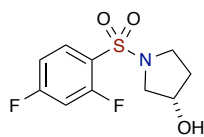
**9-Bromo-2-butyl-3,4,5,6-tetrahydro-2H-3,7-methanobenzo[h][1,2,7]thiadiazonine
1,1-dioxide (2.8.7)**



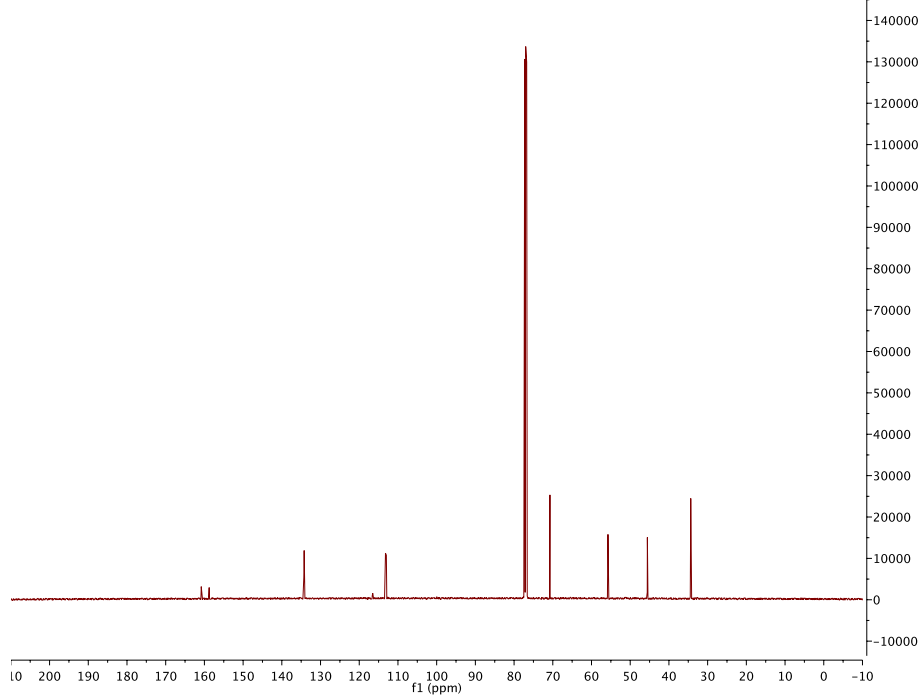
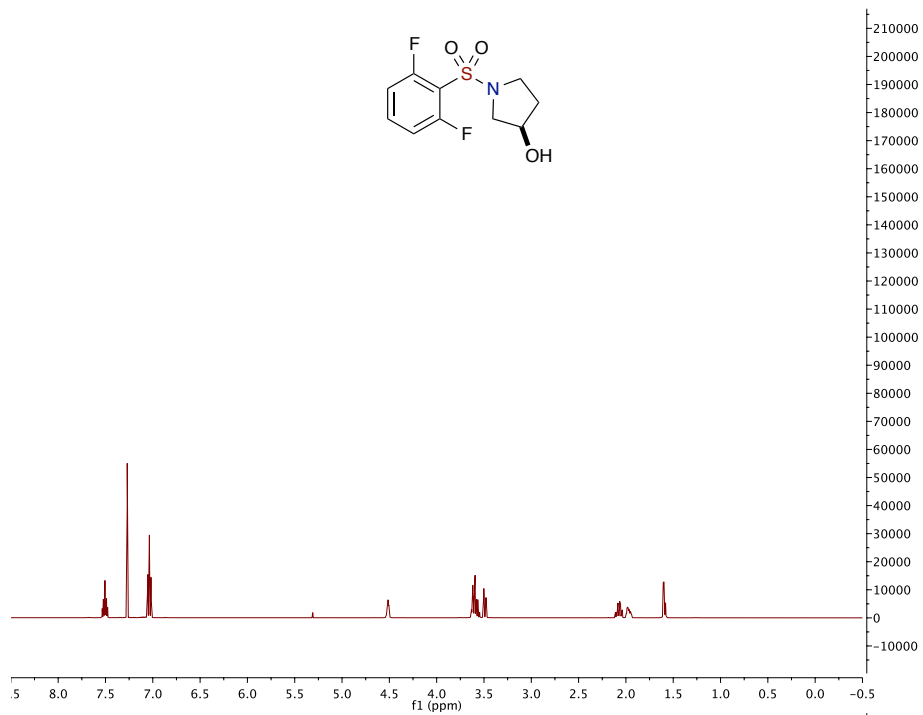
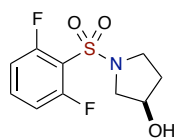
(R)-1-((2,4-difluorophenyl)sulfonyl)pyrrolidin-3-ol (2.9.3)



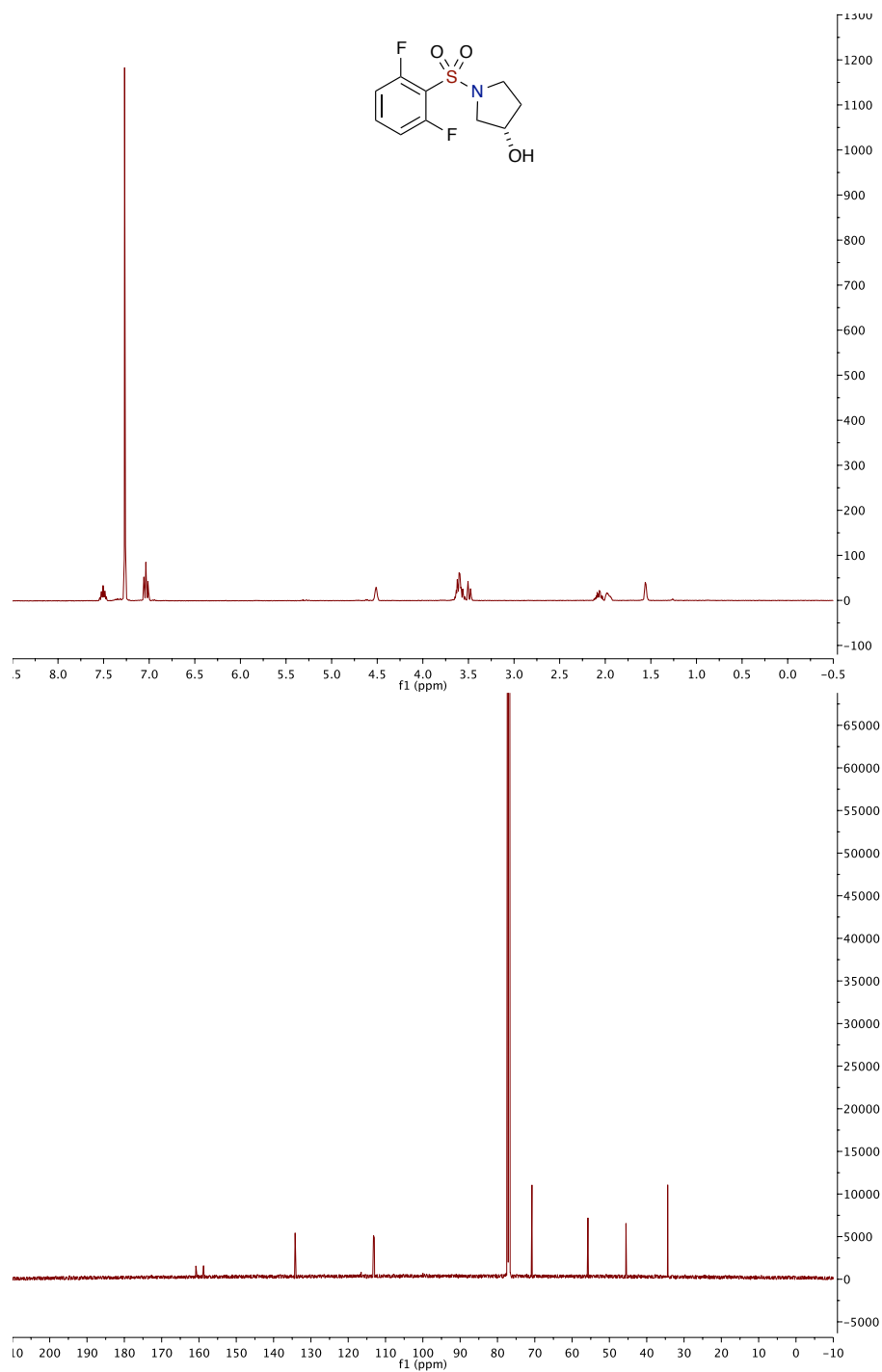
(S)-1-((2,4-difluorophenyl)sulfonyl)pyrrolidin-3-ol (2.9.4)



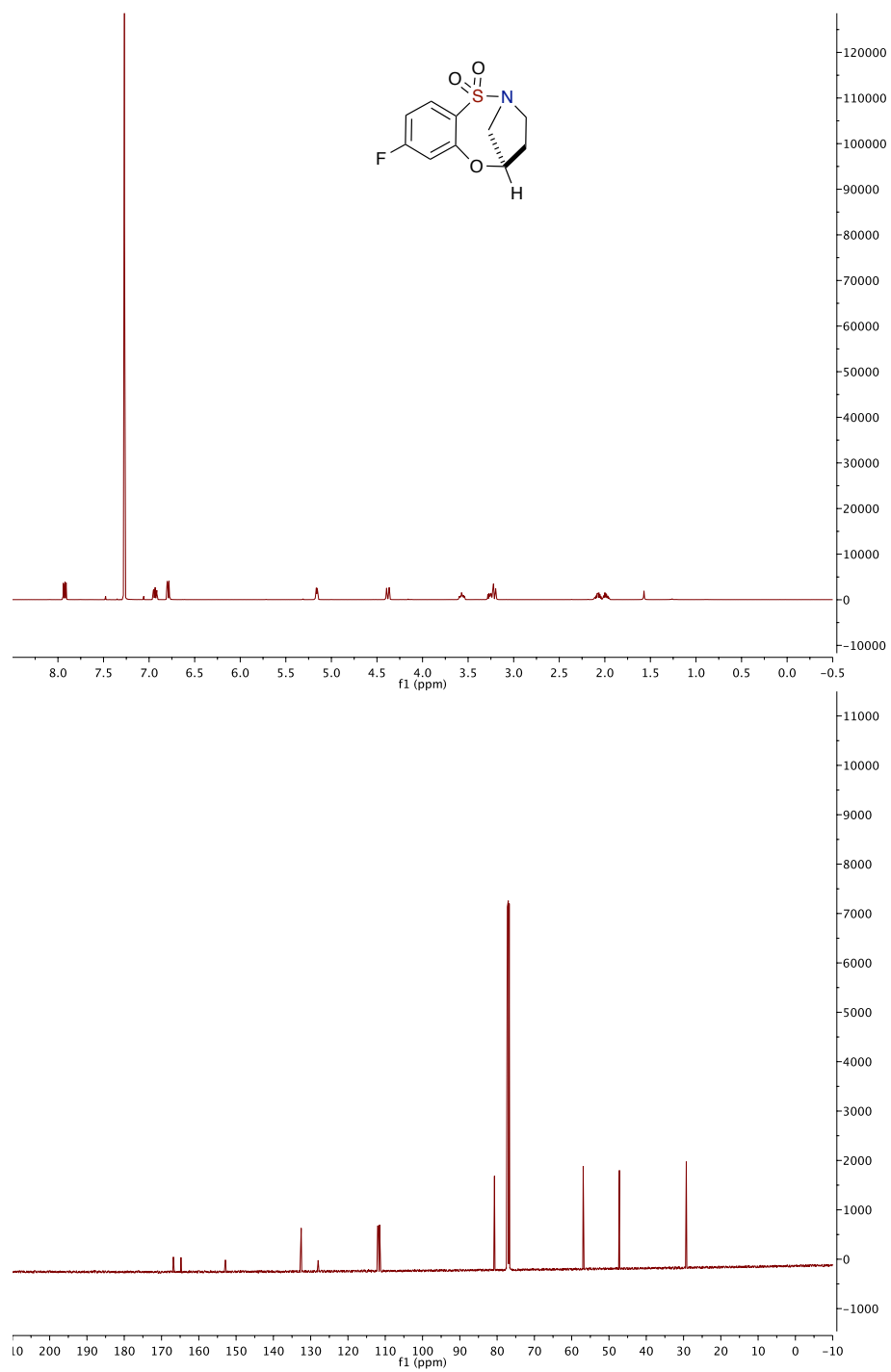
(R)-1-((2,6-difluorophenyl)sulfonyl)pyrrolidin-3-ol (2.9.5)



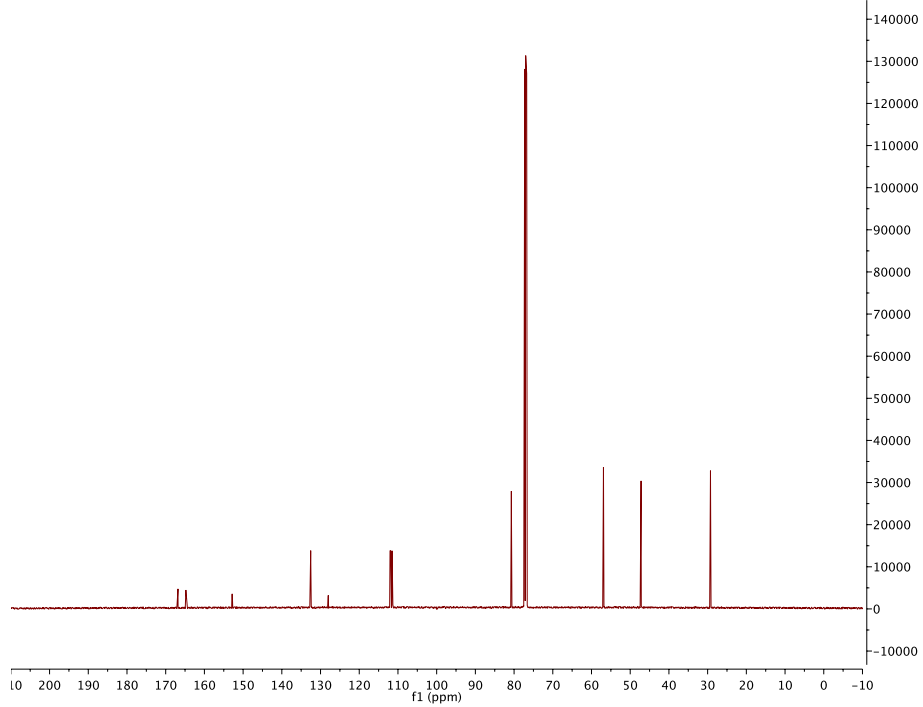
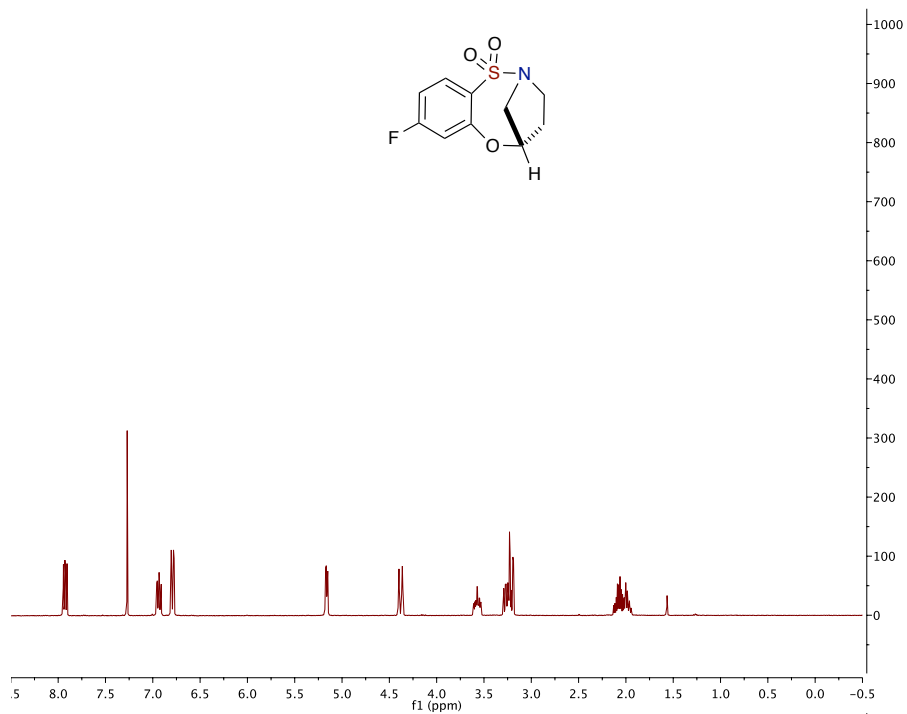
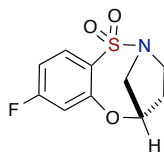
(S)-1-((2,6-difluorophenyl)sulfonyl)pyrrolidin-3-ol (2.9.6)



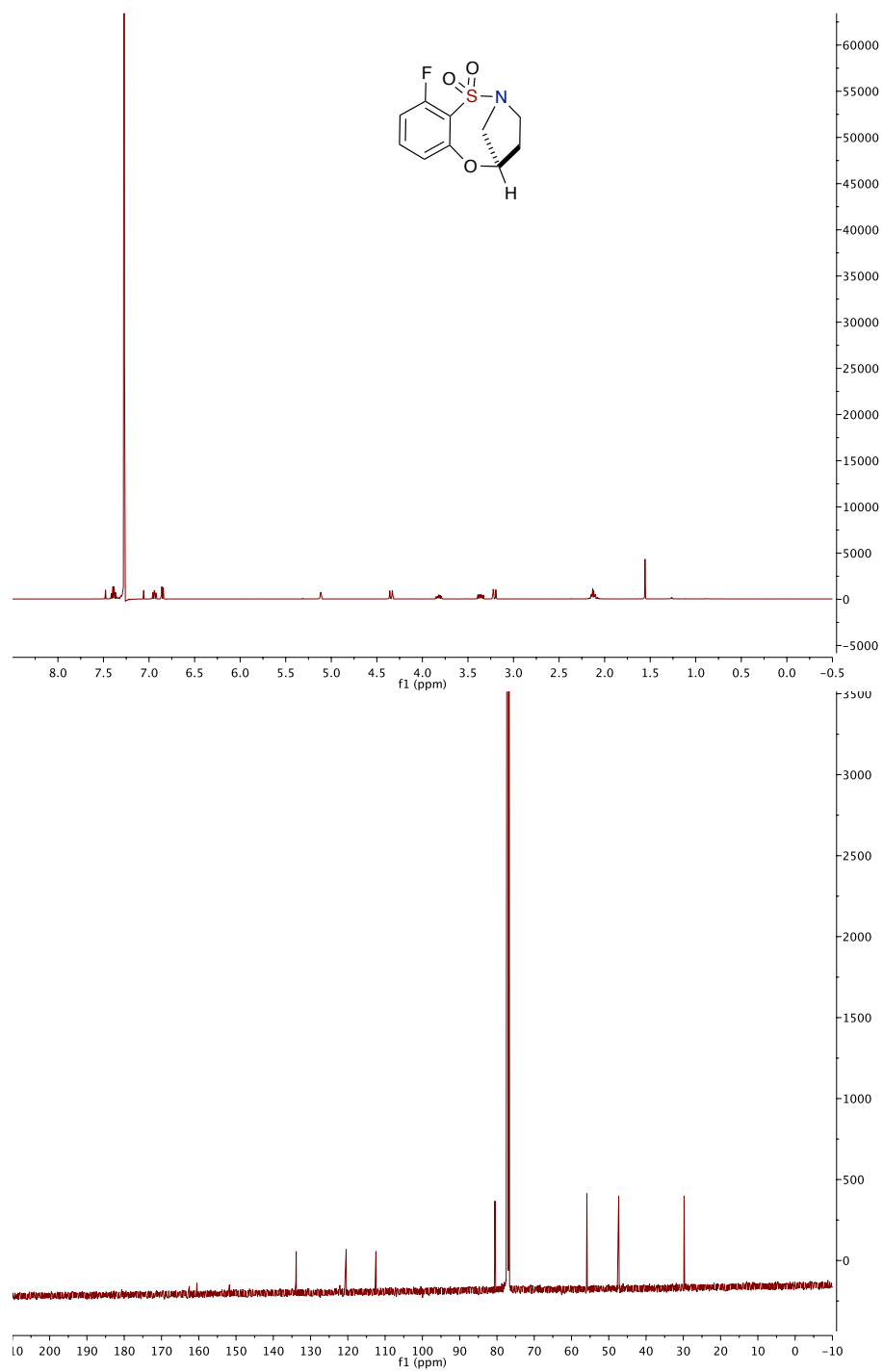
(5R)-8-fluoro-4,5-dihydro-3H-2,5-methanobenzo[*b*][1,4,5]oxathiazocine 1,1-dioxide
(2.9.7)



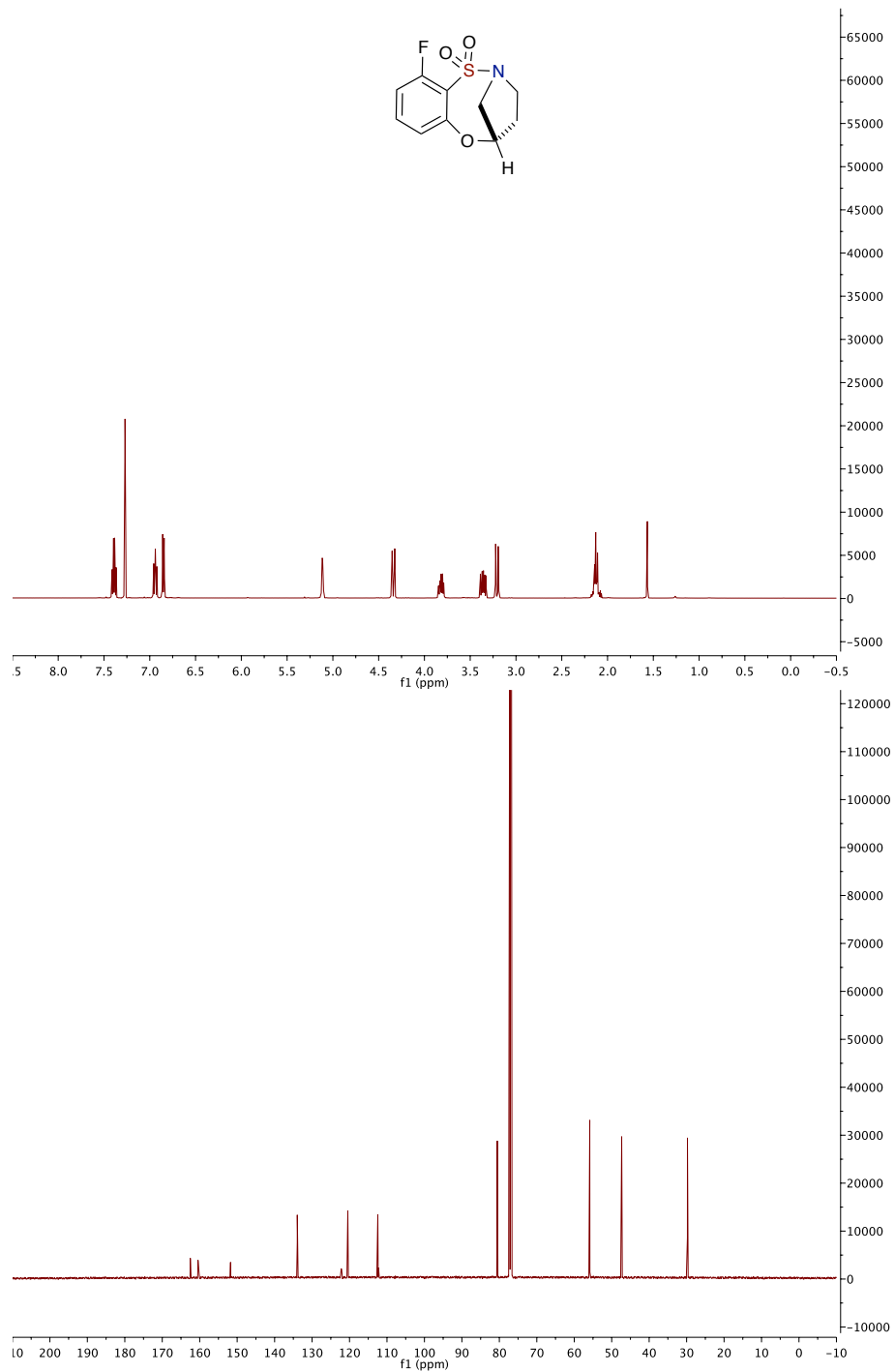
(5*S*)-8-fluoro-4,5-dihydro-3*H*-2,5-methanobenzo[*b*][1,4,5]oxathiazocine 1,1-dioxide
(2.9.8)



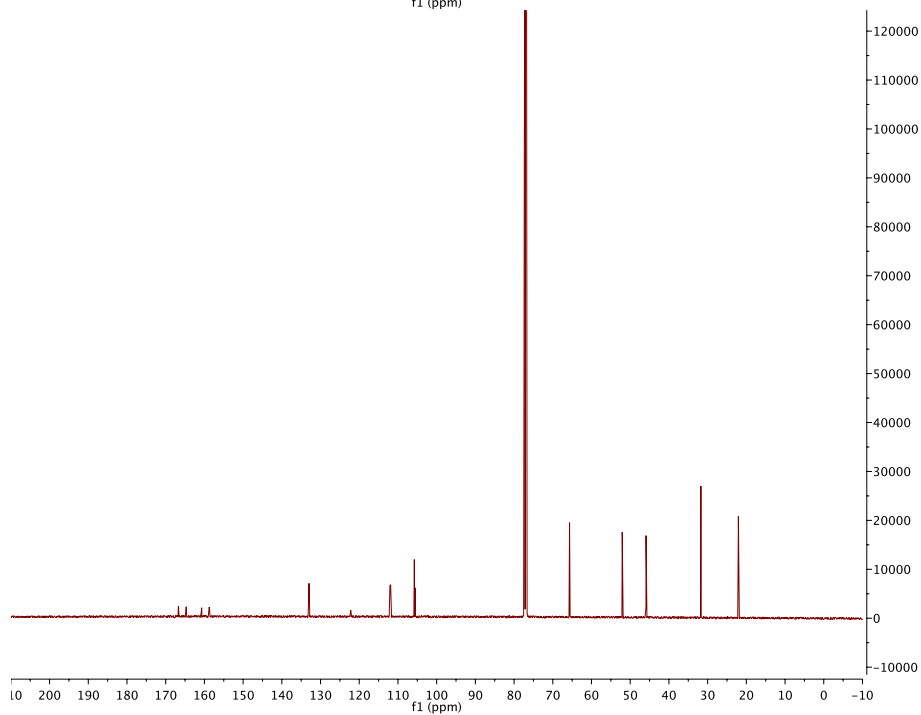
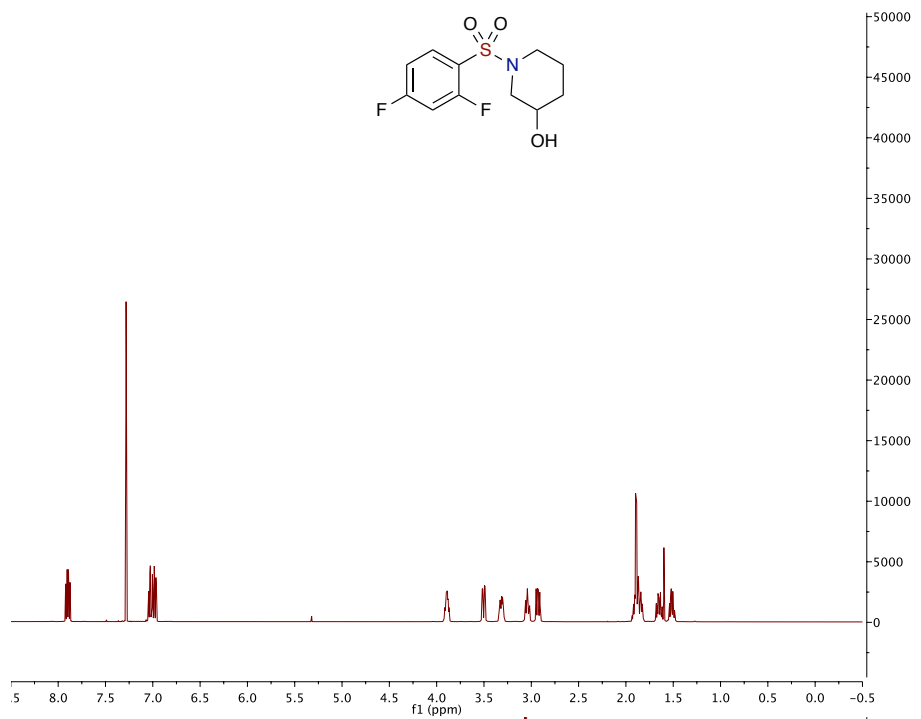
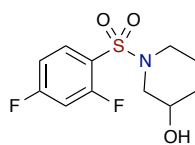
(5R)-10-fluoro-4,5-dihydro-3H-2,5-methanobenzo[*b*][1,4,5]oxathiazocine 1,1-dioxide
(2.9.9)



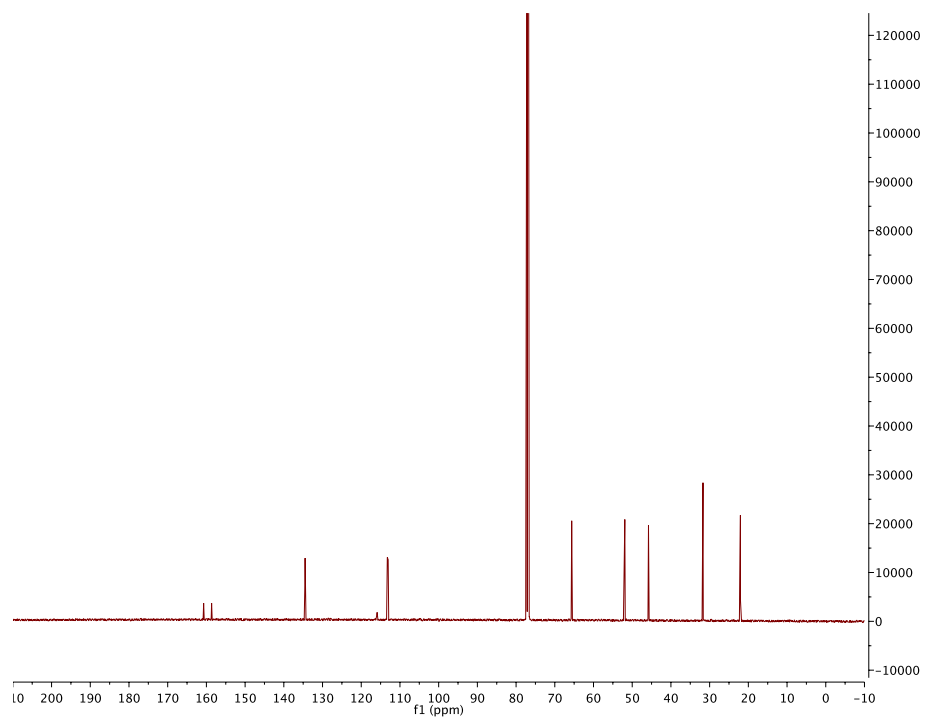
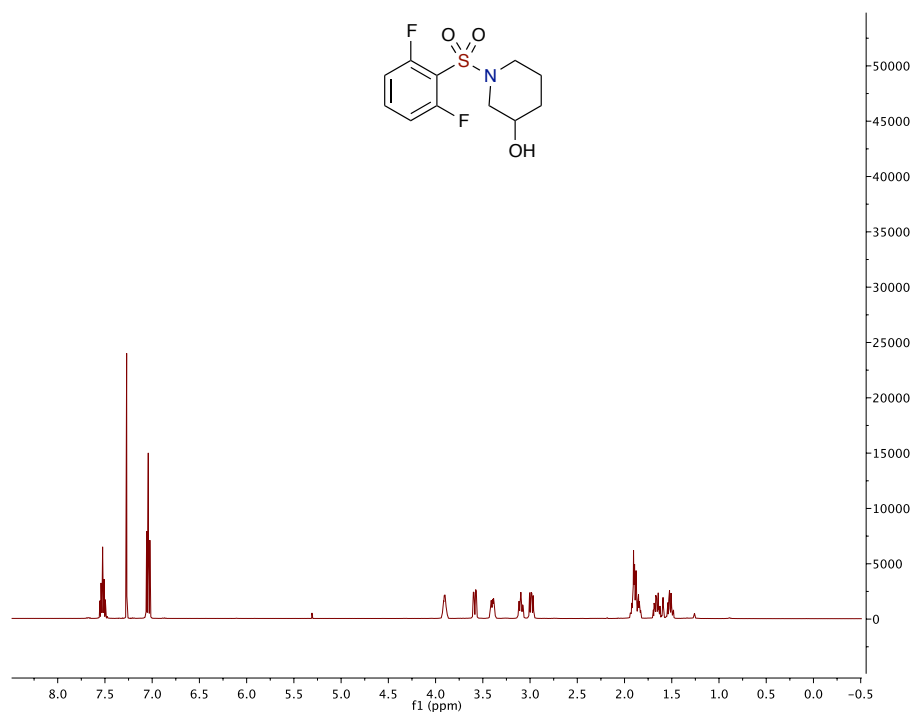
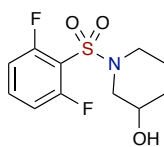
(5S)-10-fluoro-4,5-dihydro-3H-2,5-methanobenzo[*b*][1,4,5]oxathiazocine 1,1-dioxide
(2.9.10)



1-((2,4-difluorophenyl)sulfonyl)piperidin-3-ol (2.9.11)

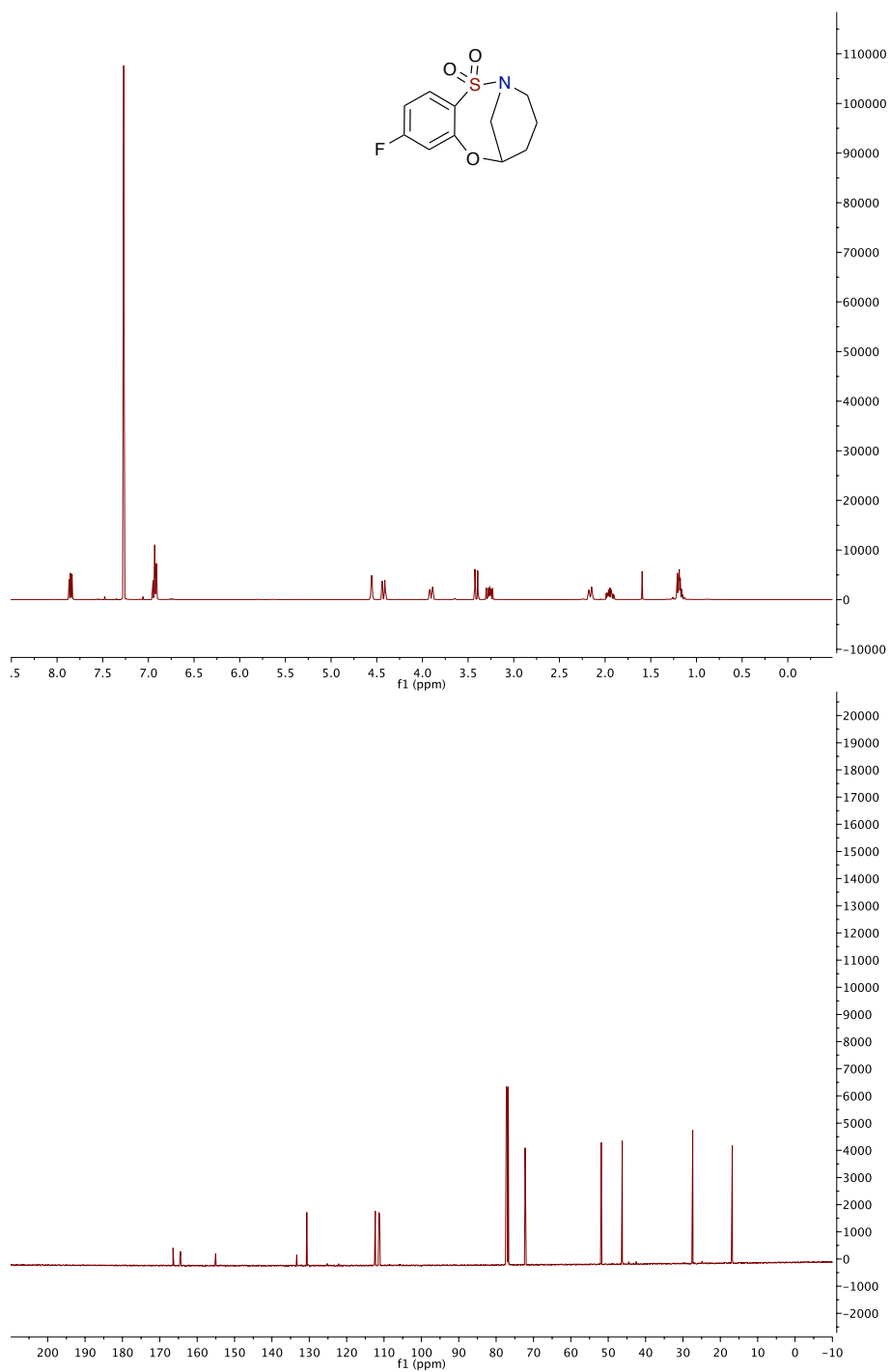


1-((2,6-difluorophenyl)sulfonyl)piperidin-3-ol (2.9.12)

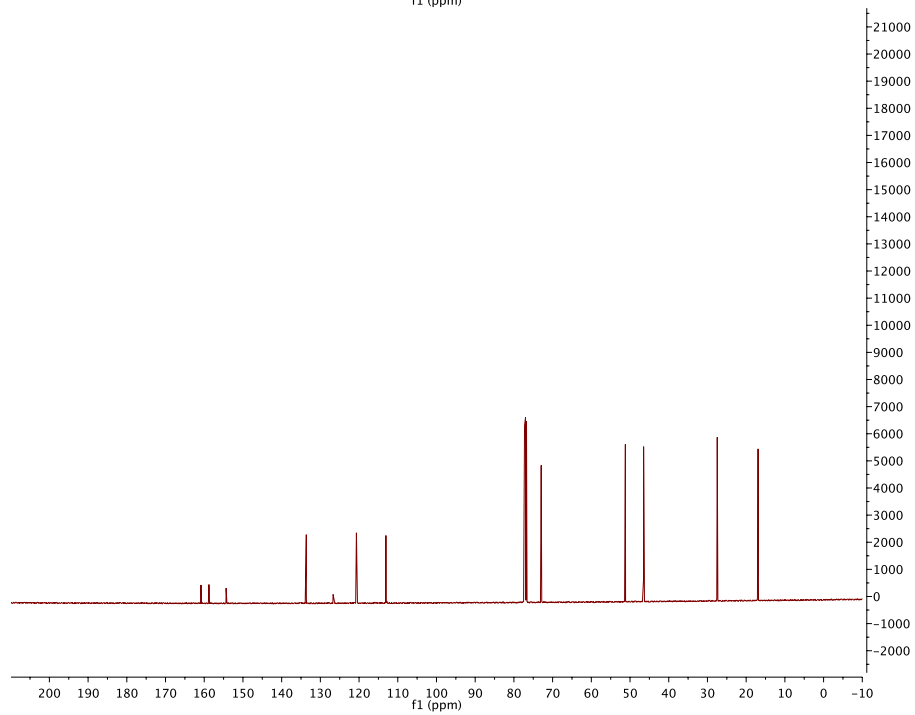
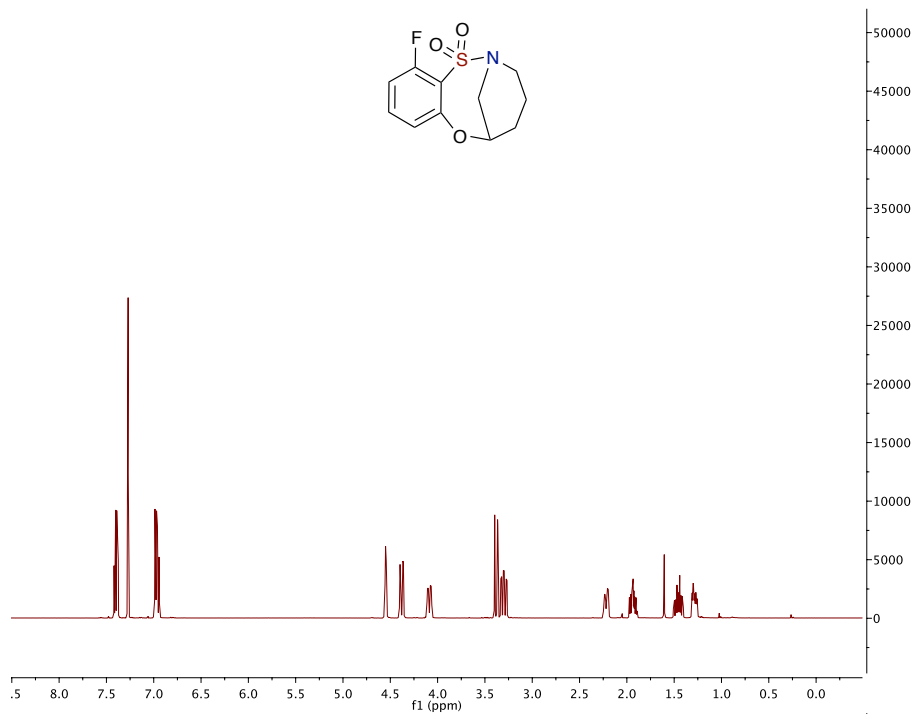
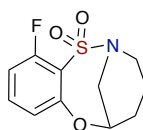


**9-fluoro-3,4,5,6-tetrahydro-2,6-methanobenzo[*b*][1,4,5]oxathiazonine
(2.9.13)**

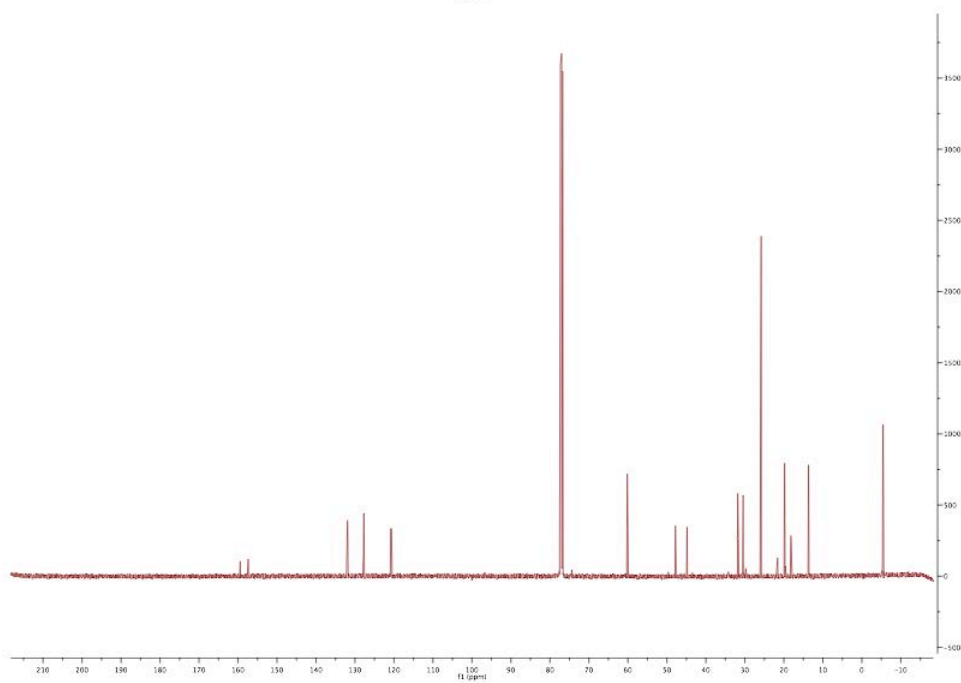
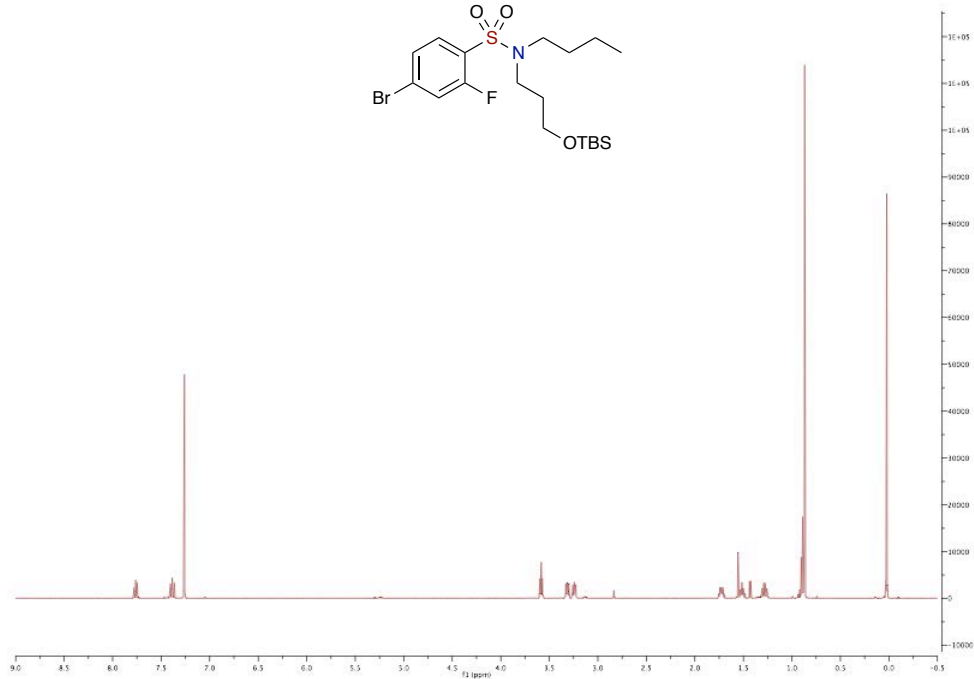
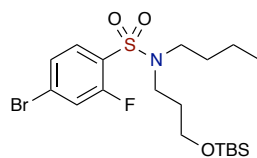
1,1-dioxide



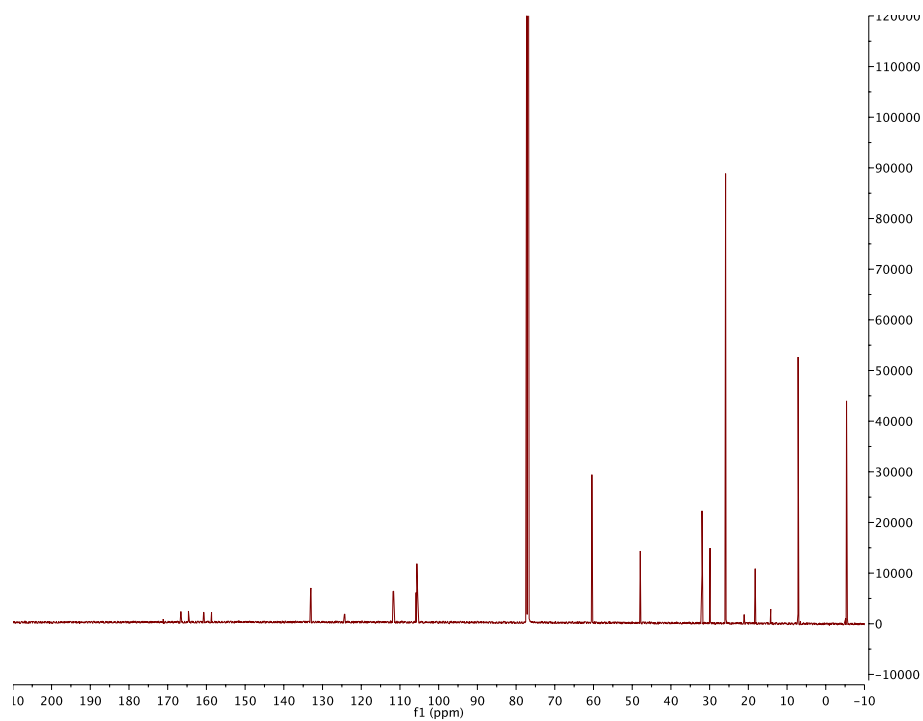
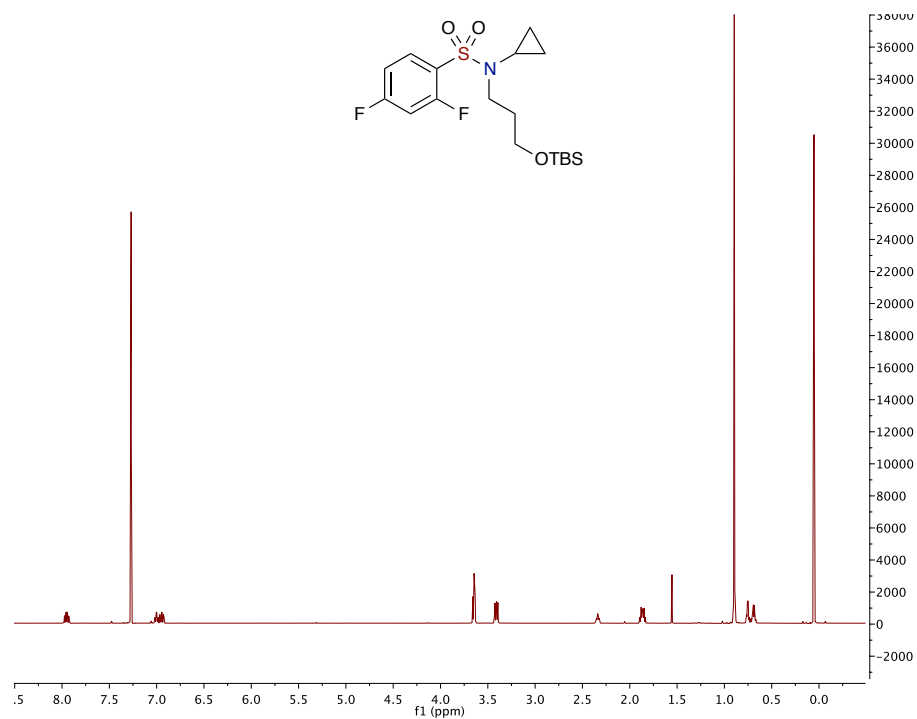
**11-fluoro-3,4,5,6-tetrahydro-2,6-methanobenzo[*b*][1,4,5]oxathiazonine 1,1-dioxide
(2.9.14)**



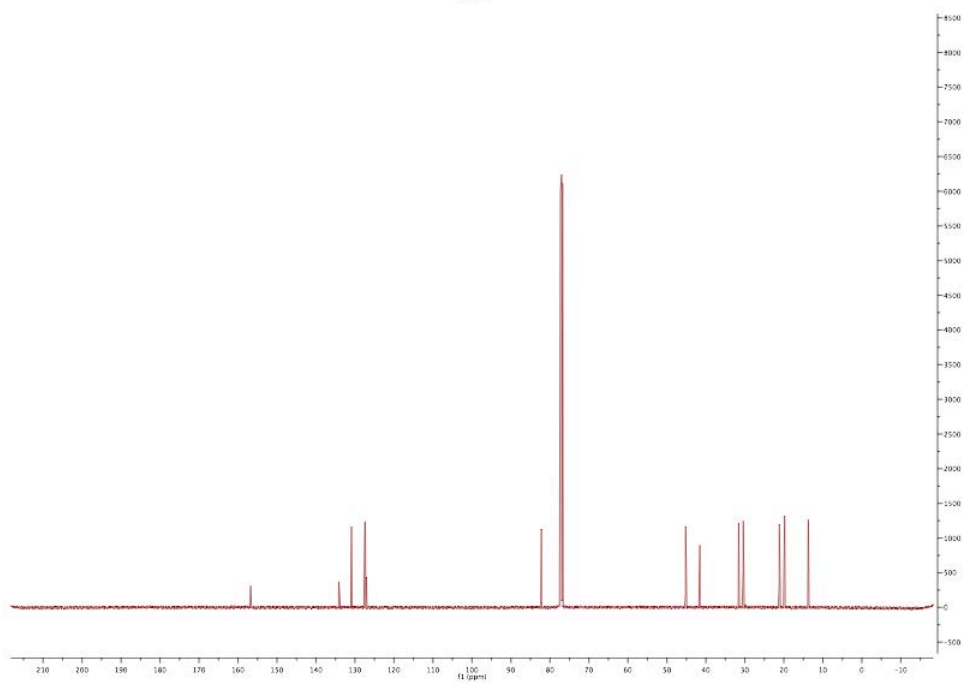
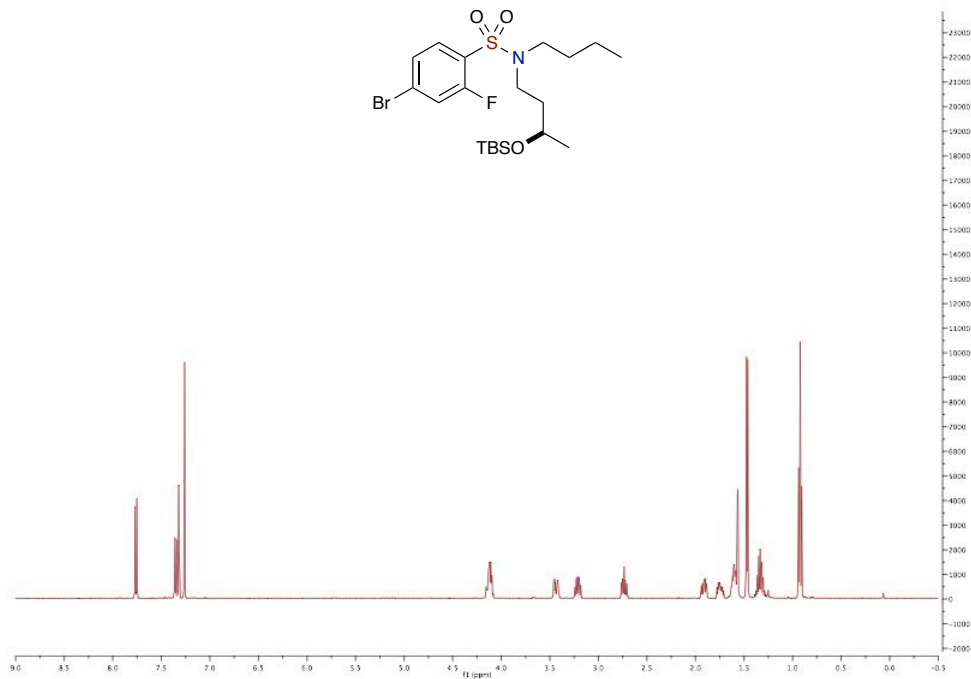
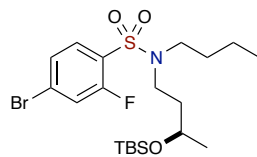
4-Bromo-N-butyl-N-(3-(*tert*-butyldimethylsilyloxy)propyl)-2-fluorobenzene-sulfonamide (2.10.1)



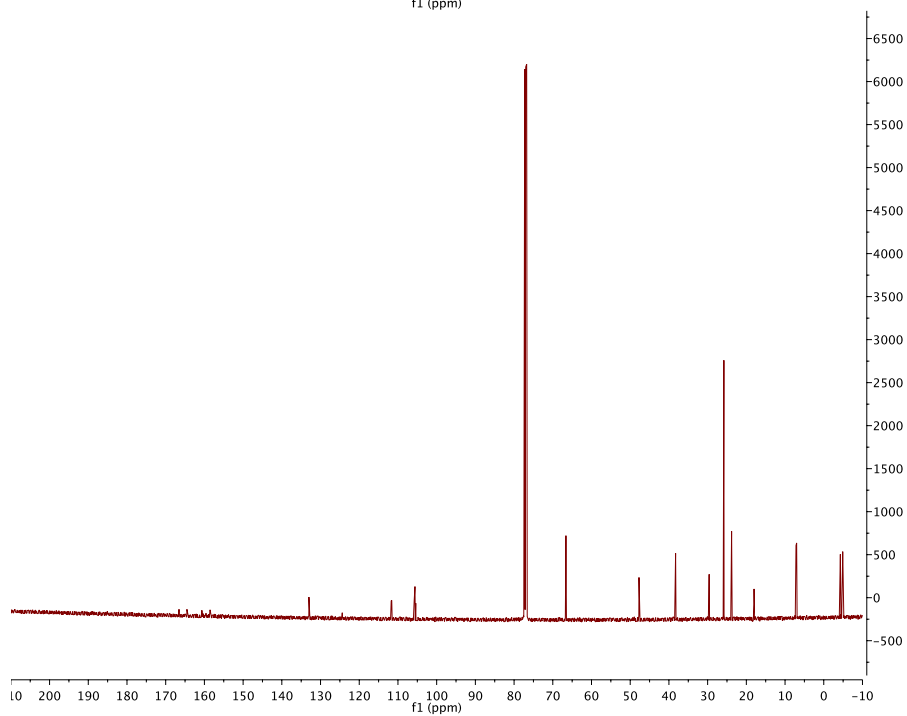
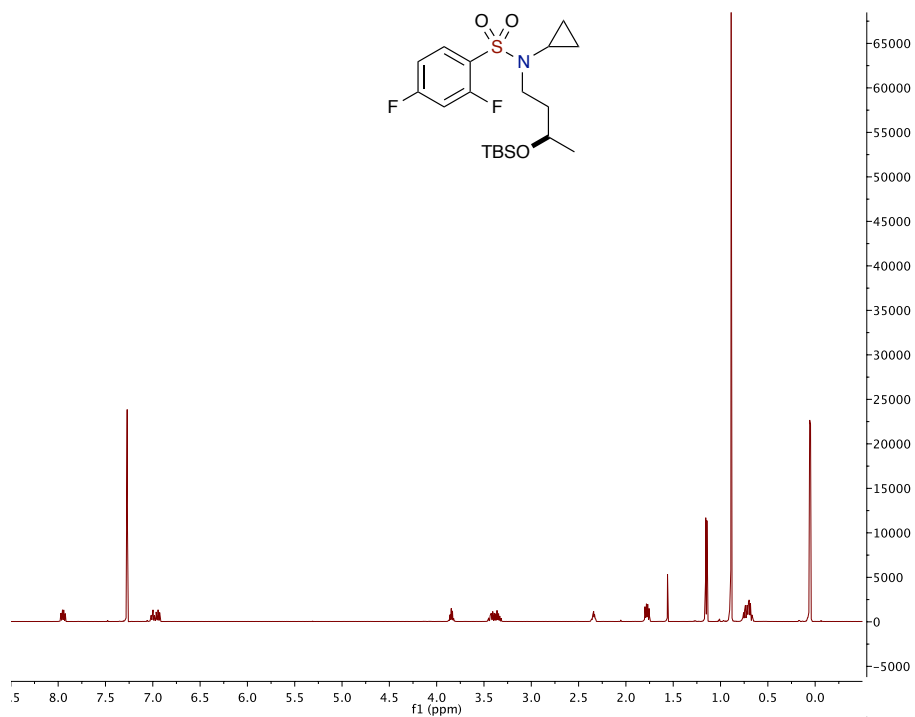
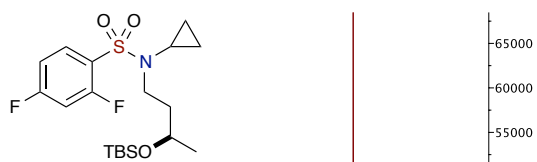
***N*-(3-((*tert*-butyldimethylsilyl)oxy)propyl)-*N*-cyclopropyl-2,4-difluorobenzene-sulfonamide (2.10.2)**



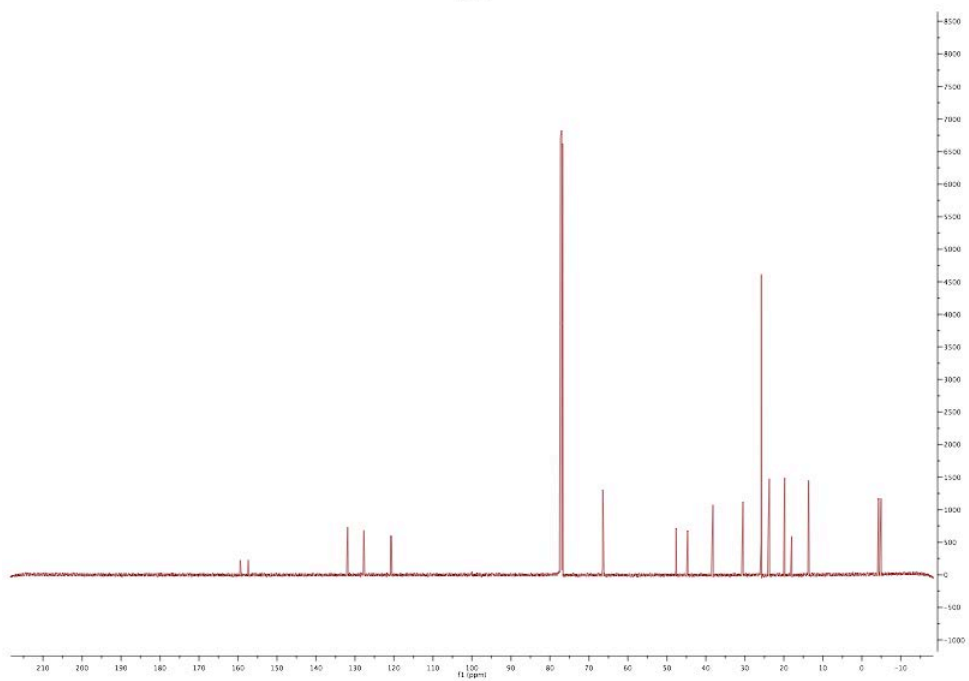
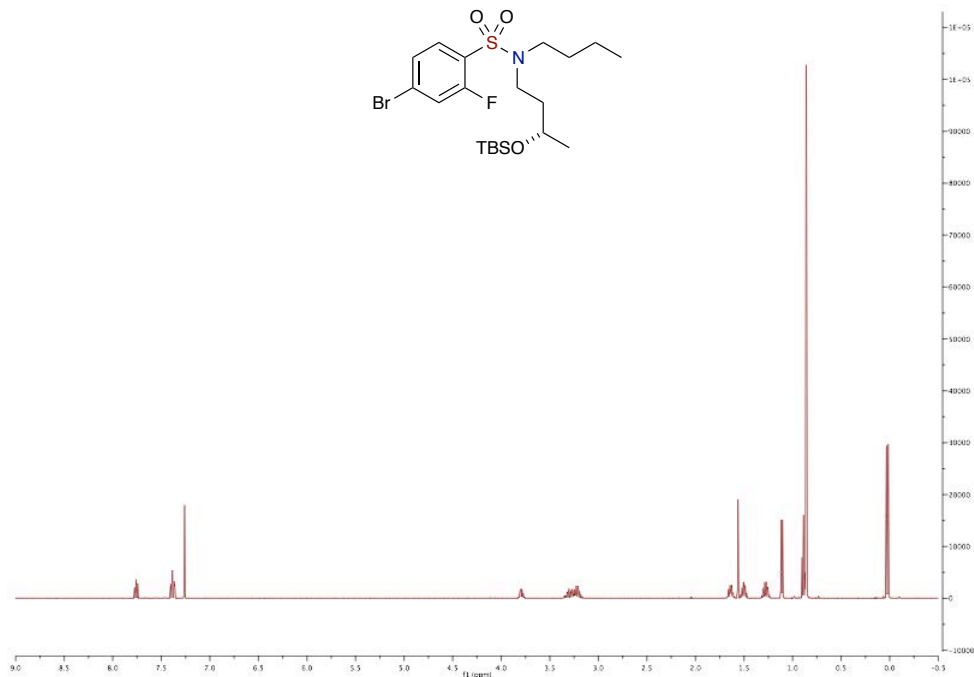
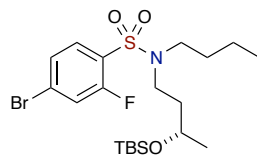
(R)-4-Bromo-N-butyl-N-(3-(*tert*-butyldimethylsilyloxy)butyl)-2-fluorobenzene-sulfonamide (2.10.4)



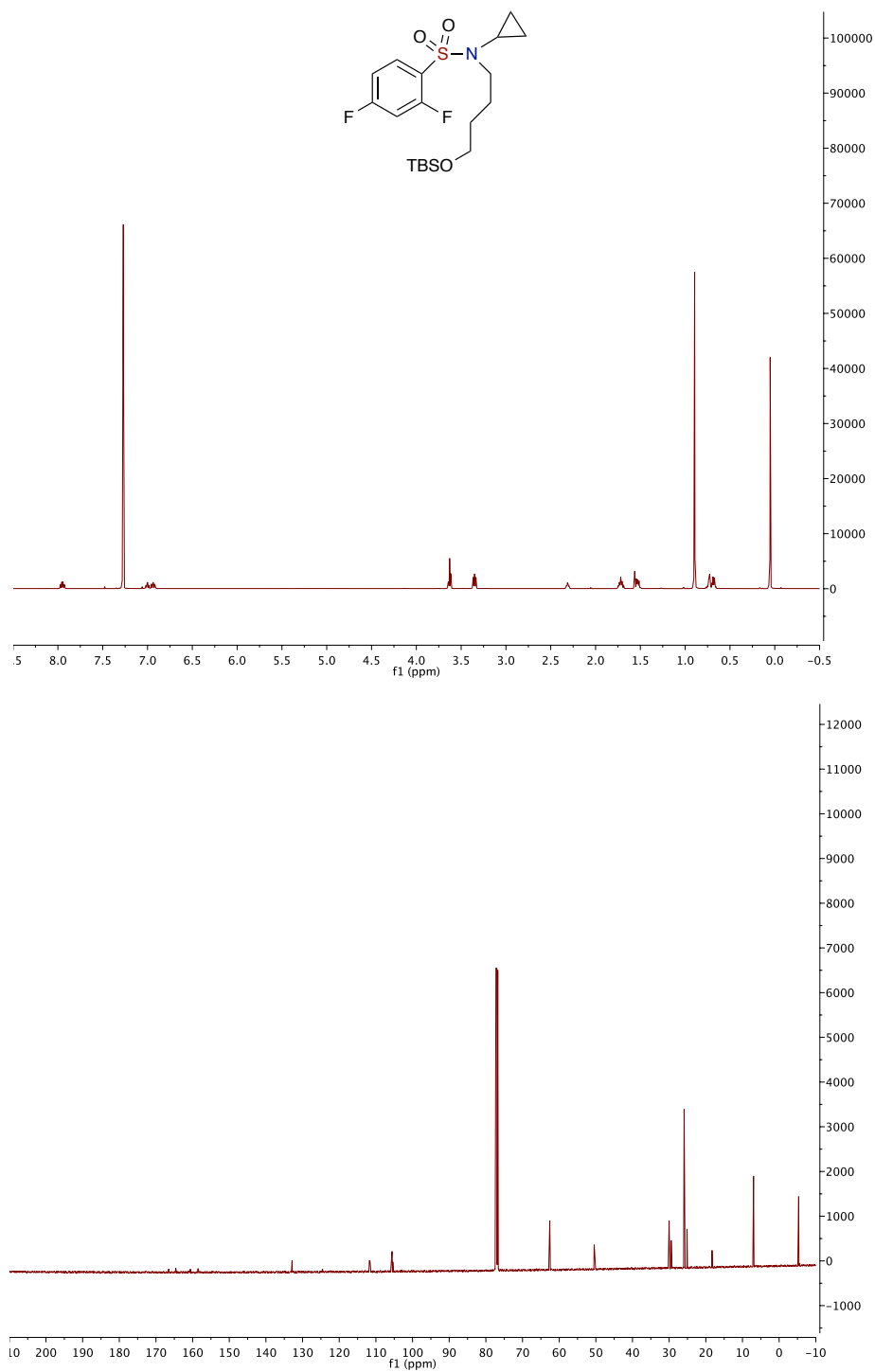
(R)-N-(3-((*tert*-butyldimethylsilyl)oxy)butyl)-N-cyclopropyl-2,4-difluorobenzene-sulfonamide (2.10.5)



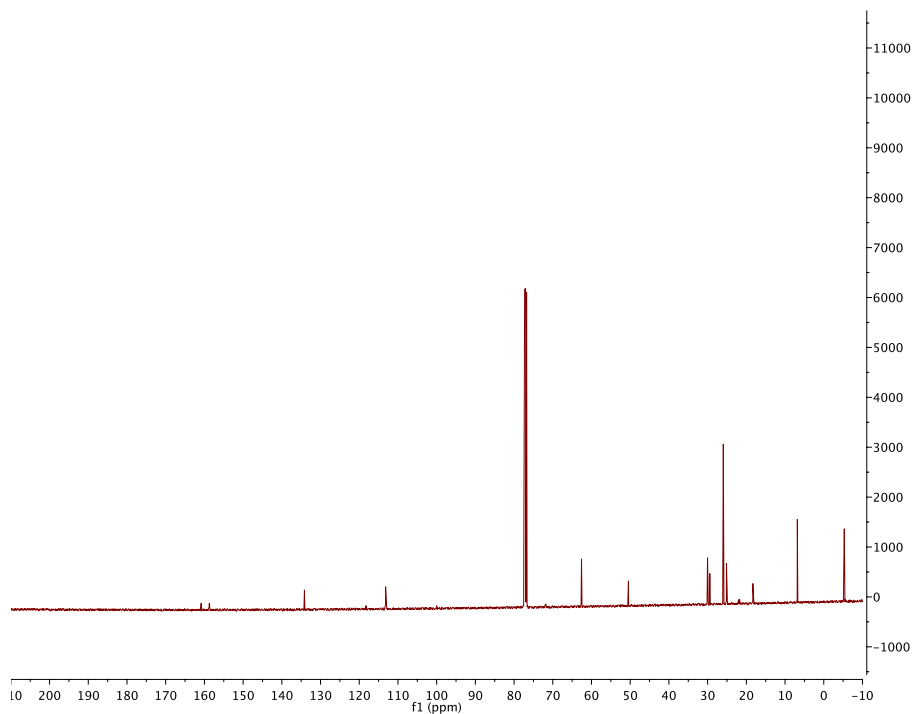
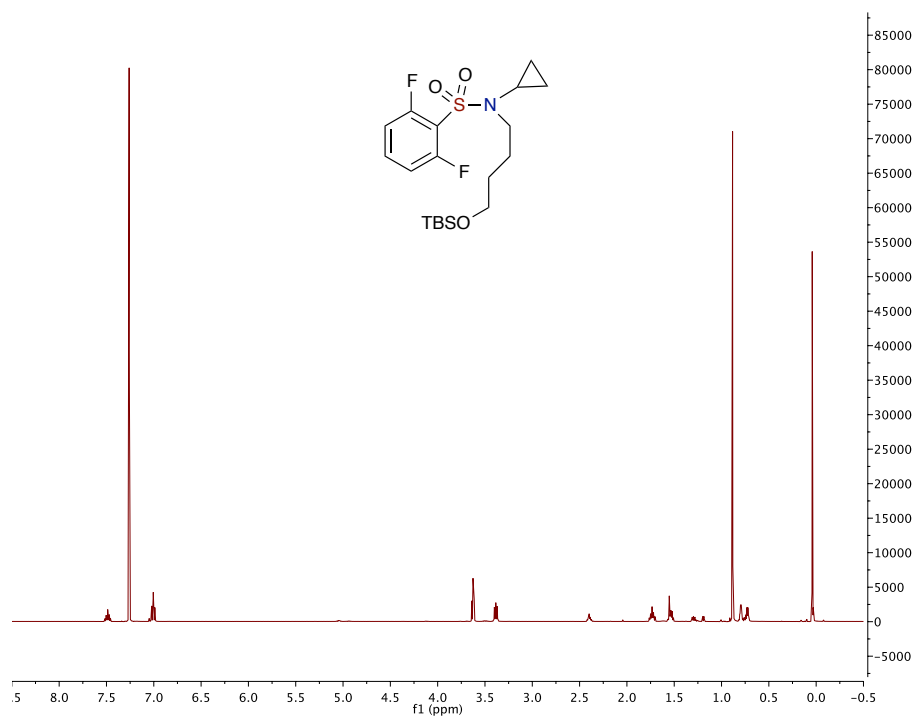
(S)-4-Bromo-N-butyl-N-(3-(*tert*-butyldimethylsilyloxy)butyl)-2-fluorobenzene-sulfonamide (2.10.7)



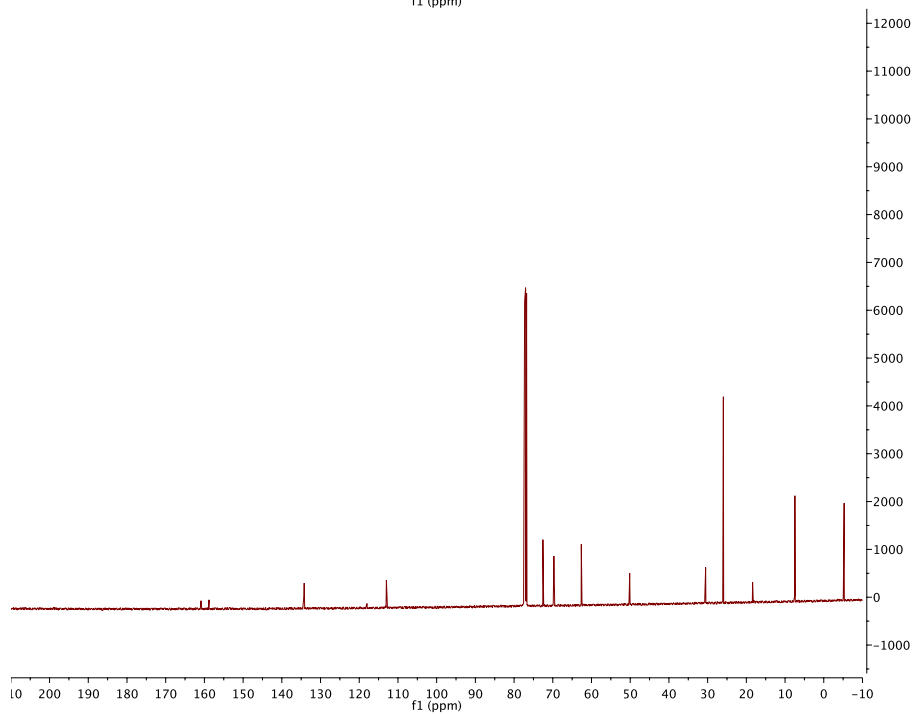
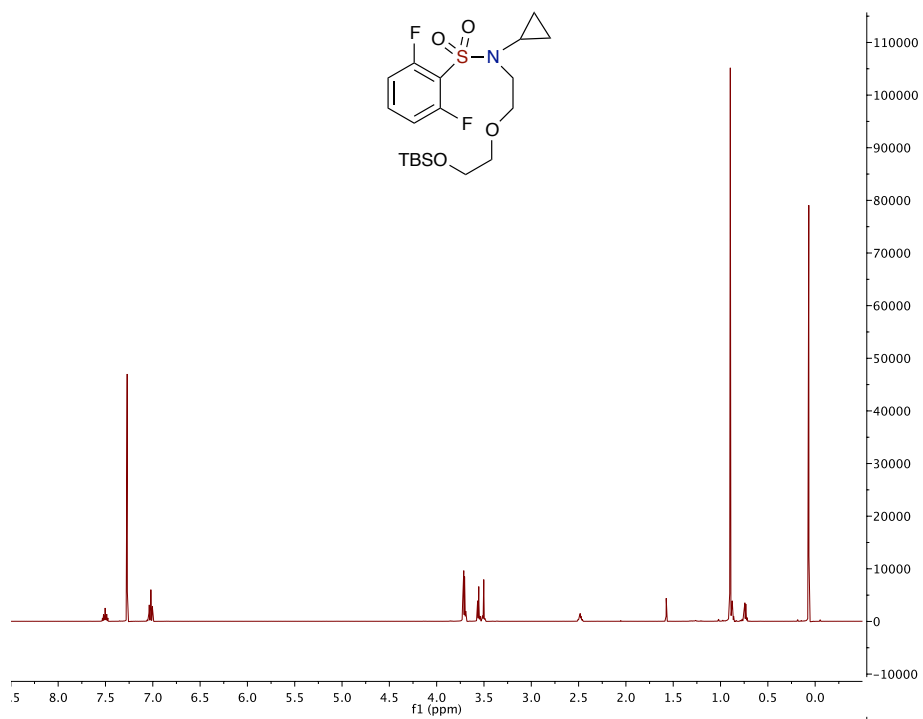
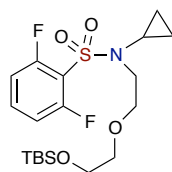
***N*-(4-((*tert*-butyldimethylsilyl)oxy)butyl)-*N*-cyclopropyl-2,4-difluorobenzene-sulfonamide (2.10.8)**



***N*-[4-(*tert*-butyldimethylsilyloxy)butyl]-*N*-cyclopropyl-2,6-difluorobenzene-sulfonamide (2.10.9)**

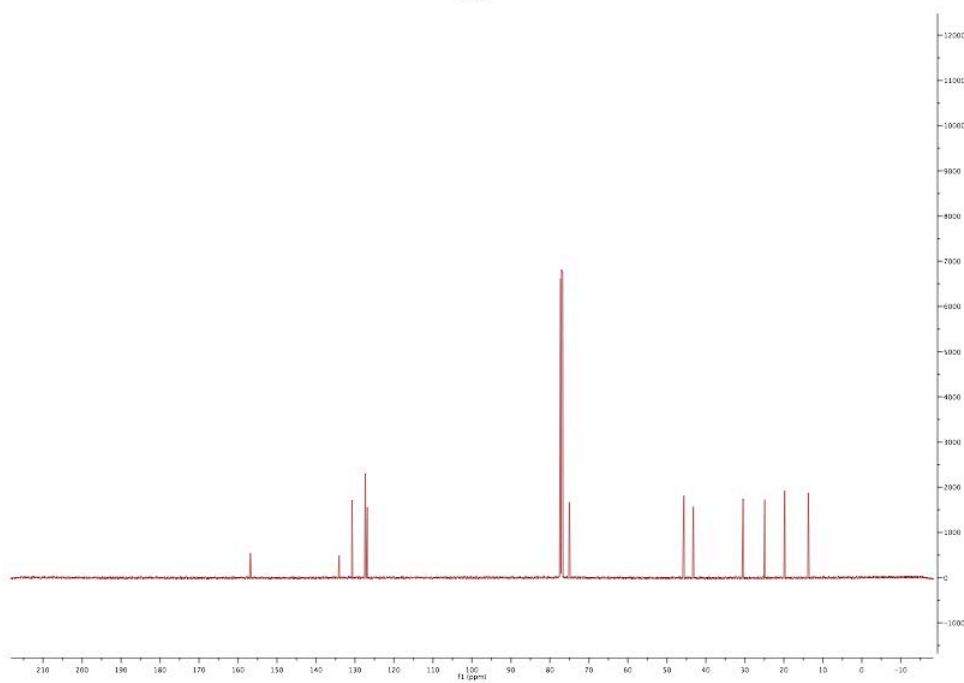
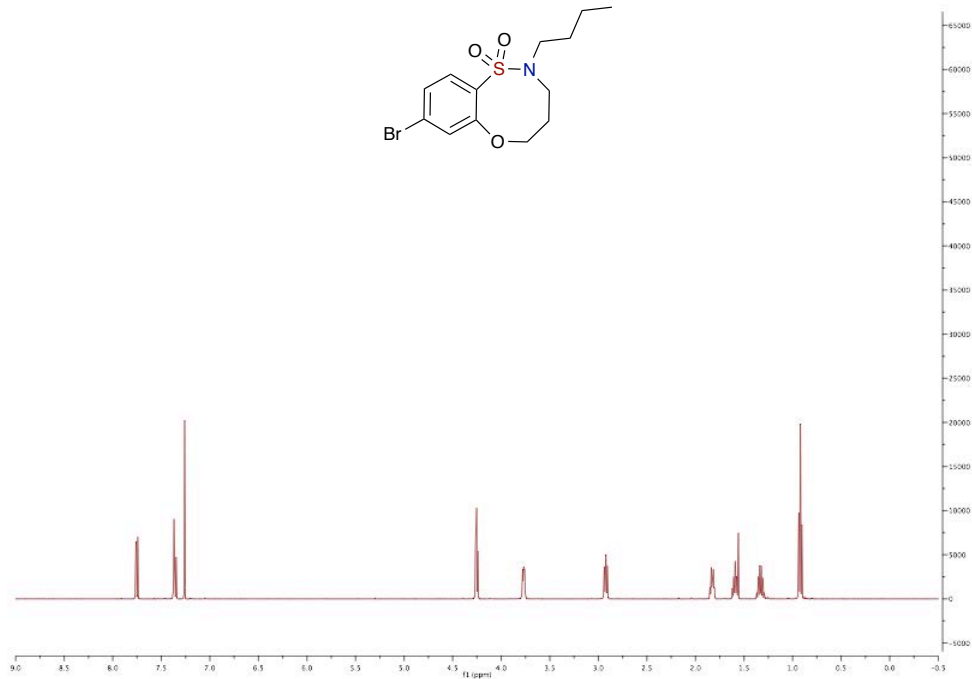
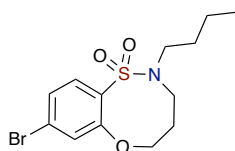


***N*-(2-(2-((*tert*-butyldimethylsilyl)oxy)ethoxy)ethyl)-*N*-cyclopropyl-2,6-difluorobenzenesulfonamide (SI-4)**

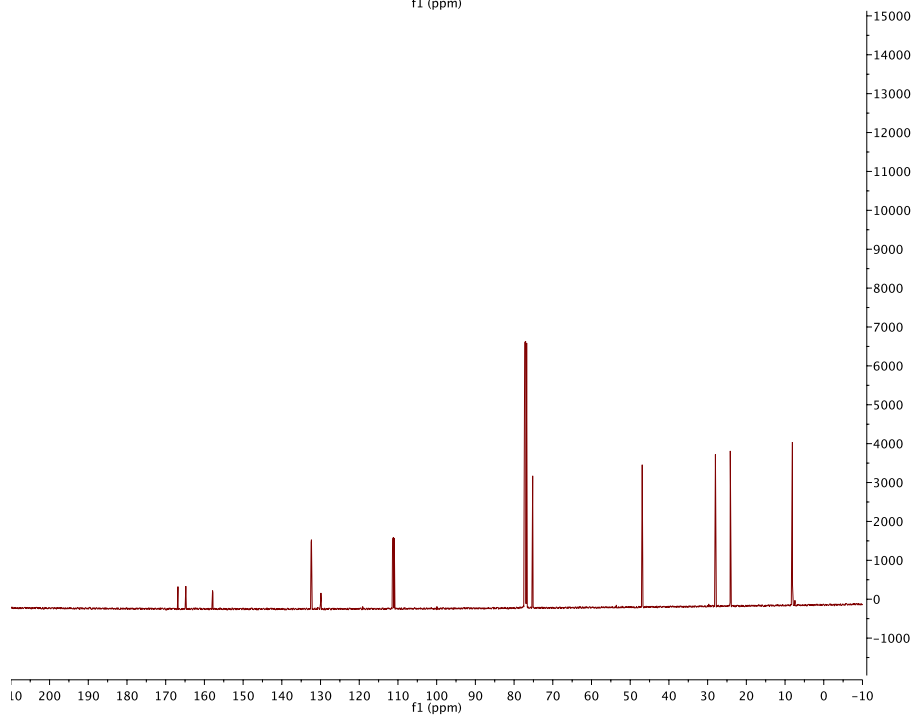
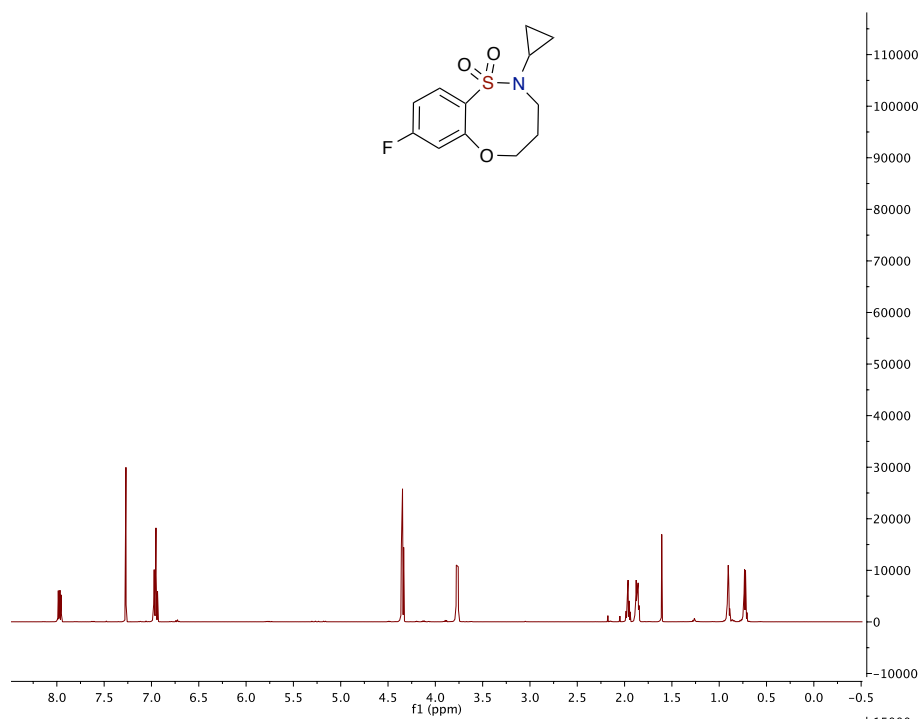
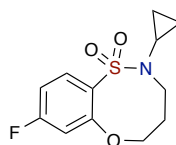


**8-Bromo-2-butyl-2,3,4,5-tetrahydrobenzo[*b*][1,4,5]oxathiazocine
(2.10.11)**

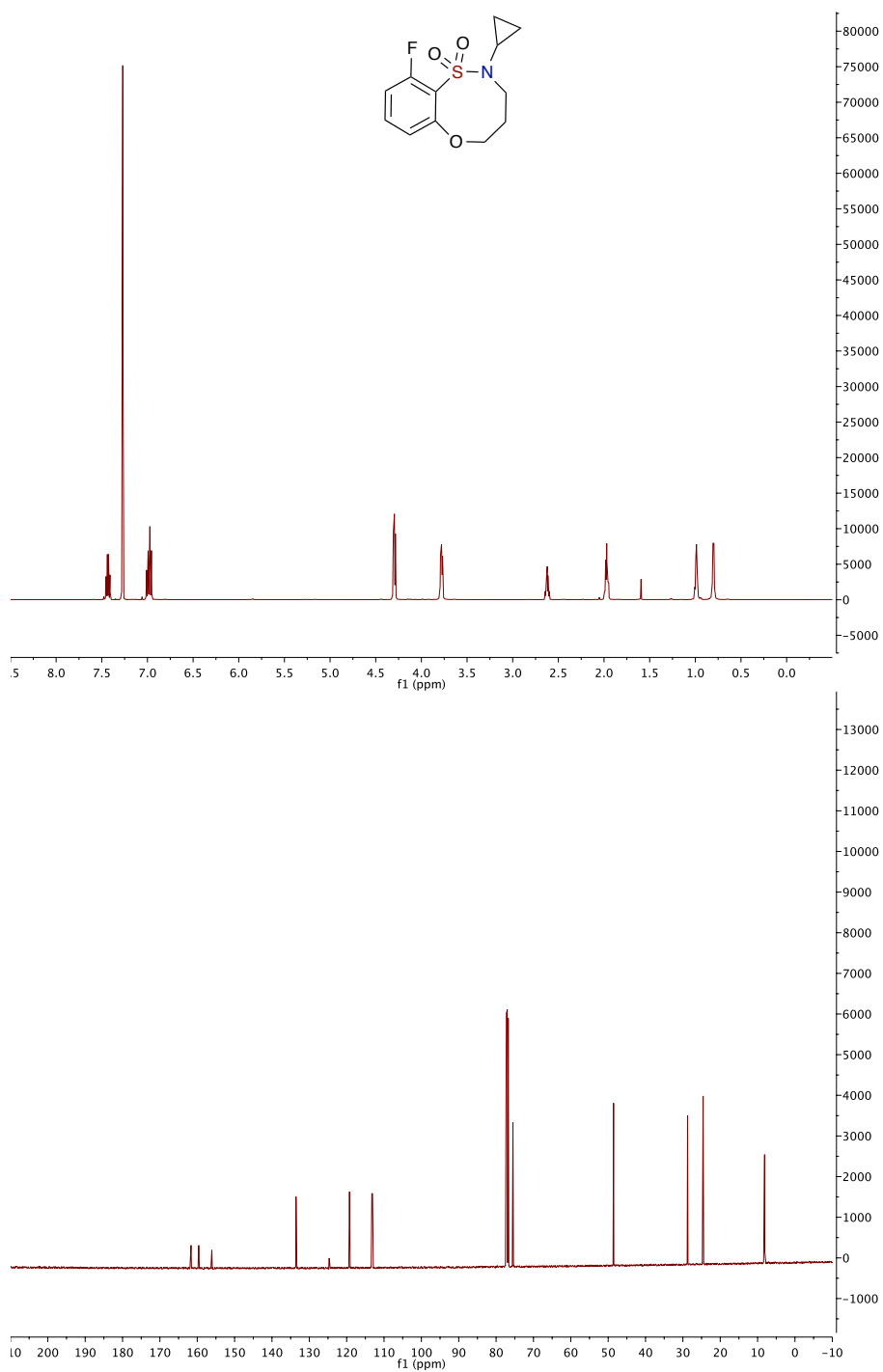
1,1-dioxide



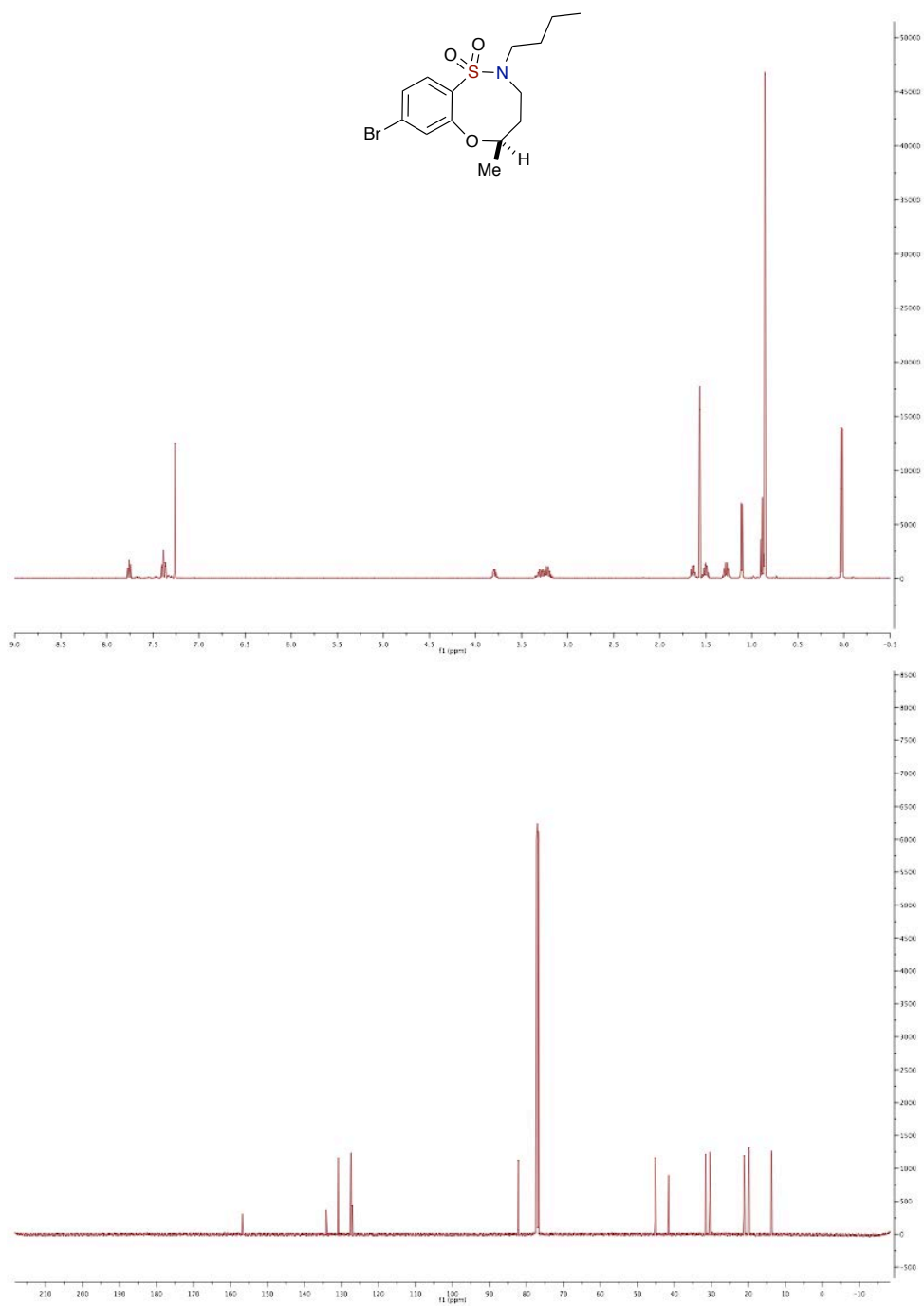
2-cyclopropyl-8-fluoro-2,3,4,5-tetrahydrobenzo[*b*][1,4,5]oxathiazocine 1,1-dioxide
(2.10.12)



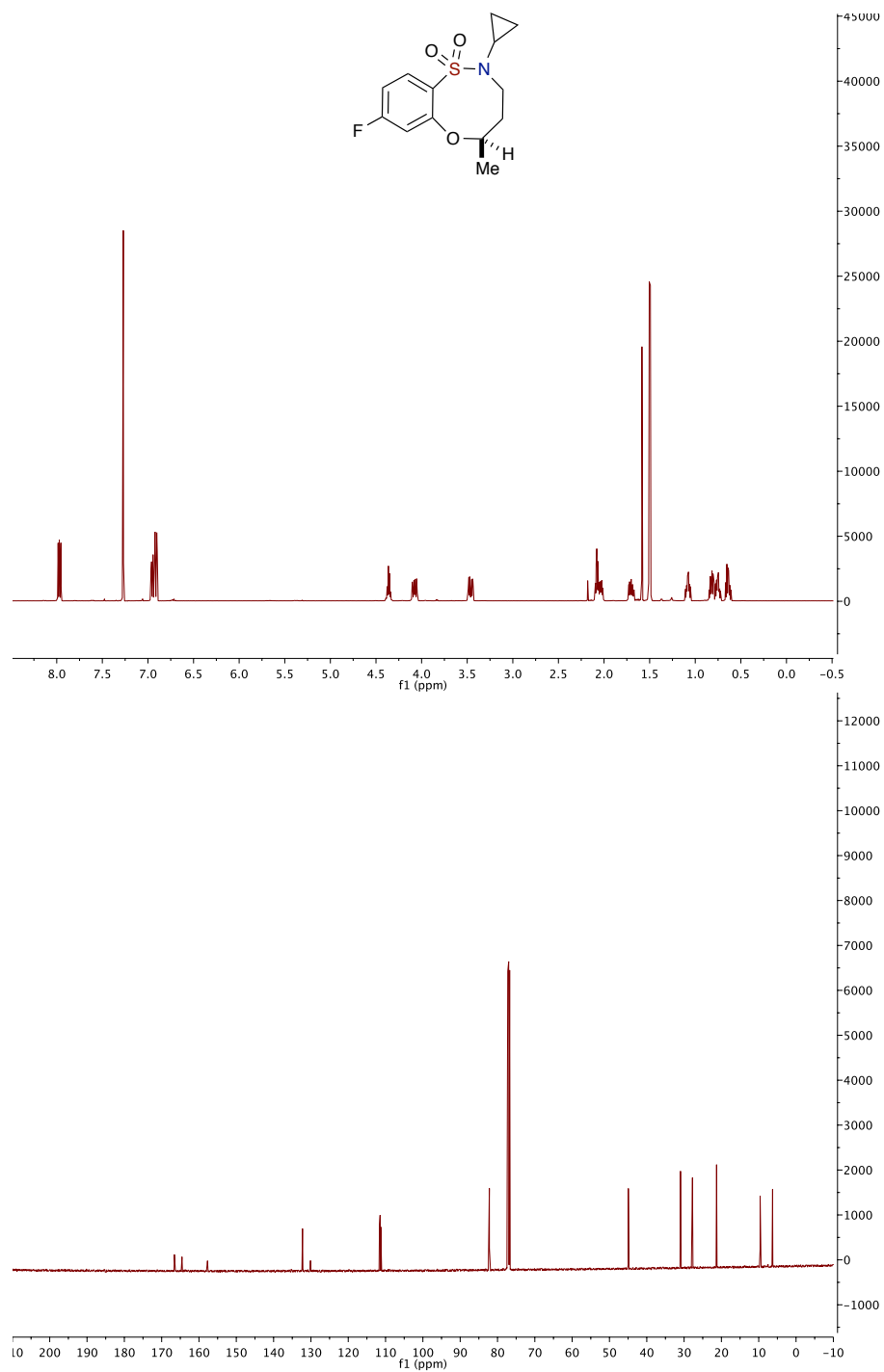
2-cyclopropyl-10-fluoro-2,3,4,5-tetrahydrobenzo[*b*][1,4,5]oxathiazocine 1,1-dioxide (2.10.13)



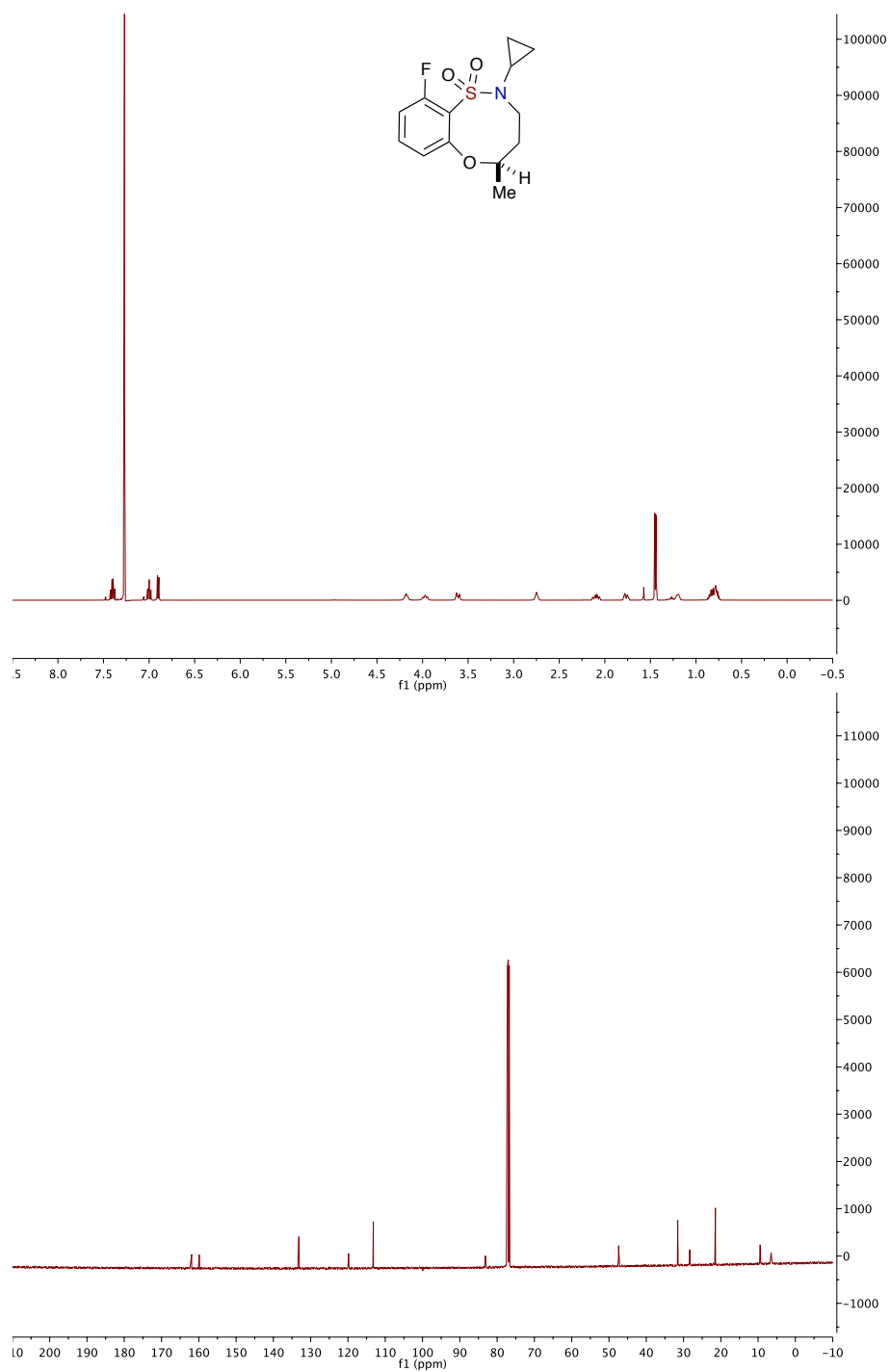
(R)-8-Bromo-2-butyl-5-methyl-2,3,4,5-tetrahydrobenzo[*b*][1,4,5]oxathiazocine 1,1-dioxide (2.10.14)



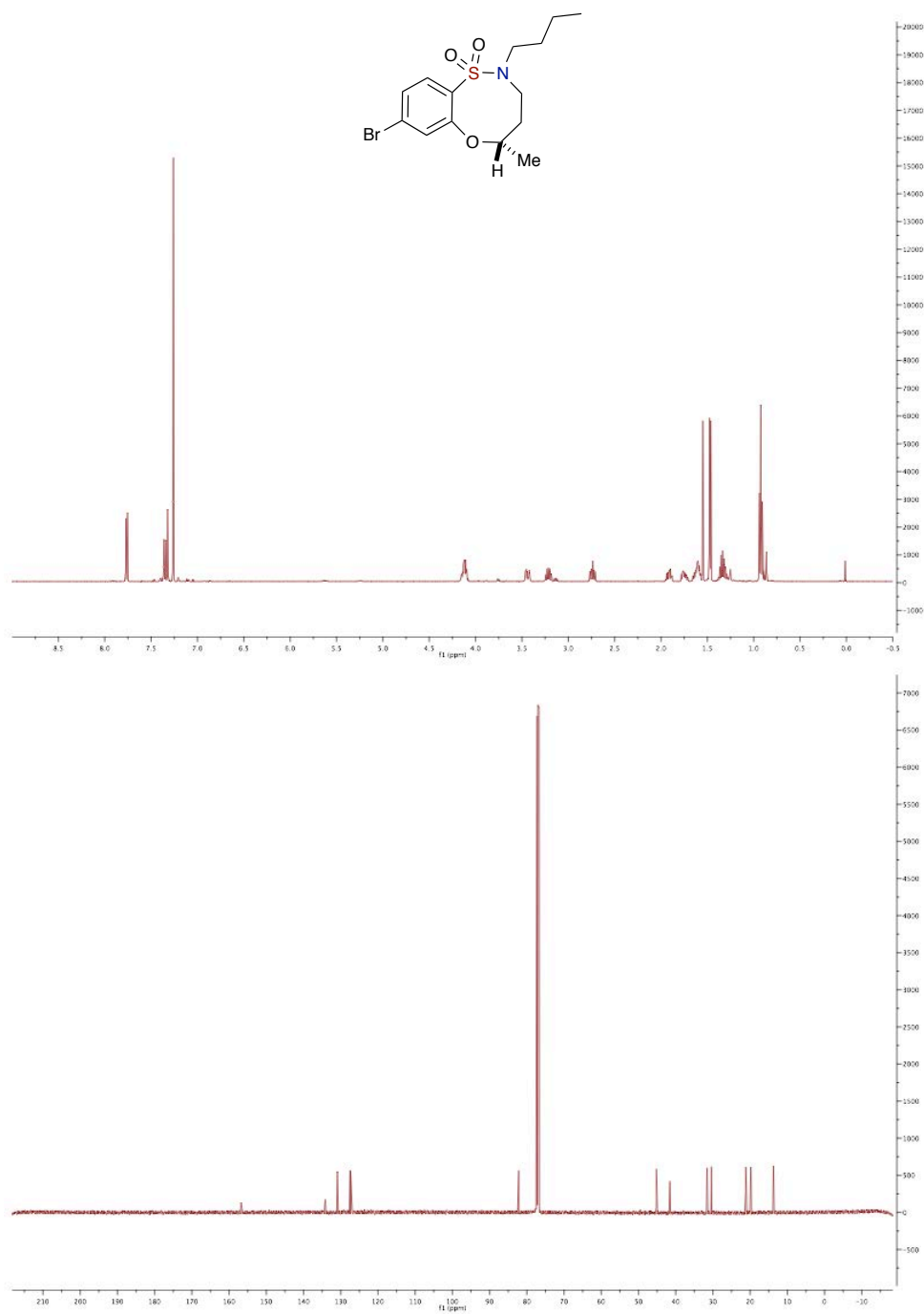
(R)-2-cyclopropyl-8-fluoro-5-methyl-2,3,4,5-tetrahydrobenzo[*b*][1,4,5]oxathiazocine 1,1-dioxide (2.10.15)



(R)-2-cyclopropyl-10-fluoro-5-methyl-2,3,4,5-tetrahydrobenzo[*b*][1,4,5]oxathiazocine 1,1-dioxide (2.10.16)

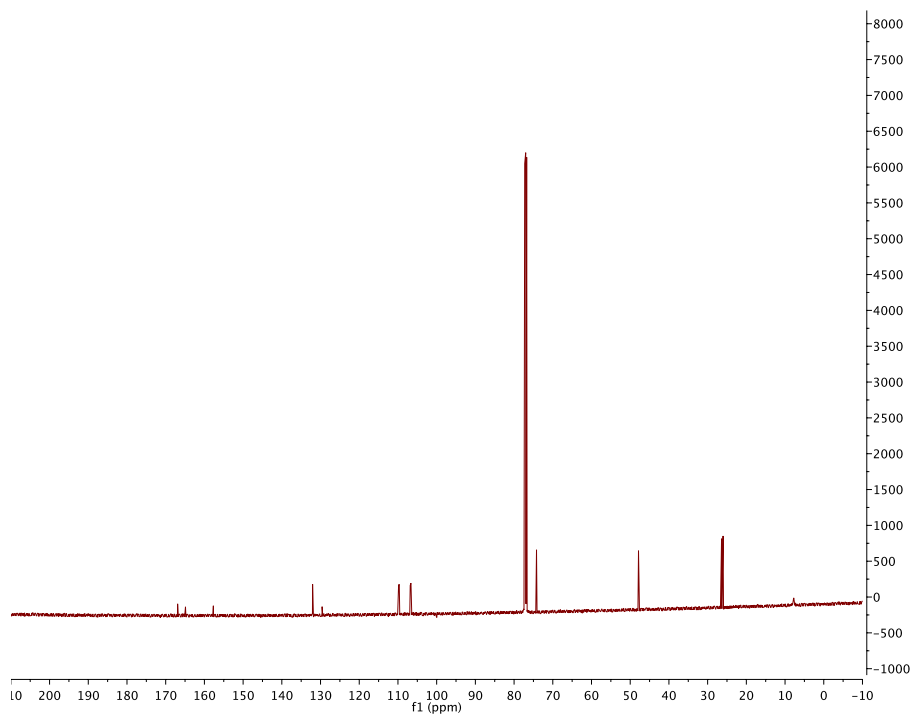
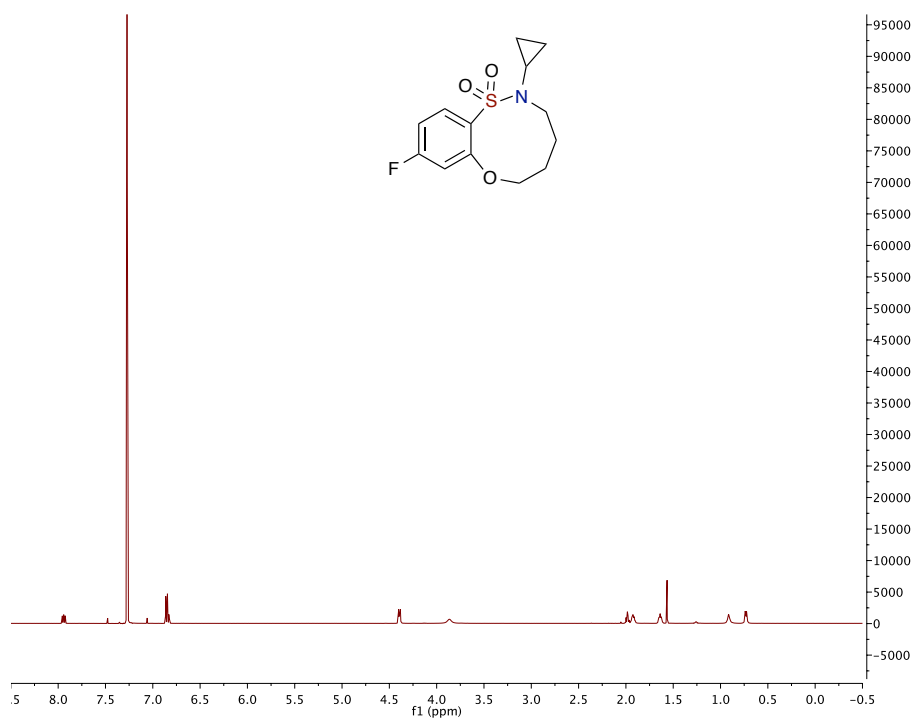


(S)-8-Bromo-2-butyl-5-methyl-2,3,4,5-tetrahydrobenzo[*b*][1,4,5]oxathiazocine 1,1-dioxide (2.10.17)



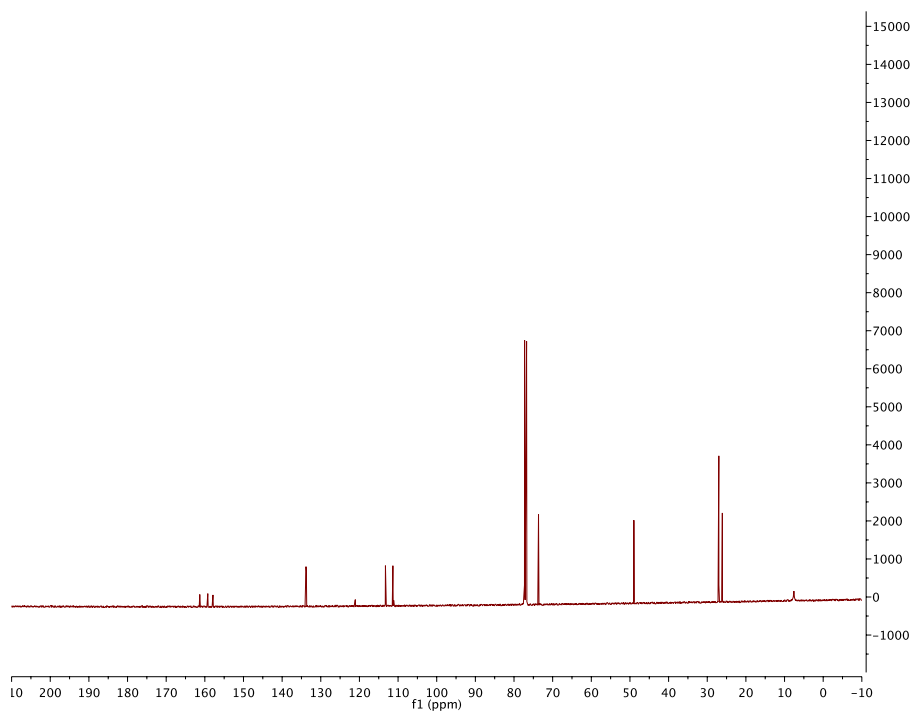
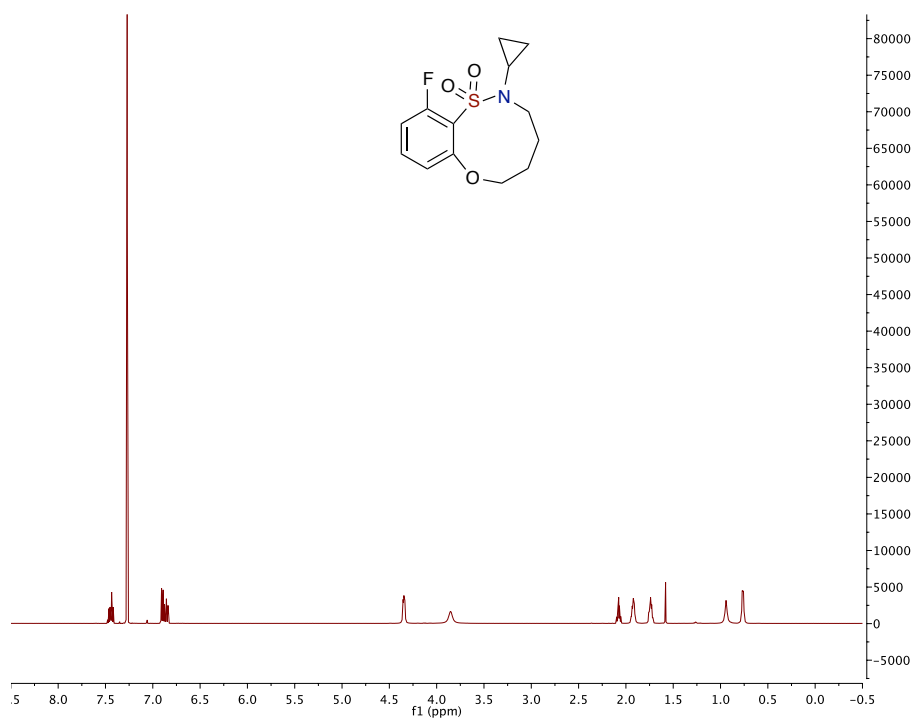
2-cyclopropyl-9-fluoro-3,4,5,6-tetrahydro-2H-benzo[b][1,4,5]oxathiazonine dioxide (2.10.18)

1,1-

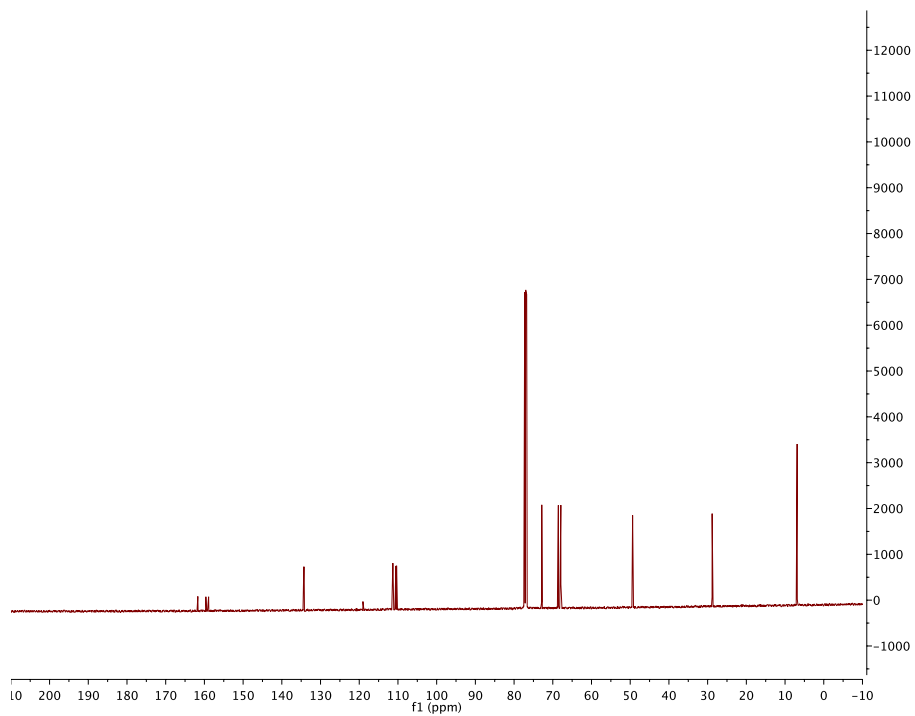
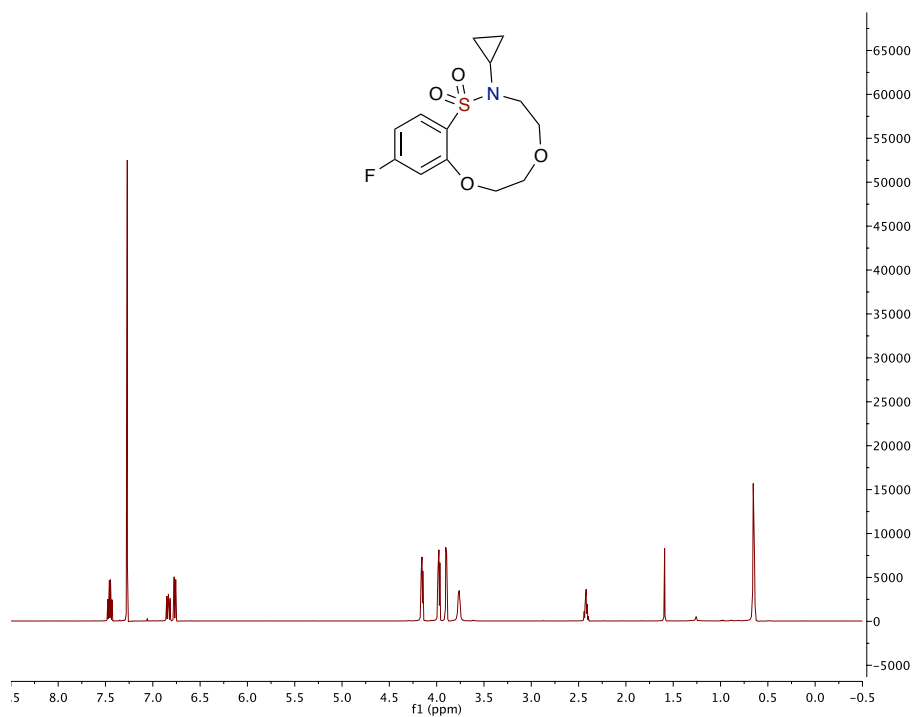


**2-cyclopropyl-11-fluoro-3,4,5,6-tetrahydro-2H-benzo[*b*][1,4,5]oxathiazonine
dioxide (2.10.19)**

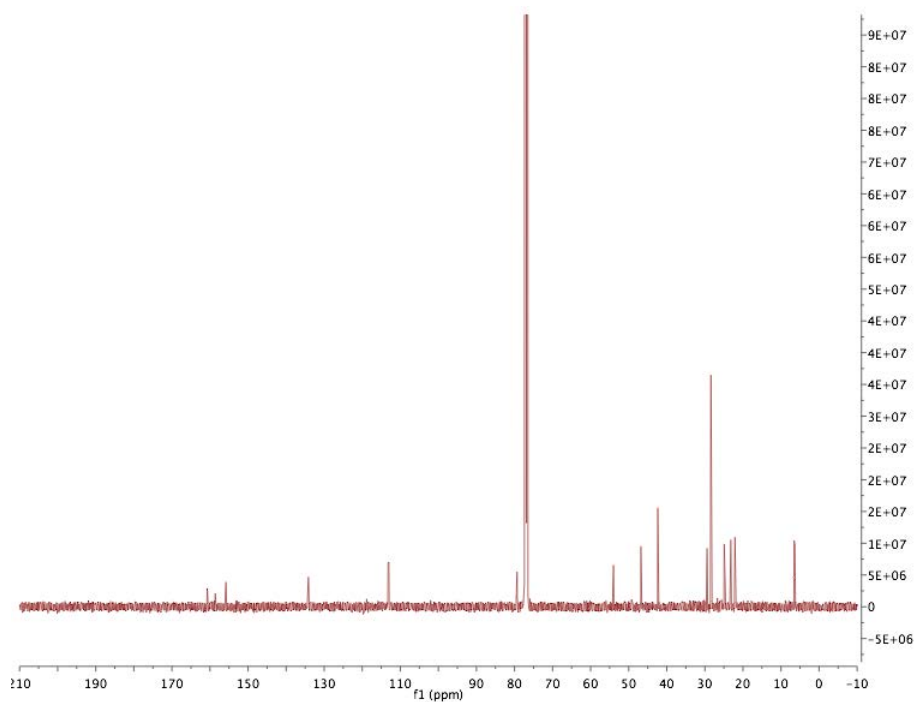
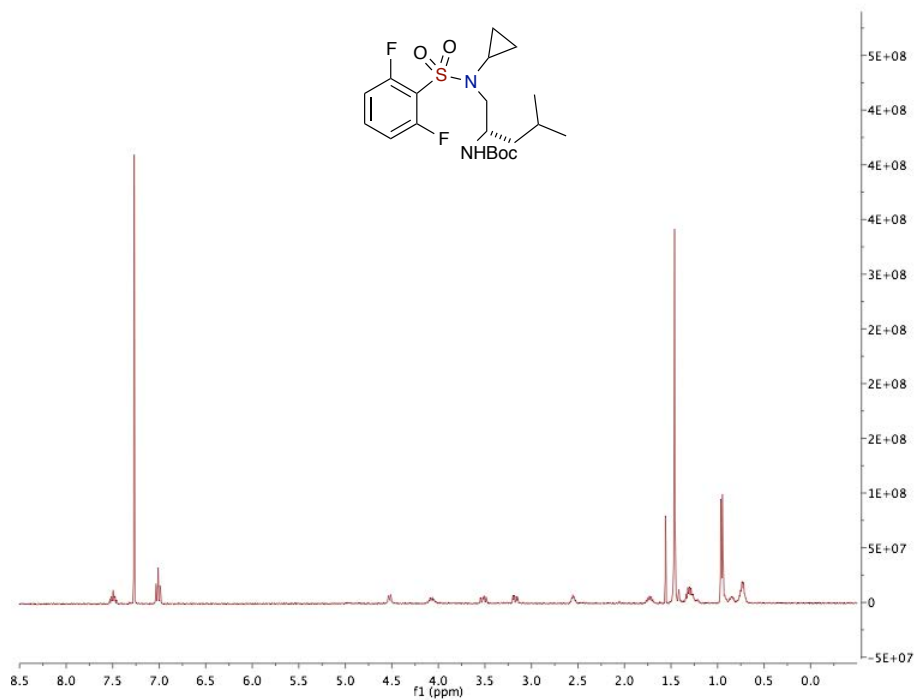
1,1-



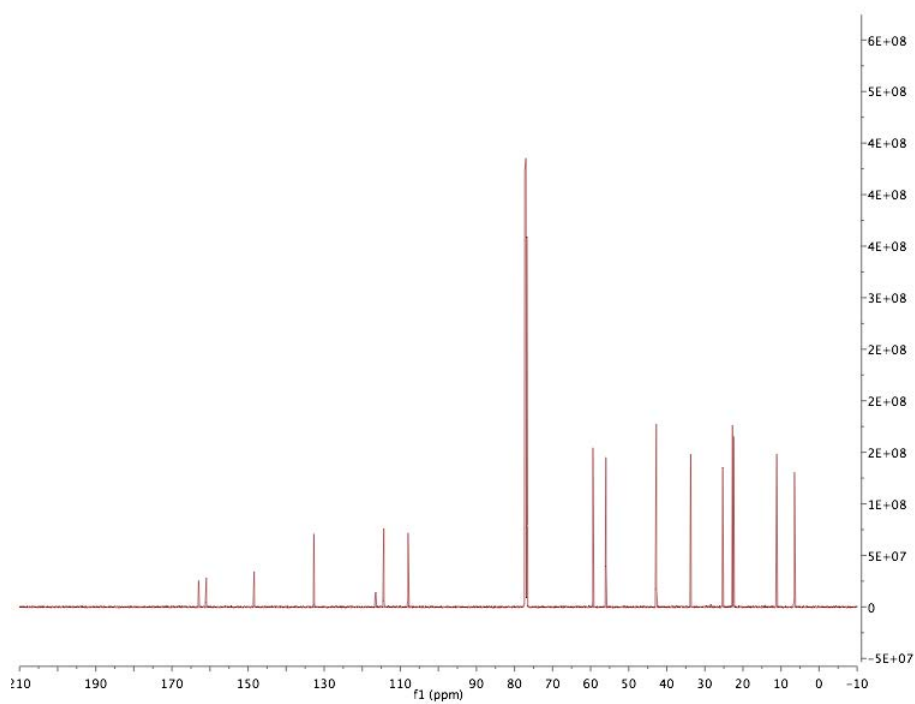
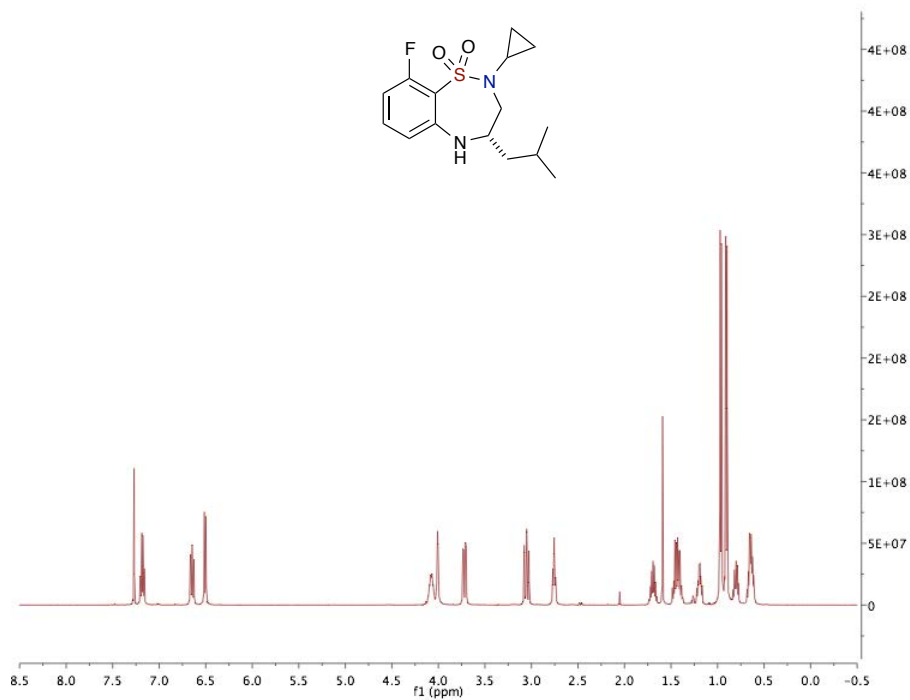
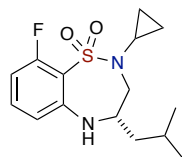
2-cyclopropyl-10-fluoro-3,4,6,7-tetrahydro-2H-benzo[e][1,4,7,8]dioxathiazecine 1,1-dioxide (2.10.20)



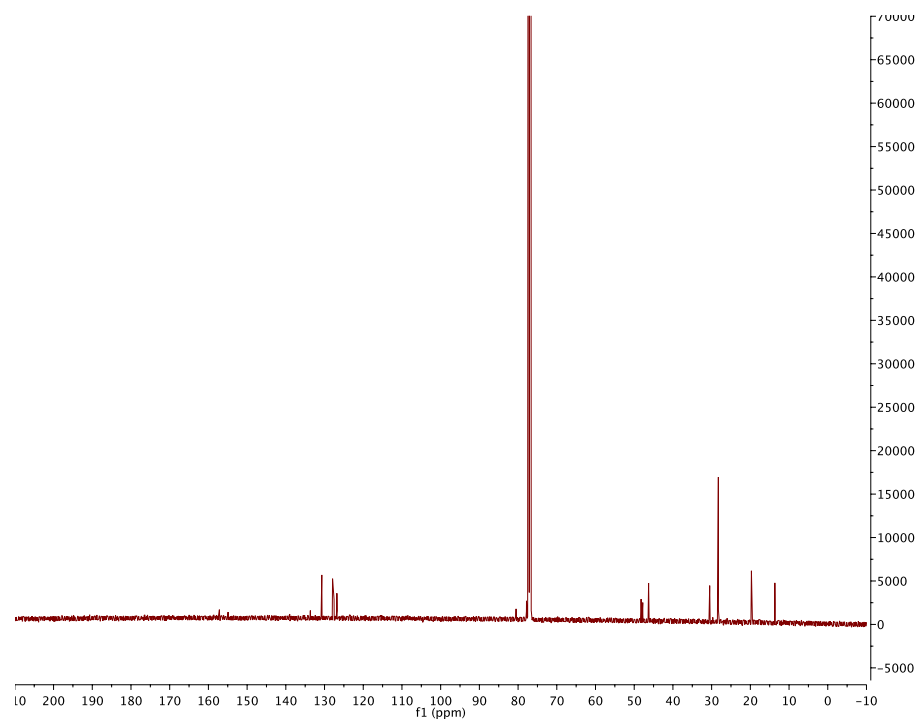
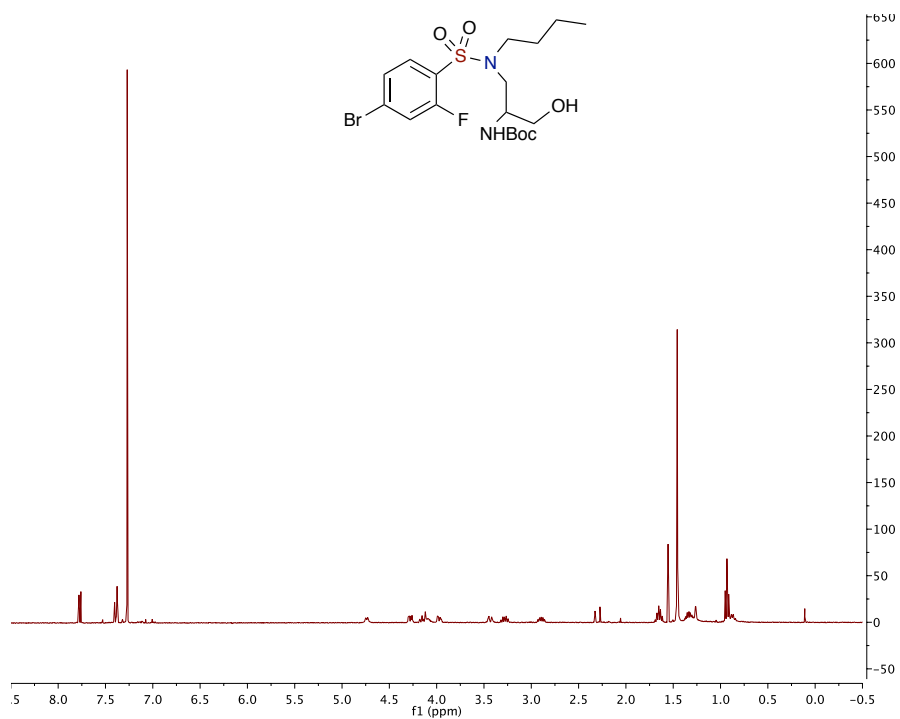
(S)-tert-butyl (1-(N-cyclopropyl-2,6-difluorophenylsulfonamido)-4-methylpentan-2-yl)carbamate (2.11.2)



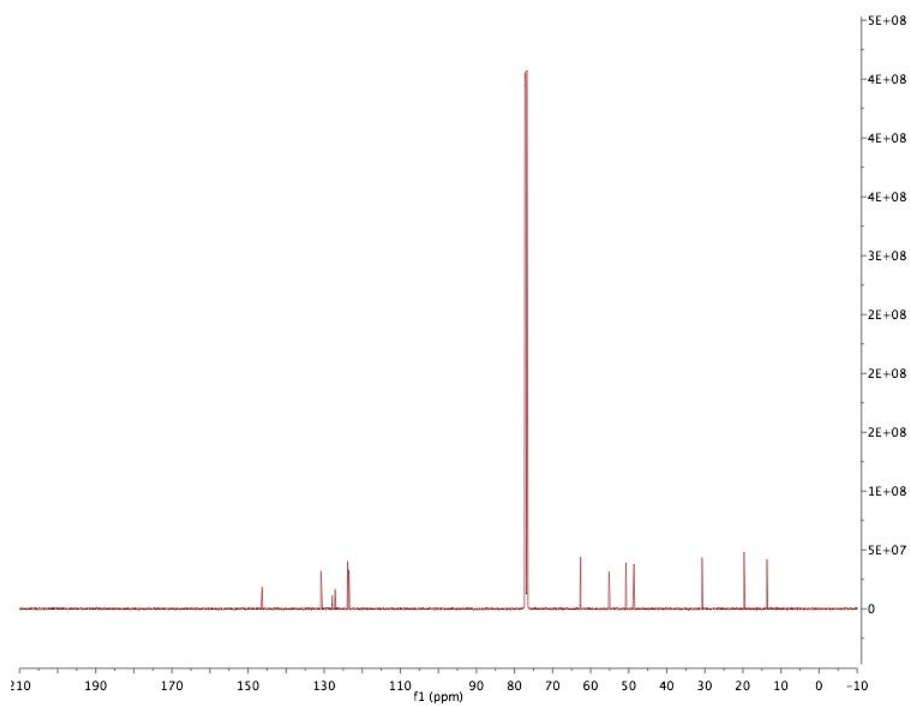
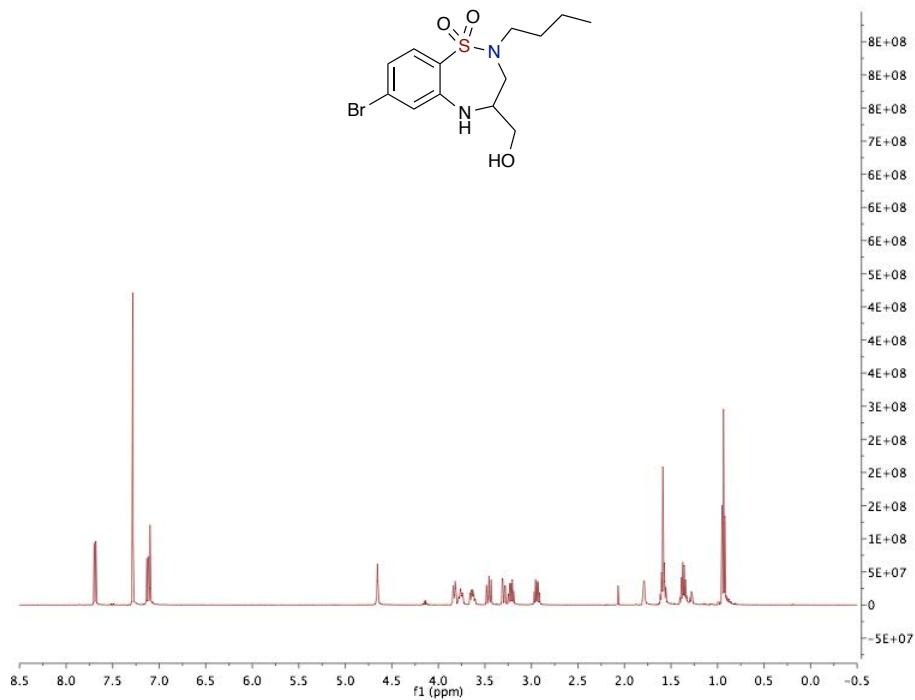
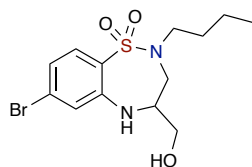
(S)-2-cyclopropyl-9-fluoro-4-isobutyl-2,3,4,5-tetrahydrobenzo[f][1,2,5]thiadiazepine 1,1-dioxide (2.11.3)



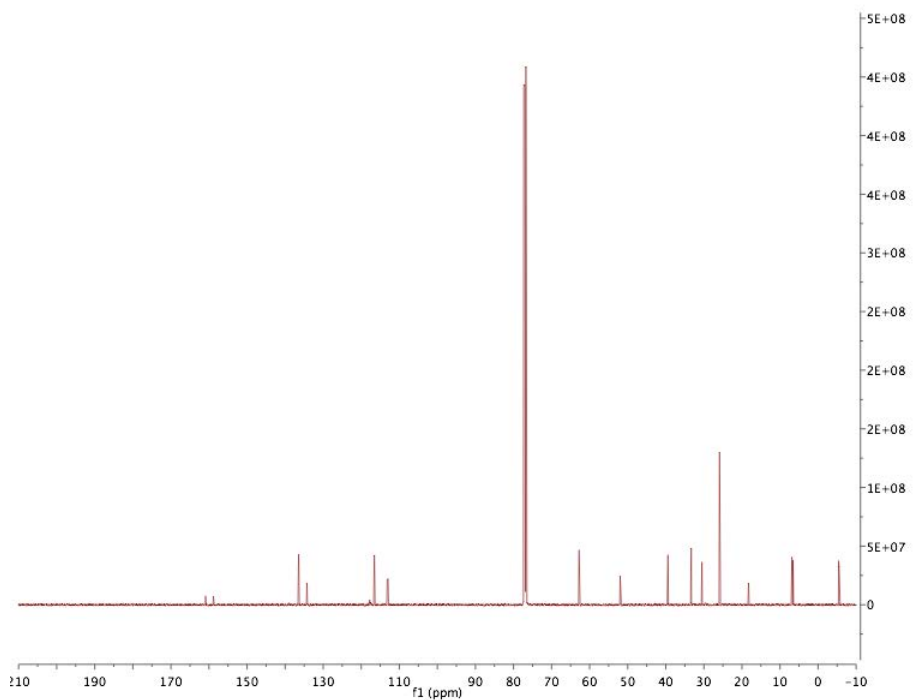
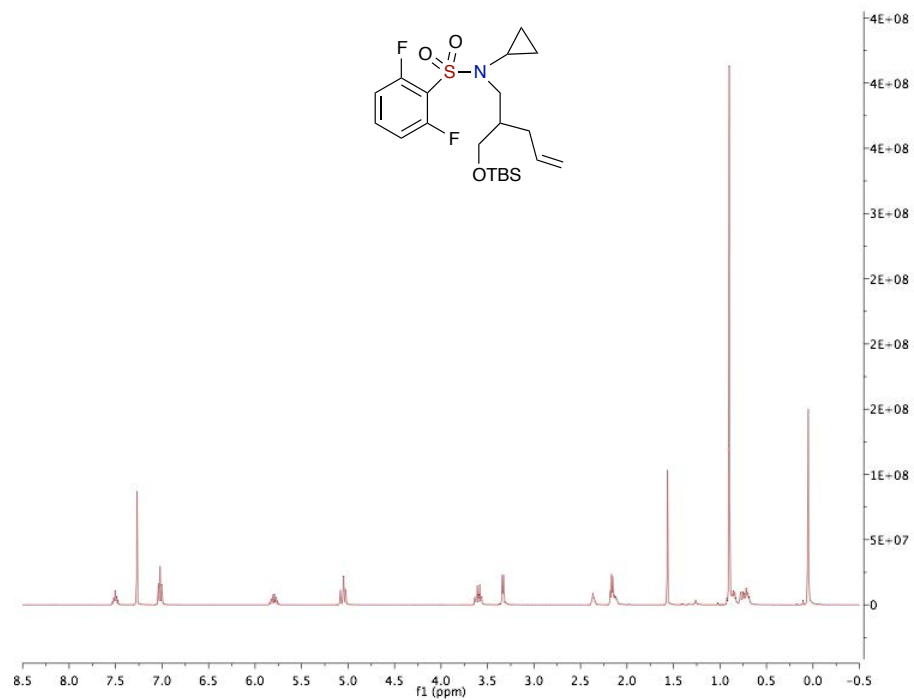
***tert*-butyl (1-(4-bromo-*N*-butyl-2-fluorophenylsulfonamido)-3-hydroxypropan-2-yl)-
carbamate (SI-5)**



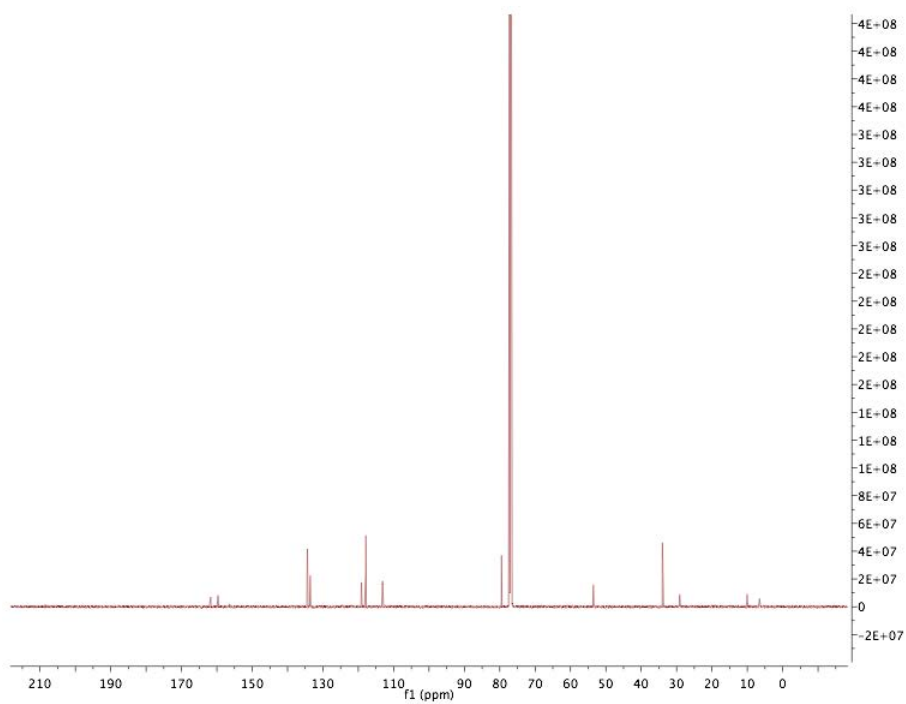
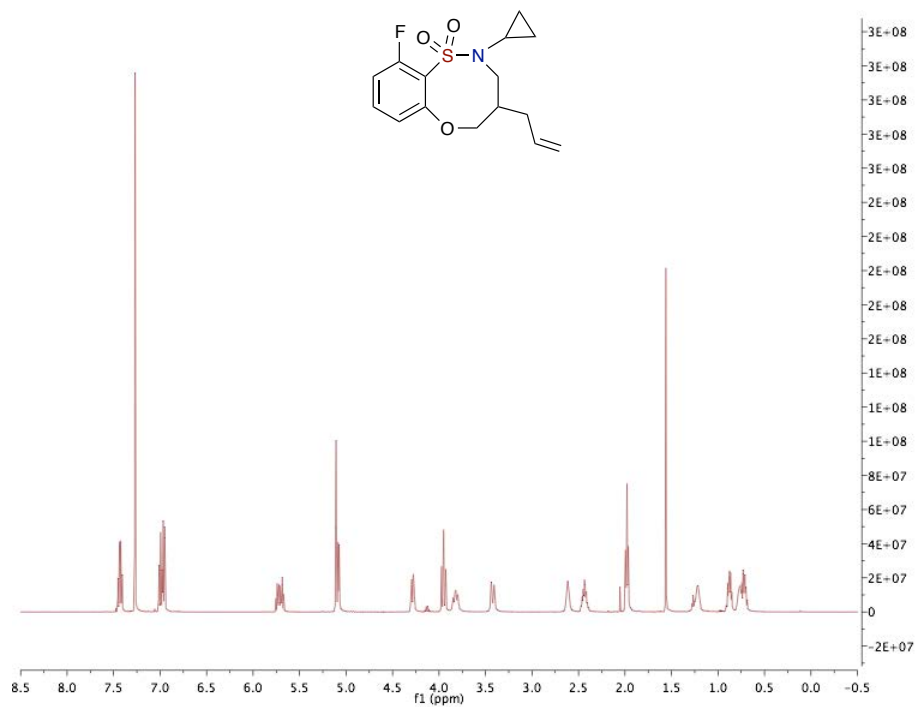
7-bromo-2-butyl-4-(hydroxymethyl)-2,3,4,5-tetrahydrobenzo[f][1,2,5]thiadiazepine 1,1-dioxide (2.11.4)



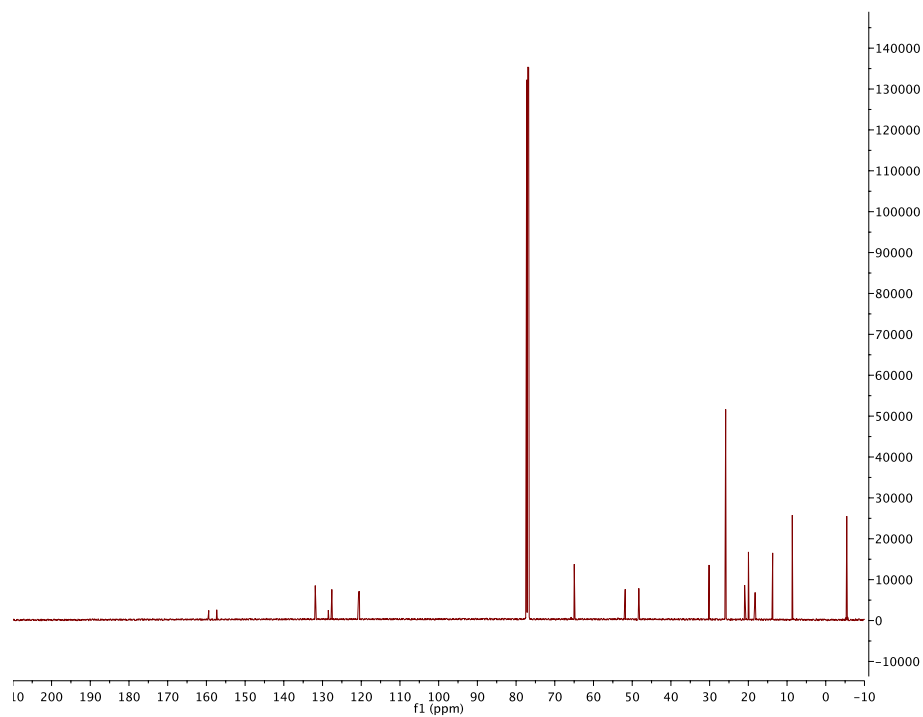
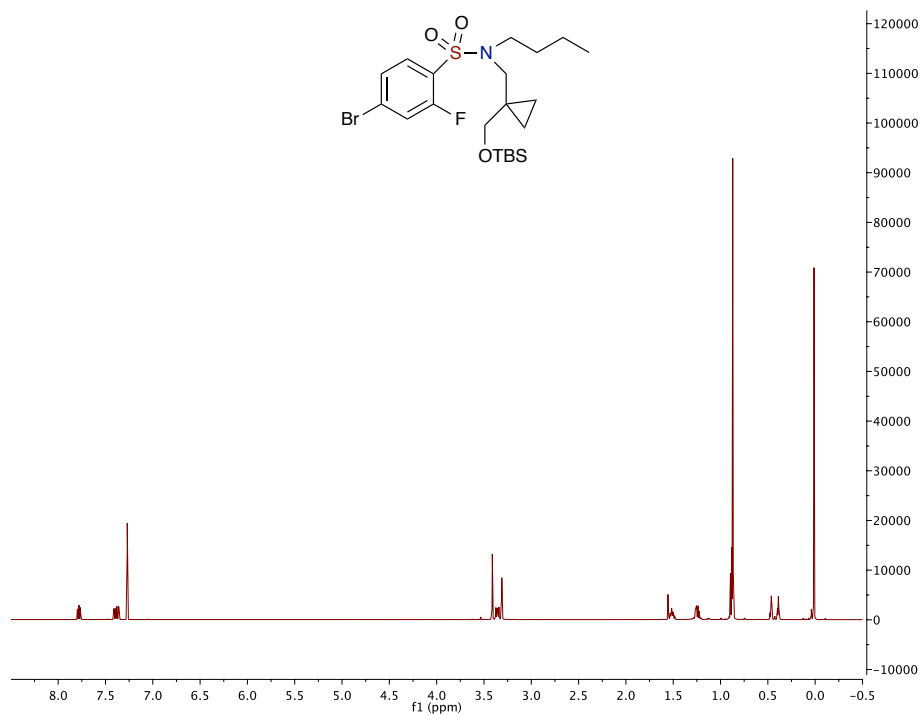
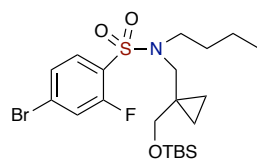
(R)-N-(2-(((*tert*-butyldimethylsilyl)oxy)methyl)pent-4-en-1-yl)-N-cyclopropyl-2,6-difluorobenzenesulfonamide (SI-6)



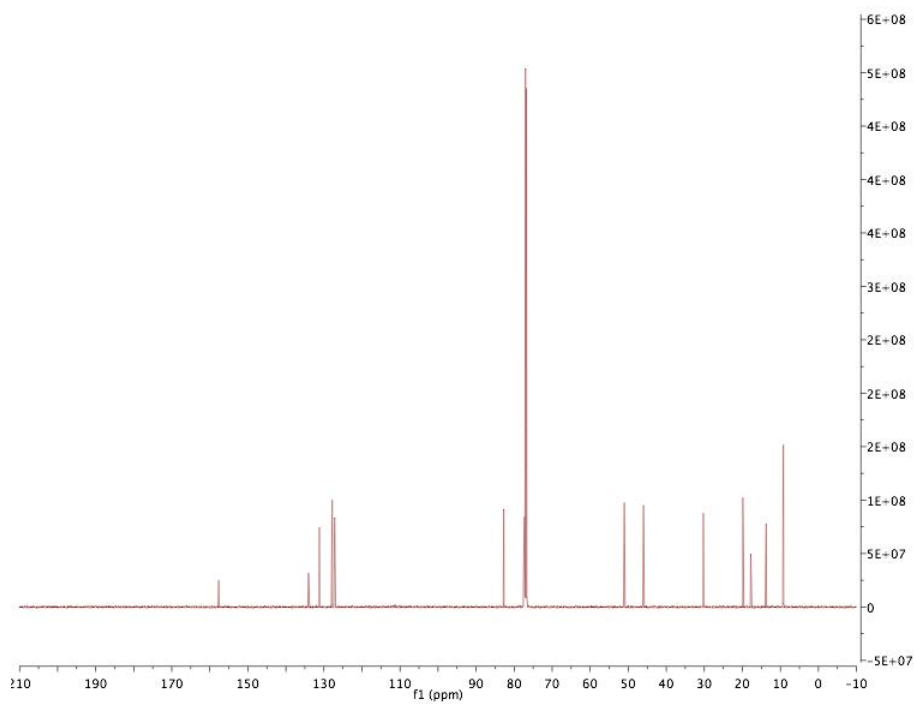
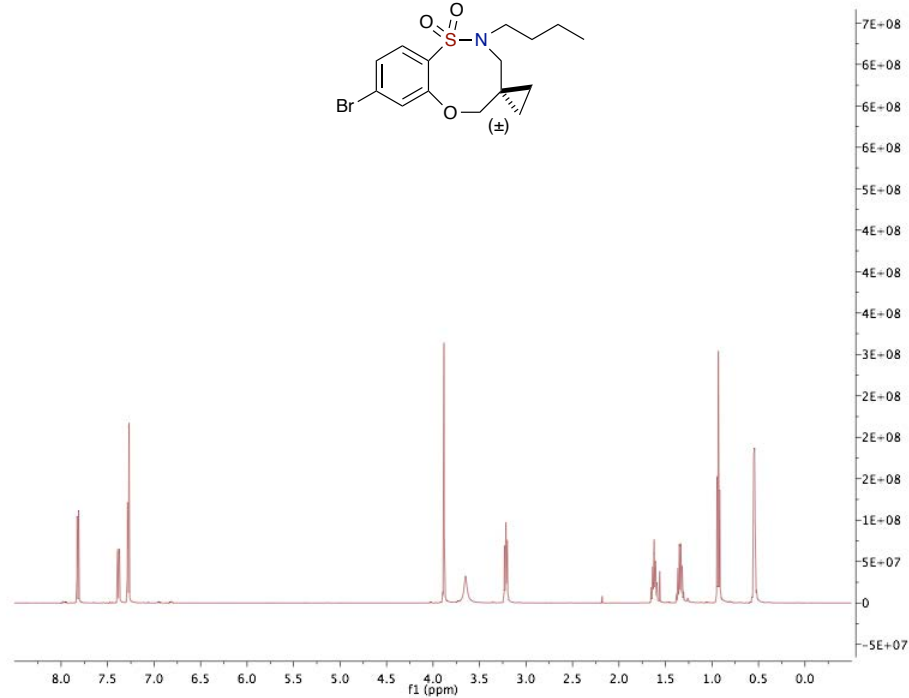
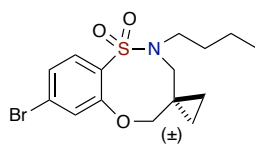
4-allyl-2-cyclopropyl-10-fluoro-2,3,4,5-tetrahydrobenzo[*b*][1,4,5]oxathiazocine 1,1-dioxide (2.11.5)



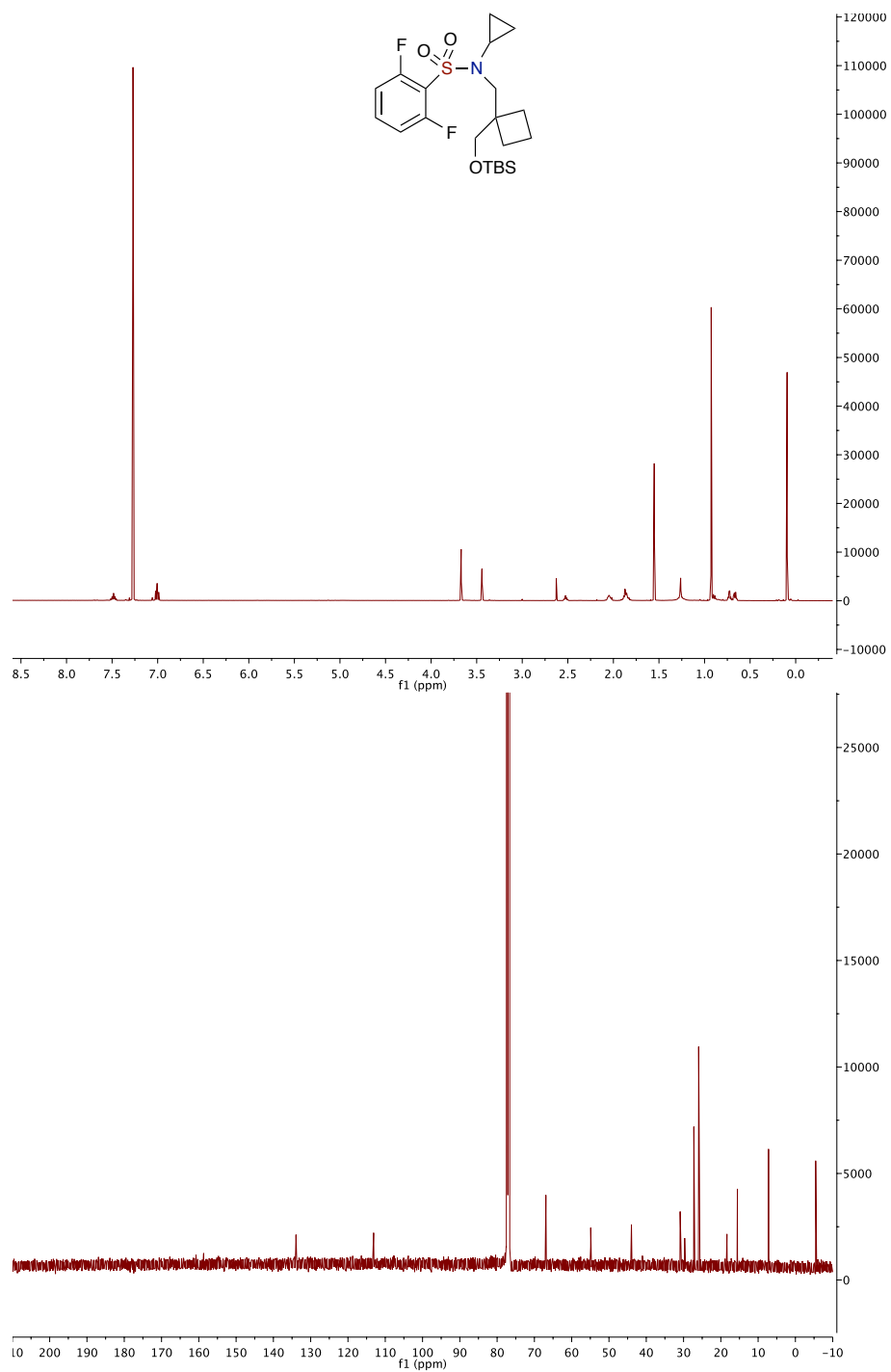
4-bromo-N-butyl-N-((1-(((*tert*-butyldimethylsilyl)oxy)methyl)cyclopropyl)methyl)-2-fluorobenzenesulfonamide (SI-7)



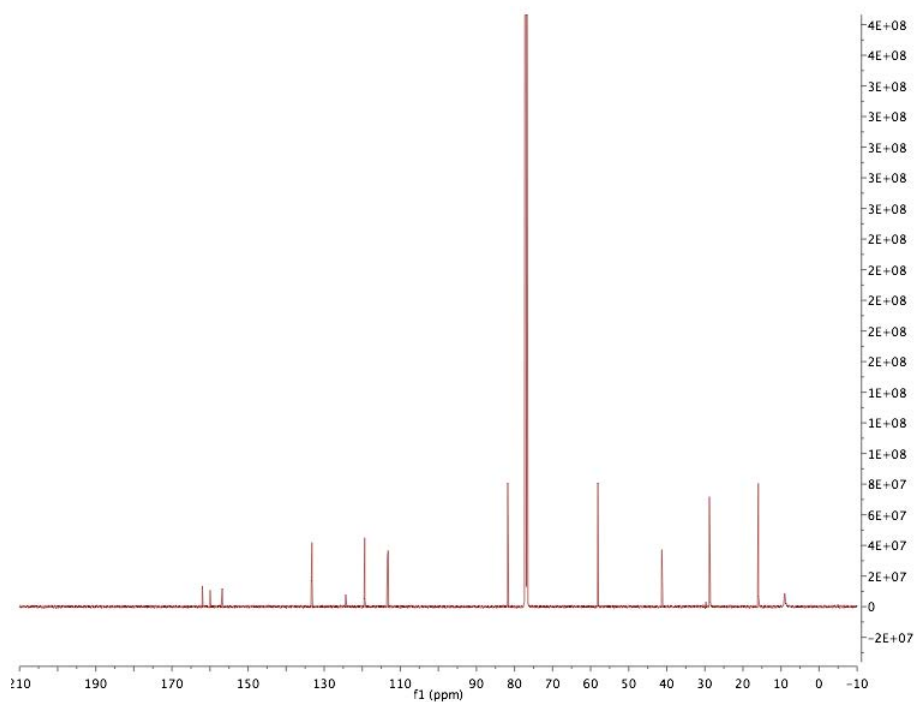
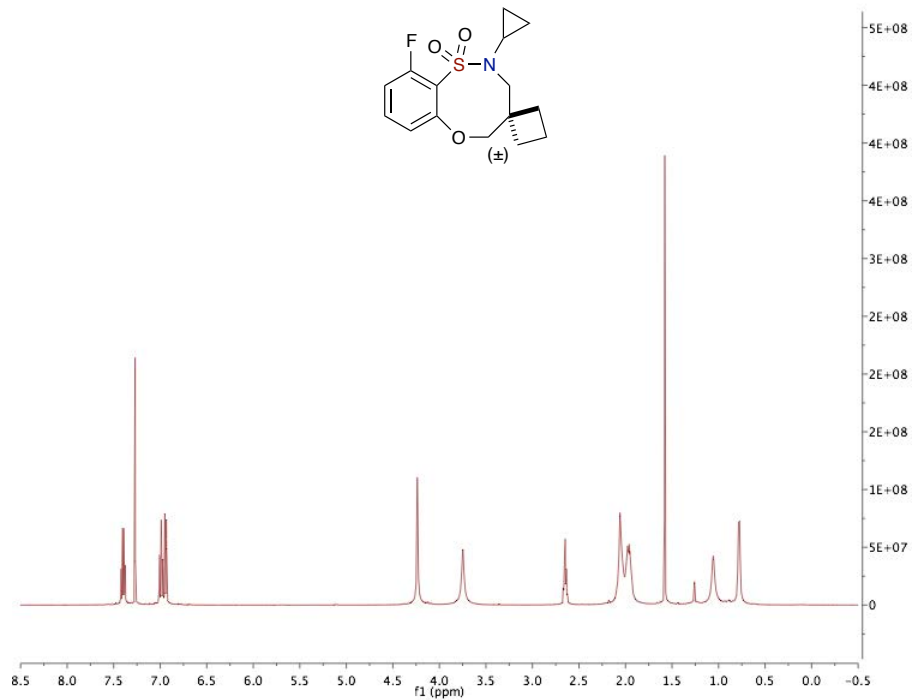
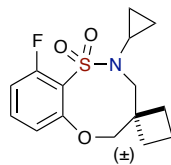
8-bromo-2-butyl-3,5-dihydro-2H-spiro[benzo[*b*][1,4,5]oxathiazocine-4,1'-cyclopropane] 1,1-dioxide (2.11.6)



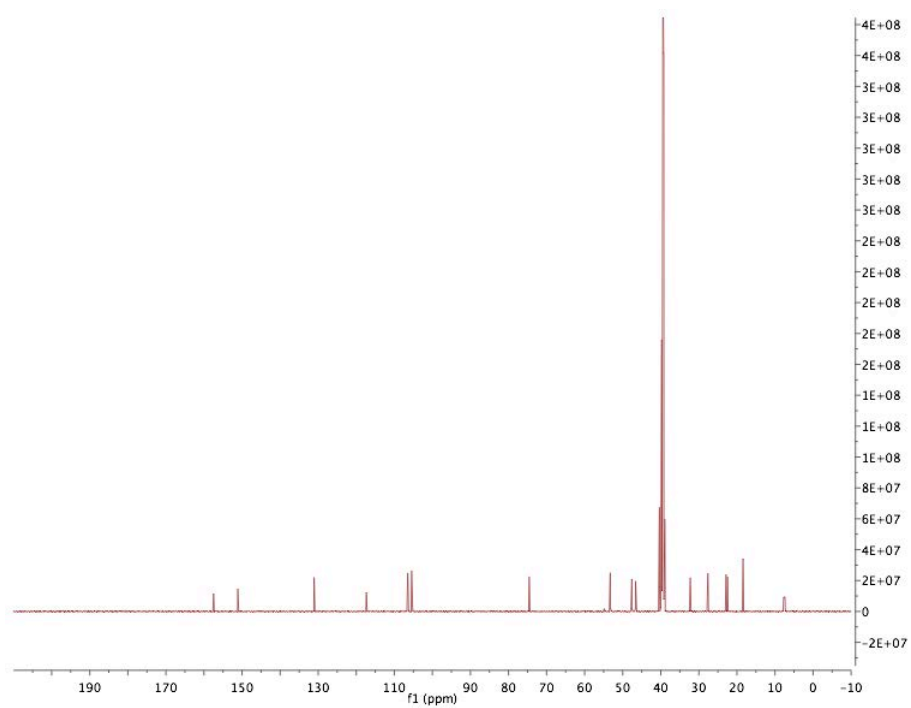
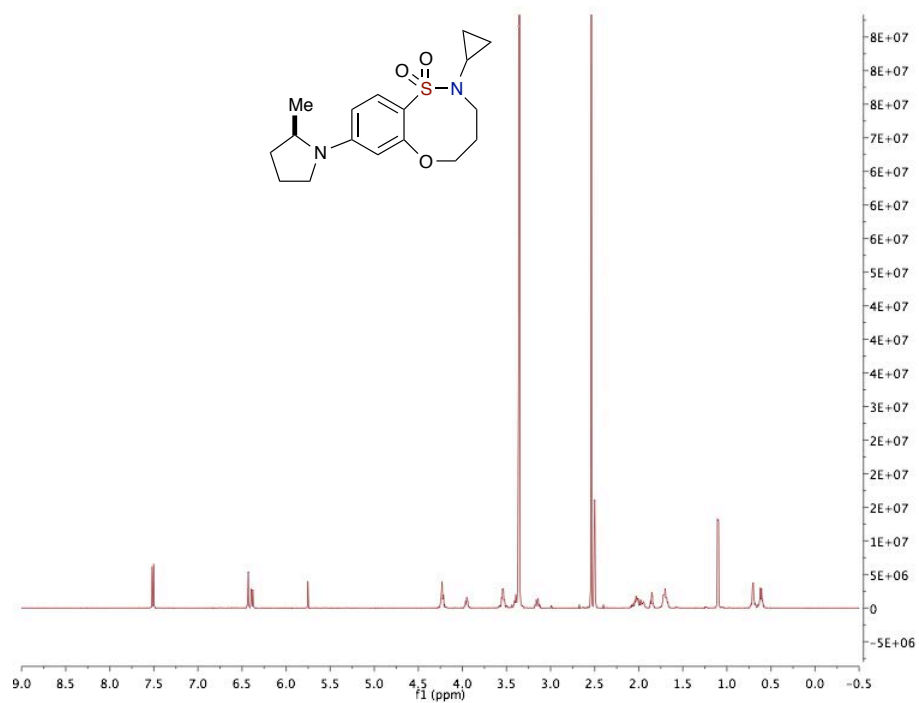
***N*-((1-(((*tert*-butyldimethylsilyl)oxy)methyl)cyclobutyl)methyl)-*N*-cyclopropyl-2,6-difluorobenzenesulfonamide (SI-8)**



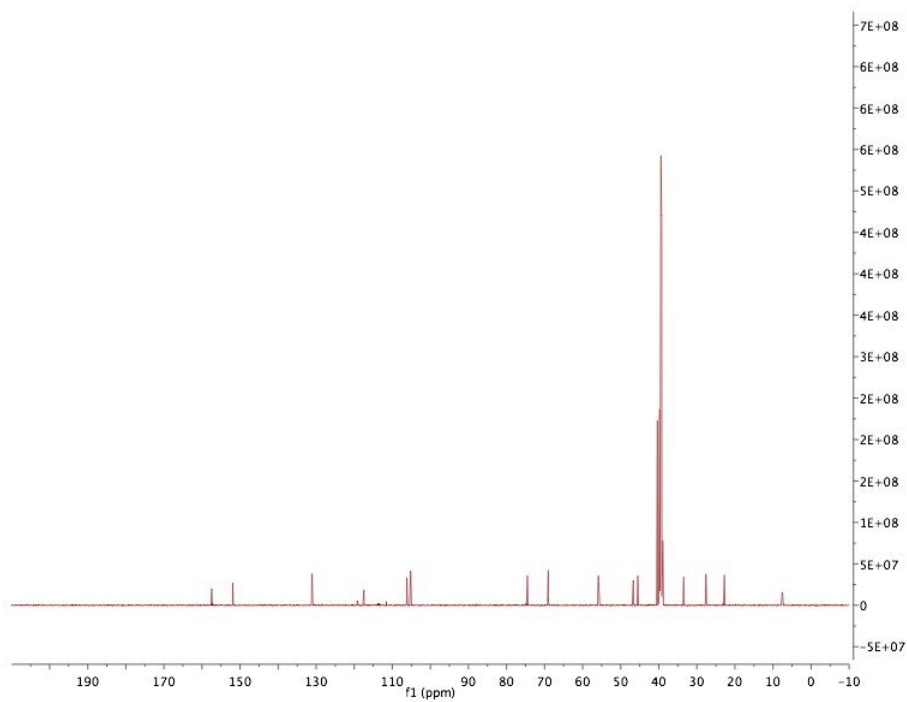
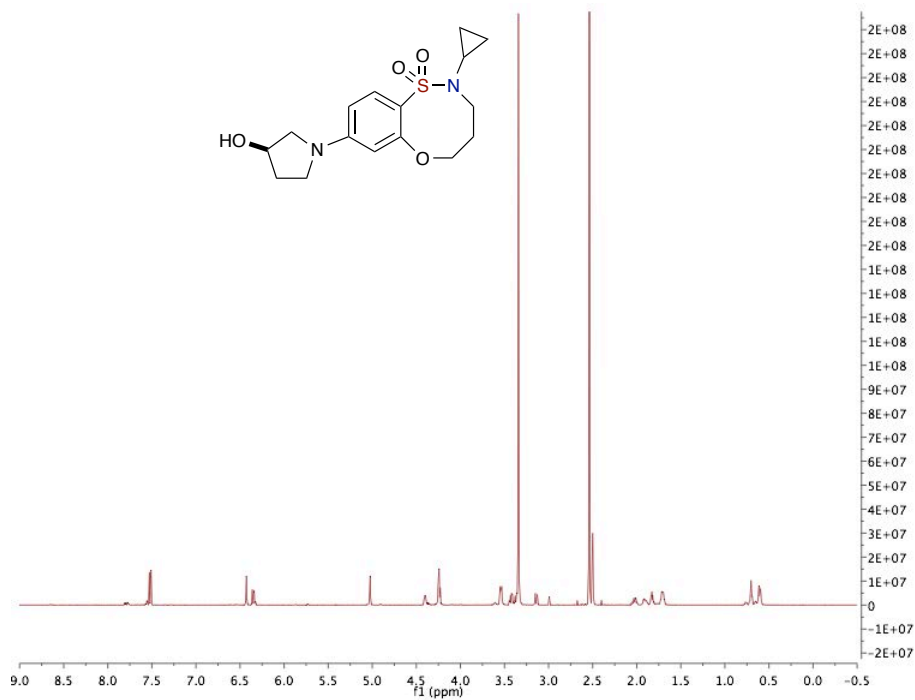
2-cyclopropyl-10-fluoro-3,5-dihydro-2*H*-spiro[benzo[*b*][1,4,5]oxathiazocine-4,1'-cyclobutane] 1,1-dioxide (2.11.7)



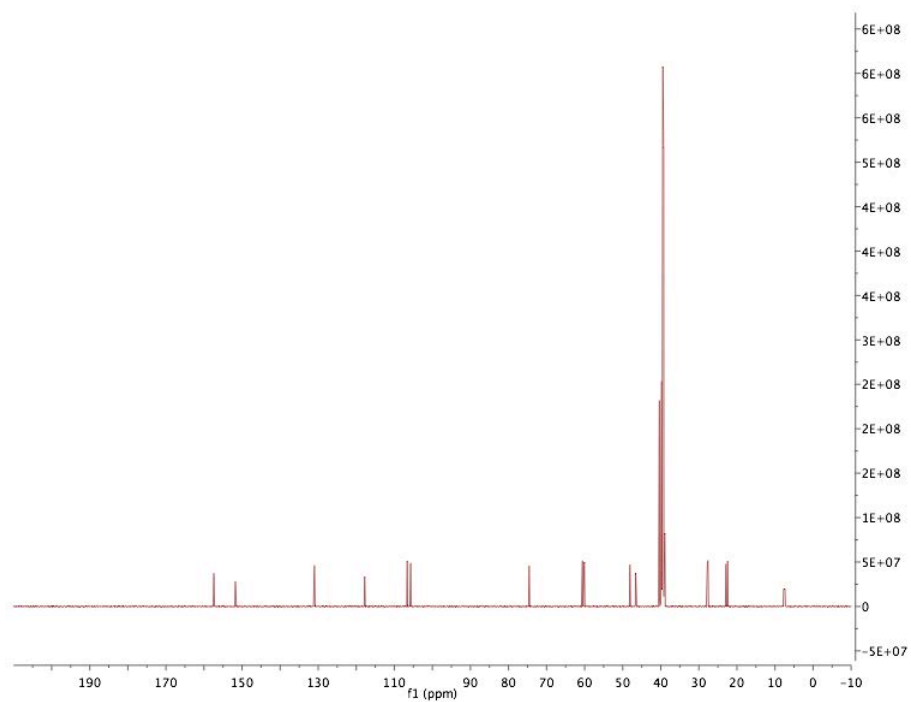
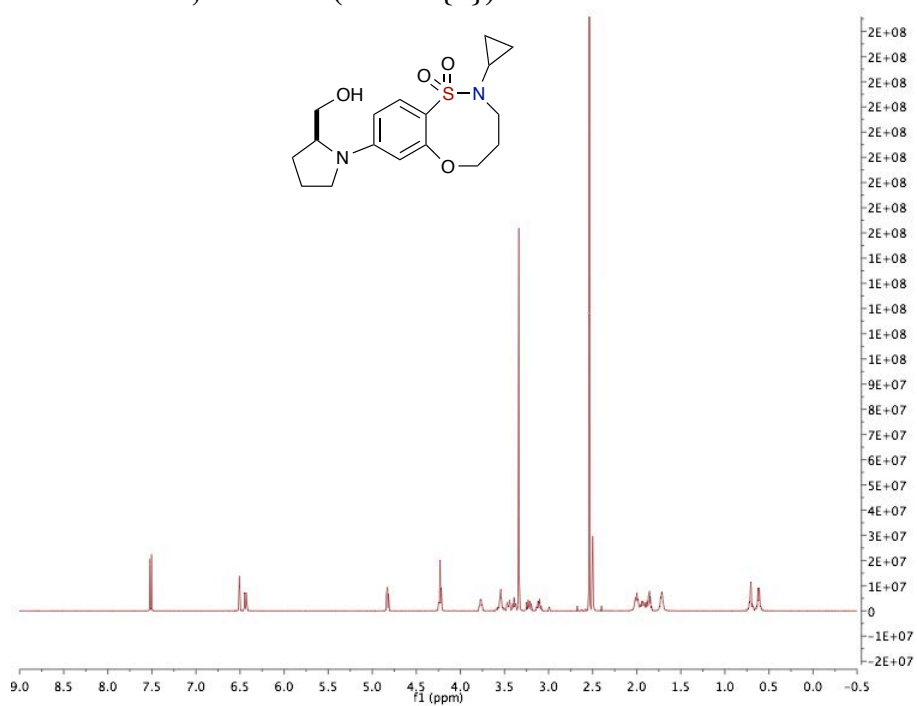
(R)-2-cyclopropyl-8-(2-methylpyrrolidin-1-yl)-2,3,4,5-tetrahydrobenzo[*b*][1,4,5]oxathiazocine 1,1-dioxide (2.10.12{1})



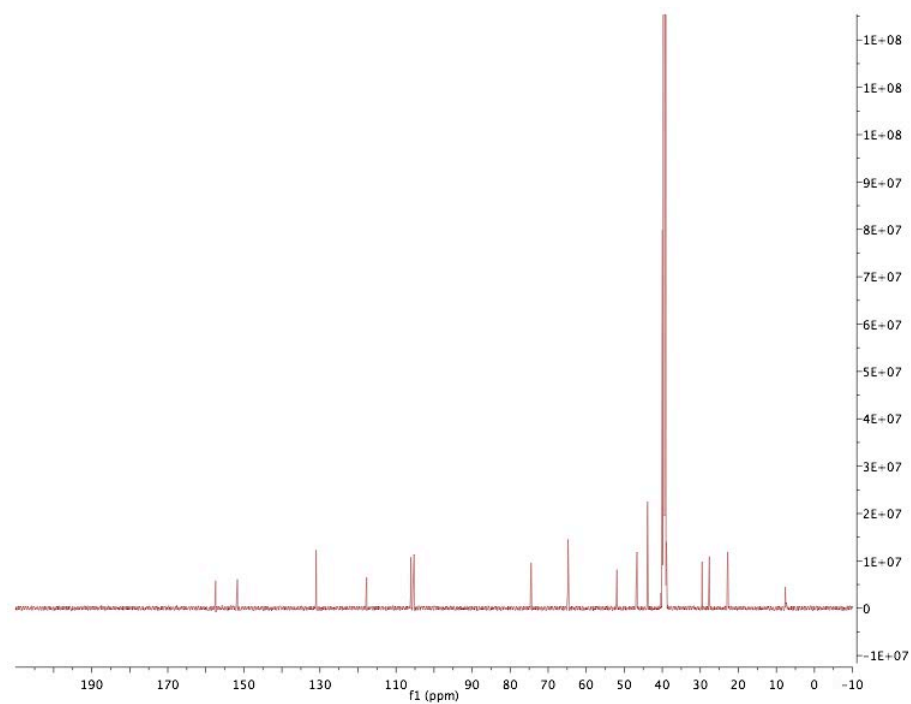
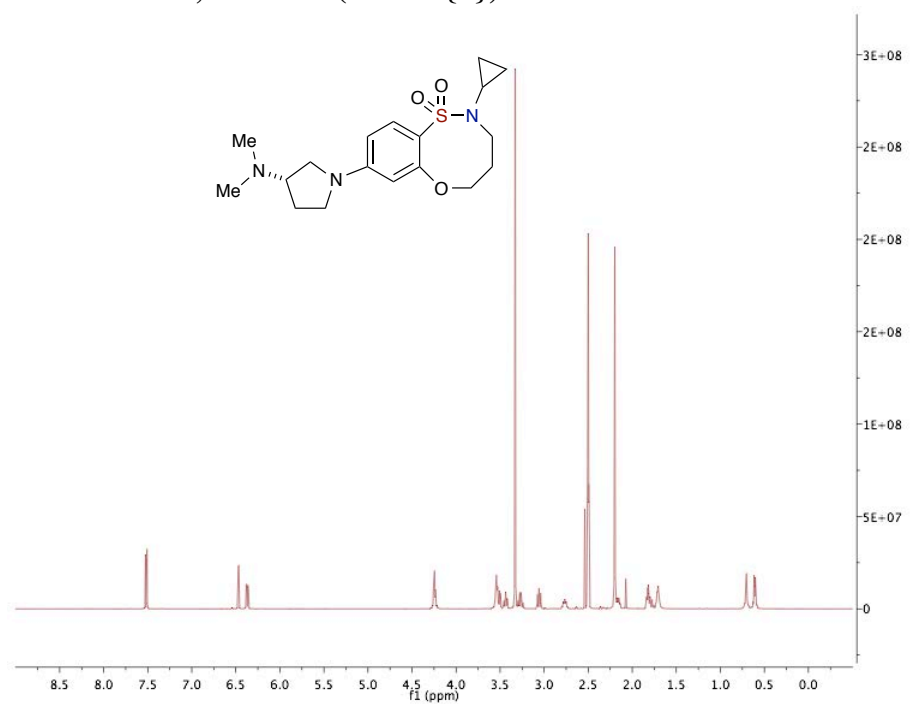
(R)-2-cyclopropyl-8-(3-hydroxypyrrolidin-1-yl)-2,3,4,5-tetrahydrobenzo[b][1,4,5]oxathiazine 1,1-dioxide (2.10.12{3})



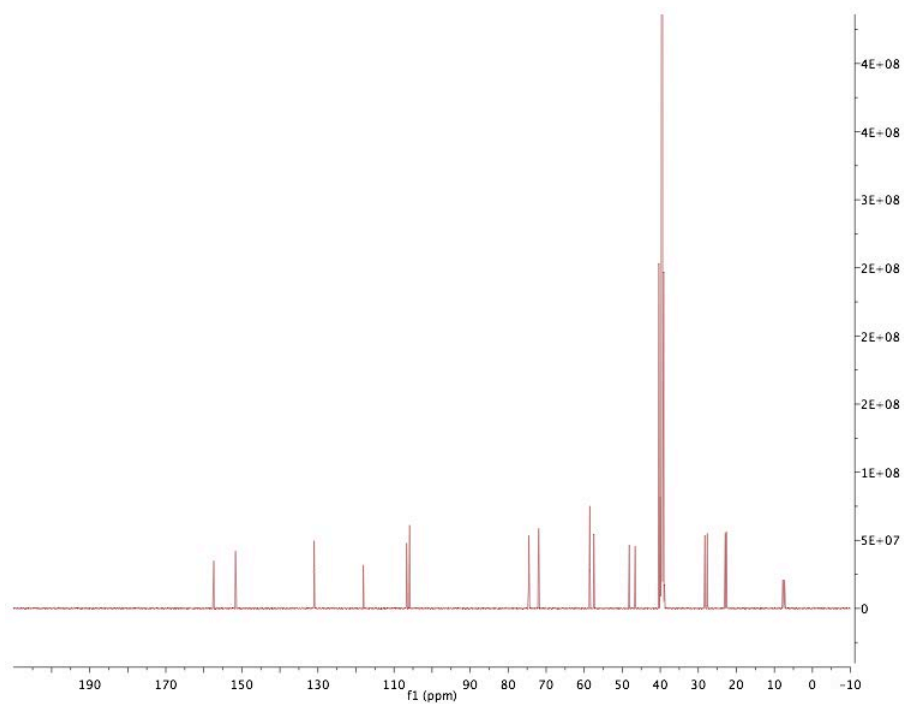
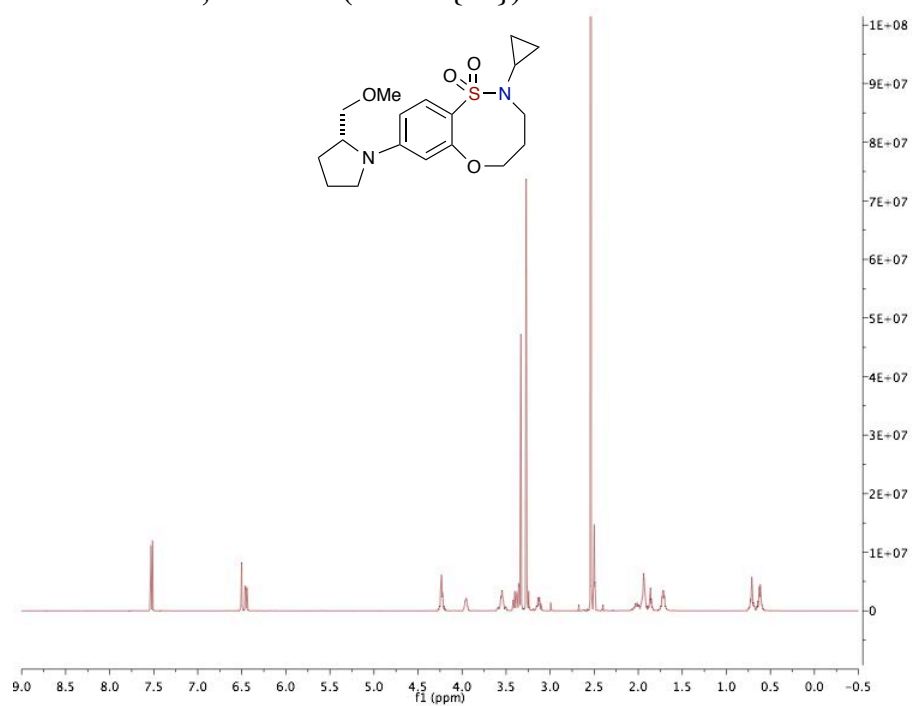
(S)-2-cyclopropyl-8-(2-(hydroxymethyl)pyrrolidin-1-yl)-2,3,4,5 tetrahydrobenzo[*b*]-[1,4,5]oxa thiazocine1,1-dioxide (2.10.12{5})



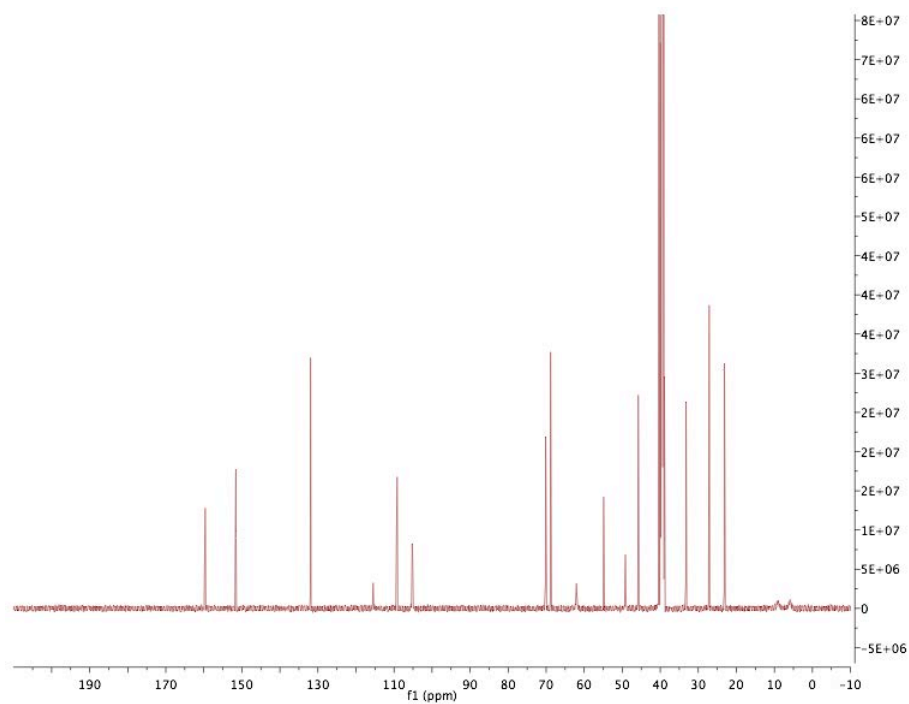
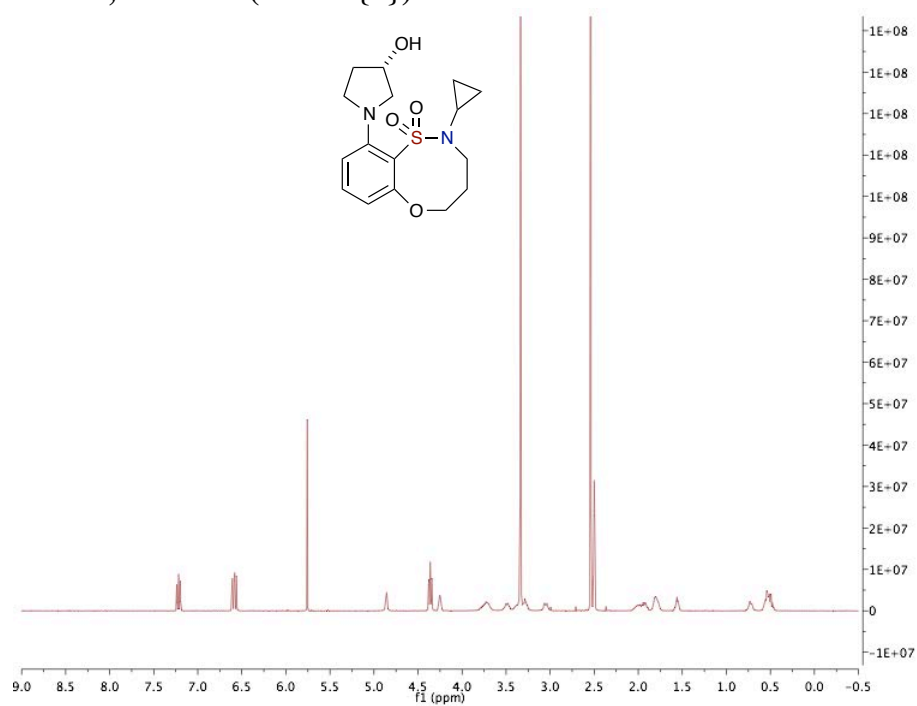
(S)-2-cyclopropyl-8-(3-(dimethylamino)pyrrolidin-1-yl)-2,3,4,5 tetrahydrobenzo[*b*]-[1,4,5] oxathiazocine 1,1-dioxide (2.10.12{8})



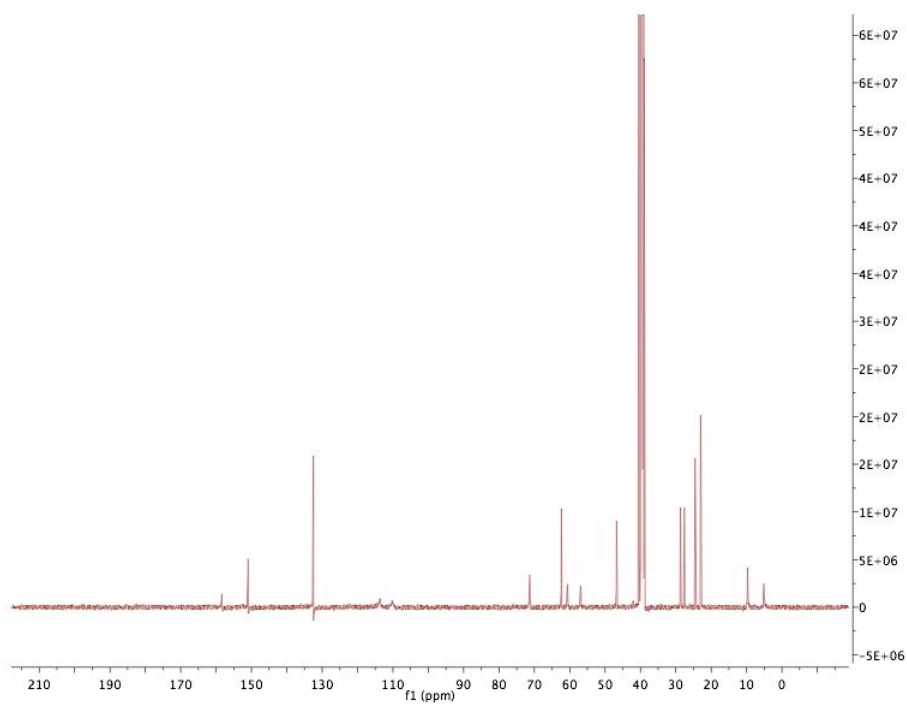
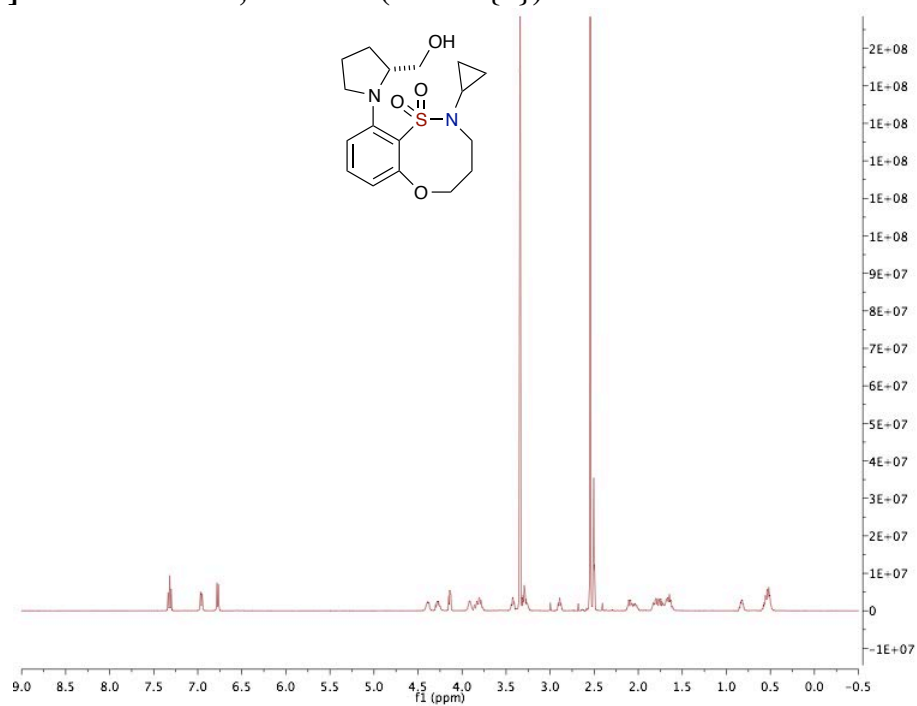
(R)-2-cyclopropyl-8-(2-(methoxymethyl)pyrrolidin-1-yl)-2,3,4,5 tetrahydrobenzo[*b*]-[1,4,5] oxathiazocine 1,1-dioxide (2.10.12{10})



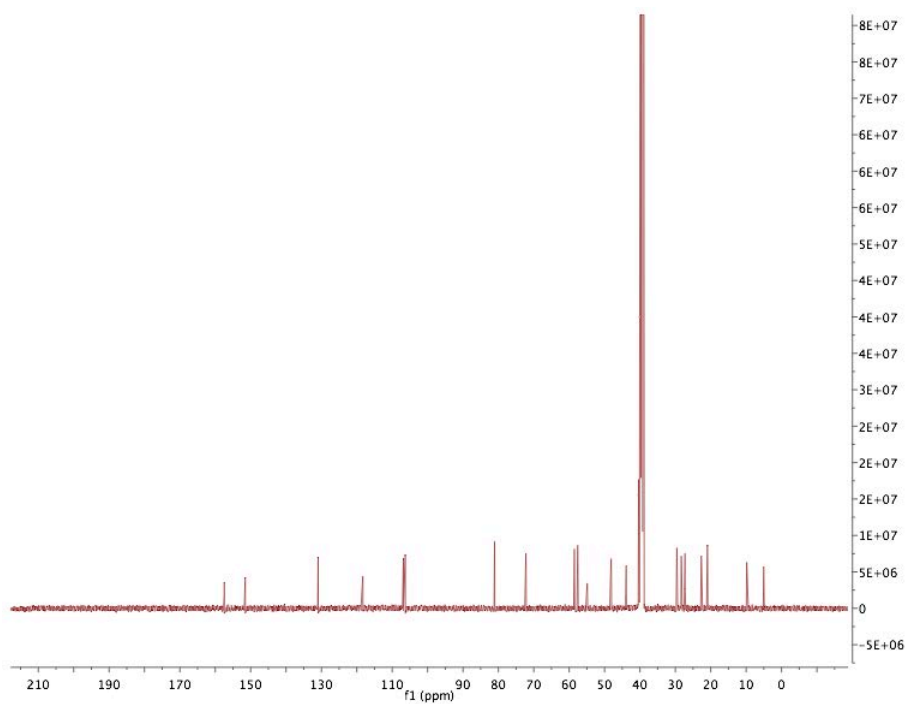
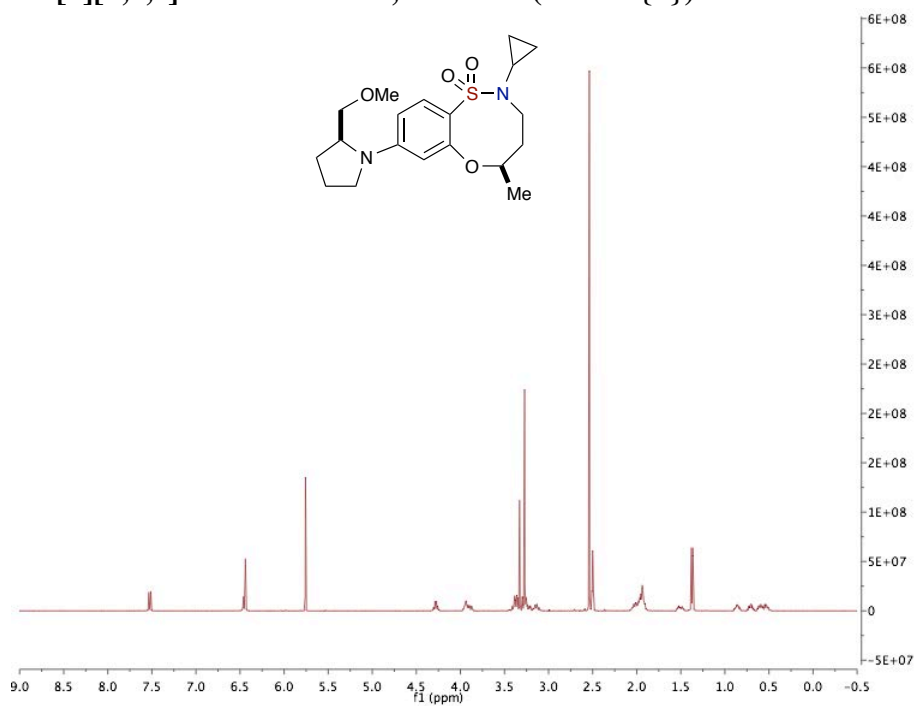
(S)-2-cyclopropyl-10-(3-hydroxypyrrolidin-1-yl)-2,3,4,5-tetrahydrobenzo[*b*][1,4,5]oxathiazocine 1,1-dioxide (2.10.13{4})



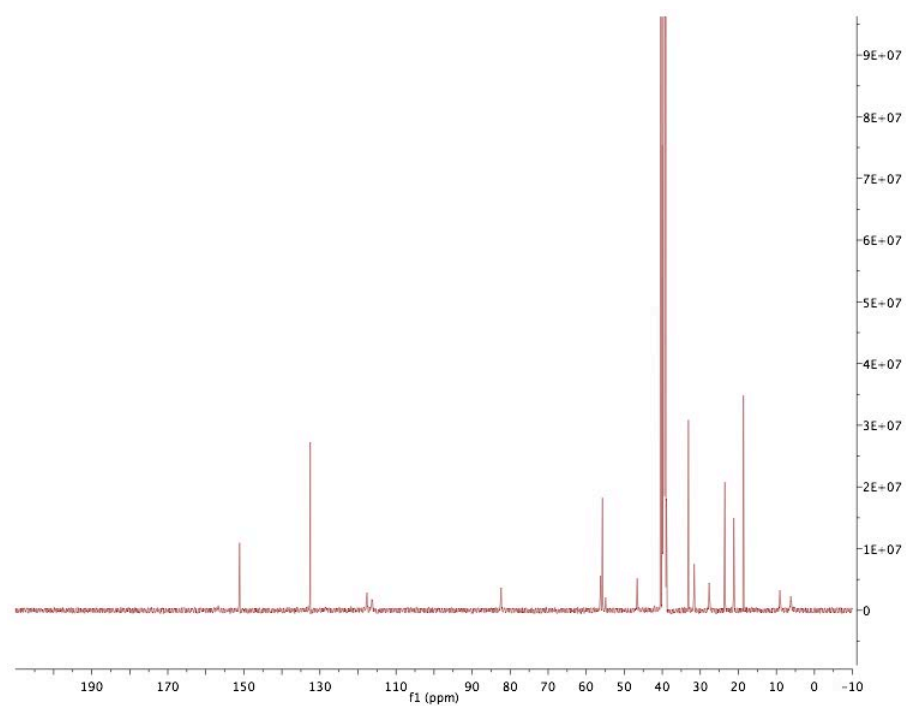
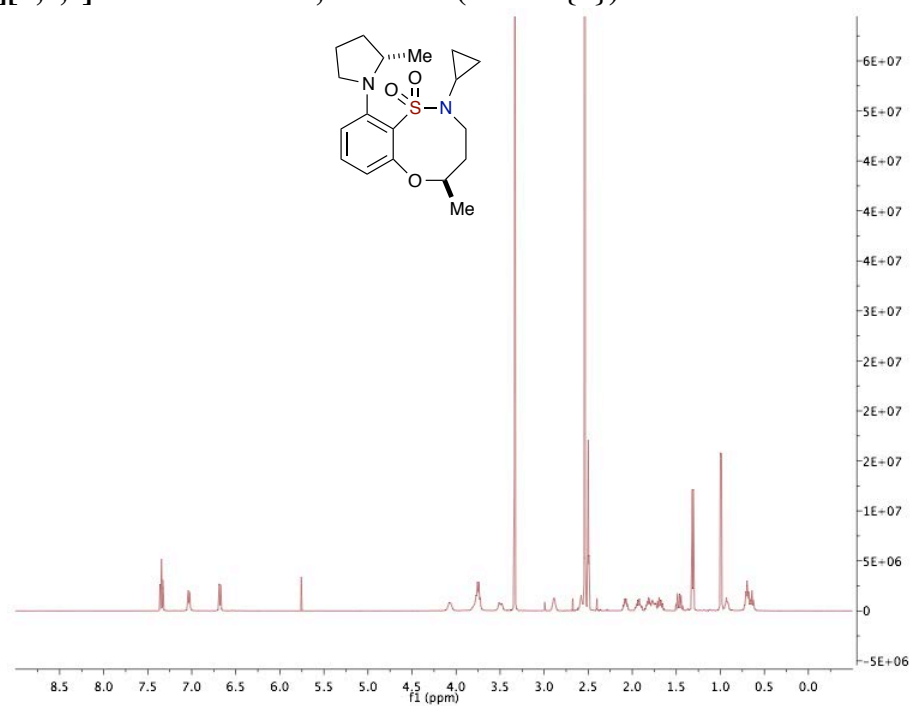
**(R)-2-cyclopropyl-10-(2-(hydroxymethyl)pyrrolidin-1-yl)-2,3,4,5-tetrahydrobenzo-
[b][1,4,5] oxathiazocine 1,1-dioxide (2.10.13{6})**



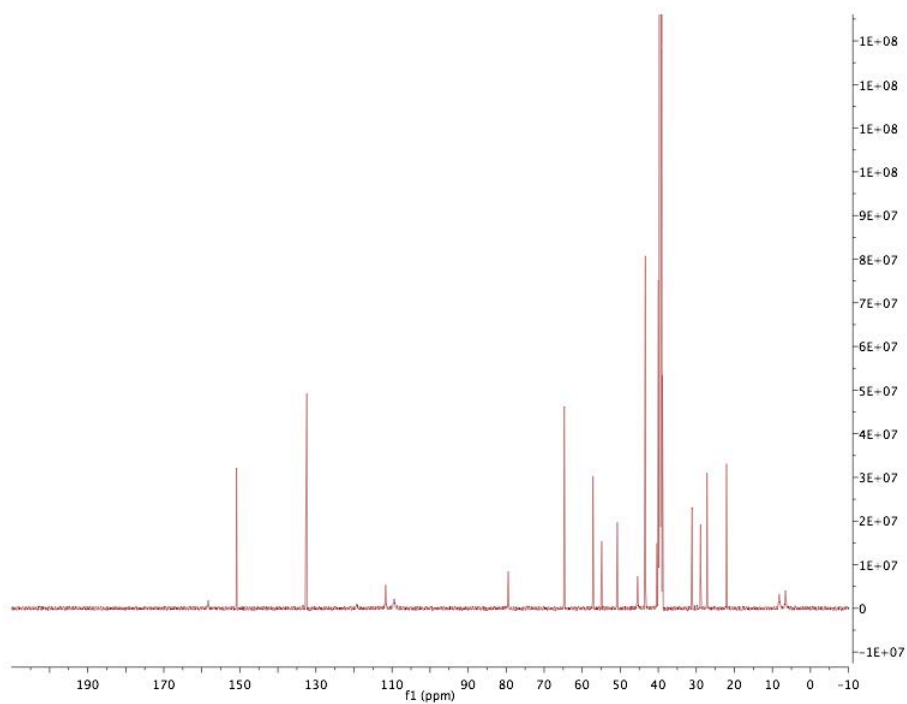
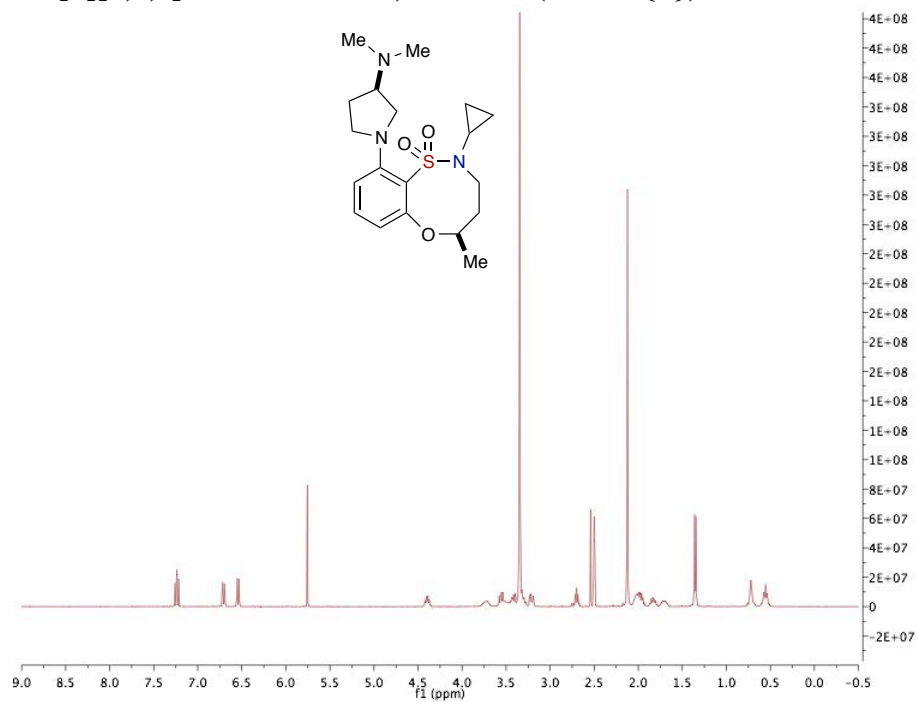
(R)-2-cyclopropyl-8-((S)-2-(methoxymethyl)pyrrolidin-1-yl)-5-methyl-2,3,4,5 tetrahydrobenzo[*b*][1,4,5]oxathiazocine 1,1-dioxide (2.10.15{9})



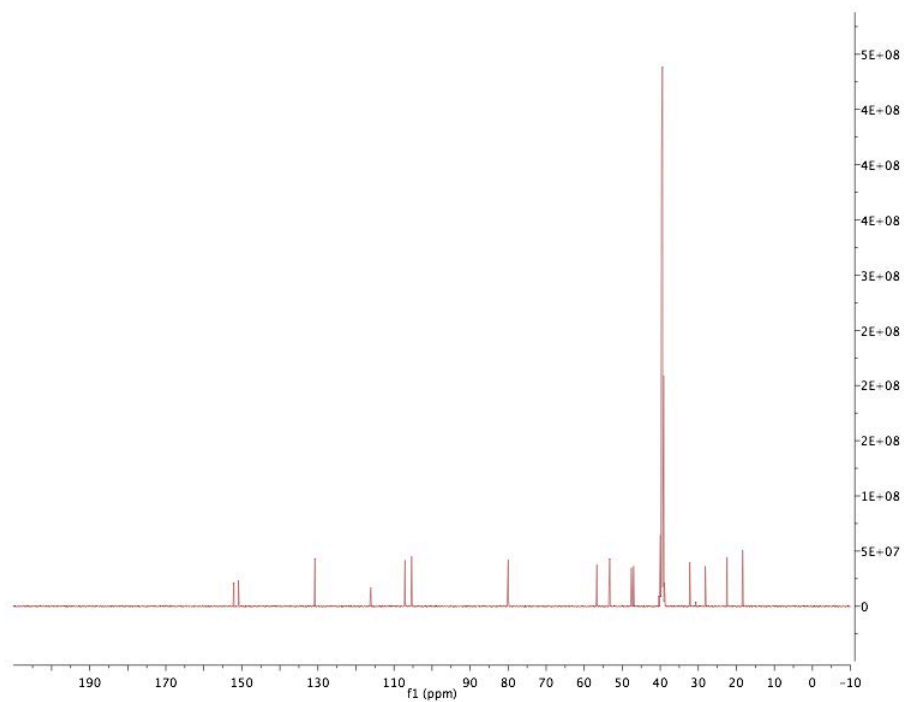
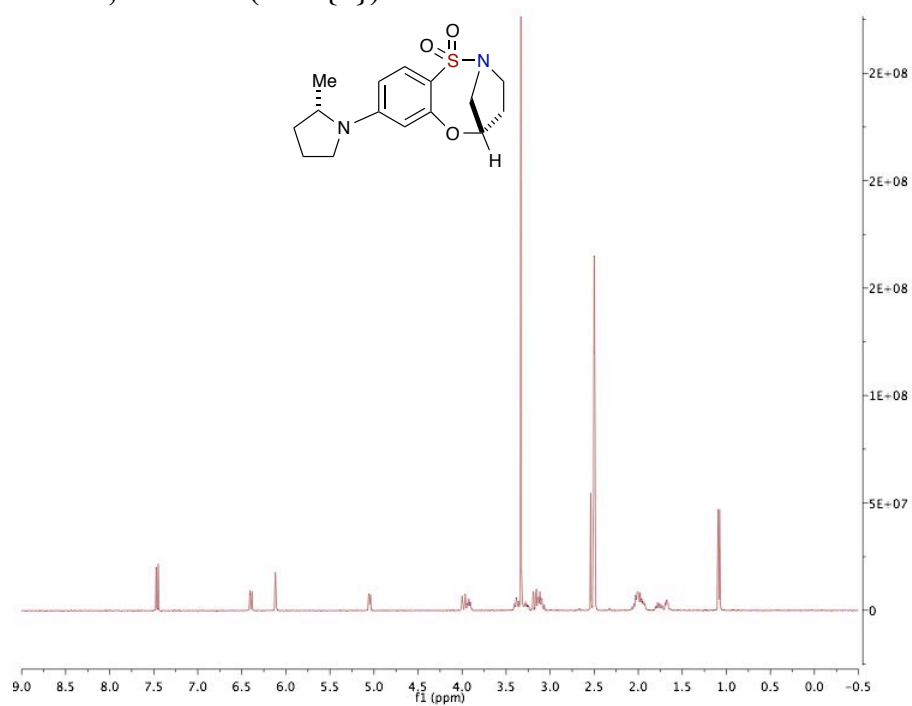
(R)-2-cyclopropyl-5-methyl-10-((S)-2-methylpyrrolidin-1-yl)-2,3,4,5 tetrahydrobenzo[*b*][1,4,5]oxa-thiazocine 1,1-dioxide (2.10.16{2})



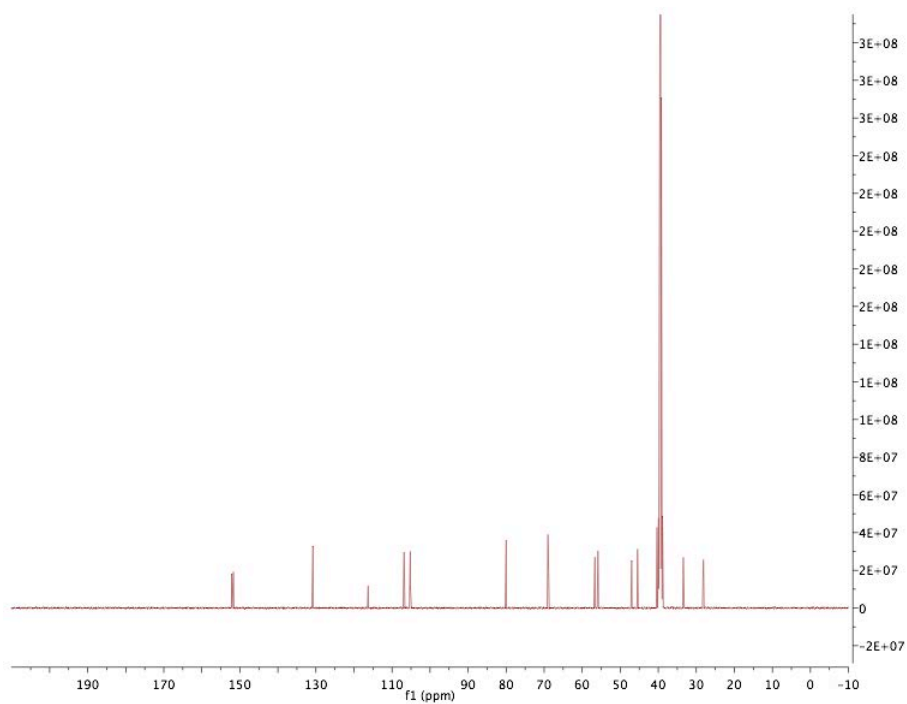
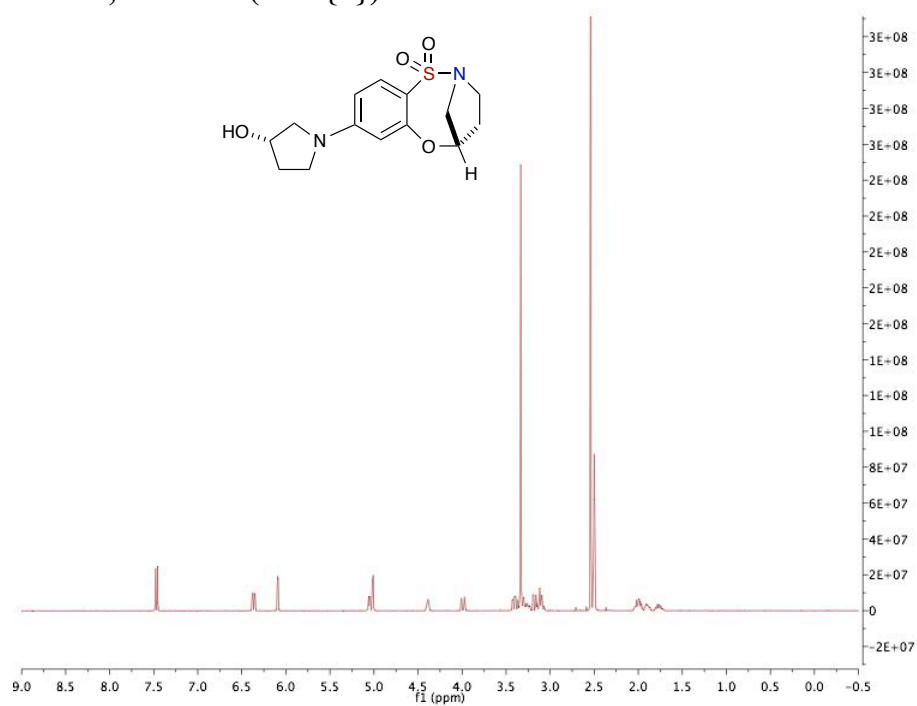
(R)-2-cyclopropyl-10-((R)-3-(dimethylamino)pyrrolidin-1-yl)-5-methyl-2,3,4,5 tetrahydrobenzo[b][1,4,5]oxathiazocine 1,1-dioxide (2.10.16{7})



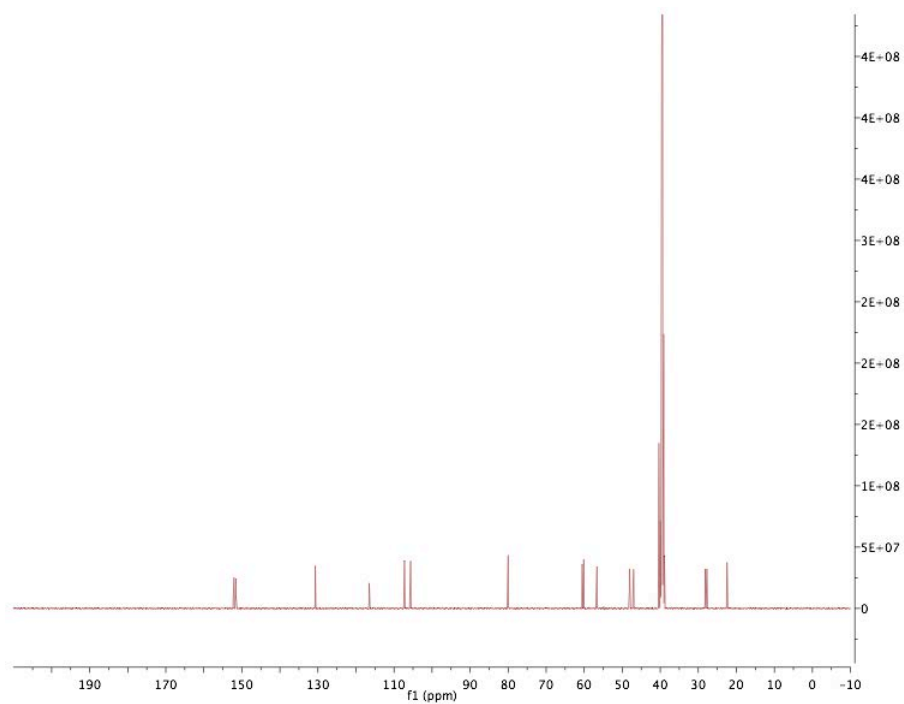
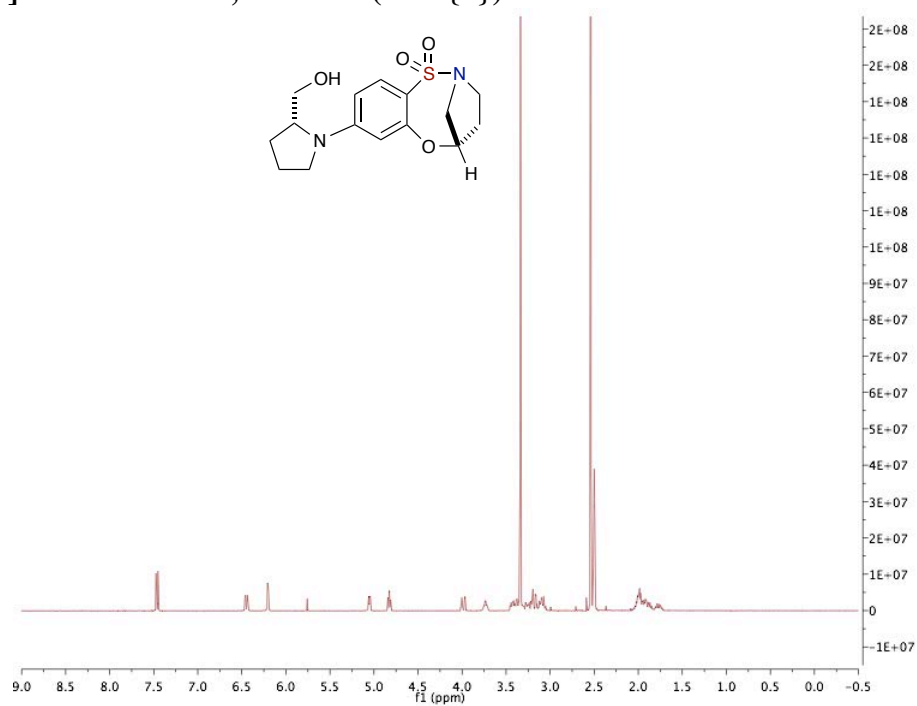
(5S)-8-((S)-2-methylpyrrolidin-1-yl)-4,5-dihydro-3H-2,5 methanobenzo[b][1,4,5] oxathiazocine 1,1-dioxide (2.9.3{2})



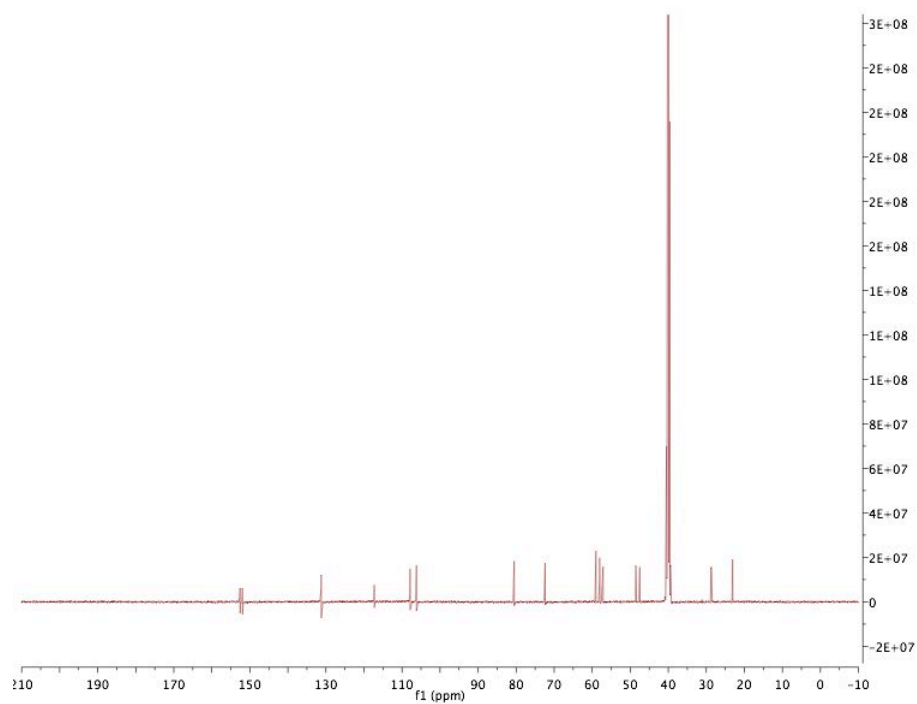
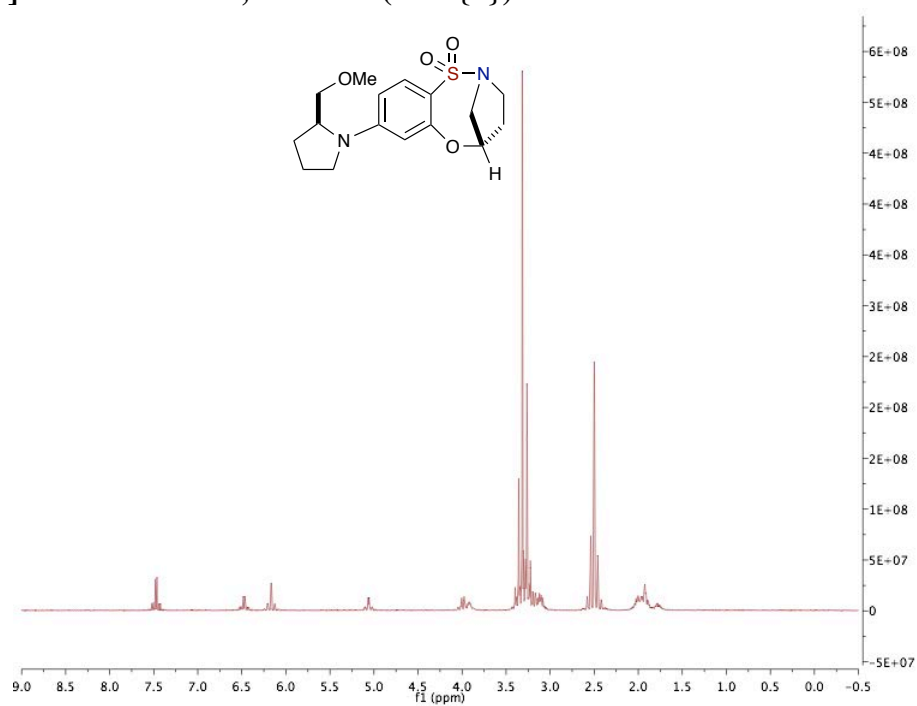
(5*S*)-8-((*S*)-3-hydroxypyrrolidin-1-yl)-4,5-dihydro-3*H*-2,5 methanobenzo[*b*][1,4,5]-oxathiazocine 1,1-dioxide (2.9.3{4})



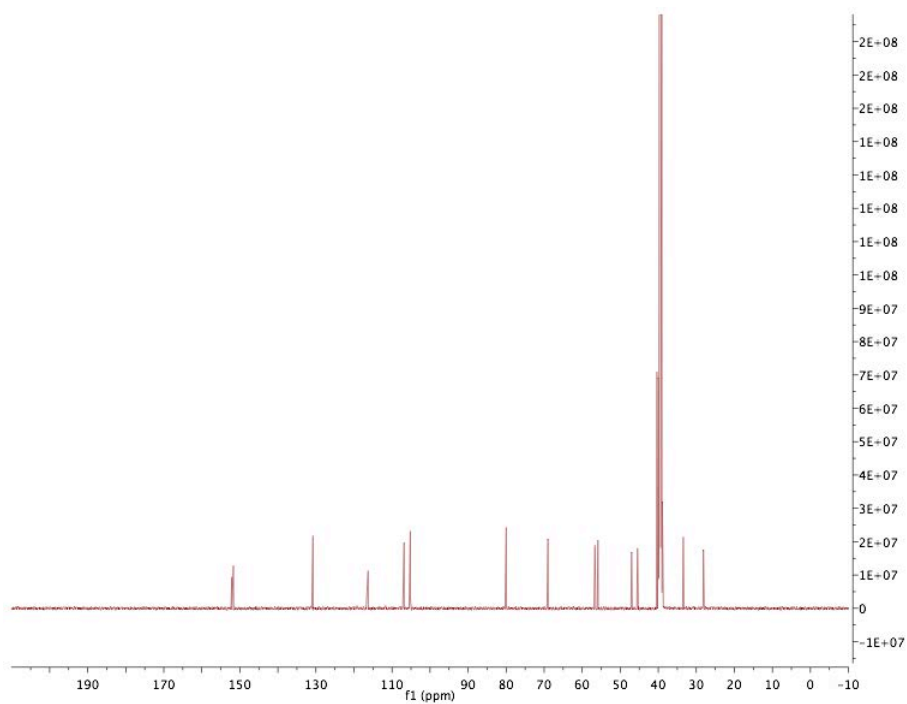
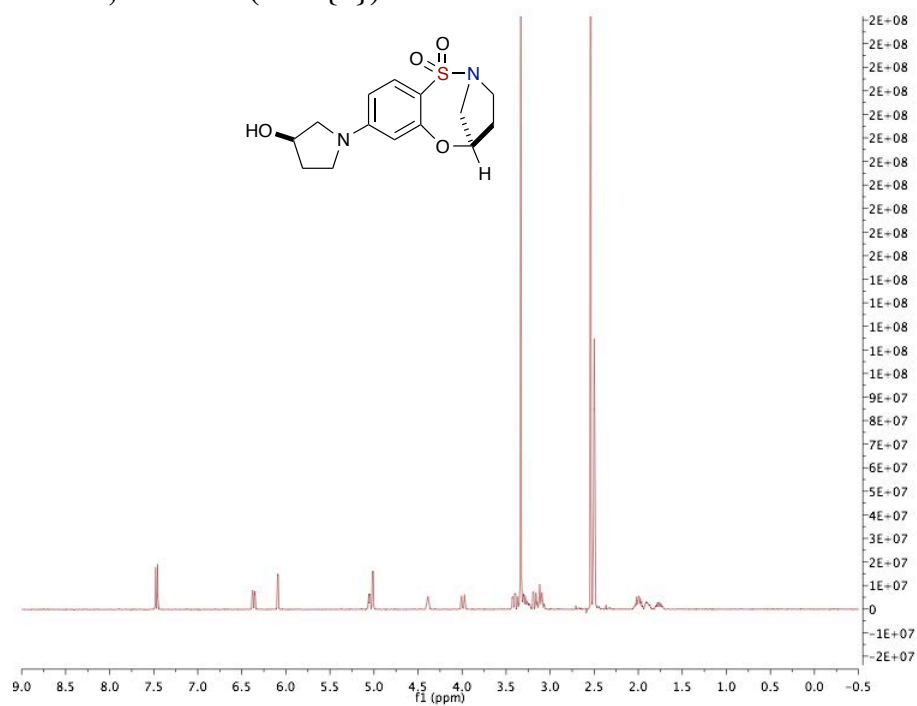
**(5S)-8-((R)-2-(hydroxymethyl)pyrrolidin-1-yl)-4,5-dihydro-3H-2,5-methanobenzo-
[b][1,4,5]oxathiazocine 1,1-dioxide (2.9.3{6})**



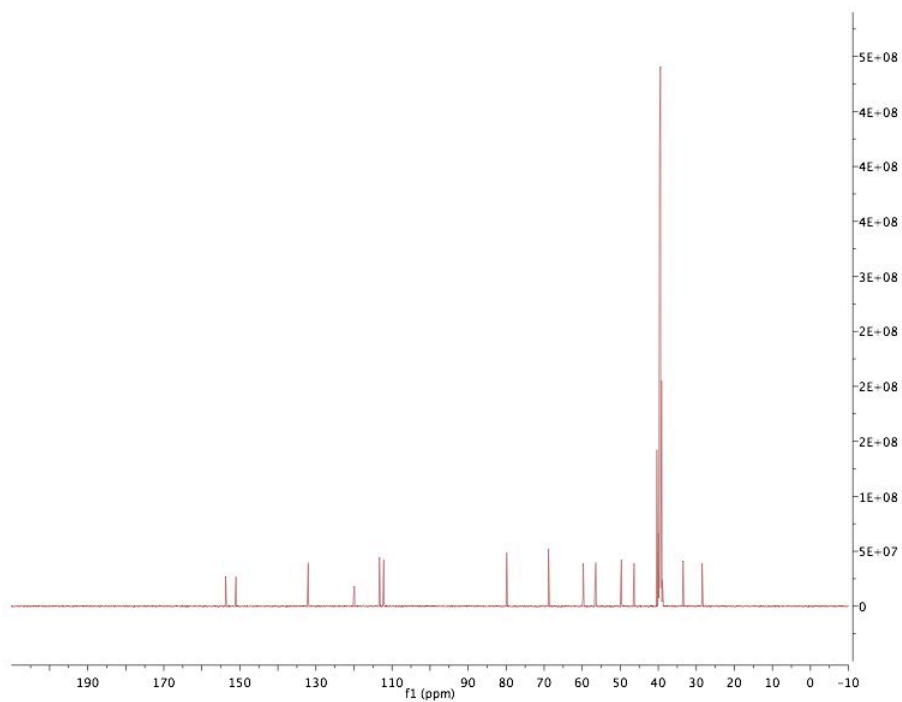
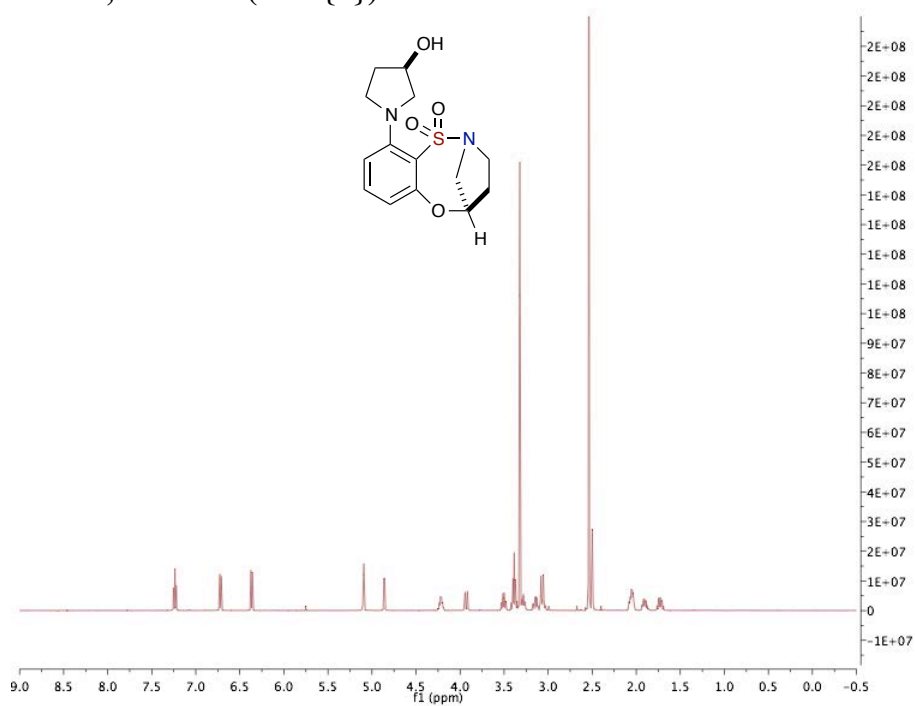
**(5S)-8-((S)-2-(methoxymethyl)pyrrolidin-1-yl)-4,5-dihydro-3H-2,5-methanobenzo
[b][1,4,5]oxa-thiazocine 1,1-dioxide (2.9.3{9})**



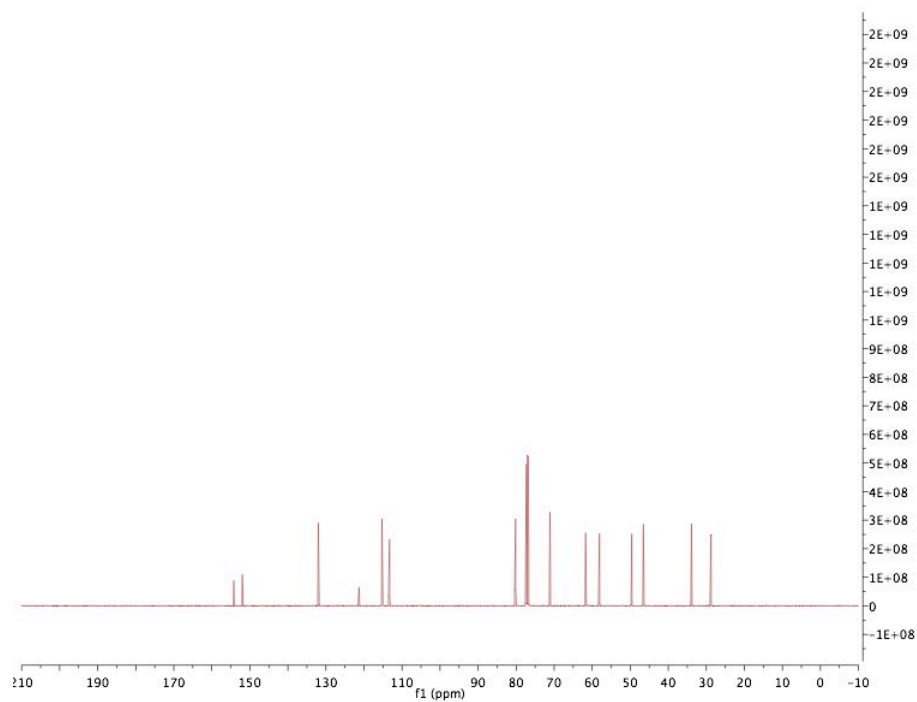
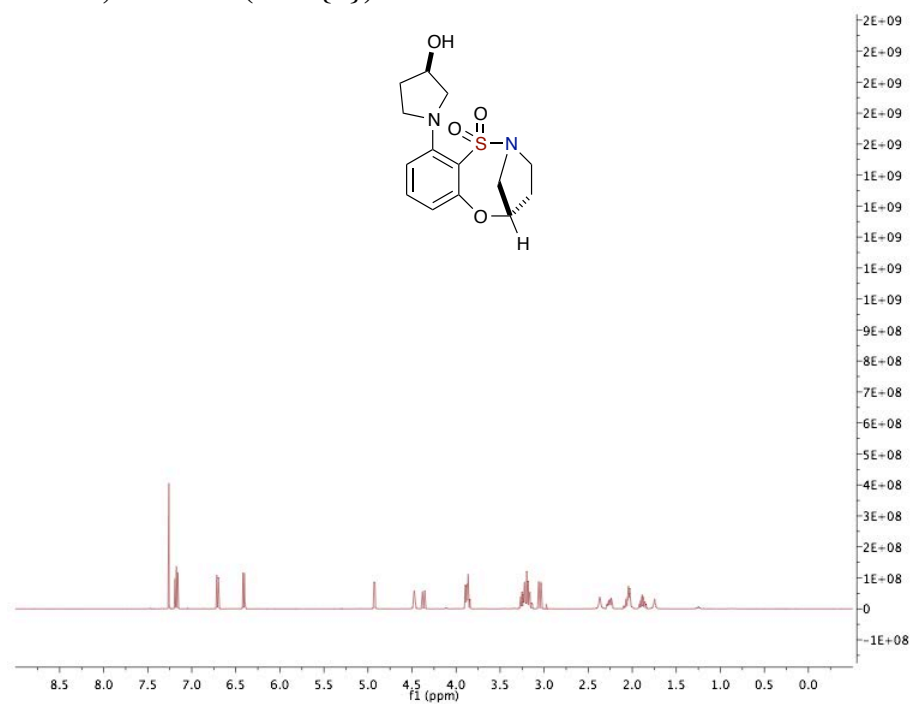
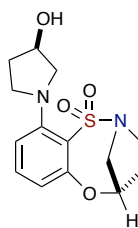
(5*R*)-8-((*R*)-3-hydroxypyrrolidin-1-yl)-4,5-dihydro-3*H*-2,5-methanobenzo[*b*][1,4,5]-oxathiazocine 1,1-dioxide (2.9.4{3})



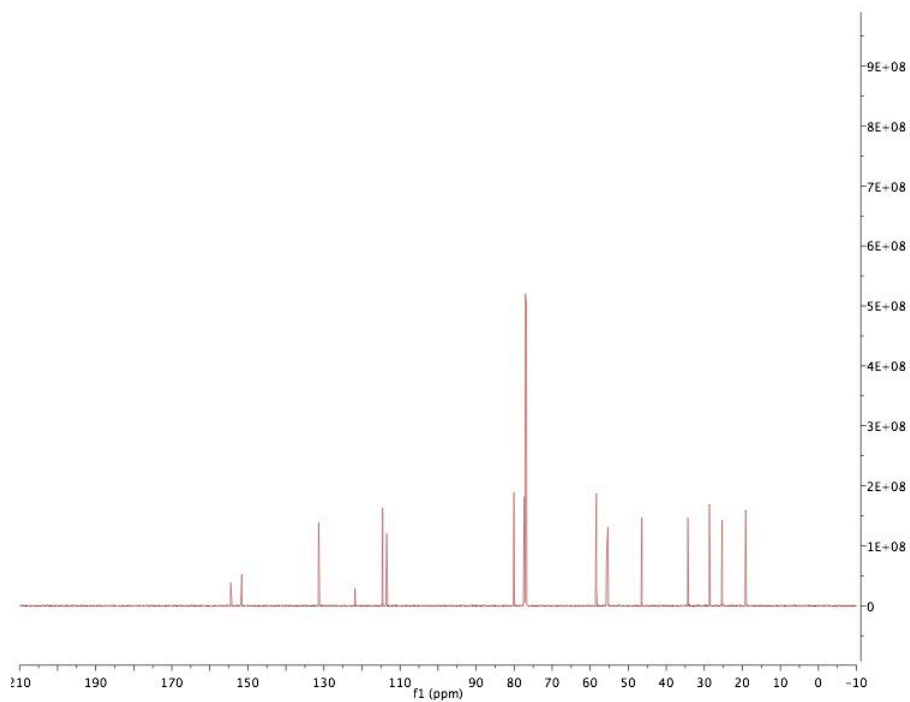
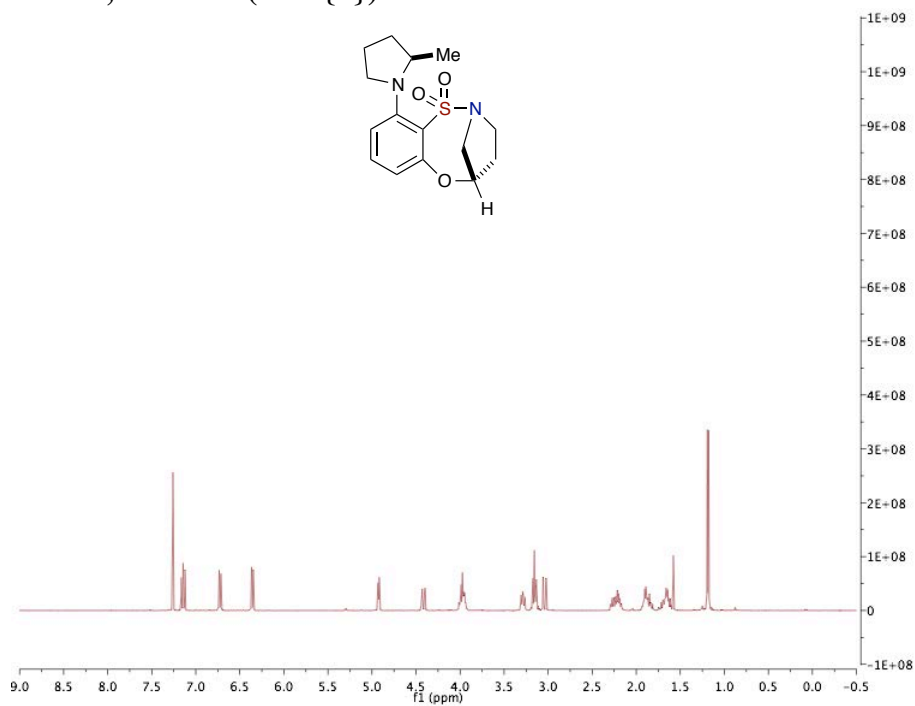
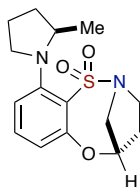
(5*R*)-10-((*R*)-3-hydroxypyrrolidin-1-yl)-4,5-dihydro-3*H*-2,5-methanobenzo[*b*][1,4,5]oxathiazocine 1,1-dioxide (2.9.5{3})



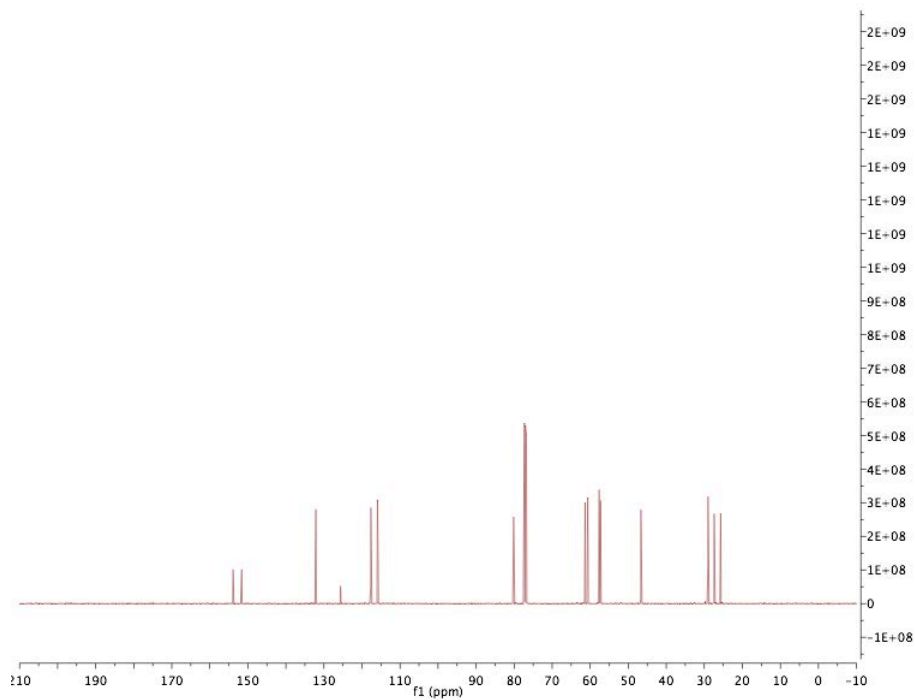
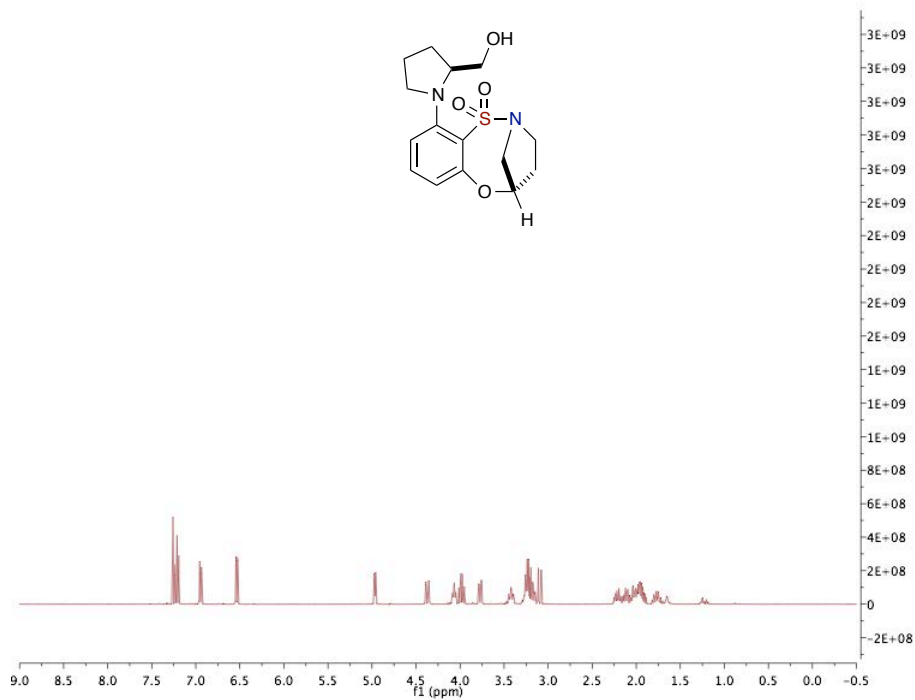
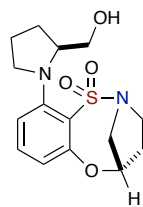
(5S)-10-((R)-3-hydroxypyrrolidin-1-yl)-4,5-dihydro-3H-2,5-methanobenzo[b][1,4,5]oxathiazocine 1,1-dioxide (2.9.6{3})



(5*S*)-10-((*R*)-2-methylpyrrolidin-1-yl)-4,5-dihydro-3*H*-2,5-methanobenzo[*b*][1,4,5]-oxathiazocine 1,1-dioxide (2.9.6{1})



**(5S)-10-((S)-2-(hydroxymethyl)pyrrolidin-1-yl)-4,5-dihydro-3H-2,5-methanobenzo
[b][1,4,5]oxa-thiazocine 1,1-dioxide 2.9.6{5}**



**(5S)-10-((S)-3-(dimethylamino)pyrrolidin-1-yl)-4,5-dihydro-3H-2,5-methanobenzo
[b][1,4,5]oxa-thiazocine 1,1-dioxide 2.9.6{8}**

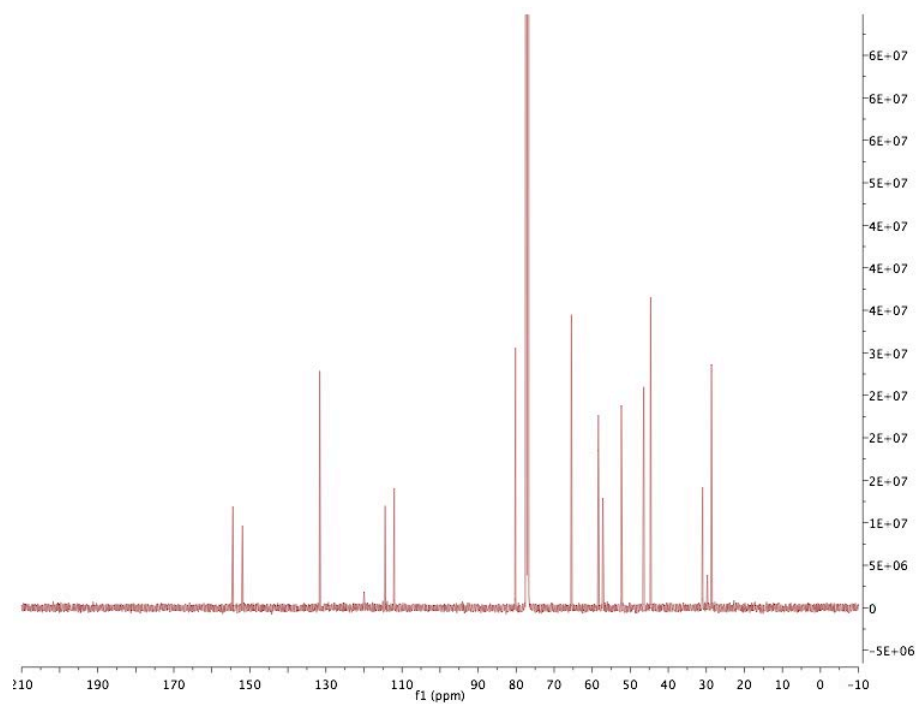
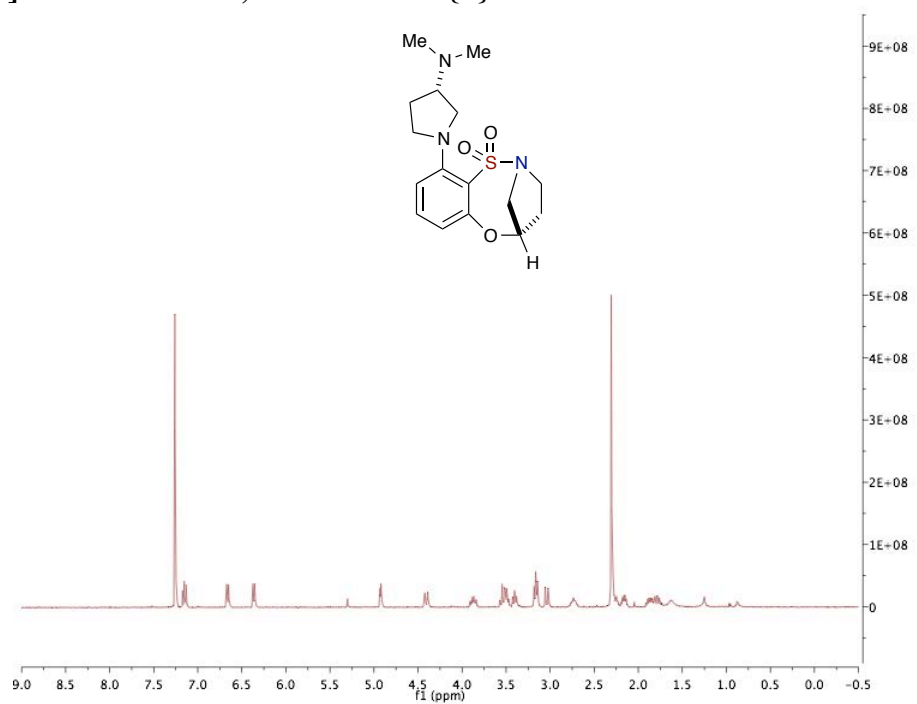


Table of Mass Spectroscopy Data, Final Mass and Purity for all Library Compounds

Comp.	HRMS Expected M/z (M) ⁺	HRMS Found M/z (M+H) ⁺	Mass (mg) ^a	Purity (%)
2.9.3 {1}	308.1195	309.1271	71.7	100
2.9.3 {2}	308.1195	309.1243	73.4	100
2.9.3 {3}	310.0987	311.1057	79.5	99.8
2.9.3 {4}	310.0987	311.1032	76.7	99.8
2.9.3 {5}	324.1144	325.1189	73.6	99.7
2.9.3 {6}	324.1144	325.1183	90.2	99.6
2.9.3 {7}	337.1460	338.1500	21.2	99.1
2.9.3 {8}	337.1460	338.1493	94.9	100
2.9.3 {9}	338.1300	339.1345	84.7	100
2.9.3 {10}	338.1300	339.1363	93.9	100
2.9.4 {1}	308.1195	309.1249	80.5	99.6
2.9.4 {2}	308.1195	309.1248	69.8	99.5
2.9.4 {3}	310.0987	311.1014	70.0	99.4
2.9.4 {4}	310.0987	311.1046	46.1	98.7
2.9.4 {5}	324.1144	325.1216	83.8	99.1
2.9.4 {6}	324.1144	325.1199	82.9	99
2.9.4 {7}	337.1460	338.1511	78.5	99.2
2.9.4 {8}	337.1460	338.1511	18.2	98.5
2.9.4 {9}	338.1300	339.1357	39.6	99.9
2.9.4 {10}	338.1300	339.1364	78.8	100
2.9.5 {1}	308.1195	309.1248	70.1	99.5
2.9.5 {2}	308.1195	309.1262	64.5	99.6
2.9.5 {3}	310.0987	311.1028	49.3	100
2.9.5 {4}	310.0987	311.1028	63.9	99.3
2.9.5 {5}	324.1144	325.1205	72.1	99.6
2.9.5 {6}	324.1144	325.1203	65.3	100
2.9.5 {7}	337.1460	338.1520	69.4	99.1
2.9.5 {8}	337.1460	338.1519	69.7	98.6
2.9.5 {9}	338.1300	339.1353	80.6	99.7
2.9.5 {10}	338.1300	339.1356	69.4	100
2.9.6 {1}	308.1195	309.1259	70.8	99.1
2.9.6 {2}	308.1195	309.1260	70.4	99
2.9.6 {3}	310.0987	311.1051	54.1	99.7
2.9.6 {4}	310.0987	311.1035	41.3	99.5
2.9.6 {5}	324.1144	325.1194	72.9	100
2.9.6 {6}	324.1144	325.1208	82.2	99.5
2.9.6 {7}	337.1460	338.1516	83.7	98.6
2.9.6 {8}	337.1460	338.1517	86.3	99.1

2.9.6{9}	338.1300	339.1367	88.5	99.1
2.9.6{10}	338.1300	339.1368	83.5	99.7
2.10.12{1}	336.1508	337.1580	79.8	100
2.10.12{2}	336.1508	337.1584	79.4	100
2.10.12{3}	338.1300	339.1339	75.8	100
2.10.12{4}	338.1300	339.1344	79.1	100
2.10.12{5}	352.1457	353.1510	85.7	100
2.10.12{6}	352.1457	353.1508	83.1	100
2.10.12{7}	365.1773	366.1813	18.7	98.2
2.10.12{8}	365.1773	366.1826	49.2	99.9
2.10.12{9}	366.1613	367.1661	85.3	99.1
2.10.12{10}	366.1613	367.1680	83.7	99.1
2.10.13{1}	336.1508	337.1581	66.1	98.8
2.10.13{2}	336.1508	337.1578	69.5	98
2.10.13{3}	338.1300	339.1376	77.2	97.6
2.10.13{4}	338.1300	339.1356	61.0	97.7
2.10.13{5}	352.1457	353.1501	68.6	99.7
2.10.13{6}	352.1457	353.1519	67.7	99.6
2.10.13{7}	365.1773	366.1834	76.2	96.9
2.10.13{8}	365.1773	366.1840	75.2	98.1
2.10.13{9}	366.1613	367.1668	76.1	100
2.10.13{10}	366.1613	367.1677	81.5	99.9
2.10.15{1}	350.1664	351.1730	72.7	99
2.10.15{2}	350.1664	351.1709	44.2	99.5
2.10.15{3}	352.1457	353.1500	74.0	97.7
2.10.15{4}	352.1457	353.1539	61.8	97.7
2.10.15{5}	366.1613	367.1680	76.9	98.7
2.10.15{6}	366.1613	367.1686	76.7	98.6
2.10.15{7}	379.1930	380.1978	46.5	99.5
2.10.15{8}	379.1930	380.1995	77.9	99.3
2.10.15{9}	380.1770	381.1831	67.4	99.9
2.10.15{10}	380.1770	381.1830	92.6	100
2.10.16{1}	350.1664	351.1712	50.8	98.6
2.10.16{2}	350.1664	351.1700	33.9	98.6
2.10.16{3}	352.1457	353.1500	49.9	99.6
2.10.16{4}	352.1457	353.1517	42.7	99.6
2.10.16{5}	366.1613	367.1684	70.1	99.6
2.10.16{6}	366.1613	367.1682	46.1	99.4
2.10.16{7}	379.1930	380.1976	37.9	95.5
2.10.16{8}	379.1930	380.1981	127.4	97.3
2.10.16{9}	380.1770	381.1844	34.6	99.6
2.10.16{10}	380.1770	381.1821	22.3	98.9

^aLow yields obtained are due to several reasons including:

1. Peaks having bad shouldering problems
2. Only a small amount of the peak that could satisfies the 90% purity threshold
3. Mechanical/instrumental error: over-pressured.

In-Silico Analysis

Sketched electronic versions of the library compounds were imported into the Tripos Molecular Spreadsheet [2] wherein standard Lipinski's Rule of 5 parameters (molecular weight, ClogP, number of H-acceptors, and number of H-donors [3]) plus the number of rotatable bonds and polar surface area were computed. Lipinski violations were specified according to molecular weight > 500, ClogP > 5.0, number of acceptors > 10, number of donors > 5, and number of rotatable bonds > 5. The structures were then exported into SDF format and converted into three-dimensional protonated structures via Concord [4]. Absorption, distribution, metabolism and excretion (ADME) profiles of these compounds was then generated via Volsurf [5]. Descriptors were generated using three probes (water, hydrophobic and carbonyl oxygen) with a grid space distribution of 1.0 Å. Predictions were then projected onto internal ADME models at the 5-component level. Finally diversity analysis was carried out using DiverseSolutions [6] using standard H-aware 3D BCUT descriptors. The library was then projected onto a chemical space defined by the following descriptors: gastchrg_invdist2_000.550_K_L, gastchrg_invdist6_000.500_K_H, haccept_invdist2_001.000_K_H, tabpolar_invdist_000.250_K_H, tabpolar_invdist_000.500_K_L and populated (for comparison) by a recent version of the MLSMR screening set (ca. 7/2010; ~330,000 unique chemical

structures). Diversity scores ($div(A)$) for our library were then generated for each of our compounds (A) according to the expression:

$$div(A) = \frac{pop[Cell(A)]}{\sum_{i \in Occ} pop(i) / N_{occ}}$$

where N_{occ} is the number of cells occupied by PubChem compounds in an evenly distributed $10 \times 10 \times 10 \times 10 \times 10$ grid decomposition of the chemistry space, and $pop(i)$ is the population of cell i .

In-Silico Analysis

Molecule	CLOGP	Mol. Wt	Acceptor	Donor	Rot Bond	LIP_VI OLS	PSA	DI VS	BB B	SO LY	CAC O2	SP S	SP P	PB	VO LD	HE RG	SoL_D MSO	METST AB
2.9.3(1)	2.31	308.40	4	1	1	0	82.29	0.12	0.81	4.32	0.86	0.28	0.64	76.01	0.27	0.52	0.69	-0.18
2.9.3(2)	2.31	308.40	4	1	1	0	82.30	0.12	0.79	4.24	0.78	0.26	0.66	76.31	0.23	0.46	0.77	-0.22
2.9.3(3)	0.45	310.37	5	2	2	0	131.01	0.13	0.19	3.64	0.29	0.48	0.11	64.50	0.18	0.65	1.76	0.44
2.9.3(4)	0.45	310.37	5	2	2	0	130.95	0.13	0.30	3.63	0.23	0.50	0.17	63.82	0.14	0.73	1.87	0.43
2.9.3(5)	1.07	324.40	5	2	3	0	134.37	0.39	0.17	3.38	0.35	0.43	0.24	62.71	0.28	0.74	1.91	0.49
2.9.3(6)	1.07	324.40	5	2	3	0	130.54	0.39	0.03	3.93	0.53	0.44	0.12	64.56	0.40	0.44	1.71	0.37
2.9.3(7)	1.40	337.44	4	2	2	0	85.01	0.33	0.59	4.40	0.67	0.19	0.42	74.82	0.21	0.36	0.99	-0.29
2.9.3(8)	1.40	337.44	4	2	2	0	85.03	0.33	0.37	4.13	0.66	0.19	0.41	74.36	0.36	0.39	0.87	-0.21
2.9.3(9)	1.83	338.42	5	1	3	0	91.49	0.13	0.40	3.90	0.63	0.26	0.57	69.78	0.41	0.69	1.18	0.09
2.9.3(10)	1.83	338.42	5	1	3	0	90.32	0.13	0.55	4.30	0.72	0.27	0.45	74.93	0.33	0.46	1.10	-0.23
2.9.4(1)	2.31	308.40	4	1	1	0	82.29	0.12	0.81	4.32	0.86	0.28	0.64	76.01	0.27	0.52	0.69	-0.18
2.9.4(2)	2.31	308.40	4	1	1	0	82.30	0.12	0.79	4.24	0.78	0.26	0.66	76.31	0.23	0.46	0.77	-0.22
2.9.4(3)	0.45	310.37	5	2	2	0	131.01	0.13	0.19	3.64	0.29	0.48	0.11	64.50	0.18	0.65	1.76	0.44
2.9.4(4)	0.45	310.37	5	2	2	0	130.95	0.13	0.30	3.63	0.23	0.50	0.17	63.82	0.14	0.73	1.87	0.43
2.9.4(5)	1.07	324.40	5	2	3	0	134.37	0.39	0.17	3.38	0.35	0.43	0.24	62.71	0.28	0.74	1.91	0.49
2.9.4(6)	1.07	324.40	5	2	3	0	130.54	0.39	0.03	3.93	0.53	0.44	0.12	64.56	0.40	0.44	1.71	0.37
2.9.4(7)	1.40	337.44	4	2	2	0	85.01	0.33	0.59	4.40	0.67	0.19	0.42	74.82	0.21	0.36	0.99	-0.29
2.9.4(8)	1.40	337.44	4	2	2	0	85.03	0.33	0.37	4.13	0.66	0.19	0.41	74.36	0.36	0.39	0.87	-0.21
2.9.4(9)	1.83	338.42	5	1	3	0	91.49	0.13	0.40	3.90	0.63	0.26	0.57	69.78	0.41	0.69	1.18	0.09
2.9.4(10)	1.83	338.42	5	1	3	0	90.32	0.13	0.55	4.30	0.72	0.27	0.45	74.93	0.33	0.46	1.10	-0.23
2.9.5(1)	2.31	308.40	4	1	1	0	49.01	0.12	1.24	4.39	1.10	0.25	0.86	86.48	0.54	0.83	0.44	-0.31
2.9.5(2)	2.31	308.40	4	1	1	0	61.58	0.12	0.75	4.01	1.09	0.19	0.92	81.13	0.67	0.66	0.65	-0.03
2.9.5(3)	0.45	310.37	5	2	2	0	113.67	0.04	0.13	3.50	0.59	0.35	0.46	75.01	0.60	0.95	1.50	0.42
2.9.5(4)	0.45	310.37	5	2	2	0	113.88	0.04	0.09	3.27	0.51	0.38	0.48	74.02	0.54	0.99	1.73	0.53
2.9.5(5)	1.07	324.40	5	2	3	0	87.94	0.25	0.56	3.95	0.84	0.39	0.41	70.00	0.35	0.37	1.28	0.23
2.9.5(6)	1.07	324.40	5	2	3	0	109.05	0.10	0.01	4.16	0.74	0.36	0.34	74.32	0.58	0.56	1.25	0.48
2.9.5(7)	1.40	337.44	4	2	2	0	68.08	0.33	0.79	4.16	0.85	0.12	0.68	85.87	0.44	0.63	0.94	-0.01
2.9.5(8)	1.40	337.44	4	2	2	0	68.46	0.33	0.82	4.11	0.91	0.08	0.72	81.83	0.53	0.53	0.77	0.01
2.9.5(9)	1.83	338.42	5	1	3	0	52.34	0.51	1.07	4.60	1.08	0.26	0.72	78.22	0.45	0.45	0.69	-0.33
2.9.5(10)	1.83	338.42	5	1	3	0	71.81	0.15	0.39	4.14	0.93	0.24	0.67	74.36	0.71	0.57	0.81	-0.09
2.9.6(1)	2.31	308.40	4	1	1	0	49.01	0.12	1.24	4.39	1.10	0.25	0.86	86.48	0.54	0.83	0.44	-0.31
2.9.6(2)	2.31	308.40	4	1	1	0	61.58	0.12	0.75	4.01	1.09	0.19	0.92	81.13	0.67	0.66	0.65	-0.03
2.9.6(3)	0.45	310.37	5	2	2	0	113.67	0.04	0.13	3.50	0.59	0.35	0.46	75.01	0.60	0.95	1.50	0.42

2.9.6(4)	0.45	310.37	5	2	2	0	113.88	0.04	-	-	0.51	0.38	0.48	74.02	-	0.54	0.99	1.73	0.53
2.9.6(5)	1.07	324.40	5	2	3	0	87.94	0.25	0.56	3.95	0.84	0.39	0.41	70.00	-	0.35	0.37	1.28	0.23
2.9.6(6)	1.07	324.40	5	2	3	0	109.05	0.10	0.01	4.16	0.74	0.36	0.34	74.32	-	0.58	0.56	1.25	0.48
2.9.6(7)	1.40	337.44	4	2	2	0	68.08	0.33	0.79	4.16	0.85	0.12	0.68	85.87	-	0.44	0.63	0.94	-0.01
2.9.6(8)	1.40	337.44	4	2	2	0	68.46	0.33	0.82	4.11	0.91	0.08	0.72	81.83	-	0.53	0.53	0.77	0.01
2.9.6(9)	1.83	338.42	5	1	3	0	52.34	0.15	1.07	4.60	1.08	0.26	0.72	78.22	-	0.45	0.45	0.69	-0.33
2.9.6(10)	1.83	338.42	5	1	3	0	71.81	0.15	0.39	4.14	0.93	0.24	0.67	74.36	-	0.71	0.57	0.81	-0.09
2.10.12(1)	3.16	336.45	4	1	2	0	44.72	0.45	0.91	4.50	0.91	0.14	0.66	86.30	-	0.51	0.14	0.55	-0.40
2.10.12(2)	3.16	336.45	4	1	2	0	44.75	0.45	0.85	4.62	0.96	0.15	0.62	84.26	-	0.47	0.03	0.58	-0.35
2.10.12(3)	1.31	338.42	5	2	3	0	93.34	0.04	0.06	4.14	0.31	0.34	0.32	81.54	-	0.33	0.58	1.50	0.01
2.10.12(4)	1.31	338.42	5	2	3	0	93.33	0.04	0.01	4.04	0.30	0.33	0.34	76.43	-	0.35	0.66	1.46	-0.04
2.10.12(5)	1.93	352.45	5	2	4	0	97.12	0.79	0.15	4.35	0.46	0.30	0.17	72.36	-	0.22	0.49	1.78	0.11
2.10.12(6)	1.93	352.45	5	2	4	0	96.63	0.79	0.19	4.14	0.54	0.38	0.26	67.72	-	0.23	0.60	1.74	0.22
2.10.12(7)	2.26	365.49	4	2	3	0	47.44	0.33	0.82	4.71	0.68	0.09	0.49	83.36	-	0.41	0.18	0.66	-0.56
2.10.12(8)	2.26	365.49	4	2	3	0	47.39	0.33	0.91	4.89	0.72	0.04	0.48	83.16	-	0.40	0.01	0.60	-0.61
2.10.12(9)	2.68	366.48	5	1	4	0	53.95	0.13	0.74	4.78	0.74	0.11	0.50	84.42	-	0.49	0.36	0.90	-0.42
2.10.12(10)	2.68	366.48	5	1	4	0	53.76	0.13	0.64	4.67	0.76	0.14	0.52	78.18	-	0.39	0.24	1.14	-0.43
2.10.13(1)	3.16	336.45	4	1	2	0	24.09	0.45	1.12	5.07	1.35	0.01	0.88	93.64	-	0.82	0.19	0.10	-0.32
2.10.13(2)	3.16	336.45	4	1	2	0	25.72	0.45	1.13	4.58	1.41	0.23	0.89	82.01	-	0.71	0.01	0.41	-0.24
2.10.13(3)	1.31	338.42	5	2	3	0	72.90	0.28	0.02	4.11	0.67	0.27	0.52	85.13	-	0.61	0.80	1.44	0.14
2.10.13(4)	1.31	338.42	5	2	3	0	73.01	0.28	0.06	3.96	0.71	0.26	0.47	82.31	-	0.55	0.66	1.67	0.43
2.10.13(5)	1.93	352.45	5	2	4	0	73.24	0.10	0.19	4.46	0.77	0.25	0.45	81.75	-	0.37	0.61	1.89	0.22
2.10.13(6)	1.93	352.45	5	2	4	0	60.10	0.13	0.30	4.12	1.10	0.29	0.62	77.94	-	0.63	0.24	1.43	0.16
2.10.13(7)	2.26	365.49	4	2	3	0	27.03	0.33	0.96	5.08	1.05	0.00	0.63	95.81	-	0.49	0.16	0.83	-0.17
2.10.13(8)	2.26	365.49	4	2	3	0	27.10	0.33	0.90	4.92	1.07	0.00	0.67	94.22	-	0.50	0.03	0.81	-0.14
2.10.13(9)	2.68	366.48	5	1	4	0	31.99	0.15	0.83	4.91	1.09	0.05	0.73	91.30	-	0.63	0.33	0.98	-0.34
2.10.13(10)	2.68	366.48	5	1	4	0	25.16	0.71	0.91	4.85	1.35	0.11	0.84	84.46	-	0.61	0.13	0.68	-0.28
2.10.15(1)	3.68	350.48	4	1	2	0	43.13	0.45	0.73	4.54	0.96	0.07	0.70	85.66	-	0.58	0.13	0.67	-0.48
2.10.15(2)	3.68	350.48	4	1	2	0	43.15	0.45	0.74	4.49	1.01	0.09	0.66	81.46	-	0.53	0.00	0.67	-0.37
2.10.15(3)	1.83	352.45	5	2	3	0	91.74	0.79	0.11	4.19	0.38	0.25	0.38	80.29	-	0.40	0.55	1.62	-0.05
2.10.15(4)	1.83	352.45	5	2	3	0	91.73	0.79	0.15	4.11	0.38	0.24	0.41	76.13	-	0.42	0.62	1.57	-0.11
2.10.15(5)	2.45	366.48	5	2	4	0	95.53	0.79	0.04	4.32	0.51	0.25	0.22	70.80	-	0.24	0.52	1.84	0.04
2.10.15(6)	2.45	366.48	5	2	4	0	95.04	0.79	0.14	4.19	0.55	0.31	0.27	69.69	-	0.36	0.64	1.79	0.21
2.10.15(7)	2.78	379.52	4	2	3	0	45.84	0.35	0.65	4.76	0.71	0.01	0.54	83.56	-	0.46	0.15	0.83	-0.63
2.10.15(8)	2.78	379.52	4	2	3	0	45.79	0.33	0.73	4.97	0.74	0.03	0.53	83.74	-	0.45	0.03	0.76	-0.67
2.10.15	3.20	380.	5	1	4	0	52.30	0.10	0.6	-	0.77	0.00	0.5	81.	-	0.42	0.98	-0.40	

{9}		50					5	3	1	4.7 0		9	3	86	0.49				
2.10.15 {10}	3.20	380. 50	5	1	4	0	52.1 7	0.1 3	0.4 8	- 4.6 3	0.83	0.1 4	0.5 7	78. 23	- 0.49	0.39	1.07	-0.32	
2.10.16 {1}	3.68	350. 48	4	1	2	0	22.4 9	0.4 5	1.2 6	- 5.3 7	1.41	0.0 6	0.8 7	93. 74	- 0.71	0.00	0.29	-0.61	
2.10.16 {2}	3.68	350. 48	4	1	2	0	21.9 3	0.4 5	1.0 5	- 4.8 6	1.40	0.1 5	0.8 9	86. 02	- 0.68	- 0.01	0.55	-0.33	
2.10.16 {3}	1.83	352. 45	5	2	3	0	71.3 0	0.7 9	0.0 0	- 4.2 2	0.70	0.2 2	0.5 4	83. 46	- 0.63	0.73	1.38	-0.02	
2.10.16 {4}	1.83	352. 45	5	2	3	0	71.4 2	0.7 9	0.1 0	- 4.0 3	0.75	0.2 1	0.5 0	81. 02	- 0.57	0.60	1.63	0.26	
2.10.16 {5}	2.45	366. 48	5	2	4	0	71.6 8	0.8 9	0.2 8	- 4.3 8	0.83	0.2 5	0.4 7	77. 40	- 0.41	0.53	1.59	0.10	
2.10.16 {6}	2.45	366. 48	5	2	4	0	58.9 5	0.4 0	0.5 6	- 4.4 8	1.09	0.2 7	0.6 3	79. 78	- 0.65	0.13	1.16	-0.09	
2.10.16 {7}	2.78	379. 52	4	2	3	0	25.4 7	0.0 6	0.9 2	- 5.1 1	1.09	0.0 4	0.6 7	94. 33	- 0.54	- 0.25	0.82	-0.29	
2.10.16 {8}	2.78	379. 52	4	2	3	0	25.5 5	0.0 6	0.8 6	- 4.9 7	1.10	0.0 2	0.7 0	92. 80	- 0.55	- 0.08	0.80	-0.25	
2.10.16 {9}	3.20	380. 50	5	1	4	0	30.4 4	0.1 7	0.9 3	- 4.8 1	1.14	0.0 7	0.7 3	86. 24	- 0.67	0.26	0.70	-0.39	
2.10.16 {10}	3.20	380. 50	5	1	4	0	23.6 6	0.1 6	1.0 0	- 4.6 7	1.24	0.1 8	0.8 1	80. 85	- 0.65	- 0.07	0.64	-0.37	
Averages	1.97	341. 34	5	2	3	0	73.3 8	0.2 9	0.4 9	- 4.2 9	0.79	0.2 2	0.5 3	78. 49	- 0.46	0.44	1.10	-0.06	

References

1. Grubbs, R. H.; Rosen, R. K.; Timmers, F. J. *Organometallics* **1996**, *15*, 1518–1520.
2. SYBYL 8.0, The Tripos Associates, St. Louis MO, 2008.
3. Lipinski, C.A., Lombardo, F., Dominy, B.W., Feeney, P.J. Experimental and computational approaches to estimate solubility and permeability in drug discovery and development settings. *Adv. Drug Delivery Rev.* **1997**, *23*, 3–25.
4. Concord 8.0, The Tripos Associates, St. Louis MO, 2008.
5. Cruciani, G., Meniconi, M., Carosati, E., Zamora, I., Mannhold, R. VOLSURF: A Tool for Drug ADME-Properties Prediction. In: *Methods and Principles in Medicinal Chemistry*. Eds. van de Waterbeemd, H., Lennernäs, H., Artursson, P. (Wiley-VCH Verlag GmbH & Co., Weinheim, 2003).
6. Pearlman, R.S.; Smith, K.M. Metric Validation and the Receptor-Relevant Subspace Concept. *J. Chem. Inf. Comput. Sci.* **1999**, *39*, 28–35.

5.2 Experimental for Chapter 3

General Procedure A: preparation of *o*-fluorobenzyl aziridinyl sulfonamides. To a round bottom flask containing a solution of aziridine (2.2 mmol, 2.0 eq.) in dry CH₂Cl₂ (0.5 M), was added Et₃N (2.2 mmol, 2.0 eq.). The reaction mixture was cooled to -40 °C, stirred for 10 min and sulfonyl chloride (1.1 mmol, 1.0 eq.) was added to the reaction mixture in a drop-wise fashion. The reaction was then stirred for 0.5–2 h at -40 °C after, which conversion of starting material was monitored by TLC. Upon completion of reaction, the mixture was warmed to rt, quenched with cold water (2.2 mL) and the layers were separated. The organic portion was washed with cold 10% aq. HCl and resulting layers were separated. This partitioning was then repeated with cold water, cold sat. NaHCO₃, cold water again and finally brine. The final organic layer was dried (Na₂SO₄), and concentrated under reduced pressure to afford the desired aziridinyl sulfonamide.

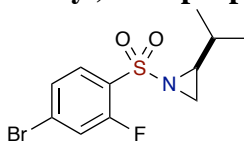
General Procedure B: one-pot, sequential (aziridine ring-opening and S_NAr). To a microwave vial containing a solution of aziridinyl sulfonamide (1.0 eq.) in DMF (0.3 M), was added amine/amino alcohol (1.05–1.2 eq.). The reaction vessel was capped and heated in the Biotage® Initiator microwave at 130 °C for 30–40 mins, after which, conversion of starting material was monitored by TLC. To the crude mixture, DMF (0.08 M) and Cs₂CO₃ (2.5 eq) were added and the mixture underwent microwave irradiation again at 150 °C for 30–50 mins. Water was added to the crude mixture, which was extracted with EtOAc (4x). The organic layer was separated and the combined organic layers were washed with water, brine, dried (Na₂SO₄) and concentrated under reduced

pressure to afford the crude product, which was purified by automated flash column chromatography system.

General Procedure C: one-pot, sequential (aziridine ring-opening and S_NAr). To a microwave vial containing a solution of sulfonamide (1.0 eq.) in DMF (0.3 M), was added amine/amino alcohol (1.05–1.2 eq.). The reaction vessel was capped and heated in the Biotage® Initiator microwave at 130 °C for 30–40 mins, after which, conversion of starting material was monitored by TLC. To the crude mixture, Cs₂CO₃ (2.5 eq) was added and the mixture underwent microwave irradiation again at 150 °C for 30–50 mins. Water was added to the crude mixture, which was extracted with EtOAc (4x). The organic layer was separated and the combined organic layers were washed with water, brine, dried (Na₂SO₄) and concentrated under reduced pressure to afford the crude product, which was purified by automated flash column chromatography system.

General Procedure D: Mitsunobu reaction. To a flame-dried round bottom flask containing a solution of sultam (0.0466 mmol, 1.0 eq.) in dry THF (0.05 M), was added triphenylphosphine (0.140 mmol, 3.0 eq.). The reaction mixture was stirred for 10 min and diisopropyl azodicarboxylate (0.117 mmol, 2.5 eq.) was added to the mixture in a drop-wise fashion. The reaction was then stirred overnight at rt, which conversion of starting material was monitored by TLC. The solvent was removed *in vacuo* to yield yellow oil and was purified by automated flash column chromatography system.

(S)-1-((4-bromo-2-fluorophenyl)sulfonyl)-2-isopropylaziridine (3.8.4b)



According to general procedure **A**, **3.8.4b** (854.4 mg, 72%) was isolated as yellow oil.

$[\alpha]_D^{20} = -47.6$ ($c = 0.675$, CHCl_3);

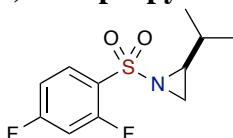
FTIR (thin film) 3094, 2962, 1589, 1472, 1398, 1333, 1167, 879, 735 cm^{-1} ;

^1H NMR (500 MHz, CDCl_3) δ ppm 7.88–7.76 (m, 1H, aromatic), 7.53–7.41 (m, 2H, aromatic), 2.80 (dd, $J = 7.1, 1.1$ Hz, 1H, $\text{NCH}_a\text{H}_b\text{CH}$), 2.72 (ddd, $J = 7.3, 7.2, 4.8$ Hz, 1H, NCHCH), 2.24 (d, $J = 4.8$ Hz, 1H, $\text{NCH}_a\text{H}_b\text{CH}$), 1.59–1.39 (m, 1H, CH_3CHCH_3), 0.96 (d, $J = 6.8$ Hz, 3H, CH_3CHCH_3), 0.91 (d, $J = 6.7$ Hz, 3H, CH_3CHCH_3);

^{13}C NMR (126 MHz, CDCl_3) δ ppm 159.1 (d, $^1J_{\text{C-F}} = 262.2$ Hz), 131.4, 129.4 (d, $^3J_{\text{C-F}} = 9.0$ Hz), 127.9 (d, $^3J_{\text{C-F}} = 3.8$ Hz), 121.0 (d, $^2J_{\text{C-F}} = 24.5$ Hz), 120.5 (d, $^2J_{\text{C-F}} = 24.2$ Hz), 46.6, 33.8, 30.1, 19.5, 18.9;

HRMS calculated for $\text{C}_{11}\text{H}_{13}\text{BrFNO}_2\text{SH}$ ($\text{M}+\text{N}$) $^+$ 321.9913; found 321.9865 (TOF MS ES^+).

(S)-1-((2,4-difluorophenyl)sulfonyl)-2-isopropylaziridine (3.8.4d)



According to general procedure **A**, **3.8.4d** (889.4 mg, 72%) was isolated as yellow oil.

$[\alpha]_D^{20} = -5.0$ ($c = 1.43$, CHCl_3);

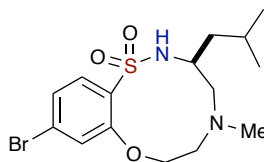
FTIR (thin film) 3103, 2964, 1603, 1481, 1429, 1335, 1167, 854, 741, 727 cm^{-1} ;

$^1\text{H NMR}$ (500 MHz, CDCl_3) δ ppm 8.10–7.85 (m, 1H, aromatic), 7.12–6.88 (m, 2H, aromatic), 2.80 (dd, $J = 7.1, 1.1$ Hz, 1H, $\text{NCH}_a\text{H}_b\text{CH}$), 2.70 (ddd, $J = 7.3, 7.2, 4.6$ Hz, 1H, NCHCH), 2.24 (d, $J = 3.8$ Hz, 1H, $\text{NCH}_a\text{H}_b\text{CH}$), 1.61–1.43 (m, 1H, CH_3CHCH_3), 0.96 (d, $J = 6.8$ Hz, 3H, CH_3CHCH_3), 0.90 (d, $J = 6.7$ Hz, 3H, CH_3CHCH_3);

$^{13}\text{C NMR}$ (126 MHz, CDCl_3) δ ppm 166.3 (dd, $J = 258.5, 11.4$ Hz), 160.4 (dd, $J = 260.8, 12.8$ Hz), 132.4 (dd, $J = 10.6, 1.6$ Hz), 111.9 (dd, $J = 22.0, 3.8$ Hz), 105.8 (dd, $J = 25.5, 25.4$ Hz), 105.4 (dd, $J = 26.0, 25.9$ Hz), 46.5, 33.7, 30.1, 19.4, 18.9;

HRMS calculated for $\text{C}_{11}\text{H}_{13}\text{F}_2\text{NO}_2\text{SH}$ ($\text{M}+\text{H}$) $^+$ 262.0713; found 262.0720 (TOF MS ES^+).

(S)-10-bromo-3-isobutyl-5-methyl-2,3,4,5,6,7-hexahydrobenzo[*b*][1,4,5,8]oxathiazine 1,1-dioxide (3.1.2a)



According to general procedure **B**, **3.1.2a** (38.7 mg, 66%) was isolated as a white solid.

mp 192–195 °C;

$[\alpha]_D^{20} = +167.5$ ($c = 1.02$, CHCl_3);

FTIR (thin film) 3267, 3090, 2966, 1576, 1558, 1462, 1400, 1323, 1165, 1059, 824, 781, 748, 725 cm^{-1} ;

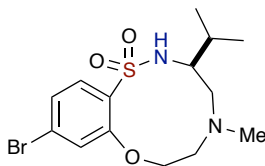
$^1\text{H NMR}$ (500 MHz, CDCl_3) δ ppm 7.85 (d, $J = 8.3$ Hz, 1H, aromatic), 7.34–7.28 (m, 2H, aromatic), 7.09 (s, 1H, NH), 4.41–4.31 (m, 2H, OCH_2CH_2), 2.73 (dddd, $J = 9.2, 9.0, 4.7, 4.6$ Hz, 1H, NHCHCH_2N), 2.66 (dd, $J = 12.6, 4.9$ Hz, 1H, $\text{NHCHCH}_a\text{H}_b\text{N}$), 2.58 (ddd, $J = 14.8, 10.8, 3.3$ Hz, 1H, $\text{NCH}_a\text{H}_b\text{CH}_2\text{O}$), 2.46 (s, 3H, NCH_3), 2.34 (ddd, $J = 15.2,$

1.7, 1.6 Hz, 1H, NCH_aH_bCH₂O), 2.24 (dd, $J = 12.6, 10.5$ Hz, 1H, NHCHCH_aH_bN), 1.85 (ddd, $J = 13.7, 9.4, 4.2$ Hz, 1H, NHCHCH_aH_b), 1.62–1.49 (m, 1H, CH₃CHCH₃), 1.33 (ddd, $J = 13.8, 8.8, 5.0$ Hz, 1H, NHCHCH_aH_b), 0.86 (d, $J = 6.6$ Hz, 3H, CH₃CHCH₃), 0.73 (d, $J = 6.6$ Hz, 3H, CH₃CHCH₃);

¹³C NMR (126 MHz, CDCl₃) δ ppm 155.1, 132.8, 129.3, 128.4, 125.7, 120.6, 69.7, 60.0, 53.2, 49.8, 44.3, 43.1, 24.4, 23.6, 21.9;

HRMS calculated for C₁₅H₂₃BrN₂O₃SH (M+H)⁺ 391.0691; found 391.0670 (TOF MS ES⁺).

(S)-10-bromo-3-isopropyl-5-methyl-2,3,4,5,6,7-hexahydrobenzo[*b*][1,4,5,8]oxathiazine-1,1-dioxide (3.9.2b)



According to general procedure **B**, **3.9.2b** (41.0 mg, 70%) was isolated as a white solid.

mp 175–180 °C;

$[\alpha]_D^{20} = +170.4$ ($c = 0.545$, CHCl₃);

FTIR (thin film) 3263, 2968, 1578, 1560, 1452, 1371, 1323, 1163 1057, 820, 737 cm⁻¹;

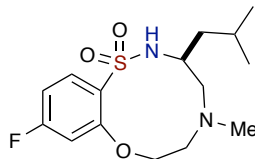
¹H NMR (500 MHz, CDCl₃) δ ppm 7.84 (d, $J = 8.4$ Hz, 1H, aromatic), 7.36–7.29 (m, 2H, aromatic), 7.05 (s, 1H, NH), 4.43–4.27 (m, 2H, OCH₂CH₂), 2.68 (ddd, $J = 11.2, 4.6, 4.5$ Hz, 1H, NHCHCH₂N), 2.60 (ddd, $J = 14.5, 10.6, 3.5$ Hz, 1H, NHCHCH_aH_bN), 2.49 (dd, $J = 12.7, 5.1$ Hz, 1H, NCH_aH_bCH₂O), 2.46 (s, 3H, NCH₃), 2.38–2.23 (m, 3H,

NHCHCH_aH_bN, NCH_aH_bCH₂O, CH₃CHCH₃), 0.98 (d, $J = 6.9$ Hz, 3H, CH₃CHCH₃), 0.79 (d, $J = 7.3$ Hz, 3H, CH₃CHCH₃);

¹³C NMR (126 MHz, CDCl₃) δ ppm 155.2, 132.9, 129.2, 128.3, 125.7, 120.7, 69.7, 55.6, 53.7, 53.1, 44.3, 28.9, 18.3, 15.6;

HRMS calculated for C₁₄H₂₁BrN₂O₃SH (M+H)⁺ 377.0535; found 377.0495 (TOF MS ES⁺).

(S)-10-fluoro-3-isobutyl-5-methyl-2,3,4,5,6,7-hexahydrobenzo[*b*][1,4,5,8]oxathiazine 1,1-dioxide (3.9.2c)



According to general procedure C, **3.9.2c** (26.8 mg, 43%) was isolated as a white solid.

mp 145–148 °C;

$[\alpha]_D^{20} = +148.7$ ($c = 0.87$, CHCl₃);

FTIR (thin film) 3265, 2962, 1603, 1587, 1458, 1350, 1323, 1163, 1057, 818, 785, 733, 704 cm⁻¹;

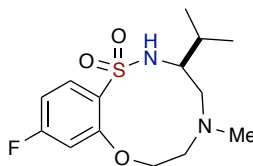
¹H NMR (400 MHz, CDCl₃) δ ppm 7.99 (dd, $J = 8.6, 6.4$ Hz, 1H, aromatic), 7.07 (s, 1H, NH), 6.92–6.78 (m, 2H, aromatic), 4.46–4.19 (m, 2H, OCH₂CH₂), 2.70 (dddd, $J = 9.0, 8.8, 4.6, 4.4$ Hz, 1H, NHCHCH₂N), 2.65 (dd, $J = 12.4, 4.9$ Hz, 1H, NHCHCH_aH_bN), 2.58 (ddd, $J = 14.9, 8.9, 5.5$ Hz, 1H, NCH_aH_bCH₂O), 2.46 (s, 3H, NCH₃), 2.34 (ddd, $J = 15.1, 1.8, 1.7$ Hz, 1H, NCH_aH_bCH₂O), 2.23 (dd, $J = 12.4, 10.5$ Hz, 1H, NHCHCH_aH_bN), 1.85 (ddd, $J = 13.7, 9.5, 3.9$ Hz, 1H, NHCHCH_aH_b), 1.61–1.52 (m, 1H, CH₃CHCH₃), 1.33

(ddd, $J = 13.8, 8.6, 5.0$ Hz, 1H, NHCHCH_aH_b), 0.86 (d, $J = 6.6$ Hz, 3H, CH₃CHCH₃), 0.72 (d, $J = 6.6$ Hz, 3H, CH₃CHCH₃);

¹³C NMR (126 MHz, CDCl₃) δ ppm 166.3 (d, $^1J_{C-F} = 254.8$ Hz), 156.3 (d, $^3J_{C-F} = 10.5$ Hz), 133.7 (d, $^3J_{C-F} = 10.8$ Hz), 126.2 (d, $^4J_{C-F} = 3.2$ Hz), 109.7 (d, $^2J_{C-F} = 22.1$ Hz), 104.9 (d, $^2J_{C-F} = 25.0$ Hz), 69.7, 60.0, 53.2, 49.9, 44.4, 43.1, 24.4, 23.6, 21.8;

HRMS calculated for C₁₅H₂₃FN₂O₃SH (M+H)⁺ 331.1492; found 331.1519 (TOF MS ES⁺).

(S)-10-fluoro-3-isopropyl-5-methyl-2,3,4,5,6,7-hexahydrobenzo[*b*][1,4,5,8]oxathia-diazecine-1,1-dioxide (3.9.2d)



According to general procedure C, **3.9.2d** (44.6 mg, 40%) was isolated as a white solid.

mp 183–188 °C;

$[\alpha]_D^{20} = +128.8$ ($c = 0.745$, CHCl₃);

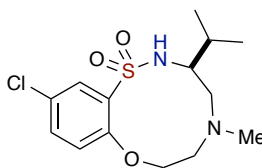
FTIR (thin film) 3257, 2974, 1603, 1587, 1470, 1448, 1373, 1323, 1163, 1067, 818, 777, 756, 729 cm⁻¹;

¹H NMR (400 MHz, CDCl₃) δ ppm 7.99 (dd, $J = 8.6, 6.4$ Hz, 1H, aromatic), 7.04 (s, 1H, NH), 6.93–6.73 (m, 2H, aromatic), 4.43–4.25 (m, 2H, OCH₂CH₂), 2.71–2.56 (m, 2H, NHCHCH₂N, NHCHCH_aH_bN), 2.50 (dd, $J = 12.8, 5.0$ Hz, 1H, NCH_aH_bCH₂O), 2.47 (s, 3H, NCH₃), 2.37–2.29 (m, 3H, NHCHCH_aH_bN, NCH_aH_bCH₂O, CH₃CHCH₃), 0.99 (d, $J = 6.9$ Hz, 3H, CH₃CHCH₃), 0.80 (d, $J = 7.2$ Hz, 3H, CH₃CHCH₃);

^{13}C NMR (126 MHz, CDCl_3) δ ppm 166.3 (d, $^1J_{\text{C-F}} = 254.7$ Hz), 156.4 (d, $^3J_{\text{C-F}} = 10.6$ Hz), 133.7 (d, $^3J_{\text{C-F}} = 10.8$ Hz), 126.2 (d, $^4J_{\text{C-F}} = 3.4$ Hz), 109.7 (d, $^2J_{\text{C-F}} = 22.1$ Hz), 105.1 (d, $^2J_{\text{C-F}} = 25.0$ Hz), 69.7, 55.7, 53.8, 53.1, 44.4, 28.9, 18.4, 15.6;

HRMS calculated for $\text{C}_{14}\text{H}_{21}\text{FN}_2\text{O}_3\text{SH}$ (M+H) $^+$ 317.1335; found 317.1320 (TOF MS ES $^+$).

(S)-11-chloro-3-isopropyl-5-methyl-2,3,4,5,6,7-hexahydrobenzo[b][1,4,5,8]oxathiazine 1,1-dioxide (3.9.2e)



According to general procedure **B**, **3.9.2e** (45.8 mg, 51%) was isolated as yellow oil.

$[\alpha]_D^{20} = +89.0$ ($c = 0.125$, CHCl_3);

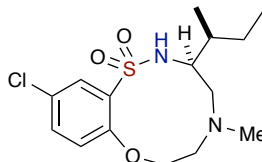
FTIR (thin film) 3149, 2962, 1587, 1469, 1371, 1307, 1222, 1161, 1060, 835, 729 cm^{-1} ;

^1H NMR (500 MHz, CDCl_3) δ ppm 7.95 (d, $J = 2.7$ Hz, 1H, aromatic), 7.50 (dd, $J = 8.8$, 2.7 Hz, 1H, aromatic), 7.14 (s, 1H, NH), 7.12 (d, $J = 8.9$ Hz, 1H, aromatic), 4.39–4.29 (m, 2H, OCH_2CH_2), 2.75–2.69 (m, 1H, NHCHCH_2N), 2.56 (ddd, $J = 14.5$, 10.5, 3.6 Hz, 1H, $\text{NCH}_2\text{H}_b\text{CH}_2\text{O}$), 2.48 (dd, $J = 12.6$, 5.1 Hz, 1H, $\text{NCH}_a\text{H}_b\text{CH}_2\text{O}$), 2.45 (s, 3H, NCH_3), 2.38–2.25 (m, 3H, $\text{NHCHCH}_a\text{H}_b$, $\text{NHCHCH}_a\text{H}_b\text{N}$, CH_3CHCH_3), 0.98 (d, $J = 6.9$ Hz, 3H, CH_3CHCH_3), 0.81 (d, $J = 7.2$ Hz, 3H, CH_3CHCH_3);

^{13}C NMR (126 MHz, CDCl_3) δ ppm 153.2, 134.1, 131.6, 131.3, 127.5, 118.7, 69.7, 55.4, 53.6, 53.0, 44.2, 28.9, 18.3, 15.5;

HRMS calculated for $C_{14}H_{21}ClN_2O_3SH$ ($M+H$)⁺ 333.1040; found 333.1022 (TOF MS ES⁺).

(S)-3-((S)-sec-butyl)-11-chloro-5-methyl-2,3,4,5,6,7-hexahydrobenzo[*b*][1,4,5,8]oxathiadiazecine 1,1-dioxide (3.9.2f)



According to general procedure **B**, **3.9.2f** (42.1 mg, 45%) was isolated as a white solid.

mp 138–142 °C;

$[\alpha]_D^{20} = -93.2$ ($c = 0.125$, $CHCl_3$);

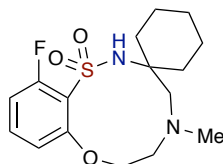
FTIR (thin film) 2962, 1588, 1467, 1371, 1159, 1060, 831, 819, 750 cm^{-1} ;

¹H NMR (500 MHz, $CDCl_3$) δ ppm 7.95 (d, $J = 2.7$ Hz, 1H, aromatic), 7.50 (dd, $J = 8.8$, 2.7 Hz, 1H, aromatic), 7.11 (d, $J = 8.8$ Hz, 1H, aromatic), 7.05 (s, 1H, NH), 4.44–4.24 (m, 2H, OCH_2CH_2), 2.83–2.72 (m, 1H, $NHCHCH_2N$), 2.58 (ddd, $J = 14.5$, 10.6, 3.5 Hz, 1H, $NCH_aH_bCH_2O$), 2.50 (dd, $J = 12.6$, 5.1 Hz, 1H, $NCH_aH_bCH_2O$), 2.44 (s, 3H, NCH_3), 2.35–2.25 (m, 2H, $NHCHCH_aH_bN$, $NHCHCH_aH_b$), 2.01–1.92 (m, 1H, $CH_3CHCH_aH_bCH_3$), 1.92–1.82 (m, 1H, $CH_3CHCH_aH_bCH_3$), 1.03–0.95 (m, 1H, $CH_3CHCH_aH_bCH_3$), 0.95–0.90 (m, 3H, $CH_3CHCH_2CH_3$), 0.80 (d, $J = 7.1$ Hz, 3H, $CH_3CHCH_2CH_3$);

¹³C NMR (126 MHz, $CDCl_3$) δ ppm 153.3, 134.1, 131.6, 131.3, 127.5, 118.6, 69.6, 55.7, 54.6, 52.8, 44.2, 36.0, 23.0, 15.3, 12.4;

HRMS calculated for $C_{15}H_{23}ClN_2O_3SH$ (M+H)⁺ 347.1196; found 347.1200 (TOF MS ES⁺).

12-fluoro-5-methyl-4,5,6,7-tetrahydro-2H-spiro[benzo[*b*][1,4,5,8]oxathiadiazecine-3,1'-cyclohexane] 1,1-dioxide (3.9.2g)



According to general procedure **B**, **3.9.2g** (42.6 mg, 46%) was isolated as brown oil.

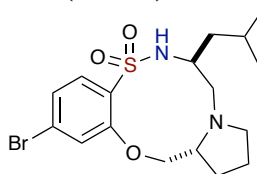
FTIR (thin film) 3245, 2956, 2931, 1591, 1488, 1458, 1319, 1153, 1062, 821, 705 cm^{-1} ;

¹H NMR (500 MHz, CDCl₃) δ ppm 7.47 (ddd, $J = 8.2, 8.2, 5.9$ Hz, 1H, aromatic), 7.13 (ddd, $J = 8.2, 1.1, 1.0$ Hz, 1H, aromatic), 6.98 (ddd, $J = 10.5, 8.4, 1.1$ Hz, 1H, aromatic), 6.55 (s, 1H, NH), 5.61–5.56 (m, 1H, OCH_aH_bCH₂), 3.79 (dd, $J = 5.1, 4.9$ Hz, 1H, OCH_aH_bCH₂), 3.38 (d, $J = 5.8$ Hz, 2H, NCH₂CH₂O), 3.25–3.09 (m, 2H, NHCC_H₂N), 2.82 (s, 3H, NCH₃), 1.99–1.87 (m, 4H, cyclohexyl), 1.70–1.44 (m, 6H, cyclohexyl);

¹³C NMR (126 MHz, CDCl₃) δ ppm 160.3(d, $^1J_{C-F} = 257.2$ Hz), 154.5, 133.5 (d, $^3J_{C-F} = 11.2$ Hz), 123.8 (d, $^3J_{C-F} = 10.2$ Hz), 119.5 (d, $^4J_{C-F} = 3.2$ Hz), 113.4 (d, $^2J_{C-F} = 24.5$ Hz), 59.5, 58.9, 50.1, 42.7, 26.4 (2C), 25.0, 22.4, 22.1 (2C);

HRMS calculated for $C_{16}H_{23}FN_2O_3SH$ (M+H)⁺ 343.1492; found 343.1485 (TOF MS ES⁺).

(6*S*,14*aR*)-11-bromo-6-isobutyl-1,2,3,5,6,7,14,14*a*-octahydrobenzo[*b*]pyrrolo[1,2*h*]-[1,4,5,8]oxathiadiazecine 8,8-dioxide (3.9.2h)



According to general procedure C, **3.9.2h** (57.7 mg, 57%) was isolated as colorless oil.

$[\alpha]_D^{20} = -48.1$ ($c = 1.805$, CHCl_3);

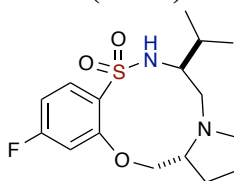
FTIR (thin film) 3275, 2955, 1578, 1466, 1317, 1159, 1063, 852, 733, 702 cm^{-1} ;

^1H NMR (400 MHz, CDCl_3) δ ppm 7.93–7.71 (m, 1H, aromatic), 7.26–7.18 (m, 2H, aromatic), 5.69 (s, 1H, NH), 4.48 (dd, $J = 11.5, 3.3$ Hz, 1H, $\text{OCH}_a\text{H}_b\text{CHN}$), 3.90 (dd, $J = 11.4, 11.3$ Hz, 1H, $\text{OCH}_a\text{H}_b\text{CHN}$), 3.40–3.26 (m, 1H, NHCHCH_2N), 3.17 (ddt, $J = 12.0, 8.1, 3.8$ Hz, 1H, NCHCH_2O), 3.14–3.03 (m, 1H, $\text{NCH}_a\text{H}_b\text{CH}_2\text{CH}_2$), 2.50–2.38 (m, 3H, NHCHCH_2N , $\text{NCH}_a\text{H}_b\text{CH}_2\text{CH}_2$), 2.01–1.90 (m, 1H, $\text{NCH}_2\text{CH}_2\text{CH}_a\text{H}_b$), 1.88–1.77 (m, 3H, $\text{NCH}_2\text{CH}_2\text{CH}_2$, CH_3CHCH_3), 1.67 (ddd, $J = 14.3, 8.4, 6.2$ Hz, 1H, $\text{NHCHCH}_a\text{H}_b$), 1.40 (td, $J = 11.4, 4.6$ Hz, 1H, $\text{NCH}_2\text{CH}_2\text{CH}_a\text{H}_b$), 1.10 (ddd, $J = 14.0, 7.8, 6.2$ Hz, 1H, $\text{NHCHCH}_a\text{H}_b$), 0.90 (dd, $J = 6.9, 6.8$ Hz, 6H, CH_3CHCH_3);

^{13}C NMR (126 MHz, CDCl_3) δ ppm 156.0, 131.1, 130.8, 128.0, 124.5, 118.2, 74.0, 62.8, 61.4, 56.7, 55.5, 40.9, 27.4, 24.7, 24.7, 22.7, 22.3;

HRMS calculated for $\text{C}_{17}\text{H}_{25}\text{BrN}_2\text{O}_3\text{SH}$ ($\text{M}+\text{H}$)⁺ 417.0848; found 417.0836 (TOF MS ES⁺).

(6*S*,14*aR*)-11-fluoro-6-isopropyl-1,2,3,5,6,7,14,14*a*-octahydrobenzo[*b*]pyrrolo[1,2-*h*][1,4,5,8]oxathia-diazecine 8,8-dioxide (3.9.2i)



According to general procedure **C**, **3.9.2i** (26.1 mg, 37%) was isolated as semi-white sticky oil.

$[\alpha]_D^{20} = -6.6$ ($c = 1.33$, CHCl_3);

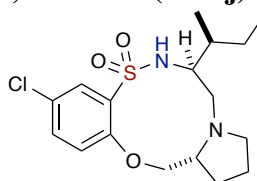
FTIR (thin film) 3300, 2961, 1603, 1587, 1468, 1387, 1323, 1157, 1070, 839 cm^{-1} ;

^1H NMR (500 MHz, CDCl_3) δ ppm 7.99–7.76 (m, 1H, aromatic), 6.82–6.64 (m, 2H, aromatic), 4.84 (d, $J = 6.9$ Hz, 1H, NH), 4.45 (dd, $J = 11.6, 3.1$ Hz, 1H, $\text{OCH}_a\text{H}_b\text{CHN}$) 3.99 (dd, $J = 11.2, 11.1$ Hz, 1H, $\text{OCH}_a\text{H}_b\text{CHN}$), 3.32 (ddd, $J = 11.3, 5.9, 5.7$ Hz, 1H, NHCHCH_2N), 3.08 (dddd, $J = 11.2, 8.7, 5.8, 3.1$ Hz, 1H, NCHCH_2O), 2.97 (ddd, $J = 9.6, 6.2, 4.5$ Hz, 1H, $\text{NCH}_a\text{H}_b\text{CH}_2\text{CH}_2$), 2.71 (dd, $J = 14.4, 5.6$ Hz, 1H, $\text{NHCHCH}_a\text{H}_b\text{N}$), 2.56–2.43 (m, 2H, $\text{NCH}_a\text{H}_b\text{CH}_2\text{CH}_2$, $\text{NHCHCH}_a\text{H}_b\text{N}$), 2.00–1.85 (m, 2H, CH_3CHCH_3 , $\text{NCH}_2\text{CH}_2\text{CH}_a\text{H}_b$), 1.79–1.69 (m, 2H, $\text{NCH}_2\text{CH}_2\text{CH}_2$), 1.45–1.31 (m, 1H, $\text{NCH}_2\text{CH}_2\text{CH}_a\text{H}_b$), 0.97 (dd, $J = 6.9, 4.4$ Hz, 6H, CH_3CHCH_3);

^{13}C NMR (126 MHz, CDCl_3) δ ppm 166.0 (d, $^1J_{\text{C-F}} = 253.8$ Hz), 157.5 (d, $^3J_{\text{C-F}} = 10.8$ Hz), 132.0 (d, $^3J_{\text{C-F}} = 10.9$ Hz), 126.7 (d, $^4J_{\text{C-F}} = 3.2$ Hz), 107.9 (d, $^2J_{\text{C-F}} = 22.2$ Hz), 102.6 (d, $^2J_{\text{C-F}} = 25.6$ Hz), 74.0, 64.9, 62.8, 59.4, 57.5, 31.3, 27.2, 23.8, 18.7, 18.2;

HRMS calculated for $\text{C}_{16}\text{H}_{23}\text{FN}_2\text{O}_3\text{SH}$ ($\text{M}+\text{H}$) $^+$ 343.1492; found 343.1492 (TOF MS ES^+).

(6*S*,14*aR*)-6-((*S*)-*sec*-butyl)-10-chloro-1,2,3,5,6,7,14,14*a*-octahydrobenzo[*b*]pyrrolo-[1,2-*h*][1,4,5,8]oxathiadiazecine 8,8-dioxide (3.9.2j)



According to general procedure **B, 3.9.2j** (54.4 mg, 54%) was isolated as yellow oil.

$[\alpha]_D^{20} = -68.4$ ($c = 0.125$, CHCl_3);

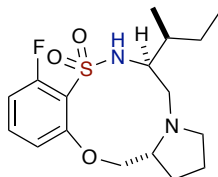
FTIR ((**thin film**)) 2962, 2875, 1598, 1467, 1407, 1380, 1338, 1163, 1064, 786, 761 cm^{-1} ;

^1H NMR (500 MHz, CDCl_3) δ ppm 7.91 (d, $J = 2.7$ Hz, 1H, aromatic), 7.46 (dd, $J = 8.8$, 2.7 Hz, 1H, aromatic), 7.06 (d, $J = 8.8$ Hz, 1H, aromatic), 6.85 (d, $J = 5.7$ Hz, 1H, NH), 4.35 (dd, $J = 11.8$, 3.2 Hz, 1H, $\text{OCH}_a\text{H}_b\text{CHN}$), 3.90 (t, $J = 11.6$ Hz, 1H, $\text{OCH}_a\text{H}_b\text{CHN}$), 3.20–2.95 (m, 2H, NHCHCH_2N , NCHCH_2O), 2.92–2.78 (m, 1H, $\text{NCH}_a\text{H}_b\text{CH}_2\text{CH}_2$), 2.63–2.50 (m, 2H, $\text{NHCHCH}_a\text{H}_b\text{N}$, $\text{NCH}_a\text{H}_b\text{CH}_2\text{CH}_2$), 2.41 (dd, $J = 13.5$, 5.1 Hz, 1H, $\text{NHCHCH}_a\text{H}_b\text{N}$), 2.02–1.86 (m, 1H, $\text{NCH}_2\text{CH}_a\text{H}_b\text{CH}_2$), 1.86–1.75 (m, 2H, $\text{NCH}_2\text{CH}_a\text{H}_b\text{CH}_2$, $\text{NCH}_2\text{CH}_a\text{H}_b\text{CH}_a\text{H}_b$), 1.76–1.62 (m, 2H, $\text{NCH}_2\text{CH}_a\text{H}_b\text{CH}_a\text{H}_b$, $\text{CH}_3\text{CHCH}_a\text{H}_b\text{CH}_3$), 1.40–1.29 (m, 1H, $\text{CH}_3\text{CHCH}_a\text{H}_b\text{CH}_3$), 1.11–0.97 (m, 1H, $\text{CH}_3\text{CHCH}_a\text{H}_b\text{CH}_3$), 0.95 (d, $J = 6.8$ Hz, 3H, $\text{CH}_3\text{CHCH}_2\text{CH}_3$), 0.90 (t, $J = 7.3$ Hz, 3H, $\text{CH}_3\text{CHCH}_2\text{CH}_3$);

^{13}C NMR (126 MHz, CDCl_3) δ ppm 153.1, 133.6, 131.6, 130.3, 126.7, 116.4, 73.5, 61.9, 58.0, 57.2, 55.7, 37.0, 27.0, 25.4, 24.2, 15.8, 11.6;

HRMS calculated for $\text{C}_{17}\text{H}_{25}\text{ClN}_2\text{O}_3\text{SH}$ ($\text{M}+\text{H}$) $^+$ 373.1353; found 373.1334 (TOF MS ES^+).

(6*S*,14*aR*)-6-((*S*)-*sec*-butyl)-9-fluoro-1,2,3,5,6,7,14,14*a*-octahydrobenzo[*b*]pyrrolo-[1,2-*h*][1,4,5,8]oxathia-diazecine 8,8-dioxide (3.9.2k)



According to general procedure **B**, **3.9.2k** (54.9 mg, 57%) was isolated as a yellow/white solid.

mp 152–156 °C;

$[\alpha]_D^{20} = -58.3$ ($c = 0.125$, CHCl_3);

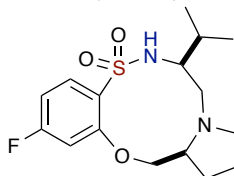
FTIR ((**thin film**)) 2962, 2875, 1598, 1467, 1380, 1338, 1163, 1064, 786, 761 cm^{-1} ;

^1H NMR (500 MHz, CDCl_3) δ ppm 7.42 (ddd, $J = 8.4, 5.8$ Hz, 1H, aromatic), 7.07 (d, $J = 6.2$ Hz, 1H, NH), 6.89 (ddd, $J = 8.5, 1.1, 1.1$ Hz, 1H, aromatic), 6.82 (ddd, $J = 9.6, 8.4, 1.0$ Hz, 1H, aromatic), 4.42 (dd, $J = 11.8, 3.2$ Hz, 1H, $\text{OCH}_a\text{H}_b\text{CHN}$), 3.92 (dd, $J = 11.5, 11.2$ Hz, 1H, $\text{OCH}_a\text{H}_b\text{CHN}$), 3.19–3.04 (m, 2H, NHCHCH_2N , NCHCH_2O), 3.03–2.93 (m, 1H, $\text{NCH}_a\text{H}_b\text{CH}_2\text{CH}_2$), 2.64 (dd, $J = 13.8, 5.4$ Hz, 1H, $\text{NHCHCH}_a\text{H}_b\text{N}$), 2.57 (ddd, $J = 9.3, 9.2, 6.1$ Hz, 1H, $\text{NCH}_a\text{H}_b\text{CH}_2\text{CH}_2$), 2.46 (dd, $J = 13.8, 4.9$ Hz, 1H, $\text{NHCHCH}_a\text{H}_b\text{N}$), 1.99–1.88 (m, 1H, $\text{NCH}_2\text{CH}_a\text{H}_b\text{CH}_2$), 1.88–1.61 (m, 4H, $\text{NCH}_2\text{CH}_a\text{H}_b\text{CH}_2$, $\text{NCH}_2\text{CH}_a\text{H}_b\text{CH}_2$, $\text{CH}_3\text{CHCH}_a\text{H}_b\text{CH}_3$), 1.38 (dddd, $J = 13.1, 6.8, 3.6, 3.5$ Hz, 1H, $\text{CH}_3\text{CHCH}_a\text{H}_b\text{CH}_3$), 1.10–1.00 (m, 1H, $\text{CH}_3\text{CHCH}_a\text{H}_b\text{CH}_3$), 0.99 (d, $J = 6.8$ Hz, 3H, $\text{CH}_3\text{CHCH}_2\text{CH}_3$), 0.89 (t, $J = 7.3$ Hz, 3H, $\text{CH}_3\text{CHCH}_2\text{CH}_3$);

^{13}C NMR (126 MHz, CDCl_3) δ ppm 161.1 (d, $^1J_{\text{C-F}} = 259.8$ Hz), 155.6, 133.5 (d, $^3J_{\text{C-F}} = 11.0$ Hz), 119.2 (d, $^3J_{\text{C-F}} = 13.1$ Hz), 110.6 (d, $^2J_{\text{C-F}} = 24.2$ Hz), 109.9 (d, $^4J_{\text{C-F}} = 3.6$ Hz), 73.5, 62.1, 58.5, 57.6, 55.6, 36.8, 27.1, 25.6, 24.3, 15.9, 11.5;

HRMS calculated for $C_{17}H_{25}FN_2O_3SH$ (M+H)⁺ 357.1648; found 357.1635 (TOF MS ES⁺).

(6*S*,14*aS*)-11-fluoro-6-isopropyl-1,2,3,5,6,7,14,14*a*-octahydrobenzo[*b*]pyrrolo[1,2-*h*][1,4,5,8]oxathia-diazecine 8,8-dioxide (3.9.21)



According to general procedure **B**, **3.9.21** (25.7 mg, 42%) was isolated as colorless oil.

$[\alpha]_D^{20} = +74.4$ ($c = 0.36$, $CHCl_3$);

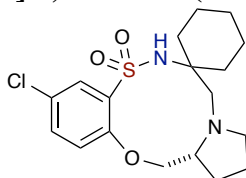
FTIR (thin film) 3286, 2962, 1603, 1587, 1475, 1383, 1329, 1163, 1070, 735, 698 cm^{-1} ;

¹H NMR (500 MHz, CDCl₃) δ ppm 7.94 (dd, $J = 8.6, 6.5$ Hz, 1H, aromatic), 6.92–6.76 (m, 3H, aromatic, NH), 4.33 (dd, $J = 11.9, 3.3$ Hz, 1H, OCH_aH_bCHN), 3.92 (dd, $J = 11.8, 11.7$ Hz, 1H, OCH_aH_bCHN), 3.16 (ddd, $J = 10.2, 5.5, 4.8$ Hz, 1H, NHCH_cCH₂N), 3.06 (ddt, $J = 11.9, 8.6, 3.1$ Hz, 1H, NCH_dCH₂O), 2.71 (dt, $J = 11.9, 5.9$ Hz, 1H, NCH_aH_bCH₂CH₂), 2.64–2.50 (m, 2H, NCH_aH_bCH₂CH₂, NHCHCH_aH_bN), 2.37 (dd, $J = 13.5, 5.0$ Hz, 1H, NHCHCH_aH_bN), 2.02–1.89 (m, 2H, CH₃CH_bCH₃, NCH₂CH₂CH_aH_b), 1.87–1.78 (m, 2H, NCH₂CH₂CH₂), 1.36 (ddt, $J = 12.6, 6.6, 3.4$ Hz, 1H, NCH₂CH₂CH_aH_b), 0.95 (dd, $J = 17.2, 6.8$ Hz, 6H, CH₃CHCH₃);

¹³C NMR (126 MHz, CDCl₃) δ ppm 166.0 (d, $^1J_{C-F} = 254.3$ Hz), 156.2 (d, $^3J_{C-F} = 10.5$ Hz), 132.5 (d, $^3J_{C-F} = 10.8$ Hz), 126.4 (d, $^4J_{C-F} = 3.3$ Hz), 108.8 (d, $^2J_{C-F} = 22.2$ Hz), 103.1 (d, $^2J_{C-F} = 25.4$ Hz), 73.7, 62.0, 59.1, 57.3, 55.2, 30.5, 27.0, 25.6, 19.6, 17.5;

HRMS calculated for $C_{16}H_{23}FN_2O_3SH$ (M+H)⁺ 343.1492; found 343.1459 (TOF MS ES⁺).

(R)-10-chloro-2,3,5,7,14,14a-hexahydro-1H-spiro[benzo[*b*]pyrrolo[1,2-*h*][1,4,5,8]-oxathiadiazecine-6,1'-cyclohexane] 8,8-dioxide (3.9.2m)



According to general procedure **B**, **3.9.2m** (53.0 mg, 51%) was isolated as a white solid.

mp 154–159 °C;

$[\alpha]_D^{20} = -24.0$ ($c = 0.125$, $CHCl_3$);

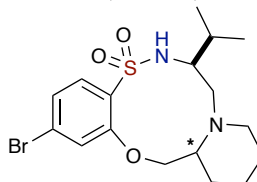
FTIR (thin film) 2937, 1585, 1465, 1315, 1228, 1157, 1064, 819, 732 cm^{-1} ;

¹H NMR (500 MHz, CDCl₃) δ ppm 7.92 (d, $J = 2.7$ Hz, 1H, aromatic), 7.45 (dd, $J = 8.8$, 2.7 Hz, 1H, aromatic), 7.05 (d, $J = 8.8$ Hz, 1H, aromatic), 6.30 (s, 1H, NH), 4.46 (dd, $J = 11.9$, 3.2 Hz, 1H, OCH_aH_bCHN), 3.93 (dd, $J = 11.8$, 11.5 Hz, 1H, OCH_aH_bCHN), 3.24–3.18 (m, 1H, NCH_bCH₂O), 3.13 (dddd, $J = 12.2$, 9.3, 3.4, 3.3 Hz, 1H, NCH_aH_bCH₂CH₂), 2.50–2.37 (m, 2H, NHCCH_aH_bN, NCH_aH_bCH₂CH₂), 2.17 (d, $J = 14.1$ Hz, 1H, NHCCH_aH_bN), 2.03–1.86 (m, 2H, NCH₂CH_aH_bCH_aH_b, NCH₂CH₂CH_aH_b), 1.84–1.76 (m, 2H, NCH₂CH_aH_bCH_aH_b, NCH₂CH₂CH_aH_b), 1.75–1.63 (m, 2H, cyclohexyl), 1.58–1.50 (m, 1H, cyclohexyl), 1.50–1.41 (m, 1H, cyclohexyl), 1.41–1.20 (m, 5H, cyclohexyl), 1.14–1.04 (m, 1H, cyclohexyl);

¹³C NMR (126 MHz, CDCl₃) δ ppm 153.0, 133.6, 133.3, 129.6, 126.5, 116.3, 73.6, 63.7, 60.3, 59.6, 38.4, 31.3, 27.3, 26.1, 25.4, 21.6, 21.4 (2C);

HRMS calculated for $C_{18}H_{25}ClN_2O_3SH (M+H)^+$ 385.1353; found 385.1336 (TOF MS ES⁺).

(7S)-2-bromo-7-isopropyl-7,8,10,11,12,13,13a,14-octahydro-6H-benzo[*b*]pyrido[1,2-*h*][1,4,5,8]oxathia-diazecine 5,5-dioxide (3.9.2n)



According to general procedure **C**, **3.9.2n** (44.7 mg, 36%) was isolated as sticky colorless oil.

$[\alpha]_D^{20} = +30.1$ ($c = 0.59$, $CHCl_3$);

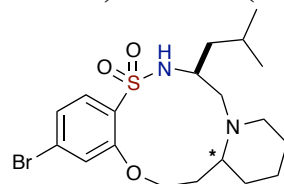
FTIR (thin film) 3259, 2934, 1578, 1464, 1391, 1327, 1159, 1063, 812, 762, 733 cm^{-1} ;

¹H NMR (400 MHz, CDCl₃) δ ppm 7.80 (d, $J = 8.3$ Hz, 1H, aromatic), 7.29 (d, $J = 1.8$ Hz, 1H, aromatic), 7.20 (d, $J = 1.8$ Hz, 1H, aromatic), 4.39 (dd, $J = 10.7, 4.6$ Hz, 1H, OCH_aH_bCHN), 3.75–3.60 (m, 1H, OCH_aH_bCHN), 3.42–3.25 (m, 1H, NCHCH₂O), 2.79–2.60 (m, 4H, NCH₂CH₂CH₂CH₂, NHCHCH₂N, NHCHCH_aH_bN), 2.49–2.31 (m, 1H, NHCHCH_aH_bN), 1.99–1.86 (m, 1H, CH₃CHCH₃), 1.87–1.77 (m, 1H, NCH₂CH₂CH_aH_bCH₂), 1.59–1.36 (m, 4H, NCH₂CH₂CH_aH_bCH_aH_b), 1.30–1.16 (m, 1H, NCH₂CH₂CH_aH_b), 0.94 (d, $J = 6.8$ Hz, 3H, CH₃CHCH₃), 0.89 (d, $J = 7.0$ Hz, 3H, CH₃CHCH₃);

¹³C NMR (126 MHz, CDCl₃) δ ppm 156.5, 131.9, 127.7, 127.7, 125.7, 120.3, 73.7, 59.4, 57.4 (2C), 54.2, 31.2, 23.8, 22.9, 21.6, 18.3, 17.2;

HRMS calculated for $C_{17}H_{25}BrN_2O_3SH$ ($M+H$)⁺ 417.0848; found 417.0838 (TOF MS ES⁺).

(7*S*)-2-bromo-7-isobutyl-6,7,8,10,11,12,13,13a,14,15-decahydrobenzo[*b*]pyrido[1,2-*h*][1,4,5,8]oxathiadiazacycloundecine 5,5-dioxide (3.9.2o)



According to general procedure **C**, **3.9.2o** (14.5 mg, 20%) was isolated as light yellow oil.

$[\alpha]_D^{20} = +132.4$ ($c = 0.69$, $CHCl_3$);

FTIR (thin film) 3202, 2935, 1580, 1470, 1389, 1325, 1163, 1065, 812, 733 cm^{-1} ;

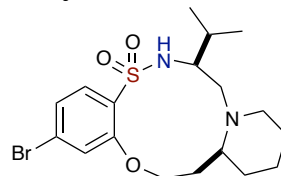
¹H NMR (500 MHz, CDCl₃) δ ppm 7.82 (d, $J = 8.3$ Hz, 1H, aromatic), 7.21 (dd, $J = 8.3$, 1.7 Hz, 1H, aromatic), 7.13 (d, $J = 1.7$ Hz, 1H, aromatic), 6.68 (s, 1H, NH), 4.56 (ddd, $J = 11.9$, 9.9, 4.4 Hz, 1H, OCH_aH_bCH₂CHN), 4.43 (ddd, $J = 11.9$, 4.7, 4.6 Hz, 1H, OCH_aH_bCH₂CHN), 3.20–2.99 (m, 2H, NHCHCH_aH_bN, NCH_aH_bCH₂CH₂CH₂), 2.81 (ddd, $J = 12.8$, 8.9, 4.3 Hz, 1H, NHCH_aH_bCH₂N), 2.50 (dt, $J = 14.1$, 3.9 Hz, 1H, NCH_aH_bCH₂CH₂CH₂), 2.35 (dt, $J = 12.9$, 4.4 Hz, 1H, NCH_aH_bCH₂CH₂O), 2.15–2.05 (m, 2H, NHCHCH_aH_bN, NCHCH_aH_bCH₂O), 2.01 (dt, $J = 15.1$, 5.0 Hz, 1H, NCHCH_aH_bCH₂O), 1.94 (ddd, $J = 13.6$, 9.2, 4.1 Hz, 1H, NCH₂CH₂CH_aH_bCH₂), 1.77–1.68 (m, 1H, NCH₂CH₂CH_aH_b), 1.68–1.50 (m, 4H, NCH₂CH₂CH₂CH₂, CH₃CHCH₃, NHCHCH_aH_b), 1.38–1.28 (m, 2H, NCH₂CH₂CH_aH_bCH₂, NHCHCH_aH_b), 1.22–1.13 (m,

1H, NCH₂CH₂CH₂CH_aH_b), 0.87 (d, *J* = 6.6 Hz, 3H, CH₃CHCH₃), 0.79 (d, *J* = 6.6 Hz, 3H, CH₃CHCH₃);

¹³C NMR (126 MHz, CDCl₃) δ ppm 154.5, 132.3, 128.1, 126.3, 123.7, 116.2, 65.5, 55.5, 50.5 (2C), 49.0, 43.6, 28.1, 24.7, 23.9, 23.5, 22.0, 21.3, 20.6;

HRMS calculated for C₁₉H₂₉BrN₂O₃SH (M+H)⁺ 445.1161; found 445.1157 (TOF MS ES⁺).

(7*S*,13*aS*)-2-bromo-7-isopropyl-6,7,8,10,11,12,13,13*a*,14,15-decahydrobenzo[*b*]pyrido[1,2-*h*][1,4,5,8]oxa-thiadiazacycloundecine 5,5-dioxide (3.9.2p)



According to general procedure C, **3.9.2p** (23.3 mg, 22%) was isolated as a white solid.

mp 152–157 °C;

[α]_D²⁰ = +107.4 (*c* = 0.81, CHCl₃);

FTIR (thin film) 3205, 2934, 1580, 1470, 1387, 1327, 1163, 1065, 821, 733 cm⁻¹;

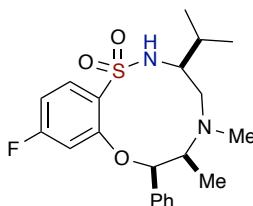
¹H NMR (400 MHz, CDCl₃) δ ppm 7.81 (d, *J* = 8.3 Hz, 1H, aromatic), 7.20 (dd, *J* = 8.3, 1.7 Hz, 1H, aromatic), 7.13 (d, *J* = 1.7 Hz, 1H, aromatic), 6.62 (s, 1H, NH), 4.54 (ddd, *J* = 11.6, 9.4, 4.4 Hz, 1H, OCH_aH_bCH₂CHN), 4.40 (ddd, *J* = 11.6, 5.0, 4.9 Hz, 1H, OCH_aH_bCH₂CHN), 3.17–3.03 (m, 1H, NCH_aH_bCH₂CH₂CH₂), 2.96 (dd, *J* = 12.9, 4.6 Hz, 1H, NHCHCH_aH_bN), 2.73 (ddd, *J* = 10.4, 4.6, 4.4 Hz, 1H, NHCHCH_aH_bN), 2.51 (d, *J* = 14.3 Hz, 1H, NCH_aH_bCH₂CH₂CH₂), 2.47–2.32 (m, 2H, CH₃CHCH₃, NCHCH₂CH₂O), 2.29–2.08 (m, 2H, NHCHCH_aH_bN, NCHCH_aH_bCH₂O), 1.95 (dddd, *J* = 14.6, 9.3, 5.1, 4.9 Hz, 1H, NCHCH_aH_bCH₂O), 1.81–1.67 (m, 1H, NCH₂CH₂CH₂CH_aH_b), 1.67–1.45 (m, 3H,

NCH₂CH_aH_bCH₂CH₂), 1.37–1.20 (m, 1H, NCH₂CH_aH_bCH₂CH₂), 1.19–1.09 (m, 1H, NCH₂CH₂CH₂CH_aH_b), 0.98 (d, *J* = 6.9 Hz, 3H, CH₃CHCH₃), 0.87 (d, *J* = 7.2 Hz, 3H, CH₃CHCH₃);

¹³C NMR (126 MHz, CDCl₃) δ ppm 154.8, 132.4, 128.1, 126.3, 123.7, 116.3, 66.0, 55.1, 50.4, 50.2, 49.4, 29.1, 28.4, 23.6, 21.1, 20.5, 18.9, 15.6;

HRMS calculated for C₁₈H₂₇BrN₂O₃SH (M+H)⁺ 431.1004; found 431.0976 (TOF MS ES⁺).

(3*S*,6*S*,7*R*)-10-fluoro-3-isopropyl-5,6-dimethyl-7-phenyl-2,3,4,5,6,7-hexahydrobenzo-*b*[1,4,5,8]oxathia-diazecine 1,1-dioxide (3.10.2a)



According to general procedure **C**, **3.10.2a** (37.2 mg, 46%) was isolated as sticky colorless oil.

[α]_D²⁰ = +43.1 (*c* = 1.145, CHCl₃);

FTIR (thin film) 3267, 2962, 1603, 1585, 1475, 1454, 1371, 1323, 1163, 1068, 812, 764, 737, 704 cm⁻¹;

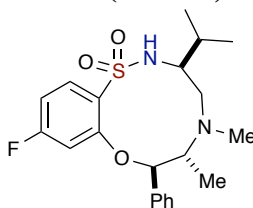
¹H NMR (500 MHz, CDCl₃) δ ppm 8.02 (dd, *J* = 8.8, 6.5 Hz, 1H, aromatic), 7.60–7.54 (m, 2H, aromatic), 7.48 (s, 1H, NH), 7.45–7.35 (m, 3H, aromatic), 6.94 (dd, *J* = 10.3, 2.4 Hz, 1H, aromatic), 6.87 (ddd, *J* = 8.7, 7.7, 2.3 Hz, 1H, aromatic), 5.25 (d, *J* = 2.5 Hz, 1H, OCHPh), 2.93 (qd, *J* = 7.1, 2.6 Hz, 1H, NCHCH₃), 2.63 (ddd, *J* = 11.3, 4.6, 4.5 Hz, 1H,

NHCHCH₂N), 2.55 (dd, $J = 12.9, 5.2$ Hz, 1H, NHCHCH_aH_bN), 2.32 (m, 1H, CH₃CHCH₃), 2.11 (dd, $J = 12.1, 12.0$ Hz, 1H, NHCHCH_aH_bN), 1.51 (s, 3H, NCH₃), 1.09 (d, $J = 7.1$ Hz, 3H, NCHCH₃), 0.98 (d, $J = 6.9$ Hz, 3H, CH₃CHCH₃), 0.78 (d, $J = 7.2$ Hz, 3H, CH₃CHCH₃);

¹³C NMR (126 MHz, CDCl₃) δ ppm 166.3 (d, $^1J_{C-F} = 254.6$ Hz), 155.6 (d, $^3J_{C-F} = 10.7$ Hz), 135.0, 134.0 (d, $^3J_{C-F} = 10.8$ Hz), 128.4, 128.3 (2C), 127.1 (2C), 125.1 (d, $^4J_{C-F} = 3.4$ Hz), 109.5 (d, $^2J_{C-F} = 22.0$ Hz), 104.3 (d, $^2J_{C-F} = 25.2$ Hz), 85.3, 56.7, 55.1, 52.9, 38.9, 28.6, 18.3, 15.5, 10.6;

HRMS calculated for C₂₁H₂₇FN₂O₃SH (M+H)⁺ 407.1805; found 407.1790 (TOF MS ES⁺).

(3*S*,6*R*,7*R*)-10-fluoro-3-isopropyl-5,6-dimethyl-7-phenyl-2,3,4,5,6,7-hexahydrobenzo-*[b]*[1,4,5,8]oxathia-diazecine 1,1-dioxide (3.10.2b)



According to general procedure **B**, **3.10.2b** (39.0 mg, 47%) was isolated as a white solid.

mp 87–93 °C;

$[\alpha]_D^{20} = +12.8$ ($c = 0.69$, CHCl₃);

FTIR (thin film) 3300, 2962, 1603, 1583, 1479, 1456, 1369, 1325, 1157, 1068, 843, 770, 735, 700 cm⁻¹;

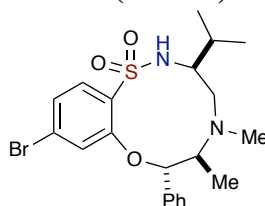
¹H NMR (400 MHz, CDCl₃) δ ppm 7.97 (dd, $J = 8.8, 6.6$ Hz, 1H, aromatic), 7.56–7.45 (m, 2H, aromatic), 7.45–7.32 (m, 3H, aromatic), 6.76 (ddd, $J = 8.7, 7.7, 2.4$ Hz, 1H,

aromatic), 6.66 (dd, $J = 10.6, 2.4$ Hz, 1H, aromatic), 6.47 (s, 1H, NH), 4.78 (d, $J = 9.9$ Hz, 1H, OCHPh), 3.10 (dq, $J = 9.8, 6.5$ Hz, 1H, NCHCH₃), 2.82–2.59 (m, 2H, NHCHCH₂N, NHCHCH_aH_bN), 2.40 (dd, $J = 13.9, 7.2$ Hz, 1H, NHCHCH_aH_bN), 2.15 (s, 3H, NCH₃), 1.98–1.79 (m, 1H, CH₃CHCH₃), 0.97 (d, $J = 6.9$ Hz, 6H, CH₃CHCH₃), 0.86 (d, $J = 6.6$ Hz, 3H, NCHCH₃);

¹³C NMR (126 MHz, CDCl₃) δ ppm 165.9 (d, $^1J_{C-F} = 253.7$ Hz), 158.7 (d, $^3J_{C-F} = 10.8$ Hz), 138.5, 133.0 (d, $^3J_{C-F} = 10.7$ Hz), 129.0 (2C), 128.8, 127.1 (2C), 124.2 (d, $^4J_{C-F} = 3.2$ Hz), 108.5 (d, $^2J_{C-F} = 22.0$ Hz), 104.7 (d, $^2J_{C-F} = 25.3$ Hz), 88.3, 67.8, 58.4, 52.5, 37.7, 32.1, 19.0, 17.7, 10.6;

HRMS calculated for C₂₁H₂₇FN₂O₃SH (M+H)⁺ 407.1805; found 407.1765 (TOF MS ES⁺).

(3*S*,6*S*,7*S*)-10-bromo-3-isopropyl-5,6-dimethyl-7-phenyl-2,3,4,5,6,7-hexahydrobenzo-*b*[[1,4,5,8]oxathia-diazecine 1,1-dioxide (3.10.2c)



According to general procedure C, **3.10.2c** (9.7 mg, 13%) was isolated as colorless oil.

$[\alpha]_D^{20} = +73.2$ ($c = 0.335$, CHCl₃);

FTIR (thin film) 3285, 2964, 1578, 1468, 1452, 1319, 1155, 1064, 804, 756, 702 cm⁻¹;

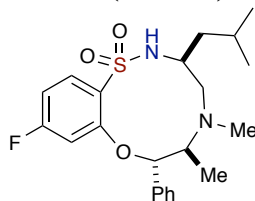
¹H NMR (400 MHz, CDCl₃) δ ppm 7.78 (d, $J = 8.4$ Hz, 1H, aromatic), 7.52–7.47 (m, 2H, aromatic), 7.46–7.40 (m, 2H, aromatic), 7.40–7.33 (m, 1H, aromatic), 7.07 (dd, $J = 8.4, 1.8$ Hz, 1H, aromatic), 6.95 (d, $J = 1.8$ Hz, 1H, aromatic), 4.71 (d, $J = 9.3$ Hz, 1H,

OCHPh), 4.41 (s, 1H, NH), 4.01 (bs, 1H, NHCHCH₂N), 3.19–3.08 (m, 1H, NCHCH₃), 2.78 (dd, *J* = 13.3, 2.9 Hz, 1H, NHCHCH_aH_bN), 2.23 (m, 4H, NHCHCH_aH_bN, NCH₃), 1.96–1.79 (m, 1H, CH₃CHCH₃), 1.09 (d, *J* = 6.8 Hz, 3H, CH₃CHCH₃), 1.00 (d, *J* = 6.9 Hz, 3H, CH₃CHCH₃), 0.75 (d, *J* = 7.0 Hz, 3H, NCHCH₃);

¹³C NMR (126 MHz, CDCl₃) δ ppm 157.8, 138.5, 131.0, 130.8, 128.9 (2C), 128.6, 127.7, 126.7 (2C), 123.4, 118.8, 87.0, 60.4, 58.8, 58.0, 37.3, 32.3, 19.0, 18.0, 10.4;

HRMS calculated for C₂₁H₂₇BrN₂O₃SH (M+H)⁺ 467.1004; found 467.1004 (TOF MS ES⁺).

(3*S*,6*S*,7*S*)-10-fluoro-3-isobutyl-5,6-dimethyl-7-phenyl-2,3,4,5,6,7-hexahydrobenzo-*b*][1,4,5,8]oxathia-diazecine 1,1-dioxide (3.10.2d)



According to general procedure C, **3.10.2d** (33.2 mg, 30%) was isolated as a white solid.

mp 165–169 °C;

$[\alpha]_D^{20} = +20.0$ (*c* = 0.145, CHCl₃);

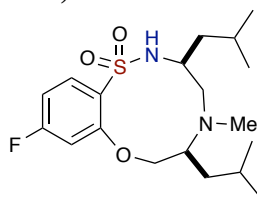
FTIR (thin film) 3265, 2960, 1602, 1586, 1473, 1451, 1373, 1323, 1163, 1066, 815, 762, 734, 706 cm⁻¹;

¹H NMR (400 MHz, CDCl₃) δ ppm 7.94 (dd, *J* = 8.8, 6.6 Hz, 1H, aromatic), 7.51–7.31 (m, 5H, aromatic), 6.65 (ddd, *J* = 8.5, 8.3, 2.4 Hz, 1H, aromatic), 6.52 (dd, *J* = 10.4, 2.4 Hz, 1H, aromatic), 4.68 (d, *J* = 9.3 Hz, 1H, OCHPh), 4.40 (d, *J* = 7.3 Hz, 1H, NH), 4.18 (bs, 1H, NHCHCH₂N), 3.17 (dd, *J* = 8.8, 7.1 Hz, 1H, NCHCH₃), 2.79 (dd, *J* = 13.6, 3.4

Hz, 1H, NHCHCH_aH_bN), 2.26 (s, 3H, NCH₃), 2.22–2.14 (m, 1H, NHCHCH_aH_bN), 1.94 (dt, $J = 13.3, 6.7$ Hz, 1H, CH₃CHCH₃), 1.50 (dd, $J = 14.0, 7.0$ Hz, 1H, NHCHCH_aH_b), 1.32 (ddd, $J = 13.9, 7.7, 6.0$ Hz, 1H, NHCHCH_aH_b), 1.04 (d, $J = 6.6$ Hz, 3H, CH₃CHCH₃), 1.02 (d, $J = 6.8$ Hz, 3H, CH₃CHCH₃), 0.77 (d, $J = 7.0$ Hz, 3H, NCHCH₃);
¹³C NMR (126 MHz, CDCl₃) δ ppm 165.9 (d, $^1J_{C-F} = 253.3$ Hz), 158.7 (d, $^3J_{C-F} = 11.0$ Hz), 138.6, 131.6 (d, $^3J_{C-F} = 10.9$ Hz), 129.0 (2C), 128.6, 127.9 (d, $^4J_{C-F} = 3.5$ Hz), 126.7 (2C), 107.3 (d, $^2J_{C-F} = 22.3$ Hz), 103.2 (d, $^2J_{C-F} = 25.5$ Hz), 86.9, 60.9, 60.7, 52.5, 45.4, 37.2, 24.7, 23.1, 22.8, 10.9;

HRMS calculated for C₂₂H₂₉FN₂O₃SH (M+H)⁺ 421.1956; found 421.1956 (TOF MS ES⁺).

(3*S*,6*S*)-10-fluoro-3,6-diisobutyl-5-methyl-2,3,4,5,6,7-hexahydrobenzo[*b*][1,4,5,8]-oxathiadiazecine-1,1-dioxide (3.10.2e)



According to general procedure **B**, **3.10.2e** (26.6 mg, 39%) was isolated as a white solid.

mp 133–137 °C;

$[\alpha]_D^{20} = +106.8$ ($c = 0.825$, CHCl₃);

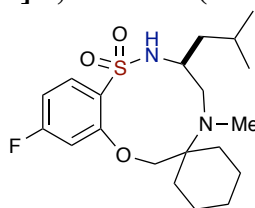
FTIR (thin film) 2957, 1601, 1585, 1475, 1387, 1325, 1165, 1068, 849, 731 cm⁻¹;

¹H NMR (500 MHz, CDCl₃) δ ppm 8.04–7.96 (m, 1H, aromatic), 7.22 (s, 1H, NH), 6.89–6.83 (m, 2H, aromatic), 4.22–4.08 (m, 2H, OCH₂CHN), 2.86 (dd, $J = 13.0, 4.8$ Hz, 1H, NHCHCH_aH_bN), 2.74–2.63 (m, 1H, NHCHCH₂N), 2.51 (tdd, $J = 9.0, 5.3, 3.5$ Hz,

1H, NCHCH₂), 2.35 (s, 3H, NCH₃), 2.13 (dd, $J = 13.0, 11.0$ Hz, 1H, NHCHCH_aH_bN), 1.87 (ddd, $J = 13.7, 9.8, 3.7$ Hz, 1H, NHCHCH_aH_b), 1.64–1.44 (m, 2H, NHCHCH₂CH, NCHCH₂CH), 1.39–1.20 (m, 2H, NHCHCH_aH_b, NCHCH_aH_b), 1.10 (ddd, $J = 14.2, 8.7, 5.8$ Hz, 1H, NCHCH_aH_b), 0.91 (d, $J = 6.6$ Hz, 3H, CH₃CHCH₃), 0.85 (d, $J = 6.6$ Hz, 3H, CH₃CHCH₃), 0.77 (d, $J = 6.6$ Hz, 3H, CH₃CHCH₃), 0.71 (d, $J = 6.5$ Hz, 3H, CH₃CHCH₃); ¹³C NMR (126 MHz, CDCl₃) δ ppm 166.2 (d, $^1J_{C-F} = 254.8$ Hz), 156.6 (d, $^3J_{C-F} = 10.5$ Hz), 133.6 (d, $^3J_{C-F} = 10.6$ Hz), 126.1 (d, $^4J_{C-F} = 3.4$ Hz), 109.6 (d, $^2J_{C-F} = 22.1$ Hz), 104.6 (d, $^2J_{C-F} = 25.0$ Hz), 71.4, 57.7, 55.0, 49.4, 42.8, 36.1, 34.8, 25.3, 24.4, 23.7, 23.1, 22.0, 21.5;

HRMS calculated for C₁₉H₃₁FN₂O₃SH (M+H)⁺ 387.2118; found 387.2093 (TOF MS ES⁺).

(S)-10-fluoro-3-isobutyl-5-methyl-3,4,5,7-tetrahydro-2H-spiro[benzo[*b*][1,4,5,8]-oxathiadiazecine-6,1'-cyclohexane] 1,1-dioxide (3.10.2f)



According to general procedure **B**, **3.10.2f** (30.9 mg, 46%) was isolated as sticky colorless oil.

$[\alpha]_D^{20} = +8.7$ ($c = 0.695$, CHCl₃);

FTIR (thin film) 2953, 1605, 1589, 1468, 1425, 1391, 1317, 1159, 1070, 847, 733 cm⁻¹;

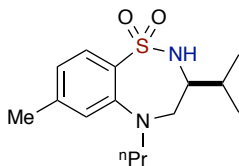
¹H NMR (500 MHz, CDCl₃) δ ppm 7.97 (dd, $J = 8.7, 6.5$ Hz, 1H, aromatic), 6.84 (ddd, $J = 8.8, 7.9, 2.4$ Hz, 1H, aromatic), 6.79 (dd, $J = 9.9, 2.4$ Hz, 1H, aromatic), 4.69 (d, $J =$

10.2 Hz, 1H, OCH_aH_bC), 3.70 (d, $J = 9.8$ Hz, 1H, OCH_aH_bC), 2.99–2.84 (m, 2H, NHCH, NCH_aH_b), 2.43 (s, 3H, NCH₃), 2.25–2.12 (m, 1H, NCH_aH_b), 1.94–1.66 (m, 8H, NHCHCH₂CH, NHCHCH_aH_b, cyclohexyl), 1.64–1.47 (m, 1H, cyclohexyl), 1.43 (d, $J = 12.8$ Hz, 1H, cyclohexyl), 1.36–1.11 (m, 3H, NHCHCH_aH_b, cyclohexyl), 0.84 (dd, $J = 6.6, 6.5$ Hz, 6H, CH₃CHCH₃);

¹³C NMR (126 MHz, CDCl₃) δ ppm 165.9 (d, $^1J_{C-F} = 254.3$ Hz), 157.7 (d, $^3J_{C-F} = 10.6$ Hz), 132.5 (d, $^3J_{C-F} = 10.7$ Hz), 124.8, 109.3 (d, $^2J_{C-F} = 22.0$ Hz), 104.2 (d, $^2J_{C-F} = 24.9$ Hz), 73.2, 59.8, 52.5, 49.3, 47.3, 36.8, 30.6, 28.1, 25.5, 24.3, 23.1, 22.8, 22.7, 22.4;

HRMS calculated for C₂₀H₃₁FN₂O₃SH (M+H)⁺ 399.2118; found 399.2126 (TOF MS ES⁺).

(S)-3-isopropyl-7-methyl-5-propyl-2,3,4,5-tetrahydrobenzo[*f*][1,2,5]thiadiazepine 1,1-dioxide (3.11.2a)



According to general procedure **B**, **3.11.2a** (33.1 mg, 44%) was isolated as yellow oil.

$[\alpha]_D^{20} = -140.3$ ($c = 0.125$, CHCl₃);

FTIR (thin film) 3267, 2927, 1595, 1461, 1325, 1161, 790, 732 cm⁻¹;

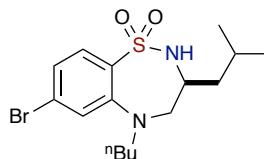
¹H NMR (500 MHz, CDCl₃) δ ppm 7.77 (d, $J = 8.1$ Hz, 1H, aromatic), 6.84 (s, 1H), 6.81 (ddd, $J = 8.0, 1.5, 0.7$ Hz, 1H), 4.18 (d, $J = 9.2$ Hz, 1H, NHCHCH₂N), 3.46 (dd, $J = 14.8, 2.5$ Hz, 1H, NHCHCH₂N), 3.41–3.24 (m, 2H, NHCHCH_aH_bN, NCH_aH_bCH₂CH₃), 3.18 (ddd, $J = 13.1, 7.1, 6.9$ Hz, 1H, NCH_aH_bCH₂CH₃), 3.01 (dd, $J = 14.9, 9.4$ Hz, 1H,

NHCHCH_aH_bN), 2.35 (s, 3H, PhCH₃), 2.02–1.85 (m, 1H, CH₃CHCH₃), 1.66 (dddd, $J = 7.3, 7.3, 7.3, 7.3, 7.3$ Hz, 2H, NCH₂CH₂CH₃), 1.04 (dd, $J = 6.8, 5.0$ Hz, 6H, CH₃CHCH₃), 0.99 (t, $J = 7.3$ Hz, 3H, NCH₂CH₂CH₃);

¹³C NMR (126 MHz, CDCl₃) δ ppm 148.6, 143.5, 131.1, 128.4, 121.7, 119.8, 61.4, 56.9, 56.0, 30.3, 21.7, 21.5, 19.6, 19.0, 11.5;

HRMS calculated for C₁₅H₂₄N₂O₂SH (M+H)⁺ 297.1637; found 297.1615 (TOF MS ES⁺).

(S)-7-bromo-5-butyl-3-isobutyl-2,3,4,5-tetrahydrobenzo[f][1,2,5]thiadiazepine 1,1-dioxide (3.11.2b)



According to general procedure **B**, **3.11.2b** (29.0 mg, 50%) was isolated as colorless oil.

$[\alpha]_D^{20} = -90.2$ ($c = 3.3$, CHCl₃);

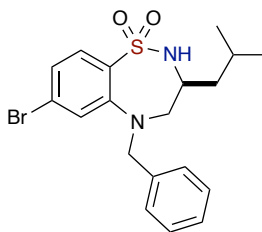
FTIR (thin film) 3258, 2957, 1578, 1468, 1369, 1319, 1151, 802, 733 cm⁻¹;

¹H NMR (400 MHz, CDCl₃) δ ppm 7.68 (d, $J = 8.5$ Hz, 1H, aromatic), 7.12 (d, $J = 1.8$ Hz, 1H, aromatic), 7.07 (dd, $J = 8.5, 1.7$ Hz, 1H, aromatic), 4.33 (d, $J = 8.1$ Hz, 1H, NH), 3.68–3.55 (m, 1H, NHCHCH₂N), 3.51 (dd, $J = 15.2, 2.9$ Hz, 1H, NHCHCH_aH_bN), 3.45–3.34 (m, 1H, NCH_aH_bCH₂CH₂CH₃), 3.28–3.17 (m, 1H, NCH_aH_bCH₂CH₂CH₃), 3.05 (dd, $J = 15.2, 8.3$ Hz, 1H, NHCHCH_aH_bN), 1.86 (ddq, $J = 12.9, 8.3, 6.5$ Hz, 1H, CH₃CHCH₃), 1.68–1.57 (m, 2H, NCH₂CH₂CH₂CH₃), 1.57–1.49 (m, 1H, NHCHCH_aH_bCH), 1.48–1.36 (m, 2H, NCH₂CH₂CH₂CH₃), 1.29 (ddd, $J = 13.9, 8.5, 5.5$ Hz, 1H, NHCHCH_aH_bCH), 1.01–0.94 (m, 9H);

^{13}C NMR (126 MHz, CDCl_3) δ ppm 149.3, 131.9, 129.7, 127.0, 123.1, 121.4, 58.5, 54.3, 53.9, 40.8, 29.8, 24.6, 23.0, 21.9, 20.1, 13.9;

HRMS calculated for $\text{C}_{16}\text{H}_{25}\text{BrN}_2\text{O}_2\text{SH}$ ($\text{M}+2+\text{H}$) $^+$ 391.0873; found 391.0872 (TOF MS ES^+).

(S)-5-benzyl-7-bromo-3-isobutyl-2,3,4,5-tetrahydrobenzo[f][1,2,5]thiadiazepine 1,1-dioxide (3.11.2c)



According to general procedure C, **3.11.2c** (41.1 mg, 50%) was isolated as a white solid.

mp 140–144 °C;

$[\alpha]_D^{20} = -75.5$ ($c = 0.14$, CHCl_3);

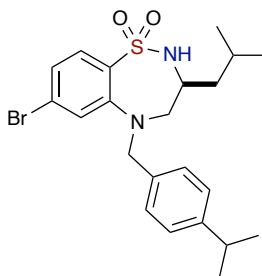
FTIR (thin film) 3275, 2957, 1578, 1458, 1325, 1155, 800, 783, 698 cm^{-1} ;

^1H NMR (400 MHz, CDCl_3) δ ppm 7.76 (d, $J = 8.5$ Hz, 1H, aromatic), 7.42–7.29 (m, 5H, aromatic), 7.23 (d, $J = 1.8$ Hz, 1H, aromatic), 7.16 (dd, $J = 8.4, 1.8$ Hz, 1H, aromatic), 4.65 (d, $J = 14.3$ Hz, 1H, $\text{NCH}_a\text{H}_b\text{Ph}$), 4.38 (d, $J = 14.3$ Hz, 1H, $\text{NCH}_a\text{H}_b\text{Ph}$), 4.30–4.17 (m, 1H, NH), 3.51–3.28 (m, 2H, NHCHCH_2N , $\text{NHCHCH}_a\text{H}_b\text{N}$), 3.01–2.79 (m, 1H, $\text{NHCHCH}_a\text{H}_b\text{N}$), 1.59–1.48 (m, 1H, CH_3CHCH_3), 1.35 (ddd, $J = 14.2, 7.4, 7.0$ Hz, 1H, $\text{NHCHCH}_a\text{H}_b$), 1.09–0.96 (m, 1H, $\text{NHCHCH}_a\text{H}_b$), 0.79 (d, $J = 6.5$ Hz, 3H, CH_3CHCH_3), 0.70 (d, $J = 6.6$ Hz, 3H, CH_3CHCH_3);

^{13}C NMR (126 MHz, CDCl_3) δ ppm 149.8, 136.7, 129.7, 128.9 (2C), 128.3 (2C), 127.9, 127.4, 127.35, 124.2, 122.4, 58.3, 57.8, 53.7, 41.0, 24.5, 22.4, 22.0;

HRMS calculated for $\text{C}_{19}\text{H}_{23}\text{BrN}_2\text{O}_2\text{SH}$ ($\text{M}+\text{H}$) $^+$ 423.0742; found 423.0742 (TOF MS ES^+).

(S)-7-bromo-3-isobutyl-5-(4-isopropylbenzyl)-2,3,4,5-tetrahydrobenzo[f][1,2,5]thiadiazepine 1,1-dioxide (3.11.2d)



According to general procedure C, **3.11.2d** (23.5 mg, 42%) was isolated as a light yellow solid.

mp 155–161 °C;

$[\alpha]_D^{20} = -102.9$ ($c = 0.485$, CHCl_3);

FTIR (thin film) 3258, 2959, 1578, 1468, 1375, 1325, 1155, 843, 798, 700 cm^{-1} ;

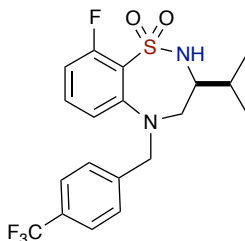
^1H NMR (500 MHz, CDCl_3) δ ppm 7.74 (dd, $J = 8.4, 2.0$ Hz, 1H, aromatic), 7.32 (d, $J = 7.9$ Hz, 2H, aromatic), 7.26 (d, $J = 5.0$ Hz, 2H, aromatic), 7.27–7.21 (m, 1H, aromatic), 7.19–7.11 (m, 1H, aromatic), 4.60 (d, $J = 13.9$ Hz, 1H, $\text{NCH}_a\text{H}_b\text{Ph}$), 4.32 (d, $J = 13.9$ Hz, 1H, $\text{NCH}_a\text{H}_b\text{Ph}$), 4.23 (s, 1H, NH), 3.41 (dd, $J = 14.9, 2.4$ Hz, 1H, NHCHCH_2N), 3.38–3.30 (m, 1H, $\text{NHCHCH}_a\text{H}_b\text{N}$), 3.03–2.80 (m, 1H, $\text{NHCHCH}_a\text{H}_b\text{N}$), 1.60–1.46 (m, 1H, CH_3CHCH_3), 1.40–1.26 (m, 1H, CCHCH_3), 1.25 (d, $J = 6.9$ Hz, 6H, CH_3CHCH_3), 1.06–

0.93 (m, 1H, NHCHCH_aH_b), 0.95–0.83 (m, 1H, NHCHCH_aH_b), 0.76 (d, $J = 6.6$ Hz, 3H, CH₃CHCH₃), 0.64 (d, $J = 6.6$ Hz, 3H, CH₃CHCH₃);

¹³C NMR (126 MHz, CDCl₃) δ ppm 150.0 (2C), 148.7, 134.0, 129.6, 128.5 (2C), 127.4, 126.9 (2C), 124.0, 122.3, 57.9, 57.5, 53.8, 41.0, 33.9, 24.6, 24.0, 23.9, 22.3, 22.1;

HRMS calculated for C₂₂H₂₉BrN₂O₂SH (M+H)⁺ 465.1211; found 465.1184 (TOF MS ES⁺).

(S)-9-fluoro-3-isopropyl-5-(4-(trifluoromethyl)benzyl)-2,3,4,5-tetrahydrobenzo[*f*]-[1,2,5]thiadiazepine 1,1-dioxide (3.11.2e)



According to general procedure **B**, **3.11.2e** (59.6 mg, 53%) was isolated as brown oil.

$[\alpha]_D^{20} = -149.9$ ($c = 0.125$, CHCl₃);

FTIR (thin film) 3267, 2968, 1604, 1573, 1477, 1433, 1325, 1161, 854, 742 cm⁻¹;

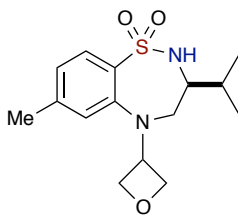
¹H NMR (500 MHz, CDCl₃) δ ppm 7.93 (dd, $J = 8.8, 6.4$ Hz, 1H, aromatic), 7.65 (d, $J = 8.0$ Hz, 2H, aromatic), 7.55 (d, $J = 8.0$ Hz, 2H, aromatic), 6.78–6.69 (m, 2H, aromatic), 4.68 (d, $J = 14.7$ Hz, 1H, NCH_aH_bPh), 4.44 (d, $J = 14.7$ Hz, 1H, NCH_aH_bPh), 4.32 (d, $J = 9.1$ Hz, 1H, NH), 3.43 (dd, $J = 14.8, 2.2$ Hz, 1H, NHCHCH₂N), 3.29–3.14 (m, 1H, NHCHCH_aH_bN), 3.13–2.96 (m, 1H, NHCHCH_aH_bN), 1.85–1.66 (m, 1H, CH₃CHCH₃), 0.86 (d, $J = 6.8$ Hz, 3H, CH₃CHCH₃), 0.79 (d, $J = 6.7$ Hz, 3H, CH₃CHCH₃);

¹³C NMR (126 MHz, CDCl₃) δ ppm 165.3 (d, $^1J_{C-F} = 253.5$ Hz), 150.6 (d, $^3J_{C-F} = 10.1$ Hz), 140.9 (d, $^4J_{C-F} = 0.9$ Hz), 130.8 (d, $^3J_{C-F} = 10.9$ Hz), 130.2 (q, $^2J_{C-CF_3} = 32.6$ Hz),

130.1, 128.5 (2C), 125.8 (q, $^3J_{C-CF_3} = 3.7$ Hz, 2C), 124.0 (q, $^1J_{C-CF_3} = 273.1$ Hz), 108.7 (d, $^2J_{C-F} = 22.6$ Hz), 106.5 (d, $^2J_{C-F} = 24.4$ Hz), 60.7, 58.0, 56.4, 30.0, 19.0, 18.7;

HRMS calculated for $C_{19}H_{20}F_4N_2O_2SH$ (M+H)⁺ 417.1260; found 417.1271 (TOF MS ES⁺).

(S)-3-isopropyl-7-methyl-5-(oxetan-3-yl)-2,3,4,5-tetrahydrobenzo[*f*][1,2,5]thiadiazepine 1,1-dioxide (3.11.2f)



According to general procedure **B**, **3.11.2f** (46.1 mg, 55%) was isolated as a white solid.

mp 145–148 °C;

$[\alpha]_D^{20} = -27.0$ ($c = 0.125$, $CHCl_3$);

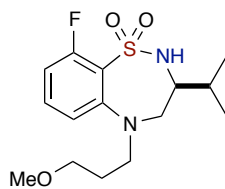
FTIR (thin film) 3267, 2960, 1602, 1471, 1369, 1326, 1218, 1145, 1068, 815, 729 cm^{-1} ;

1H NMR (500 MHz, $CDCl_3$) δ ppm 7.79 (d, $J = 8.0$ Hz, 1H, aromatic), 7.27–7.24 (m, 1H, aromatic), 7.13 (bs, 1H, aromatic), 3.80 (ddd, $J = 14.6, 7.7, 1.6$ Hz, 1H, $NCHCH_aH_bOCH_2$), 3.70–3.62 (m, 1H, $NCHCH_2OCH_aH_b$), 3.59 (dd, $J = 10.9, 9.2$ Hz, 1H, $NCHCH_aH_bOCH_2$), 3.54–3.42 (m, 1H, $NCHCH_2OCH_aH_b$), 3.31 (dddd, $J = 9.7, 9.7, 7.7, 1.6$ Hz, 1H, $NHCHCH_2N$), 3.20–3.12 (m, 1H, $NCHCH_2OCH_2$), 2.94 (dd, $J = 14.5, 9.6$ Hz, 1H, $NHCHCH_aH_bN$), 2.70 (dd, $J = 14.5, 10.0$ Hz, 1H, $NHCHCH_aH_bN$), 2.56 (s, 1H, NH), 2.40 (s, 3H, $PhCH_3$), 1.92–1.80 (m, 1H, CH_3CHCH_3), 1.09 (d, $J = 6.5$ Hz, 3H, CH_3CHCH_3), 0.84 (d, $J = 6.6$ Hz, 3H, CH_3CHCH_3);

^{13}C NMR (126 MHz, CDCl_3) δ ppm 144.5, 141.1, 140.1, 130.4, 129.1, 128.7, 61.9, 60.1, 58.7, 47.6, 41.1, 29.3, 21.3, 20.6, 18.5;

HRMS calculated for $\text{C}_{15}\text{H}_{22}\text{N}_2\text{O}_3\text{SH}$ ($\text{M}+\text{H}$) $^+$ 311.1429; found 311.1415 (TOF MS ES^+).

(S)-9-fluoro-3-isopropyl-5-(3-methoxypropyl)-2,3,4,5-tetrahydrobenzo[f][1,2,5]thiadiazepine 1,1-dioxide (3.11.2g)



According to general procedure **B**, **3.11.2g** (50.0 mg, 56%) was isolated as yellow oil.

$[\alpha]_D^{20} = -140.7$ ($c = 0.125$, CHCl_3);

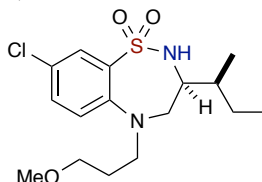
FTIR (thin film) 3263, 2962, 1608, 1569, 1456, 1386, 1319, 1201, 1149, 1068, 723 cm^{-1} ;

^1H NMR (500 MHz, CDCl_3) δ ppm 7.85 (dd, $J = 8.8, 6.5$ Hz, 1H, aromatic), 6.74 (dd, $J = 11.5, 2.4$ Hz, 1H, aromatic), 6.66 (ddd, $J = 8.8, 7.5, 2.4$ Hz, 1H, aromatic), 4.54 (d, $J = 7.2$ Hz, 1H, NH), 3.58–3.42 (m, 4H, NHCHCH_aH_bN, NHCH_bCH₂N, NCH₂CH₂CH₂OCH₃), 3.34 (s, 3H, NCH₂CH₂CH₂OCH₃), 3.33–3.30 (m, 1H, NCH_aH_bCH₂CH₂OCH₃), 3.28–3.19 (m, 2H, NHCHCH_aH_bN, NCH_aH_bCH₂CH₂OCH₃), 2.01–1.93 (m, 1H, CH₃CHCH₃), 1.92–1.83 (m, 2H, NCH₂CH₂CH₂OCH₃), 1.06 (d, $J = 6.8$ Hz, 3H, CH₃CHCH₃), 1.03 (d, $J = 6.7$ Hz, 3H, CH₃CHCH₃);

^{13}C NMR (126 MHz, CDCl_3) δ ppm 165.2 (d, $^1J_{\text{C-F}} = 252.1$ Hz), 150.3 (d, $^3J_{\text{C-F}} = 10.5$ Hz), 130.8 (d, $^3J_{\text{C-F}} = 10.9$ Hz), 129.2, 107.7 (d, $^2J_{\text{C-F}} = 22.7$ Hz), 105.6 (d, $^2J_{\text{C-F}} = 24.7$ Hz), 69.7, 61.6, 58.7, 56.8, 51.0, 30.2, 28.0, 19.6, 19.0;

HRMS calculated for $C_{15}H_{23}FN_2O_3SH$ (M+H)⁺ 331.1492; found 331.1481 (TOF MS ES⁺).

(S)-3-((S)-sec-butyl)-8-chloro-5-(3-methoxypropyl)-2,3,4,5-tetrahydrobenzo[f][1,2,5]-thiadiazepine 1,1-dioxide (3.11.2h)



According to general procedure **B**, **3.11.2h** (44.8 mg, 46%) was isolated as colorless oil.

$[\alpha]_D^{20} = +132.5$ ($c = 0.125$, $CHCl_3$);

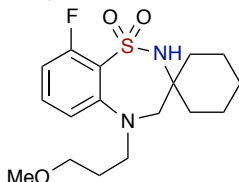
FTIR (thin film) 3267, 2931, 1506, 1488, 1458, 1386, 1326, 1220, 1157, 1058, 821 cm^{-1} ;

¹H NMR (500 MHz, $CDCl_3$) δ ppm 7.83 (d, $J = 2.5$ Hz, 1H, aromatic), 7.34 (dd, $J = 8.8$, 2.6 Hz, 1H, aromatic), 7.05 (d, $J = 8.8$ Hz, 1H, aromatic), 4.49 (d, $J = 9.4$ Hz, 1H, NH), 3.60–3.48 (m, 2H, NHCH_aCH₂N, NCH₂CH₂CH_aH_bOCH₃), 3.48–3.42 (m, 2H, NCH₂CH₂CH_aH_bOCH₃, NCH_aH_bCH₂CH₂OCH₃), 3.38 (dd, $J = 14.8$, 2.5 Hz, 1H, NHCHCH_aH_bN), 3.33 (s, 3H, NCH₂CH₂CH₂OCH₃), 3.29 (dd, $J = 13.5$, 6.8 Hz, 1H, NCH_aH_bCH₂CH₂OCH₃), 3.04 (dd, $J = 14.8$, 9.6 Hz, 1H, NHCHCH_aH_bN), 1.90–1.78 (m, 2H, NCH₂CH₂CH₂OCH₃), 1.74–1.64 (m, 1H, CH₃CHCH₂CH₃), 1.59–1.49 (m, 1H, CH₃CHCH_aH_bCH₃), 1.36–1.25 (m, 1H, CH₃CHCH_aH_bCH₃), 1.01–0.93 (m, 6H, CH₃CHCH₂CH₃);

¹³C NMR (126 MHz, $CDCl_3$) δ ppm 146.7, 134.8, 132.6, 128.1, 125.9, 120.7, 77.2, 69.8, 61.5, 58.7, 57.1, 51.2, 30.2, 28.2, 19.6, 18.9;

HRMS calculated for $C_{16}H_{25}ClN_2O_3SH$ (M+H)⁺ 361.1353; found 361.1338 (TOF MS ES⁺).

9-fluoro-5-(3-methoxypropyl)-4,5-dihydro-2H-spiro[benzo[f][1,2,5]thiadiazepine-3,1'-cyclohexane] 1,1-dioxide (3.11.2i)



According to general procedure **B**, **3.11.2i** (54.0 mg, 56%) was isolated as brown oil.

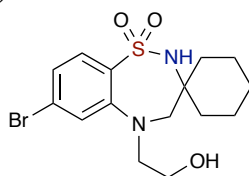
FTIR (thin film) 3326, 2928, 1612, 1573, 1469, 1338, 1147, 1041, 773 cm^{-1} ;

¹H NMR (500 MHz, CDCl₃) δ ppm 7.27–7.22 (m, 1H, aromatic), 6.97 (s, 1H, NH), 6.48 (d, $J = 8.8$, Hz, 1H, aromatic), 6.35 (ddd, $J = 11.2$, 8.1, 1.0 Hz, 1H, aromatic), 5.61–5.54 (m, 1H, NCH₂CH₂CH_aH_bOCH₃), 4.95 (dd, $J = 6.6$, 6.5 Hz, 1H, NCH₂CH₂CH_aH_bOCH₃), 3.54–3.44 (m, 4H, NHCCH₂N, NCH₂CH₂CH₂OCH₃), 3.36 (s, 3H, OCH₃), 3.25 (ddd, $J = 6.7$, 6.6, 5.0 Hz, 2H, NCH₂CH₂CH₂OCH₃), 2.00–1.84 (m, 5H, cyclohexyl), 1.65–1.55 (m, 1H, cyclohexyl), 1.54–1.39 (m, 4H, cyclohexyl);

¹³C NMR (126 MHz, CDCl₃) δ ppm 161.1 (d, $^1J_{C-F} = 248.9$ Hz), 148.6 (d, $^4J_{C-F} = 3.4$ Hz), 134.2 (d, $^3J_{C-F} = 12.7$ Hz), 109.4 (d, $^3J_{C-F} = 14.0$ Hz), 107.8, 101.1 (d, $^2J_{C-F} = 23.5$ Hz), 70.2, 58.8, 50.0, 40.8, 29.0, 26.2 (2C), 25.0, 22.3, 21.9 (2C);

HRMS calculated for $C_{17}H_{25}FN_2O_3SH$ (M+H)⁺ 357.1648; found 357.1627 (TOF MS ES⁺).

7-bromo-5-(2-hydroxyethyl)-4,5-dihydro-2H-spiro[benzo[f][1,2,5]thiadiazepine-3,1'-cyclohexane] 1,1-dioxide (3.11.2j)



According to general procedure C, **3.11.2j** (24.8 mg, 46%) was isolated as a white solid.

mp 178–182 °C;

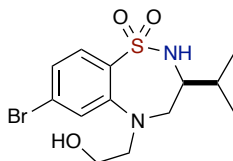
FTIR (thin film) 3454, 3263, 2934, 1580, 1487, 1369, 1312, 1150, 1057, 795, 733 cm⁻¹;

¹H NMR (400 MHz, CDCl₃) δ ppm 7.68 (dd, *J* = 8.4, 1.7 Hz, 1H, aromatic), 7.25 (s, 1H, aromatic), 7.19 (dd, *J* = 8.4, 1.7 Hz, 1H, aromatic), 4.44 (s, 1H, NH), 3.81–3.66 (m, 2H, NCH₂CH₂OH), 3.57 (bs, 2H, NCH₂CH₂OH), 3.26 (bs, 2H, NCH₂CNH), 2.85 (s, 1H, OH), 1.75–1.53 (m, 6H, cyclohexyl), 1.50–1.27 (m, 4H, cyclohexyl);

¹³C NMR (126 MHz, CDCl₃) δ ppm 148.1, 129.5, 127.1, 125.8, 125.3, 122.6, 65.3, 59.5, 59.1, 56.5, 25.6 (2C), 21.0 (3C);

HRMS calculated for C₁₅H₂₁BrN₂O₃SH (M+H)⁺ 387.0383; found 387.0372 (TOF MS ES⁺).

(S)-7-bromo-5-(2-hydroxyethyl)-3-isopropyl-2,3,4,5-tetrahydrobenzo[f][1,2,5]thiadiazepine 1,1-dioxide (3.11.2k)



According to general procedure C, **3.11.2k** (50.4 mg, 46%) was isolated as colorless oil.

[α]_D²⁰ = -175.5 (*c* = 0.125, CHCl₃);

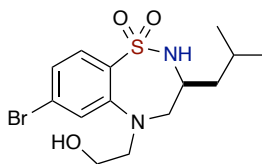
FTIR (thin film) 3466, 3252, 2964, 1578, 1470, 1371, 1319, 1157, 1059, 795, 731 cm^{-1} ;

^1H NMR (400 MHz, CDCl_3) δ ppm 7.74 (dd, $J = 8.6, 2.1$ Hz, 1H, aromatic), 7.37 (d, $J = 2.0$ Hz, 1H, aromatic), 7.29–7.22 (m, 1H, aromatic), 4.17 (d, $J = 9.4$ Hz, 1H, NH), 3.88–3.76 (m, 1H, HOCH_aH_b), 3.68–3.57 (m, 2H, NCH_2CH_2), 3.51–3.36 (m, 3H, $\text{NCH}_a\text{H}_b\text{CHNH}$, NHCH_2CH_2 , OH), 3.33–3.22 (m, 1H, HOCH_aH_b), 2.85 (dd, $J = 15.0, 10.4$ Hz, 1H, $\text{NCH}_a\text{H}_b\text{CHNH}$), 1.92–1.79 (m, 1H, CH_3CHCH_3), 1.06 (d, $J = 6.8$ Hz, 3H, CH_3CHCH_3), 1.02 (d, $J = 6.9$ Hz, 3H, CH_3CHCH_3);

^{13}C NMR (126 MHz, CDCl_3) δ ppm 148.9, 135.6, 129.6, 127.7, 126.1, 125.5, 60.9, 60.0, 58.9, 57.9, 30.0, 19.5, 18.3;

HRMS calculated for $\text{C}_{13}\text{H}_{19}\text{BrN}_2\text{O}_3\text{SH}$ ($\text{M}+\text{H}$) $^+$ 363.0378; found 363.0375 (TOF MS ES^+).

(S)-7-bromo-5-(2-hydroxyethyl)-3-isobutyl-2,3,4,5-tetrahydrobenzo[*f*][1,2,5]thiadiazepine 1,1-dioxide (3.11.2i)



According to general procedure C, **3.11.2i** (31.0 mg, 43%) was isolated as colorless oil.

$[\alpha]_D^{20} = -120.8$ ($c = 0.085$, CHCl_3);

FTIR (thin film) 3454, 3250, 2957, 1576, 1470, 1367, 1319, 1155, 1061, 808, 789, 745, 700 cm^{-1} ;

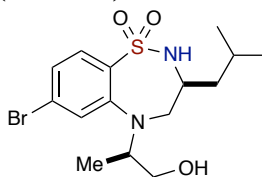
^1H NMR (500 MHz, CDCl_3) δ ppm 7.69 (d, $J = 8.4$ Hz, 1H, aromatic), 7.36 (d, $J = 1.8$ Hz, 1H, aromatic), 7.23 (dd, $J = 8.5, 1.8$ Hz, 1H, aromatic), 4.27 (d, $J = 9.0$ Hz, 1H, NH),

3.82 (ddd, $J = 13.6, 5.6, 3.9$ Hz, 1H, HOCH_aH_b), 3.73–3.57 (m, 3H, NHCH_cCH₂, NCH₂CH₂OH), 3.42 (s, 1H, OH), 3.36 (dd, $J = 15.0, 2.1$ Hz, 1H, NHCHCH_aH_bN), 3.32–3.21 (m, 1H, HOCH_aH_b), 2.85–2.71 (m, 1H, NHCHCH_aH_bN), 1.93–1.79 (m, 1H, CH₃CH_cCH₃), 1.36 (ddd, $J = 14.3, 9.1, 5.7$ Hz, 1H, NHCHCH_aH_b), 1.30–1.18 (m, 1H, NHCHCH_aH_b), 0.98 (dd, $J = 6.5, 6.4$ Hz, 6H, CH₃CH_cCH₃);

¹³C NMR (126 MHz, CDCl₃) δ ppm 148.9, 135.6, 129.6, 127.7, 126.1, 125.5, 61.3, 60.1, 58.0, 54.1, 40.7, 24.6, 23.0, 21.9;

HRMS calculated for C₁₄H₂₁BrN₂O₃SH (M+H)⁺ 377.0535; found 377.0485 (TOF MS ES⁺).

(S)-7-bromo-5-((R)-1-hydroxypropan-2-yl)-3-isobutyl-2,3,4,5-tetrahydrobenzo[*f*]-[1,2,5]thiadiazepine 1,1-dioxide (3.11.2m)



According to general procedure C, **3.11.2m** (28.5 mg, 12%) was isolated as a white solid.
mp 150–154 °C;

$[\alpha]_D^{20} = -143.5$ ($c = 0.365$, CHCl₃);

FTIR (thin film) 3475, 3253, 2957, 1576, 1470, 1381, 1321, 1161, 1055, 808, 777, 727, 694 cm⁻¹;

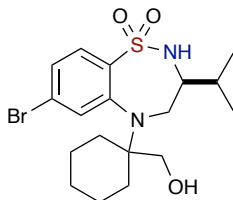
¹H NMR (500 MHz, CDCl₃) δ ppm 7.76 (d, $J = 8.4$ Hz, 1H, aromatic), 7.35 (d, $J = 1.8$ Hz, 1H, aromatic), 7.27–7.24 (m, 1H, aromatic), 3.98 (s, 1H, NH), 3.88–3.74 (m, 1H, NCH_cCH₃), 3.62 (s, 1H, OH), 3.58–3.47 (m, 3H, NHCH_cCH₂N, NHCHCH_aH_bN),

HOCH_aH_b), 3.40 (dd, $J = 11.0, 10.4$ Hz, 1H, HOCH_aH_b), 2.47–2.26 (m, 1H, NHCHCH_aH_bN), 1.95–1.78 (m, 1H, CH₃CHCH₃), 1.40–1.19 (m, 5H, CH₃CHN, NHCHCH₂), 1.00 (dd, $J = 6.3$ Hz, 6H, CH₃CHCH₃);

¹³C NMR (126 MHz, CDCl₃) δ ppm 150.7, 134.6, 129.5, 127.8, 125.7, 125.5, 65.6, 60.9, 54.0, 51.7, 41.1, 24.7, 23.0, 21.9, 13.9;

HRMS calculated for C₁₅H₂₃BrN₂O₃SH (M+H)⁺ 391.0691; found 391.0656 (TOF MS ES⁺).

(S)-7-bromo-5-(1-(hydroxymethyl)cyclohexyl)-3-isopropyl-2,3,4,5-tetrahydrobenzo-[f][1,2,5]thiadiazepine 1,1-dioxide (3.11.2n)



According to general procedure C, **3.11.2n** (34.0 mg, 26%) was isolated as a white solid.

mp 164–168 °C;

$[\alpha]_D^{20} = -187.1$ ($c = 1.29$, CHCl₃);

FTIR (thin film) 3445, 3261, 2959, 1574, 1462, 1398, 1321, 1163, 1063, 808, 733 cm⁻¹;

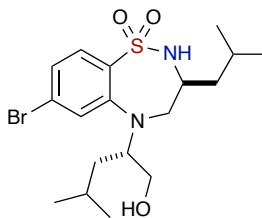
¹H NMR (400 MHz, CDCl₃) δ ppm 7.76 (d, $J = 8.5$ Hz, 1H, aromatic), 7.68 (d, $J = 1.8$ Hz, 1H, aromatic), 7.35 (dd, $J = 8.4, 1.8$ Hz, 1H, aromatic), 4.06 (d, $J = 9.2$ Hz, 1H, NH), 3.92–3.77 (m, 2H, NCH_aH_bCHNH, CH_aH_bOH), 3.68 (dd, $J = 12.6, 4.8$ Hz, 1H, CH_aH_bOH), 3.45 (ddd, $J = 8.9, 8.8, 8.6$ Hz, 1H, NHCHCH₂N), 3.36–3.21 (m, 1H, OH), 2.35 (dd, $J = 15.6, 10.4$ Hz, 1H, NCH_aH_bCHNH), 2.09 (d, $J = 12.9$ Hz, 1H, cyclohexyl), 1.88–1.68 (m, 6H, cyclohexyl, CH₃CHCH₃), 1.57 (ddd, $J = 13.1, 12.8, 3.7$ Hz, 1H,

cyclohexyl), 1.48–1.34 (m, 2H, cyclohexyl), 1.31–1.17 (m, 1H, cyclohexyl), 1.06 (d, $J = 6.8$ Hz, 3H, CH_3CHCH_3), 1.00 (d, $J = 6.9$ Hz, 3H, CH_3CHCH_3);

^{13}C NMR (126 MHz, CDCl_3) δ ppm 147.9, 139.0, 131.8, 129.3, 127.6, 126.2, 63.6, 61.5, 61.2, 50.3, 31.6, 31.2, 30.1, 25.5, 23.0, 22.8, 19.3, 18.2;

HRMS calculated for $\text{C}_{18}\text{H}_{27}\text{BrN}_2\text{O}_3\text{SH}$ ($\text{M}+\text{H}$) $^+$ 431.1004; found 431.1019 (TOF MS ES^+).

(S)-7-bromo-5-((S)-1-hydroxy-4-methylpentan-2-yl)-3-isobutyl-2,3,4,5 tetrahydrobenzo[*f*][1,2,5]thiadiazepine 1,1-dioxide (3.11.2o)



According to general procedure **C**, **3.11.2o** (70.0 mg, 21%) was isolated as a white solid.

mp 86–90 °C;

$[\alpha]_D^{20} = +117.3$ ($c = 0.92$, CHCl_3);

FTIR (thin film) 3470, 3250, 2955, 1578, 1470, 1402, 1323, 1163, 1068, 812 cm^{-1} ;

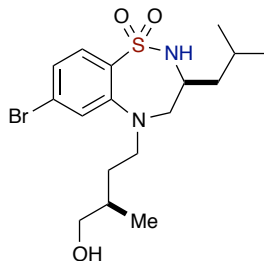
^1H NMR (400 MHz, CDCl_3) δ ppm 7.83 (d, $J = 8.1$ Hz, 1H, aromatic), 7.25–7.14 (m, 2H, aromatic), 6.70 (d, $J = 6.4$ Hz, 1H, NH), 4.41 (dd, $J = 11.7, 2.9$ Hz, 1H, $\text{NCHCH}_a\text{H}_b\text{OH}$), 3.87 (dd, $J = 11.8, 11.0$ Hz, 1H, $\text{NCHCH}_a\text{H}_b\text{OH}$), 3.16–2.99 (m, 1H, NHCHCH_2N), 2.77–2.57 (m, 2H, NCHCH_2OH , $\text{NCH}_a\text{H}_b\text{CHNH}$), 2.40 (dd, $J = 13.6, 4.8$ Hz, 1H, $\text{NCH}_a\text{H}_b\text{CHNH}$), 1.80–1.68 (m, 2H, CH_3CHCH_3 , CH_3CHCH_3), 1.63 (ddd, $J = 14.1, 7.2, 7.1$ Hz, 1H, $\text{NHCHCH}_a\text{H}_b$), 1.24 (dd, $J = 7.8, 6.3$ Hz, 2H, NCHCH_2), 1.13 (ddd,

$J = 13.7, 7.0, 6.9$ Hz, 1H, NHCHCH_aH_b), 0.98–0.88 (m, 9H, CH₃CHCH₃, CH₃CHCH₃), 0.84 (d, $J = 6.6$ Hz, 3H, CH₃CHCH₃);

¹³C NMR (126 MHz, CDCl₃) δ ppm 155.2, 131.8, 129.7, 128.0, 124.9, 118.5, 75.2, 54.0, 51.4, 51.3, 43.4, 42.0, 24.9, 24.3, 23.0, 22.7, 22.5, 22.4;

HRMS calculated for C₁₈H₂₉BrN₂O₃SH (M+H)⁺ 435.1136; found 435.1147 (TOF MS ES⁺).

(S)-7-bromo-5-((R)-4-hydroxy-3-methylbutyl)-3-isobutyl-2,3,4,5-tetrahydrobenzo-[f][1,2,5]thiadiazepine 1,1-dioxide (3.11.2p)



According to general procedure C, **3.11.2p** (43.1 mg, 43%) was isolated as colorless oil.

$[\alpha]_D^{20} = -103.1$ ($c = 0.66$, CHCl₃);

FTIR (thin film) 3512, 3252, 2957, 1578, 1543, 1470, 1371, 1315, 1150, 1040, 800, 731, 700 cm⁻¹;

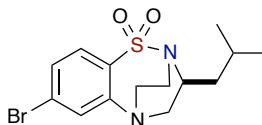
¹H NMR (500 MHz, CDCl₃) δ ppm 7.67 (d, $J = 8.5$ Hz, 1H, aromatic), 7.20 (d, $J = 1.8$ Hz, 1H, aromatic), 7.10 (dd, $J = 8.5, 1.8$ Hz, 1H, aromatic), 4.41 (d, $J = 8.2$ Hz, 1H, NH), 3.68–3.56 (m, 2H, NHCHCH₂N, NCH_aH_bCH₂CHMe), 3.55–3.49 (m, 1H, HOCH_aH_bCHMe), 3.46 (dd, $J = 15.1, 2.7$ Hz, 1H, NHCHCH_aH_bN), 3.43–3.39 (m, 1H, HOCH_aH_bCHMe), 3.21 (ddd, $J = 13.7, 8.3, 5.9$ Hz, 1H, NCH_aH_bCH₂CHMe), 2.95 (dd, $J = 15.1, 9.0$ Hz, 1H, NHCHCH_aH_bN), 1.91–1.79 (m, 2H, HOCH₂CHMe, CH₃CHCH₃),

1.79–1.70 (m, 2H, NCH₂CH_aH_bCHMe, OH), 1.53–1.43 (m, 2H, NHCHCH_aH_bCH, NCH₂CH_aH_bCHMe), 1.27 (ddd, *J* = 14.0, 8.4, 5.6 Hz, 1H, NHCHCH_aH_bCH), 1.03–0.93 (m, 9H, CH₃CHCH₃, HOCH₂CHCH₃);

¹³C NMR (126 MHz, CDCl₃) δ ppm 149.3, 132.4, 129.7, 127.3, 123.8, 122.1, 67.7, 59.2, 54.0, 52.3, 40.9, 33.4, 31.4, 24.6, 22.9, 21.9, 17.0;

HRMS calculated for C₁₇H₂₇BrN₂O₃SH (M+H)⁺ 421.0979; found 421.0980 (TOF MS ES⁺).

(3*S*)-7-bromo-3-isobutyl-3,4-dihydro-2,5-ethanobenzo[*f*][1,2,5]thiadiazepine 1,1-dioxide (3.12.1a)



According to general procedure **D**, **3.12.1a** (14.6 mg, 87%.) was isolated as colorless oil.

$[\alpha]_D^{20} = -29.1$ (*c* = 0.945, CHCl₃);

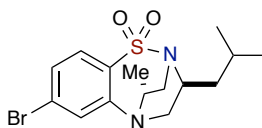
FTIR (thin film) 2957, 1574, 1448, 1391, 1333, 1165, 839, 797, 694 cm⁻¹;

¹H NMR (500 MHz, CDCl₃) δ ppm 7.74 (d, *J* = 8.4 Hz, 1H, aromatic), 7.56 (dd, *J* = 8.4, 2.0 Hz, 1H, aromatic), 7.48 (d, *J* = 2.0 Hz, 1H, aromatic), 3.97–3.82 (m, 1H, NCHCH₂N), 3.72 (dddd, *J* = 14.7, 8.6, 2.4, 1.7 Hz, 1H, SNCH_aH_b), 3.42 (ddd, *J* = 14.1, 7.7, 2.5 Hz, 1H, CNCH_aH_bCH₂NS), 3.39–3.32 (m, 1H, CNCH_aH_bCH₂NS), 3.26–3.21 (m, 1H, NCH_aH_bCHN), 3.21–3.16 (m, 1H, SNCH_aH_b), 2.73 (dd, *J* = 14.4, 9.1 Hz, 1H, NCH_aH_bCHN), 1.89–1.75 (m, 1H, CH₃CHCH₃), 1.68 (ddd, *J* = 14.3, 9.8, 4.7 Hz, 1H, NCHCH_aH_bCH), 1.14 (ddd, *J* = 13.8, 9.0, 4.6 Hz, 1H, NCHCH_aH_bCH), 0.95 (d, *J* = 6.8 Hz, 3H, CH₃CHCH₃), 0.93 (d, *J* = 6.5 Hz, 3H, CH₃CHCH₃);

^{13}C NMR (126 MHz, CDCl_3) δ ppm 148.1, 143.2, 133.9, 131.3, 129.8, 126.8, 53.3, 51.1, 51.07, 39.1, 38.3, 24.6, 23.2, 21.6;

HRMS calculated for $\text{C}_{14}\text{H}_{19}\text{BrN}_2\text{O}_2\text{SH}$ ($\text{M}+\text{H}$) $^+$ 359.0429; found 359.0430 (TOF MS ES $^+$).

(4*R*,11*S*)-7-bromo-11-isobutyl-4-methyl-3,4-dihydro-2,5-ethanobenzo[*f*][1,2,5]thiadiazepine 1,1-dioxide (3.12.1b)



According to general procedure **D 3.12.1b** (12.5 mg, 46%) was isolated as colorless oil.

$[\alpha]_D^{20} = -2.1$ ($c = 0.25$, CHCl_3);

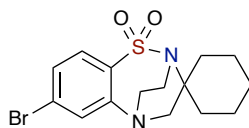
FTIR (thin film) 2957, 1574, 1456, 1381, 1331, 1161, 816, 789, 756, 698 cm^{-1} ;

^1H NMR (500 MHz, CDCl_3) δ ppm 7.72 (d, $J = 8.4$ Hz, 1H, aromatic), 7.59 (dd, $J = 8.4$, 2.0 Hz, 1H, aromatic), 7.45 (d, $J = 1.9$ Hz, 1H, aromatic), 4.09–3.90 (m, 1H, NCHCH_2N), 3.51–3.29 (m, 4H, $\text{SNCH}_2\text{CHCH}_3$, $\text{NCHCH}_a\text{H}_b\text{N}$), 2.81 (dd, $J = 14.3$, 6.6 Hz, 1H, $\text{NCHCH}_a\text{H}_b\text{N}$), 1.84–1.77 (m, 1H, CH_3CHCH_3), 1.73 (ddd, $J = 13.9$, 10.2, 4.7 Hz, 1H, $\text{NCHCH}_a\text{H}_b\text{CH}$), 1.21 (ddd, $J = 14.1$, 9.0, 5.0 Hz, 1H, $\text{NCHCH}_a\text{H}_b\text{CH}$), 0.96 (dd, $J = 6.5$, 3.8 Hz, 9H, NCHCH_3 , CH_3CHCH_3);

^{13}C NMR (126 MHz, CDCl_3) δ ppm 144.3, 143.6, 136.0, 131.6, 129.1, 126.6, 56.2, 54.5, 49.2, 44.8, 40.3, 25.1, 23.2, 21.5, 20.2;

HRMS calculated for $\text{C}_{15}\text{H}_{21}\text{BrN}_2\text{O}_2\text{SH}$ ($\text{M}+\text{H}$) $^+$ 373.0585; found 373.0565 (TOF MS ES $^+$).

7-bromo-4*H*-spiro[2,5-ethanobenzo[*f*][1,2,5]thiadiazepine-3,1'-cyclohexane] 1,1-dioxide (3.12.1c)



According to general procedure **D**, **3.12.1c** (8.1 mg, 40%) was isolated as a white solid.

mp 182–185 °C;

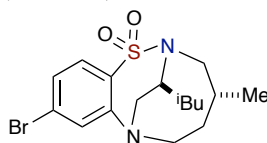
FTIR (thin film) 2935, 1574, 1452, 1393, 1327, 1167, 804, 694 cm⁻¹;

¹H NMR (500 MHz, CDCl₃) δ ppm 7.67 (d, *J* = 8.4 Hz, 1H, aromatic), 7.53 (dd, *J* = 8.4, 2.0 Hz, 1H, aromatic), 7.47 (d, *J* = 2.0 Hz, 1H, aromatic), 3.88 (ddd, *J* = 14.8, 6.9, 5.7 Hz, 1H, SNCH_aH_b), 3.44 (ddd, *J* = 14.7, 8.5, 7.1 Hz, 1H, SNCH_aH_b), 3.38–3.30 (m, 2H, CNCH₂CH₂NS), 3.15 (ddd, *J* = 14.3, 1.3, 1.2 Hz, 1H, NCH_aH_bCNS), 2.94 (dd, *J* = 14.5, 0.9 Hz, 1H, NCH_aH_bCNS), 2.20–2.09 (m, 1H, cyclohexyl), 1.89–1.77 (m, 3H, cyclohexyl), 1.75–1.65 (m, 1H, cyclohexyl), 1.49–1.35 (m, 3H, cyclohexyl), 1.34–1.21 (m, 2H, cyclohexyl);

¹³C NMR (126 MHz, CDCl₃) δ ppm 148.9, 144.8, 133.7, 131.2, 128.7, 126.8, 60.5, 58.8, 49.8, 41.3, 37.1, 36.9, 25.1, 22.8, 22.4;

HRMS calculated for C₁₅H₁₉BrN₂O₂SH (M+2+H)⁺ 373.0403; found 373.0399 (TOF MS ES⁺).

(4*R*,13*S*)-9-bromo-13-isobutyl-4-methyl-3,4,5,6-tetrahydro-2,7-ethanobenzo[*h*]-[1,2,7]thiadiazonine 1,1-dioxide (3.13.1a)



According to general procedure **C**, **3.13.1a** (2 mg, 5%) was isolated as colorless oil.

$[\alpha]_D^{20} = -377.9$ ($c = 0.08$, CHCl_3);

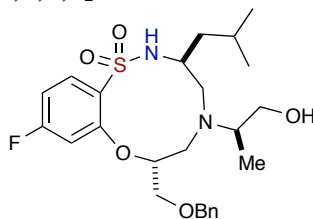
FTIR (thin film) 2955, 1574, 1454, 1385, 1327, 1151, 789, 711 cm^{-1} ;

^1H NMR (400 MHz, CDCl_3) δ ppm 7.58 (d, $J = 8.5$ Hz, 1H, aromatic), 7.26 (d, $J = 2.0$ Hz, 1H, aromatic), 7.20 (dd, $J = 8.5, 1.9$ Hz, 1H, aromatic), 4.03 (ddd, $J = 15.6, 3.9, 2.6$ Hz, 1H, $\text{NCH}_a\text{H}_b\text{CH}_2\text{CHMe}$), 3.88–3.68 (m, 2H, $\text{NCH}_a\text{H}_b\text{CHN}$), 3.37 (dd, $J = 15.0, 3.7$ Hz, 1H, $\text{NCH}_a\text{H}_b\text{CHMe}$), 3.30–3.16 (m, 2H, $\text{NCH}_a\text{H}_b\text{CHN}$, $\text{NCH}_a\text{H}_b\text{CHMe}$), 3.03 (ddd, $J = 15.6, 12.1, 1.6$ Hz, 1H, $\text{NCH}_a\text{H}_b\text{CH}_2\text{CHMe}$), 2.10 (ddd, $J = 13.9, 9.4, 5.0$ Hz, 2H, NCH_2CHMe , $\text{NCHCH}_a\text{H}_b\text{CH}$), 1.94–1.80 (m, 1H, CH_3CHCH_3), 1.42 (dd, $J = 15.5, 2.7$ Hz, 1H, $\text{NCH}_2\text{CH}_a\text{H}_b\text{CHMe}$), 1.27–1.15 (m, 2H, $\text{NCHCH}_a\text{H}_b\text{CH}$, $\text{NCH}_2\text{CH}_a\text{H}_b\text{CHMe}$), 1.00 (d, $J = 6.7$ Hz, 3H, CH_3CHCH_3), 0.96 (d, $J = 6.6$ Hz, 3H CH_3CHCH_3), 0.90 (d, $J = 6.6$ Hz, 3H, $\text{NCH}_2\text{CHCH}_3$);

^{13}C NMR (126 MHz, CDCl_3) δ ppm 147.7, 137.0, 129.5, 129.1, 126.5, 126.1, 57.3, 57.0, 56.1, 54.3, 40.3, 34.7, 33.5, 25.4, 23.4, 22.3, 20.9;

HRMS calculated for $\text{C}_{17}\text{H}_{25}\text{BrN}_2\text{O}_2\text{SH}$ ($\text{M}+\text{H}$) $^+$ 403.0873; found 403.0870 (TOF MS ES $^+$).

(3*S*,7*R*)-7-((benzyloxy)methyl)-10-fluoro-5-((*R*)-1-hydroxypropan-2-yl)-3-isobutyl-2,3,4,5,6,7hexahydrobenzo[*b*][1,4,5,8]oxathiadiazecine 1,1-dioxide (3.14.7)



According to general procedure **B**, **3.14.7** (33.4 mg, 42%) was isolated as a white solid.

mp 50–55 °C;

$[\alpha]_D^{20} = +22.5$ ($c = 1.315$, CHCl_3);

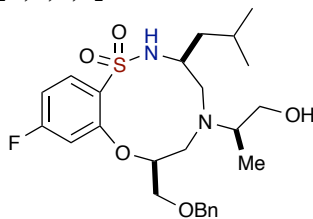
FTIR (thin film) 3514, 2953, 1601, 1587, 1477, 1454, 1389, 1321, 1155, 1070, 808, 741, 700 cm^{-1} ;

^1H NMR (500 MHz, CDCl_3) δ ppm 7.98 (dd, $J = 8.8, 6.5$ Hz, 1H, aromatic), 7.41–7.25 (m, 5H, aromatic), 6.79 (ddd, $J = 8.7, 7.8, 2.4$ Hz, 1H, aromatic), 6.72 (dd, $J = 9.9, 2.4$ Hz, 1H, aromatic), 5.75 (s, 1H, NH), 4.46 (d, $J = 11.8$ Hz, 1H, $\text{OCH}_a\text{H}_b\text{C}$), 4.40 (d, $J = 11.9$ Hz, 1H, $\text{OCH}_a\text{H}_b\text{C}$), 4.37 (dd, $J = 12.3, 5.1$ Hz, 1H, $\text{OCHCH}_a\text{H}_b\text{O}$), 3.90 (dd, $J = 11.9$ Hz, 1H, $\text{OCHCH}_a\text{H}_b\text{O}$), 3.64 (bs, 1H, NHCHCH_2N), 3.37–3.23 (m, 2H, OCHCH_2O , NCHCH_3), 3.14 (dd, $J = 9.4, 4.1$ Hz, 1H, $\text{HOCH}_a\text{H}_b\text{CH}$), 3.09–2.99 (m, 2H, $\text{NHCHCH}_a\text{H}_b\text{N}$, $\text{HOCH}_a\text{H}_b\text{CH}$), 2.53 (d, $J = 12.7$ Hz, 1H, $\text{NCH}_a\text{H}_b\text{CHO}$), 2.36–2.28 (m, 2H, $\text{NCH}_a\text{H}_b\text{CHO}$, OH), 2.14 (dd, $J = 15.1, 10.8$ Hz, 1H, $\text{NHCHCH}_a\text{H}_b\text{N}$), 1.95–1.81 (m, 1H, CH_3CHCH_3), 1.42 (ddd, $J = 13.7, 7.7, 6.0$ Hz, 1H, $\text{NHCHCH}_a\text{H}_b$), 1.14 (ddd, $J = 13.6, 7.9, 5.6$ Hz, 1H, $\text{NHCHCH}_a\text{H}_b$), 0.98 (d, $J = 6.5$ Hz, 3H, NCHCH_3), 0.93 (d, $J = 6.5$ Hz, 3H, CH_3CHCH_3), 0.89 (d, $J = 6.6$ Hz, 3H, CH_3CHCH_3);

^{13}C NMR (126 MHz, CDCl_3) δ ppm 165.7 (d, $^1J_{\text{C-F}} = 254.0$ Hz), 157.2, 137.7, 132.2 (d, $^3J_{\text{C-F}} = 10.8$ Hz), 128.5 (2C), 127.9 (2C), 127.7 (2C), 108.6 (d, $^2J_{\text{C-F}} = 22.2$ Hz), 104.1 (d, $^2J_{\text{C-F}} = 24.5$ Hz), 73.4, 72.2, 71.9, 69.4 (2C), 57.4, 56.3, 53.7, 46.1, 24.2, 23.0, 22.5, 9.5;

HRMS calculated for $\text{C}_{25}\text{H}_{35}\text{FN}_2\text{O}_5\text{SH}$ ($\text{M}+\text{H}$) $^+$ 495.2329; found 495.2348 (TOF MS ES $^+$).

3*S*,7*S*)-7-((benzyloxy)methyl)-10-fluoro-5-((*R*)-1-hydroxypropan-2-yl)-3-isobutyl-2,3,4,5,6,7hexahydro-benzo[*b*][1,4,5,8]oxathiadiazecine 1,1-dioxide (3.14.8)



According to general procedure **B**, **3.14.8** (30.5 mg, 42%) was isolated as colorless sticky oil.

$[\alpha]_D^{20} = +45.9$ ($c = 0.535$, CHCl_3);

FTIR (thin film) 3450, 3259, 2957, 1603, 1587, 1477, 1454, 1387, 1323, 1161, 1070, 808, 733, 698 cm^{-1} ;

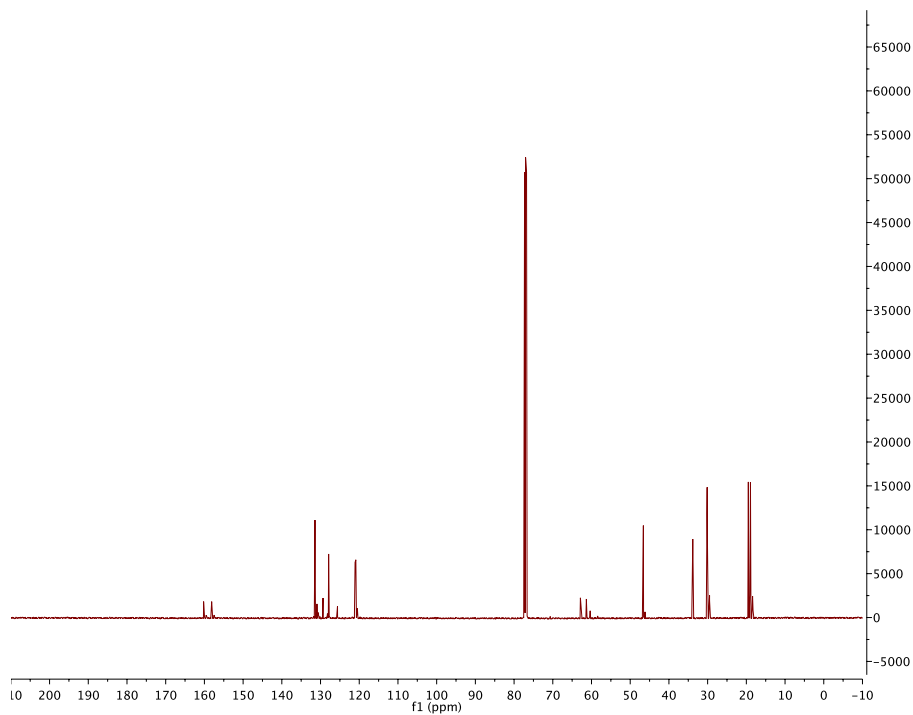
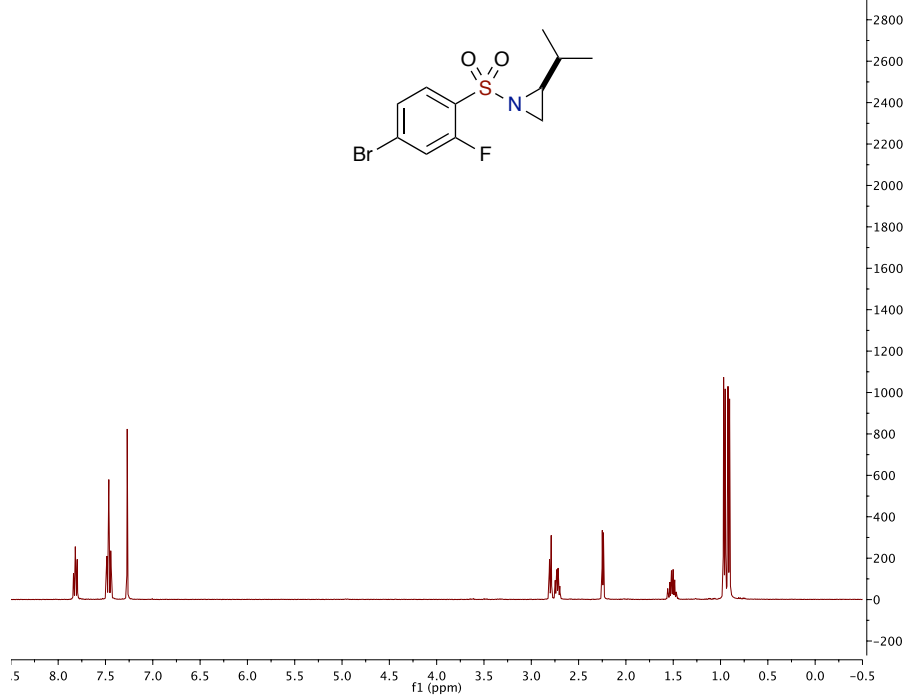
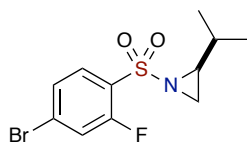
^1H NMR (500 MHz, CDCl_3) δ ppm 7.96 (ddd, $J = 8.6, 6.4, 1.6$ Hz, 1H, aromatic), 7.53–7.44 (m, 2H, aromatic), 7.44–7.37 (m, 2H, aromatic), 7.38–7.29 (m, 1H, aromatic), 6.87–6.79 (m, 1H, aromatic), 6.79 (ddd, $J = 10.0, 1.8$ Hz, 1H, aromatic), 6.42 (s, 1H, NH), 4.66 (s, 2H, OCH_2C), 4.56 (dd, $J = 5.4, 3.1$ Hz, 1H, OCHCH_2O), 4.01 (dd, $J = 10.5, 5.1$ Hz, 1H, $\text{OCHCH}_a\text{H}_b\text{O}$), 3.98–3.89 (m, 1H, $\text{OCHCH}_a\text{H}_b\text{O}$), 3.44–3.26 (m, 2H, HOCH_2CH), 3.06–2.96 (m, 1H, NHCHCH_2N), 2.95–2.87 (m, 3H, NCH_2CHO , OH), 2.77–2.64 (m, 1H, NCHCH_3), 2.33 (dd, $J = 14.8, 4.9$ Hz, 1H, $\text{NHCHCH}_a\text{H}_b\text{N}$), 2.26 (dd, $J = 14.9, 3.8$ Hz, 1H, $\text{NHCHCH}_a\text{H}_b\text{N}$), 1.65–1.53 (m, 1H, CH_3CHCH_3), 1.54–1.43 (m, 1H, $\text{NHCHCH}_a\text{H}_b$), 0.96 (ddd, $J = 13.5, 7.9, 5.6$ Hz, 1H, $\text{NHCHCH}_a\text{H}_b$), 0.84 (dd, $J = 6.5, 1.5$ Hz, 3H, CH_3CHCH_3), 0.81 (dd, $J = 6.7, 1.6$ Hz, 3H, NCHCH_3), 0.72 (dd, $J = 6.6, 1.5$ Hz, 3H, CH_3CHCH_3);

^{13}C NMR (126 MHz, CDCl_3) δ ppm 165.9 (d, $^1J_{\text{C-F}} = 254.8$ Hz), 155.5, 136.2, 132.3 (d, $^3J_{\text{C-F}} = 10.2$ Hz), 129.0 (2C), 128.6 (2C), 128.4, 127.3, 109.2 (d, $^2J_{\text{C-F}} = 22.0$ Hz), 104.1

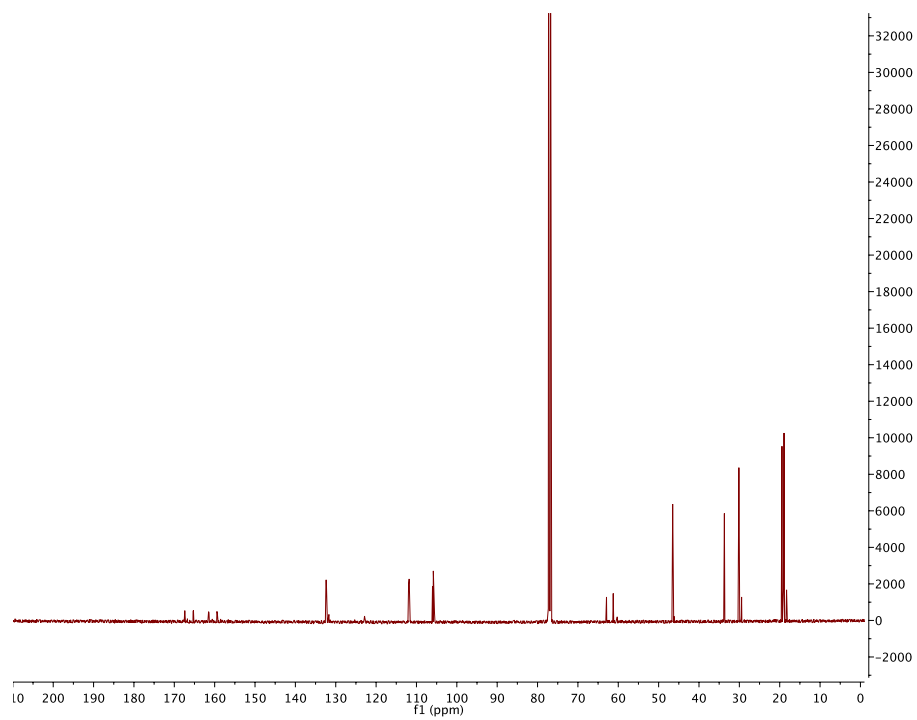
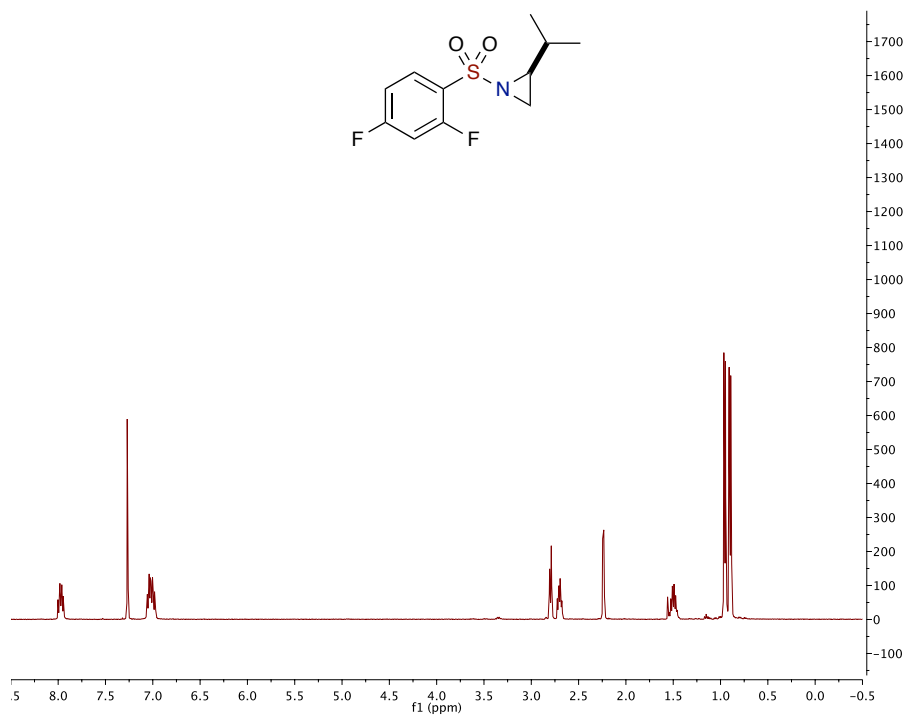
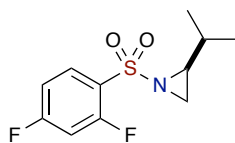
(d, $^2J_{C-F} = 25.2$ Hz), 78.6, 75.0, 71.0, 64.8, 61.4, 55.8, 53.5, 51.6, 43.4, 24.1, 23.1, 21.8, 10.0;

HRMS calculated for $C_{25}H_{35}FN_2O_5SH$ (M+H)⁺ 495.2329; found 495.2298 (TOF MS ES⁺).

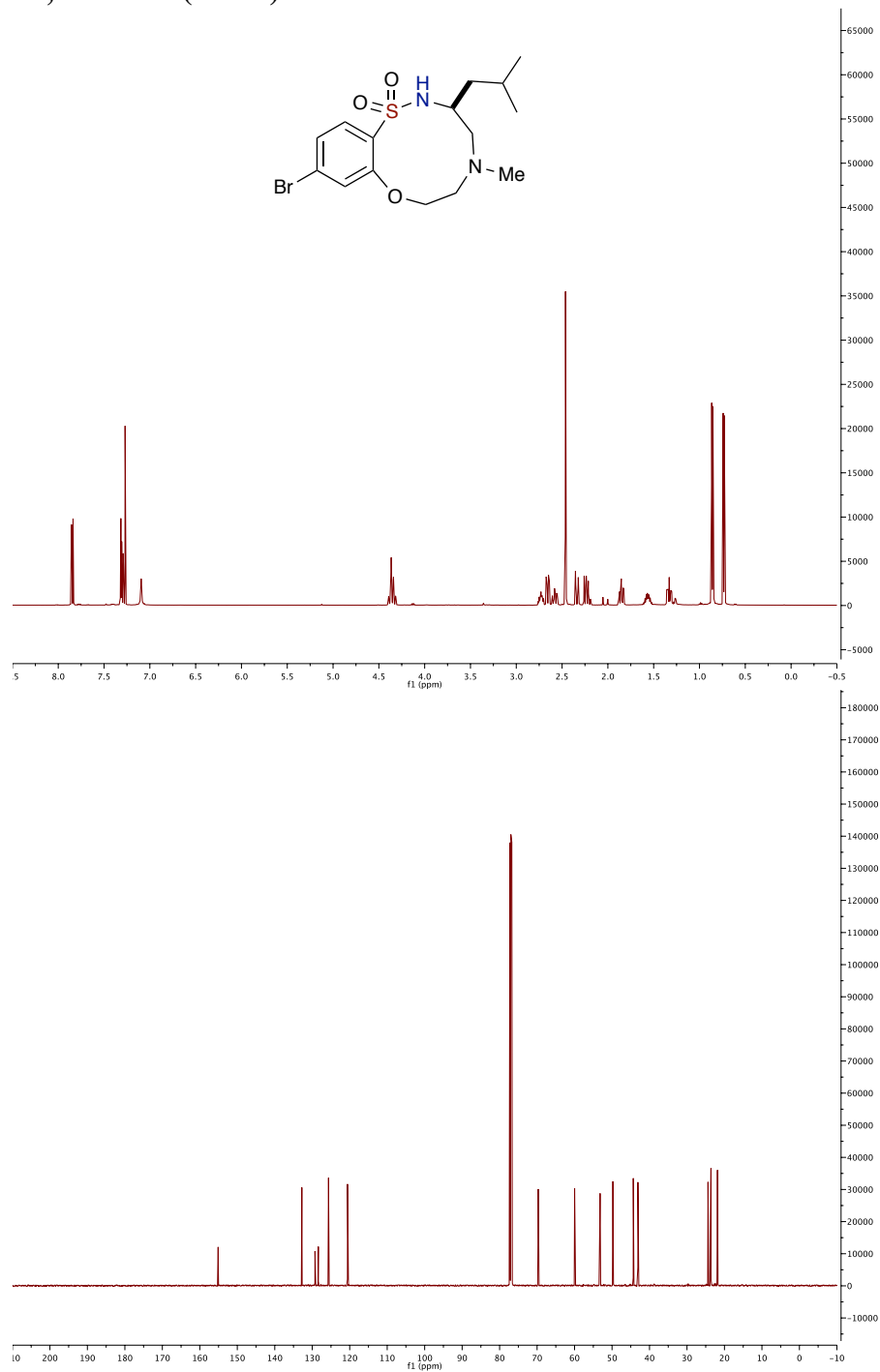
(S)-1-((4-bromo-2-fluorophenyl)sulfonyl)-2-isopropylaziridine (3.8.4b)



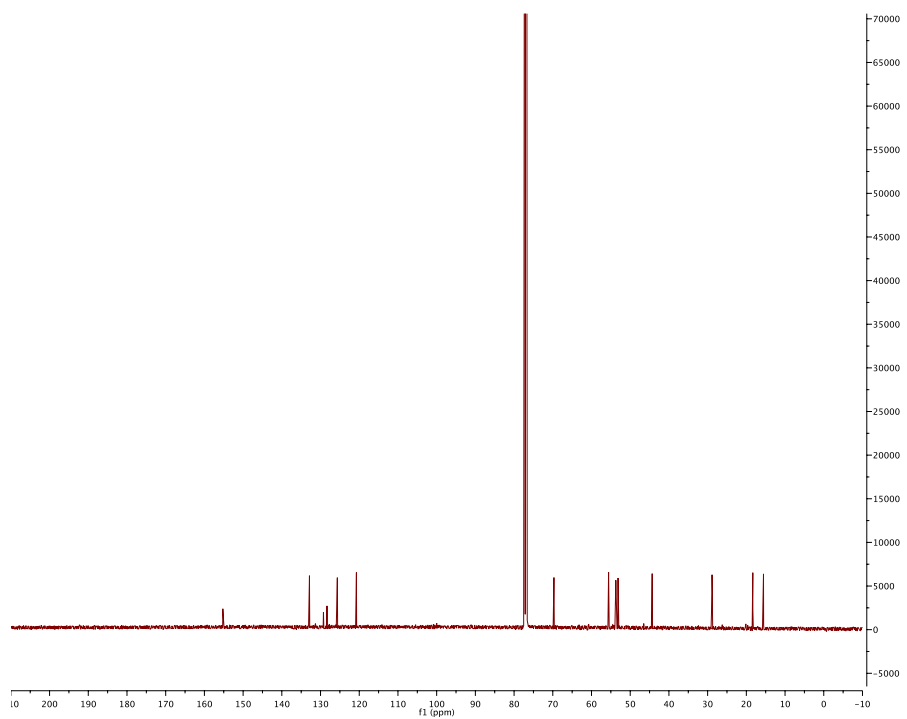
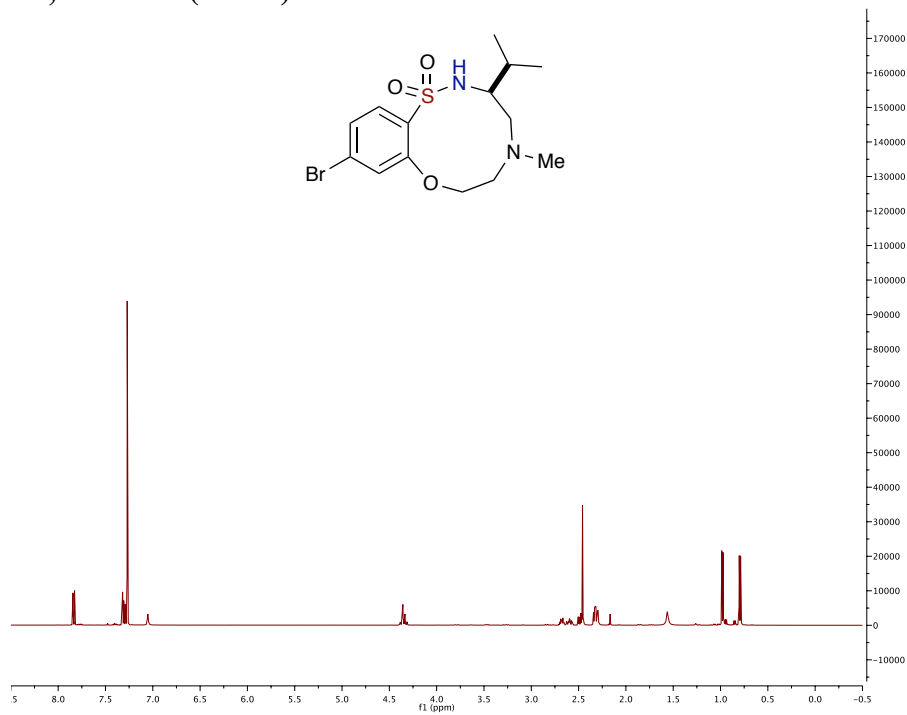
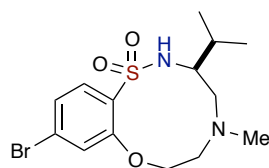
(S)-1-((2,4-difluorophenyl)sulfonyl)-2-isopropylaziridine (3.8.4d)



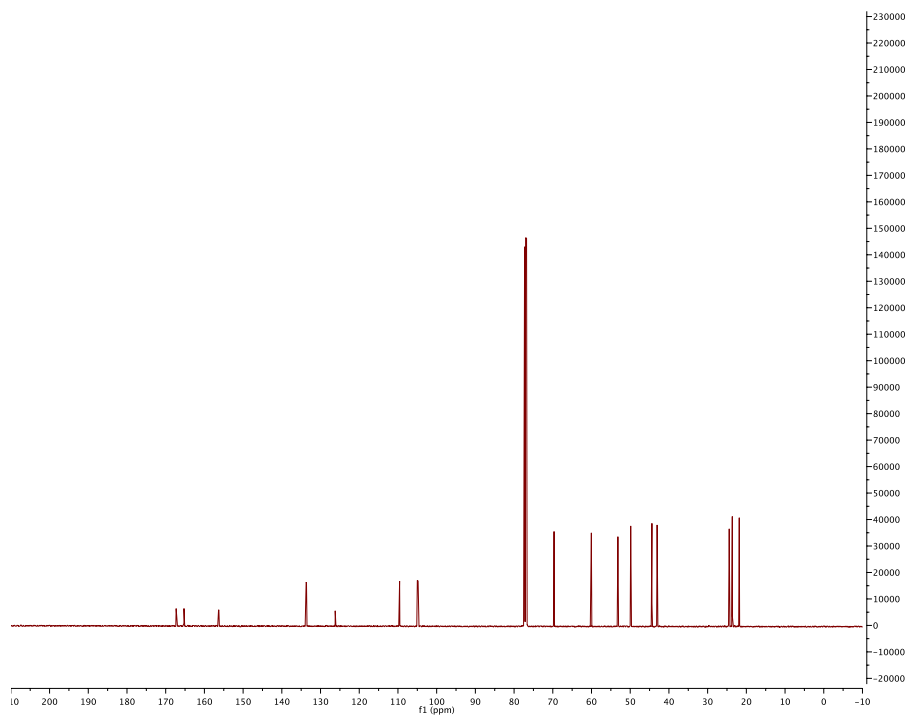
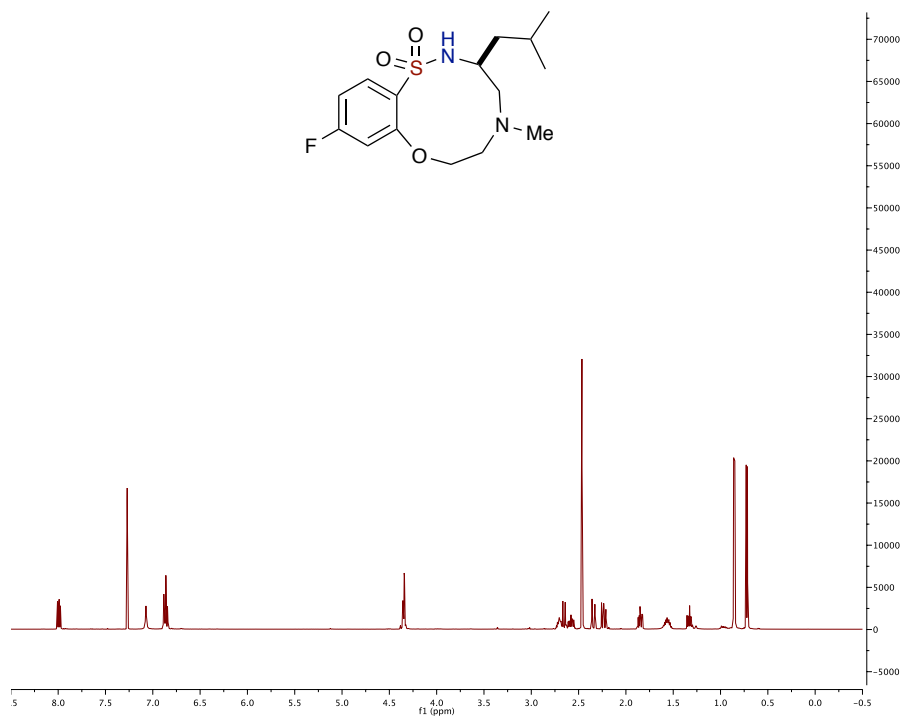
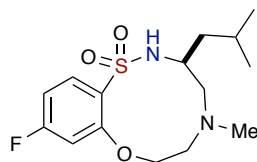
(S)-10-bromo-3-isobutyl-5-methyl-2,3,4,5,6,7-hexahydrobenzo[*b*][1,4,5,8]oxathiazine 1,1-dioxide (3.1.2a)



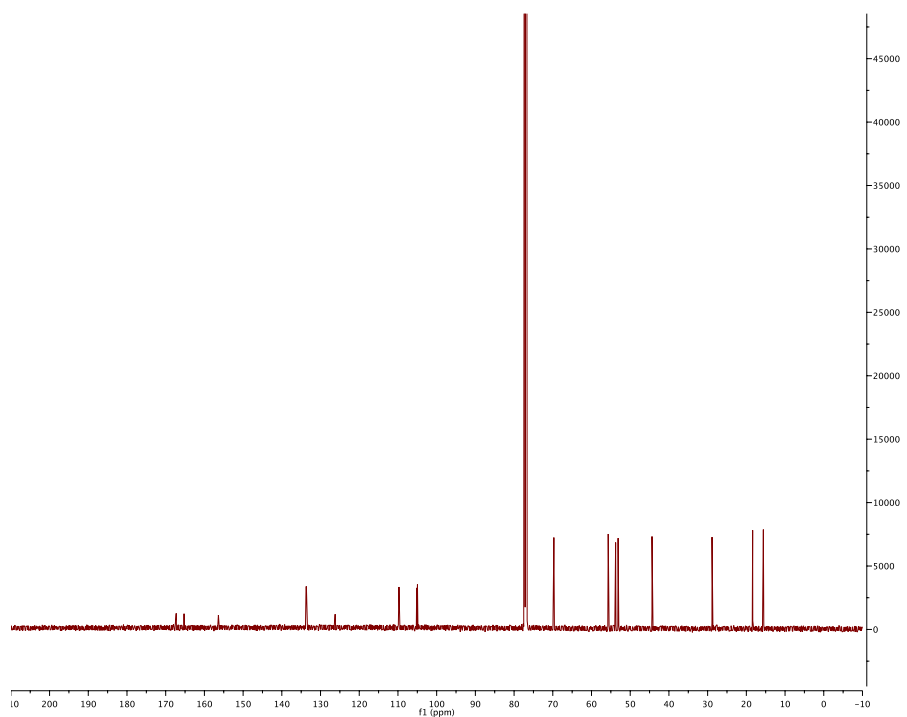
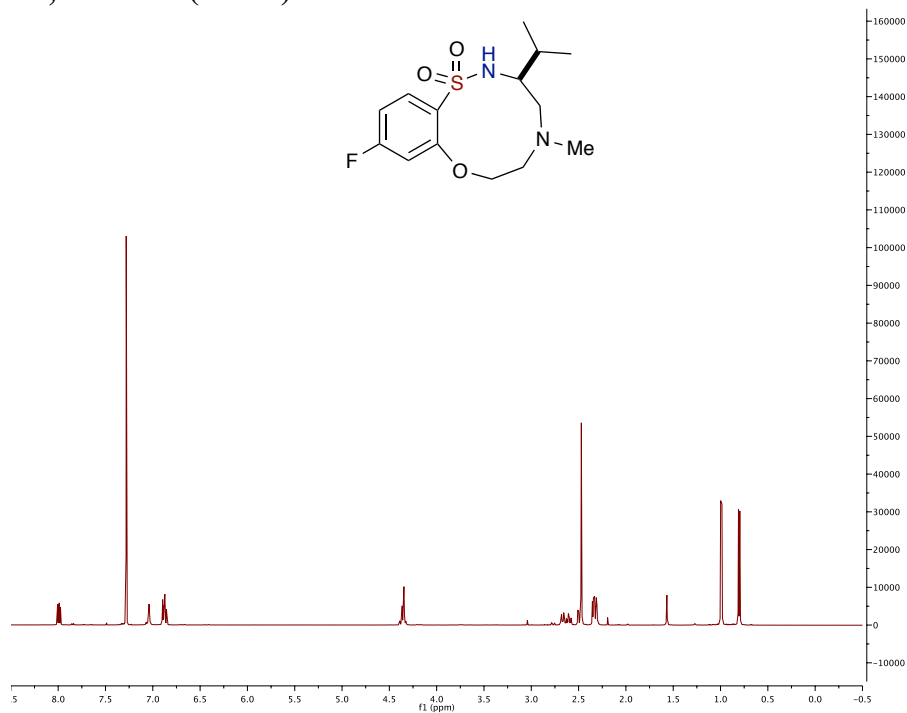
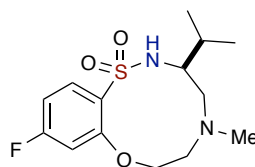
(S)-10-bromo-3-isopropyl-5-methyl-2,3,4,5,6,7-hexahydrobenzo[*b*][1,4,5,8]oxathiazine-1,1-dioxide (3.9.2b)



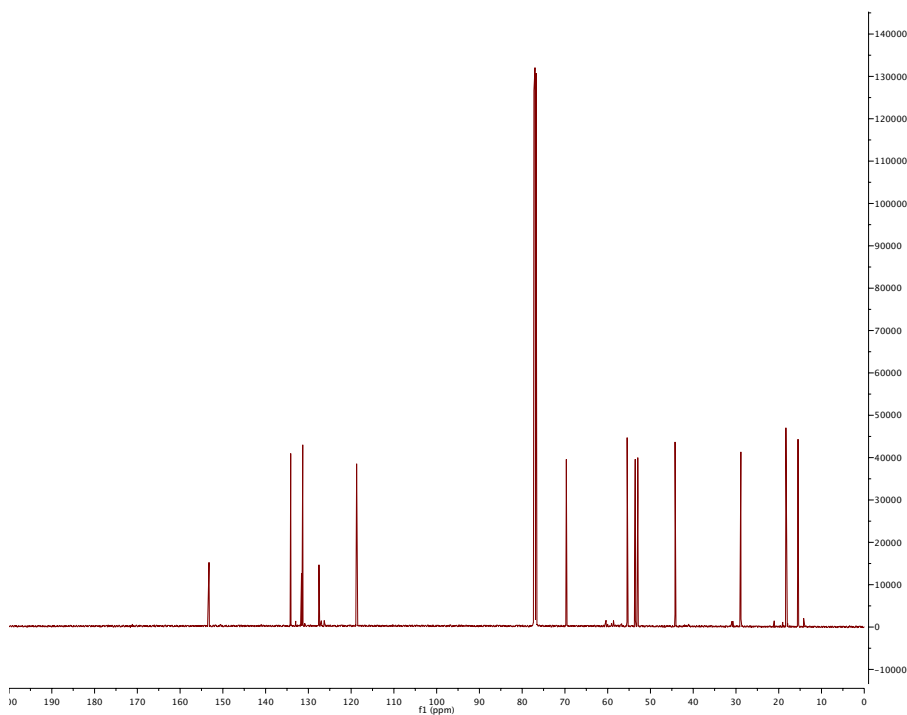
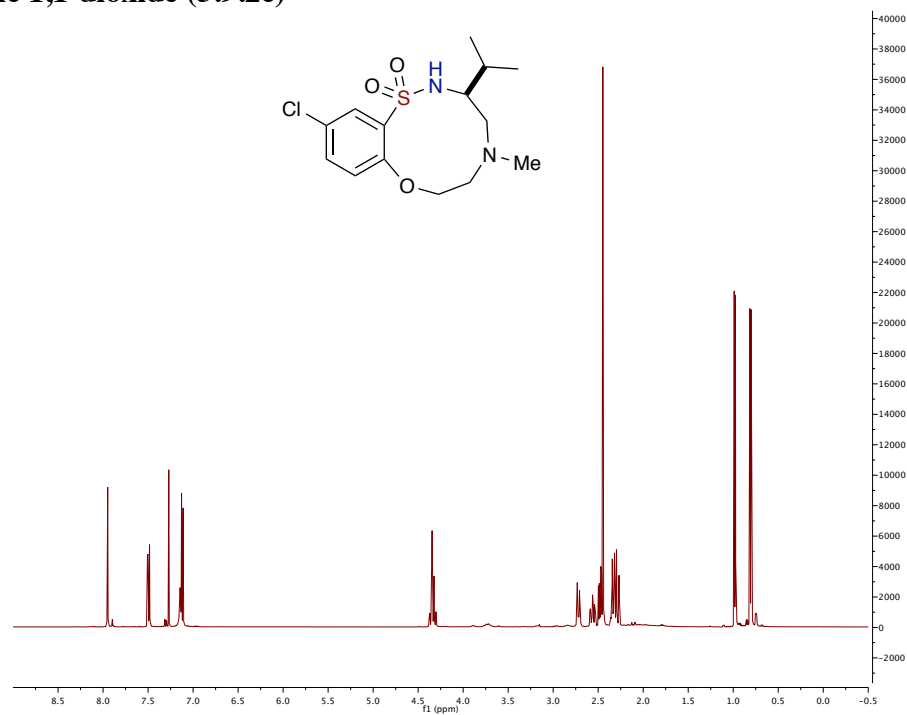
(S)-10-fluoro-3-isobutyl-5-methyl-2,3,4,5,6,7-hexahydrobenzo[*b*][1,4,5,8]oxathiazine 1,1-dioxide (3.9.2c)



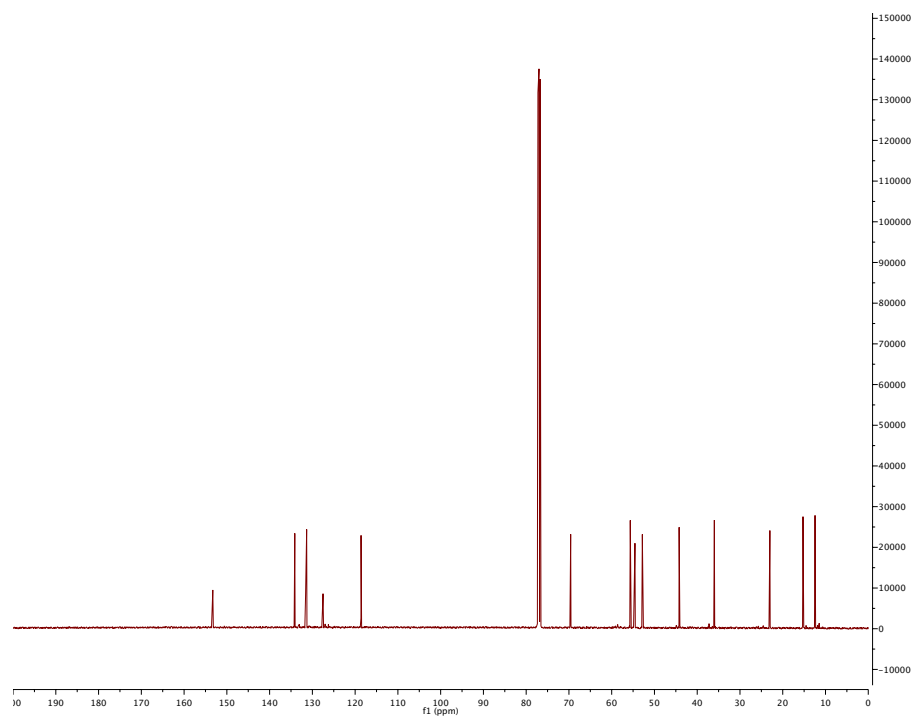
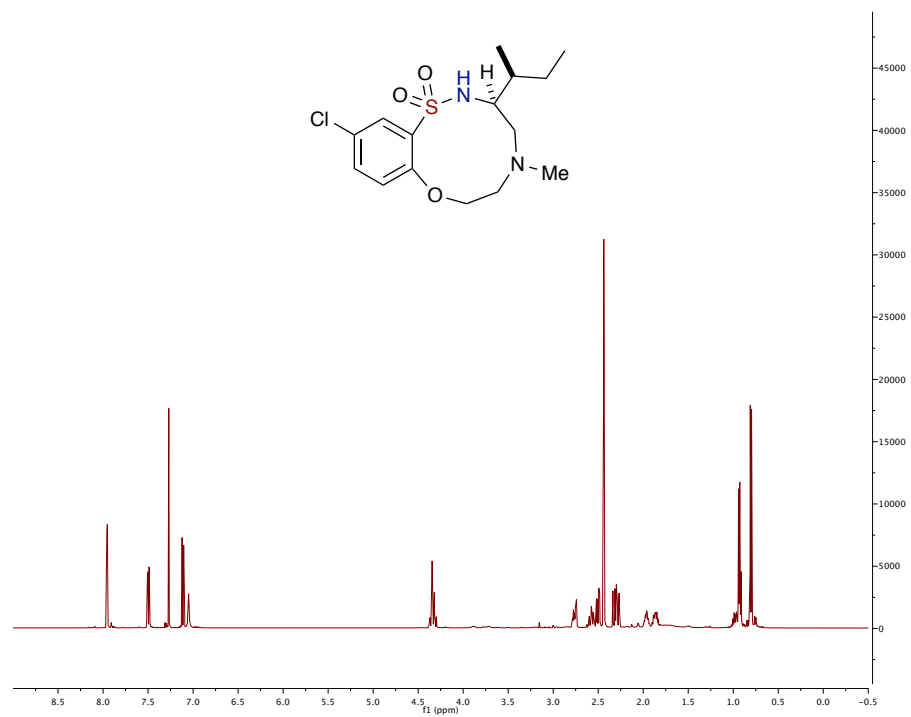
(S)-10-fluoro-3-isopropyl-5-methyl-2,3,4,5,6,7-hexahydrobenzo[*b*][1,4,5,8]oxathiazine-1,1-dioxide (3.9.2d)



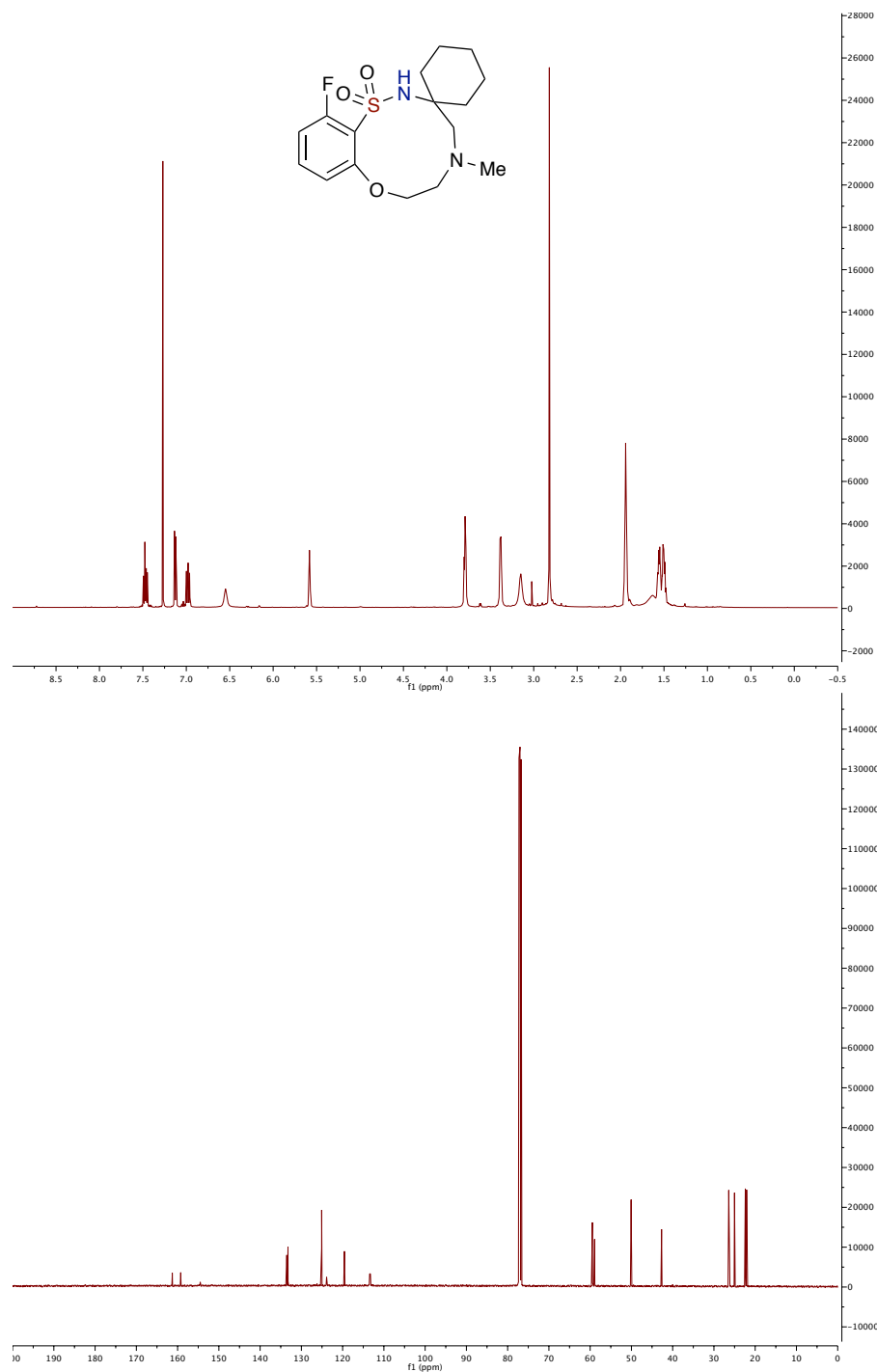
(S)-11-chloro-3-isopropyl-5-methyl-2,3,4,5,6,7-hexahydrobenzo[*b*][1,4,5,8]oxathiazine 1,1-dioxide (3.9.2e)



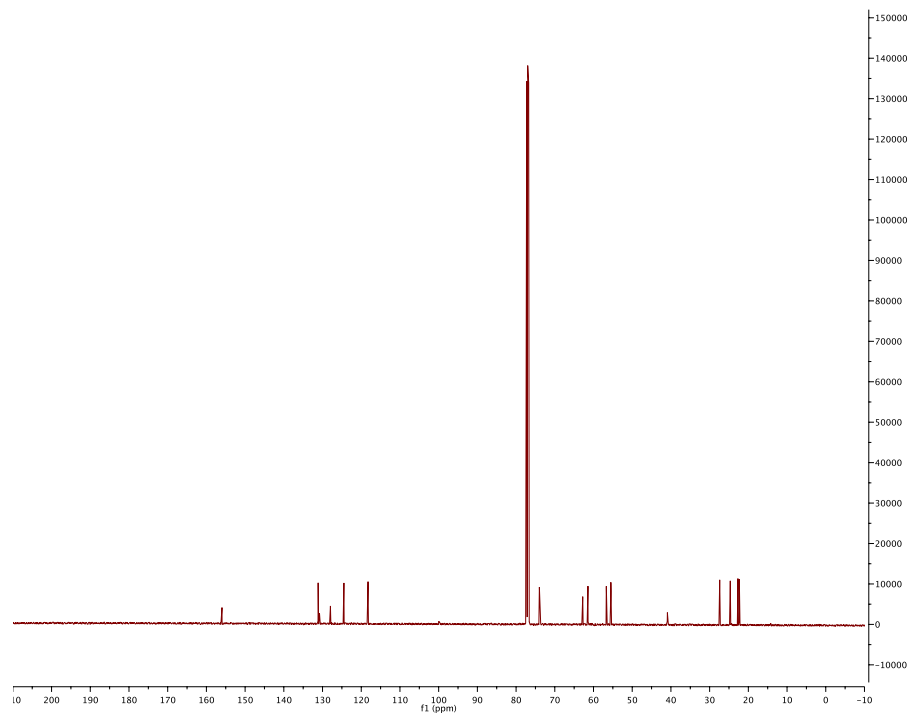
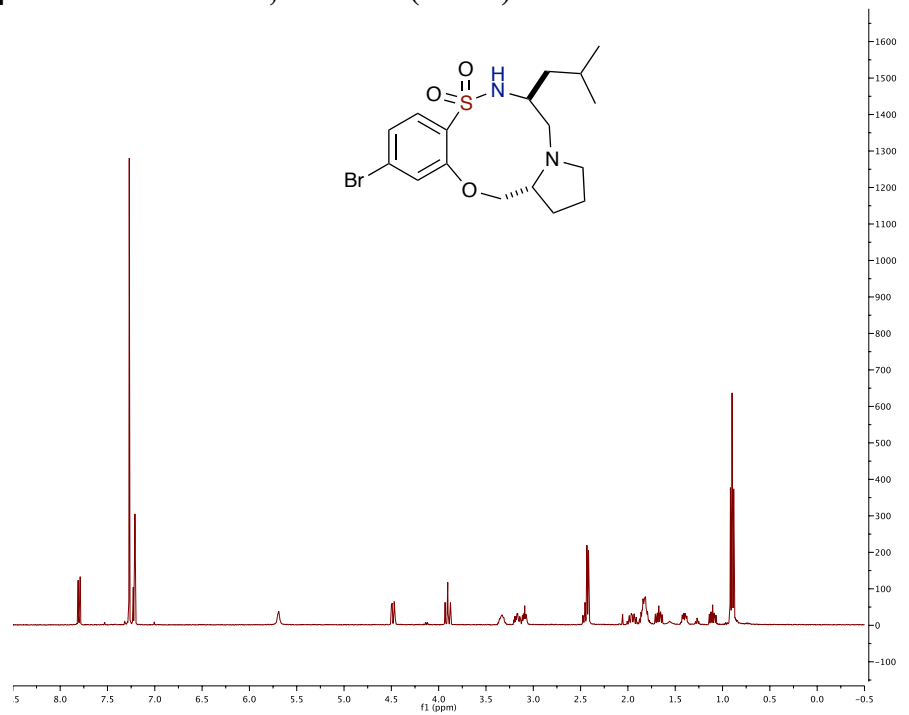
(S)-3-((S)-*sec*-butyl)-11-chloro-5-methyl-2,3,4,5,6,7-hexahydrobenzo[*b*][1,4,5,8]-oxathiadiazecine 1,1-dioxide (3.9.2f)



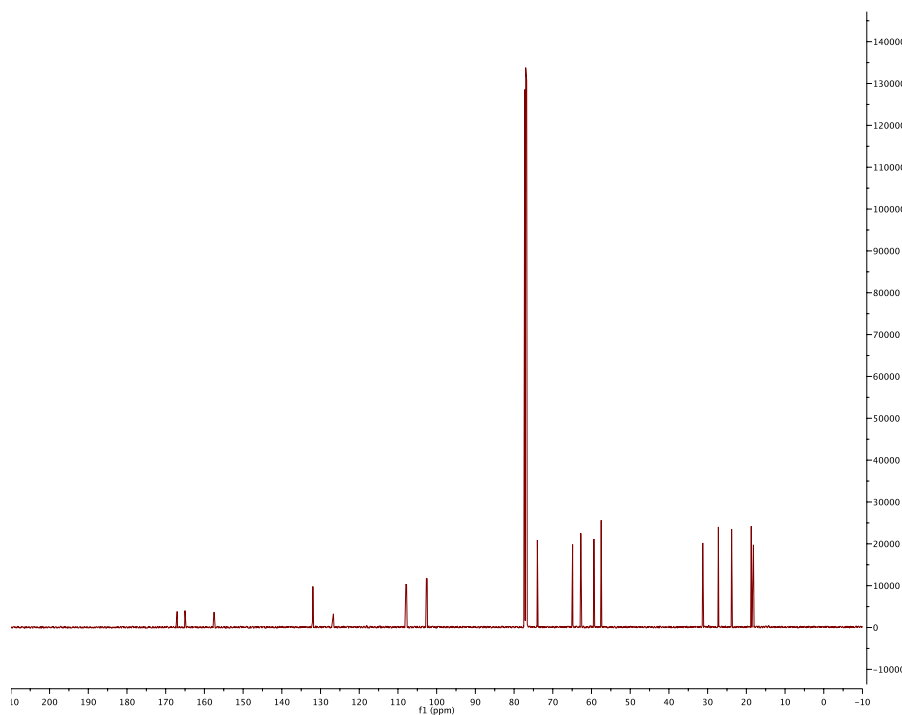
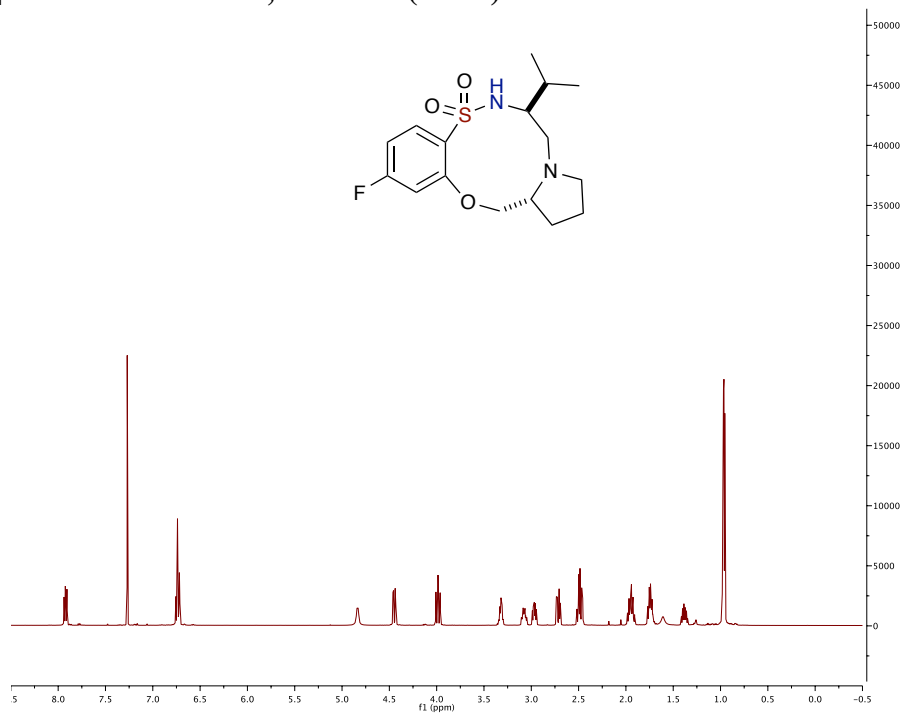
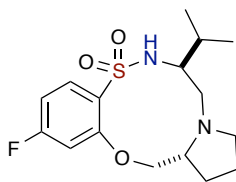
12-fluoro-5-methyl-4,5,6,7-tetrahydro-2H-spiro[benzo[b][1,4,5,8]oxathiadiazecine-3,1'-cyclohexane] 1,1-dioxide (3.92g)



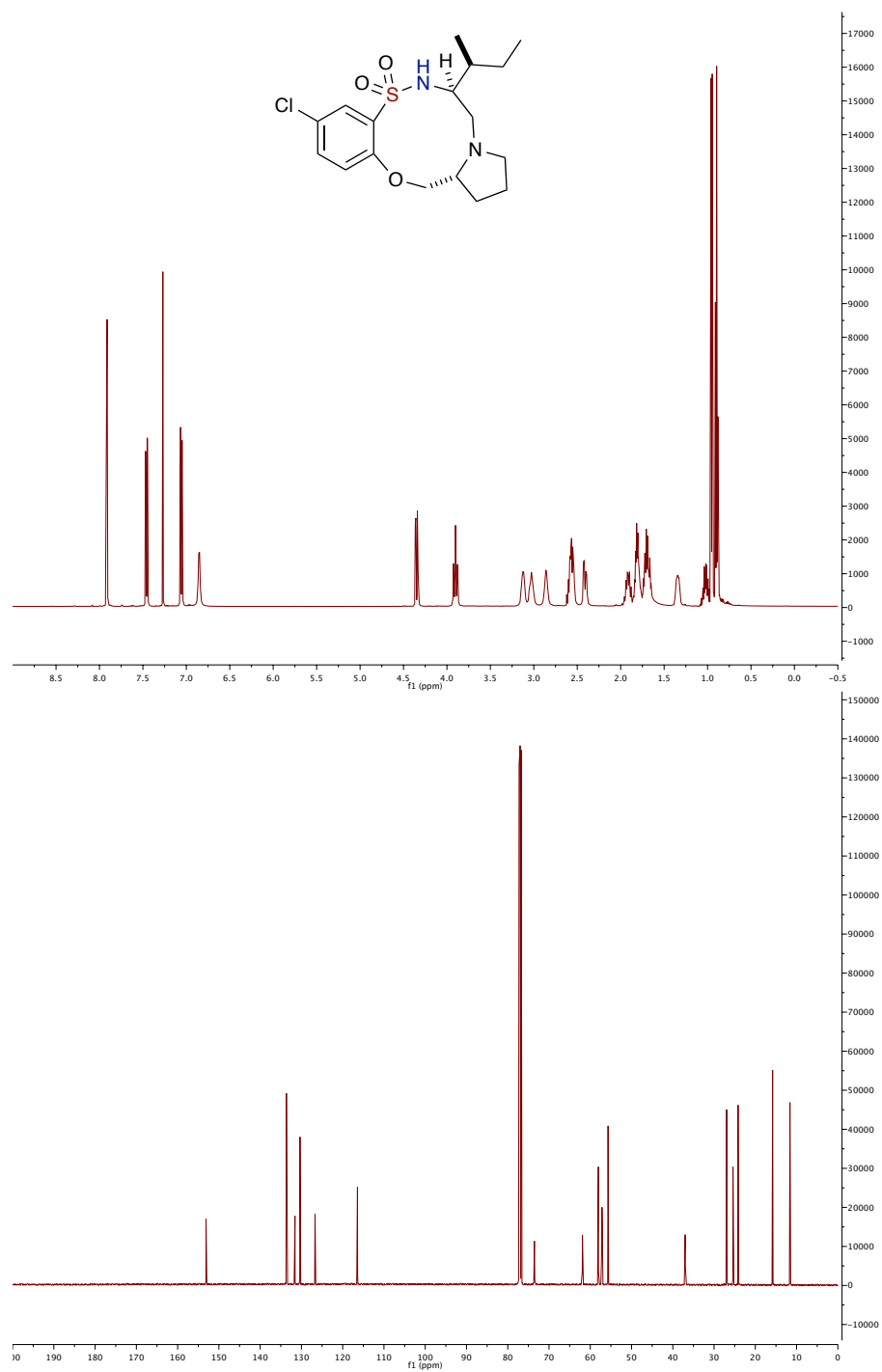
(6*S*,14*aR*)-11-bromo-6-isobutyl-1,2,3,5,6,7,14,14*a*-octahydrobenzo[*b*]pyrrolo[1,2*h*]-[1,4,5,8]oxathia-diazecine 8,8-dioxide (3.9.2h)



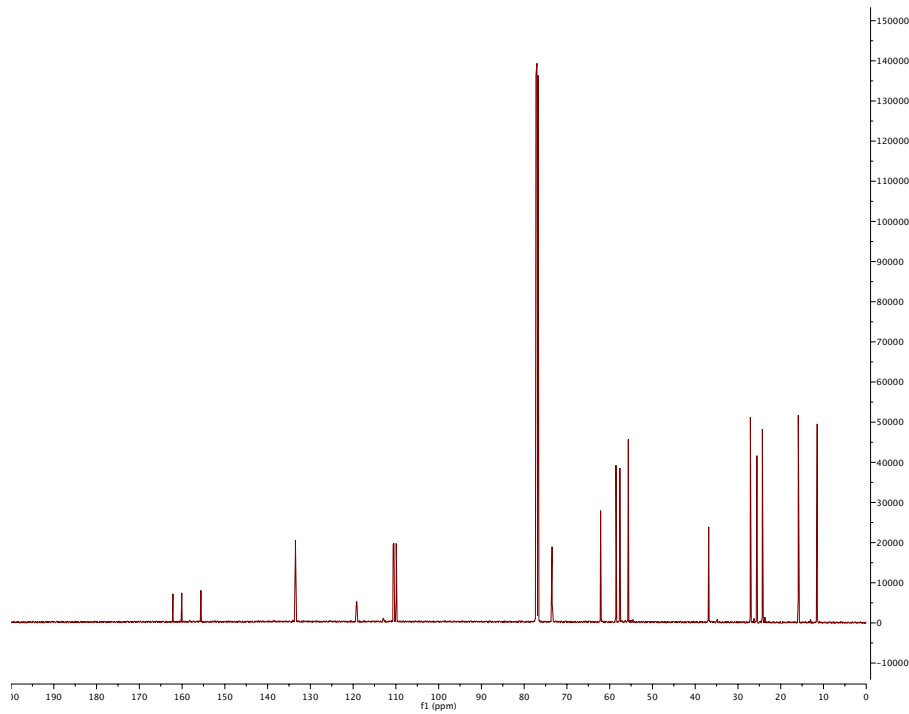
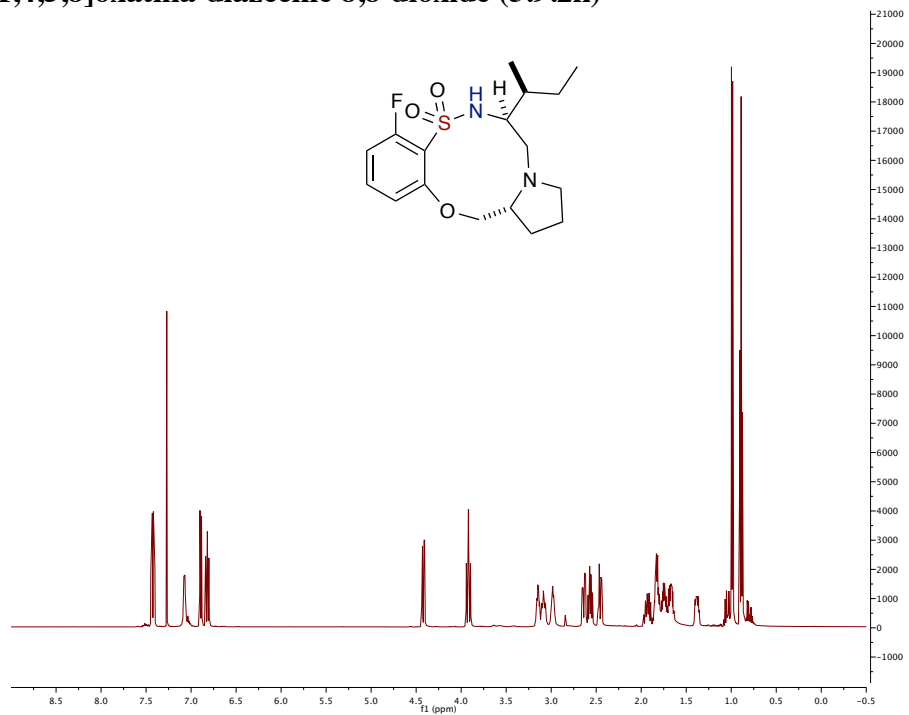
(6*S*,14*aR*)-11-fluoro-6-isopropyl-1,2,3,5,6,7,14,14a-octahydrobenzo[*b*]pyrrolo[1,2*h*]-[1,4,5,8]oxathia-diazecine 8,8-dioxide (3.9.2i)



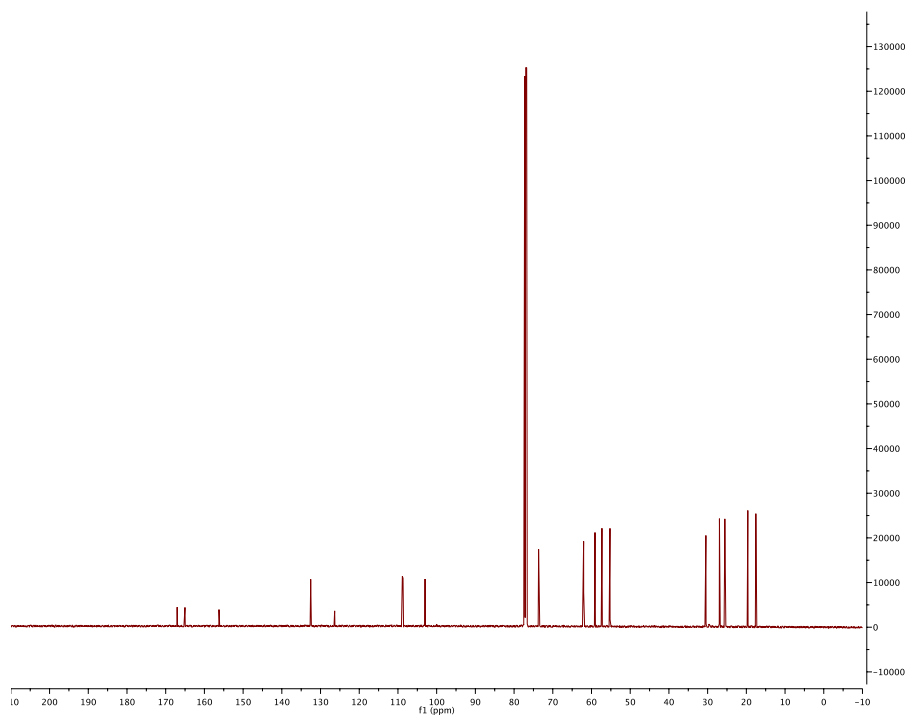
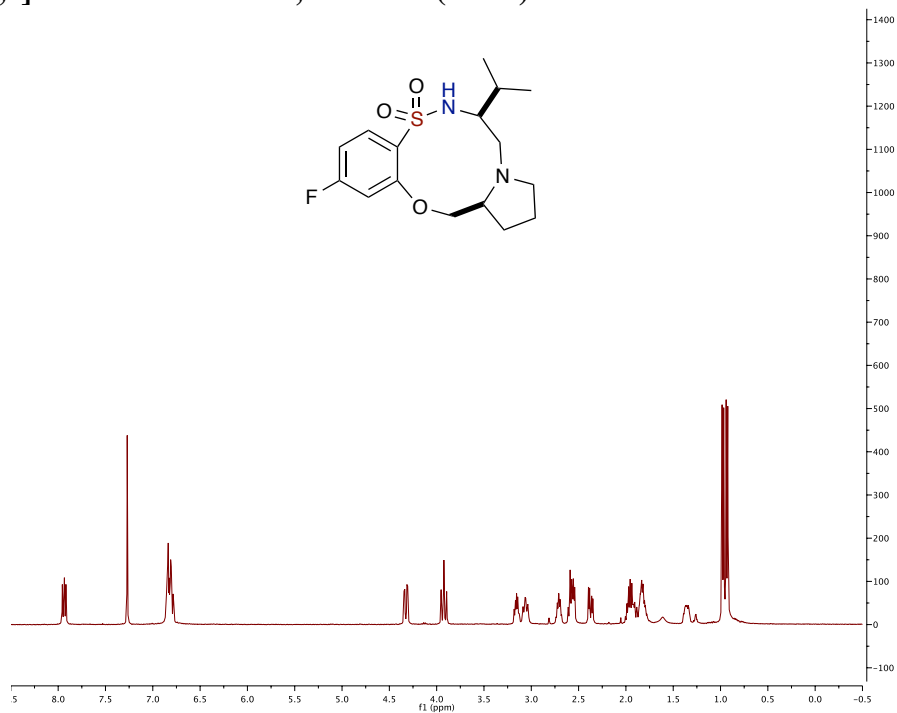
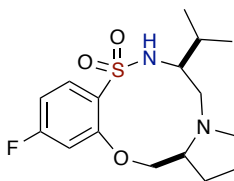
(6*S*,14*aR*)-6-((*S*)-*sec*-butyl)-10-chloro-1,2,3,5,6,7,14,14*a*-octahydrobenzo[*b*]-pyrrolo[1,2-*h*][1,4,5,8]oxathia-diazecine 8,8-dioxide (3.9.2j)



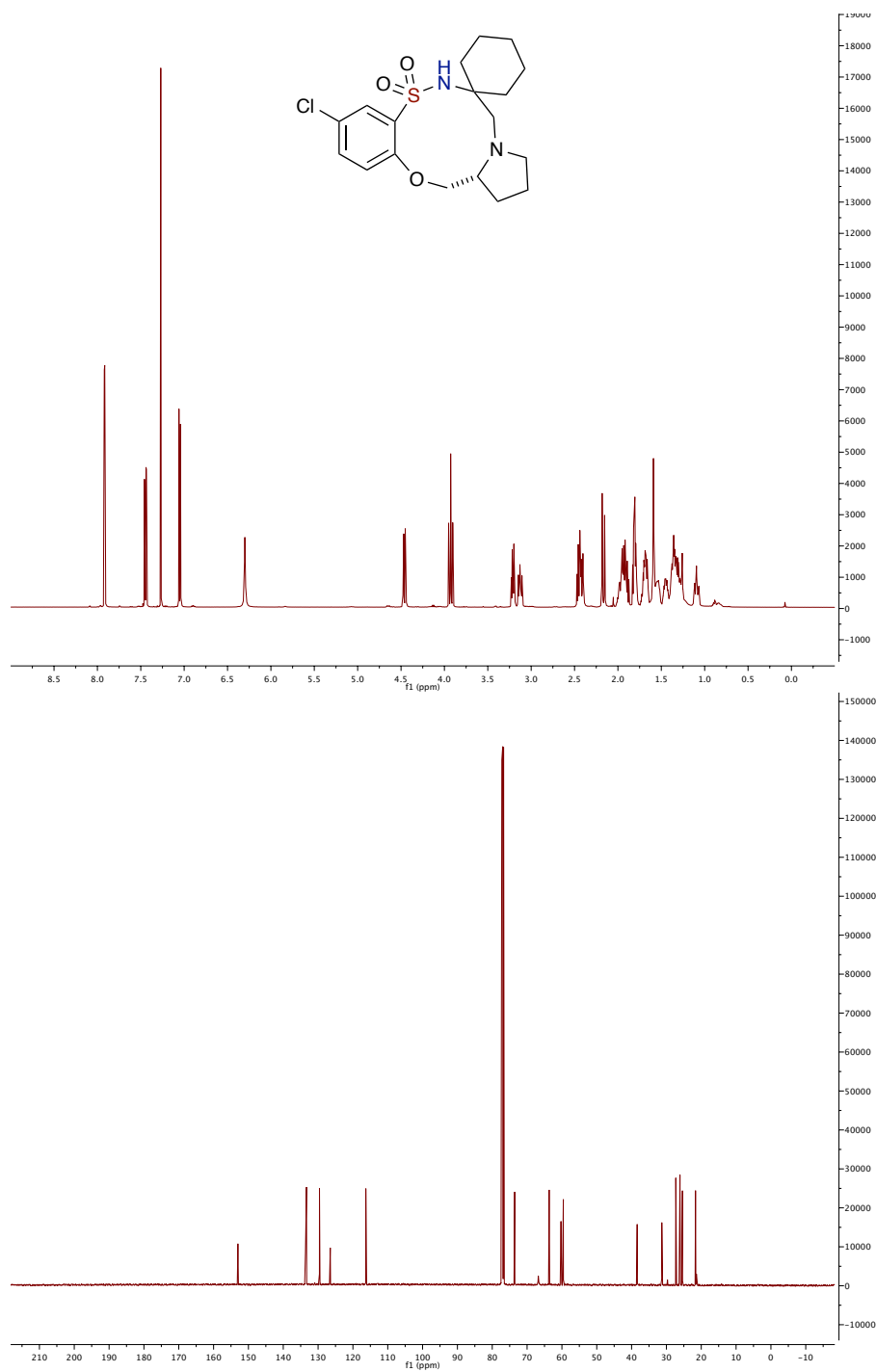
(6*S*,14*aR*)-6-((*S*)-*sec*-butyl)-9-fluoro-1,2,3,5,6,7,14,14*a*-octahydrobenzo[*b*]pyrrolo-[1,2-*h*][1,4,5,8]oxathia-diazecine 8,8-dioxide (3.9.2k)



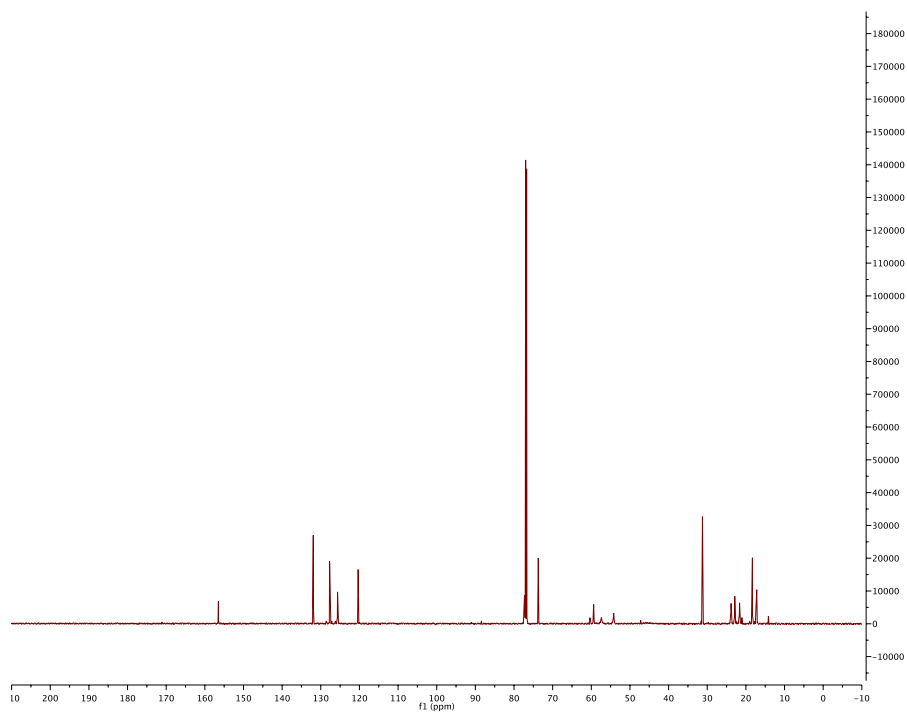
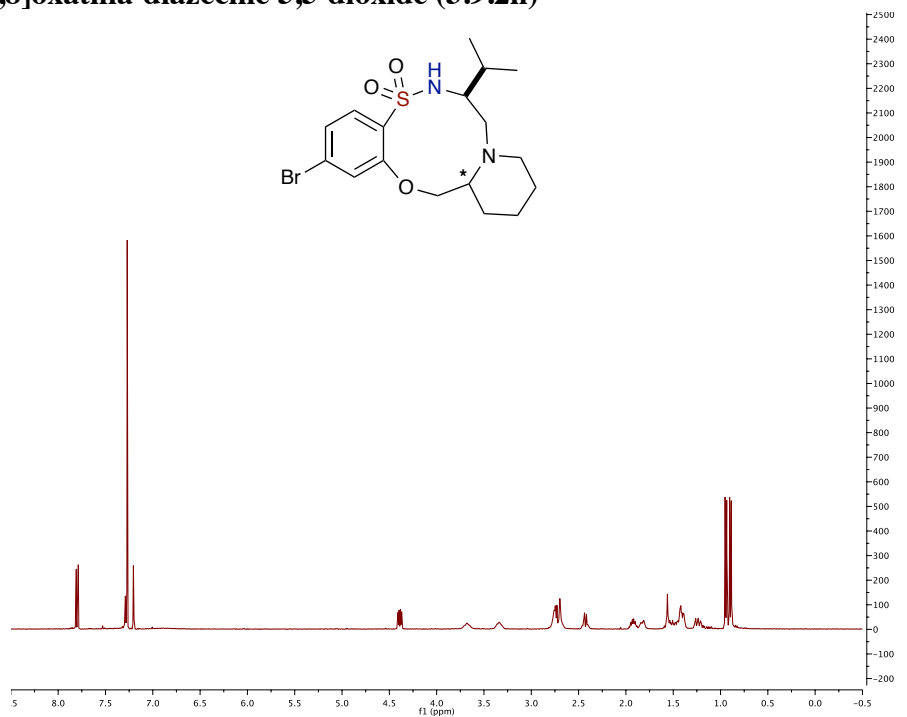
(6*S*,14*aS*)-11-fluoro-6-isopropyl-1,2,3,5,6,7,14,14*a*-octahydrobenzo[*b*]pyrrolo[1,2-*h*][1,4,5,8]oxathia-diazecine 8,8-dioxide (3.9.21)



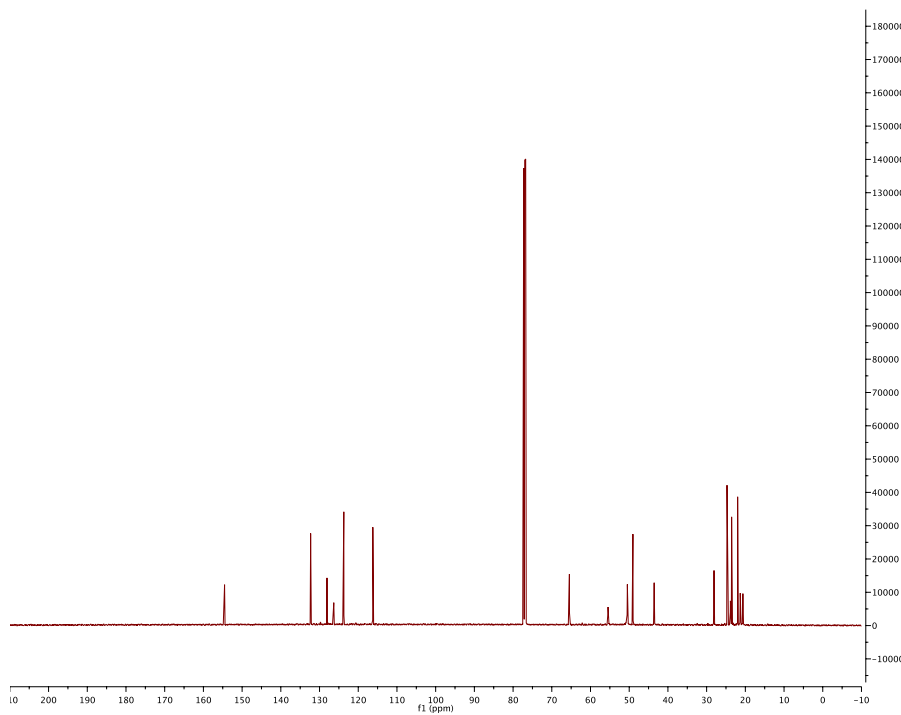
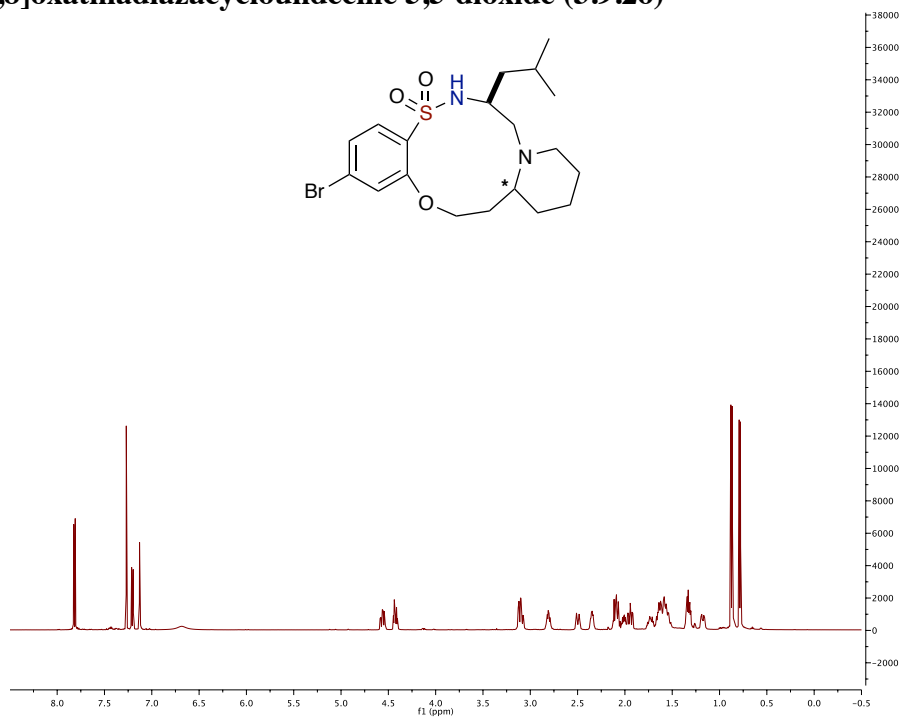
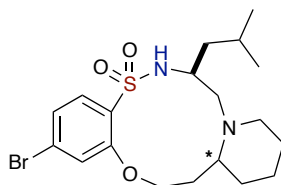
(R)-9-fluoro-2,3,5,7,14,14a-hexahydro-1H-spiro[benzo[*b*]pyrrolo[1,2-*h*][1,4,5,8]-oxathiadiazecine-6,1'-cyclohexane] 8,8-dioxide (3.9.2m)



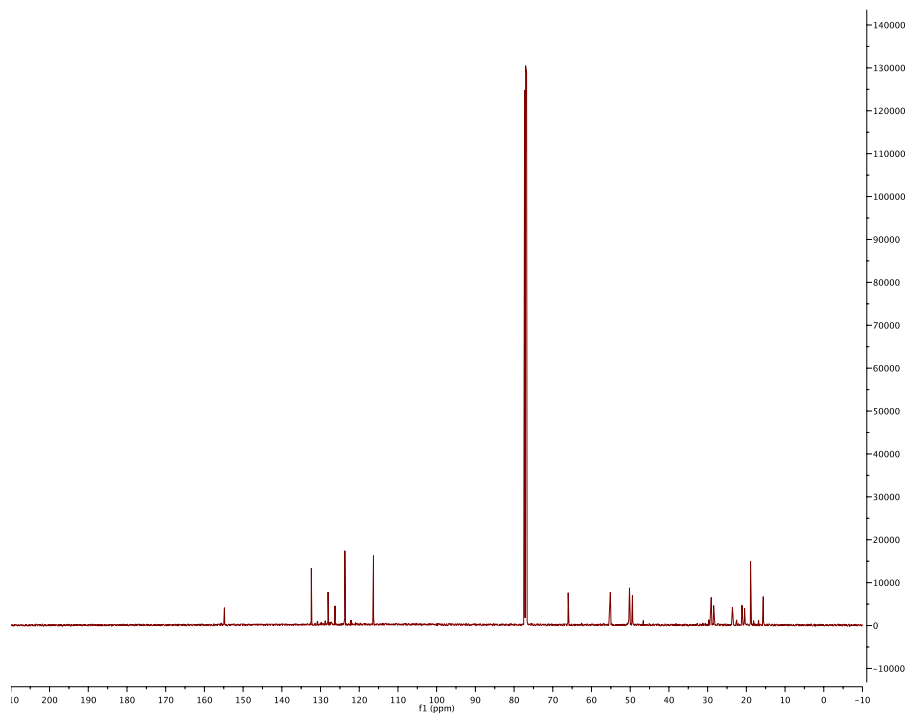
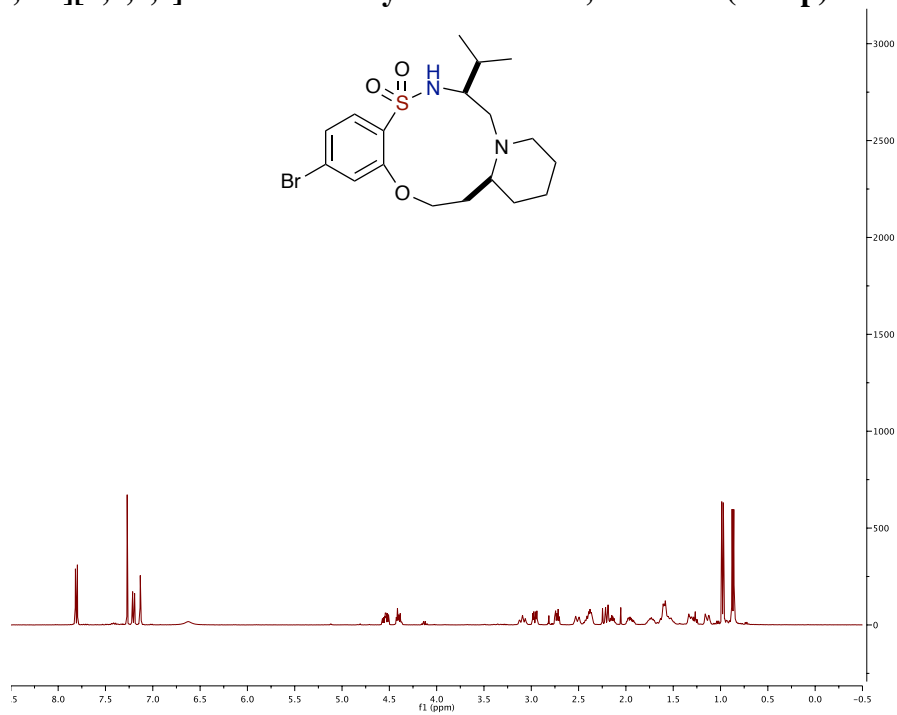
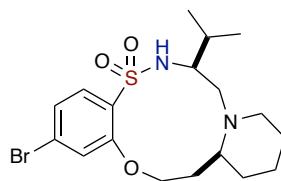
(7S)-2-bromo-7-isopropyl-7,8,10,11,12,13,13a,14-octahydro-6H-benzo[b]pyrido[1,2-h][1,4,5,8]oxathia-diazecine 5,5-dioxide (3.9.2n)



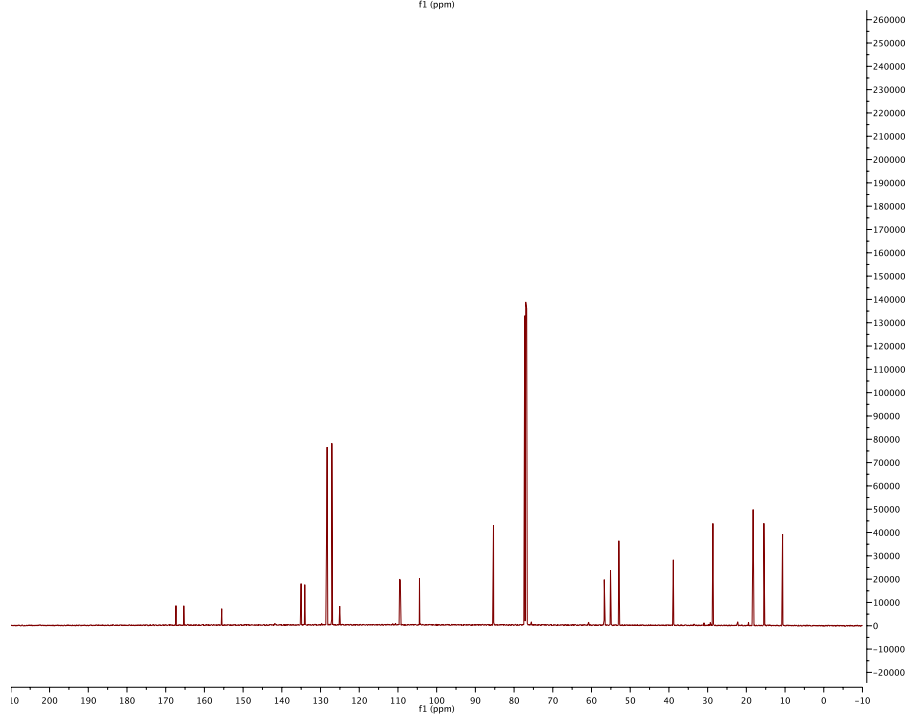
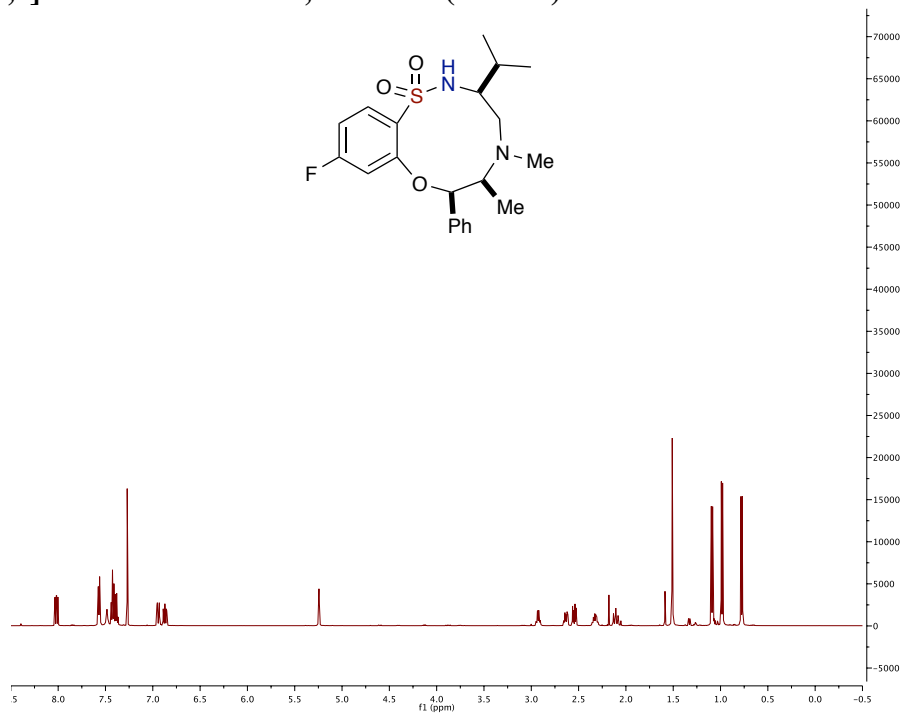
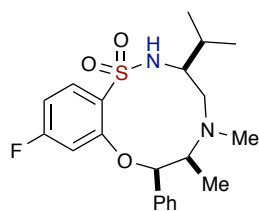
(7S)-2-bromo-7-isobutyl-6,7,8,10,11,12,13,13a,14,15-decahydrobenzo[*b*]pyrido[1,2-*h*][1,4,5,8]oxathiadiazacycloundecine 5,5-dioxide (3.9.2o)



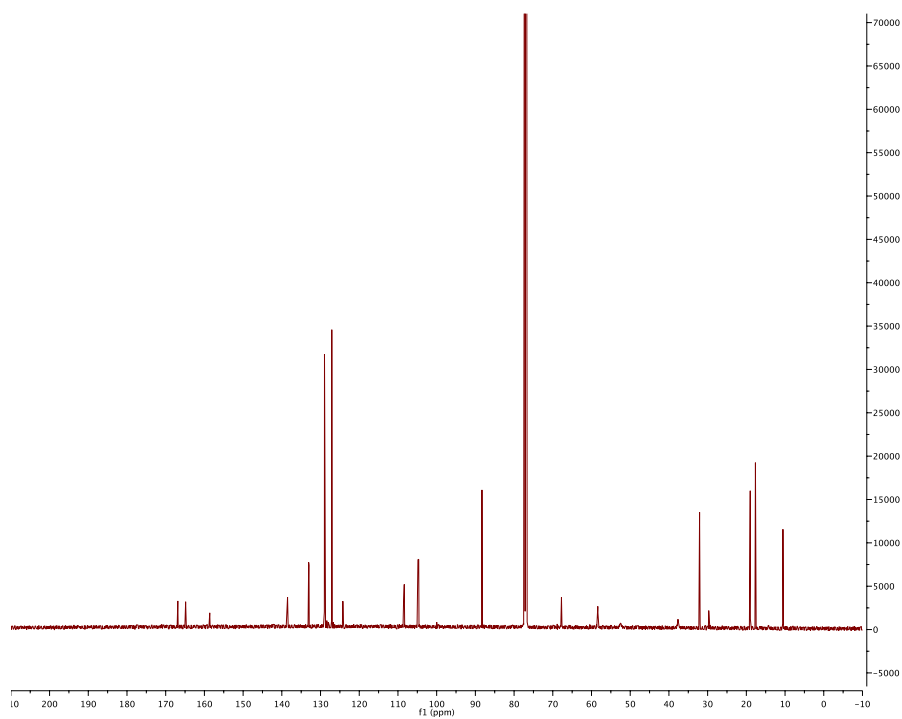
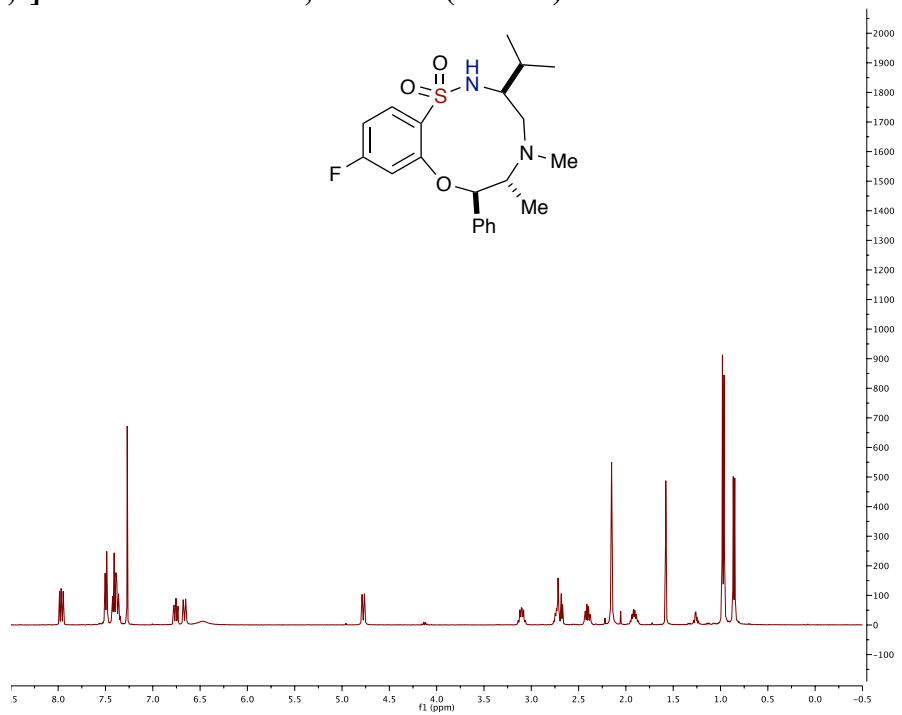
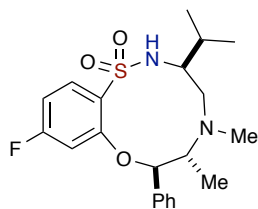
(7*S*,13*aS*)-2-bromo-7-isopropyl-6,7,8,10,11,12,13,13*a*,14,15-decahydrobenzo[*b*]-pyrido[1,2-*h*][1,4,5,8]oxa-thiadiazacycloundecine 5,5-dioxide (3.9.2p)



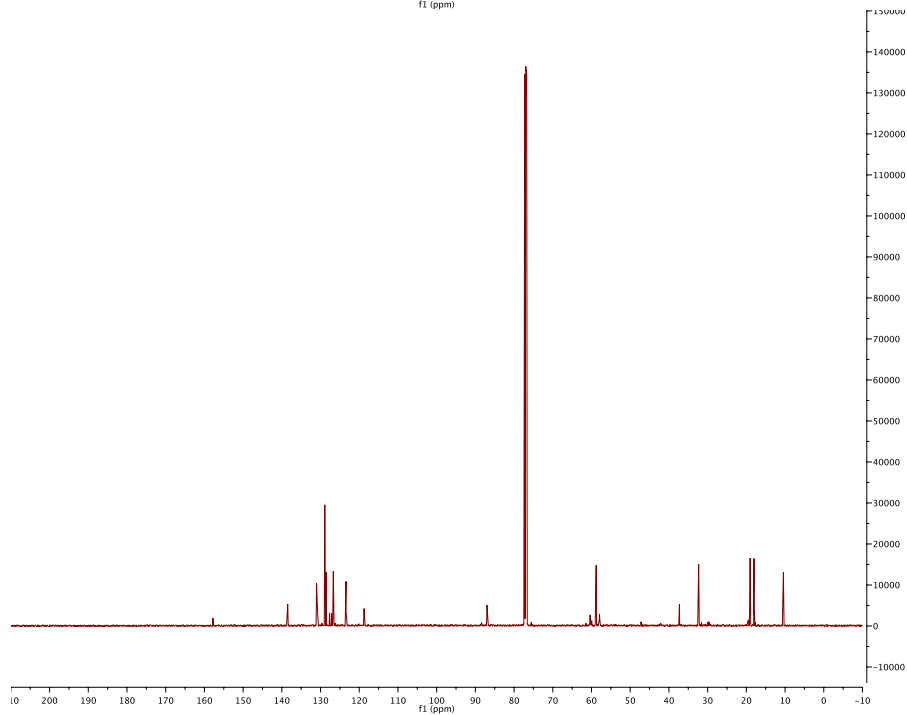
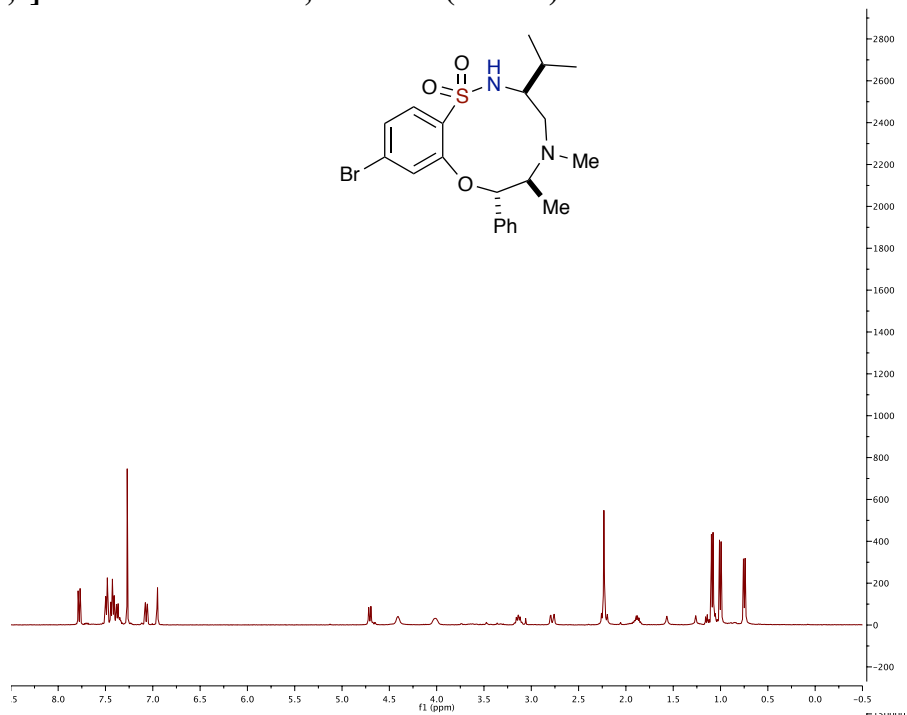
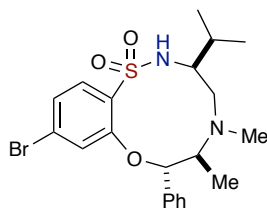
**(3*S*,6*S*,7*R*)-10-fluoro-3-isopropyl-5,6-dimethyl-7-phenyl-2,3,4,5,6,7-hexahydrobenzo-
[*b*][1,4,5,8]oxathia-diazecine 1,1-dioxide (3.10.2a)**



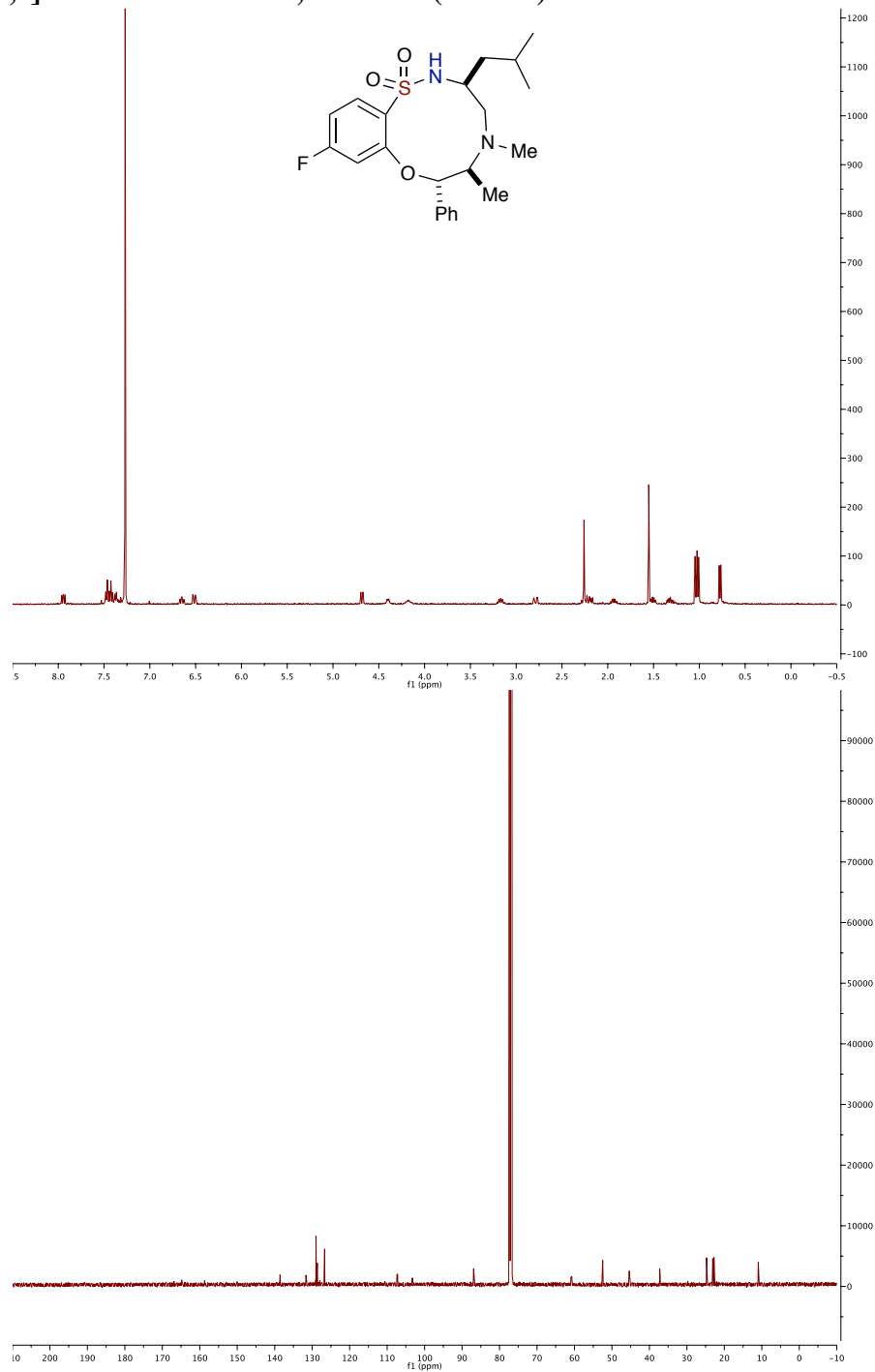
**(3*S*,6*R*,7*R*)-10-fluoro-3-isopropyl-5,6-dimethyl-7-phenyl-2,3,4,5,6,7-hexahydrobenzo-
[*b*][1,4,5,8]oxathia-diazecine 1,1-dioxide (3.10.2b)**



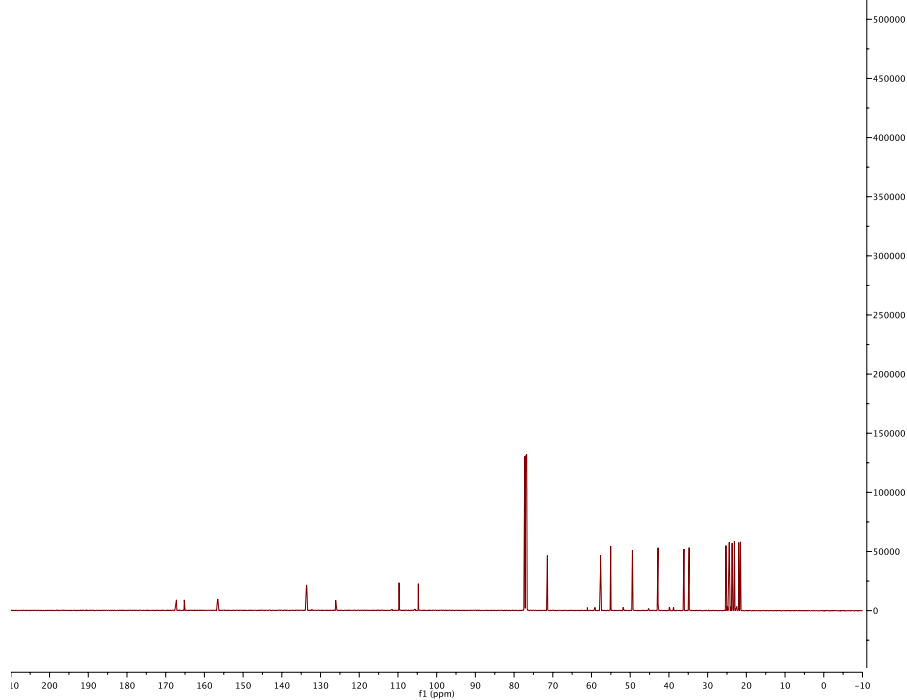
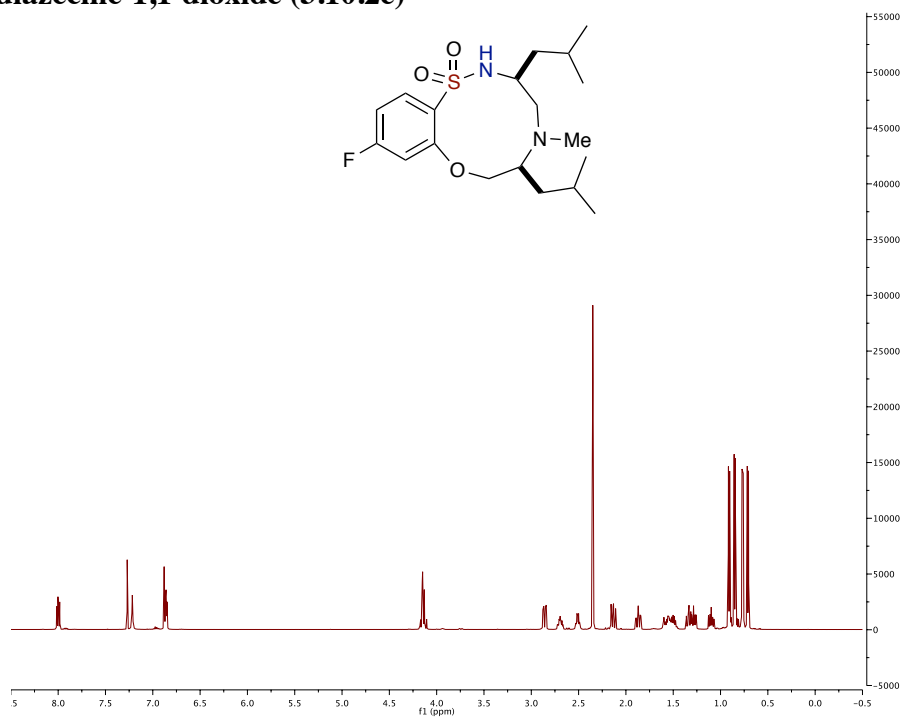
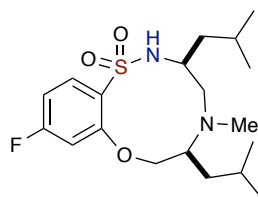
**(3*S*,6*S*,7*S*)-10-bromo-3-isopropyl-5,6-dimethyl-7-phenyl-2,3,4,5,6,7-hexahydrobenzo-
[*b*][1,4,5,8]oxathia-diazecine 1,1-dioxide (3.10.2c)**



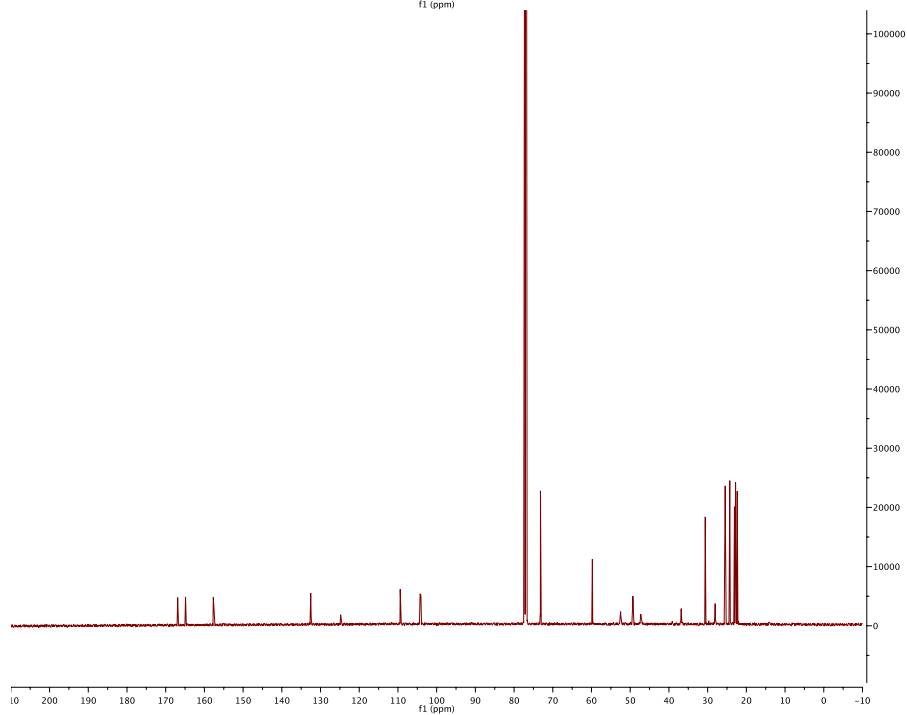
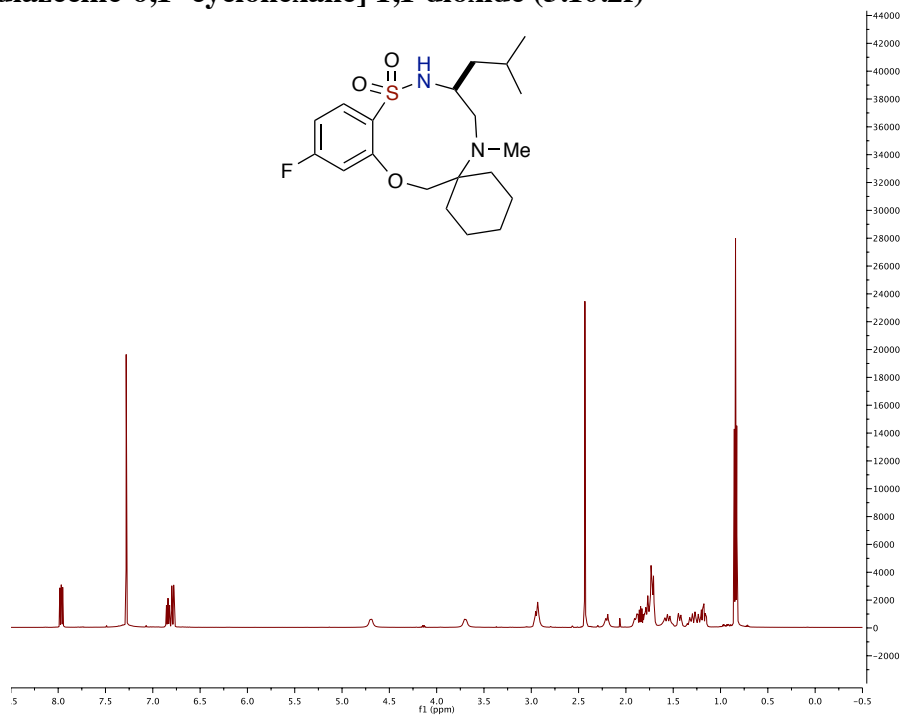
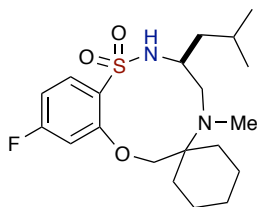
**(3*S*,6*S*,7*S*)-10-fluoro-3-isobutyl-5,6-dimethyl-7-phenyl-2,3,4,5,6,7-hexahydrobenzo-
[*b*][1,4,5,8]oxathia-diazecine 1,1-dioxide (3.10.2d)**



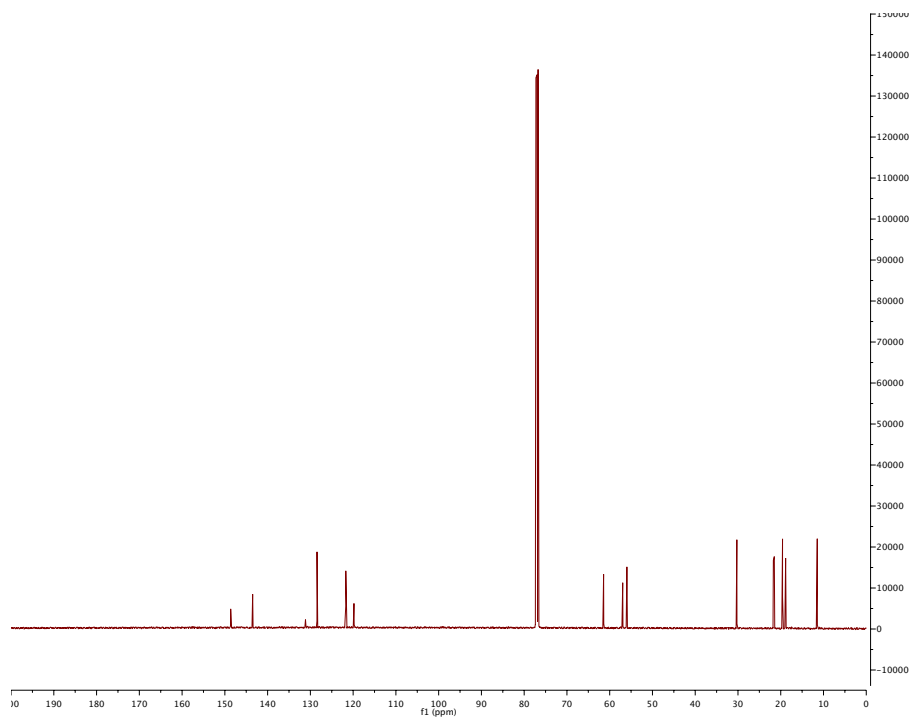
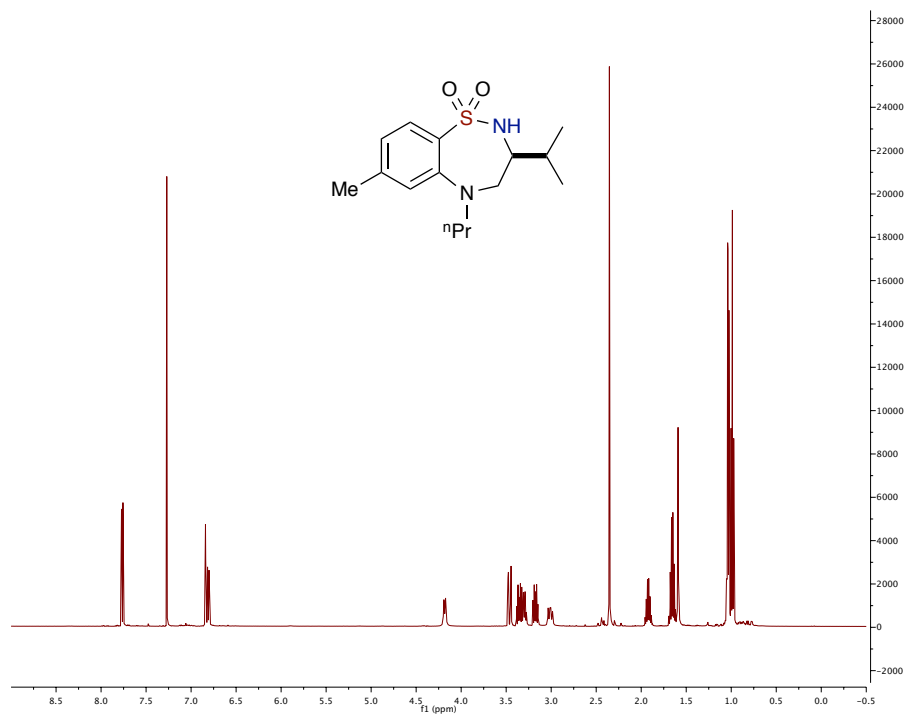
(3*S*,6*S*)-10-fluoro-3,6-diisobutyl-5-methyl-2,3,4,5,6,7-hexahydrobenzo[*b*][1,4,5,8]-oxathiadiazecine-1,1-dioxide (3.10.2e)



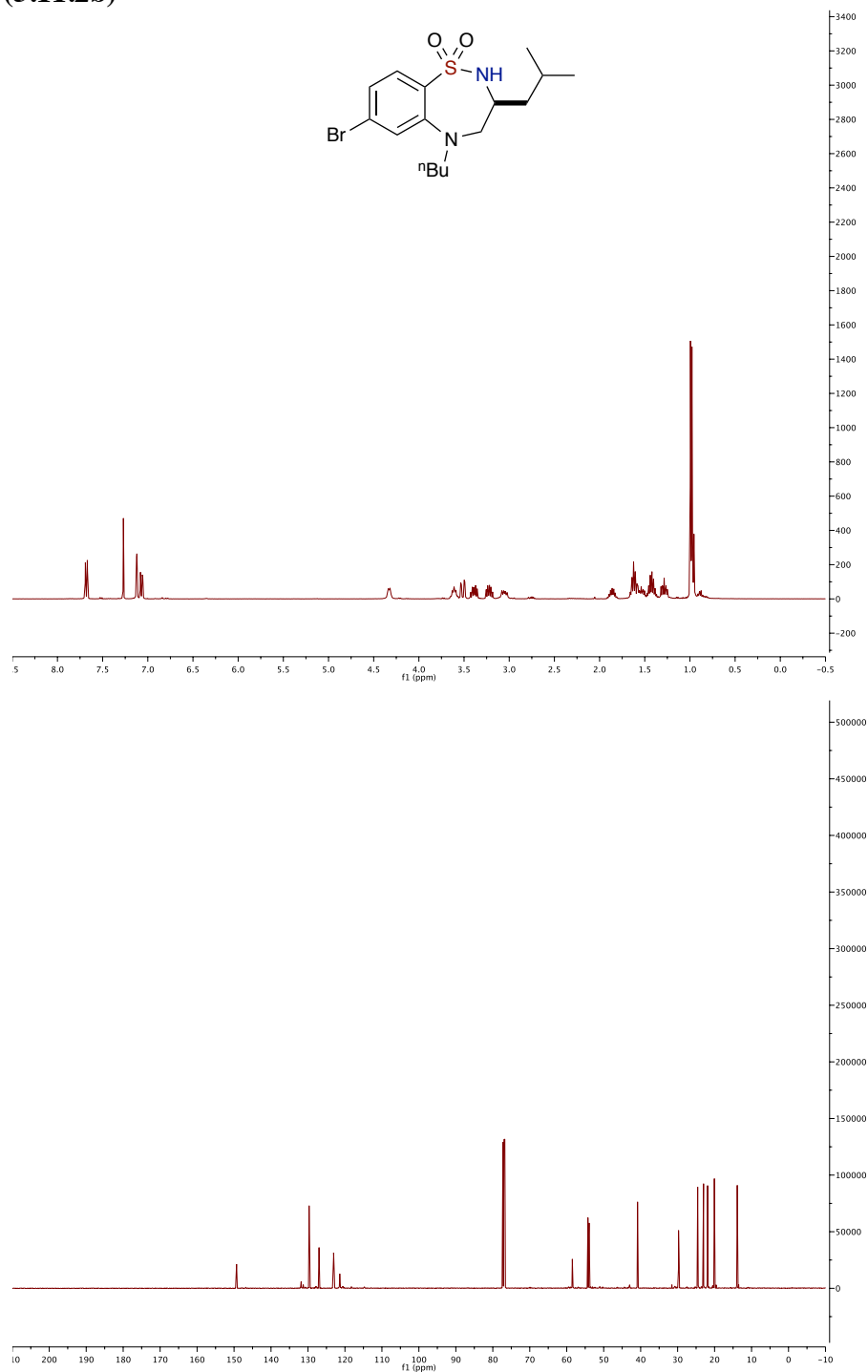
(S)-10-fluoro-3-isobutyl-5-methyl-3,4,5,7-tetrahydro-2H-spiro[benzo[*b*][1,4,5,8]-oxathiadiazecine-6,1'-cyclohexane] 1,1-dioxide (3.10.2f)



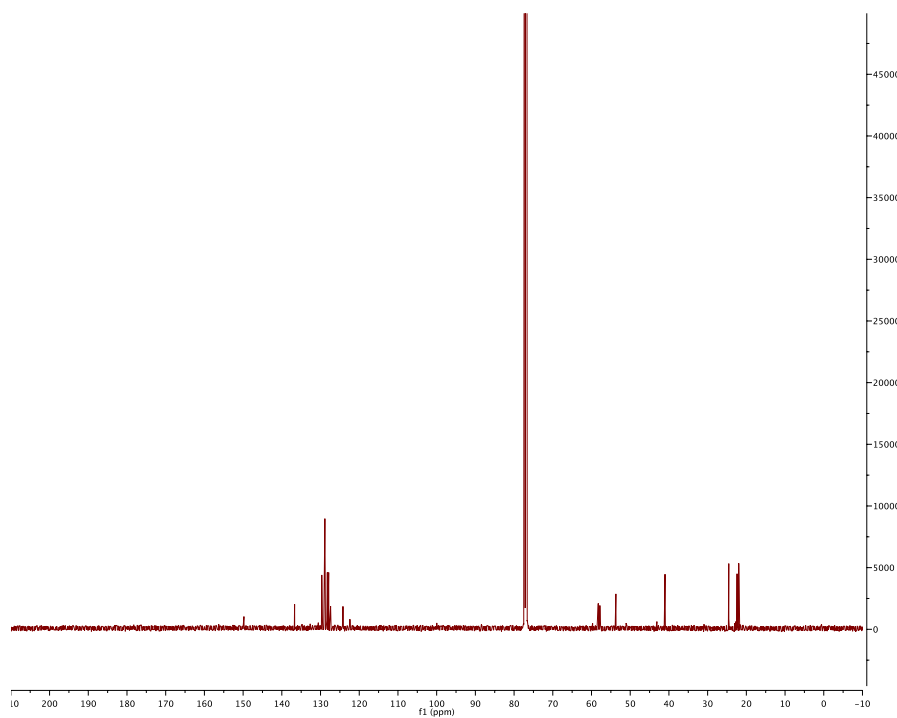
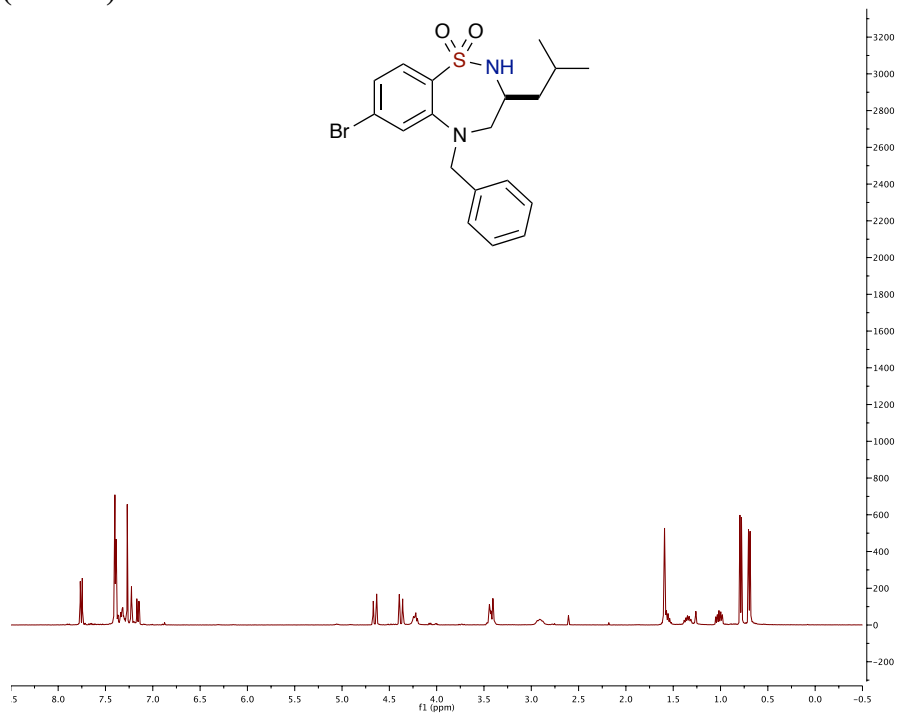
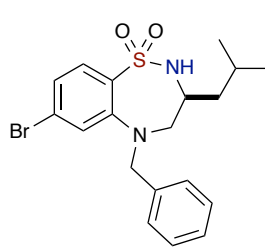
(S)-3-isopropyl-7-methyl-5-propyl-2,3,4,5-tetrahydrobenzo[f][1,2,5]thiadiazepine 1,1-dioxide (3.11.2a)



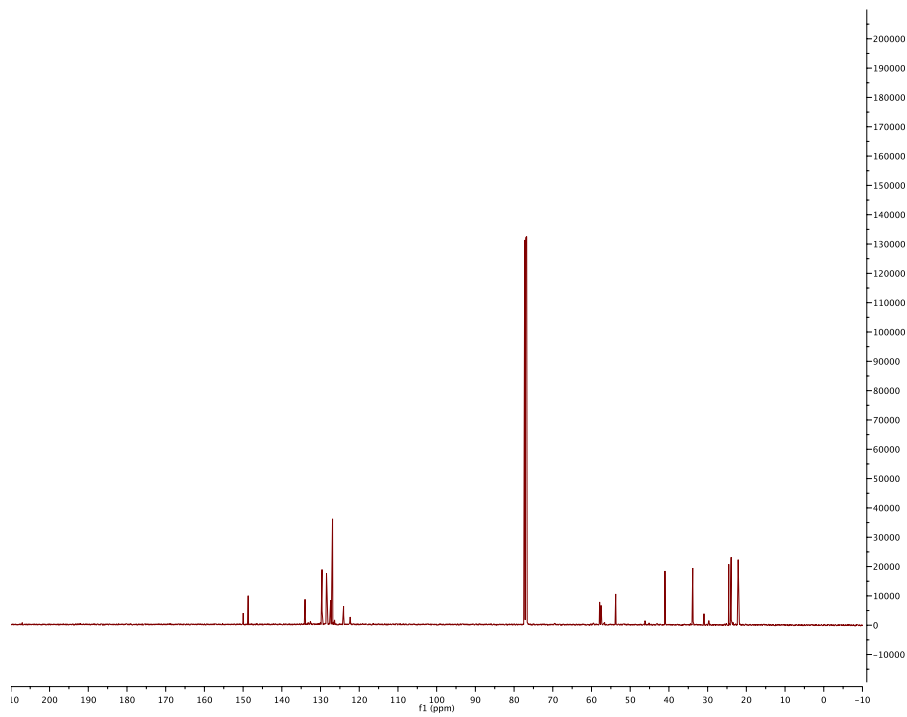
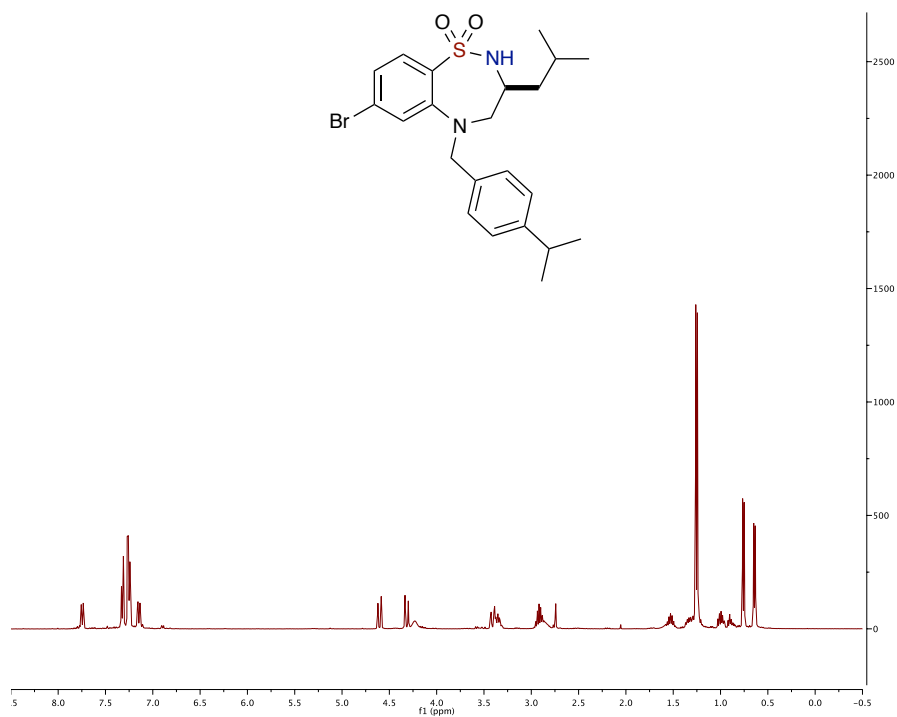
(S)-7-bromo-5-butyl-3-isobutyl-2,3,4,5-tetrahydrobenzo[f][1,2,5]thiadiazepine 1,1-dioxide (3.11.2b)



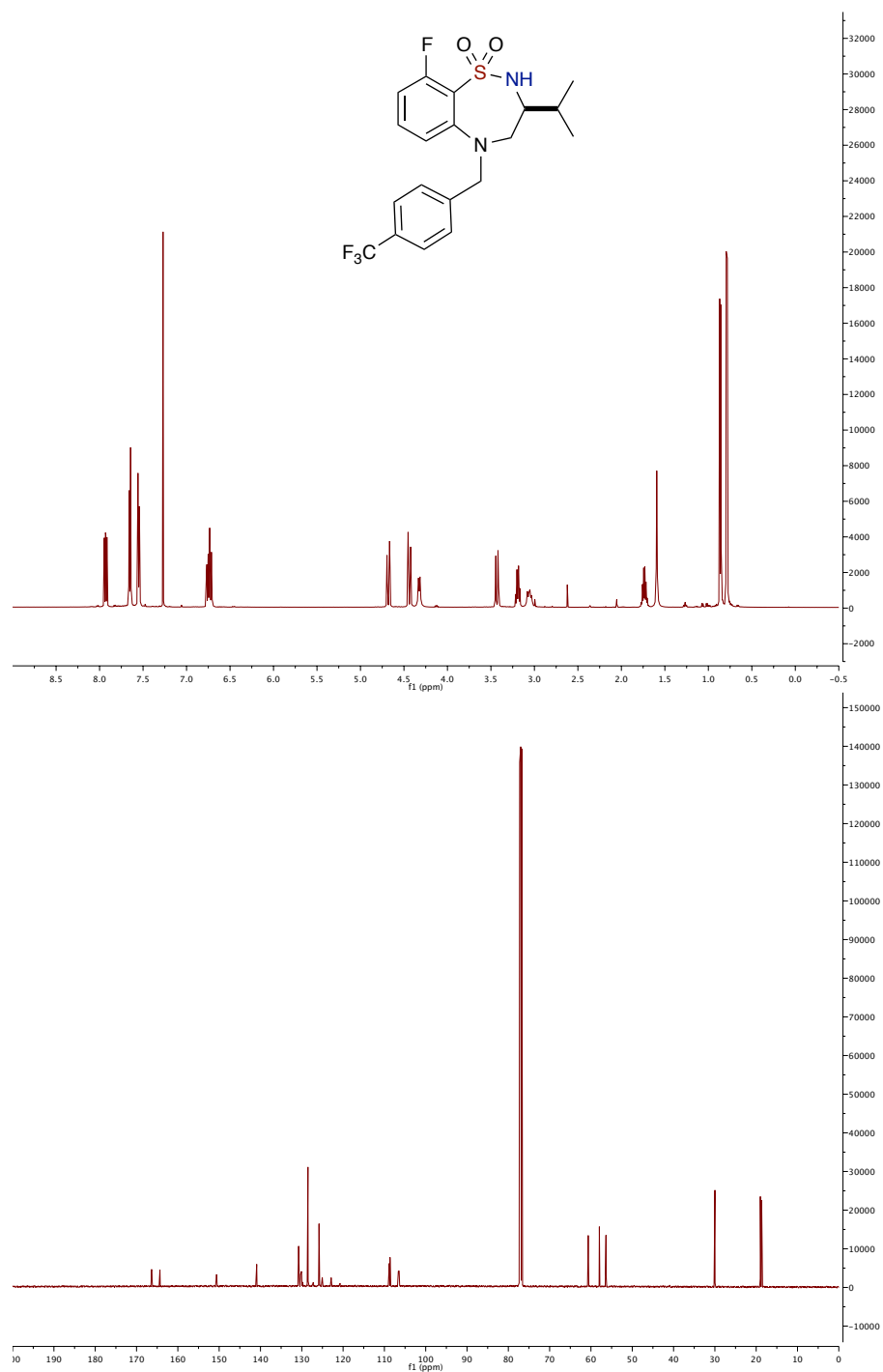
(S)-5-benzyl-7-bromo-3-isobutyl-2,3,4,5-tetrahydrobenzo[f][1,2,5]thiadiazepine 1,1-dioxide (3.11.2c)



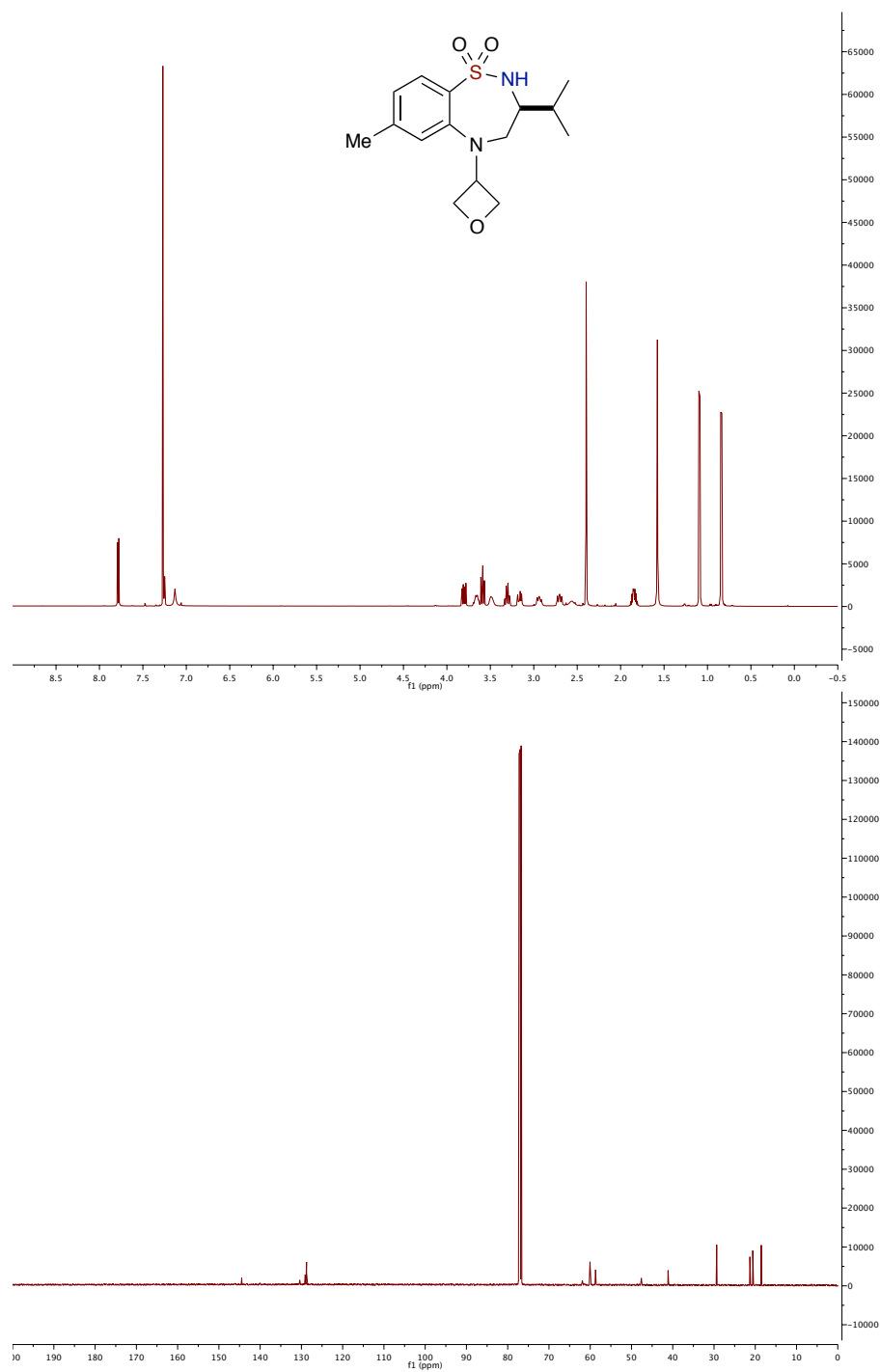
(S)-7-bromo-3-isobutyl-5-(4-isopropylbenzyl)-2,3,4,5-tetrahydrobenzo[f][1,2,5]-thiadiazepine 1,1-dioxide (3.11.2d)



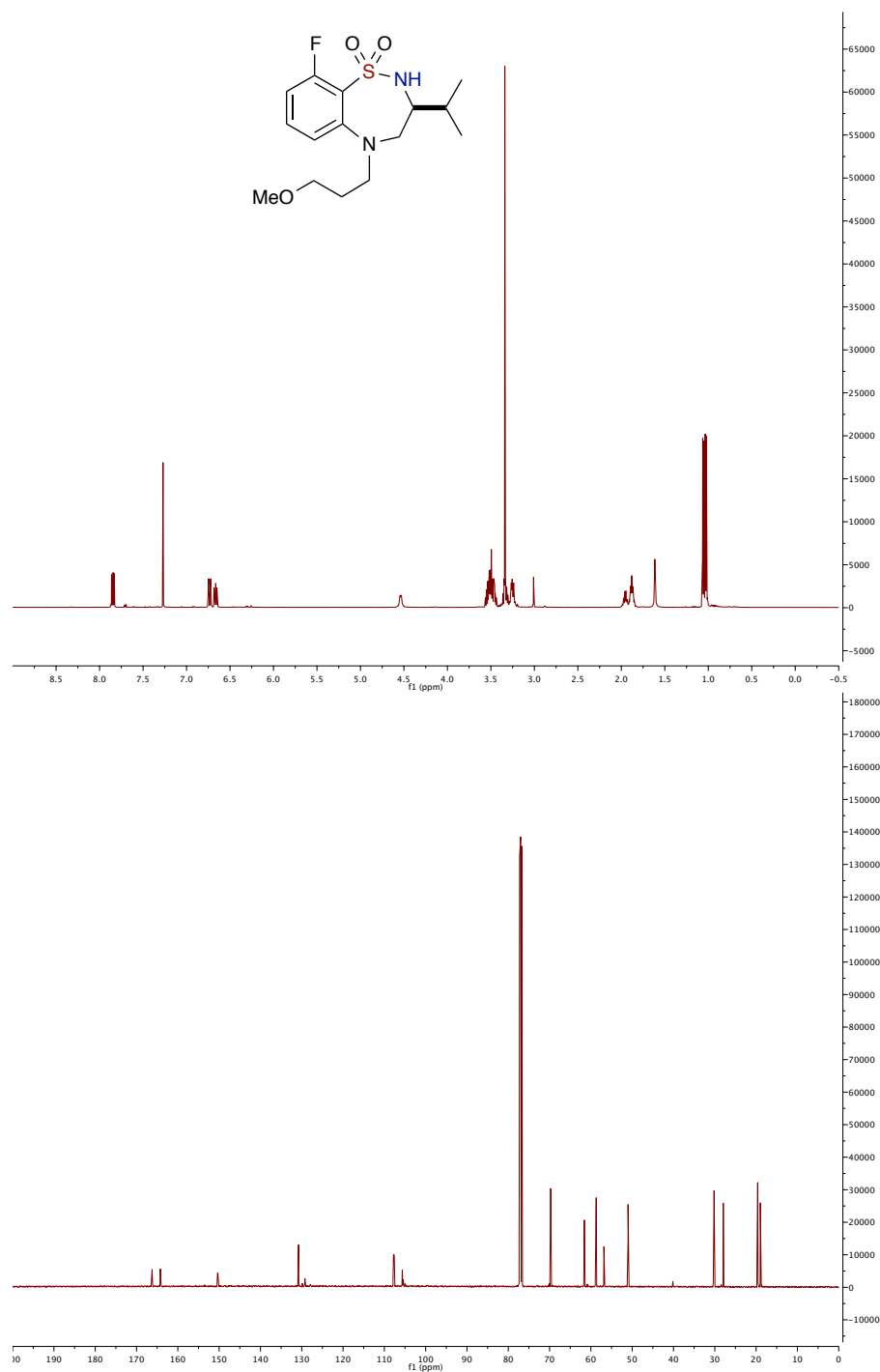
**(S)-9-fluoro-3-isopropyl-5-(4-(trifluoromethyl)benzyl)-2,3,4,5-tetrahydrobenzo-
[f][1,2,5]thiadiazepine 1,1-dioxide (3.11.2e)**



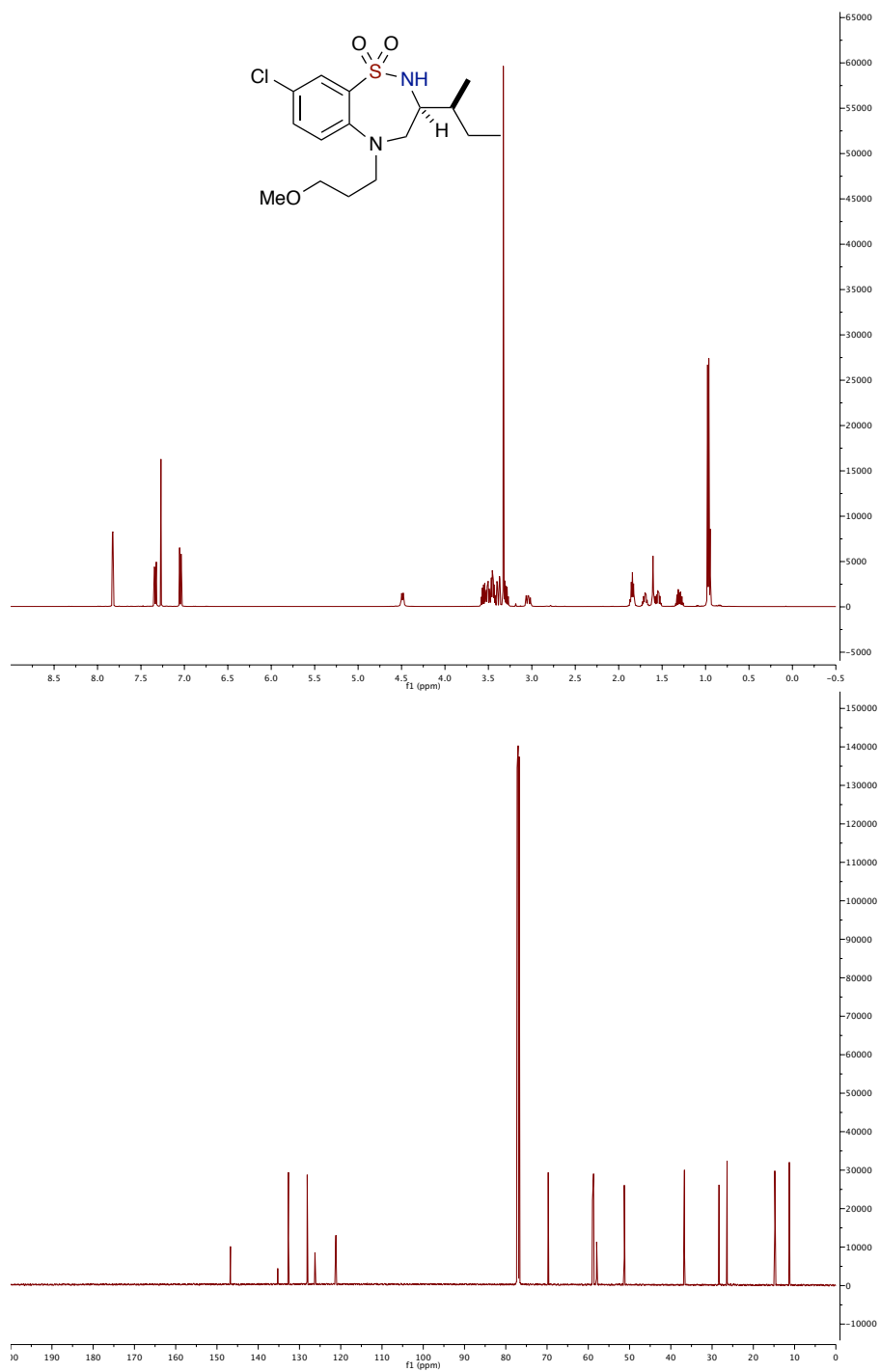
(S)-3-isopropyl-7-methyl-5-(oxetan-3-yl)-2,3,4,5-tetrahydrobenzo[f][1,2,5]-thiadiazepine 1,1-dioxide (3.11.2f)



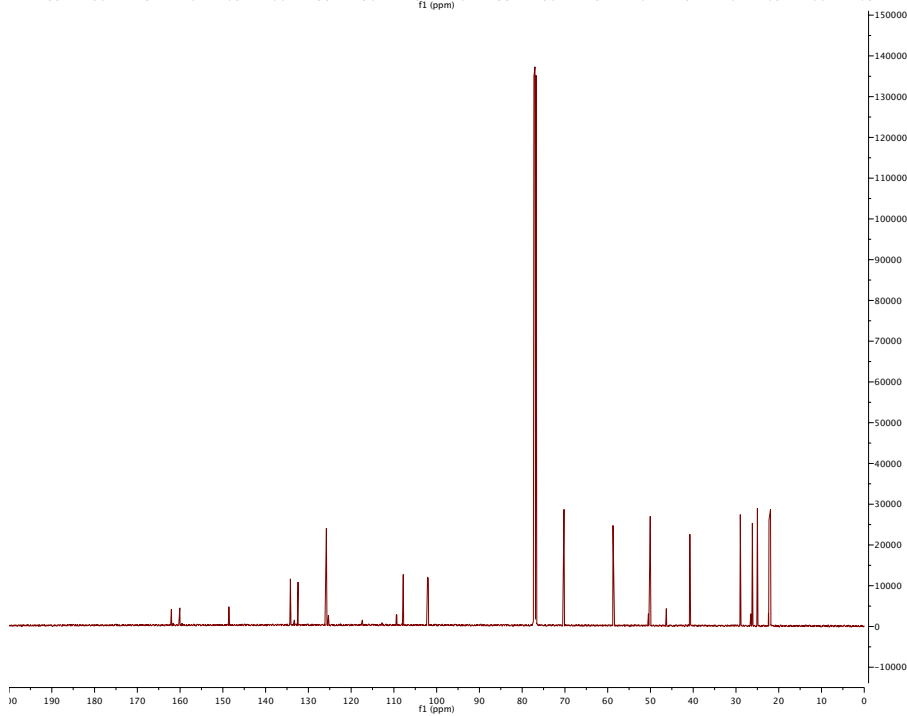
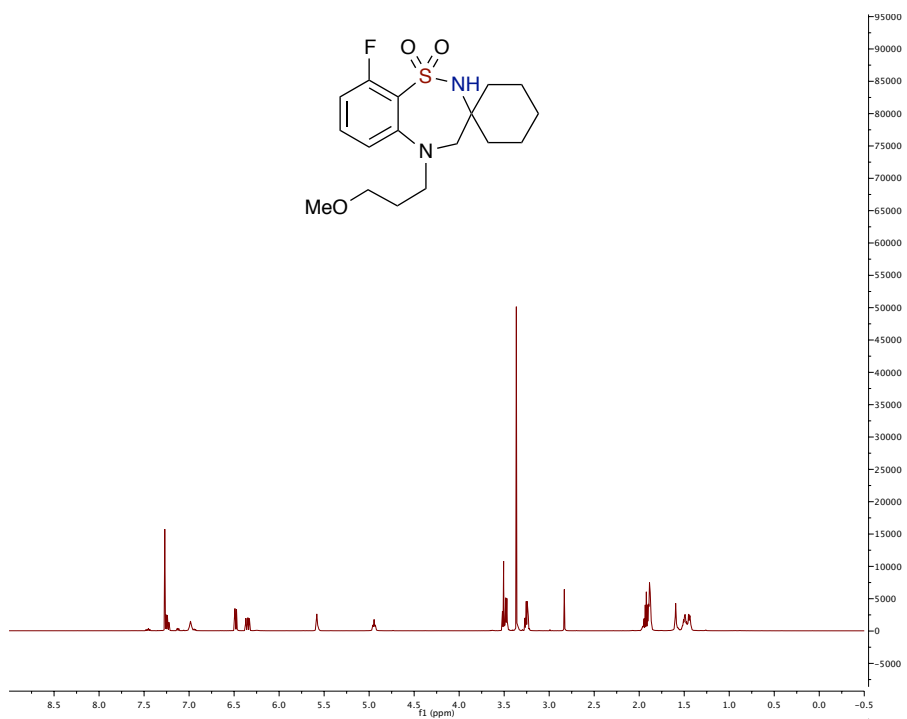
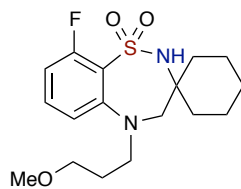
(S)-9-fluoro-3-isopropyl-5-(3-methoxypropyl)-2,3,4,5-tetrahydrobenzo[f][1,2,5]-thiadiazepine 1,1-dioxide (3.11.2g)



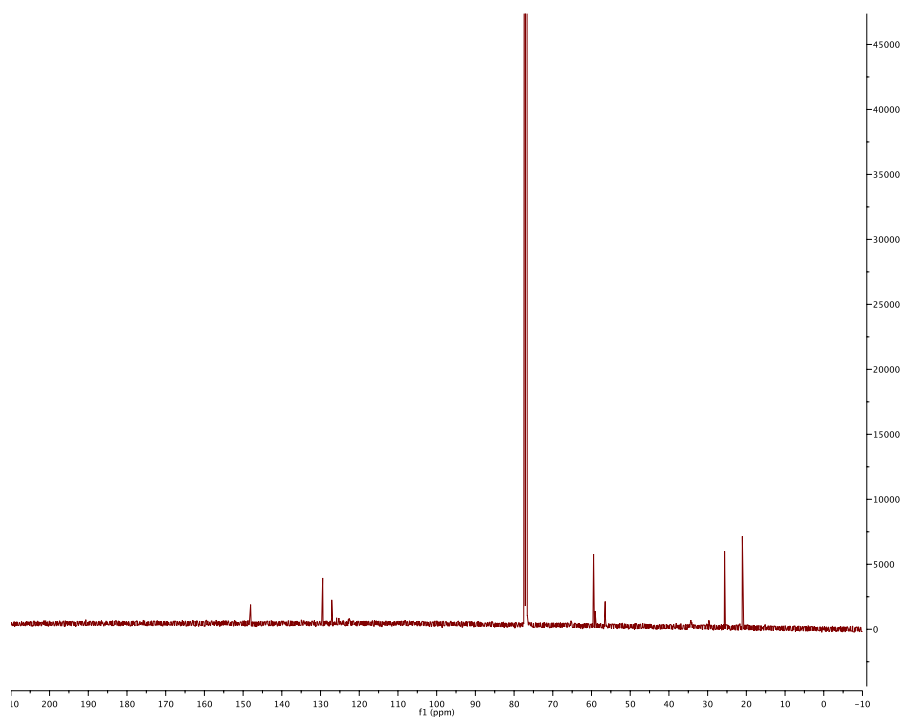
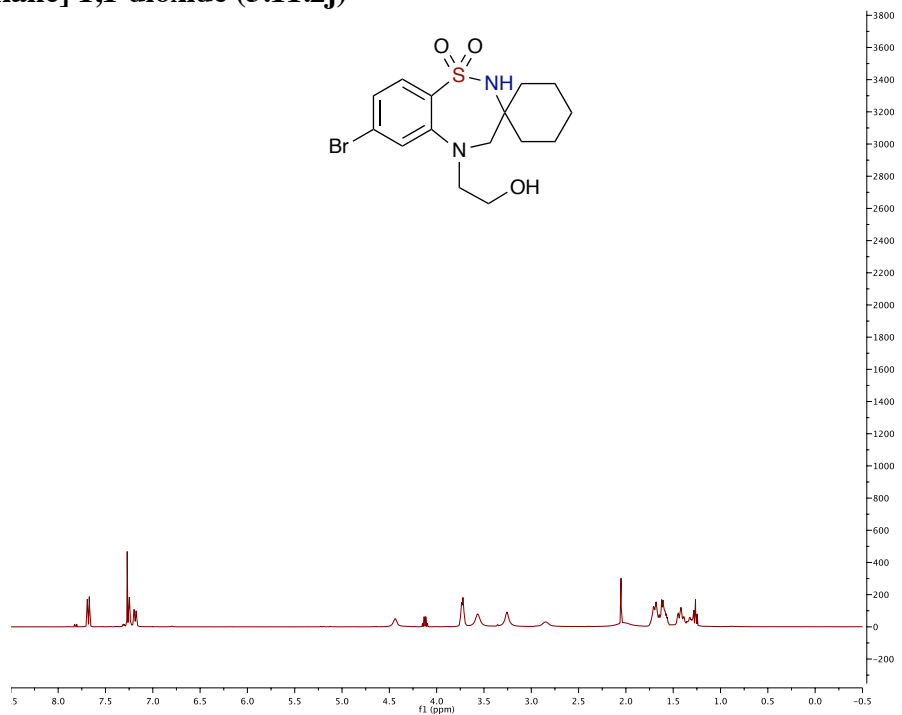
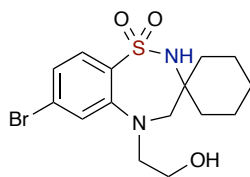
(S)-3-((S)-*sec*-butyl)-8-chloro-5-(3-methoxypropyl)-2,3,4,5-tetrahydrobenzo[*f*][1,2,5]-thiadiazepine 1,1-dioxide (3.11.2h)



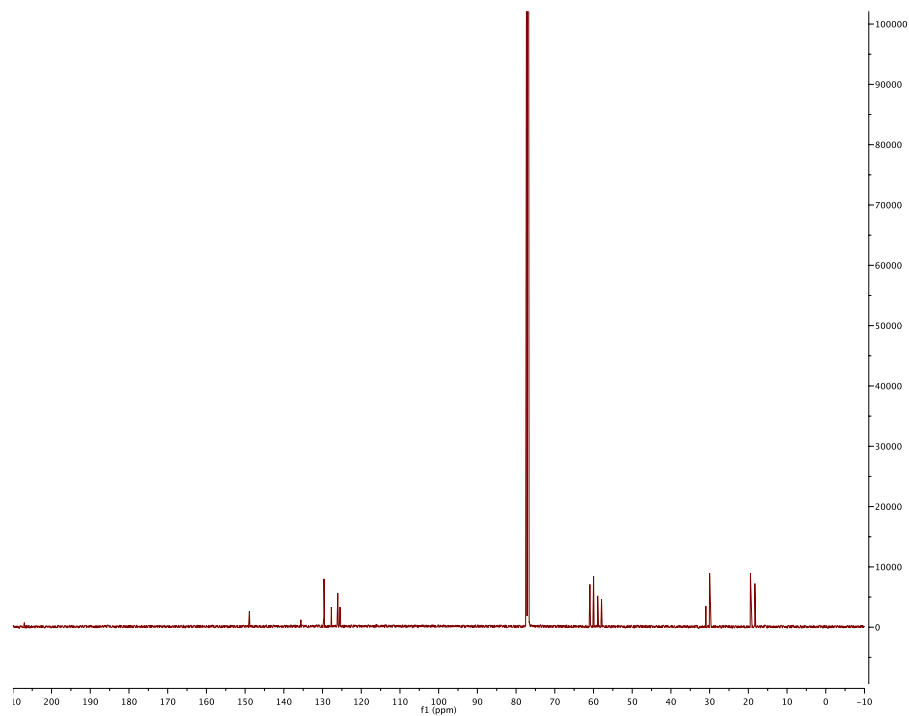
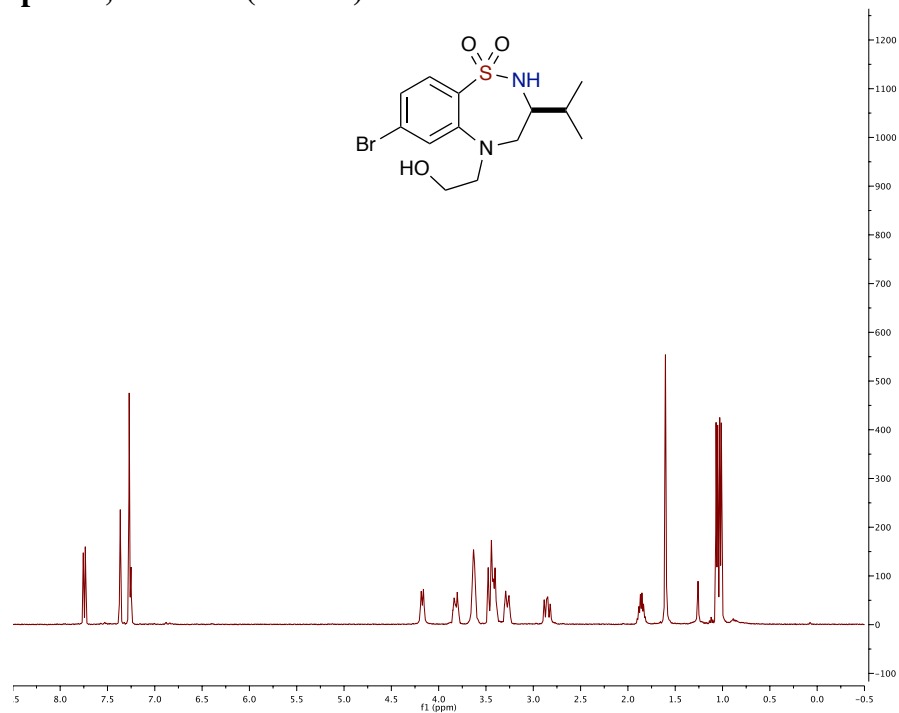
9-fluoro-5-(3-methoxypropyl)-4,5-dihydro-2H-spiro[benzo[f][1,2,5]thiadiazepine-3,1'-cyclohexane] 1,1-dioxide (3.11.2i)



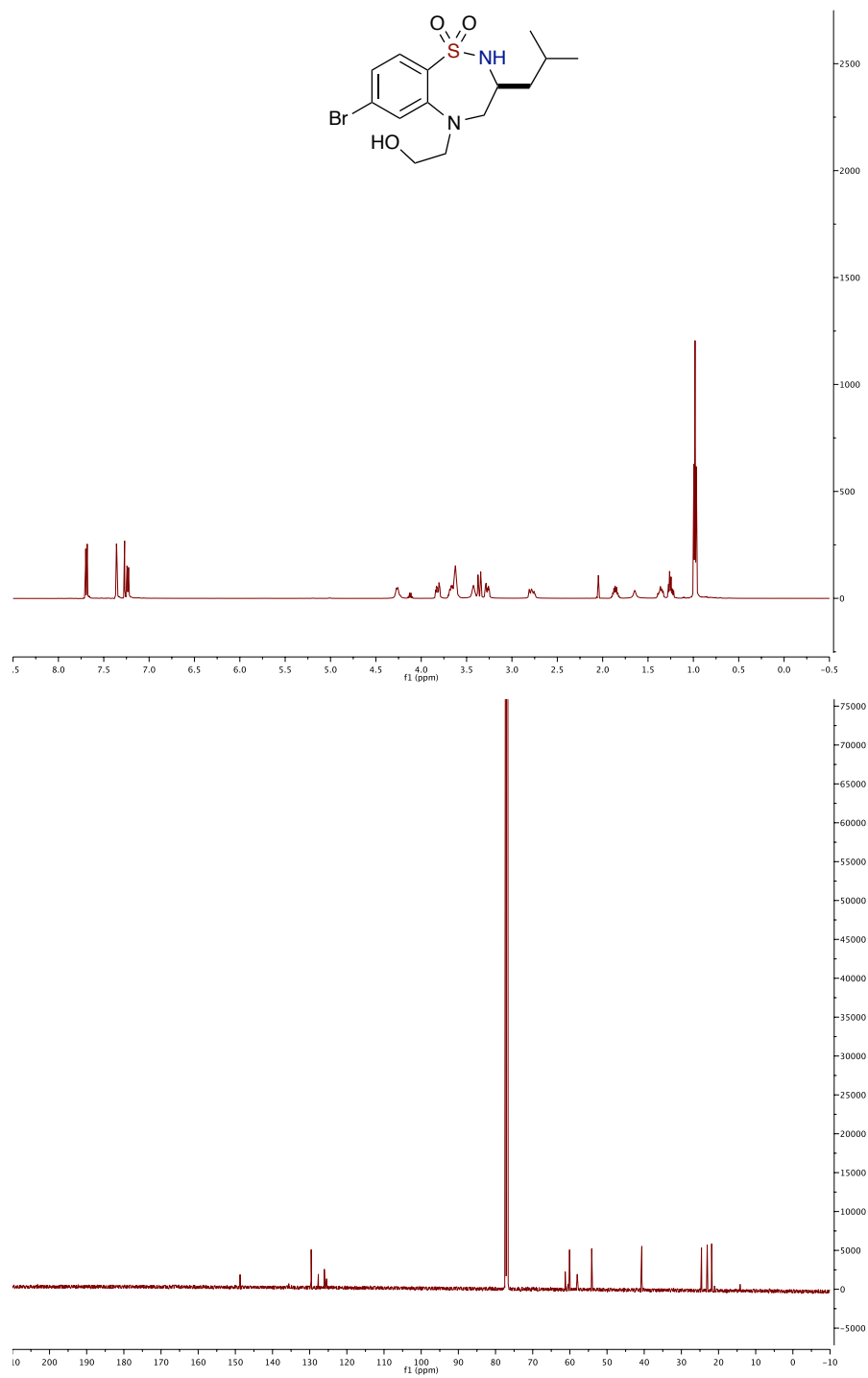
7-bromo-5-(2-hydroxyethyl)-4,5-dihydro-2H-spiro[benzo[f][1,2,5]thiadiazepine-3,1'-cyclohexane] 1,1-dioxide (3.11.2j)



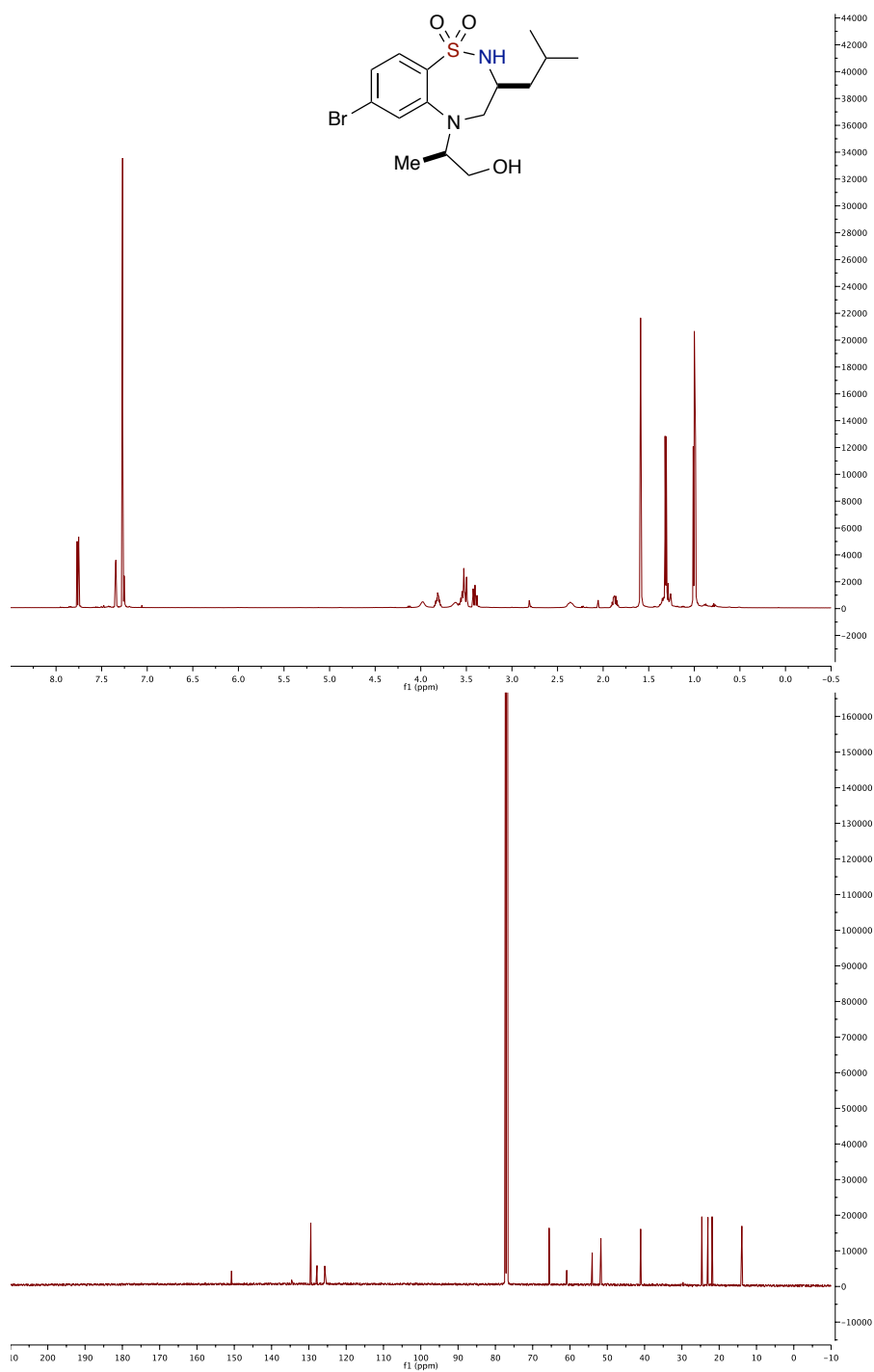
(S)-7-bromo-5-(2-hydroxyethyl)-3-isopropyl-2,3,4,5-tetrahydrobenzo[f][1,2,5]-thiadiazepine 1,1-dioxide (3.11.2k)



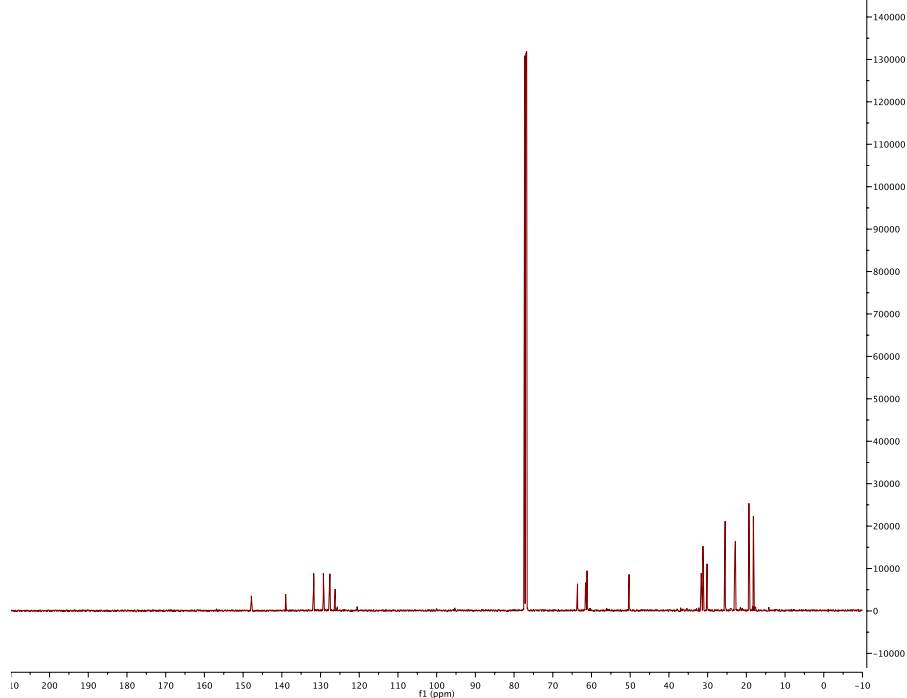
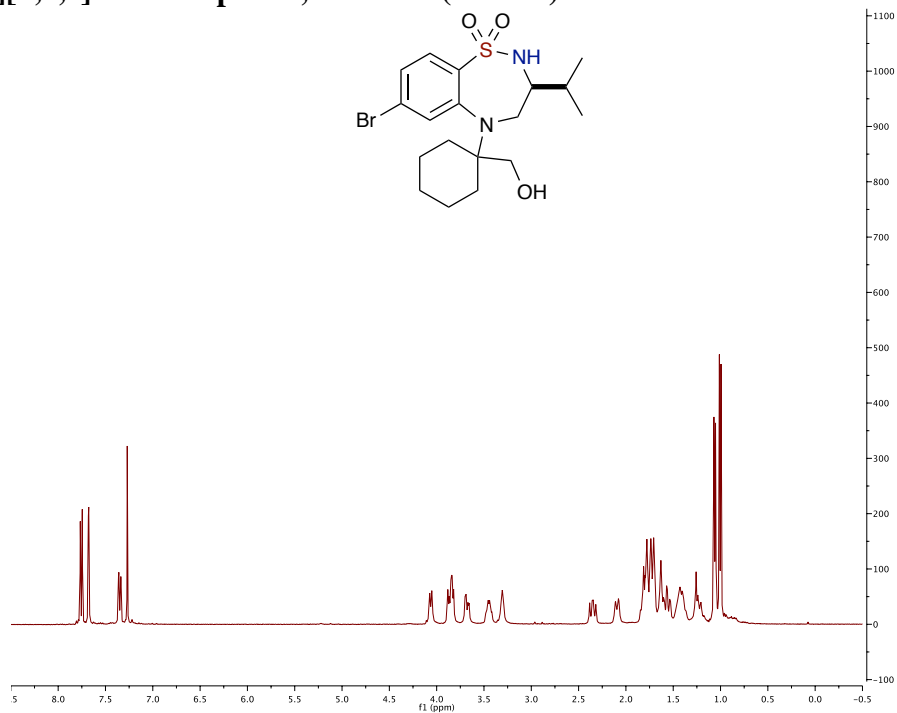
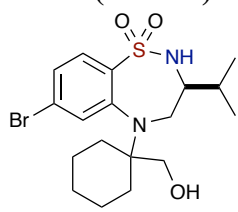
(S)-7-bromo-5-(2-hydroxyethyl)-3-isobutyl-2,3,4,5-tetrahydrobenzo[*f*][1,2,5]-thiadiazepine 1,1-dioxide (3.11.21)



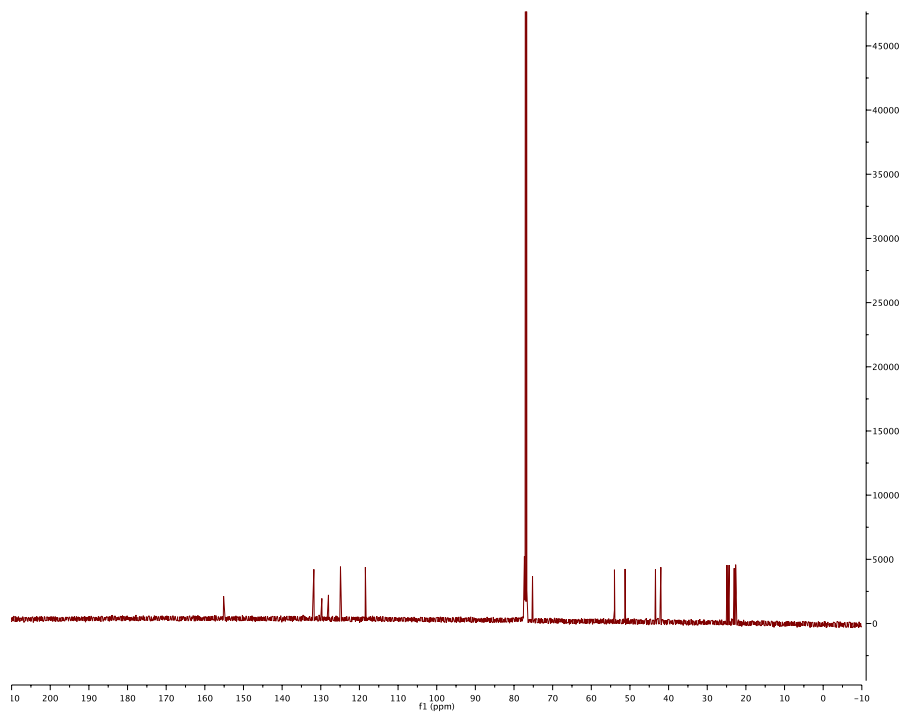
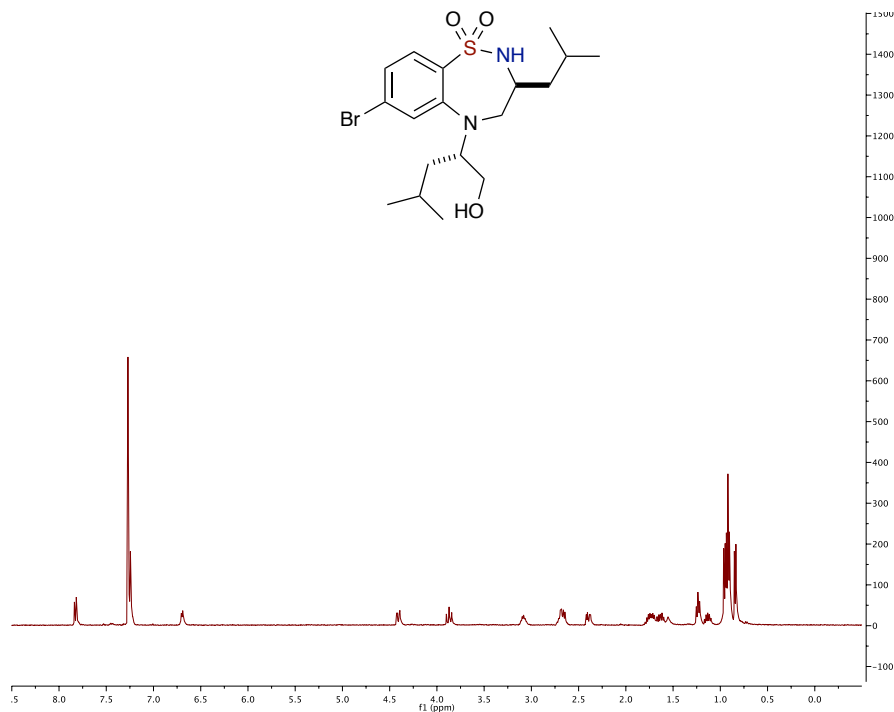
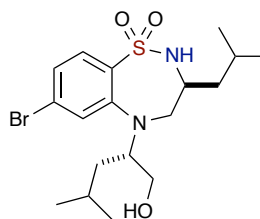
**(S)-7-bromo-5-((R)-1-hydroxypropan-2-yl)-3-isobutyl-2,3,4,5-tetrahydrobenzo-
[f][1,2,5]thiadiazepine 1,1-dioxide (3.11.2m)**



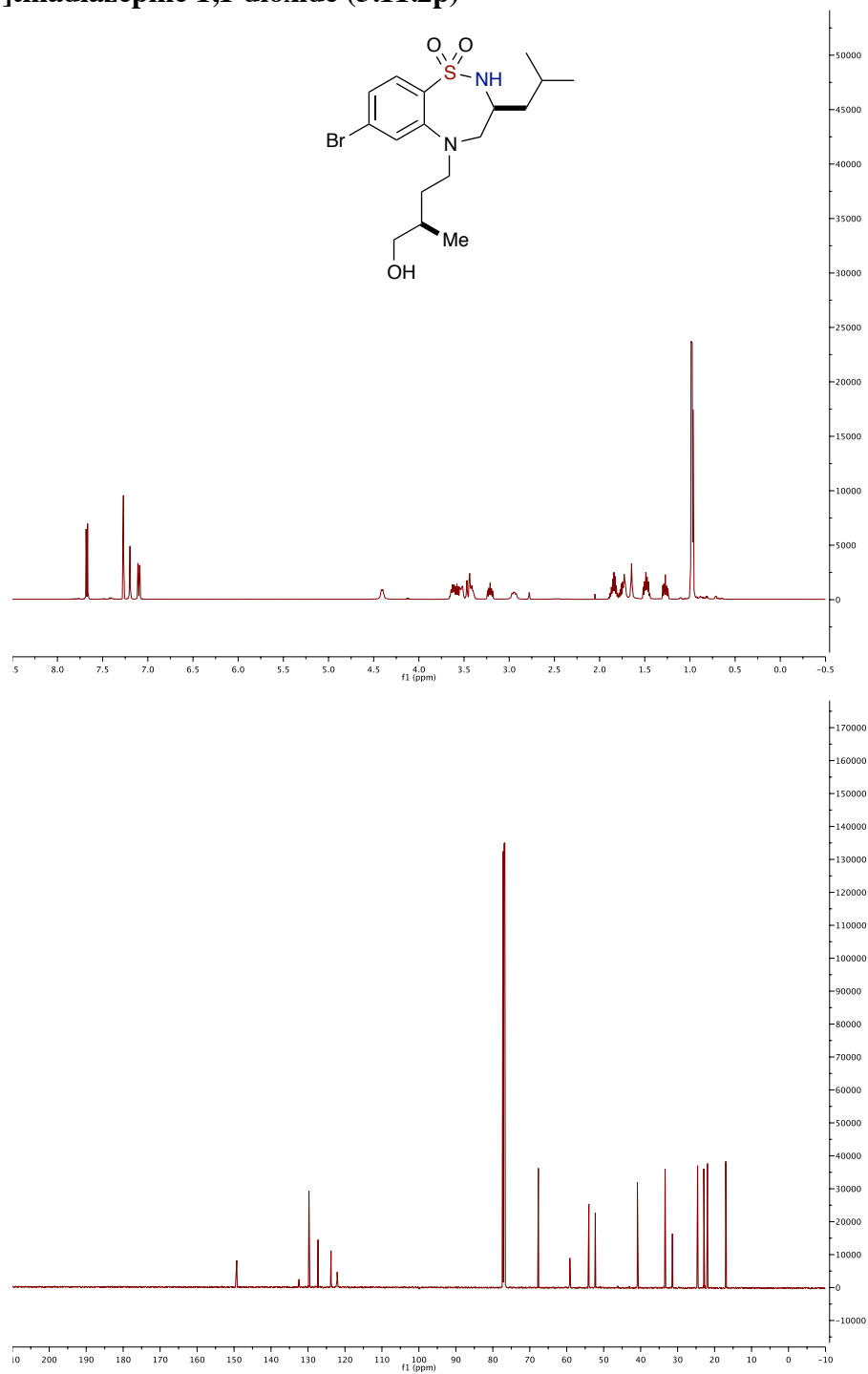
(S)-7-bromo-5-(1-(hydroxymethyl)cyclohexyl)-3-isopropyl-2,3,4,5-tetrahydrobenzo[*f*][1,2,5]thiadiazepine 1,1-dioxide (3.11.2n)



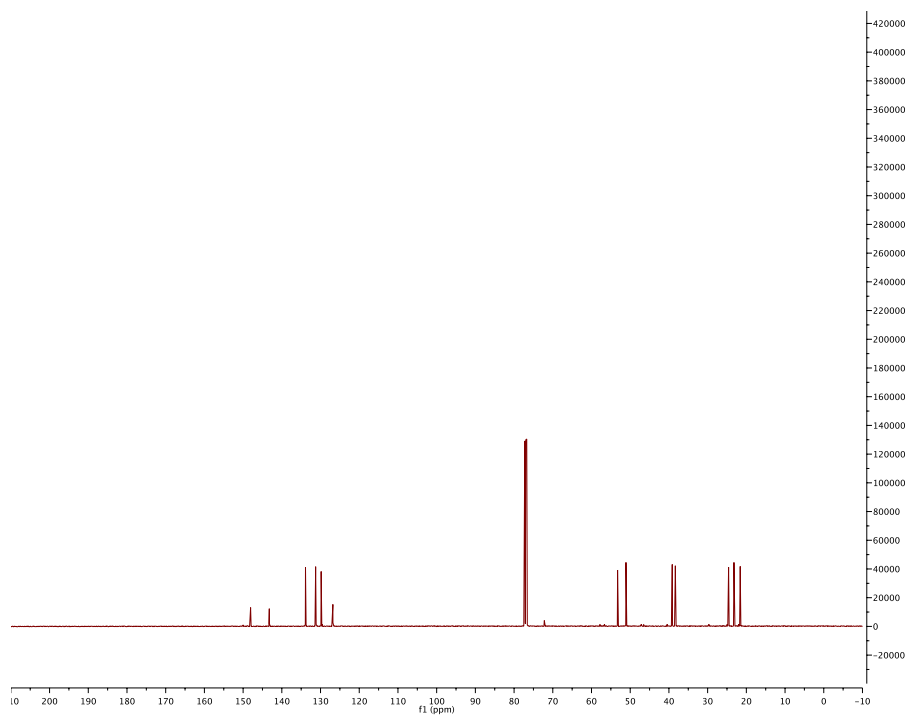
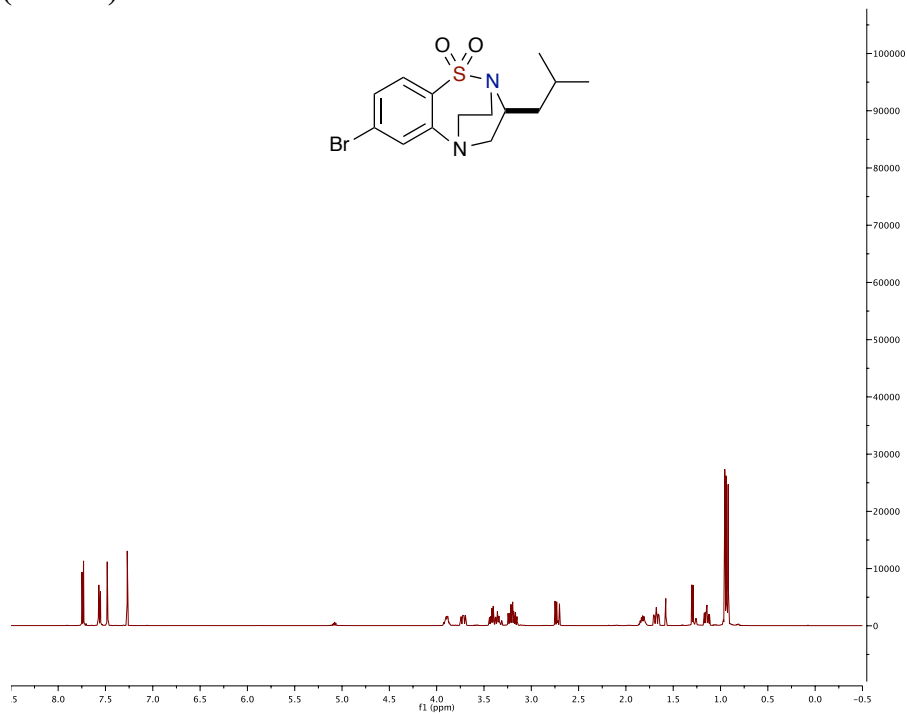
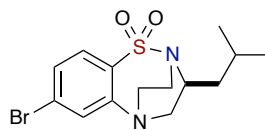
(S)-7-bromo-5-((S)-1-hydroxy-4-methylpentan-2-yl)-3-isobutyl-2,3,4,5-tetrahydrobenzo[f][1,2,5]thiadiazepine 1,1-dioxide (3.11.2o)



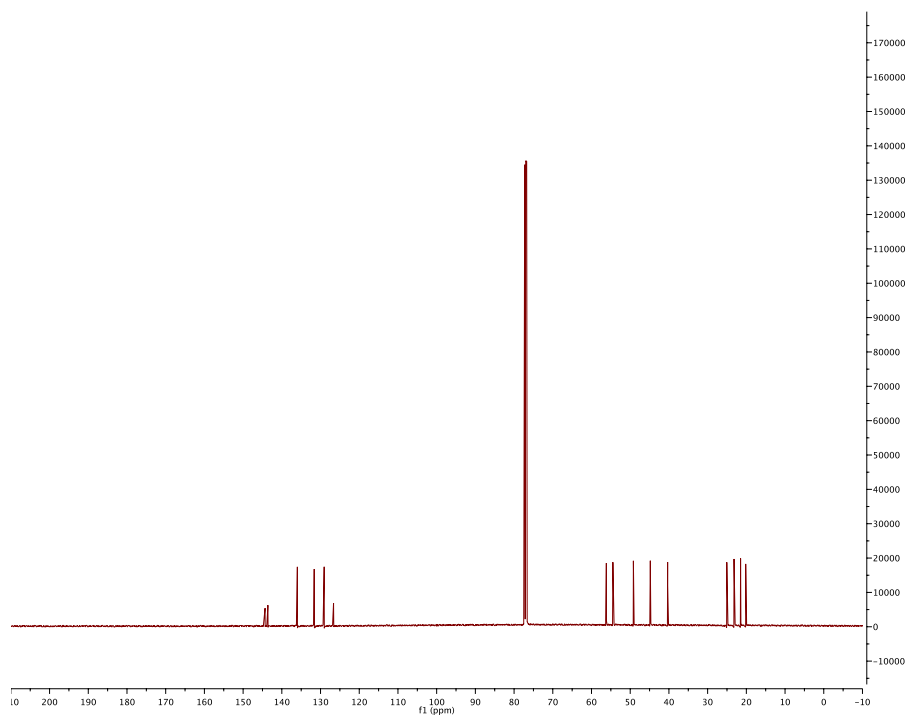
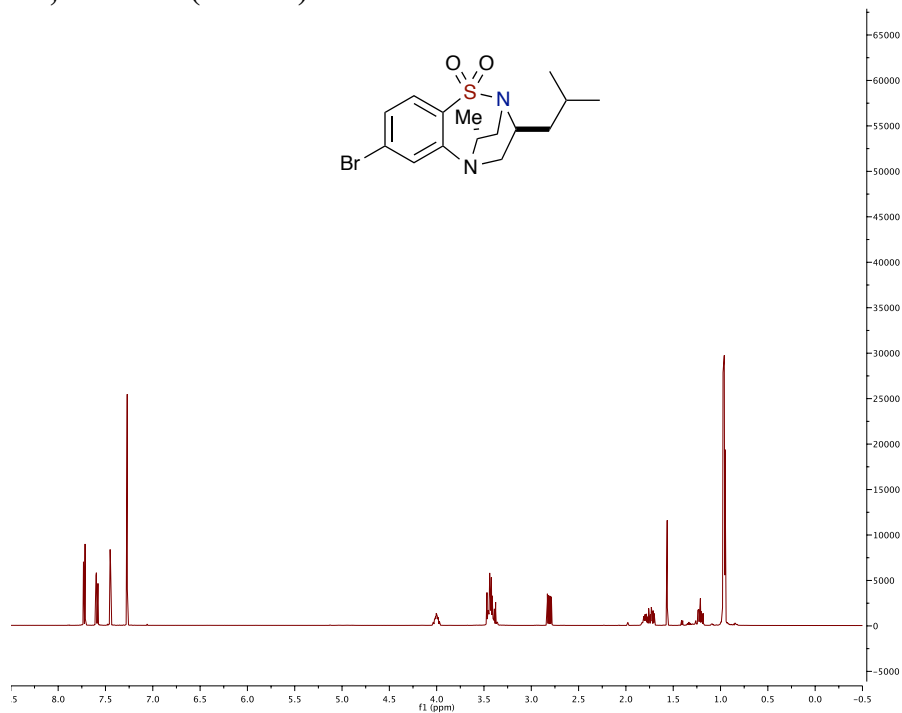
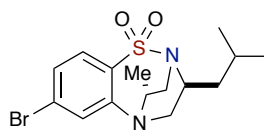
**(S)-7-bromo-5-((R)-4-hydroxy-3-methylbutyl)-3-isobutyl-2,3,4,5-tetrahydrobenzo-
[f][1,2,5]thiadiazepine 1,1-dioxide (3.11.2p)**



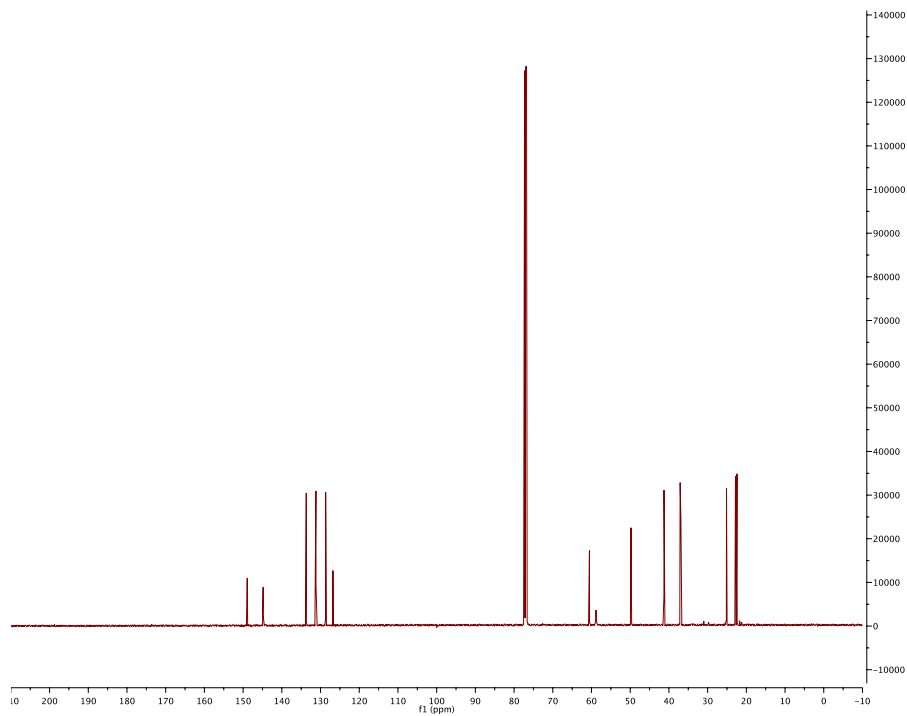
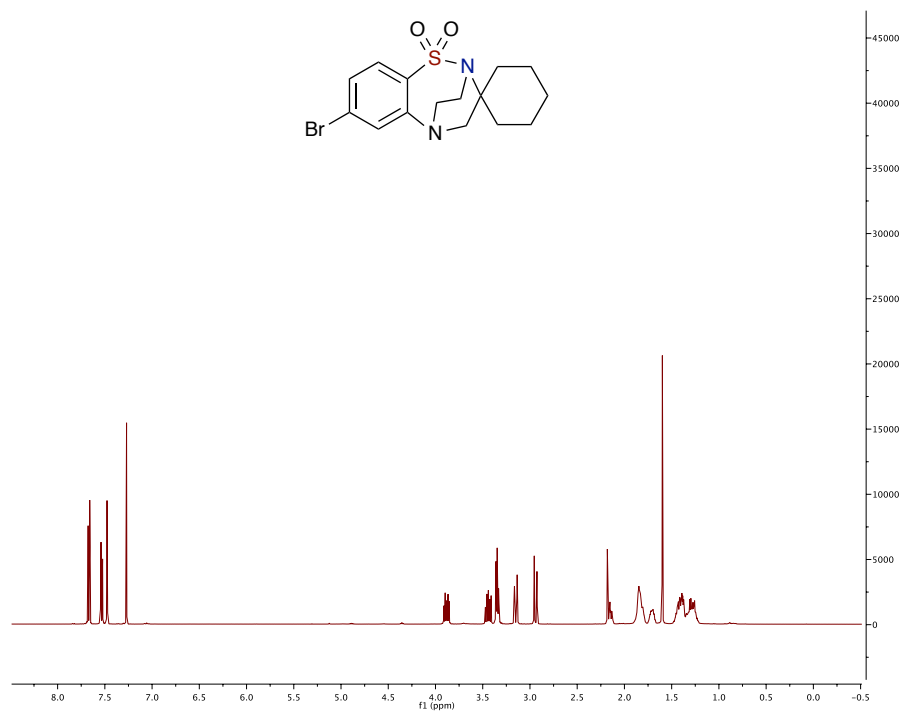
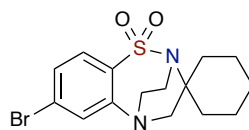
(3S)-7-bromo-3-isobutyl-3,4-dihydro-2,5-ethanobenzo[f][1,2,5]thiadiazepine 1,1-dioxide (3.12.1a)



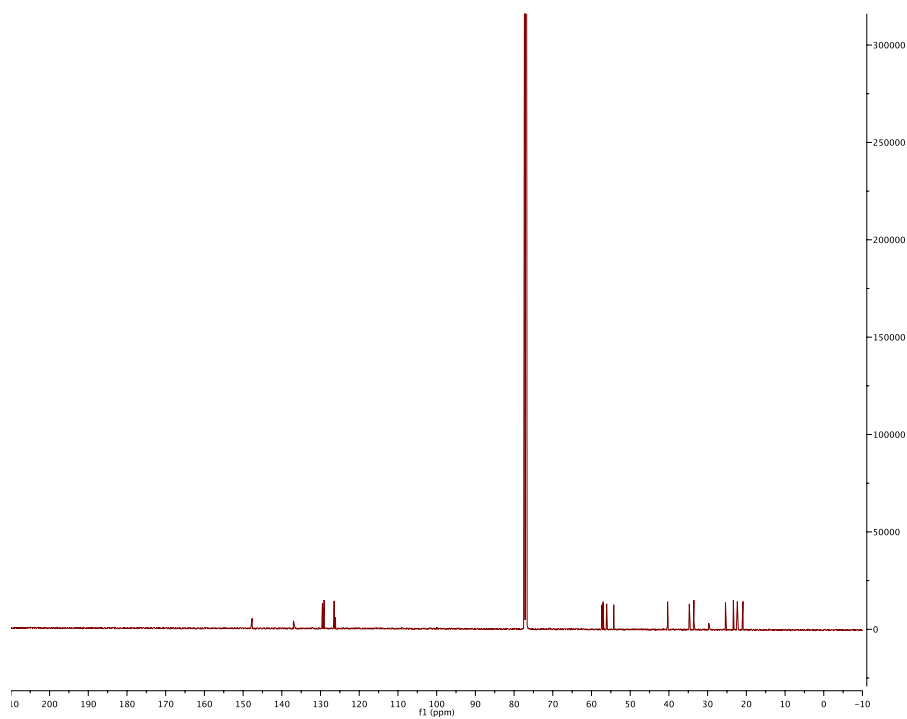
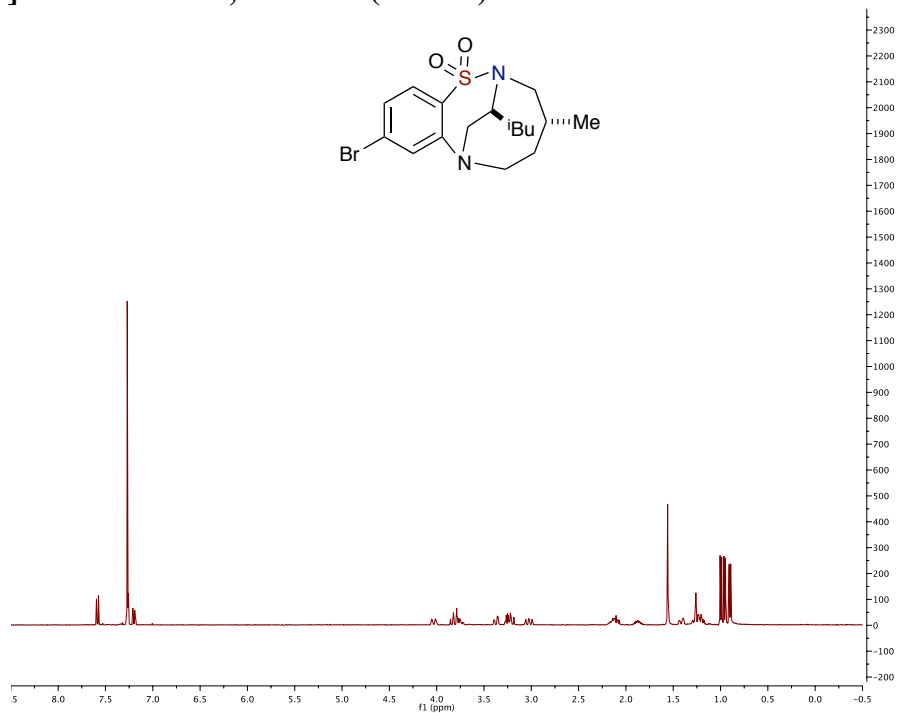
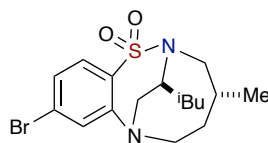
(4*R*,11*S*)-7-bromo-11-isobutyl-4-methyl-3,4-dihydro-2,5-ethanobenzo[*f*][1,2,5]thiazepine 1,1-dioxide (3.12.1b)



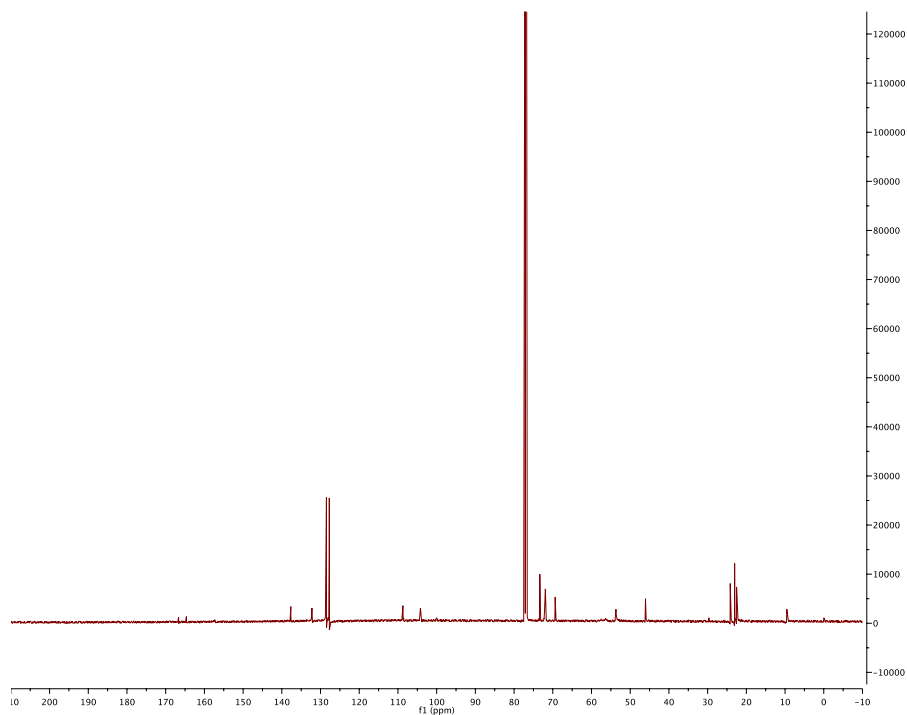
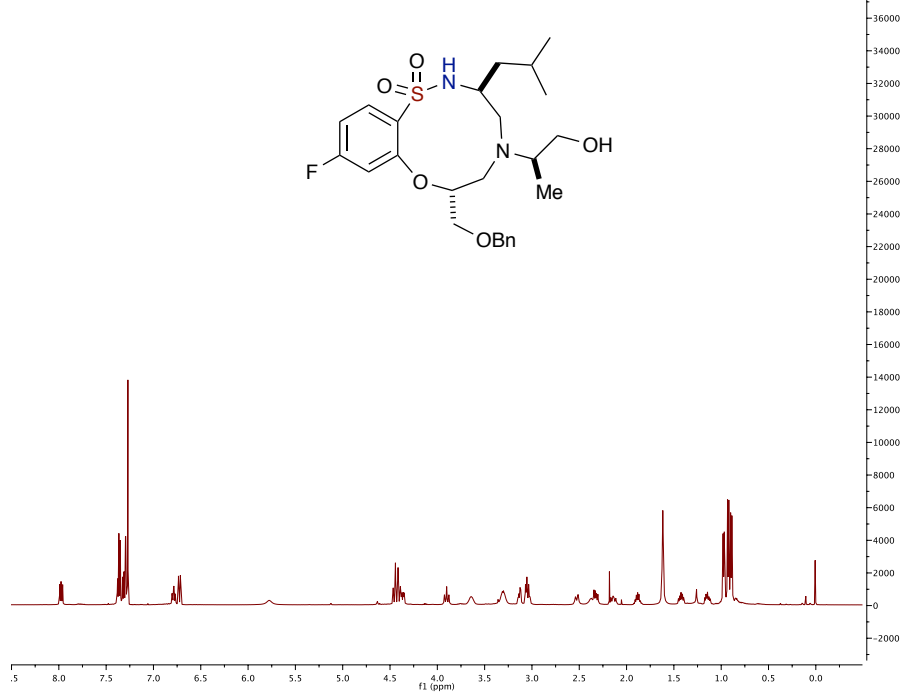
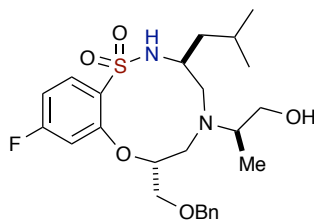
7-bromo-4H-spiro[2,5-ethanobenzo[*f*][1,2,5]thiadiazepine-3,1'-cyclohexane] 1,1-dioxide (3.12.1c)



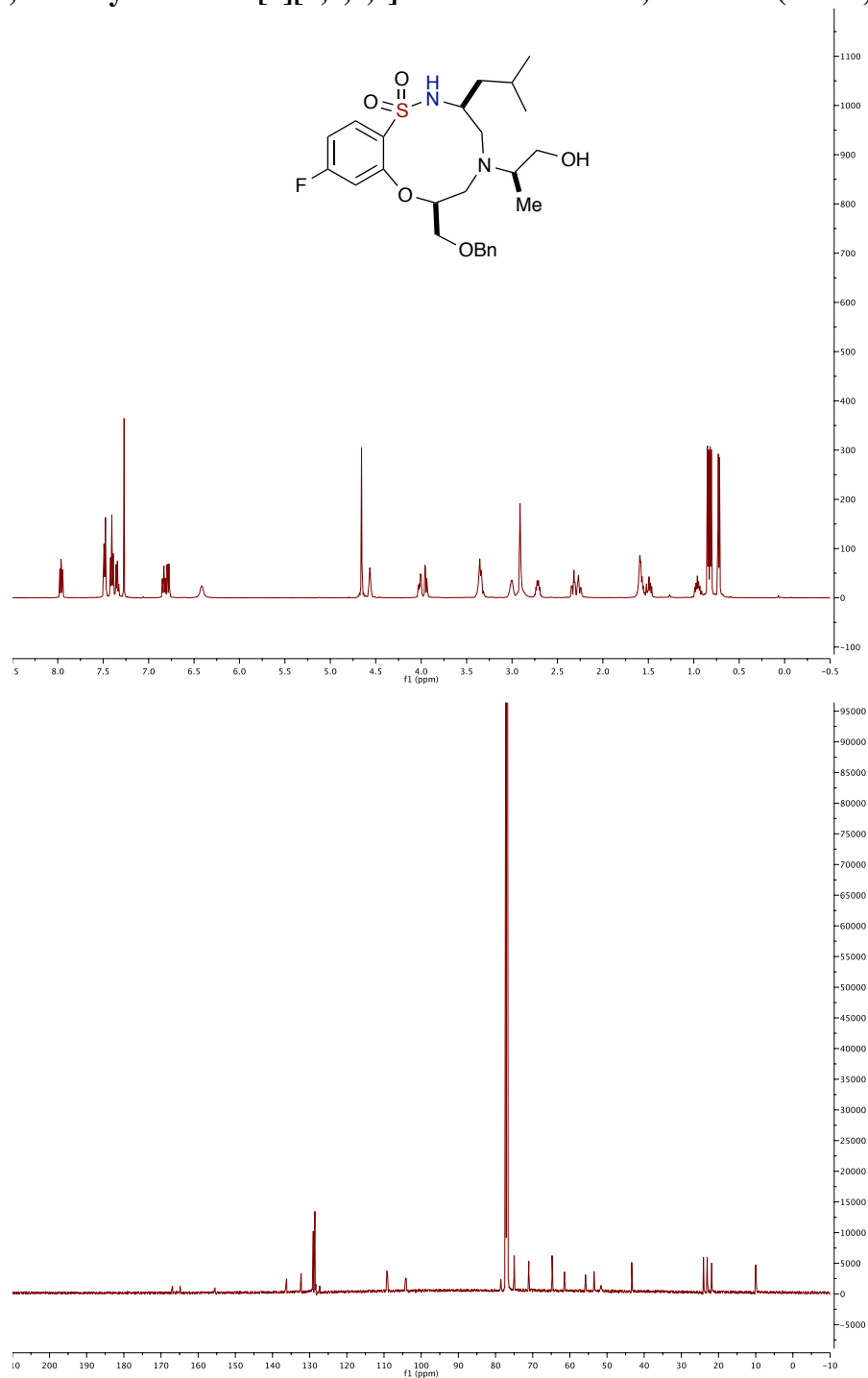
**(4*R*,13*S*)-9-bromo-13-isobutyl-4-methyl-3,4,5,6-tetrahydro-2,7-ethanobenzo-
[*h*][1,2,7]thiadiazonine 1,1-dioxide (3.13.1d)**



(3*S*,7*R*)-7-((benzyloxy)methyl)-10-fluoro-5-((*R*)-1-hydroxypropan-2-yl)-3-isobutyl-2,3,4,5,6,7hexahydro-benzo[*b*][1,4,5,8]oxathiadiazecine 1,1-dioxide (3.14.7)



(3*S*,7*S*)-7-((benzyloxy)methyl)-10-fluoro-5-((*R*)-1-hydroxypropan-2-yl)-3-isobutyl-2,3,4,5,6,7hexahydro-benzo[*b*][1,4,5,8]oxathiadiazecine 1,1-dioxide (3.14.8)

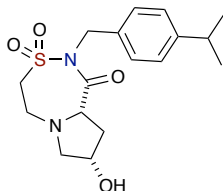


5.3 Experimental for Chapter 4

General Procedure A: one-pot, sequential 3-component (sulfonylation, Michael and amide coupling). To a pressure tube containing a solution of amine (1.44 mmol, 1.5 eq.) in dry CH_2Cl_2 (0.5 M), was added Et_3N (1.91 mmol, 2.0 eq.). The reaction mixture was stirred for 20 min and 2-chloroethane sulfonyl chloride (0.96 mmol, 1.0 eq.) was added in a drop-wise fashion. The reaction was stirred overnight and CH_2Cl_2 was removed *in vacuo* upon completion of the reaction. MeOH/water (0.5 M, 6:1), Et_3N (1.91 mmol, 2.0 eq.) and amino acid (1.15 mmol, 1.2 eq.) were added to the reaction mixture, which was stirred at 60 °C for 12 h, after which solvents were evaporated to dryness. DMF (0.08 M) (for cyclic amino acids), EDC (1.91 mmol, 2.0 eq.), HOBt (1.44 mmol, 1.5 eq.) and Et_3N (1.91 mmol, 2.0 eq.) were added to the crude mixture. The reaction was stirred at rt for 12 h, followed by evaporation of DMF. Water was added to the crude mixture, which was extracted with EtOAc (2x). Layers were separated and solvent was removed under reduced pressure to afford the crude product. The crude product was QC/purified by an automated preparative reverse phase HPLC (detected by mass spectroscopy). For acyclic amino acids, CHCl_3 was utilized as the solvent, followed by addition of EDC (1.91 mmol, 2.0 eq.), HOBt (1.44 mmol, 1.5 eq.) and Et_3N (1.91 mmol, 2.0 eq.). The reaction was stirred at 50 °C for 12 h after which time; water (equal volume of CHCl_3 used) was added to the crude mixture and extraction of aqueous layer with EtOAc (2x). Layers were separated and solvent was removed under reduced pressure to afford the crude product. The crude product was QC/purified by an automated preparative reverse phase HPLC (detected by mass spectroscopy).

General Procedure B: one-pot, sequential 3-component (sulfonylation, Michael and amide coupling). To a pressure tube containing a solution of amine (1.0 mmol, 1.05 eq.) in dry CH_2Cl_2 (0.5 M), was added Et_3N (1.91 mmol, 2.0 eq.). The reaction mixture was stirred for 20 min and 2-chloroethane sulfonyl chloride (0.96 mmol, 1.0 eq.) was added in a drop-wise fashion. The reaction was left to stir overnight and CH_2Cl_2 was removed *in vacuo* upon completion of the reaction. MeOH/water (0.5 M, 5:1), Et_3N (2.87 mmol, 3.0 eq.) and amino acid (1.0 mmol, 1.05 eq.) were added to the reaction mixture, and stirred at 60 °C for 12 h, after which solvents were evaporated to dryness. DMF (0.08 M) (for cyclic amino acids), EDC (1.91 mmol, 2.0 eq.), HOBt (0.48 mmol, 0.5 eq.) and Et_3N (1.91 mmol, 2.0 eq.) were added to the crude mixture. The reaction was stirred at rt for 12 h, followed by evaporation of DMF. Water was added to the crude mixture, which was extracted with EtOAc (2x). Layers were separated and solvent was removed under reduced pressure to afford the crude product. The crude product was QC/purified by an automated preparative reverse phase HPLC (detected by mass spectroscopy). For acyclic amino acids, CHCl_3 was utilized as the solvent, followed by addition of EDC (1.91 mmol, 2.0 eq.), HOBt (0.48 mmol, 0.5 eq.) and Et_3N (1.91 mmol, 2.0 eq.). The reaction was stirred at 50 °C for 12 h after which time; water (equal volume of CHCl_3 used) was added to the crude mixture and extraction of aqueous layer with EtOAc (2x). Layers were separated and solvent was removed under reduced pressure to afford the crude product. The crude product was QC/purified by an automated preparative reverse phase HPLC (detected by mass spectroscopy).

(8*S*,9*aS*)-8-hydroxy-2-(4-isopropylbenzyl)hexahydropyrrolo[2,1-*d*][1,2,5]thiadiazepin-1(2*H*)-one 3,3-dioxide (4.1.4{5,6})



According to general procedure **A**, **4.1.4{5,6}** (40.4 mg, 12%) was isolated as yellow oil.

$[\alpha]_D^{20} = +79.1$ ($c = 0.239$, CH_2Cl_2);

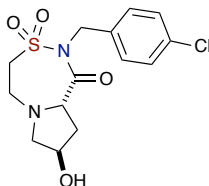
FTIR (thin film) 3281, 2959, 1778, 1512, 1445, 1383, 1325, 1143, 1086, 1059, 820 cm^{-1} ;

^1H NMR (500 MHz, MeOD) δ ppm 7.28 (d, $J = 7.6$ Hz, 2H), 7.22 (d, $J = 7.8$ Hz, 2H), 4.91 (s, 1H), 4.19 (s, 2H), 3.56 (s, 1H), 3.27–3.23 (m, 1H), 3.18–3.08 (m, 1H), 3.07–2.99 (m, 1H), 2.96–2.82 (m, 2H), 2.71–2.65 (m, 1H), 2.11 (d, $J = 10.9$ Hz, 1H), 2.09–2.04 (m, 1H), 1.90 (ddd, $J = 10.8, 1.6, 1.6$ Hz, 1H), 1.24–1.17 (m, 6H);

^{13}C NMR (126 MHz, MeOD) δ ppm 173.6, 149.7, 136.8, 129.2 (2C), 127.7 (2C), 81.5, 63.8, 56.7, 52.6, 48.9, 47.5, 40.0, 35.1, 24.5 (2C);

HRMS calculated for $\text{C}_{17}\text{H}_{24}\text{N}_2\text{O}_4\text{SH}$ ($\text{M}+\text{H}^+$) 353.1535; found 353.1527 (TOF MS ES^+).

(8*R*,9*aS*)-2-(4-chlorobenzyl)-8-hydroxyhexahydropyrrolo[2,1-*d*][1,2,5]thiadiazepin-1(2*H*)-one 3,3-dioxide (4.1.4{4,7})



According to general procedure **A**, **4.1.4{4,7}** (70.3 mg, 14%) was isolated as light yellow oil.

$[\alpha]_D^{20} = +13.8$ ($c = 0.485$, MeOH);

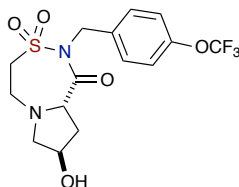
FTIR (thin film) 3364, 3339, 2947, 1701, 1632, 1493, 1352, 1217, 1151, 1091, 835 cm^{-1} ;

^1H NMR (500 MHz, CDCl_3) δ ppm 7.37–7.32 (m, 2H), 7.31–7.28 (m, 2H), 5.07 (d, $J = 15.1$ Hz, 1H), 4.87 (d, $J = 15.1$ Hz, 1H), 4.45–4.35 (m, 2H), 3.45 (ddd, $J = 13.2, 11.9, 2.3$ Hz, 1H), 3.42–3.33 (m, 2H), 3.27–3.16 (m, 2H), 2.72 (m, 1H), 2.65 (ddd, $J = 9.9, 5.2, 1.2$ Hz, 1H), 2.18 (s, 1H), 1.96 (dddd, $J = 13.3, 8.7, 5.6, 1.2$ Hz, 1H);

^{13}C NMR (126 MHz, CDCl_3) δ ppm 171.4, 135.1, 133.6, 129.9 (2C), 128.7 (2C), 70.1, 64.1, 56.5, 52.5, 47.9, 36.6, 30.9;

HRMS calculated for $\text{C}_{14}\text{H}_{17}\text{ClN}_2\text{O}_4\text{SH}$ ($\text{M}+\text{H}$) $^+$ 345.0676; found 345.0662 (TOF MS ES $^+$).

(8*R*,9*aS*)-8-hydroxy-2-(4-(trifluoromethoxy)benzyl)hexahydropyrrolo[2,1-*d*]-[1,2,5]thiadiazepin-1(2*H*)-one 3,3-dioxide (4.1.4{6,7})



According to general procedure **A**, **4.1.4{6,7}** (143 mg, 38%) was isolated as light yellow oil.

$[\alpha]_D^{20} = +8.4$ ($c = 0.45$, MeOH);

FTIR (thin film) 3350, 3337, 2947, 1703, 1510, 1435, 1352, 1221, 1151, 1109, 825 cm^{-1} ;

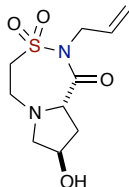
^1H NMR (500 MHz, CDCl_3) δ ppm 7.43 (d, $J = 8.6$ Hz, 2H), 7.17 (d, $J = 8.2$ Hz, 2H), 5.08 (d, $J = 15.2$ Hz, 1H), 4.92 (d, $J = 15.2$ Hz, 1H), 4.48–4.35 (m, 2H), 3.52–3.35 (m,

3H), 3.28–3.16 (m, 2H), 2.72 (ddd, $J = 13.3, 5.9, 5.8$ Hz, 1H), 2.69–2.64 (m, 1H), 1.97 (ddd, $J = 13.7, 8.6, 5.5$ Hz, 1H), 1.87 (s, 1H);

^{13}C NMR (126 MHz, CDCl_3) δ ppm 171.7, 148.9, 135.5, 130.1 (2C), 121.2 (2C), 120.6 (q, $J_{\text{C-F}} = 257.2$ Hz), 70.4, 64.4, 56.8, 52.7, 48.0, 41.2, 36.8;

HRMS calculated for $\text{C}_{15}\text{H}_{17}\text{F}_3\text{N}_2\text{O}_5\text{SH}$ ($\text{M}+\text{H}$) $^+$ 395.0889; found 395.0885 (TOF MS ES^+).

(8*R*,9*aS*)-2-allyl-8-hydroxyhexahydropyrrolo[2,1-*d*][1,2,5]thiadiazepin-1(2*H*)-one 3,3-dioxide (4.1.4{10,7})



According to general procedure **A**, **4.1.4{10,7}** (145 mg, 39%) was isolated as a white solid.

mp 113–116 °C;

$[\alpha]_D^{20} = +25.8$ ($c = 0.36$, MeOH);

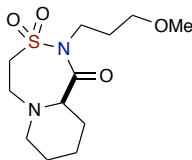
FTIR (thin film) 3373, 3331, 2928, 1705, 1647, 1447, 1344, 1150, 1082, 989, 915 cm^{-1} ;

^1H NMR (500 MHz, CDCl_3) δ ppm 5.87 (dddd, $J = 17.2, 10.3, 6.2, 5.3$ Hz, 1H), 5.34 (dd, $J = 17.1, 1.4$ Hz, 1H), 5.23 (dd, $J = 10.3, 1.2$ Hz, 1H), 4.51–4.36 (m, 4H), 3.52–3.33 (m, 4H), 3.28 (dt, $J = 12.7, 3.5$ Hz, 1H), 2.75 (dddd, $J = 12.8, 5.8, 5.8, 1.0$ Hz, 1H), 2.67 (ddd, $J = 9.9, 5.3, 1.2$ Hz, 1H), 1.96 (dddd, $J = 14.2, 8.8, 5.7, 1.2$ Hz, 1H), 1.58 (s, 1H);

^{13}C NMR (126 MHz, CDCl_3) δ ppm 171.3, 132.2, 118.5, 70.4, 64.4, 64.3, 56.7, 52.7, 47.8, 36.7;

HRMS calculated for $C_{10}H_{16}N_2O_4SH$ ($M+H$)⁺ 261.0909; found 261.0894 (TOF MS ES⁺).

(R)-2-(3-methoxypropyl)octahydro-1H-pyrido[2,1-d][1,2,5]thiadiazepin-1-one 3,3-dioxide (4.1.4{1,4})



According to general procedure **A**, **4.1.4{1,4}** (119 mg, 43%) was isolated as brown oil.

$[\alpha]_D^{20} = +157.0$ ($c = 0.595$, CH_2Cl_2);

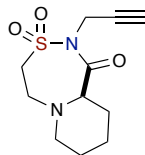
FTIR (thin film) 2930, 2872, 1690, 1443, 1369, 1344, 1148, 1020 cm^{-1} ;

¹H NMR (500 MHz, $CDCl_3$) δ ppm 4.27 (s, 1H), 3.90 (ddd, $J = 8.2, 6.3, 3.5$ Hz, 2H), 3.85–8.76 (m, 1H), 3.54 (ddd, $J = 14.4, 11.6, 3.0$ Hz, 1H), 3.45 (ddd, $J = 6.4, 5.9, 1.3$ Hz, 2H), 3.34 (s, 3H), 3.31 (ddd, $J = 15.3, 3.7, 3.6$ Hz, 1H), 3.23 (d, $J = 13.8$ Hz, 1H), 2.72–2.64 (m, 1H), 2.62–2.56 (m, 1H), 2.13–2.05 (m, 1H), 2.03–1.87 (m, 2H), 1.81–1.68 (m, 1H), 1.67–1.61 (m, 1H), 1.61–1.54 (m, 3H);

¹³C NMR (126 MHz, $CDCl_3$) δ ppm 172.8, 70.3, 60.9, 58.6, 52.7, 52.2, 47.9, 43.6, 29.8, 27.4, 25.9, 19.9;

HRMS calculated for $C_{12}H_{22}N_2O_4SH$ ($M+H$)⁺ 291.1379; found 291.1388 (TOF MS ES⁺).

(R)-2-(prop-2-yn-1-yl)octahydro-1H-pyrido[2,1-d][1,2,5]thiadiazepin-1-one 3,3-dioxide (4.1.4{7,4})



According to general procedure A, **4.1.4**{7,4} (163.8 mg, 67%) was isolated as a brown solid.

mp 125–129 °C;

$[\alpha]_D^{20} = +120.0$ ($c = 0.405$, CH_2Cl_2);

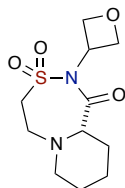
FTIR (thin film) 3285, 2926, 1699, 1346, 1148 cm^{-1} ;

^1H NMR (500 MHz, CDCl_3) δ ppm 4.79 (dd, $J = 17.5, 2.4$ Hz, 1H), 4.46 (dd, $J = 17.6, 2.4$ Hz, 1H), 4.34 (s, 1H), 3.88 (ddd, $J = 15.0, 12.0, 2.4$ Hz, 1H), 3.65 (ddd, $J = 15.0, 11.9, 3.0$ Hz, 1H), 3.39 (ddd, $J = 15.3, 3.5, 3.5$ Hz, 1H), 3.28 (s, 1H), 2.88–2.79 (m, 1H), 2.63 (s, 1H), 2.29 (t, $J = 2.5$ Hz, 1H), 2.14–2.06 (m, 1H), 1.87–1.74 (m, 1H), 1.68 (s, 1H), 1.63–1.57 (m, 3H);

^{13}C NMR (126 MHz, CDCl_3) δ ppm 174.8, 78.5, 71.8, 60.6, 52.5, 52.2, 47.7, 34.0, 27.2, 25.7, 19.6;

HRMS calculated for $\text{C}_{11}\text{H}_{16}\text{N}_2\text{O}_3\text{SH}$ ($\text{M}+\text{H}^+$) 257.0960; found 257.0960 (TOF MS ES^+).

(S)-2-(oxetan-3-yl)octahydro-1H-pyrido[2,1-d][1,2,5]thiadiazepin-1-one 3,3-dioxide (**4.1.4**{9,5})



According to general procedure A, **4.1.4**{9,5} (109.3 mg, 42%) was isolated as dark brown oil.

$[\alpha]_D^{20} = -159.0$ ($c = 0.595$, CH_2Cl_2);

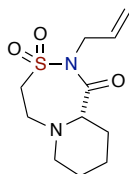
FTIR (thin film) 2939, 1693, 1346, 1151, 1067 cm^{-1} ;

¹H NMR (500 MHz, CDCl₃) δ ppm 5.03 (p, *J* = 7.3 Hz, 1H), 4.84 (dddd, *J* = 7.0, 7.0, 1.0, 0.9 Hz, 1H), 4.80 (dddd, *J* = 7.1, 6.8, 1.1, 0.9 Hz, 1H), 4.76 (dd, *J* = 7.5, 7.4 Hz, 1H), 4.50 (dd, *J* = 7.4, 7.3 Hz, 1H), 4.14 (dd, *J* = 4.0, 3.7 Hz, 1H), 3.82 (ddd, *J* = 15.1, 12.4, 2.5 Hz, 1H), 3.68 (ddd, *J* = 14.1, 12.4, 3.4 Hz, 1H), 3.44 (ddd, *J* = 15.3, 3.1, 3.1 Hz, 1H), 3.21 (ddd, *J* = 14.1, 2.7, 2.6 Hz, 1H), 3.06–2.97 (m, 1H), 2.75–2.69 (m, 1H), 2.24–2.16 (m, 1H), 1.66–1.63 (m, 1H), 1.63–1.61 (m, 2H), 1.61–1.58 (m, 1H), 1.39–1.28 (m, 1H);

¹³C NMR (126 MHz, CDCl₃) δ ppm 175.5, 76.5, 75.9, 62.5, 53.2, 52.2, 51.7, 47.2, 27.9, 25.5, 20.2;

HRMS calculated for C₁₁H₁₈N₂O₄SH (M+H)⁺ 275.1066; found 275.1075 (TOF MS ES⁺).

(S)-2-allyloctahydro-1H-pyrido[2,1-*d*][1,2,5]thiadiazepin-1-one 3,3-dioxide (4.1.4{10,5})



According to general procedure **A**, **4.1.4{10,5}** (140.6 mg, 57%) was isolated as brown oil.

$[\alpha]_D^{20} = -161.0$ (*c* = 0.395, CH₂Cl₂);

FTIR (thin film) 2943, 1693, 1344, 1147, 1003, 928 cm⁻¹;

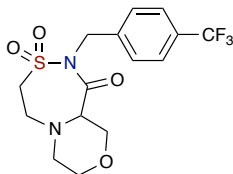
¹H NMR (500 MHz, CDCl₃) δ ppm 5.90 (ddt, *J* = 16.5, 10.2, 6.1 Hz, 1H), 5.36 (dd, *J* = 17.1, 1.3 Hz, 1H), 5.23 (dd, *J* = 10.3, 1.3 Hz, 1H), 4.46 (dddd, *J* = 15.3, 5.8, 1.4, 1.4 Hz, 1H), 4.38 (dddd, *J* = 15.2, 6.5, 1.4, 1.3 Hz, 1H), 4.30 (dd, *J* = 3.5, 3.5 Hz, 1H), 3.83 (ddd, *J* = 14.8, 11.8, 2.4 Hz, 1H), 3.49 (ddd, *J* = 14.6, 11.8, 3.0 Hz, 1H), 3.32 (ddd, *J* = 15.4,

3.5, 3.4 Hz, 1H), 3.23 (ddd, $J = 14.5, 3.0, 2.9$ Hz, 1H), 2.75–2.64 (m, 1H), 2.62–2.56 (m, 1H), 2.14–2.05 (m, 1H), 1.80–1.70 (m, 1H), 1.64 (ddd, $J = 12.7, 4.4, 4.3$ Hz, 1H), 1.62–1.55 (m, 3H);

^{13}C NMR (126 MHz, CDCl_3) δ ppm 172.6, 132.6, 119.0, 60.9, 52.9, 52.2, 47.9, 47.6, 27.4, 25.9, 19.9;

HRMS calculated for $\text{C}_{11}\text{H}_{18}\text{N}_2\text{O}_3\text{SH}$ ($\text{M}+\text{H}$) $^+$ 259.1116; found 259.1117 (TOF MS ES^+).

2-(4-(trifluoromethyl)benzyl)hexahydro-[1,4]oxazino[3,4-*d*][1,2,5]thiadiazepin-1(2*H*)-one 3,3-dioxide (4.1.4{2,8})



According to general procedure **A**, **4.1.4{2,8}** (111.1 mg, 31%) was isolated as a brown solid.

mp 108–113 °C;

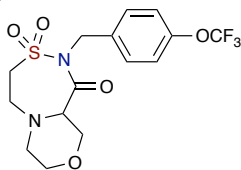
FTIR (thin film) 2916, 2856, 1693, 1615, 1429, 1325, 1150, 1067, 1053, 847 cm^{-1} ;

^1H NMR (500 MHz, CDCl_3) δ ppm 7.60 (s, 4H), 5.15 (d, $J = 15.1$ Hz, 1H), 4.99 (d, $J = 15.0$ Hz, 1H), 4.34 (dd, $J = 11.0, 2.0$ Hz, 1H), 4.13 (dd, $J = 3.1, 3.0$ Hz, 1H), 3.90 (ddd, $J = 14.7, 11.8, 2.5$ Hz, 1H), 3.78 (ddd, $J = 11.0, 3.2, 1.8$ Hz, 1H), 3.68 (dd, $J = 10.8, 3.0$ Hz, 1H), 3.63 (dd, $J = 11.1, 2.9$ Hz, 1H), 3.45 (ddd, $J = 14.5, 12.0, 2.7$ Hz, 1H), 3.36–3.25 (m, 2H), 2.83 (ddd, $J = 11.5, 11.4, 2.9$ Hz, 1H), 2.41 (ddd, $J = 11.9, 1.7, 1.5$ Hz, 1H);

^{13}C NMR (126 MHz, CDCl_3) δ ppm 171.2, 140.8, 130.1 (q, $^2J_{\text{C-F}} = 32.4$ Hz), 129.0 (2C), 125.6 (q, $^3J_{\text{C-F}} = 3.8$ Hz, 2C), 124.0 (q, $^1J_{\text{C-F}} = 272.2$ Hz), 67.5, 66.9, 61.4, 52.6, 51.8, 48.2, 47.3;

HRMS calculated for $\text{C}_{15}\text{H}_{17}\text{F}_3\text{N}_2\text{O}_4\text{SH}$ ($\text{M}+\text{H}$) $^+$ 379.0939; found 379.0962 (TOF MS ES^+).

2-(4-(trifluoromethoxy)benzyl)hexahydro-[1,4]oxazino[3,4-*d*][1,2,5]thiadiazepin-1(2*H*)-one 3,3-dioxide (4.1.4{6,8})



According to general procedure **A**, **4.1.4{6,8}** (177.9 mg, 47%) was isolated as a yellow solid.

mp 102–107 °C;

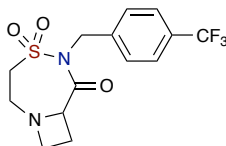
FTIR (thin film) 3121, 2962, 2916, 1682, 1508, 1435, 1346, 1219, 1151, 1043, 851 cm^{-1} ;

^1H NMR (500 MHz, CDCl_3) δ ppm 7.54 (d, $J = 8.6$ Hz, 2H), 7.18 (d, $J = 7.8$ Hz, 2H), 5.11 (d, $J = 14.9$ Hz, 1H), 4.94 (d, $J = 14.9$ Hz, 1H), 4.33 (d, $J = 10.9$ Hz, 1H), 4.10 (m, 1H), 3.93–3.83 (m, 1H), 3.75 (ddd, $J = 10.9, 3.3, 1.6$ Hz, 1H), 3.69–3.60 (m, 2H), 3.47–3.38 (m, 1H), 3.34–3.23 (m, 2H), 2.76 (dd, $J = 11.2, 11.1$ Hz, 1H), 2.37 (d, $J = 11.9$ Hz, 1H);

^{13}C NMR (126 MHz, CDCl_3) δ ppm 171.2, 148.9, 135.6, 130.6 (2C), 121.0 (2C), 120.4 (q, $J_{\text{C-F}} = 257.4$ Hz), 67.5, 66.9, 61.3, 52.7, 51.7, 47.8, 47.2;

HRMS calculated for $C_{15}H_{17}F_3N_2O_5SH$ ($M+H$)⁺ 395.0898; found 395.0913 (TOF MS ES⁺).

5-(4-(trifluoromethyl)benzyl)-4-thia-1,5-diazabicyclo[5.2.0]nonan-6-one 4,4-dioxide (4.1.4{2,1})



According to general procedure **A**, **4.1.4{2,1}** (152 mg, 46%) was isolated as a yellow solid.

mp 137–140 °C;

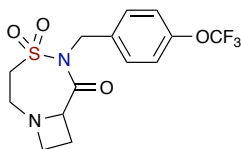
FTIR (thin film) 3016, 2974, 2934, 1711, 1620, 1452, 1325, 1234, 1163, 1150, 816 cm^{-1} ;

¹H NMR (500 MHz, CDCl₃) δ ppm 7.61 (d, $J = 8.1$ Hz, 2H), 7.53 (d, $J = 8.0$ Hz, 2H), 5.12 (d, $J = 15.5$ Hz, 1H), 4.95 (d, $J = 15.5$ Hz, 1H), 4.65 (s, 1H), 3.4–3.16 (m, 5H), 3.15–3.08 (m, 1H), 2.71–2.63 (m, 1H), 2.23–2.13 (m, 1H);

¹³C NMR (126 MHz, Acetone-*d*₆) δ ppm 173.2, 143.3, 129.9 (q, $^2J_{C-F} = 32.1$ Hz), 129.1 (2C), 126.2 (q, $^3J_{C-F} = 3.9$ Hz, 2C), 125.4 (q, $^1J_{C-F} = 271.8$ Hz), 66.7, 56.0, 52.4, 51.0, 48.5, 21.1;

HRMS calculated for $C_{14}H_{15}F_3N_2O_3SH$ ($M+H$)⁺ 349.0834; found 349.0836 (TOF MS ES⁺).

5-(4-(trifluoromethoxy)benzyl)-4-thia-1,5-diazabicyclo[5.2.0]nonan-6-one 4,4-dioxide (4.1.4{6,1})



According to general procedure **A**, **4.1.4{6,1}** (112 mg, 32%) was isolated as a yellow solid.

mp 104–108 °C;

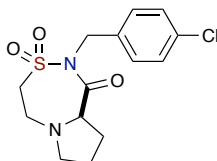
FTIR (thin film) 3020, 2974, 1709, 1510, 1450, 1431, 1352, 1223, 1163, 1150, 843 cm⁻¹;

¹H NMR (500 MHz, CDCl₃) δ ppm 7.45 (d, *J* = 8.7 Hz, 2H), 7.18 (d, *J* = 8.2 Hz, 2H), 5.09 (d, *J* = 15.3 Hz, 1H), 4.88 (d, *J* = 15.3 Hz, 1H), 4.55 (dd, *J* = 8.3, 8.2 Hz, 1H), 3.40–3.32 (m, 2H), 3.24–3.17 (m, 2H), 3.13 (ddd, *J* = 9.9, 7.7, 6.5 Hz, 1H), 3.09–3.01 (m, 1H), 2.60 (dddd, *J* = 10.3, 10.1, 8.7, 8.5 Hz, 1H), 2.13 (dddd, *J* = 10.9, 7.7, 7.6, 1.8 Hz, 1H);

¹³C NMR (126 MHz, CDCl₃) δ ppm 172.0, 148.7, 135.3, 129.8 (2C), 121.0 (2C), 120.4 (q, *J*_{C-F} = 257.3 Hz), 65.9, 55.6, 51.4, 50.6, 47.5, 20.5;

HRMS calculated for C₁₄H₁₅F₃N₂O₄SH (M+H)⁺ 365.0783; found 365.0791 (TOF MS ES⁺).

(R)-2-(4-chlorobenzyl)hexahydropyrrolo[2,1-*d*][1,2,5]thiadiazepin-1(2H)-one 3,3-dioxide (4.1.4{4,2})



According to general procedure **A**, **4.1.4{4,2}** (134.6 mg, 43%) was isolated as a white solid.

mp 105–108 °C;

$[\alpha]_D^{20} = -14.5$ ($c = 0.38$, MeOH);

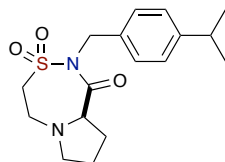
FTIR (thin film) 2970, 2945, 1703, 1493, 1352, 1151, 831 cm^{-1} ;

^1H NMR (500 MHz, CDCl_3) δ ppm 7.35 (d, $J = 8.5$ Hz, 2H), 7.30 (d, $J = 8.5$ Hz, 2H), 5.06 (d, $J = 15.1$ Hz, 1H), 4.89 (d, $J = 15.1$ Hz, 1H), 4.17 (s, 1H), 3.44–3.07 (m, 5H), 2.70–2.63 (m, 1H), 2.62–2.56 (m, 1H), 1.97–1.85 (m, 1H), 1.84–1.71 (m, 2H);

^{13}C NMR (126 MHz, MeOD) δ ppm 173.6, 137.5, 134.3, 130.8 (2C), 129.5 (2C), 65.6, 58.7, 57.0, 51.9, 48.9, 27.9, 25.6;

HRMS calculated for $\text{C}_{14}\text{H}_{17}\text{ClN}_2\text{O}_3\text{SH}$ ($\text{M}+\text{H}$) $^+$ 329.0727; found 329.0753 (TOF MS ES $^+$).

(*R*)-2-(4-isopropylbenzyl)hexahydropyrrolo[2,1-*d*][1,2,5]thiadiazepin-1(2*H*)-one 3,3-dioxide (4.1.4{5,2})



According to general procedure **A**, **4.1.4{5,2}** (294 mg, 81%) was isolated as a yellow solid.

mp 75–79 °C;

$[\alpha]_D^{20} = -43.0$ ($c = 0.27$, CH_2Cl_2);

FTIR (thin film) 3132, 2959, 1705, 1612, 1514, 1460, 1352, 1151, 831 cm^{-1} ;

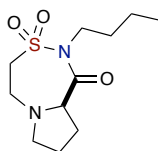
^1H NMR (500 MHz, CDCl_3) δ ppm 7.33 (d, $J = 8.1$ Hz, 2H), 7.18 (d, $J = 8.1$ Hz, 2H), 5.08 (d, $J = 15.1$ Hz, 1H), 4.90 (d, $J = 15.2$ Hz, 1H), 4.18 (s, 1H), 3.42–3.11 (m, 5H),

2.89 (hept, $J = 6.9$ Hz, 1H), 2.70–2.64 (m, 1H), 2.62–2.56 (m, 1H), 1.96–1.85 (m, 1H), 1.79 (s, 2H), 1.24 (d, $J = 6.9$ Hz, 6H);

^{13}C NMR (126 MHz, MeOD) δ ppm 173.7, 149.5, 136.1, 129.4 (2C), 127.5 (2C), 65.7, 58.8, 57.2, 52.1, 48.9, 35.3, 28.1, 25.7, 24.6 (2C);

HRMS calculated for $\text{C}_{17}\text{H}_{24}\text{N}_2\text{O}_3\text{SH}$ ($\text{M}+\text{H}$) $^+$ 337.1586; found 337.1581 (TOF MS ES $^+$).

(*R*)-2-butylhexahydropyrrolo[2,1-*d*][1,2,5]thiadiazepin-1(2*H*)-one 3,3-dioxide
(4.1.4{8,2})



According to general procedure **B**, **4.1.4{8,2}** (34.3 mg, 14%) was isolated as colorless oil.

$[\alpha]_D^{20} = -14.9$ ($c = 1.495$, MeOH);

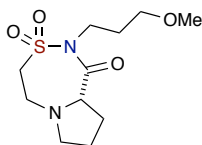
FTIR (thin film) 2959, 2872, 1703, 1454, 1383, 1352, 1148 cm^{-1} ;

^1H NMR (500 MHz, CDCl_3) δ ppm 4.10 (dd, $J = 9.8, 2.5$ Hz, 1H), 3.89–3.81 (m, 1H), 3.80–3.73 (m, 1H), 3.45–3.35 (m, 2H), 3.32–3.19 (m, 2H), 3.16–3.10 (m, 1H), 2.67–2.61 (m, 1H), 2.61–2.55 (m, 1H), 1.92–1.84 (m, 1H), 1.80–1.72 (m, 2H), 1.66–1.58 (m, 2H), 1.40–1.29 (m, 2H), 0.94 (t, $J = 7.4$ Hz, 3H);

^{13}C NMR (126 MHz, CDCl_3) δ ppm 171.7, 64.3, 57.9, 56.3, 50.8, 46.1, 31.5, 27.1, 24.7, 20.0, 13.7;

HRMS calculated for $\text{C}_{11}\text{H}_{20}\text{N}_2\text{O}_3\text{SH}$ ($\text{M}+\text{H}$) $^+$ 261.1273; found 261.1294 (TOF MS ES $^+$).

(S)-2-(3-methoxypropyl)hexahydropyrrolo[2,1-d][1,2,5]thiadiazepin-1(2H)-one 3,3-dioxide (4.1.4{1,3})



According to general procedure **A**, **4.1.4{1,3}** (147.5 mg, 56%) was isolated as a light yellow sticky oil.

$[\alpha]_D^{20} = +3.0$ ($c = 0.795$, MeOH);

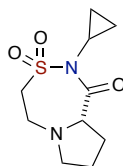
FTIR (thin film) 2968, 2930, 1701, 1445, 1383, 1352, 1151, 1115 cm^{-1} ;

^1H NMR (500 MHz, CDCl_3) δ ppm 4.10 (dd, $J = 9.8, 2.5$ Hz, 1H), 3.95 (ddd, $J = 14.2, 7.1, 7.0$ Hz, 1H), 3.87 (ddd, $J = 14.2, 7.3, 7.1$ Hz, 1H), 3.45–3.39 (m, 4H), 3.33 (s, 3H), 3.29–3.23 (m, 2H), 3.15–3.11 (m, 1H), 2.67–2.61 (m, 1H), 2.60–2.55 (m, 1H), 1.95–1.85 (m, 3H), 1.79–1.72 (m, 2H);

^{13}C NMR (126 MHz, CDCl_3) δ ppm 171.8, 70.0, 64.3, 58.5, 57.8, 56.1, 50.8, 43.8, 29.4, 27.1, 24.6;

HRMS calculated for $\text{C}_{11}\text{H}_{20}\text{N}_2\text{O}_4\text{SH}$ ($\text{M}+\text{H}^+$) 277.1222; found 277.1233 (TOF MS ES^+).

(S)-2-cyclopropylhexahydropyrrolo[2,1-d][1,2,5]thiadiazepin-1(2H)-one 3,3-dioxide (4.1.4{3,3})



According to general procedure **A**, **4.1.4{3,3}** (67.8 mg, 29%) was isolated as a light yellow solid.

mp 85–90 °C;

$[\alpha]_D^{20} = +197.0$ ($c = 0.22$, CHCl_3);

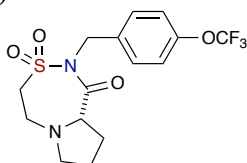
FTIR (thin film) 2968, 2945, 1711, 1354, 1157 cm^{-1} ;

^1H NMR (500 MHz, CDCl_3) δ ppm 3.98 (dd, $J = 10.3, 3.0$ Hz, 1H), 3.40 (ddd, $J = 13.9, 3.1, 2.8$ Hz, 1H), 3.35–3.25 (m, 2H), 3.25–3.17 (m, 1H), 3.16–3.10 (m, 1H), 2.73 (dddd, $J = 7.0, 6.8, 3.8, 3.8$ Hz, 1H), 2.61–2.53 (m, 2H), 1.97–1.86 (m, 1H), 1.80–1.67 (m, 2H), 1.13–1.03 (m, 2H), 0.83–0.77 (m, 1H), 0.76–0.69 (m, 1H);

^{13}C NMR (126 MHz, MeOD) δ ppm 176.0, 67.1, 58.9, 57.4, 52.1, 28.7, 28.5, 25.4, 10.1, 9.6;

HRMS calculated for $\text{C}_{10}\text{H}_{16}\text{N}_2\text{O}_3\text{SH}$ ($\text{M}+\text{H}^+$) 245.0960; found 245.0980 (TOF MS ES^+).

(S)-2-(4-(trifluoromethoxy)benzyl)hexahydropyrrolo[2,1-d][1,2,5]thiadiazepin-1(2H)-one 3,3-dioxide (4.1.4{6,3})



According to general procedure **A**, **4.1.4{6,3}** (230.5 mg, 64%) was isolated as a light yellow solid.

mp 107–111 °C;

$[\alpha]_D^{20} = +24.0$ ($c = 0.64$, CH_2Cl_2);

FTIR (thin film) 2991, 2939, 1693, 1506, 1429, 1352, 1221, 1159, 834 cm^{-1} ;

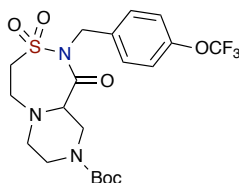
^1H NMR (500 MHz, CDCl_3) δ ppm 7.44 (d, $J = 8.6$ Hz, 2H), 7.17 (d, $J = 8.0$ Hz, 2H), 5.07 (d, $J = 15.3$ Hz, 1H), 4.92 (d, $J = 15.2$ Hz, 1H), 4.15 (dd, $J = 9.8, 2.4$ Hz, 1H), 3.44–

3.35 (m, 1H), 3.31–3.21 (m, 3H), 3.18–3.12 (m, 1H), 2.68–2.64 (m, 1H), 2.61–2.57 (m, 1H), 1.96–1.85 (m, 1H), 1.82–1.73 (m, 2H);

^{13}C NMR (126 MHz, CDCl_3) δ ppm 171.8, 148.6, 135.5, 129.9 (2C), 120.9 (2C), 120.4 (q, $J_{\text{C-F}} = 257.2$ Hz), 64.3, 57.8, 56.3, 50.7, 47.9, 27.2, 24.7;

HRMS calculated for $\text{C}_{15}\text{H}_{17}\text{F}_3\text{N}_2\text{O}_4\text{SH}$ ($\text{M}+\text{H}$) $^+$ 379.0939; found 379.0945 (TOF MS ES $^+$).

***tert*-butyl 1-oxo-2-(4-(trifluoromethoxy)benzyl)hexahydro-1*H*-pyrazino[2,1-*d*][1,2,5]-thiadiazepine-9(2*H*)-carboxylate 3,3-dioxide (4.1.4{6,9})**



According to general procedure **B**, **4.1.4{6,9}** (195 mg, 41%) was isolated as a white solid.

mp 155–158 °C;

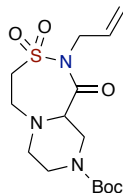
FTIR (thin film) 2978, 2924, 1693, 1510, 1454, 1425, 1366, 1350, 1259, 1150, 827 cm^{-1} ;

^1H NMR (500 MHz, CDCl_3) δ ppm 7.47 (d, $J = 7.6$ Hz, 2H), 7.18 (d, $J = 8.0$ Hz, 2H), 5.09 (d, $J = 14.9$ Hz, 1H), 4.97–4.84 (m, 1H), 4.46–4.33 (m, 1H), 4.28–4.17 (m, 1H), 3.96–3.82 (m, 2H), 3.34–3.20 (m, 3H), 3.13–2.93 (m, 2H), 2.61–2.38 (m, 2H), 1.52 (s, 9H);

^{13}C NMR (126 MHz, CDCl_3) δ ppm 170.7, 148.9, 135.6, 130.5 (2C), 129.8, 121.0 (2C), 120.4 (q, $J_{\text{C-F}} = 257.5$ Hz), 79.9, 60.6, 52.9, 51.9, 47.5, 46.5, 44.9, 42.3, 28.4 (3C);

HRMS calculated for $C_{20}H_{26}F_3N_3O_6SH$ (M+H)⁺ 494.1573; found 494.1595 (TOF MS ES⁺).

tert-butyl 2-allyl-1-oxohexahydro-1*H*-pyrazino[2,1-*d*][1,2,5]thiadiazepine-9(2*H*)-carboxylate 3,3-dioxide (4.1.4{10,9})



According to general procedure **B**, 4.1.4{10,9} (75.4 mg, 22%) was isolated as light yellow oil.

FTIR (thin film) 2976, 2918, 1693, 1425, 1366, 1348, 1165, 1148, 953, 926 cm⁻¹;

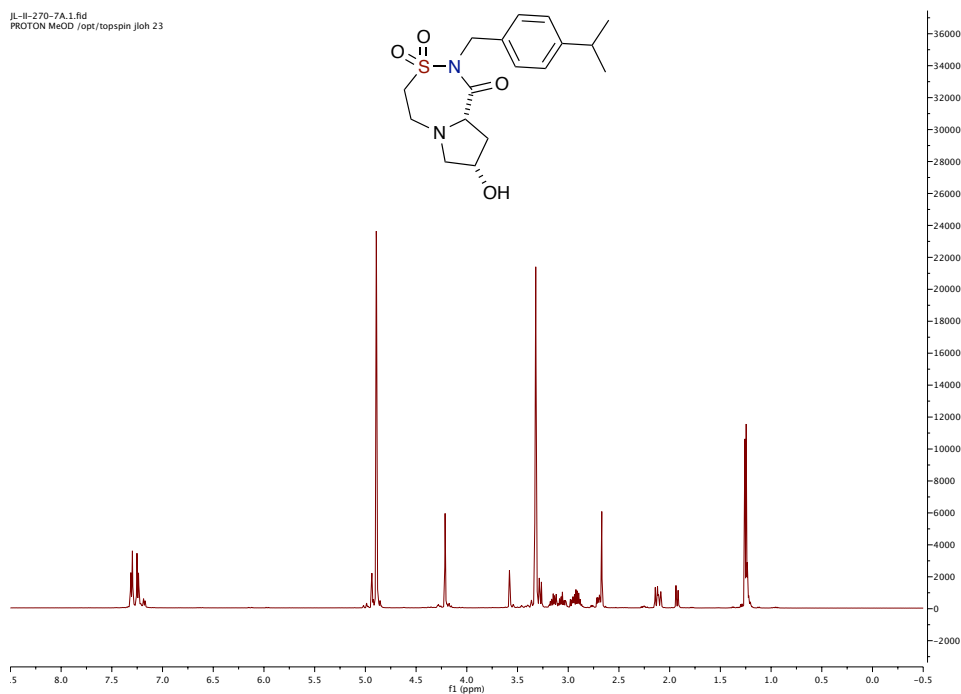
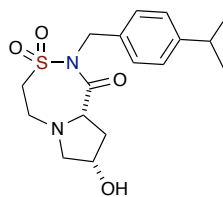
¹H NMR (500 MHz, CDCl₃) δ ppm 5.91–5.81 (m, 1H), 5.33 (ddd, *J* = 16.9, 1.4, 1.4 Hz, 1H), 5.21 (dd, *J* = 10.4, 2.7 Hz, 1H), 4.48–4.29 (m, 3H), 4.29–4.15 (m, 1H), 4.01–3.76 (m, 2H), 3.51–3.42 (m, 1H), 3.39–3.32 (m, 1H), 3.28–3.20 (m, 1H), 3.11–2.92 (m, 2H), 2.87–2.78 (m, 1H), 2.56 (d, *J* = 11.6 Hz, 1H), 1.48 (s, 9H);

¹³C NMR (126 MHz, CDCl₃) δ ppm 170.1, 154.9, 132.1, 119.3, 79.8, 60.6, 52.8, 51.9, 47.6, 46.6, 44.8, 42.4, 28.4 (3C);

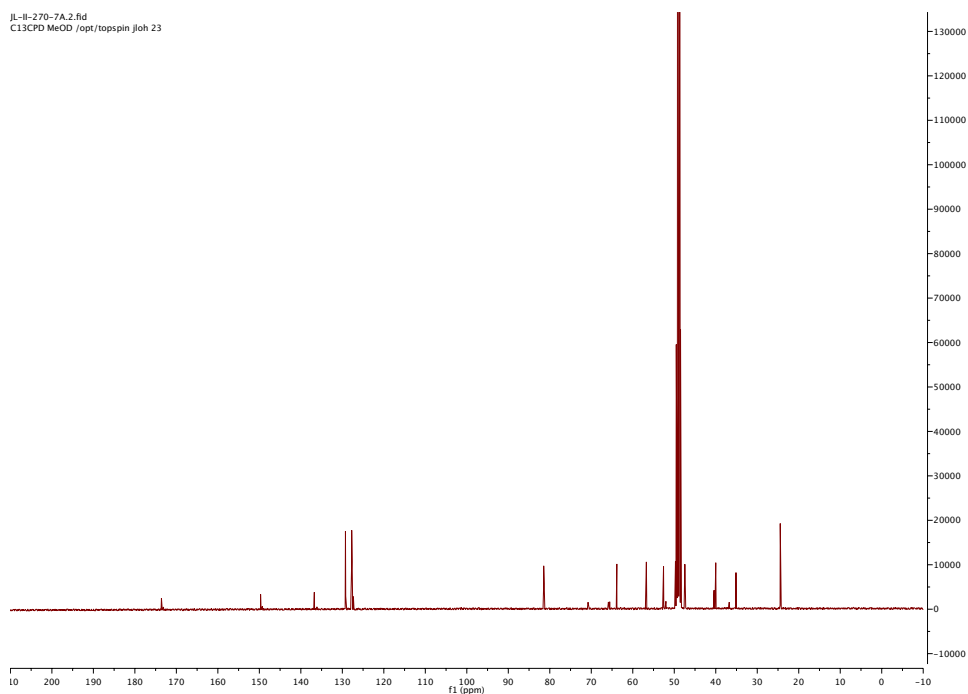
HRMS calculated for $C_{15}H_{25}N_3O_5SH$ (M+H)⁺ 360.1593; found 360.1563 (TOF MS ES⁺).

(8*S*,9*aS*)-8-hydroxy-2-(4-isopropylbenzyl)hexahydropyrrolo[2,1-*d*][1,2,5]thiadiazepin-1(2*H*)-one 3,3-dioxide (4.1.4{5,6})

JL-II-270-7A.1.fid
PROTON MeOD /opt/topspin jl0h 23

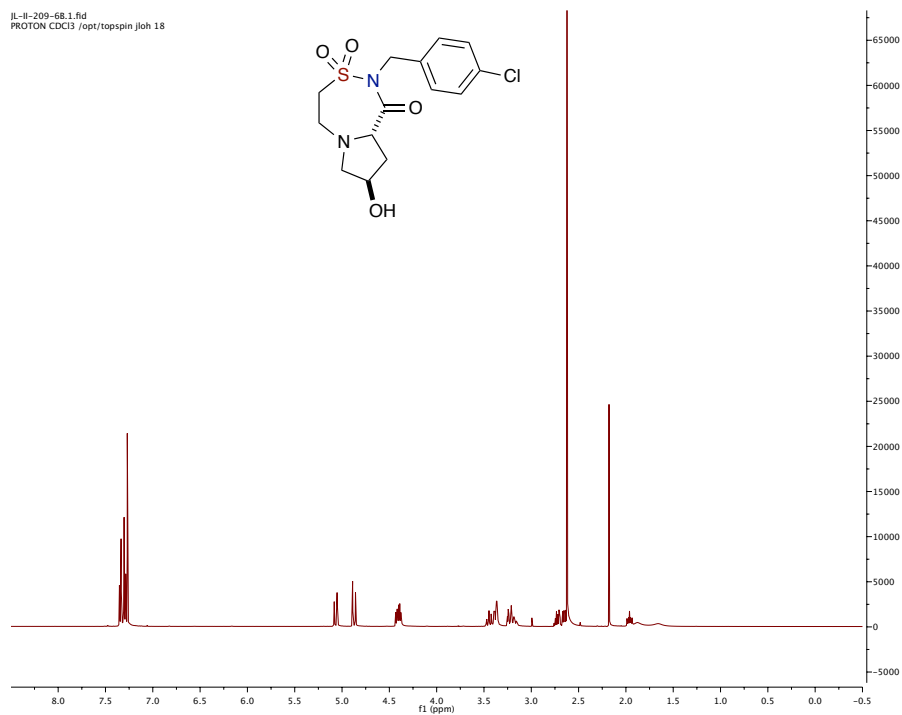
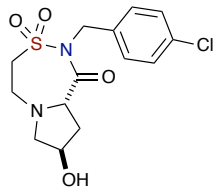


JL-II-270-7A.2.fid
C13CPD MeOD /opt/topspin jl0h 23

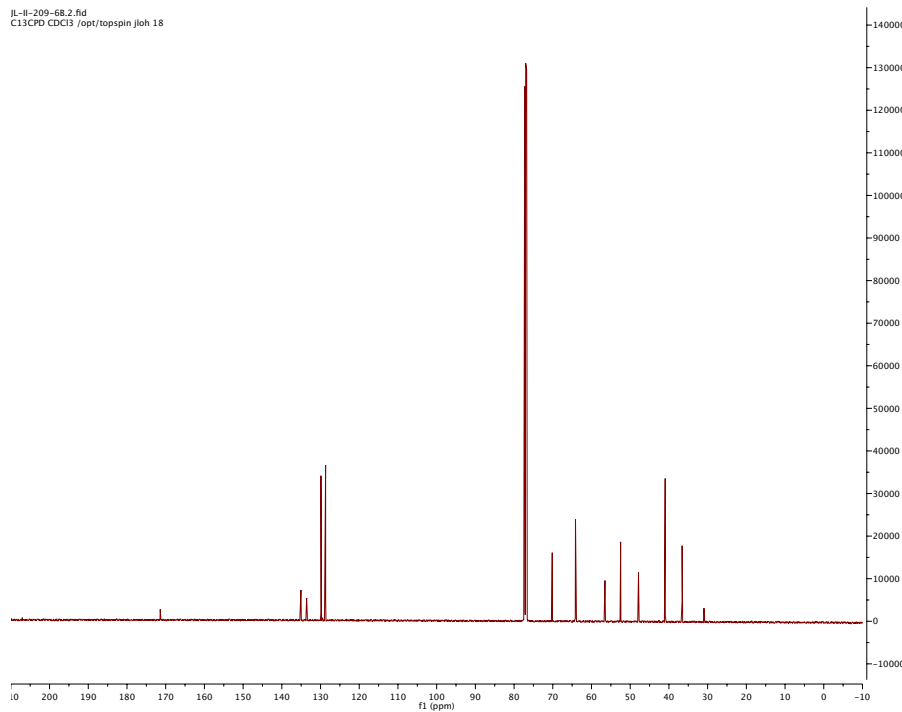


(8*R*,9*aS*)-2-(4-chlorobenzyl)-8-hydroxyhexahydropyrrolo[2,1-*d*][1,2,5]thiadiazepin-1(2*H*)-one 3,3-dioxide (4.1.4{4,7})

jl-II-209-68.1.fid
PROTON CDCI3 /opt/topspin jloh 18

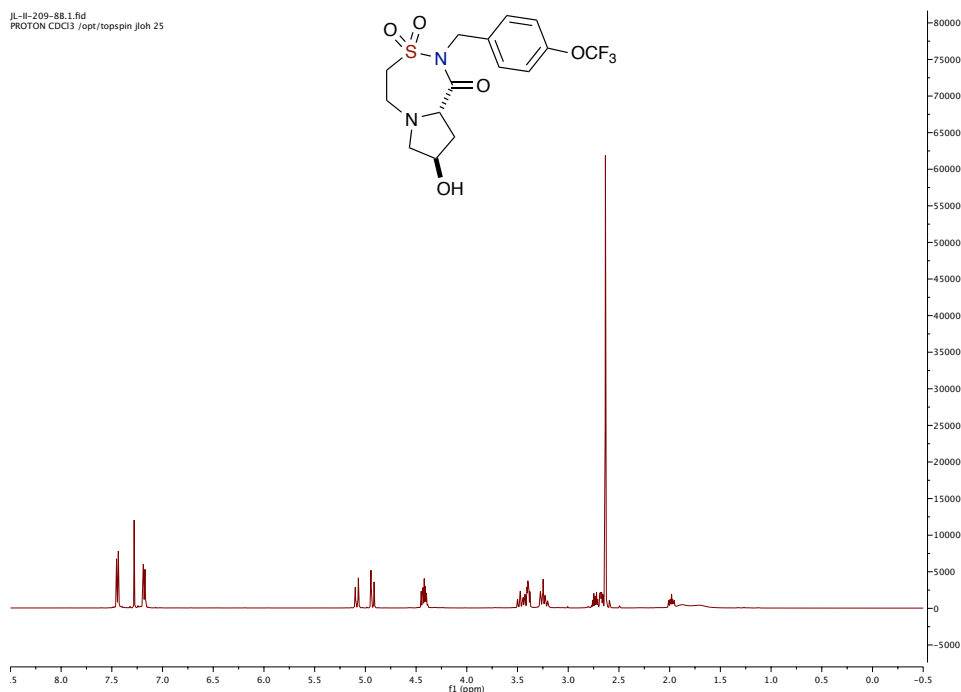
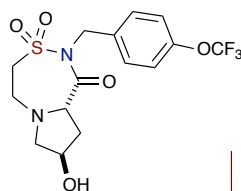


jl-II-209-68.2.fid
C13CPD CDCI3 /opt/topspin jloh 18

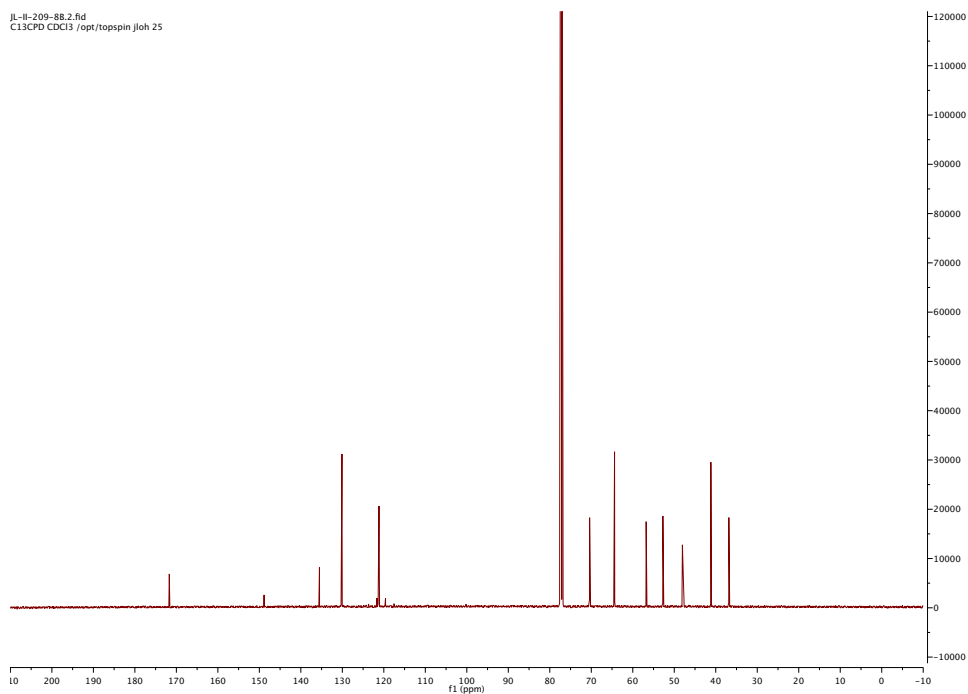


(8*R*,9*aS*)-8-hydroxy-2-(4-(trifluoromethoxy)benzyl)hexahydropyrrolo[2,1-*d*][1,2,5]-thiadiazepin-1(2*H*)-one 3,3-dioxide (4.1.4{6,7})

JL-II-209-88.1.fid
PROTON CDCl3 /opt/topspin jl0h 25

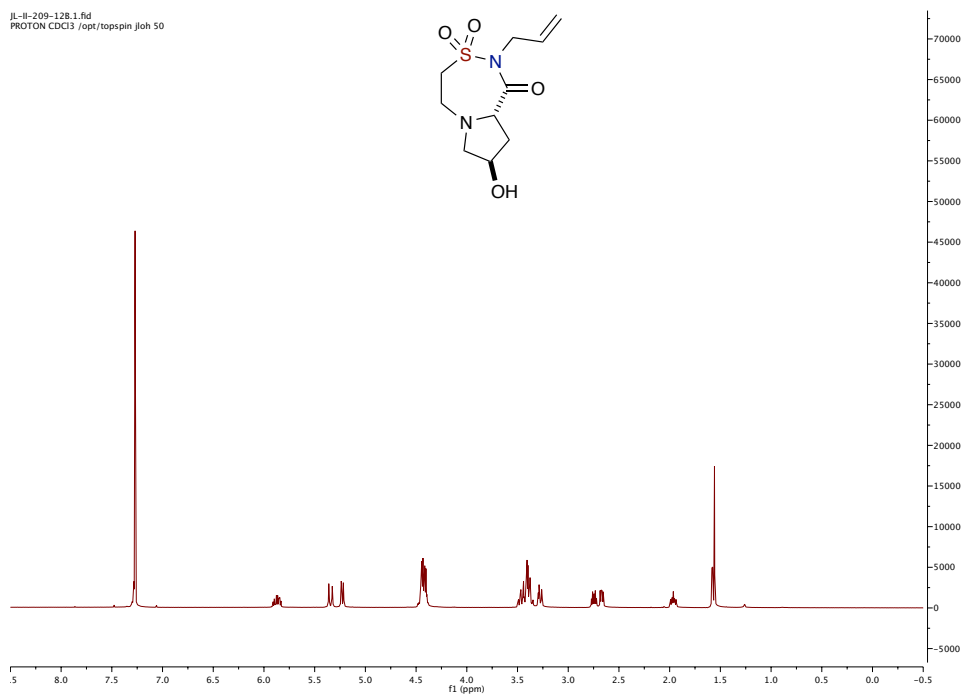
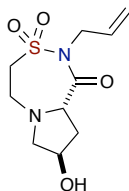


JL-II-209-88.2.fid
C13CPD CDCl3 /opt/topspin jl0h 25

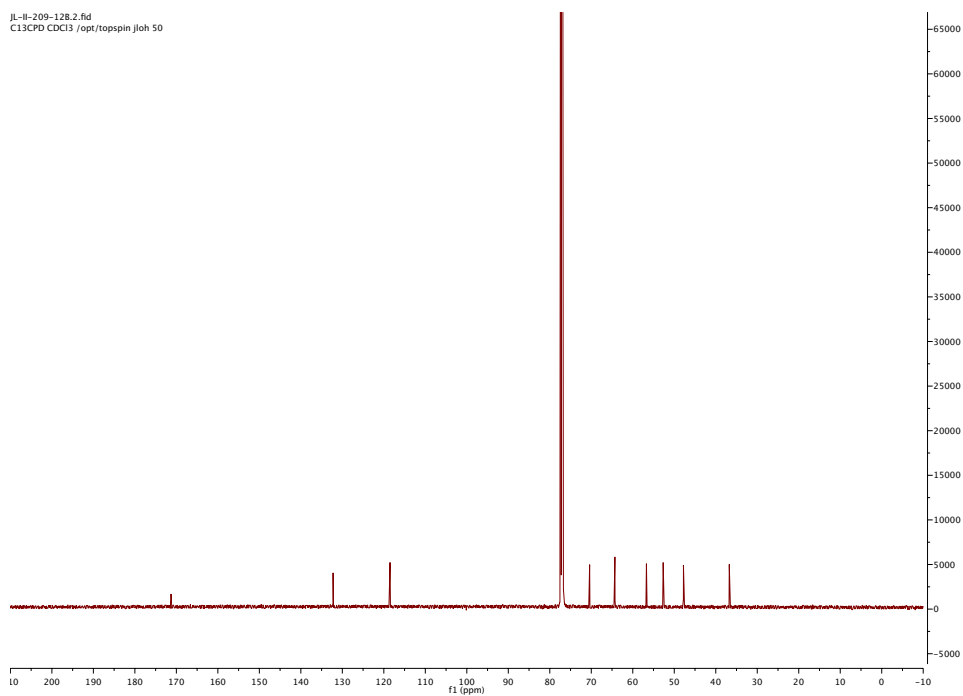


(8*R*,9*aS*)-2-allyl-8-hydroxyhexahydropyrrolo[2,1-*d*][1,2,5]thiadiazepin-1(2*H*)-one 3,3-dioxide (4.1.4{10,7})

JL-II-209-128.1.fid
PROTON CDCl₃ /opt/topspin/jloh 50

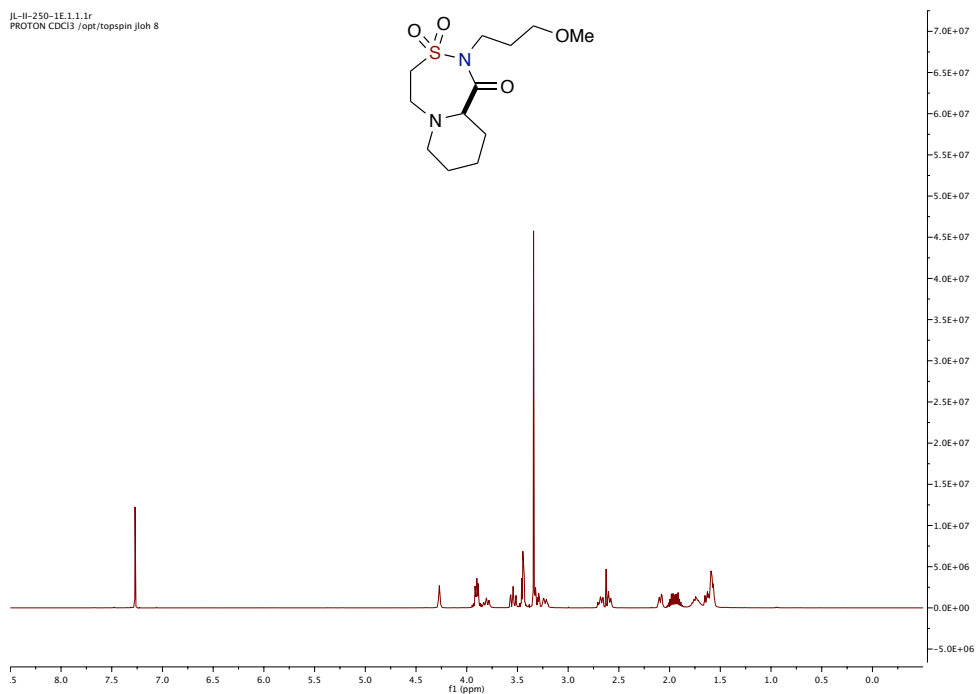
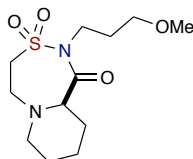


JL-II-209-128.2.fid
C13CPD CDCl₃ /opt/topspin/jloh 50

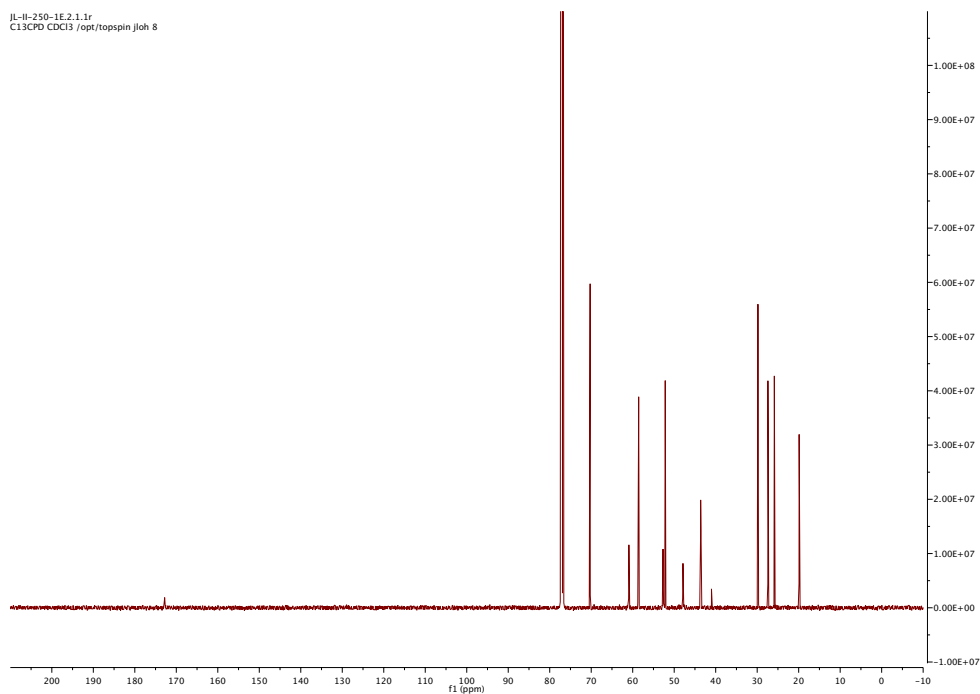


(R)-2-(3-methoxypropyl)octahydro-1H-pyrido[2,1-d][1,2,5]thiadiazepin-1-one 3,3-dioxide (4.1.4{1,4})

JL-II-250-1E.1.1.1r
PROTON CDCl3 /opt/topspin jloh 8



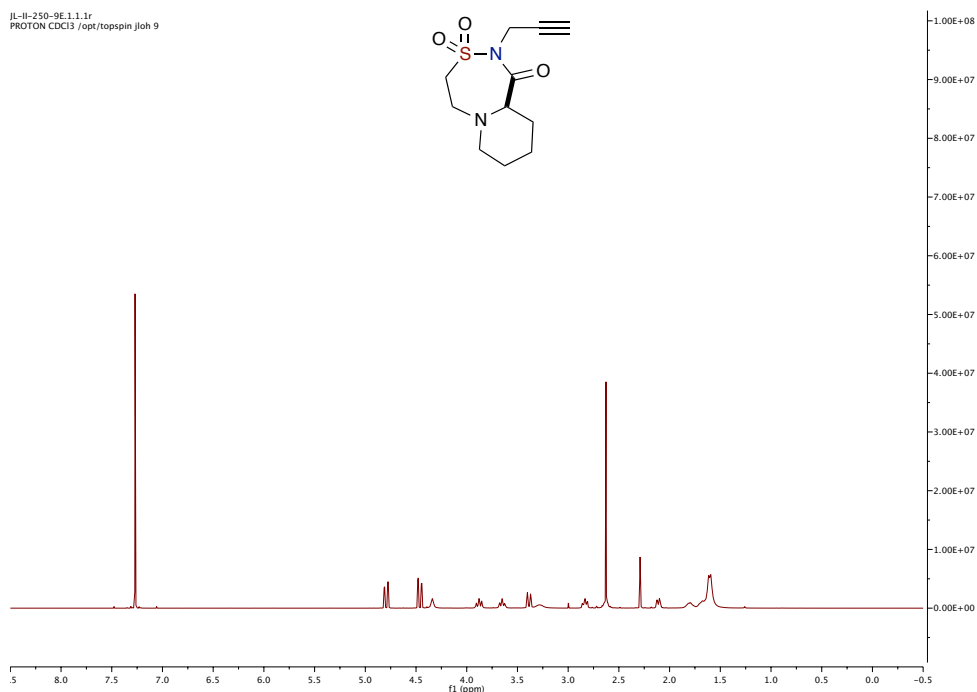
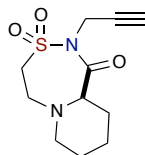
JL-II-250-1E.2.1.1r
C13CPD CDCl3 /opt/topspin jloh 8



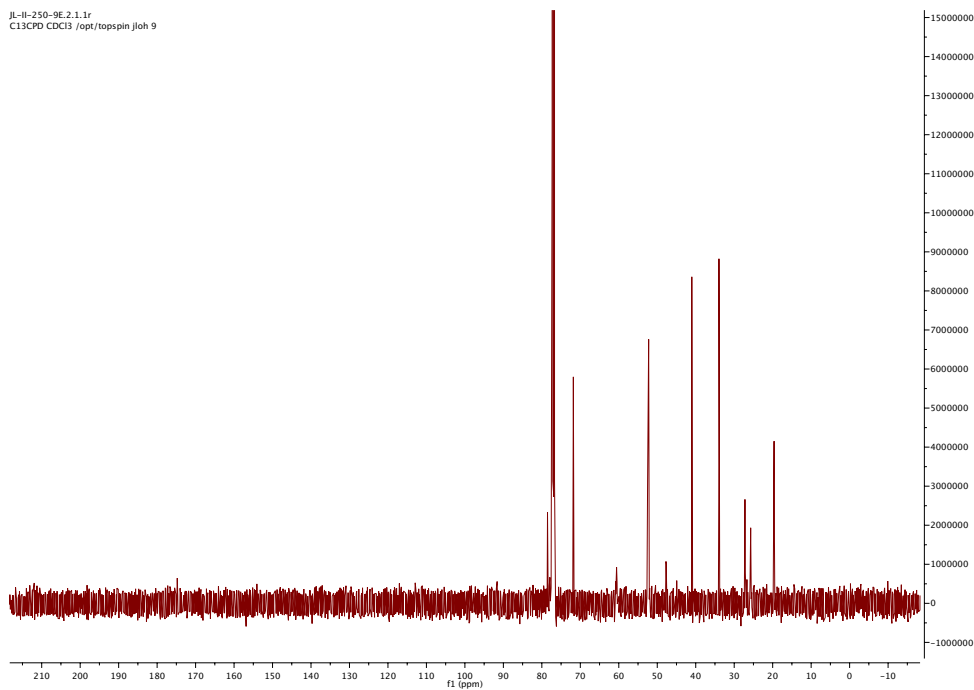
(R)-2-(prop-2-yn-1-yl)octahydro-1H-pyrido[2,1-d][1,2,5]thiadiazepin-1-one dioxide (4.1.4{7,4})

3,3-

JL-II-250-9E.1.1.1r
PROTON CDCl3 /opt/topspin jloh 9

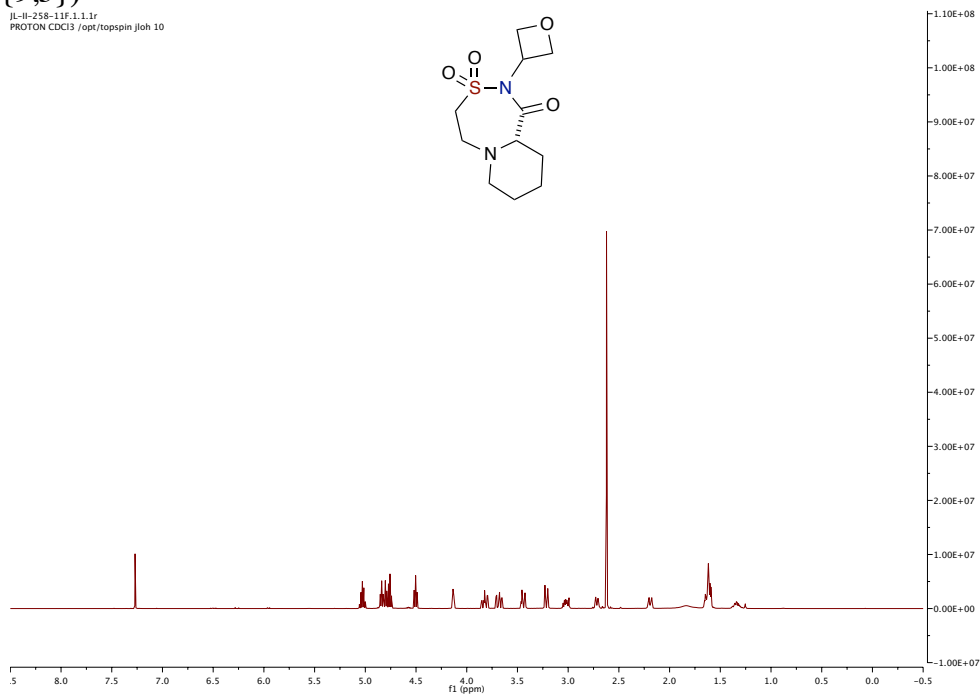
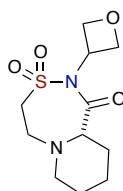


JL-II-250-9E.2.1.1r
C13CPD CDCl3 /opt/topspin jloh 9

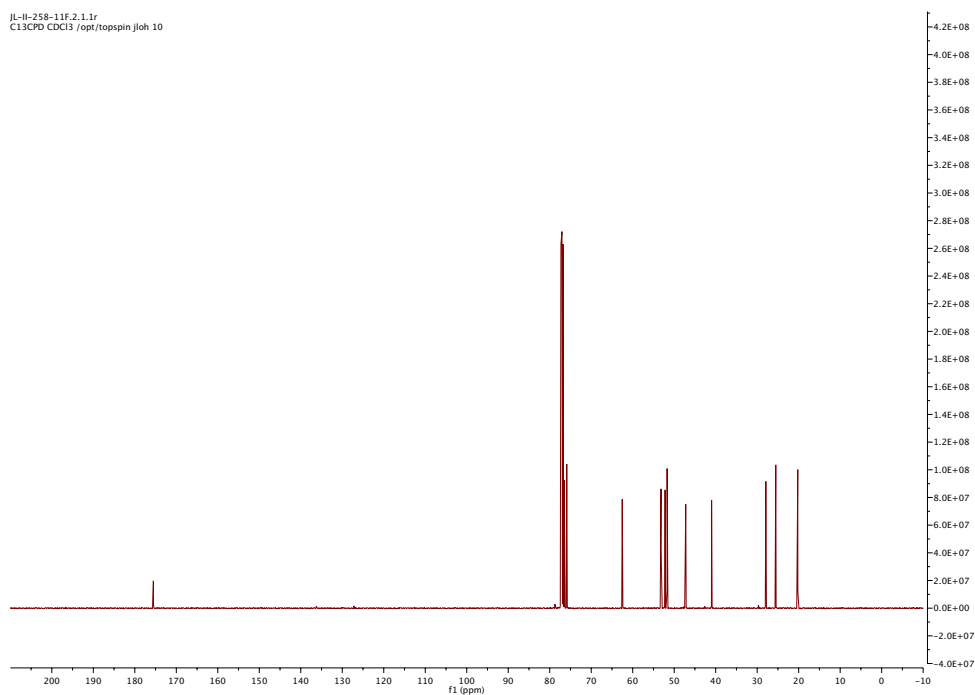


(S)-2-(oxetan-3-yl)octahydro-1H-pyrido[2,1-d][1,2,5]thiadiazepin-1-one 3,3-dioxide
(4.1.4{9,5})

JL-H-258-11F.1.1.1r
PROTON CDCl3 /opt/topspin jlloh 10



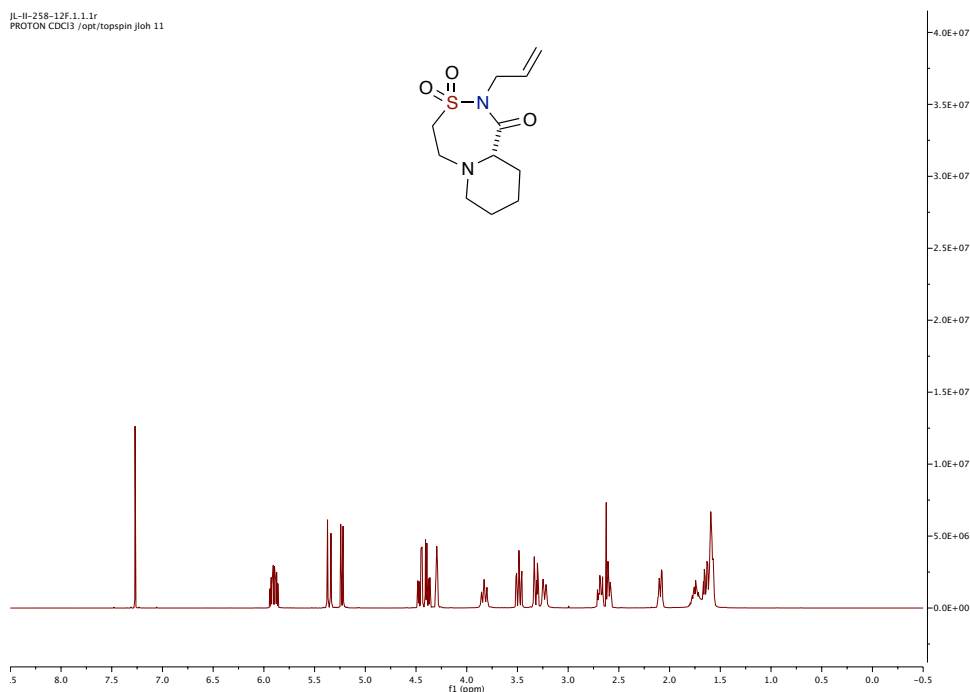
JL-H-258-11F.2.1.1r
C13CPD CDCl3 /opt/topspin jlloh 10



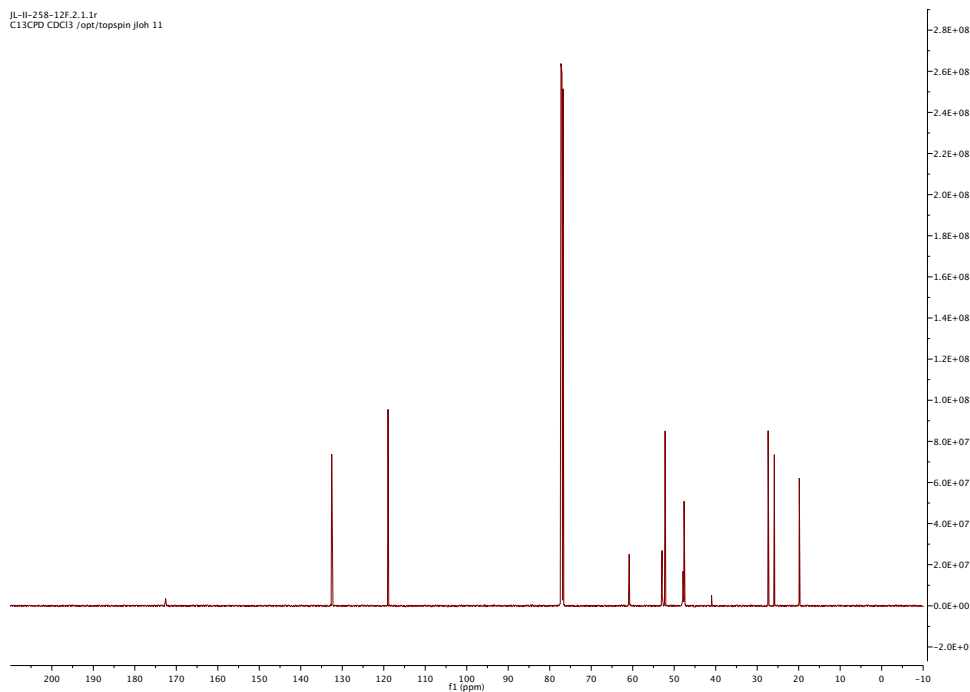
(S)-2-allyloctahydro-1H-pyrido[2,1-d][1,2,5]thiadiazepin-1-one
(4.1.4{10,5})

3,3-dioxide

JL-II-258-12F.1.1.1r
PROTON CDCl3 /opt/topspin jloh 11

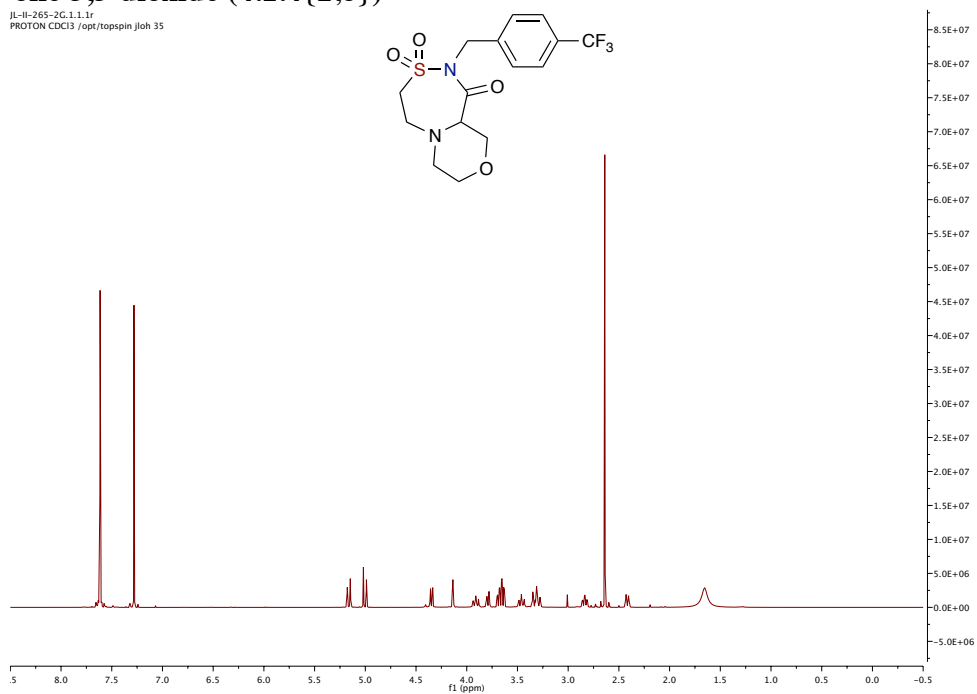
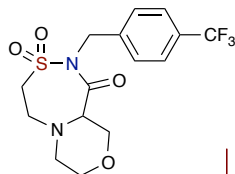


JL-II-258-12F.2.1.1r
C13CPD CDCl3 /opt/topspin jloh 11

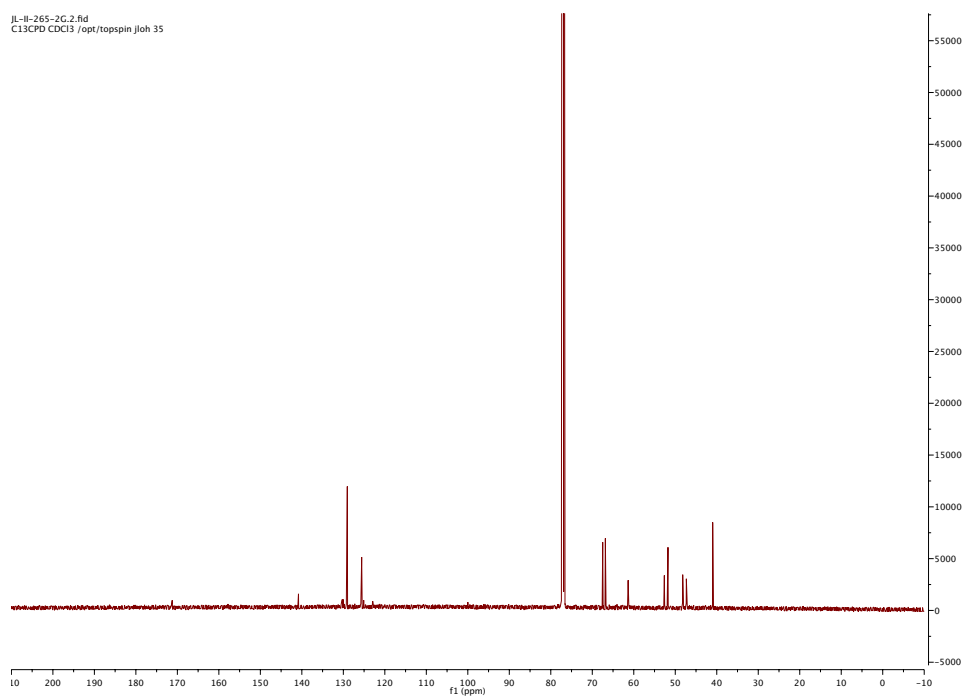


2-(4-(trifluoromethyl)benzyl)hexahydro-[1,4]oxazino[3,4-d][1,2,5]thiadiazepin-1(2H)-one 3,3-dioxide (4.1.4{2,8})

JL-II-265-2C.1.1.1r
PROTON CDCl3 /opt/topspin/jloh 35

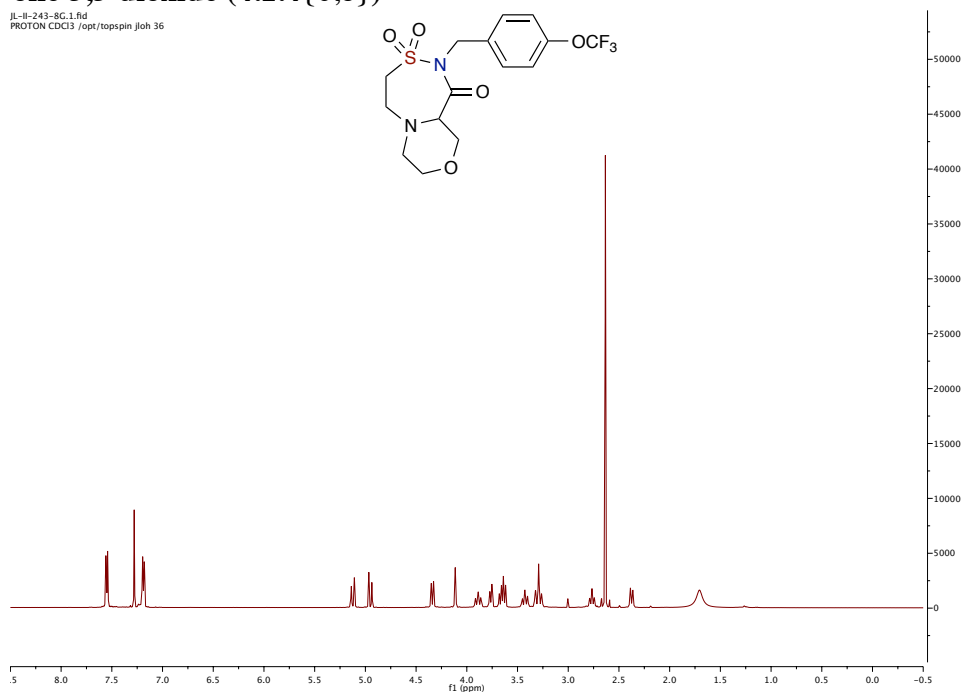
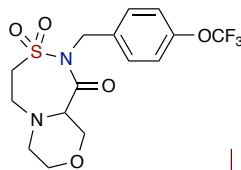


JL-II-265-2C.2.fid
C13CPD CDCl3 /opt/topspin/jloh 35

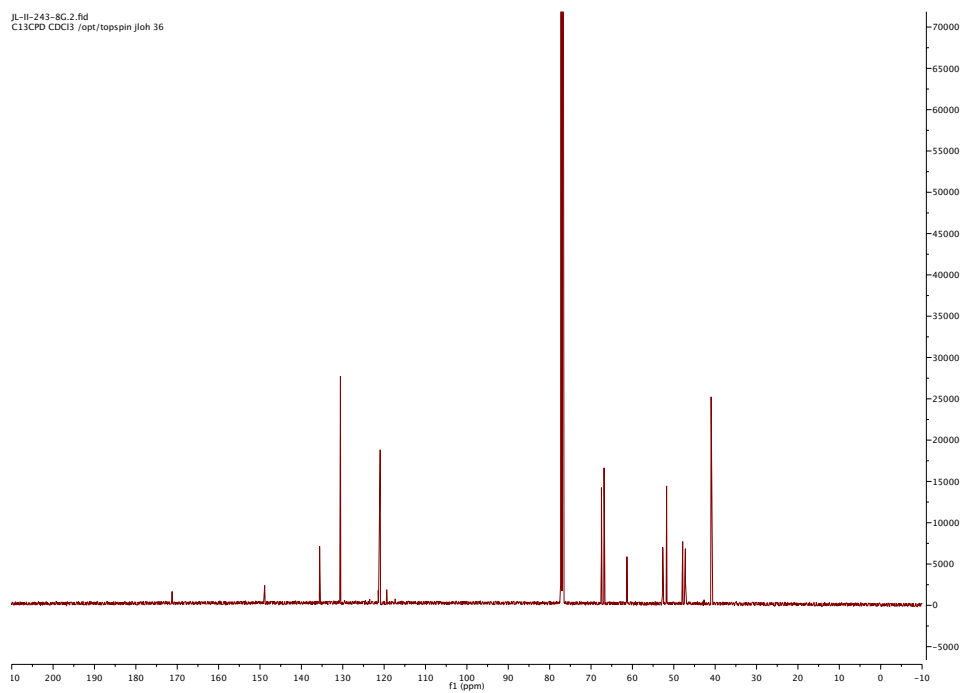


2-(4-(trifluoromethoxy)benzyl)hexahydro-[1,4]oxazino[3,4-d][1,2,5]thiadiazepin-1(2H)-one 3,3-dioxide (4.1.4{6,8})

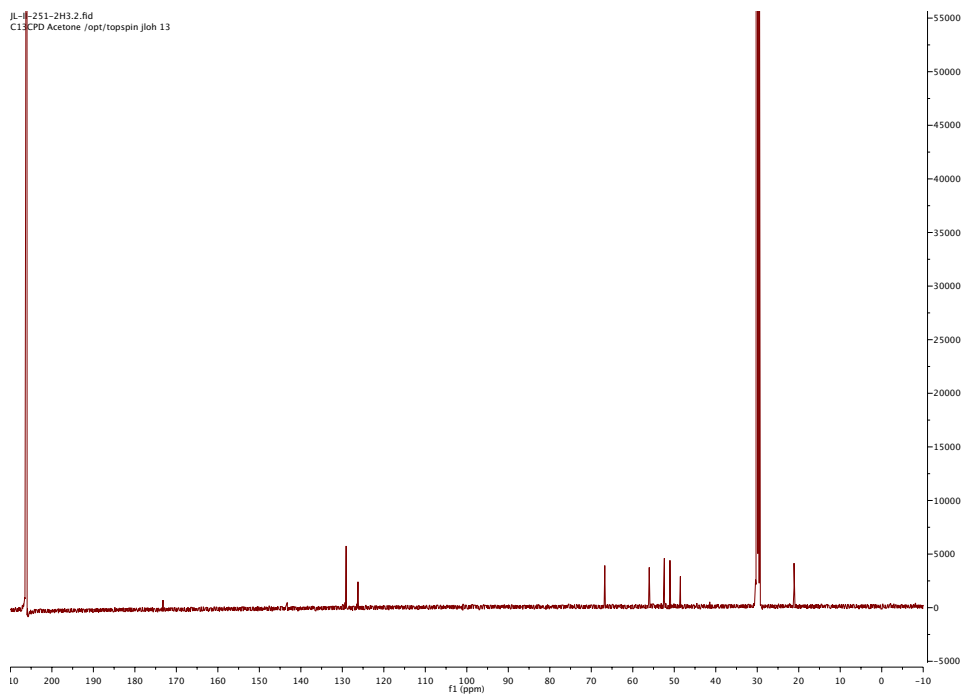
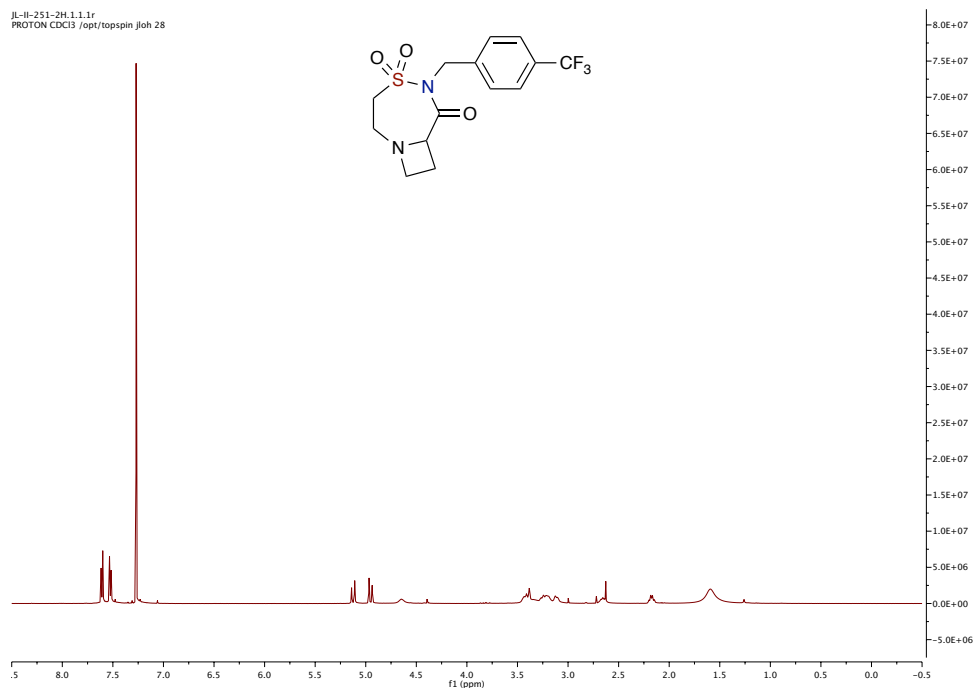
JL-II-243-8G.1.fid
PROTON CDCl3 /opr/topspin jloh 36



JL-II-243-8G.2.fid
C13CPD CDCl3 /opr/topspin jloh 36

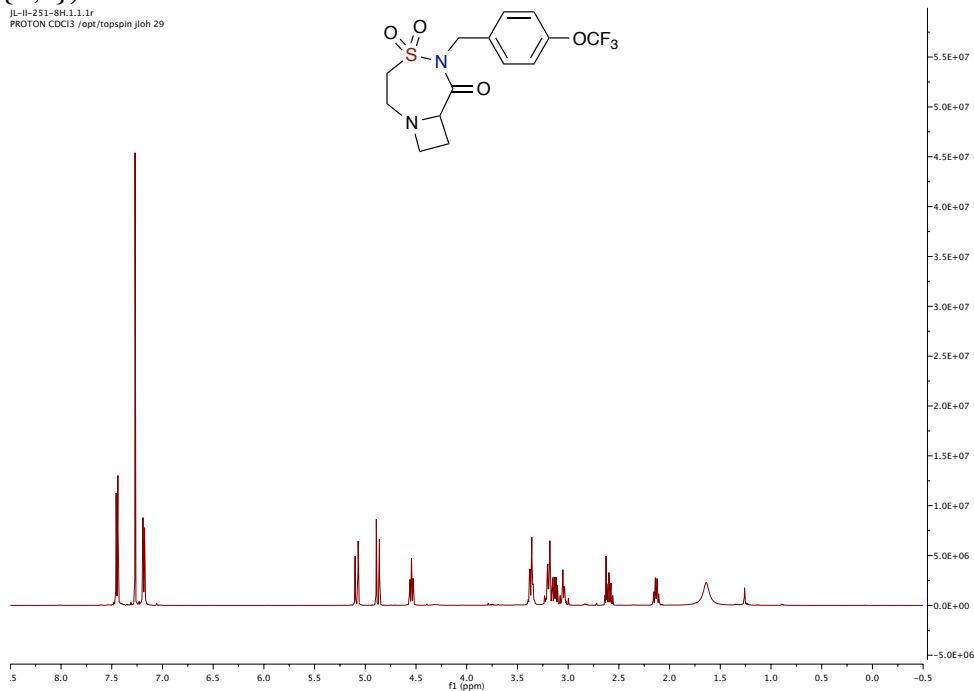
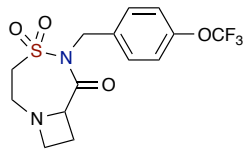


5-(4-(trifluoromethyl)benzyl)-4-thia-1,5-diazabicyclo[5.2.0]nonan-6-one 4,4-dioxide (4.1.4{2,1})

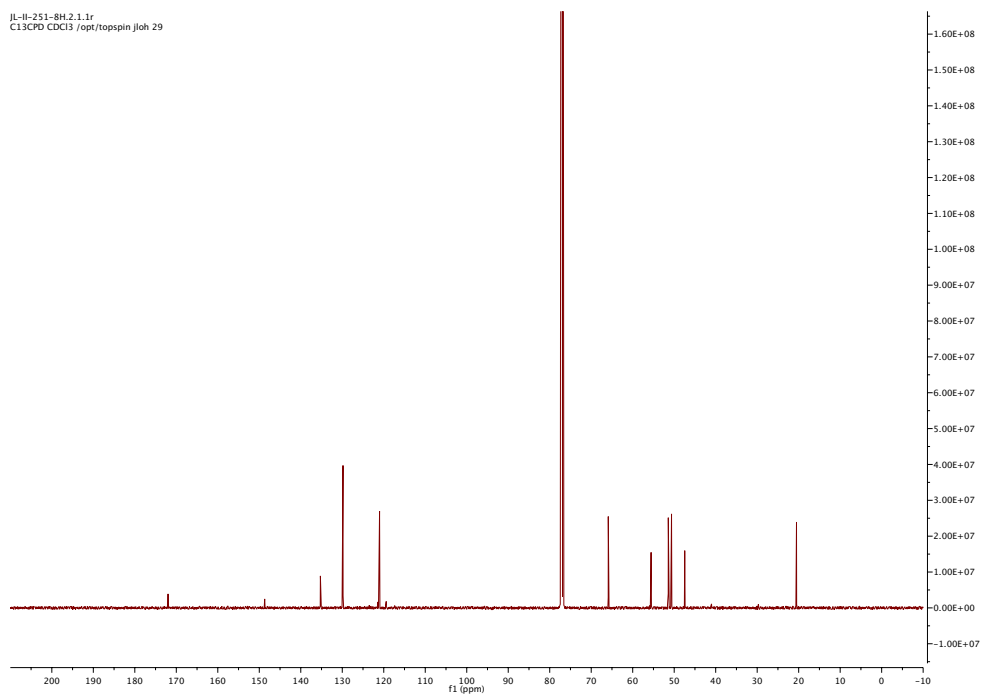


5-(4-(trifluoromethoxy)benzyl)-4-thia-1,5-diazabicyclo[5.2.0]nonan-6-one 4,4-dioxide
(4.1.4{6,1})

JL-H-251-8H.1.1.1r
PROTON CDCl3 /opt/topspin/jloh 29

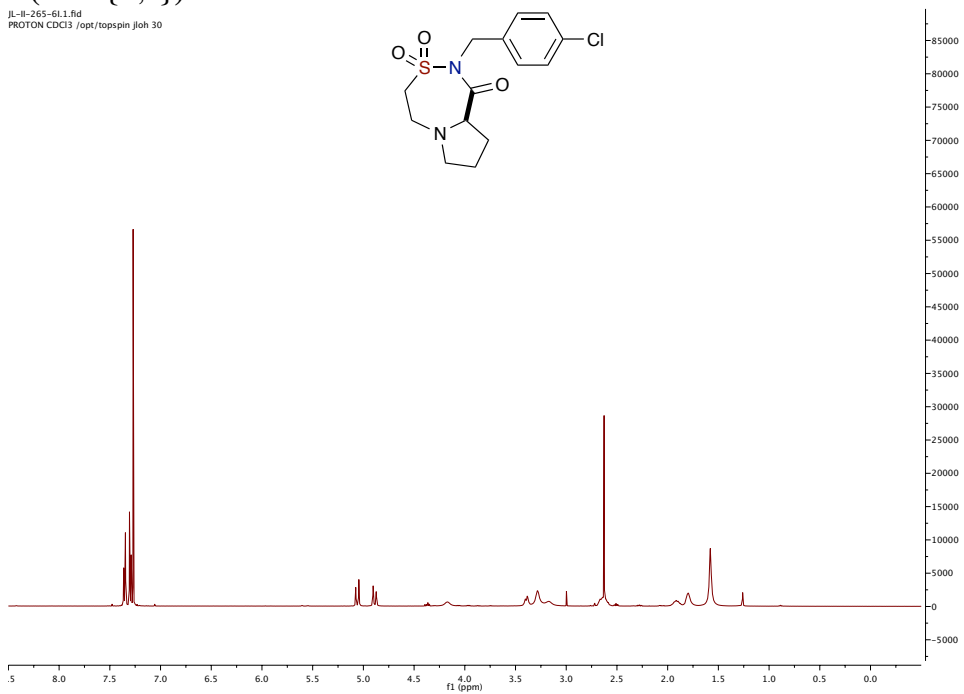
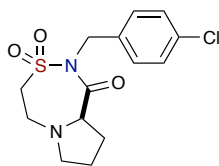


JL-H-251-8H.2.1.1r
C13CPD CDCl3 /opt/topspin/jloh 29

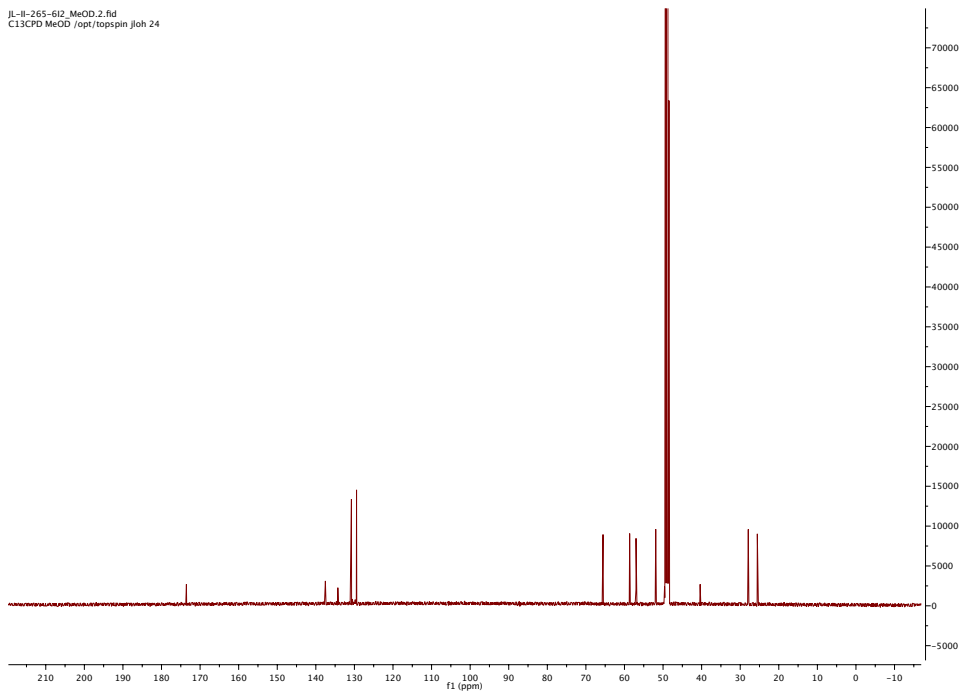


(R)-2-(4-chlorobenzyl)hexahydropyrrolo[2,1-d][1,2,5]thiadiazepin-1(2H)-one 3,3-dioxide (4.1.4{4,2})

JL-II-265-61.1.fid
PROTON CDCl3 /opt/topspin/jloh 30

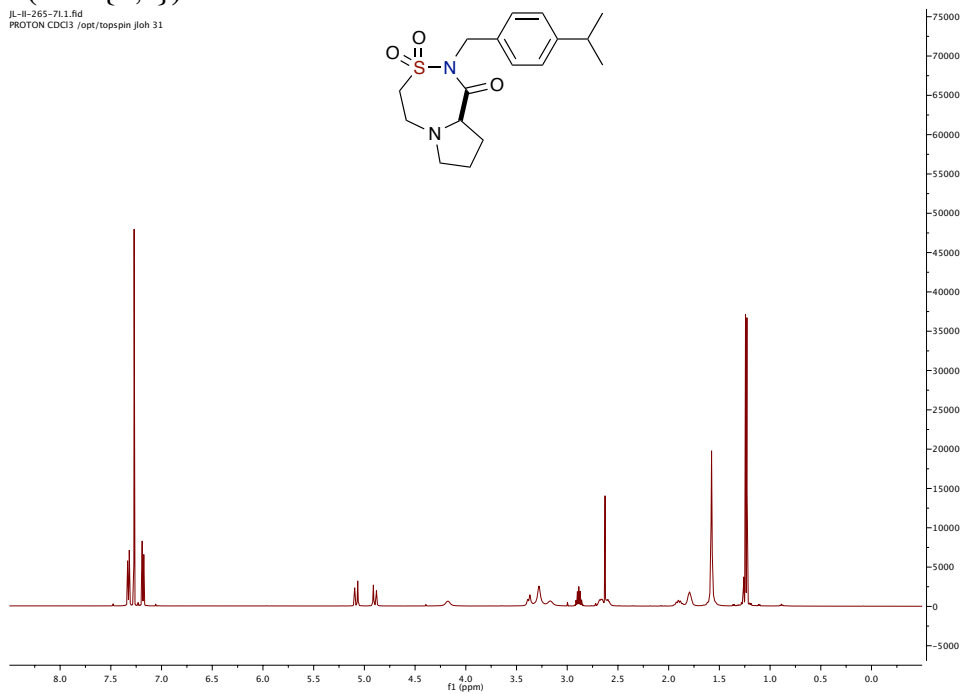
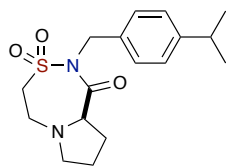


JL-II-265-612_MeOD.2.fid
C13CPD MeOD /opt/topspin/jloh 24

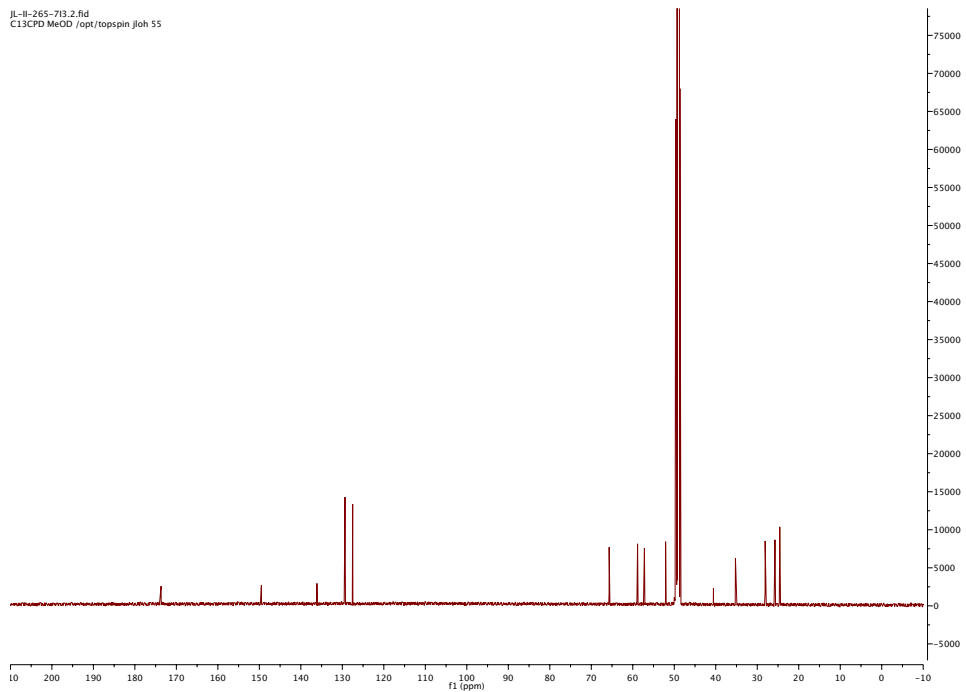


(R)-2-(4-isopropylbenzyl)hexahydropyrrolo[2,1-d][1,2,5]thiadiazepin-1(2H)-one 3,3-dioxide (4.1.4{5,2})

JL-II-265-711.1.fid
PROTON CDCl3 /opt/topspin jlsh 31

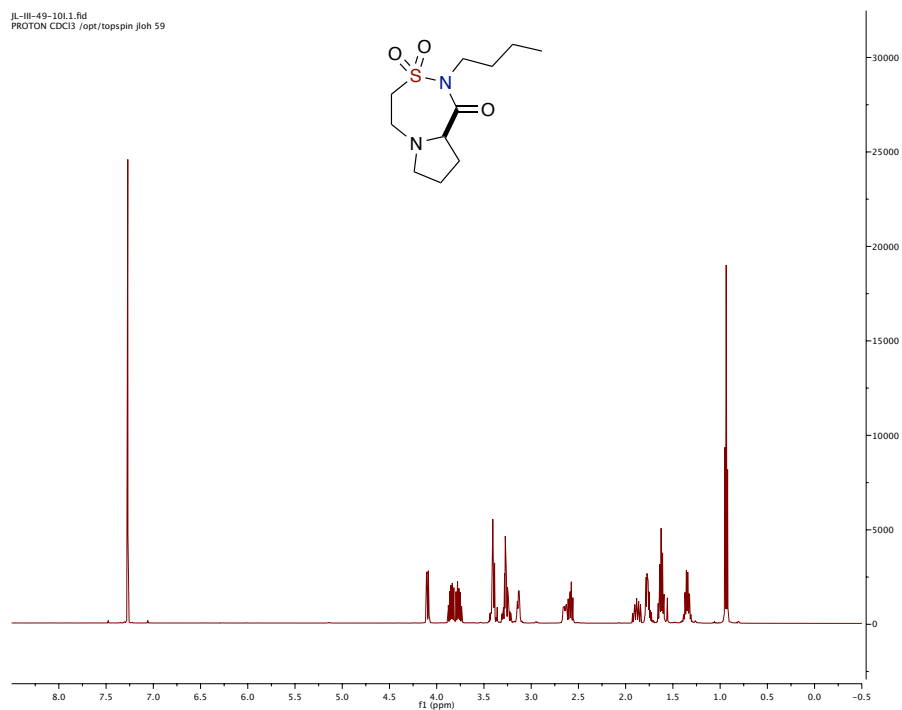


JL-II-265-713.2.fid
C13CPD MeOD /opt/topspin jlsh 55

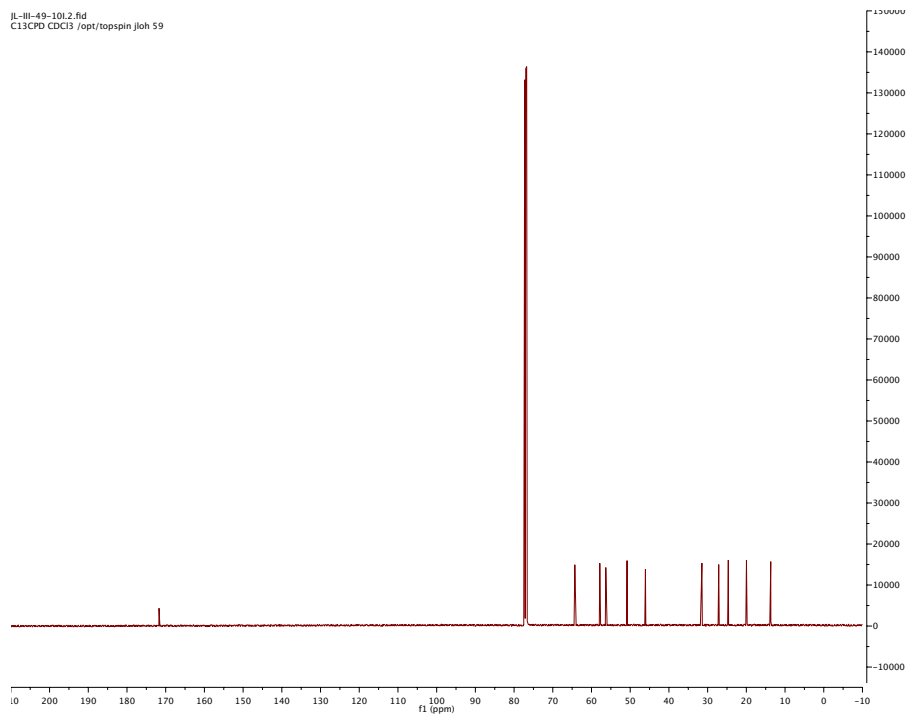


(R)-2-butylhexahydropyrrolo[2,1-d][1,2,5]thiadiazepin-1(2H)-one 3,3-dioxide
(4.1.4{8,2})

JL-III-49-101.1.fid
PROTON CDC13 /opt/topspin/jloh 59

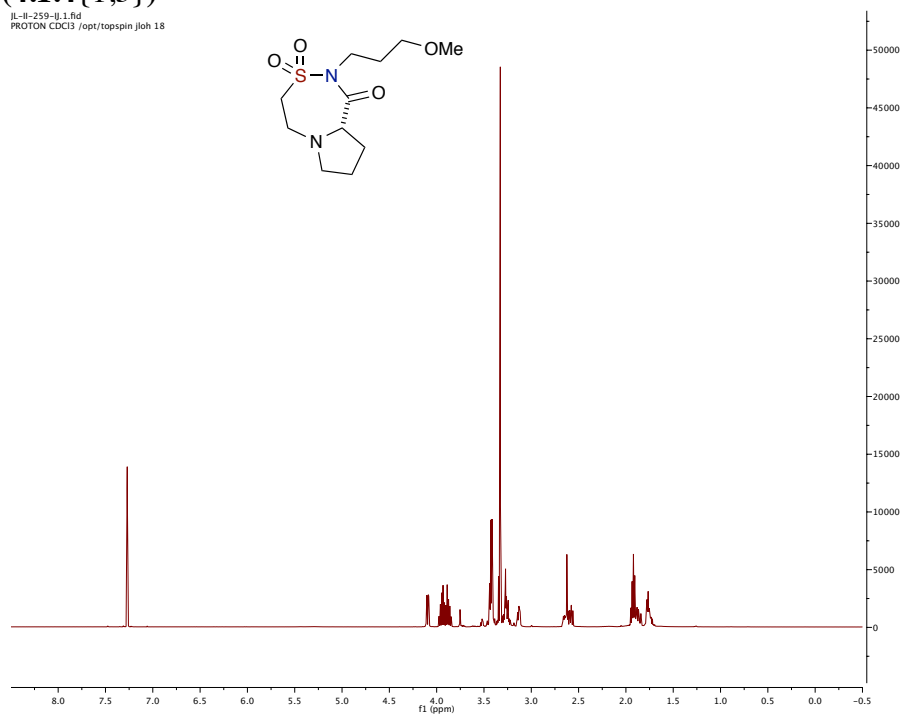


JL-III-49-101.2.fid
C13CPD CDC13 /opt/topspin/jloh 59

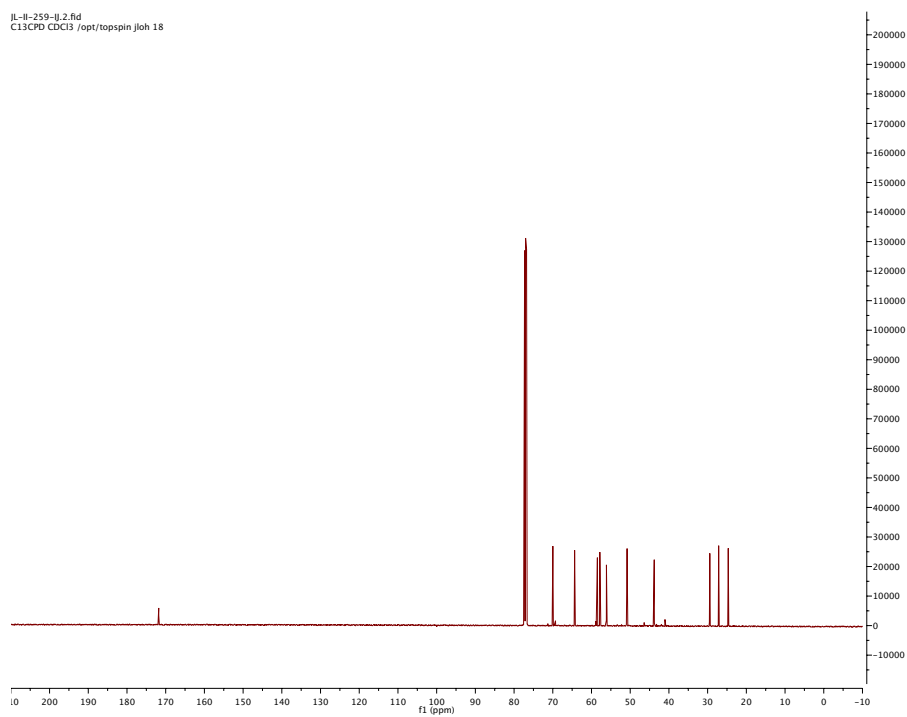


(S)-2-(3-methoxypropyl)hexahydropyrrolo[2,1-d][1,2,5]thiadiazepin-1(2H)-one 3,3-dioxide (4.1.4{1,3})

jl-ll-259-ll.1.fid
PROTON CDCI3 /opt/topspin/jloh 18

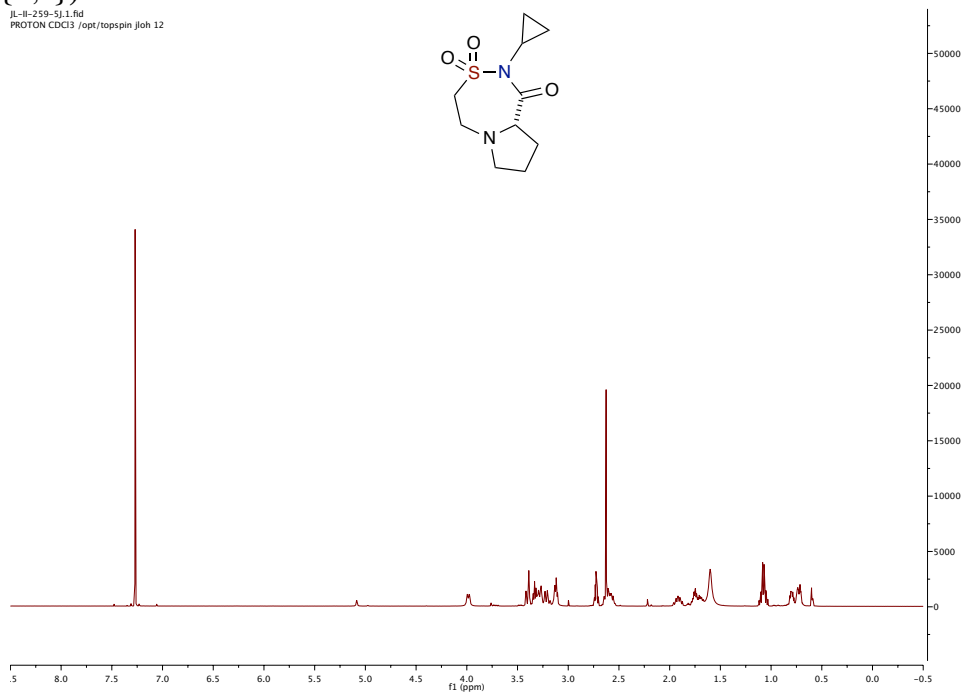
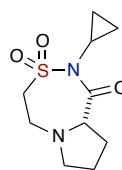


jl-ll-259-ll.2.fid
C13CPD CDCI3 /opt/topspin/jloh 18

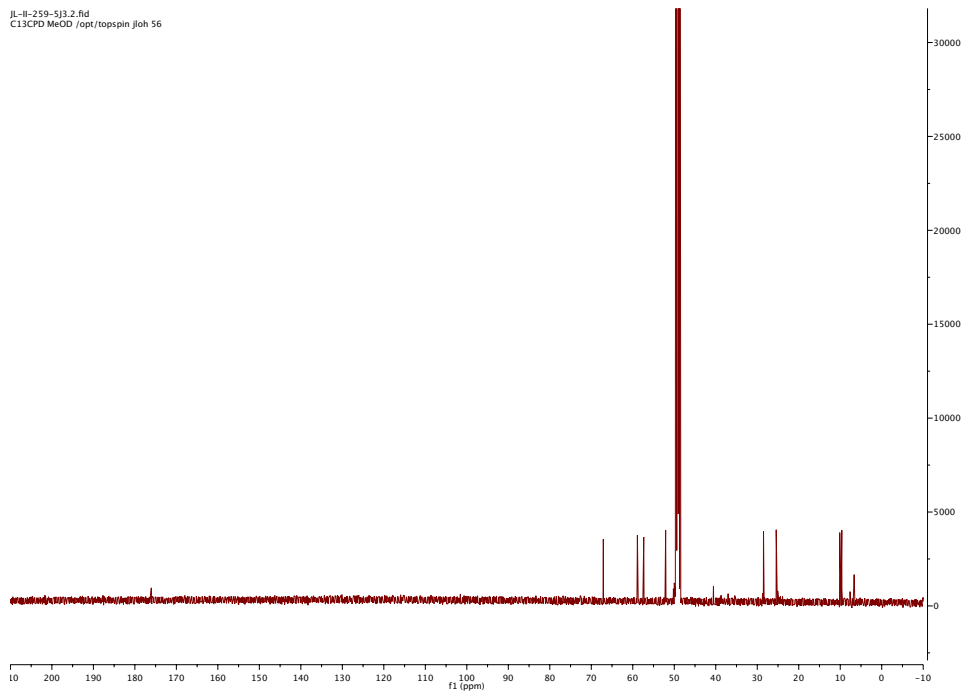


(S)-2-cyclopropylhexahydropyrrolo[2,1-d][1,2,5]thiadiazepin-1(2H)-one 3,3-dioxide
(4.1.4{3,3})

JL-II-259-Sj3.1.fid
PROTON CDCl3 /opt/topspin/jloh 12

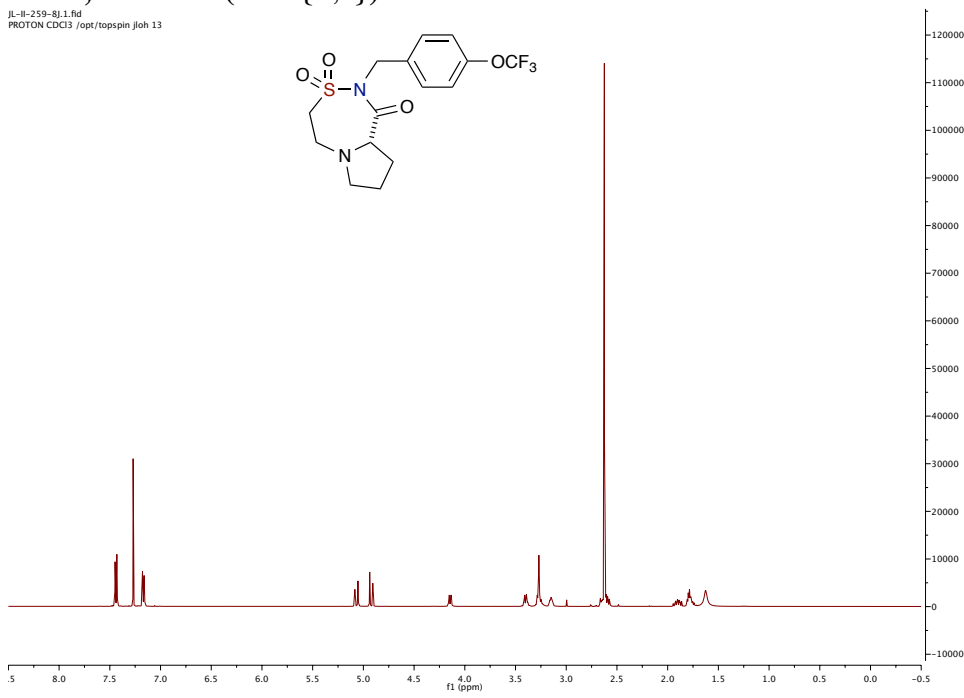
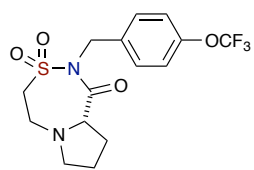


JL-II-259-Sj3.2.fid
C13CPD MeOD /opt/topspin/jloh 56

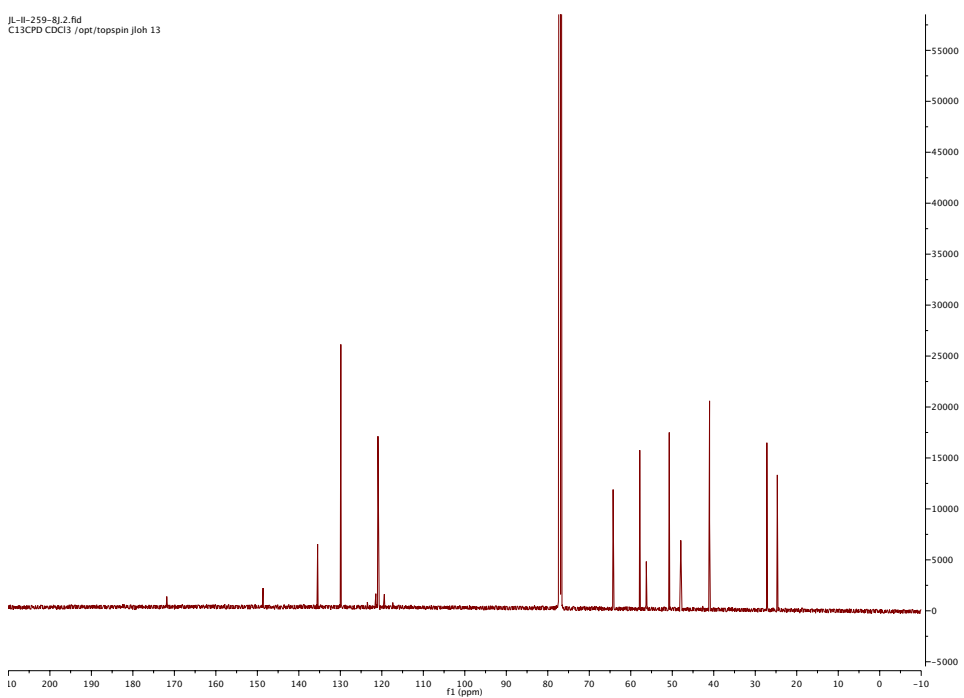


(S)-2-(4-(trifluoromethoxy)benzyl)hexahydropyrrolo[2,1-d][1,2,5]thiadiazepin-1(2H)-one 3,3-dioxide (4.1.4{6,3})

JL-II-259-8j.1.fid
PROTON CDCl3 /opt/topspin/jloh 13

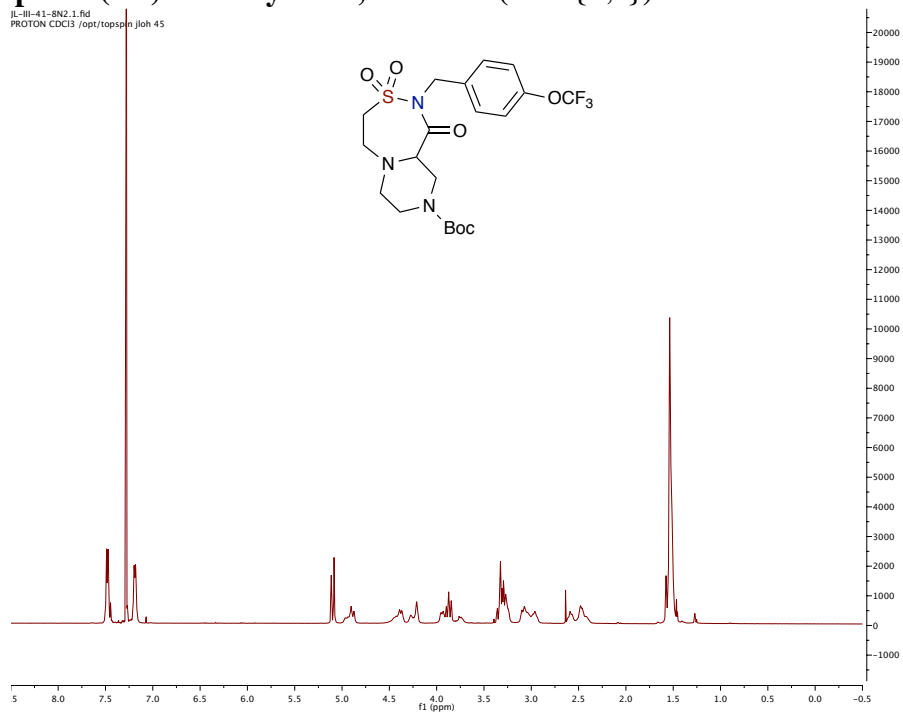


JL-II-259-8j.2.fid
C13CPD CDCl3 /opt/topspin/jloh 13

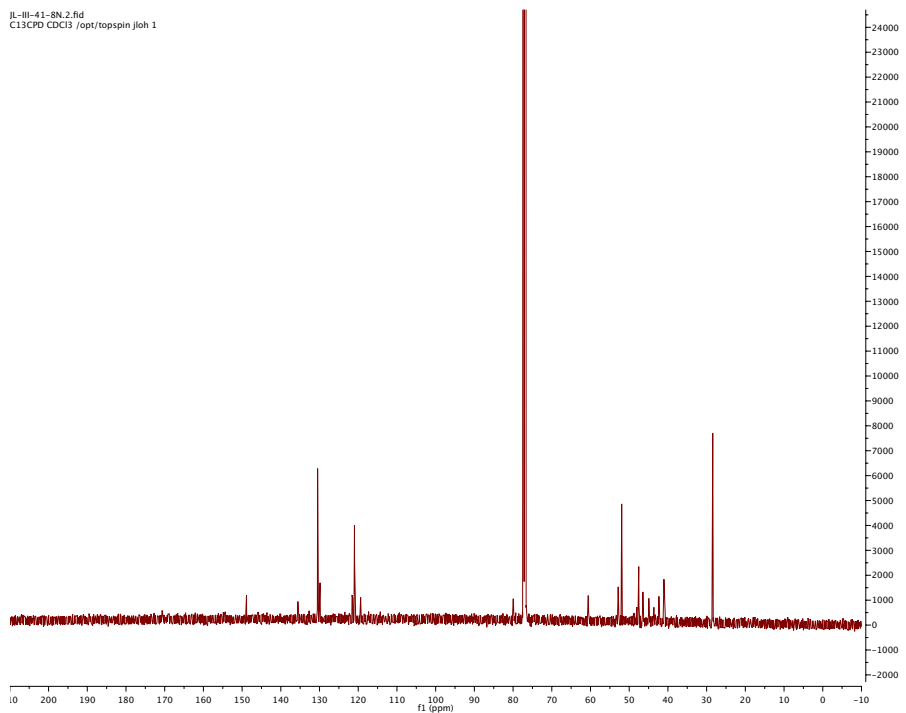


***tert*-butyl 1-oxo-2-(4-(trifluoromethoxy)benzyl)hexahydro-1*H*-pyrazino[2,1-*d*][1,2,5]-thiadiazepine-9(2*H*)-carboxylate 3,3-dioxide (4.1.4{6,9})**

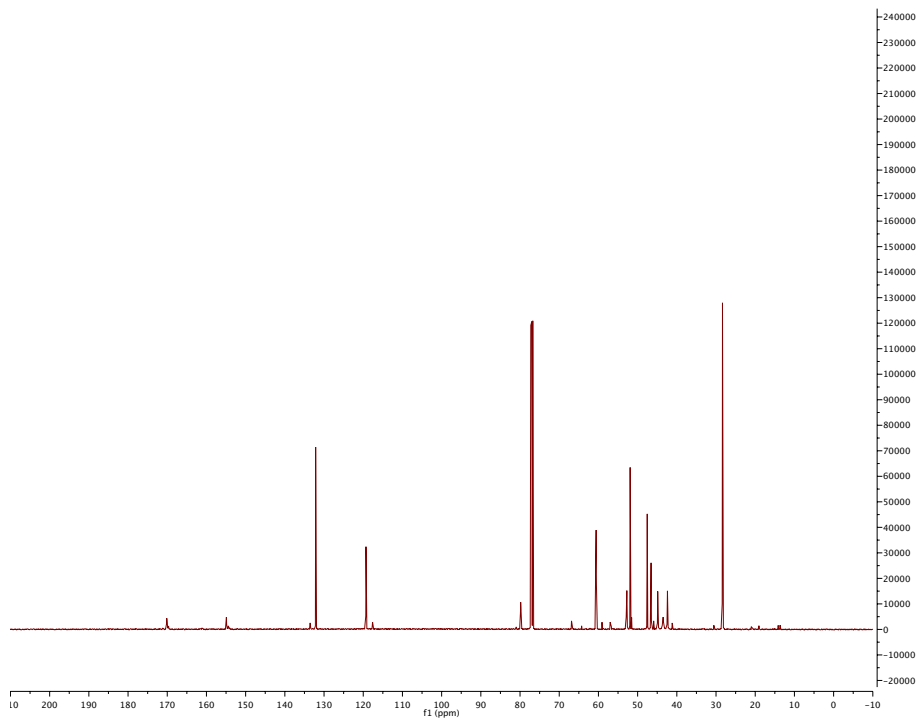
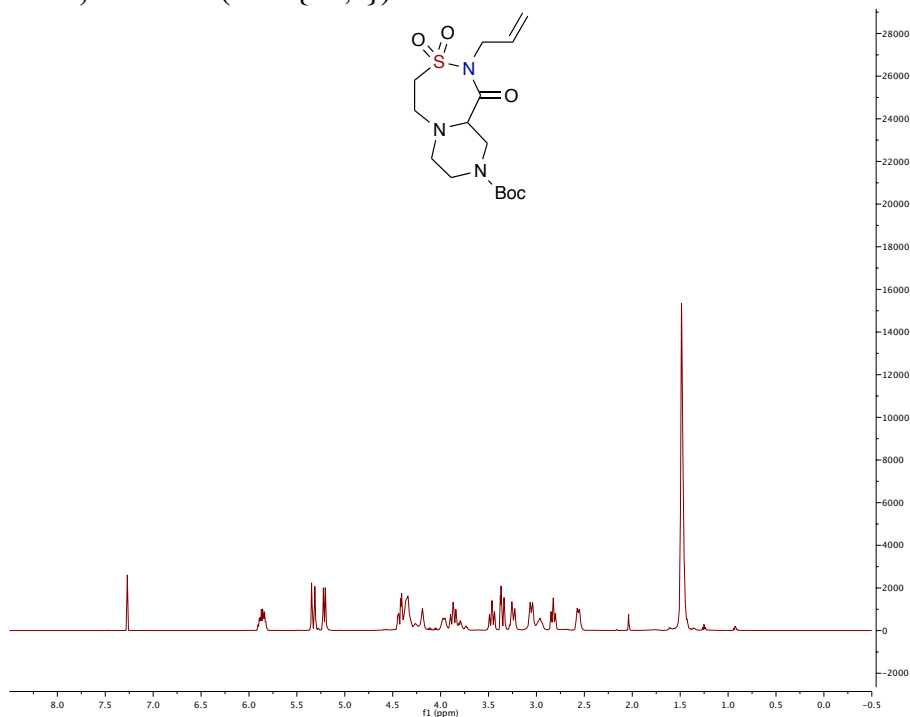
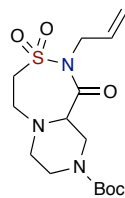
jl-III-41-SN2.1.fid
PROTON CDCl3 /opt/topspin jlsh 45



jl-III-41-SN.2.fid
C13CPD CDCl3 /opt/topspin jlsh 1



***tert*-butyl 2-allyl-1-oxohexahydro-1*H*-pyrazino[2,1-*d*][1,2,5]thiadiazepine-9(2*H*)-carboxylate 3,3-dioxide (4.1.4{10,9})**



Molecule	HRMS Expected M/z (M) ⁺	HRMS Found M/z (M+H) ⁺	Mass (mg)	Purity (%)
4.1.4{1,6}	292.1093	293.1342	21.8	90.1
4.1.4{2,6}	378.0861	379.0901	105.4	93.0
4.1.4{4,6}	344.0598	345.0694	36.3	90.0
4.1.4{5,6}	352.1457	353.1527	40.4	93.7
4.1.4{6,6}	394.0810	395.0869	66.0	97.9
4.1.4{7,6}	258.0674	-	-	-
4.1.4{8,6}	276.1144	277.1385	43.5	90.1
4.1.4{9,6}	276.0780	277.0840	33.9	100
4.1.4{10,6}	260.0831	261.1055	10.2	52.0
4.1.4{1,7}	292.1093	293.1190	11.1	90.0
4.1.4{2,7}	378.0861	379.0935	19.5	100
4.1.4{3,7}	260.0831	261.0893	38.9	90.6
4.1.4{4,7}	344.0598	345.0662	70.3	98.7
4.1.4{5,7}	352.1457	353.1518	42.2	96.1
4.1.4{6,7}	394.0810	395.0885	142.7	94.7
4.1.4{7,7}	258.0674	259.0735	118.6	92.2
4.1.4{8,7}	276.1144	277.1204	28.6	93.2
4.1.4{9,7}	276.0780	277.0837	129.2	100
4.1.4{10,7}	260.0831	261.0894	112.4	94.5
4.1.4{1,4}	290.1300	291.1388	119.0	96.0
4.1.4{2,4}	376.1068	377.1151	107.8	100
4.1.4{3,4}	258.1038	259.1096	19.6	100
4.1.4{4,4}	342.0805	343.0888	121.0	97.1
4.1.4{5,4}	350.1664	351.1736	28.1	94.9
4.1.4{6,4}	392.1018	393.1090	129.8	98.4
4.1.4{7,4}	256.0882	257.0960	163.8	93.0
4.1.4{8,4}	274.1351	275.1406	56.4	86.7
4.1.4{9,4}	274.0987	275.1081	59.8	98.8
4.1.4{10,4}	258.1038	259.1118	83.3	98.8
4.1.4{1,5}	290.1300	291.1398	39.5	100
4.1.4{2,5}	376.1068	377.1159	54.1	100
4.1.4{3,5}	258.1038	259.1097	35.0	97.6
4.1.4{4,5}	342.0805	343.0895	88.7	95.3
4.1.4{5,5}	350.1664	351.1737	142.1	91.4
4.1.4{6,5}	392.1018	393.1095	17.7	100
4.1.4{7,5}	256.0881	257.0954	178.9	100
4.1.4{8,5}	274.1351	275.1428	89.6	100
4.1.4{9,5}	274.0987	275.1075	109.3	98.8
4.1.4{10,5}	258.1038	259.1117	140.6	97.9
4.1.4{1,8}	292.1092	293.1186	50.4	100

4.1.4{2,8}	378.0861	379.0962	111.1	93.7
4.1.4{3,8}	260.0831	261.0890	29.5	96.1
4.1.4{4,8}	344.0598	345.0701	8.6	90.8
4.1.4{5,8}	352.1457	353.1554	84.6	97.9
4.1.4{6,8}	394.0810	395.0913	177.9	97.2
4.1.4{7,8}	258.0674	259.0759	-	-
4.1.4{8,8}	276.1144	277.1225	35.3	90.0
4.1.4{9,8}	276.0780	277.0822	68.1	100
4.1.4{10,8}	260.0831	-	-	-
4.1.4{1,1}	262.0987	263.1051	58.1	44.0
4.1.4{2,1}	348.0755	349.0836	151.8	97.6
4.1.4{3,1}	230.0725	231.0807	50.9	90.5
4.1.4{4,1}	314.0492	315.0560	94.1	92.7
4.1.4{5,1}	322.1351	323.1425	67.0	97.3
4.1.4{6,1}	364.0705	365.0791	111.8	95.8
4.1.4{7,1}	228.0569	229.0642	3.4	98.9
4.1.4{8,1}	246.1038	247.1119	8.1	90.0
4.1.4{9,1}	246.0674	-	-	-
4.1.4{10,1}	230.0725	231.0798	22.2	100
4.1.4{1,2}	276.1144	277.1212	254.2	91.7
4.1.4{2,2}	362.0912	363.0969	212.5	93.7
4.1.4{3,2}	244.0882	245.0984	115.0	98.9
4.1.4{4,2}	328.0648	329.0753	134.6	100
4.1.4{5,2}	336.1508	337.1581	182.0	100
4.1.4{6,2}	378.0861	379.0934	294.0	96.2
4.1.4{7,2}	242.0725	243.0789	18.7	81.4
4.1.4{8,2}	260.1195	261.1294	34.3	90.2
4.1.4{9,2}	260.0831	261.0898	6.3	87.0
4.1.4{10,2}	244.0882	245.0962	1.9	70.1
4.1.4{1,3}	276.1144	277.1233	147.5	95.3
4.1.4{2,3}	362.0912	363.0984	169.8	96.1
4.1.4{3,3}	244.0882	245.0980	67.8	94.0
4.1.4{4,3}	328.0648	329.0736	157.4	100
4.1.4{5,3}	336.1508	337.1537	133.2	92.5
4.1.4{6,3}	378.0861	379.0945	230.5	97.1
4.1.4{7,3}	242.0725	243.0823	73.0	90.3
4.1.4{8,3}	260.1195	261.1297	18.0	95.6
4.1.4{9,3}	260.0831	261.0927	38.7	92.0
4.1.4{10,3}	244.0882	245.0957	126.0	92.1
4.1.4{1,9}	391.1777	392.1824	94.0	100
4.1.4{2,9}	477.1545	478.1597	9.3	83.7
4.1.4{3,9}	359.1515	360.1583	46.8	92.2

4.1.4 {4,9}	443.1282	444.1336	74.5	96.6
4.1.4 {5,9}	451.2141	452.2207	84.0	91.6
4.1.4 {6,9}	493.1494	494.1595	195.1	91.3
4.1.4 {7,9}	357.1358	358.1418	257.9	95.4
4.1.4 {8,9}	375.1828	376.188	99.2	93.1
4.1.4 {9,9}	375.1464	376.1509	171.9	100
4.1.4 {10,9}	359.1515	360.1563	75.4	98.8

In-Silico Analysis

Sketched electronic versions of the library compounds were imported into the Tripos Molecular Spreadsheet [2] wherein standard Lipinski Rule of 5 parameters (molecular weight, ClogP, number of H-acceptors, and number of H-donors [3]) plus the number of rotatable bonds and polar surface area were computed. Lipinski violations were specified according to molecular weight > 500, ClogP > 5.0, number of acceptors > 10, number of donors > 5, and number of rotatable bonds > 5. The structures were then exported into SDF format and converted into three-dimensional protonated structures via Concord [5]. Absorption, distribution, metabolism and excretion (ADME) profiles of these compounds was then generated via Volsurf [5]. Descriptors were generated using three probes (water, hydrophobic and carbonyl oxygen) with a grid space distribution of 1.0 Å. Predictions were then projected onto internal ADME models at the 5-component level. Finally diversity analysis was carried out using DiverseSolutions [6] using standard H-aware 3D BCUT descriptors. The library was then projected onto a chemical space defined by the following descriptors: gastchrg_invdist2_000.550_K_L, gastchrg_invdist6_000.500_K_H, haccept_invdist2_001.000_K_H, tabpolar_invdist_000.250_K_H, tabpolar_invdist_000.500_K_L and populated (for comparison) by a recent version of the MLSMR screening set (ca. 7/2010; ~330,000 unique chemical

structures). Diversity scores ($div(A)$) for our library were then generated for each of our compounds (A) according to the expression:

$$div(A) = \frac{pop[Cell(A)]}{\sum_{i \in Occ} pop(i) / N_{occ}}$$

where N_{occ} is the number of cells occupied by PubChem compounds in an evenly distributed $10 \times 10 \times 10 \times 10$ grid decomposition of the chemistry space, and $pop(i)$ is the population of cell i .

In-Silico Analysis

Molecule	nH BD on	nH BA cc	nR ot B	Top oPS A	MW	XL og P	caco2 (log[cm/s])	caco2 result	DMSO (ug/ml)	DMSO result	PAMPA (log[mol/{s.cm ² }])	PAMPA result
1H	0	6	4	75.3	262.0 98728 1	- 0.8 85	1.00	Good Permeation	0.75	Poor Solubility	2.13	Good Permeation
2H	0	5	3	66.0 7	348.0 75548	0.2 86	1.00	Good Permeation	0.75	Poor Solubility	10.38	Good Permeation
5H	0	5	1	66.0 7	230.0 72513 3	- 0.5 1	1.00	Good Permeation	0.80	Poor Solubility	0.62	Good Permeation
6H	0	5	2	66.0 7	314.0 49191	- 0.0 17	1.00	Good Permeation	0.82	Poor Solubility	9.42	Good Permeation
7H	0	5	3	66.0 7	322.1 35113 6	1.3 99	1.00	Good Permeation	0.72	Poor Solubility	1.26	Good Permeation
8H	0	6	4	75.3	364.0 70462 6	0.8 98	1.00	Good Permeation	0.68	Poor Solubility	2.49	Good Permeation
9H	0	5	1	66.0 7	228.0 56863 2	- 0.7 85	1.00	Good Permeation	0.73	Poor Solubility	4.87	Good Permeation
10H	0	5	3	66.0 7	246.1 03813 4	0.2 97	1.00	Good Permeation	0.74	Poor Solubility	2.19	Good Permeation
11H	0	6	1	75.3	246.0 67427 9	- 1.4 16	1.00	Good Permeation	0.75	Poor Solubility	5.12	Good Permeation
12H	0	5	2	66.0 7	230.0 72513 3	- 0.4 38	1.00	Good Permeation	0.83	Poor Solubility	0.47	Good Permeation
1I	0	6	4	75.3	276.1 14378 1	- 0.5 27	1.00	Good Permeation	0.76	Poor Solubility	1.79	Good Permeation
2I	0	5	3	66.0 7	362.0 91198 1	0.6 44	1.00	Good Permeation	0.77	Poor Solubility	0.93	Good Permeation

5I	0	5	1	66.0 7	244.0 88163 4	- 0.1 52	1.00	Good Permeation	0.86	Poor Solubility	1.96	Good Permeation
6I	0	5	2	66.0 7	328.0 64841 1	0.3 41	1.00	Good Permeation	0.79	Poor Solubility	9.26	Good Permeation
7I	0	5	3	66.0 7	336.1 50763 6	1.7 57	1.00	Good Permeation	0.74	Poor Solubility	0.85	Good Permeation
8I	0	6	4	75.3	378.0 86112 7	1.2 56	1.00	Good Permeation	0.67	Poor Solubility	2.92	Good Permeation
9I	0	5	1	66.0 7	242.0 72513 3	- 0.4 27	1.00	Good Permeation	0.80	Poor Solubility	5.79	Good Permeation
10I	0	5	3	66.0 7	260.1 19463 5	0.6 55	1.00	Good Permeation	0.80	Poor Solubility	9.32	Good Permeation
11I	0	6	1	75.3	260.0 83078	- 1.0 58	1.00	Good Permeation	0.82	Poor Solubility	5.88	Good Permeation
12I	0	5	2	66.0 7	244.0 88163 4	- 0.0 8	1.00	Good Permeation	0.99	Poor Solubility	6.31	Good Permeation
1J	0	6	4	75.3	276.1 14378 1	- 0.5 27	1.00	Good Permeation	0.68	Poor Solubility	10.40	Good Permeation
2J	0	5	3	66.0 7	362.0 91198 1	0.6 44	1.00	Good Permeation	0.70	Poor Solubility	2.57	Good Permeation
5J	0	5	1	66.0 7	244.0 88163 4	- 0.1 52	1.00	Good Permeation	0.85	Poor Solubility	5.13	Good Permeation
6J	0	5	2	66.0 7	328.0 64841 1	0.3 41	1.00	Good Permeation	0.73	Poor Solubility	9.33	Good Permeation
7J	0	5	3	66.0 7	336.1 50763 6	1.7 57	1.00	Good Permeation	0.70	Poor Solubility	13.04	Good Permeation
8J	0	6	4	75.3	378.0 86112 7	1.2 56	1.00	Good Permeation	0.66	Poor Solubility	10.01	Good Permeation
9J	0	5	1	66.0 7	242.0 72513 3	- 0.4 27	1.00	Good Permeation	0.74	Poor Solubility	2.28	Good Permeation
10J	0	5	3	66.0 7	260.1 19463 5	0.6 55	1.00	Good Permeation	0.76	Poor Solubility	2.59	Good Permeation
11J	0	6	1	75.3	260.0 83078	- 1.0 58	1.00	Good Permeation	0.86	Poor Solubility	0.83	Good Permeation
12J	0	5	2	66.0 7	244.0 88163 4	- 0.0 8	1.00	Good Permeation	0.88	Poor Solubility	0.55	Good Permeation
1E	0	6	4	75.3	290.1 30028 2	- 0.1 69	1.00	Good Permeation	0.74	Poor Solubility	2.14	Good Permeation
2E	0	5	3	66.0 7	376.1 06848	1.0 02	1.00	Good Permeation	0.71	Poor Solubility	10.84	Good Permeation

1													
5E	0	5	1	66.0 7	258.1 03813 4	0.2 06	1.00	Good Permeation	0.90	Poor Solubility	1.97	Good Permeation	
6E	0	5	2	66.0 7	342.0 80491 1	0.6 99	1.00	Good Permeation	0.71	Poor Solubility	9.52	Good Permeation	
7E	0	5	3	66.0 7	350.1 66413 7	2.1 15	1.00	Good Permeation	0.73	Poor Solubility	2.90	Good Permeation	
8E	0	6	4	75.3	392.1 01762 7	1.6 14	1.00	Good Permeation	0.71	Poor Solubility	10.37	Good Permeation	
9E	0	5	1	66.0 7	256.0 88163 4	- 0.0 69	1.00	Good Permeation	0.86	Poor Solubility	5.80	Good Permeation	
10E	0	5	3	66.0 7	274.1 35113 6	1.0 13	1.00	Good Permeation	0.84	Poor Solubility	8.35	Good Permeation	
11E	0	6	1	75.3	274.0 98728 1	- 0.7	1.00	Good Permeation	0.93	Poor Solubility	2.07	Good Permeation	
12E	0	5	2	66.0 7	258.1 03813 4	0.2 78	1.00	Good Permeation	0.92	Poor Solubility	6.25	Good Permeation	
1F	0	6	4	75.3	290.1 30028 2	- 0.1 69	1.00	Good Permeation	0.71	Poor Solubility	8.97	Good Permeation	
2F	0	5	3	66.0 7	376.1 06848 1	1.0 02	1.00	Good Permeation	0.78	Poor Solubility	10.46	Good Permeation	
5F	0	5	1	66.0 7	258.1 03813 4	0.2 06	1.00	Good Permeation	0.90	Poor Solubility	6.30	Good Permeation	
6F	0	5	2	66.0 7	342.0 80491 1	0.6 99	1.00	Good Permeation	0.85	Poor Solubility	10.25	Good Permeation	
7F	0	5	3	66.0 7	350.1 66413 7	2.1 15	1.00	Good Permeation	0.69	Poor Solubility	12.94	Good Permeation	
8F	0	6	4	75.3	392.1 01762 7	1.6 14	1.00	Good Permeation	0.79	Poor Solubility	10.58	Good Permeation	
9F	0	5	1	66.0 7	256.0 88163 4	- 0.0 69	1.00	Good Permeation	0.99	Poor Solubility	6.19	Good Permeation	
10F	0	5	3	66.0 7	274.1 35113 6	1.0 13	1.00	Good Permeation	0.84	Poor Solubility	9.35	Good Permeation	
11F	0	6	1	75.3	274.0 98728 1	- 0.7	1.00	Good Permeation	0.95	Poor Solubility	6.49	Good Permeation	
12F	0	5	2	66.0 7	258.1 03813 4	0.2 78	1.00	Good Permeation	0.75	Poor Solubility	0.70	Good Permeation	
1A	1	7	4	95.5 3	292.1 09292 7	- 1.5 57	1.00	Good Permeation	0.95	Poor Solubility	10.40	Good Permeation	

2A	1	6	3	86.3	378.0 86112 7	- 0.3 86	1.00	Good Permeation	0.79	Poor Solubility	2.79	Good Permeation
5A	1	6	1	86.3	260.0 83078	- 1.1 82	1.00	Good Permeation	0.90	Poor Solubility	2.49	Good Permeation
6A	1	6	2	86.3	344.0 59755 7	- 0.6 89	1.00	Good Permeation	0.86	Poor Solubility	8.60	Good Permeation
7A	1	6	3	86.3	352.1 45678 2	0.7 27	1.00	Good Permeation	0.79	Poor Solubility	0.98	Good Permeation
8A	1	7	4	95.5 3	394.0 81027 3	0.2 26	1.00	Good Permeation	0.90	Poor Solubility	8.99	Good Permeation
9A	1	6	1	86.3	258.0 67427 9	- 1.4 57	1.00	Good Permeation	0.77	Poor Solubility	0.76	Good Permeation
10A	1	6	3	86.3	276.1 14378 1	- 0.3 75	1.00	Good Permeation	0.65	Poor Solubility	6.70	Good Permeation
11A	1	7	1	95.5 3	276.0 77992 6	- 2.0 88	1.00	Good Permeation	0.84	Poor Solubility	4.82	Good Permeation
12A	1	6	2	86.3	260.0 83078	- 1.1 1	1.00	Good Permeation	0.90	Poor Solubility	2.40	Good Permeation
1B	1	7	4	95.5 3	292.1 09292 7	- 1.5 57	1.00	Good Permeation	0.71	Poor Solubility	1.12	Good Permeation
2B	1	6	3	86.3	378.0 86112 7	- 0.3 86	1.00	Good Permeation	0.85	Poor Solubility	10.76	Good Permeation
5B	1	6	1	86.3	260.0 83078	- 1.1 82	1.00	Good Permeation	0.83	Poor Solubility	6.23	Good Permeation
6B	1	6	2	86.3	344.0 59755 7	- 0.6 89	1.00	Good Permeation	0.90	Poor Solubility	10.26	Good Permeation
7B	1	6	3	86.3	352.1 45678 2	0.7 27	1.00	Good Permeation	0.74	Poor Solubility	13.67	Good Permeation
8B	1	7	4	95.5 3	394.0 81027 3	0.2 26	1.00	Good Permeation	0.79	Poor Solubility	10.98	Good Permeation
9B	1	6	1	86.3	258.0 67427 9	- 1.4 57	1.00	Good Permeation	0.94	Poor Solubility	6.08	Good Permeation
10B	1	6	3	86.3	276.1 14378 1	- 0.3 75	1.00	Good Permeation	0.83	Poor Solubility	1.94	Good Permeation
11B	1	7	1	95.5 3	276.0 77992 6	- 2.0 88	1.00	Good Permeation	0.90	Poor Solubility	6.37	Good Permeation
12B	1	6	2	86.3	260.0 83078	- 1.1 1	1.00	Good Permeation	0.68	Poor Solubility	0.78	Good Permeation
1G	0	7	4	84.5 3	292.1 09292	- 1.4	1.00	Good Permeation	0.86	Poor Solubility	10.81	Good Permeation

					7	33							
2G	0	6	3	75.3	378.0 86112 7	- 0.2 62	1.00	Good Permeation	0.73	Poor Solubility	3.22	Good Permeation	
5G	0	6	1	75.3	260.0 83078	- 1.0 58	1.00	Good Permeation	0.94	Poor Solubility	2.38	Good Permeation	
6G	0	6	2	75.3	344.0 59755 7	- 0.5 65	1.00	Good Permeation	0.88	Poor Solubility	3.00	Good Permeation	
7G	0	6	3	75.3	352.1 45678 2	0.8 51	1.00	Good Permeation	0.80	Poor Solubility	0.88	Good Permeation	
8G	0	7	4	84.5 3	394.0 81027 3	0.3 5	1.00	Good Permeation	0.90	Poor Solubility	3.36	Good Permeation	
9G	0	6	1	75.3	258.0 67427 9	- 1.3 33	1.00	Good Permeation	0.63	Poor Solubility	0.74	Good Permeation	
10G	0	6	3	75.3	276.1 14378 1	- 0.2 51	1.00	Good Permeation	0.58	Poor Solubility	7.05	Good Permeation	
11G	0	7	1	84.5 3	276.0 77992 6	- 1.9 64	1.00	Good Permeation	0.85	Poor Solubility	5.20	Good Permeation	
12G	0	6	2	75.3	260.0 83078	- 0.9 86	1.00	Good Permeation	0.92	Poor Solubility	5.87	Good Permeation	
1N	0	9	7	104. 84	391.1 77706 6	- 0.1 3	1.00	Good Permeation	0.81	Poor Solubility	10.34	Good Permeation	
2N	0	8	6	95.6 1	477.1 54526 6	1.0 41	1.00	Good Permeation	0.70	Poor Solubility	2.88	Good Permeation	
5N	0	8	4	95.6 1	359.1 51491 9	0.2 45	1.00	Good Permeation	0.84	Poor Solubility	2.57	Good Permeation	
6N	0	8	5	95.6 1	443.1 28169 6	0.7 38	1.00	Good Permeation	0.78	Poor Solubility	2.85	Good Permeation	
7N	0	8	6	95.6 1	451.2 14092 2	2.1 54	1.00	Good Permeation	0.68	Poor Solubility	2.72	Good Permeation	
8N	0	9	7	104. 84	493.1 49441 2	1.6 53	1.00	Good Permeation	0.66	Poor Solubility	3.19	Good Permeation	
9N	0	8	4	95.6 1	357.1 35841 8	- 0.0 3	1.00	Good Permeation	0.67	Poor Solubility	2.44	Good Permeation	
10N	0	8	6	95.6 1	375.1 82792	1.0 52	1.00	Good Permeation	0.81	Poor Solubility	8.42	Good Permeation	
11N	0	9	4	104. 84	375.1 46406 5	- 0.6 61	1.00	Good Permeation	0.91	Poor Solubility	1.00	Good Permeation	
12N	0	8	5	95.6 1	359.1 51491 9	0.3 17	1.00	Good Permeation	0.86	Poor Solubility	0.81	Good Permeation	

References

1. Grubbs, R. H.; Rosen, R. K.; Timmers, F. J. *Organometallics* **1996**, *15*, 1518–1520.
2. SYBYL 8.0, The Tripos Associates, St. Louis MO, 2008.
3. Lipinski, C.A., Lombardo, F., Dominy, B.W., Feeney, P.J. Experimental and computational approaches to estimate solubility and permeability in drug discovery and development settings. *Adv. Drug Delivery Rev.* **1997**, *23*, 3–25.
4. Concord 8.0, The Tripos Associates, St. Louis MO, 2008.
5. Cruciani, G., Meniconi, M., Carosati, E., Zamora, I., Mannhold, R. VOLSURF: A Tool for Drug ADME-Properties Prediction. In: *Methods and Principles in Medicinal Chemistry*. Eds. van de Waterbeemd, H., Lennernäs, H., Artursson, P. (Wiley-VCH Verlag GmbH & Co., Weinheim, 2003).
6. Pearlman, R.S.; Smith, K.M. Metric Validation and the Receptor-Relevant Subspace Concept. *J. Chem. Inf. Comput. Sci.* **1999**, *39*, 28–35.

Appendix B
X-Ray Structure Reports

CONTENTS

Crystal Structure Report for C ₁₁ H ₁₂ BrNO ₃ S Compound 2.8.6 ¹	495
Crystal Structure Report for C ₁₅ H ₂₁ FN ₂ O ₂ S Compound 2.11.3 ²	499
Crystal Structure Report for C ₁₅ H ₂₃ BrN ₂ O ₃ S Compound 3.1.2a ³	502
Crystal Structure Report for C ₁₈ H ₂₇ BrN ₂ O ₃ S Compound 3.9.2p	504
Crystal Structure Report for C ₂₁ H ₂₇ FN ₂ O ₃ S Compound 3.10.2b	506
Crystal Structure Report for C ₂₁ H ₂₇ FN ₂ O ₃ S Compound 3.11.2m	509
Crystal Structure Report for C ₁₅ H ₂₃ BrN ₂ O ₃ S Compound 3.12.1c	511

- [1] X-ray data related to compound **2.8.6** can be found in the publication: Samarakoon, T. B.; Loh, J. K.; Rolfe, A.; Le, L. S.; Yoon, S. Y.; Lushington, G. H.; Hanson, P. R. A Modular Reaction Pairing Approach to the Diversity-Oriented Synthesis of Fused- and Bridged-Polycyclic Sultams. *Org. Lett.* **2011**, *13*, 5148–5151.
- [2] X-ray data related to compound **2.11.3** would be published shortly.
- [3] All X-ray data related to Chapter Three molecules (**3.1.2a**, **3.9.2p**, **3.10.2b**, **3.11.2m**, **3.12.1c**) would be submitted to *J. Org. Chem* shortly.

Crystal Structure Report

for



Compound **2.8.6**

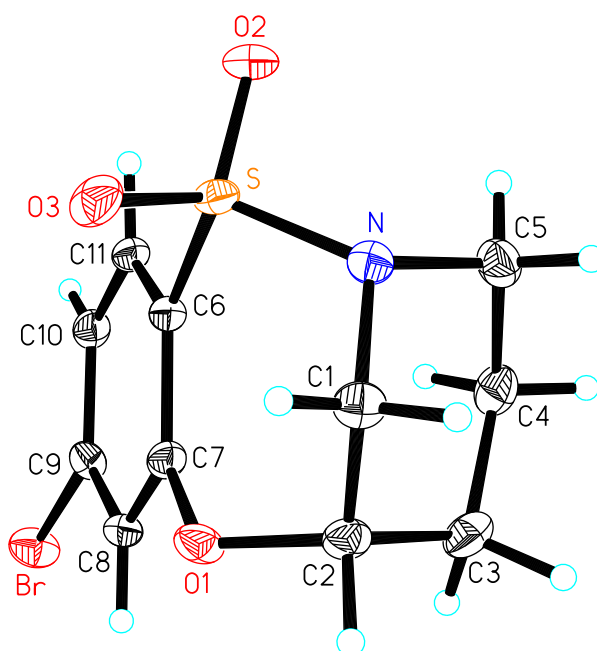
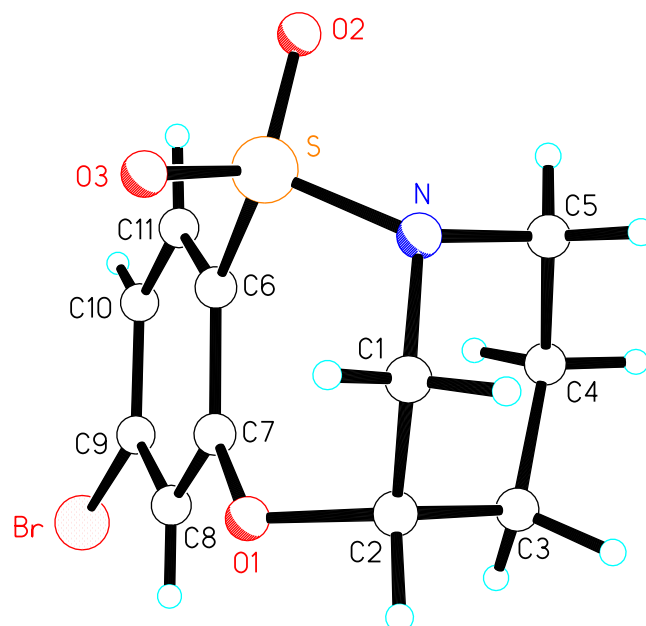
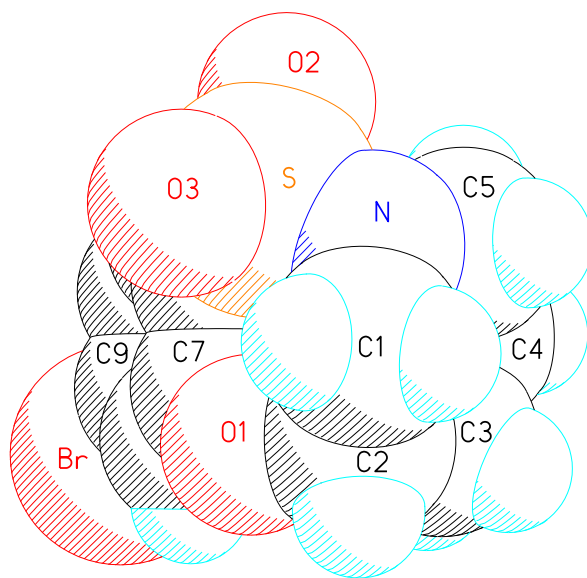
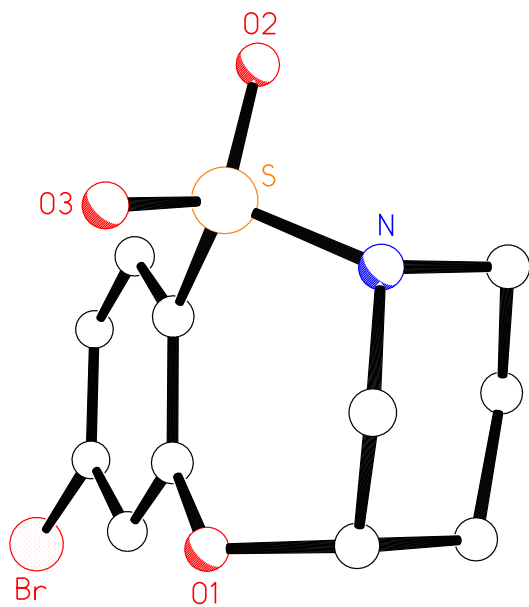


Figure 1. 50% Probability Ellipsoid Drawing of **2.8.6**



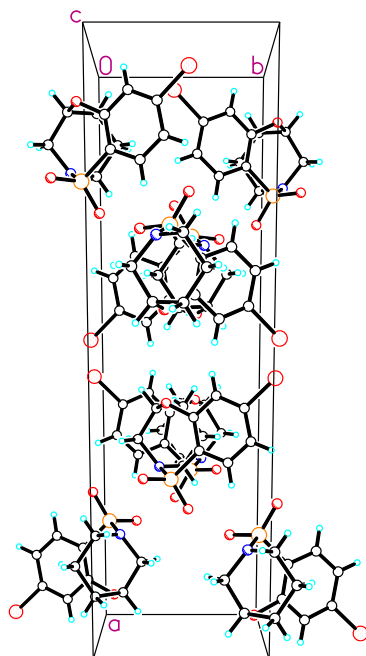
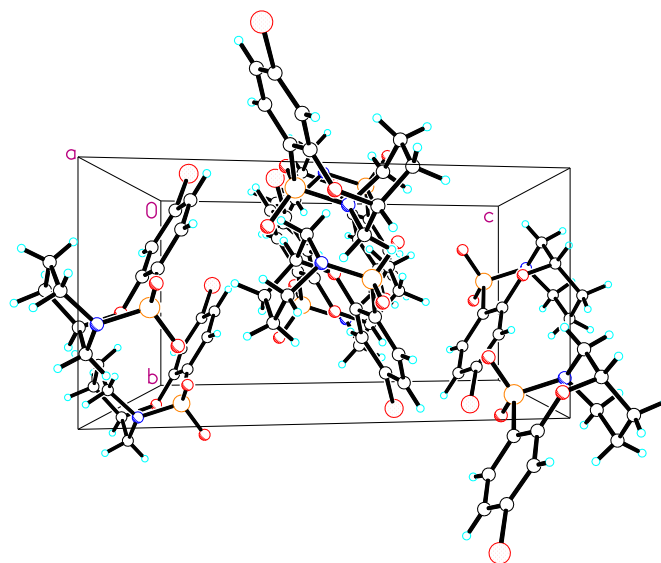
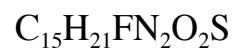


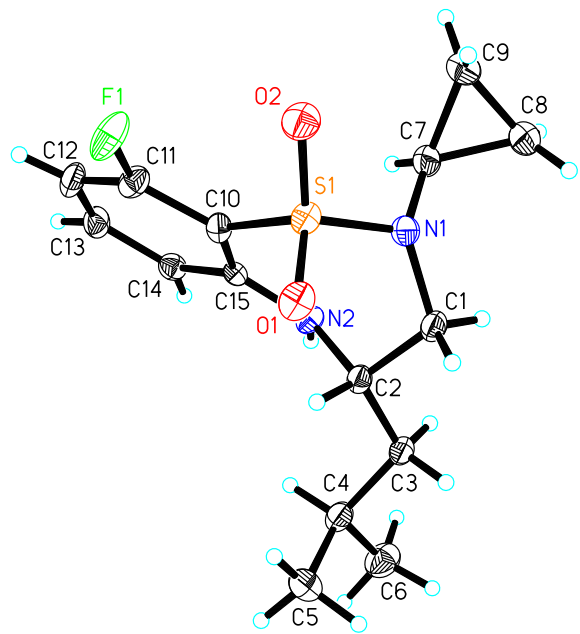
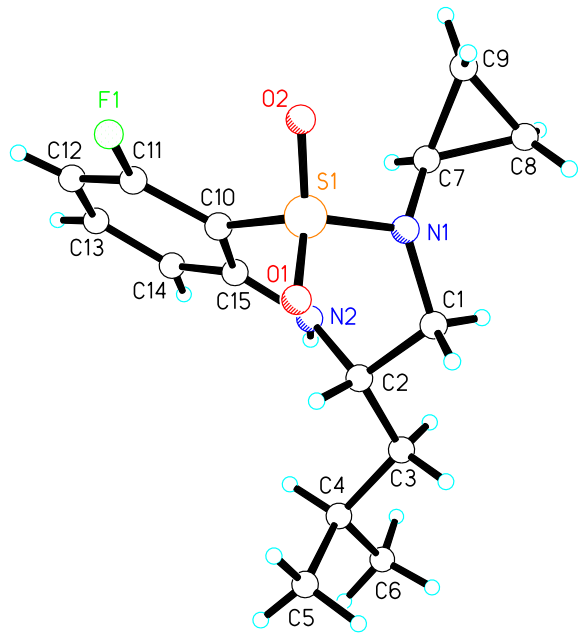
Figure 2. Packing diagram of **2.8.6**

Crystal Structure Report

for



Compound **2.11.3**



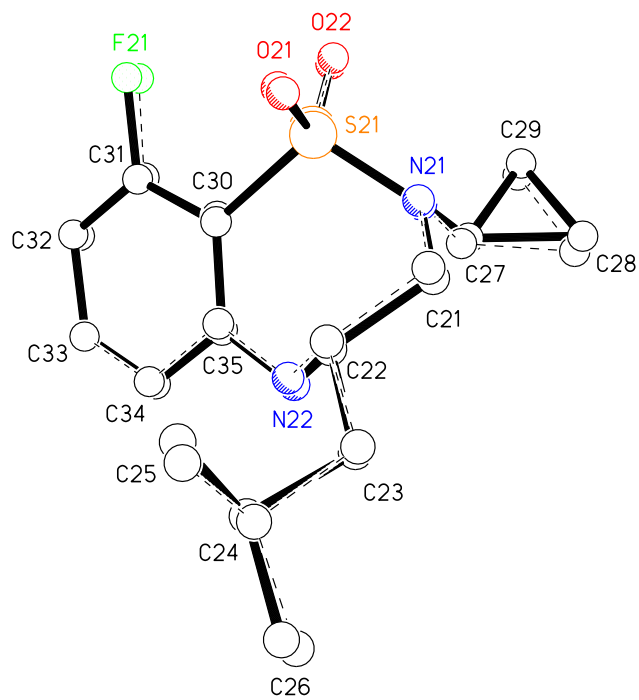


Figure 1. 50% Probability Ellipsoid Drawing of **2.11.3**

Crystal Structure Report

for



Compound **3.1.2a**

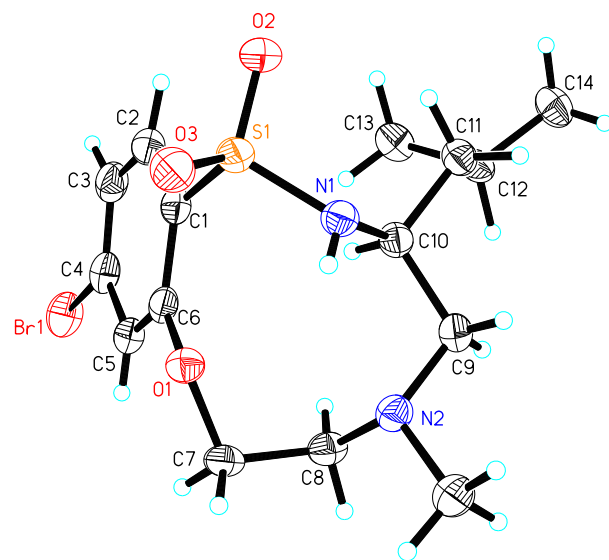
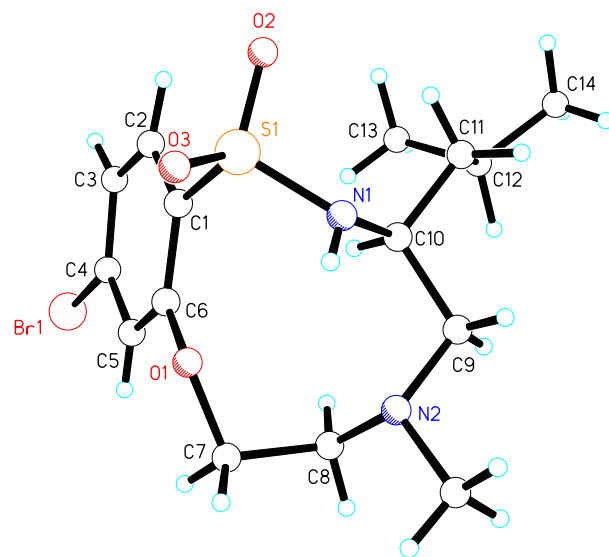


Figure 1. 50% Probability Ellipsoid Drawing of **3.1.2a**

Crystal Structure Report

for



Compound **3.9.2p**

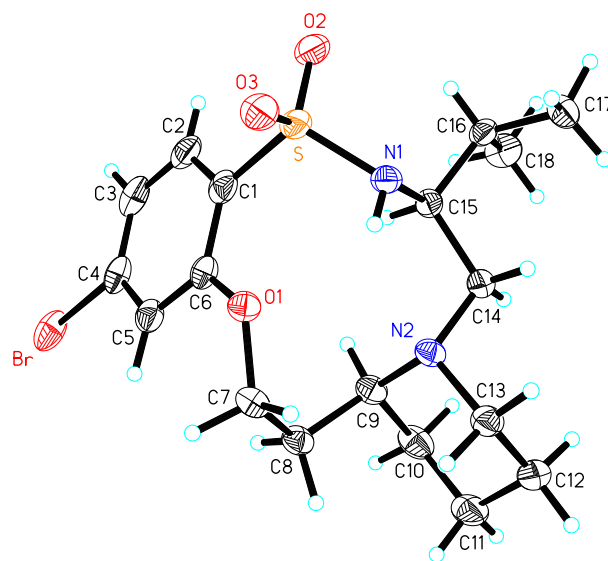
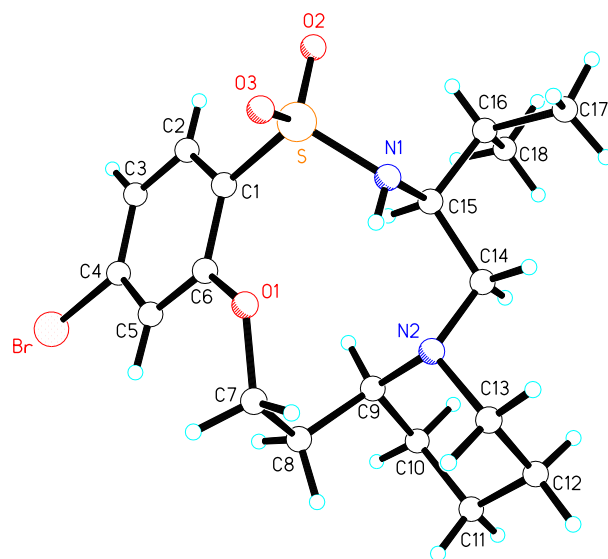
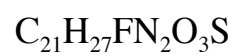


Figure 1. 50% Probability Ellipsoid Drawing of **3.9.2p**

Crystal Structure Report

for



Compound **3.10.2b**

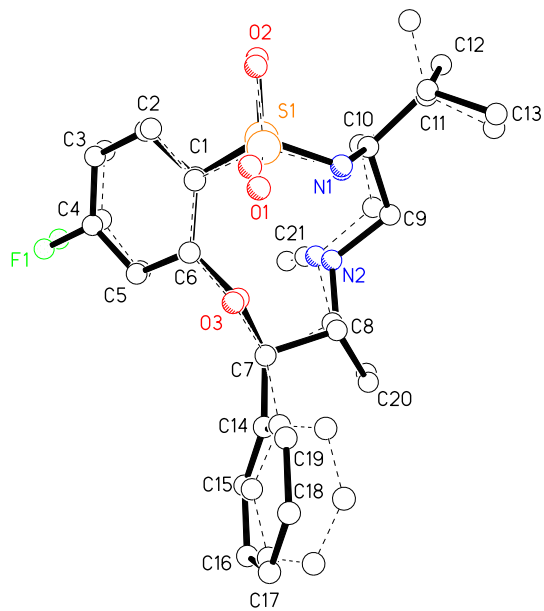
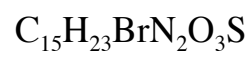


Figure 1. 50% Probability Ellipsoid Drawing of **3.10.2b**.

Crystal Structure Report

for



Compound **3.11.2m**

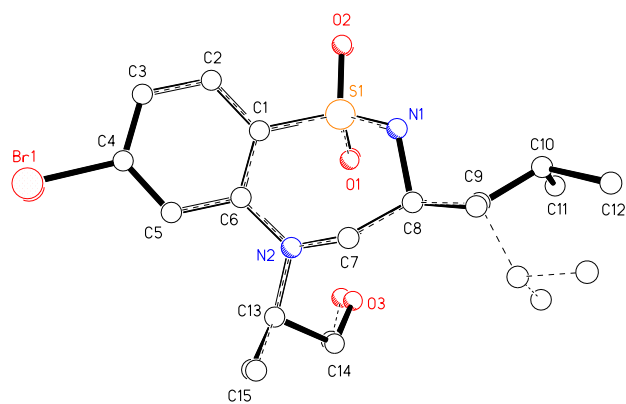
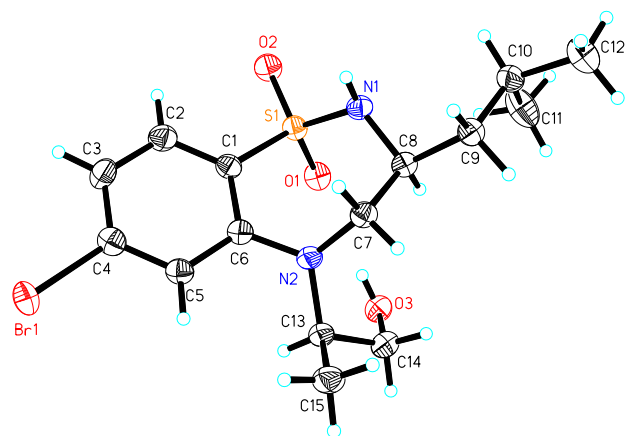
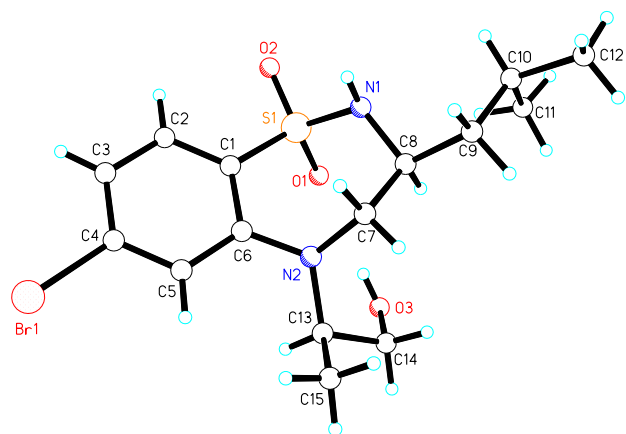


Figure 1. 50% Probability Ellipsoid Drawing of **3.11.2m**.

Crystal Structure Report

for



Compound **3.12.1c**

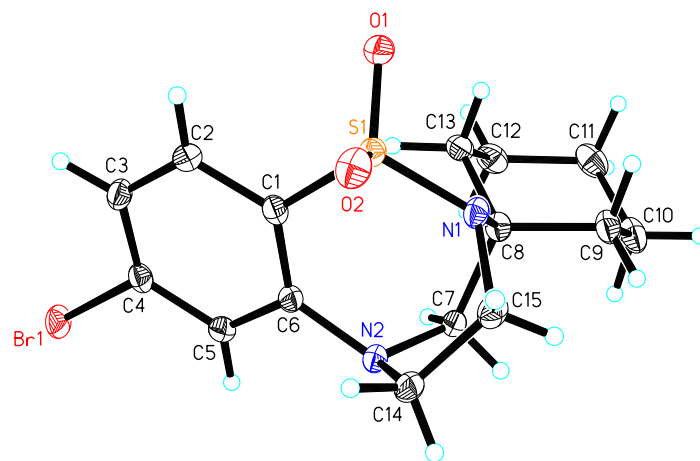
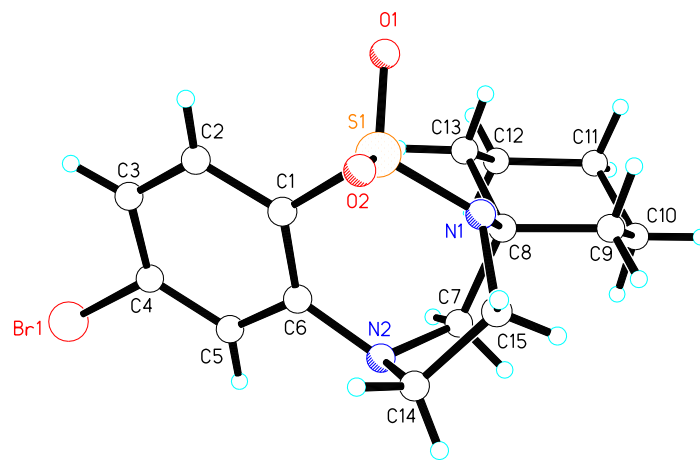


Figure 1. 50% Probability Ellipsoid Drawing of **3.12.1c**.